

**CAMPHOR-DERIVED CHIRAL AUXILIARIES: A SYNTHETIC,
MECHANISTIC AND COMPUTATIONAL STUDY**

A thesis submitted in fulfillment of the
requirements for the degree of

DOCTOR OF PHILOSOPHY

Of

RHODES UNIVERSITY

By

ANDREW ROBERT DUGGAN

March 2006

ABSTRACT

A broadly based approach has been undertaken to the development and use of camphor derivatives as chiral auxiliaries in asymmetric synthesis – an approach which has embraced synthetic, mechanistic and computational studies.

The unambiguous characterization of mono- and dihydroxy-derivatives, obtained by reduction of chiral camphor ether dimers, has been achieved through detailed one- and two-dimensional NMR spectroscopic analysis. The resulting data has been used to establish both the regio- and stereochemistry of the hydroxyl groups.

A camphor-derived cyclic iminolactone has been shown to provide a convenient platform for the synthesis of chiral α -amino acids, stereoselective monoalkylation of the iminolactone affording a range of products in yields of 52 - 65 % with up to 85 % d.e.

The attempted development of chiral bifunctional Morita-Baylis-Hillman substrates has revealed an unexpected equilibration between isomeric bornane 2,3-diol monoacrylates *via* acid-catalysed intramolecular transesterification. A detailed ^1H NMR-based kinetic study of the rearrangement in various media and at various temperatures has permitted the determination of the kinetic and thermodynamic parameters. A computational study at the DFT level has been used to explore the potential energy surfaces of the acid-catalysed and uncatalysed transesterification of the monoacrylate esters. The theoretical data supports the involvement of cyclic intermediates and has provided a rational basis for predicting the favoured reaction pathways.

Novel camphor-derived phenyl sulfonate esters and *N*-adamantylsulfonamides have been synthesised for use as chiral auxiliaries in the Morita-Baylis-Hillman reaction. Modeling at the Molecular Mechanics level has provided useful insights into possible conformational constraints and an adamantyl sulfonate auxiliary has been successfully used in the stereoselective synthesis of a range of products, generally in excellent yield and with up to 95 % d.e.

TABLE OF CONTENTS	Page
ABSTRACT	ii
TABLE OF CONTENTS	iii
ACKNOWLEDGEMENTS	vii
SELECTED ABBREVIATIONS	viii
1. INTRODUCTION	1
1.1. ASYMMETRIC SYNTHESIS	1
1.1.1. Importance of asymmetric synthesis	1
1.1.2. Methods of achieving asymmetric synthesis	2
1.2. CAMPHOR IN ASYMMETRIC SYNTHESIS	4
1.2.1. Occurrence and biosynthesis of camphor	4
1.2.2. Structure and reactivity of camphor	7
<i>1.2.2.1. C(2)-Modification</i>	8
<i>1.2.2.2. C(3)-Modification</i>	9
<i>1.2.2.3. C(5)- and C(6)-Modification</i>	10
<i>1.2.2.4. C(8)-Modification</i>	11
<i>1.2.2.5. C(9)-Modification</i>	13
<i>1.2.2.6. C(10)-Modification</i>	15
<i>1.2.2.7. C(1)-C(2)-Cleavage</i>	23
<i>1.2.2.8. C(2)-C(3)-Cleavage</i>	24
<i>1.2.2.9. C(1)-C(7)-Cleavage</i>	24
1.3. THE MORITA-BAYLIS-HILLMAN REACTION	26
1.3.1. Mechanism	27
1.3.2. Reaction Parameters	29
<i>1.3.2.1. Solvents</i>	29
<i>1.3.2.2. Temperature and microwave irradiation</i>	29
<i>1.3.2.3. Pressure and sonication</i>	30
1.3.3. Stereocontrol	30
<i>1.3.3.1. Diastereoselectivity</i>	31
<i>1.3.3.1.1 Chiral activated alkenes</i>	31

1.3.3.1.2	<i>Chiral electrophiles</i>	36
1.3.3.1.3	<i>Solvent effects</i>	40
1.3.3.2.	<i>Enantioselectivity</i>	41
1.3.3.2.1	<i>Chiral catalysts</i>	41
1.3.3.2.2	<i>Chiral co-catalysts</i>	45
1.3.3.2.3	<i>Chiral solvents</i>	47
1.3.3.2.4	<i>Resolution of adducts</i>	47
1.4.	PREVIOUS WORK BY THE RHODES RESEARCH GROUP	48
1.5.	AIMS OF THE PRESENT STUDY	51
2.	DISCUSSION	52
2.1.	SYNTHESIS AND DIMERISATION REACTIONS OF EXO-HYDROXY BORNANONES	52
2.1.1	Synthesis of α-ketols	55
2.1.2	Rearrangement and dimerisation of α-ketols	60
2.1.3	Reduction of the α-ketol dimers	74
2.2.	ASYMMETRIC SYNTHESIS OF α-ALKYLATED α-AMINO ACIDS	86
2.2.1.	Synthetic rationale	88
2.2.2.	Synthesis of the 2-iminolactone	90
2.2.3.	Alkylation of the 2-iminolactone	94
2.3.	SYNTHESIS OF CAMPHOR-DERIVED BAYLIS-HILLMAN SUBSTRATES	100
2.3.1.	Synthetic rationale	100
2.3.2.	Monoacrylate esters of dihydroxybornane	101
2.3.2.1.	<i>Synthesis of the acrylate esters</i>	102
2.3.3.	Kinetic study of the monoacrylate ester rearrangements	115
2.3.3.1.	<i>Reaction of acrylate esters in unpurified CDCl₃</i>	119
2.3.3.2.	<i>Reaction of acrylate esters in purified CDCl₃ under N₂</i>	129
2.3.3.3.	<i>Reaction of acrylate esters in purified CDCl₃ in Air</i>	136
2.3.3.4.	<i>Reaction of acrylate esters in purified DMSO-d₆</i>	138
2.3.3.5.	<i>Reaction of acrylate esters in purified DMSO-d₆ in the presence of H₂SO₄</i>	141

2.3.3.6.	<i>Reaction of acrylate esters in unpurified DMSO-d₆ in the Presence of p-TsOH</i>	142
2.3.3.7.	<i>Comparison of kinetic data for transesterification in different Media</i>	143
2.3.4.	Computational study of transesterification of the acrylate esters	146
2.3.4.1.	<i>Uncatalysed transesterification</i>	147
2.3.4.2.	<i>Catalysed transesterification</i>	154
2.3.4.3.	<i>Mechanistic conclusions of the acrylate esters</i>	160
2.3.5.	Acrylate esters of phenyl 2-hydroxybornane-10-sulfonate	162
2.3.5.1.	<i>Synthesis of phenyl camphor-10-sulfonate</i>	163
2.3.5.2.	<i>Reduction of phenyl camphor-10-sulfonate</i>	164
2.3.5.3.	<i>Acylation of the 2-hydroxybornane-10-sulfonates</i>	171
2.3.6.	Acrylate esters of N-(1-adamantyl)-2-hydroxybornane-10-sulfonamide	180
2.3.6.1.	<i>Preparation of N-(1-adamantyl)camphor-10-sulfonamide</i>	182
2.3.6.2.	<i>Reduction of N-(1-adamantyl)camphor-10-sulfonamide</i>	185
2.3.6.3.	<i>Acylation of the N-(1-adamantyl)-2-hydroxybornane-10-sulphonamides</i>	191
2.3.6.4.	<i>Use of the 2-exo-acryloyloxy-N-(1-adamantyl)bornane-10-sulphonamide auxiliary in the Morita-Baylis-Hillman reaction</i>	195
2.4.	CONCLUSIONS	201
3.	EXPERIMENTAL	203
3.1.	GENERAL	203
3.1.1.	Analysis	203
3.1.2.	Chromatography	203
3.1.3.	Solvents	204
3.1.4.	Computational Methods	204
3.1.4.1.	<i>Molecular mechanics calculations</i>	204
3.1.4.2.	<i>Density functional theory calculations</i>	204
3.2.	SYNTHETIC PROCEDURES	206
3.2.1.	Dibornyl ethers	206

3.2.2.	Iminolactones	215
3.2.3.	Acrylate esters of 2,3-dihydroxybornane	221
3.2.4.	Acrylate esters of phenyl 2-hydroxybornane-10-sulfonate	224
3.2.5.	Acrylate esters of <i>N</i> -(1-adamantyl)-2-hydroxybornane-10-sulfonamide	231
3.2.6.	Morita-Baylis-Hillman products from <i>N</i> -(1-adamantyl)-2- <i>exo</i> -acryloyloxybornane-10-sulfonamide	237
3.3.	NMR KINETIC STUDY	242
3.3.1.	General Purification, spectroscopic techniques and calculations	242
3.3.2.	Reactions in unpurified CDCl ₃	244
3.3.3.	Reactions in purified CDCl ₃ under N ₂	254
3.3.4.	Temperature effect on acrylate data in purified CDCl ₃ under N ₂	259
3.3.5.	Thermal stability study of purified CDCl ₃ in air	260
3.3.6.	Reactions in purified DMSO- <i>d</i> ₆ under N ₂	265
3.3.7.	Reactions in purified DMSO- <i>d</i> ₆ with H ₂ SO ₄ under N ₂	271
3.3.8.	Reactions in purified DMSO- <i>d</i> ₆ with <i>p</i> -TsOH under N ₂	273
4.	REFERENCES	278
5.	APPENDIX I	288
6.	APPENDIX II	CD

ACKNOWLEDGEMENTS

The source of the great majority my guidance, assistance and problem-solving has always originated from Prof. P.T. Kaye, for this and for your motivation and enthusiasm I am incredibly grateful. I am truly privileged to have been one of his many students.

Kevin Lobb's computational and mathematical skills, together with his willingness to assist, have been instrumental to much of the data acquisition and processing of this study. My deepest thanks to him. Also a very big thank you to Andy Soper and Rob Keyzer, whose tutoring and problem solving with NMR spectroscopy enabled the characterization of compounds from highly complex data.

A special thanks to the Pharmacy Department, especially to Mr and Mrs Morley and Denzil Beukes for the loan of numerous instruments, when nobody else could. For all the technical support and low-resolution mass spectrometry, my deepest thanks to Mr A. Sonneman and for routine equipment and supplies, Mr. J.J. Buys and Mr. A. Adriaan. Thanks to Professor Mino Caira from the University of Cape Town for X-ray crystallography and Mr Tommie van der Merwe from the University of Witwatersrand for the high-resolution mass spectroscopy.

To Rosa Klein, for her considerable help in proofreading this document, and all of my other fellow students and friends; Andre Daubinet, Liezel Sabbagh, Edith Antunes, Michael Wisch, Jeff Chen, Christine van den Berg, Christopher Coltman, Pierre Maclean and all the others that tirelessly offered their help and were there for me, I am indebted to you and a heartfelt thanks.

I also wish to thank the NRF and Rhodes University for the financial support.

To my parents; I could never ask for so much love, confidence and dedication from anyone. I dedicate all that I have herein to you.

SELECTED ABBREVIATIONS

$[\alpha]_D$	specific rotation (determined using the sodium D line at the temperature quoted)
Ac ₂ O	acetic anhydride
BINAP	2,2'-bis(diphenylphosphino)-1,1'-binaphthyl
br	broad
<i>c</i>	concentration (quoted in g/100mL)
BOC	<i>t</i> -butoxycarbonyl
CDCl ₃	deuterated chloroform
CDI	carbonyldiimidazole
COSY	¹ H- ¹ H homonuclear correlation spectroscopy
e.e.	enantiomeric excess
d	doublet
DABCO	1,4-diazabicyclo[2.2.2]octane
DCC	1,3-dicyclohexylcarbodiimide
d.e.	diastereomeric excess
DEPT	distortionless enhancement by polarization transfer
DMAP	4-dimethylaminopyridine
DMF	<i>N,N</i> -dimethylformamide
DMSO	dimethylsulfoxide
eq.	molar equivalent
Et ₃ N	triethylamine
Et ₂ O	diethyl ether
EtOAc	ethyl acetate
EtOH	ethanol
HMBC	heteronuclear multiple bond correlation
HMQC	¹ H - ¹³ C heteronuclear multiple quantum coherence
HRCIMS	high resolution chemical ionization mass spectrometry
HPLC	high performance liquid chromatography
HSQC	¹ H - ¹³ C heteronuclear single quantum coherence
IR	infrared
LAH	lithium aluminum hydride

LDA	lithium diisopropylamide
lit.	literature
m	multiplet
MeOH	methanol
m.p.	melting point
MS	mass spectrometry
NMR	nuclear magnetic resonance
NOESY	nuclear Overhauser enhancement spectroscopy
ppm	parts per million
<i>p</i> -TsOH	<i>p</i> -toluenesulfonic acid
pyr	pyridine
q	quartet
s	singlet
satd.	saturated
t	triplet
THF	tetrahydrofuran
TLC	thin layer chromatography
TMS	tetramethylsilane

1. INTRODUCTION

The necessity of asymmetric synthesis cannot be overstated; perhaps its importance is best exemplified by the regular, exclusive occurrence of single enantiomeric compounds in the grandest synthetic process of them all, nature itself.

1.1 ASYMMETRIC SYNTHESIS

1.1.1 Importance of Asymmetric Synthesis

The fundamental basis of asymmetric synthesis is the creation of asymmetric centres such that the resulting enantiomers or diastereomers are formed in unequal proportions. This is achieved by the creation of new asymmetric centres either in achiral molecules, through the use of asymmetric reagents or catalysts, or in molecules already possessing asymmetric centres, which generally influence the formation of new diastereomers in unequal amounts. It should be mentioned that the formation of chiral carbon compounds is by far the most widely investigated of asymmetric syntheses. However, similar approaches have been employed for the synthesis of chiral centres at sulfur, phosphorus and other elements.¹

Biological activity is most often associated with the interactions of a particular stereoisomer with a biological receptor. This distinction between stereoisomers occurs due to the asymmetric nature of the environment around typical receptors. The vast majority of drugs produced commercially contain one or more stereocentres, but only one of the stereoisomers may exhibit beneficial properties whilst the other(s) may be ineffective or even hazardous. The widely known and tragic introduction of racemic thalidomide as a sedative hypnotic drug resulted in teratogenic effects, which were attributed to one enantiomer while the other was effective in the role that it was intended.² The need for single enantiomer or diastereomer drugs is thus of vital importance and the stereoselective synthesis of these drugs is a great and fundamental challenge for organic chemists.³

1.1.2 Methods of Achieving Asymmetric Synthesis

At the forefront of asymmetric research are synthetic methods that involve the use of chiral auxiliaries, reagents or catalysts, which function as an external source that induces chirality in a reaction.⁴ While chiral auxiliaries are often without equal as exceedingly effective tools, chiral reagents and catalysts have increasingly found favour.⁴ The evolution of synthetic methodology in this area may be viewed in terms of four generations.

First generation: Substrate-controlled methods

Chiral starting materials are selected from a range of chiral molecules available from natural sources, *viz.*, the “chiral pool”,⁵ and include amino acids, carbohydrates and alkaloids. The molecules are then modified by suitable means to obtain products whose overall stereochemistry is directly influenced by the existing chiral centre(s) in the starting material.⁶

Second generation: Auxiliary-controlled methods

The chiral auxiliary is a chiral moiety that is attached to a prochiral substrate molecule, thus creating an asymmetric environment around the substrate. This molecule is then able to undergo a reaction where the very nature of the auxiliary induces some measure of stereocontrol in the formation of products. Removal, and recycling, of the auxiliary then affords a chiral product. Requirements for a chiral auxiliary include: - i) ready availability as a homochiral moiety that can be easily attached to the prochiral substrate; ii) capacity to induce a high degree of stereoselectivity; iii) easy removal from the product and recoverability in high yield.

Third generation: Reagent-controlled methods

In this approach, stereocontrol is achieved through the use of stoichiometric quantities of chiral reagent which directly influence the stereochemical outcome of the reaction of the prochiral substrate. This method characteristically involves fewer steps than with a chiral auxiliary, as there is no need to introduce or remove the auxiliary. The majority of chiral reagents are organometallic, and the most common metals involved are titanium,⁷ lithium, magnesium, aluminum⁸ and iron.⁹

Fourth generation: Catalyst-controlled methods

Chiral catalysts are typically composed of asymmetric ligands that are co-ordinated to a metal. They may be covalently attached to the substrate, forming an intermediate in the catalytic cycle, or they may act in an intermolecular manner, inducing asymmetry in a single step. Catalytic methods are often favoured due to the potential for recycling the catalyst and the small amounts of chiral material required. Furthermore, catalysts which are able to participate in a secondary interaction with substrates, in a substrate-catalyst complex, are highly valued as they have been observed to promote efficient asymmetric induction.¹⁰ Such interaction may involve the co-ordination of the catalyst not only with the functional groups undergoing chemical transformation, but also with other functional groups in the substrate.

The success of asymmetric reactions is directly related to the asymmetric environment that is achieved as a result of the chiral nature of the reactive species that surround the reactive or catalytic core. The asymmetric grouping is the ultimate source of enantioselectivity because, in order to introduce a new chiral centre into a prochiral molecule or manipulate an existing chiral centre, it is necessary to spatially direct the reaction. The chirality surrounding the reactive centre will facilitate the generation of one enantiomer, while hindering generation of the other. Computational methods have recently become powerful enough to predict, with varying degrees of success, the nature of the interactions at the reactive centre and consequently aid in the rational design of ligands for asymmetric synthesis.

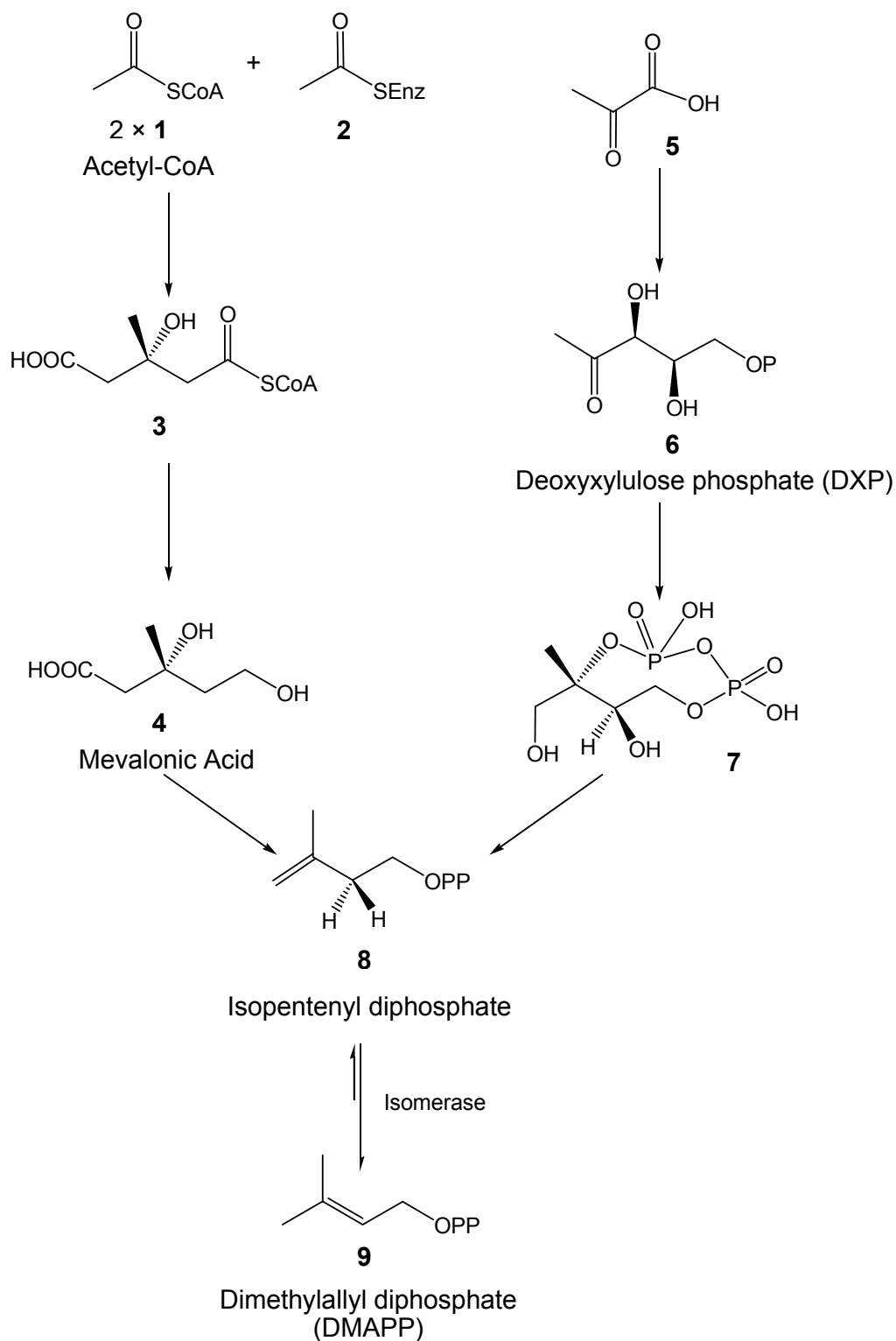
1.2 CAMPHOR IN ASYMMETRIC SYNTHESIS

Camphor has been used for hundreds of years as a rubefacient, mild analgesic, lip-balm, chilblain ointment, cold-sore ointment and in liniments against rheumatic pain, fibrositis and muscle stiffness.¹¹ Natural production of camphor has been largely replaced by the synthesis of a racemate from pinene, which is obtained from turpentine oil.¹¹

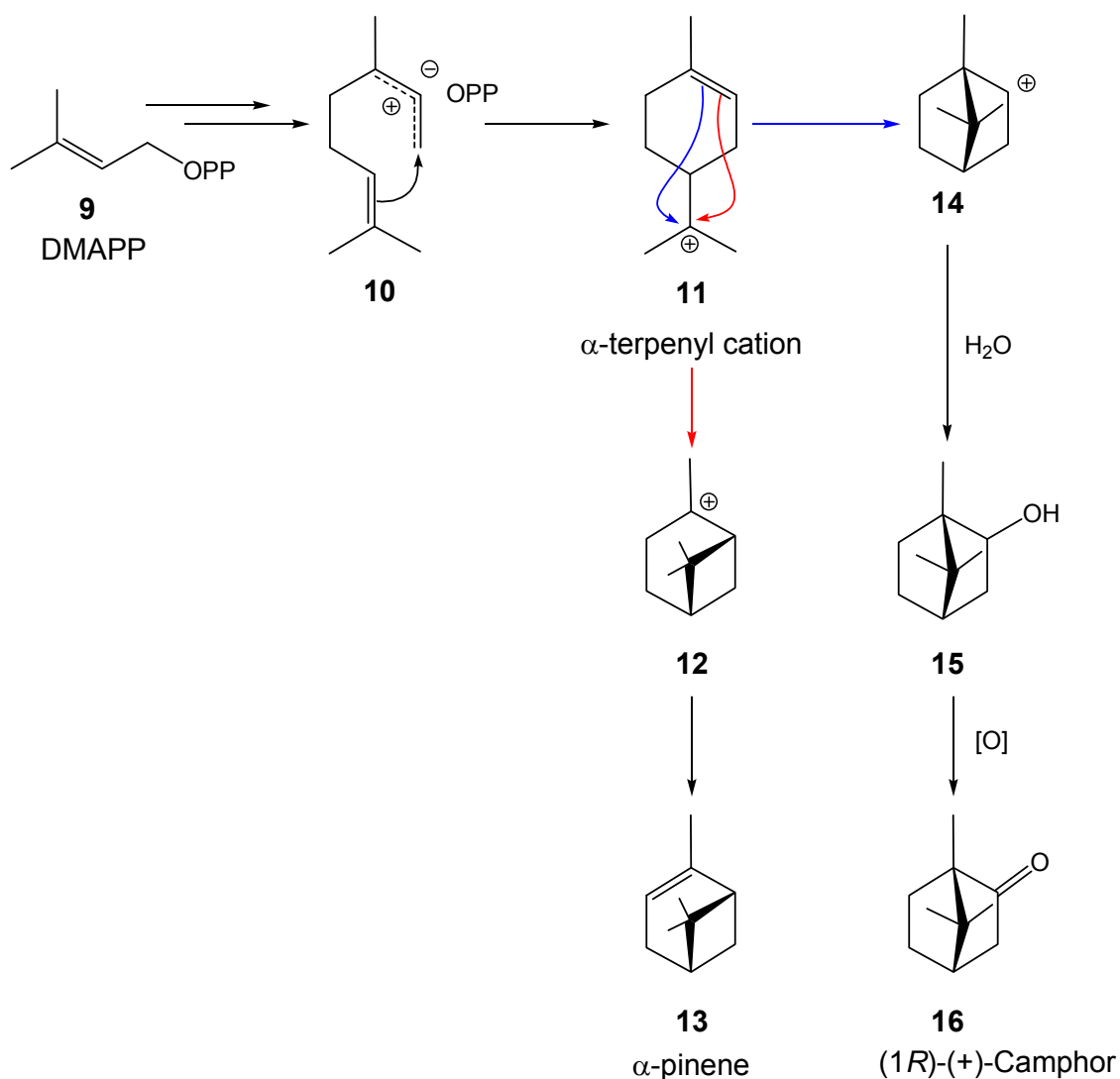
1.2.1 Occurrence and Biosynthesis of Camphor

Cinnamomum camphora (L.) J. Presl. (*Lauraceae*) is a tree in the coastal regions of South-East Asia growing up to 40m high and having coriaceous leaves and an aromatic smell. Steam distillation of the wood affords a volatile oil whose main constituent is camphor, which on cooling separates as a white crystalline solid from the mother liquor. Natural camphor is a dextrorotatory ketone with a specific rotation of $[\alpha]_D +42^\circ$.¹¹

Camphor is a terpenoid, which is biosynthetically produced by way of the intermediates, mevalonic acid (MVA) **4** or 1-deoxy-D-xylulose 5-phosphate (DXP) **6** (**Scheme 1.1**). The first steps of the mevalonate pathway have traditionally been believed to be common to the whole range of natural terpenoid derivatives, but it has subsequently been established that an alternative pathway exists, *viz.*, the mevalonate-independent pathway (also known as methylerythritol phosphate or DXP pathway) which provides an alternative pathway to the intermediates, isopentenyl diphosphate (IPP) **8** and dimethylallyl diphosphate (DMAPP) **9**. The mevalonate-independent pathway is still incompletely characterised although it undoubtedly exists and is considered the most likely pathway for the biosynthesis of IPP and DMAPP in plants.¹² The isopentenyl diphosphate pathway to (1*R*)-(+)-camphor **16** (**Scheme 1.2**) uses DMAPP produced by either the mevalonate or deoxyxylulose phosphate pathways and results in numerous compounds, including several monoterpenes. However, only the routes that specifically generate camphor **16** and α -pinene **13** are illustrated.¹²



Scheme 1.1: The mevalonic acid and deoxyxylulose phosphate pathways for the biosynthesis of isopentenyl diphosphate (IPP) **8** and dimethylallyl diphosphate (DMAPP) **9**.¹²

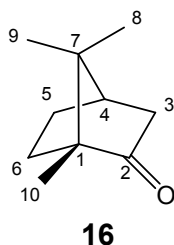


Scheme 1.2: The biosynthesis of camphor **16** and α -pinene **13** from dimethylallyl diphosphate *via* the isopentenyl diphosphate pathway.¹²

Cyclization of the α -terpenyl cation **11** occurs through enzymatic catalysis, in which the cationic side chain is folded towards the double bond, and results in the bornyl **14** and pinyll **12** cations, depending on which end of the double bond is involved in the formation of the new bond (**Scheme 1.2**). Addition of water to the bornyl cation **14** results in borneol **15**, oxidation of which leads to the ketone, (1*R*)-(+)-camphor **16**. Alternatively, loss of a proton from the pinyll cation **12** generates the alkene, α -pinene **13**.

1.2.2. Structure and Reactivity of Camphor

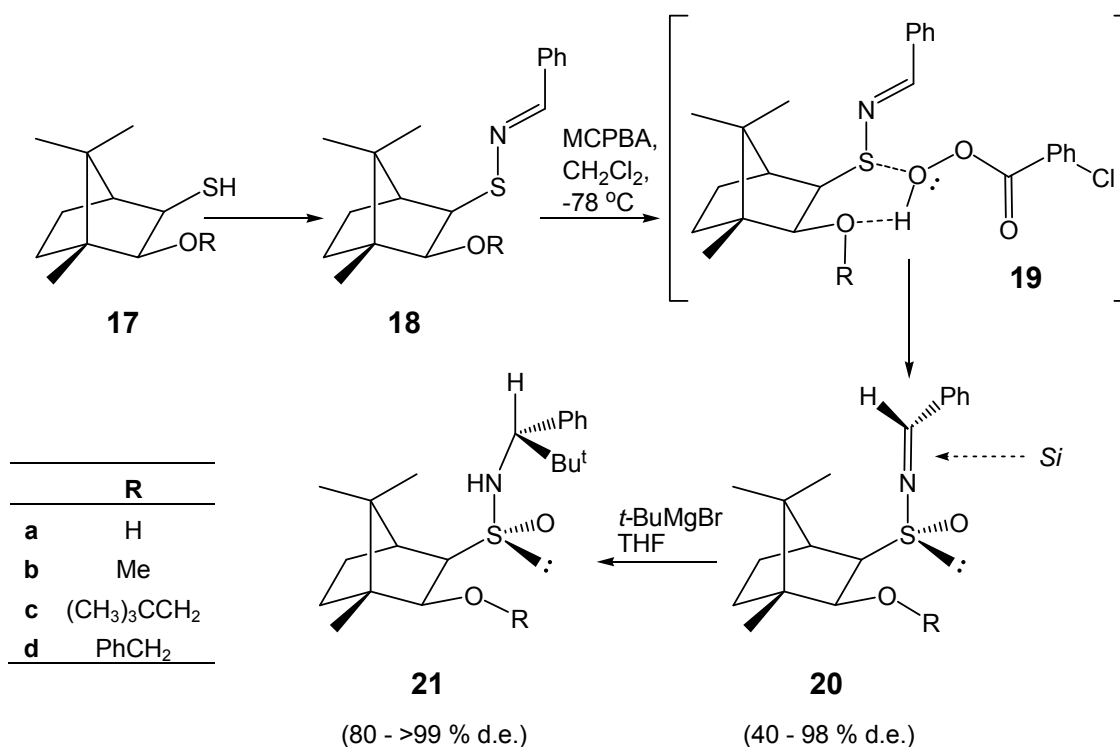
The use of camphor **16** as a starting material in asymmetric synthesis has enjoyed widespread attention, due primarily to its availability in both (+)- and (-)-enantiomeric forms and its versatility in the generation of specific derivatives, often consisting of a single stereoisomer. Functionality may be introduced at the C-3, C-5, C-8, C-9 or C-10 positions of the camphor scaffold either directly or indirectly through chemospecific, regioselective and enantioselective synthesis.¹³ Furthermore, a large number of intriguing rearrangements, observed since early the last century by Meerwein and van Emster,¹⁴ and cleavage of C(1)-C(2), C(2)-C(3) and C(1)-C(7) bonds in camphor and its derivatives are readily achieved resulting in valuable synthetic intermediates.¹⁵



Asymmetric induction in the reactions of various camphor derivatives is primarily due to the steric constraints resulting from the rigidity of the structure and the bulk of the 8-, 9- and 10-methyl groups.¹⁶ Initial attack on the camphor skeleton occurs, in most instances, from the less hindered *endo*-face to generate enantiomeric products. The resulting derivatives may, in turn, play crucial roles in stereodirecting further synthetic steps through blocking or encouraging attack from one or other face due to their steric bulk or polarity effects, which are known, collectively, as secondary interactions and which are vital for effective stereocontrol.^{17,18} Various modifications at individual positions of the camphor skeleton will be described in the following sections and illustrated by relevant examples. Specific attention will be paid to the stereodirecting characteristics of the camphor derivatives.

1.2.2.1 C(2)-Modification

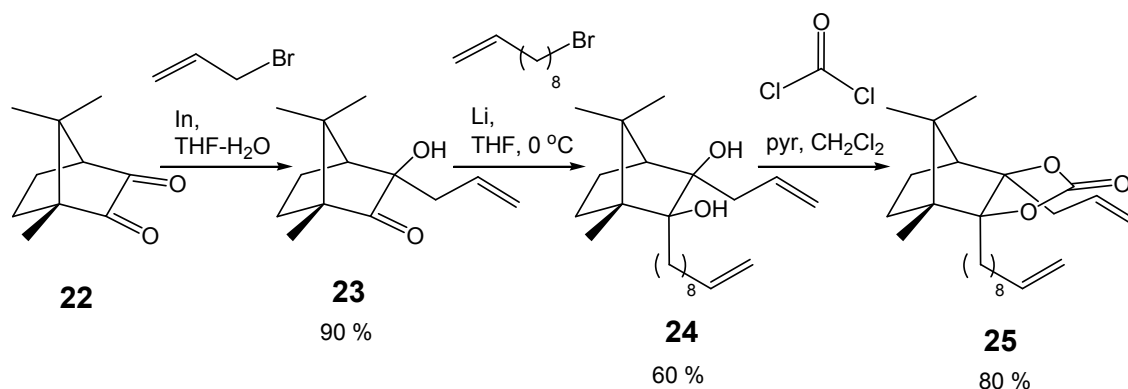
The carbonyl moiety at C-2 in camphor is already a highly reactive group that undergoes characteristic reactions to form a wide variety of synthetic intermediates. Hung *et al.*¹⁹ synthesised the hydroxythiol **17a**, which they used to achieve high stereoselective induction in Solladie-type reductions. Furthermore, the sense of induction could be reversed by changing the catalyst. Yang *et al.*²⁰ examined the use of a range of auxiliaries **17a-d** differing only at the C-2 position (**Scheme 1.3**). These thiols were used to produce the sulfenimines **18a-d**, which were oxidized to the sulfinimines **20a-d**, with moderate to excellent stereoselectivity (40 – 98 % d.e.). The high diastereoselectivity was attributed to chelation in the intermediates **19a-d**. It was suggested that *si*-face attack occurs preferentially in the final step due to chelation to the sulfinimine oxygen and/or shielding of the *re*-face by the bornane skeleton.



Scheme 1.3: Diastereoselective modification of C-2/ C-3 modified camphor derivatives.^{19,20}

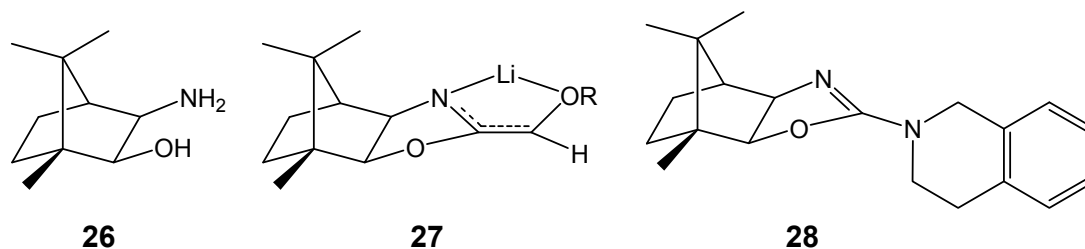
1.2.2.2 C(3)-Modification

A considerable number of C-3 substituted camphor derivatives have been reported as the reactivity of this position is extremely high, perhaps even as high as would be expected for reactive methylene groups.¹³ Oxidation of camphor is regularly performed to obtain camphorquinone **22**,^{21,22} which has been monoallylated at the less sterically congested 3-carbonyl from the *endo* π -surface to produce **23** (Scheme 1.4).²³ The high degree of steric shielding of the C-2 carbonyl in **23** necessitated harsh reaction conditions to effect further modification at this position, which was finally achieved through an alkyllithium reaction. The resulting diol **24** was subsequently cyclized to **25**.

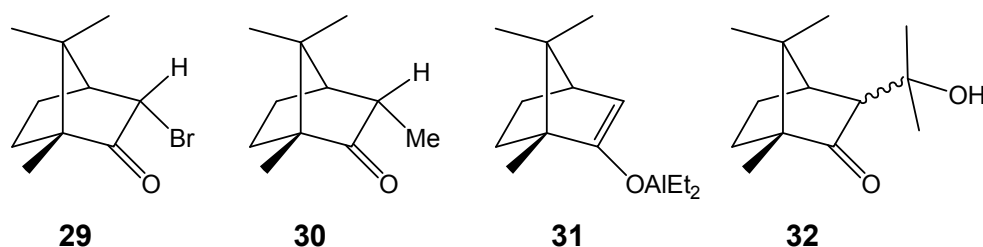


Scheme 1.4: Oxidation and stereoselective allylation at C-3, followed by stereoselective C-2 alkylation and subsequent cyclization.²³

The synthesis of the chiral auxiliary 3-*exo*-amino-2-*exo*-hydroxy camphor **26** was achieved by Chitenden *et al.*²⁴ This was subsequently used in the preparation of oxazoline intermediates **27**. Alkylation of these intermediates was achieved with a high level of diastereoselectivity (~88 % d.e.) which was relatively independent of the substrate used, suggesting that the stereochemistry of the anionic intermediate **27** is responsible for the observed stereocontrol. The auxiliary **26** has also found use in the synthesis of optically active heterohelicines²⁵ and oxazolines, such as **28**,²⁶ which was subsequently alkylated with moderate success using Grignard reagents.

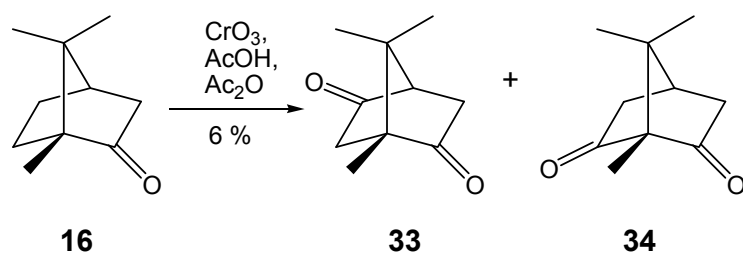


Monobromination of camphor **16** at C-3 to afford 3-*endo*-bromocamphor **29** has been achieved in excellent yield (~92 %) and high diastereoselectivity (84 % d.e.) through various methods.²⁷⁻²⁹ Furthermore, Josephy *et al.*²⁷ were amongst the first to report monomethylation at C-3 to afford 3-*endo*-methylcamphor **30** with low stereoselectivity (50 % d.e.), subsequently improved by Hutchinson *et al.*¹³ to 80 % d.e. The diethylaluminum enol derivative **31** has been proposed as an intermediate in the conversion of 3-*endo*-bromocamphor **29** into the aldol derivative **32**.³⁰ The reaction, however, proceeds with little or no stereoinduction.

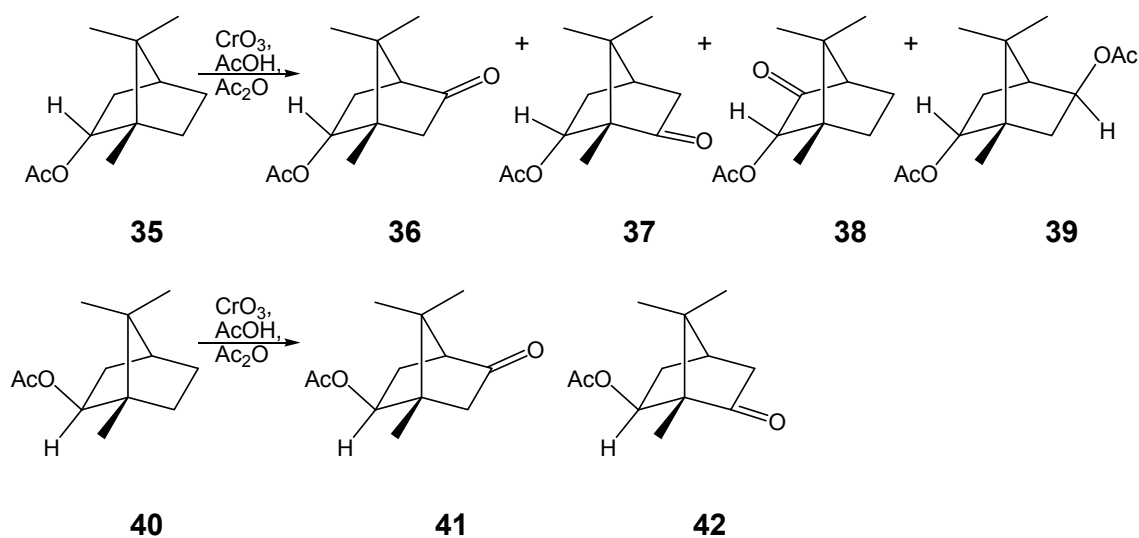


1.2.2.3 C(5)- and C(6)-Modification

A limited number of transformations have been accomplished that achieve functionalization at the C-5 or C-6 positions of (+)-camphor and very few give single products or acceptable yields. Brecht *et al.*³¹ achieved C-5 and C-6 functionalization of camphor through remote oxidation with CrO_3 and Ac_2O (**Scheme 1.5**). Although the low yield (6 %) of a mixture of bornane-2,5-dione **33** and the 2,6-isomer **34** effectively makes the reaction synthetically useless, it did provide bornanediones which assisted in the identification of the products obtained from the remote oxidation of (-)-bornyl acetate **35** and (+)-isobornyl acetate **40** (**Scheme 1.6**).^{13,32}



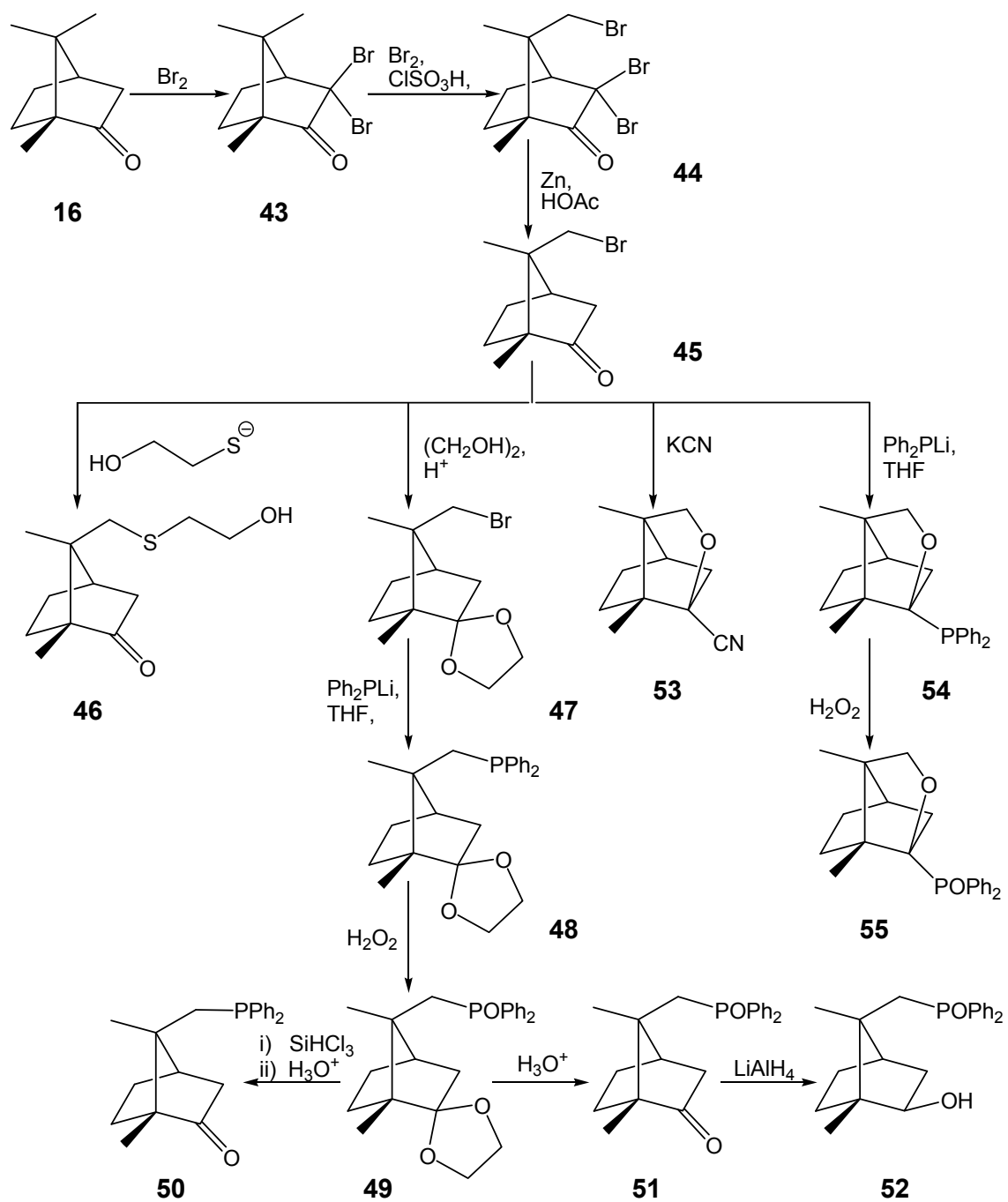
Scheme 1.5: C-5 and C-6 modification of camphor **16**.³¹



Scheme 1.6: The oxidation of (-)-bornyl acetate **35** and (+)-isobornyl acetate **40**.

1.2.2.4 C(8)-Modification

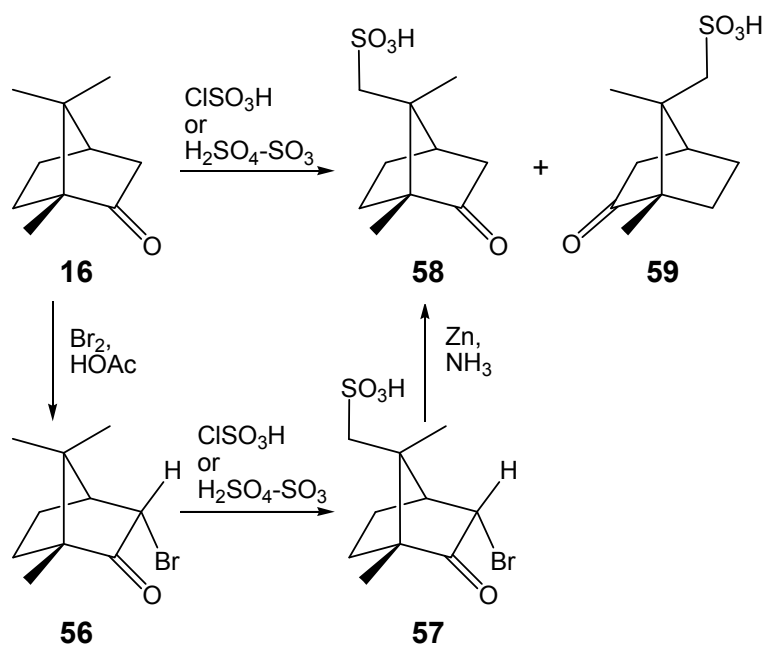
The stereospecific conversion of 3,3-dibromocamphor **43** into 8-bromocamphor **45** by Eck *et al.*³³ has permitted the synthesis of numerous other derivatives of camphor (**Scheme 1.7**). Komarov *et al.*,¹⁸ for example, made use of 8-bromocamphor **45** in the synthesis of several compounds, including the thioether **46**, the phosphines **48** and **54**, the tricyclic cyano compound **53**, the tricyclic phosphine oxide **55**, diphenylphosphanylcamphor **50** and the hydroxyphosphine oxide **52**.



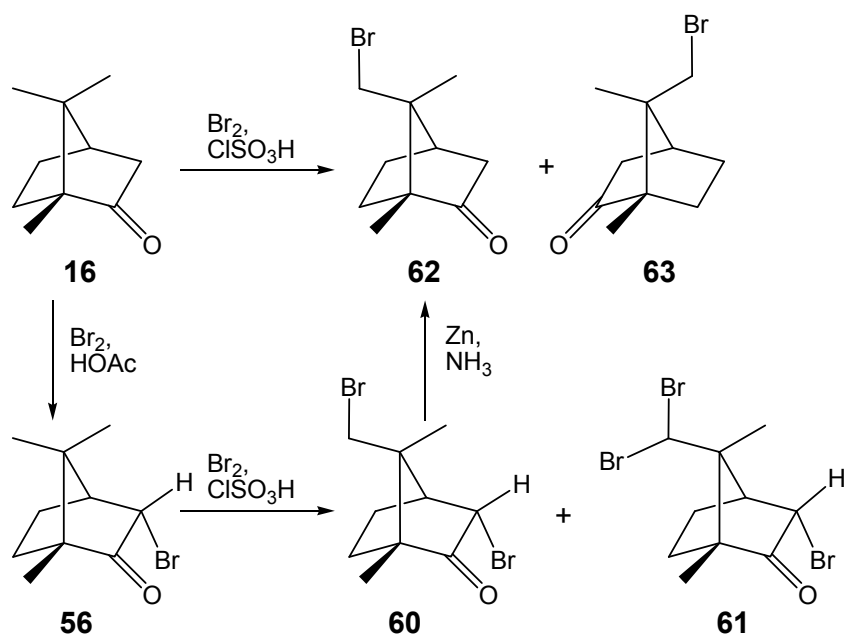
Scheme 1.7: The synthesis of 8-bromocamphor **45** and derivatives.^{18,33}

1.2.2.5 C(9)-Modification

Kipping *et al.*³⁴ achieved regiospecific sulfonation of camphor with chlorosulfonic acid or fuming sulfuric acid to afford a mixture of (+)- and (-)-camphor-9-sulfonic acid **58** and **59**, respectively (**Scheme 1.8**). The procedure was improved by several other researchers to a point where sulfonation can now be accomplished *via* 3-*endo*-bromocamphor **56** to afford (+)-camphor-9-sulfonic acid **58** exclusively.^{28,29,35} Similarly, regiospecific bromination has been achieved by reacting (1*R*)-(+)-camphor with bromine and chlorosulfonic acid to afford a mixture of (+)- and (-)-9-bromocamphor **62** and **63**, respectively (**Scheme 1.9**).^{35,36} Treatment of 3-*endo*-bromocamphor **56**, however, affords (+)-3-*endo*-9-dibromocamphor **60** and a small quantity of (+)-3-*endo*-9,9-tribromocamphor **61**. Selective debromination of **61** with zinc and acetic acid affords (+)-9-bromocamphor exclusively.

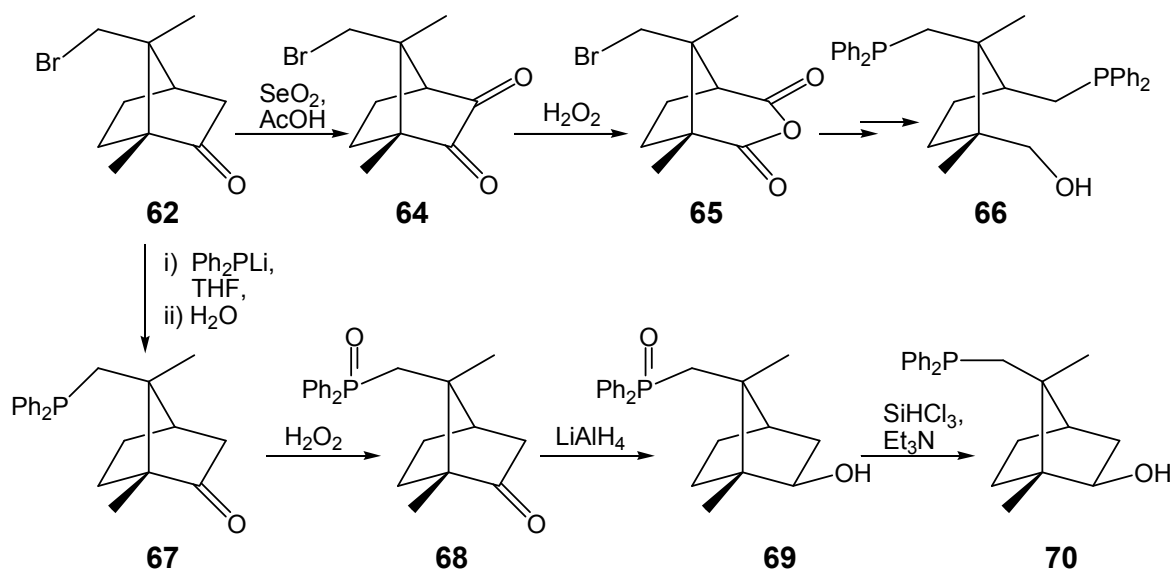


Scheme 1.8: Regiospecific sulfonation of camphor **16** at C-9.



Scheme 1.9: Regiospecific bromination of camphor **16** at C-9.

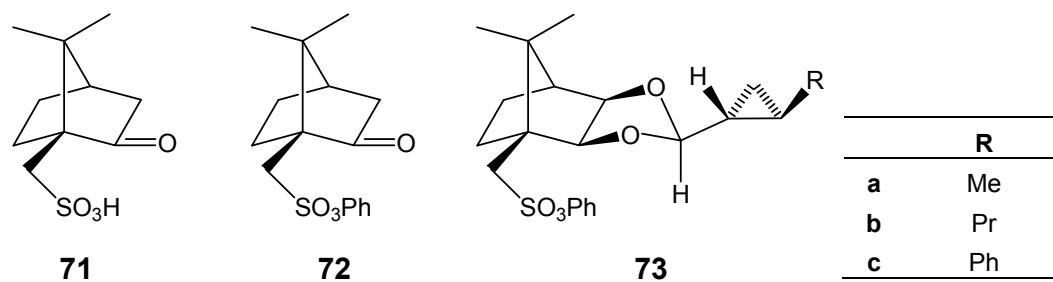
Further modification of camphor derivatives, such as **62**, has led to useful intermediates, such as the hydroxydiphosphine **66**¹⁷ and the hydroxyphosphine **70**¹⁸ (**Scheme 1.10**). Both hydroxy derivatives **66** and **70** possess no symmetry elements. In the case of **66** the hydroxy group and the *cis*-diphenylphosphine moiety are able to form eight-membered chelates upon coordination with a transition metal.



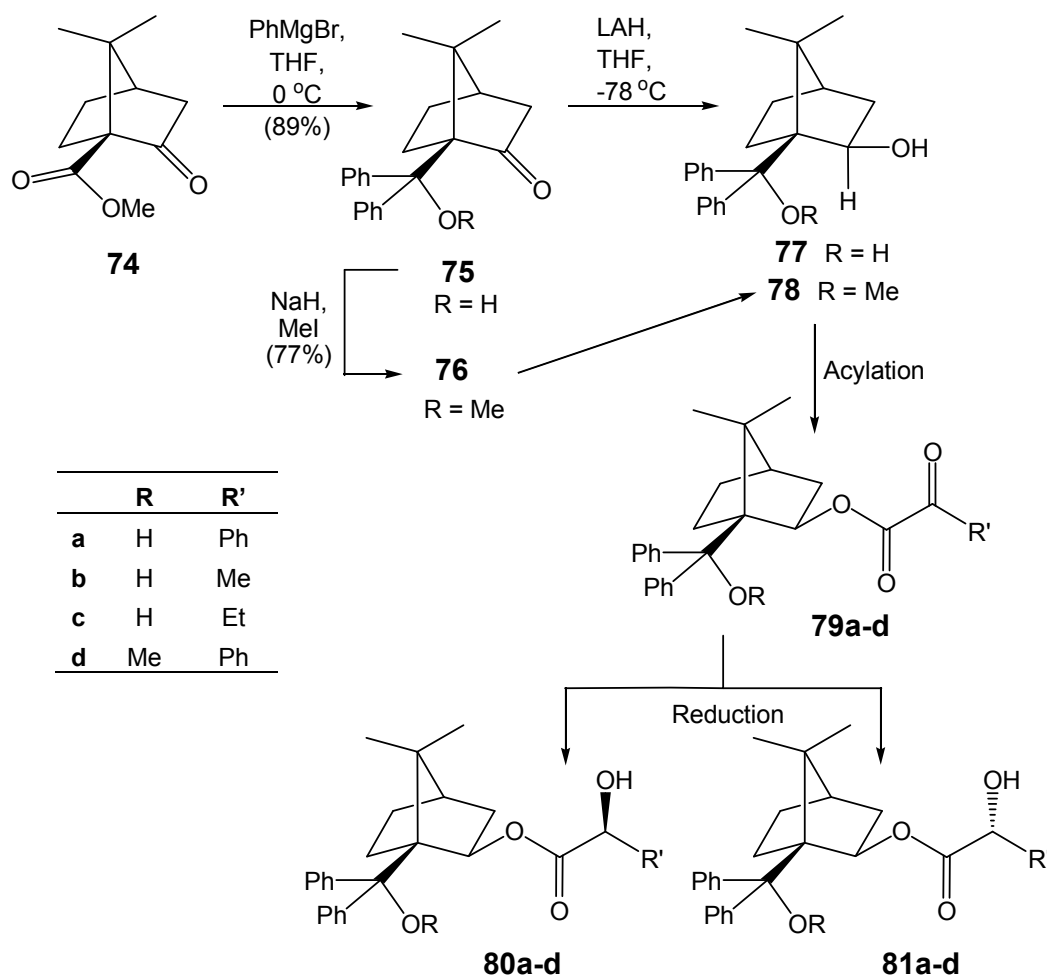
Scheme 1.10: Regiospecific synthesis of hydroxyphosphines **66** and **70**.

1.2.2.6 C(10)-Modification

C-10 functionalization of camphor is most often achieved through the use of camphor-10-sulfonic acid **71**. This is obtained through the sulfonation of camphor *via* a Wagner-Meerwein rearrangement.¹³ Kaye *et al.*³⁷ reported the diastereoselective (>99 % d.e.) cyclopropanation of α,β -unsaturated acetals resulting in the cyclopropyl derivatives **73a-c**. This was achieved by increasing the steric demand at C-10 of the bornane skeleton through use of the phenyl sulfonate derivative **72**.



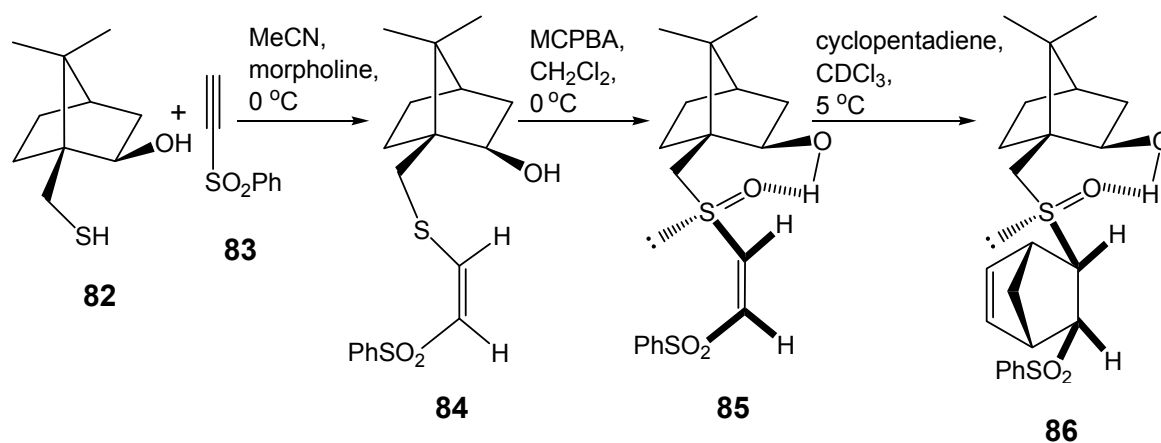
Ying-Yuan Chu *et al.*³⁸ have also achieved remarkable stereoselective induction through C-10 modification (**Scheme 1.11**). Treatment of ketopinonic acid methyl ester **74** with phenylmagnesium bromide resulted in the alcohol **75**, which afforded the ester **76** on treatment with sodium hydride and methyl iodide. *Exo*-10,10-diphenyl-2,10-camphanediol **77** and *exo*-10,10-diphenyl-10-methoxy-2-camphanol **78** were prepared under similar conditions from **75** and **76**, respectively. Various α -keto esters **79a-d**, derived from **77** and **78**, were subsequently reduced with excellent diastereomeric excesses (>99 % d.e.), affording the hydroxy esters **80a-d** and **81a-d**. In most instances the (*S*)-isomer predominated *i.e.* **80a-c**, the notable exception being predominant formation of the (*R*)-isomer **81d** from ester **79d**.



Scheme 1.11: C-10 modification and stereoselective reduction of C-2 esters.³⁸

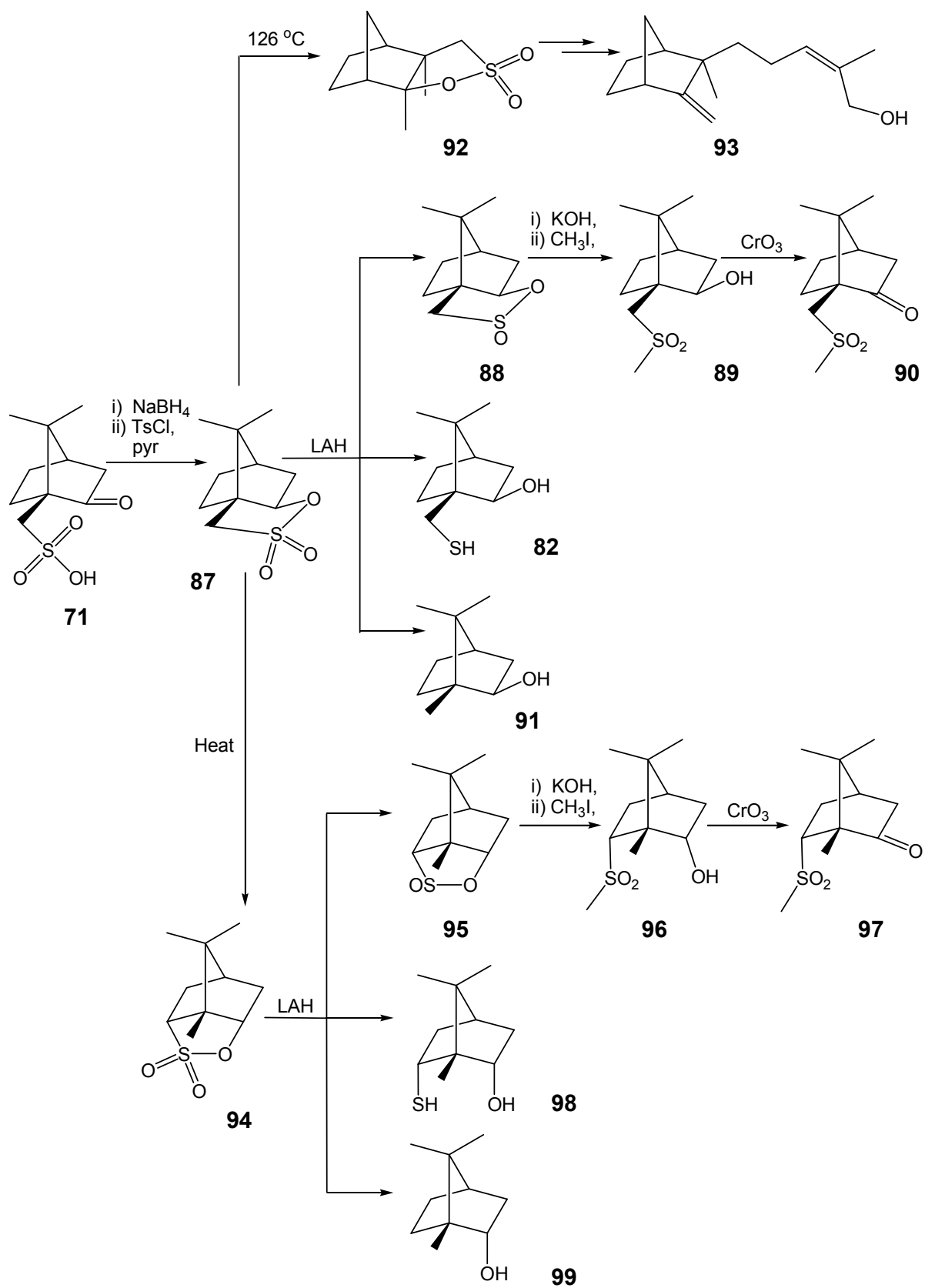
Generally, modification at the C-10 position has involved the introduction of bulky stereodirecting groups. However, Eliel *et al.*³⁹ prepared the auxiliary, 10-mercaptoisoborneol **82** with a reactive functionality at C-10. This auxiliary **82**, was used to prepare atrolactic acid methyl ester with excellent stereocontrol (97 % d.e.), *via* a hemithioacetal intermediate. De Lucchi *et al.*^{40,41} subsequently used the *exo*-hydroxy mercapto auxiliary **82** and the isomeric *endo*-alcohol in asymmetric Diels-Alder reactions; the route taken for the *exo*-isomer is shown in **Scheme 1.12**. The addition reaction between the auxiliary **82** and the alkynyl sulfone **83** produced the (*Z*)-adduct **84**. This was followed by oxidation of the thioether **84** using MCPBA to afford the chiral sulfoxide **85** with high stereoselectivity. Hydrogen bonding between the oxidizing agent, MCPBA, and the alcohol group of the auxiliary **84** is believed to be responsible for the high diastereomeric excess observed. This was verified by performing the oxidation in polar solvents, such as MeOH, where lower stereoselectivity was observed,

due to competitive hydrogen bonding interactions. Furthermore, when the oxidation was attempted with the *endo*-alcohol isomer, lower stereoselectivity was observed and this was attributed to the less favourable geometry of the alcohol group for hydrogen bonding with the oxidant. The alkenes **84** and **85** were then reacted with cyclopentadiene to give Diels-Alder products. Excellent stereoselectivity was obtained with the sulfoxide **85**, which afforded **86** in 98 % d.e; however, low stereoselectivity was observed with **84**. De Lucchi *et al.*^{40,41} deduced that chirality was directed by the asymmetric sulfoxide group of **85**. Use of polar solvents in the Diels-Alder reactions failed to change the diastereomeric excesses. Similarly, the use of the *endo*-alcohol isomer of **85** did not affect the degree of stereoselectivity indicating that hydrogen bonding was not necessary for stereocontrol in the Diels-Alder reaction and, thus, that the orientation of the alcohol group has no effect on stereoselectivity.



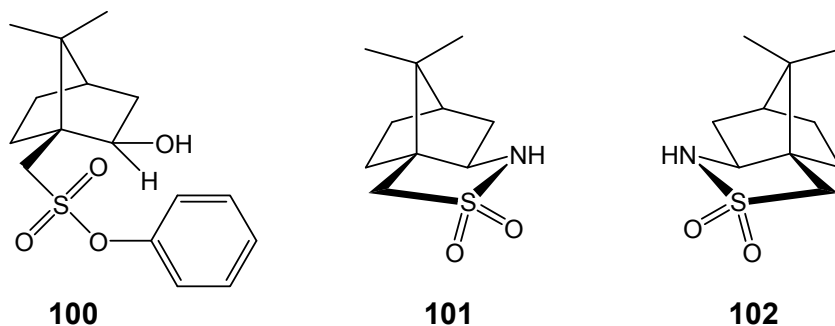
Scheme 1.12: C-10 modification and Diels-Alder reactions of sulfoxide derivatives.

In 1929, Lipp *et al.*⁴² obtained the camphene sultone **87** whilst attempting to acylate camphene with acetic anhydride in the presence of sulfur trioxide. Asahina, in 1938, suggested that the structure was in fact **92**.⁴³ Only years later, when IR and NMR techniques became powerful enough, did Wolinsky *et al.* demonstrate that a unique thermal rearrangement of **87** led to the formation of **92** or **94**,⁴⁴ and suggested that the mechanism involves 2,3- and 2,6-hydride shifts and Wagner-Meerwein type rearrangements.⁴⁵ More efficient synthetic routes to the sultones **87**, **92** and **94** were developed (**Scheme 1.13**),^{46,47} which yielded additional compounds, including β -santalol **93**, the sulfinates **88** and **95**, the methyl sulfonyl alcohols **89** and **96**, the mercapto alcohols **82** and **98**, the methyl sulfones **90** and **97** and the sulfur-free alcohols **91** and **99**.



Scheme 1.13: Camphor derivatives arising from initial C-10 modification.^{44,46,47}

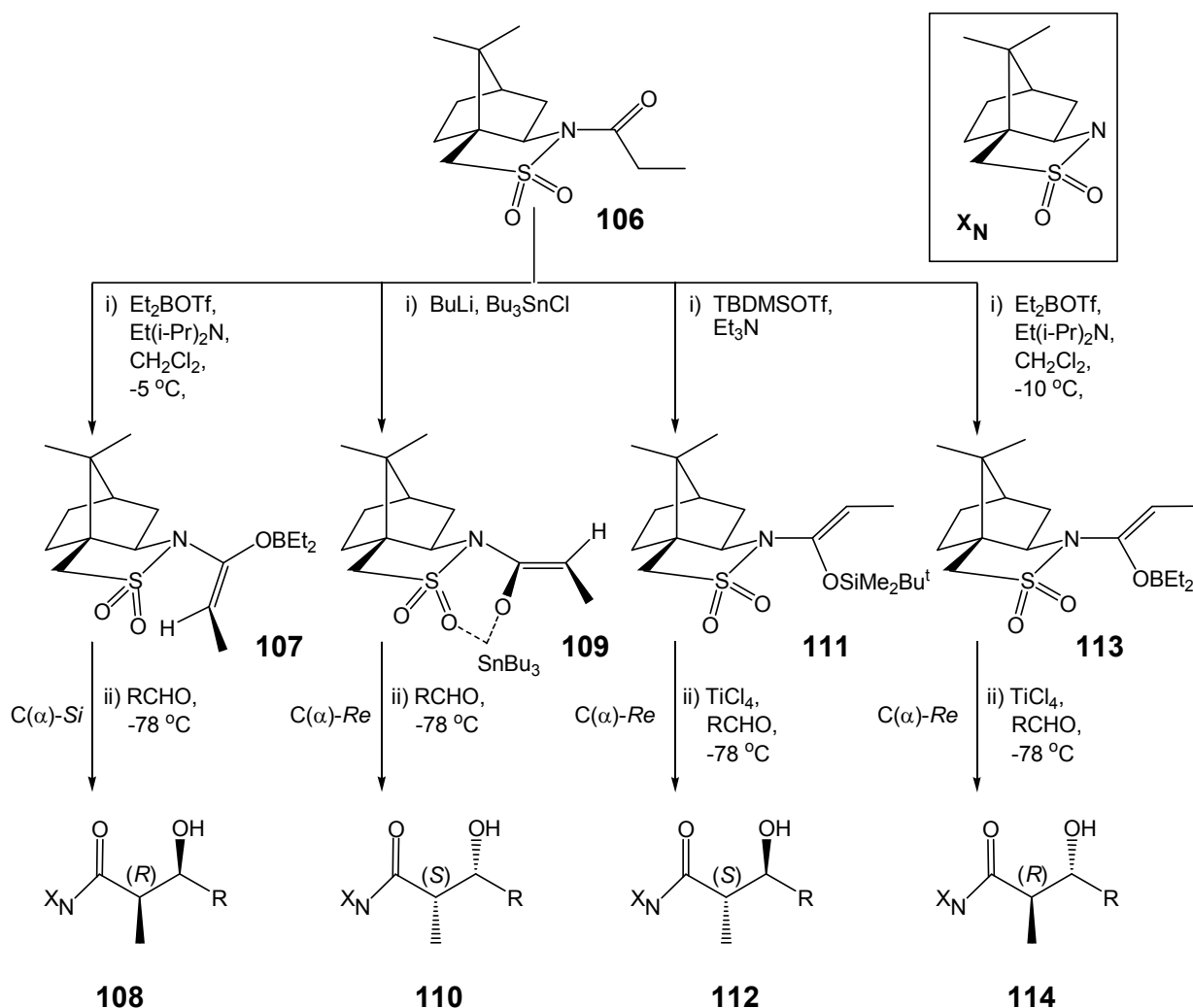
Oppolzer *et al.*⁴⁸ have subsequently reported nucleophilic ring opening of the sultone **87**, with phenyllithium in ethanol to afford the sulfonate ester **100** in moderate yield (53 %).



Perhaps the most studied of all chiral camphor auxiliaries and the basis for numerous derivatives are the sultams developed by Oppolzer *et al.*, the (-)-bornane-10,2-sultam **101** and its enantiomer **102**.⁴⁹ They are easily derived from the corresponding camphor sulfonyl chlorides in high yield (76 %) and have found use in many reactions including Diels-Alder additions,⁵⁰ aldolizations,⁵¹ alkylations⁵² and aminations.⁵³

The primary purpose of Oppolzer's sultams was initially for use in Diels-Alder additions as a dienophile auxiliary (**Scheme 1.14**).⁵⁰ The reaction was performed both in the presence of the Lewis acid, TiCl_4 ,⁵⁴ and in the absence of Lewis acid catalysts.⁴⁹ High stereoselectivity and high rates of reaction were observed with catalysis, even at low temperature, and higher than expected stereoselectivity without catalysis, albeit with slower reaction rates (**Table 1.1**). X-ray diffraction analysis showed that, while both the uncoordinated *N*-crotonyl sultam **103b** and the Lewis acid-coordinated *N*-crotonyl sultam **104b** have an *s-cis* conformation about the $\text{C}(\text{O})\text{-C}(\alpha)$ bond, they differ in the arrangement of the carbonyl and sulfonyl groups about the $\text{N-C}(\text{O})$ bond. The uncoordinated sultam **103b** has an *s-trans* arrangement about the $\text{N-C}(\text{O})$ bond as well as a pyramidal nitrogen atom, whereas the coordinated *N*-crotonyl sultam **104b** exhibits chelation to titanium resulting in an *s-cis* arrangement. The stereoselectivity observed in the uncatalyzed reactions has been attributed to a transfer of chiral information from the bornane skeleton to the distant $\text{C}(\alpha)=\text{C}(\beta)$ bond *via* the pyramidal nitrogen, resulting in *exo* $\text{C}(\alpha)\text{-Re}$ face attack.⁵³ The presence of a Lewis acid resulted in higher π -face stereoselectivity with *endo* $\text{C}(\alpha)\text{-Re}$ attack by cyclopentadiene, occurring at increased rates even at lower temperatures.

of the bornyl enolate **113** is reversed, as compared to **107**, due to the presence of a Lewis acid; the direction of attack is thus also reversed, affording the product **114**.

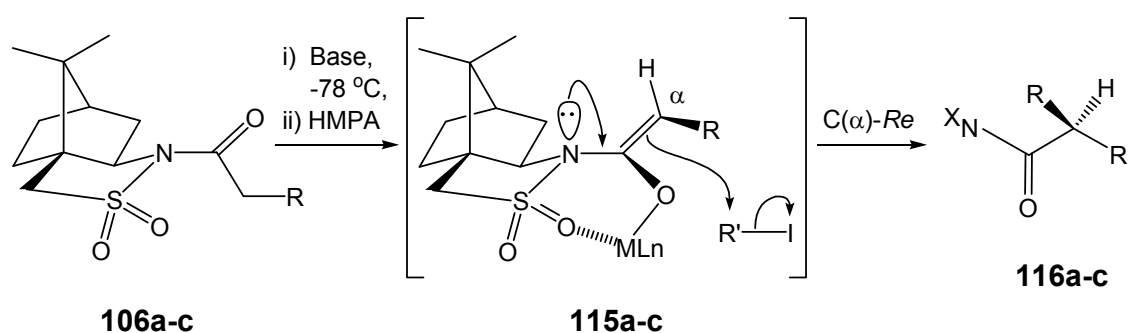


Scheme 1.15: Stereoselective aldol and anti-aldol reactions with Oppolzer's sultam derivative **106**.

Table 1.2: Aldol and anti-aldol reactions with Oppolzer's sultam derivative **106**.

Entry	Counter-ion	Lewis acid	Syn:anti	Major product	% d.e.	% Yield
1	B(III)	---	100:0	108	>99	76
2	Sn(IV)	---	97.5 : 2.5	110	>99	44
3	Si	TiCl ₄	0.8 : 99.2	112	>99	76
4	B(III)	TiCl ₄	0.6 : 99.4	114	>99	75

Derivatives of Oppolzer's sultam, such as **106a-c** have been found particularly useful in alkylation reactions (**Scheme 1.16** and **Table 1.3**).⁵² The *N*-acylsultam **106a-c** undergoes addition reactions *via* the (*Z*)-enolate **115a-c** affording disubstituted carboxylic acid derivatives **116a-c**. The sultam is very reactive permitting non-activated alkyl halides to be used. However, it is necessary to have NHMDS (sodium hexamethyldisilazide) or BuLi present to prevent competitive alkylation at C-10. Attack at the enolate π -bond occurs from the *endo*-face and opposite to the position of the nitrogen lone pair. Reversal of the alkyl groups R and R', or use of the sultam antipode **102**, results in enantiomeric products of opposite configuration at C(α).



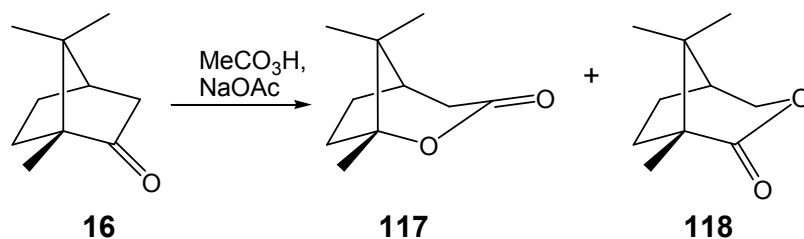
Scheme 1.16: Alkylation of Oppolzer's sultam derivative **106**.

Table 1.3: Results for the alkylation of Oppolzer's sultam derivative **106**

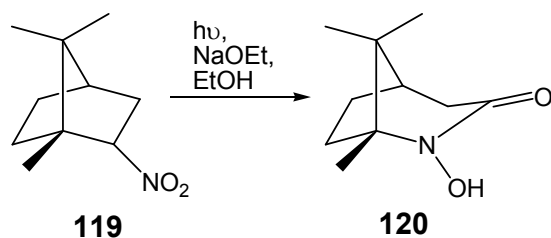
	R	R'	Base	% d.e.	% Yield
a	Me	PhCH ₂	NHMDS	>98	89
b	Me	PhCH ₂	BuLi	>98	89
c	PhCH ₂	Me	BuLi	>99	88

1.2.2.7 C(1)-C(2)-Cleavage

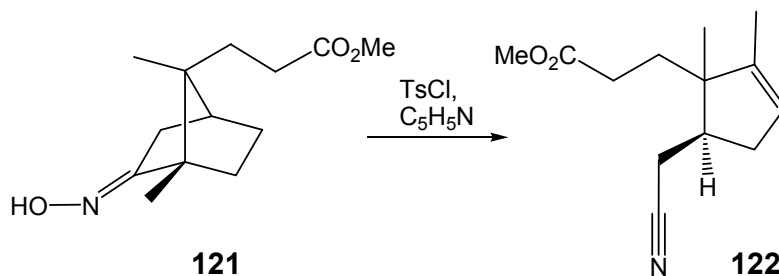
Numerous methods have been used to bring about ring cleavage between the C-1 and C-2 positions of camphor and its derivatives, examples of which are illustrated in **Schemes 1.17** to **1.20**.



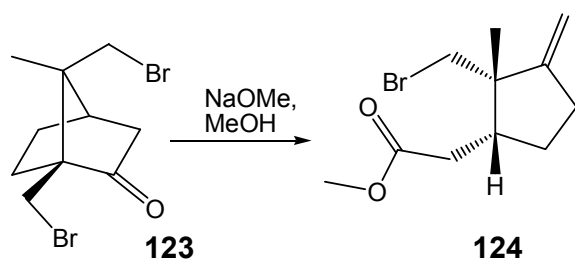
Scheme 1.17: C(1)-C(2) cleavage of camphor **16**.⁵⁷



Scheme 1.18: C(1)-C(2) cleavage of 2-nitrocamphor **119**.⁵⁸



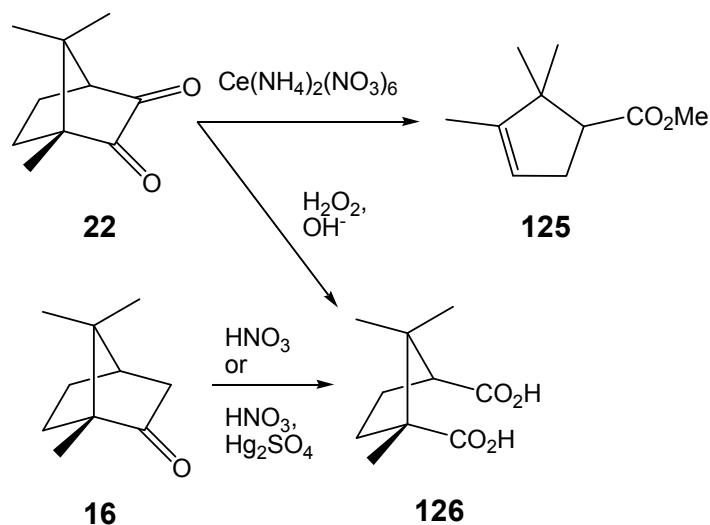
Scheme 1.19: C(1)-C(2) cleavage of the (-)-camphor derivative **121**.⁵⁹



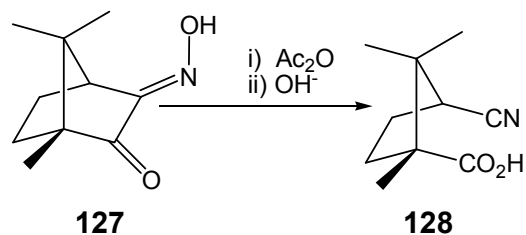
Scheme 1.20: C(1)-C(2) cleavage of the dibromocamphor derivative **123**.⁶⁰

1.2.2.8 C(2)-C(3)-Cleavage

C(2)-(3) ring cleavage has been widely observed with the use of strong acids and oxidizing agents, as illustrated in **Schemes 1.21** and **1.22**.



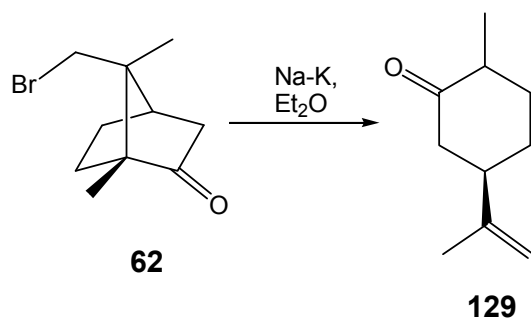
Scheme 1.21: C(2)-(3) cleavage of camphor **16** and camphorquinone **22**.^{28,62}



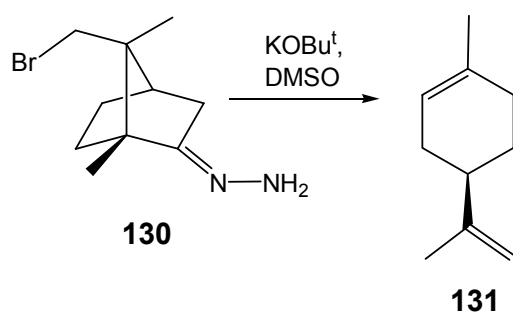
Scheme 1.22: C(2)-(3) cleavage of the camphor derivative **127**.²⁸

1.2.2.9 C(1)-C(7)-Cleavage

Few examples of cleavage of this bond exist due to the low reactivity of the quaternary carbons C-1 and C-7 compared with the highly reactive centres at C-2 and C-3. The 9-bromocamphor derivatives **62** and **130** undergo ring cleavage between C(1)-C(7) affording the alkenes **129**⁶³ and **131**,⁶⁴ respectively (**Schemes 1.23** and **1.24**).



Scheme 1.23: C(1)-C(7)-Cleavage of the 9-bromocamphor derivative **62**.⁶³

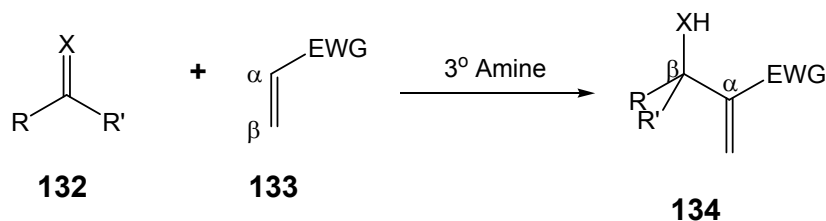


Scheme 1.24: C(1)-C(7)-Cleavage of the 9-bromocamphor derivative **130**.⁶⁴

The ability of an auxiliary to stereo-direct attack in any reaction is directly related to its conformation in the transition state, which is often a function of its ability to co-ordinate to some counterion. Consequently, the presence or absence of such a counterion is usually vital in determining which enantiomer is produced or the degree of diastereoselectivity. These factors are routinely exploited in the selective formation of a particular enantiomer. Moreover, in most reactions, attack occurs from the *endo*-face of camphor and its derivatives.

1.3 THE MORITA-BAYLIS-HILLMAN REACTION

Fundamental carbon-carbon bond forming reactions,⁶⁵⁻⁶⁸ are key steps in the total synthesis of natural products. An important, albeit initially overlooked, contribution to this type of reaction was made in a German patent application in 1972 by A.B. Baylis and M.E.D. Hillman.⁶⁹ Morita,⁷⁰ however, had reported a similar reaction involving tertiary phosphines as catalysts, five years earlier, and the reaction is sometimes referred to as the Morita-Baylis-Hillman Reaction.⁷¹ This reaction involves the formation of a carbon-carbon bond between the α -carbon of an activated alkene (Michael acceptor) **133** and carbon electrophiles **132** containing an electron-deficient sp^2 carbon atom under the influence of a suitable catalyst, usually a tertiary amine. The reaction is typically conducted using carbonyl compounds as the Michael acceptor (EWG = CO.R) resulting in the production of a β -hydroxy- α -methylene carbonyl derivative **134** as the major product (Scheme 1.25).⁷²



R = aryl, alkyl, heteroaryl

R' = H, COOR, alkyl

X = O, NCOOR, NSO₂Ph

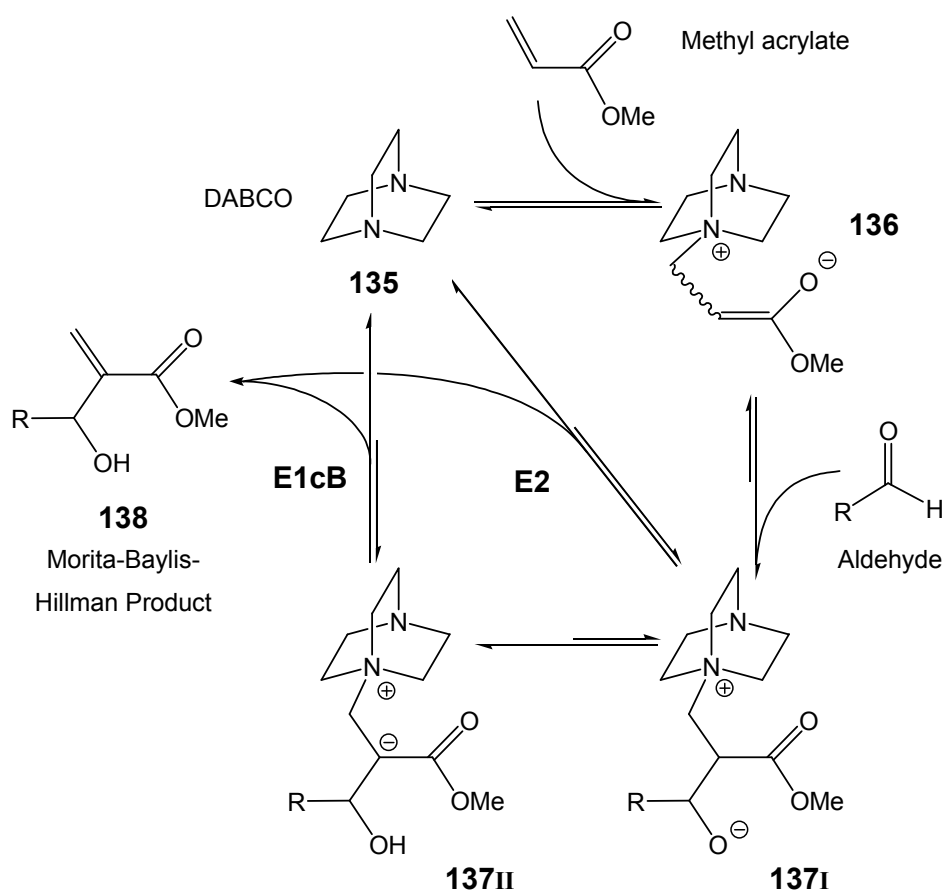
EWG = COR, CHO, CN, COOR, PO(OEt)₂, SO₂Ph, SO₃Ph, SOPh

Scheme 1.25: Generalised Morita-Baylis-Hillman reaction.⁷³

In general, the Morita-Baylis-Hillman reaction has been found to be chemo- and regioselective, requiring mild conditions and producing synthetically useful multifunctional molecules.⁷⁴ However, the greatest drawback is the prolonged reaction times that are often required. Rate acceleration has been achieved by altering the reaction temperature,⁷² applying pressure⁷⁵ or microwave irradiation,^{74,76} and by substituting trialkylphosphines⁷⁷ or 3-hydroxyquinuclidine for DABCO.⁷⁸

1.3.1 Mechanism

The mechanism of the Morita-Baylis-Hillman reaction has been investigated^{79,80} and the generalized mechanism for the DABCO-catalyzed reaction of an aldehyde with methyl acrylate is illustrated in **Scheme 1.26**.



Scheme 1.26: The Morita-Baylis-Hillman reaction mechanism.

The nucleophilic DABCO catalyst **135** attacks the activated alkene, in this case methyl acrylate, affording the zwitterion **136**, which reacts with the electrophilic aldehyde giving a second zwitterion **137I**. One of two possible elimination routes is then possible *viz*, a base-assisted anti E2 elimination of the catalyst followed by protonation, or proton transfer giving the resonance stabilized zwitterion **137II** followed by E1cB elimination. Both routes would afford the free catalyst **135** and a β -hydroxy- α -methylene carbonyl derivative **138** – the Morita-Baylis-Hillman product.

Van Rosendaal *et al.*⁷⁹ determined that both pathways exist, but the E1cB process was shown to be favoured by molecular orbital calculations. Furthermore, Roth *et al.*⁸⁰ showed that the Morita-Baylis-Hillman reaction is reversible in at least several instances. The reaction has also been shown to be first-order in each reactant and hence third-order overall.⁸¹ Neither the proton transfer nor the elimination steps have been found to be rate determining, thus the second step, involving attack of the zwitterion by the electrophile (**136** → **137I**) is considered to be the rate determining step.

Bode and Kaye⁸³ reacted acrylate esters with pyridinecarbaldehydes, in the presence of 3-hydroxyquinuclidine (3-HQ) **139** or 1,4-diazabicyclo[2.2.2]octane (DABCO) **135** and, through use of ¹H NMR spectroscopy, investigated the mechanism of the reaction. The authors determined that the data were consistent with third-order kinetics overall or, assuming the concentration of tertiary amine to be constant, pseudo second-order kinetics. Thus, the reaction rate is dependent on the concentration of both the aldehyde and the activated alkene. Rate-enhancement was observed on substitution of 3-hydroxyquinuclidine **139** for DABCO **135** – an effect rationalised in terms of hydrogen-bonding stabilization of the dipolar 3-hydroxyquinuclidine intermediate **140** (**Figure 1.1**) and a consequent increase in the equilibrium constant. However, the results of computational studies suggest that intramolecular hydrogen bonding is likely to be much more significant in the Morita-Baylis-Hillman zwitterionic adduct rather than the initial zwitterion **140**.⁸⁴

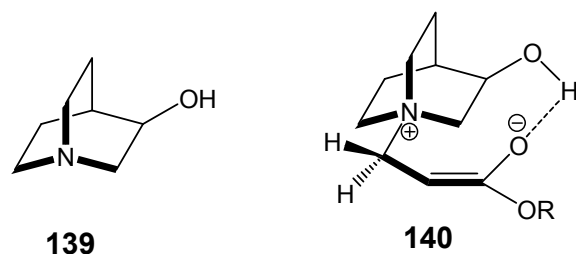


Figure 1.1: Possible hydrogen bonding interactions using 3-hydroxyquinuclidine as catalyst.

1.3.2 Reaction Parameters

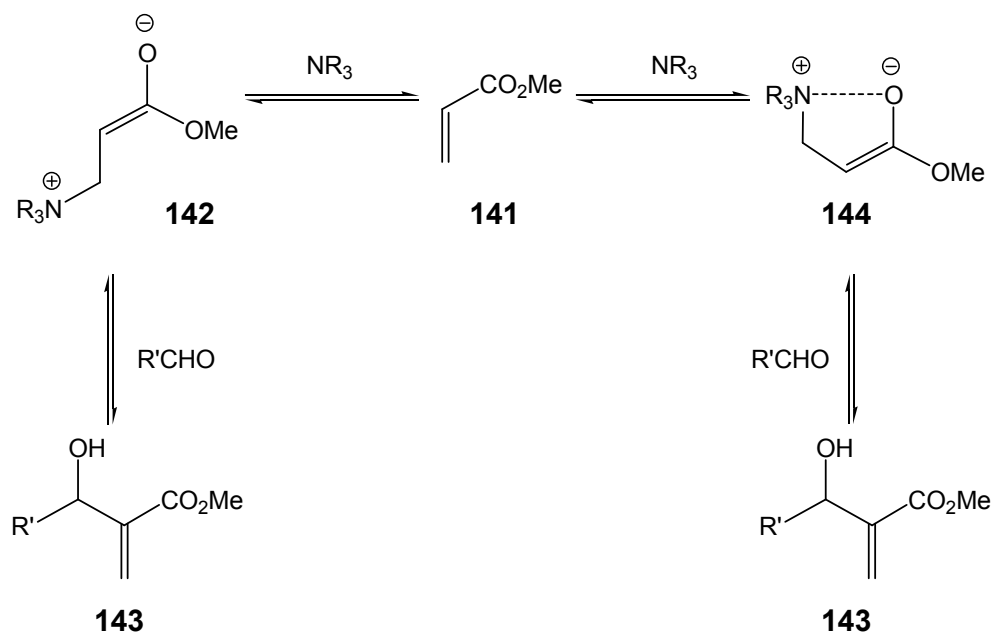
1.3.2.1 Solvents

Many Morita-Baylis-Hillman reactions are carried out neat, without the use of solvents, since the reaction is third order and dilution adversely affects the rate.⁸⁴ There are, however, instances where the use of solvent is necessary (where substrates are poorly soluble) or even beneficial (where small quantities of protic solvents have been found to increase the rate of reaction).⁷¹

1.3.2.2 Temperature and Microwave Irradiation

In general, amine catalyzed Morita-Baylis-Hillman reactions are carried out at room temperature to minimize the potential of side reactions, which are known to compete at higher temperatures especially over extended periods of time.⁷¹ The use of microwave irradiation (together with the addition of a radical inhibitor, to avoid polymerization of the activated alkene) has been shown to reduce reaction times to seconds or minutes.^{76,85}

Several studies have revealed an unprecedented increase in the rate of reaction by lowering the temperature.^{72,77} This temperature effect is counter-intuitive in that the formation of the product can apparently be accelerated by either heating or cooling the reaction! One possible explanation is that the product is formed *via* two different zwitterions (**Scheme 1.27**).^{72,77} These *E*- or *Z*-enolates should both be formed under equilibrating conditions, and are likely to react with the aldehydes at different rates. At a given temperature there could be a greater concentration of one enolate over the other while at another temperature, the relative concentrations could change.



Scheme 1.27: Competing enolates in the Morita-Baylis-Hillman reaction.

1.3.2.3 Pressure and Sonication

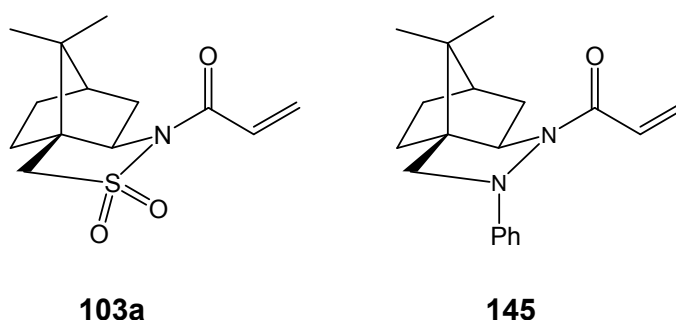
Pressure effects on the rate of the Morita-Baylis-Hillman reaction have been well documented. Hill and Isaacs^{81,86} have shown that an increase from atmospheric pressure to 5 kbar reduces the time required for the DABCO-catalyzed α -hydroxyethylation of acrylonitrile from 5 days to 5 minutes. Furthermore, previously unreactive ketones and crotonic derivatives become reactive at 10 kbar. The effect of pressure on rate acceleration has been attributed to the large negative volume of activation of the reaction as a result of bond formation and charge development prior to, and during the rate determining step.⁷¹

Subjecting reaction mixtures to ultrasound has also revealed rate enhancements⁷¹ and increased reactivity of acrylamide.⁷⁴ However, the rate acceleration is far less significant than that observed with microwave irradiation.⁸⁷

1.3.3 Stereocontrol

The production of enantiomerically pure compounds is an ongoing challenge for organic chemists. The Morita-Baylis-Hillman reaction typically involves addition to an sp^2 carbon and

the generation of a new chiral centre, thus raising the possibility for asymmetric induction.⁷⁴ In principle any of the three essential components (electrophile, activated alkene or catalyst) could be used to introduce chirality in the reaction. Numerous attempts have, in fact, been made to promote asymmetric Morita-Baylis-Hillman reactions. Use has been made of chiral catalysts,⁸⁸⁻⁹⁰ electrophiles,^{74,88,91,92} activated alkenes^{74,88} and co-catalytic Lewis acids.^{93,94} The literature on the asymmetric Morita-Baylis-Hillman reaction has grown significantly, but there are relatively few methods available for achieving effective stereocontrol,⁷¹ the most significant of these involving the use of the optically pure camphor-derived activated alkenes **103a** and **145**.^{72,95}



The role of hydrogen bonding interactions in rate enhancement and asymmetric induction in these reactions is well known.^{88,90,94,96-99} Hydrogen bonding may stabilize the reaction intermediates and/or transition state complexes and increase the steric demands for attack of the electrophile. Thus the effect of hydrogen bonding on stereocontrol is significant.

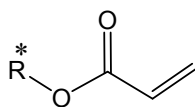
1.3.3.1 Diastereoselectivity

Reactions in which the electrophile and/or the activated alkene already contain asymmetric centres may result in two or more diastereomers being formed. Rationalization of the observed stereoselectivity has been followed by optimization procedures in an attempt to produce selected diastereomers, but with limited success.⁷¹

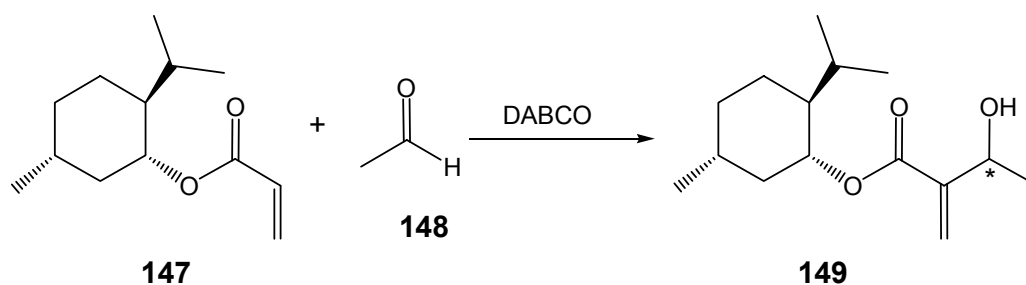
1.3.3.1.1 Chiral activated alkenes

Acrylic acid esters **146** of chiral alcohols ($\overset{*}{\text{R}}\text{OH}$) have been the most widely studied of all chiral activated alkenes as they are readily accessible and removal of the chiral auxiliary is

easily achieved. Unfortunately, the relative inaccessibility of optically active forms of vinyl ketones, sulfones and phosphonates has limited their usefulness.

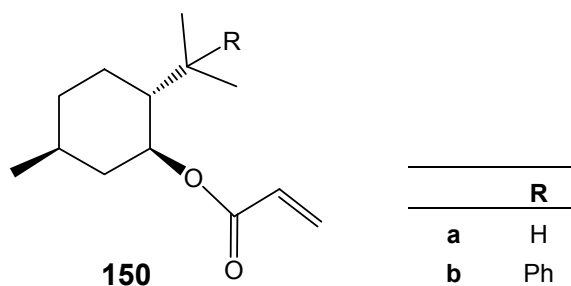
**146**

Perhaps the earliest reported study of chiral acrylates in the Morita-Baylis-Hillman reaction was undertaken by Brown *et al.*¹⁰⁰ who reacted (-)-menthyl acrylate **147** with acetaldehyde **148** in the presence of DABCO, producing **149** with low diastereoselectivity (d.e. 16 %) (Scheme 1.28).

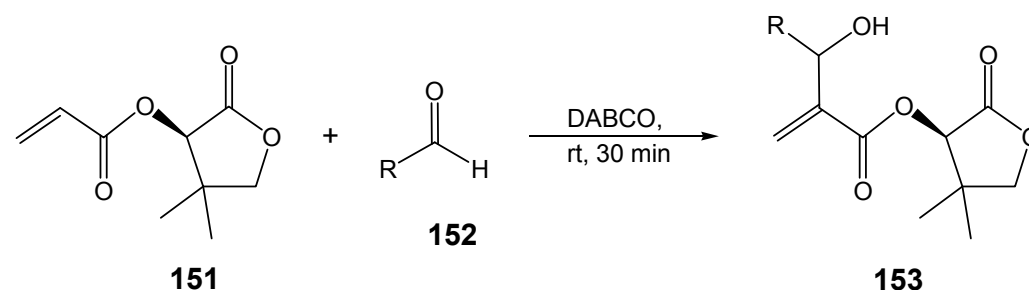


Scheme 1.28: Early diastereoselective Morita-Baylis-Hillman reaction.¹⁰⁰

Gilbert *et al.*⁸⁶ undertook similar reactions with the (+)-menthyl esters **150a-b** and a range of aldehydes. The experiments were conducted between atmospheric pressure and 8.5 kbar. In all instances, higher stereoselectivity was observed in reactions of **150b** and the stereoselectivity increased with the bulk of the aldehyde and with increasing pressure. The highest stereoselectivity (86 - 100 % d.e.) was observed using aromatic aldehydes at 8.5 kbar.



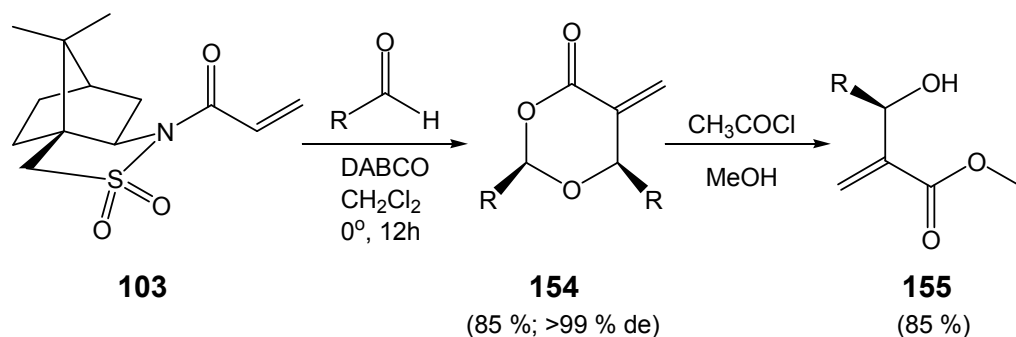
It has been suggested that, in these systems, preferential *si*-face attack of the initial zwitterion on the aldehyde results in an (*S*)-configuration at the new chiral centre and the greater diastereoselectivity exhibited by the 8-phenylmenthyl ester **150b** has been attributed to a π -stacking effect.⁶¹ It also seems that the reactivity of the aldehyde substrate influences the degree of diastereoselectivity, rather than its steric bulk, as the faster the reaction, the lower the likelihood of equilibration *via* the reverse reaction.⁶¹ The reactions of the lactone ester **151** with selected aldehydes occurs very quickly, but only moderate, if any, diastereoselectivity is observed, perhaps due to the lack of an effective blocking group (**Scheme 1.29**).¹⁰¹



	R	% d.e.	% Yield
a	CCl ₃	48	83
b	Ph	2	81

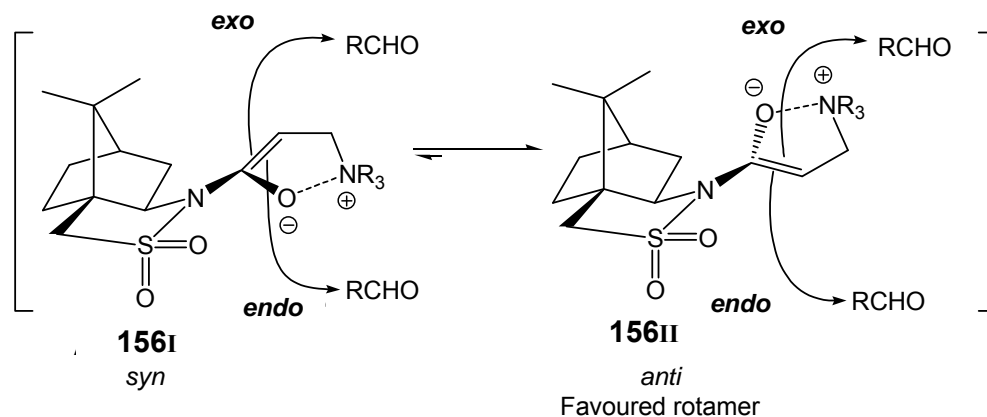
Scheme 1.29: High-rate Morita-Baylis-Hillman reaction.¹⁰¹

One of the most successful syntheses involving the asymmetric version of the Morita-Baylis-Hillman reaction⁷¹ was reported by Leahy and co-workers,^{72,102} who used the commercially available, optically pure camphor-derived Oppolzer's sultam⁴⁹ and introduced acrylate functionality. The resulting acrylamide **103** was reacted in the presence of a variety of achiral aldehydes with DABCO, as catalyst. Oppolzer's sultam was found to be an excellent chiral auxiliary, affording cyclic intermediates **154** in good yield and in excess of 99 % d.e.; subsequent cleavage gave the Morita-Baylis-Hillman product **155** (**Scheme 1.30**). However, the acrylamide **103** was noted to be inactive towards more hindered aldehydes.



Scheme 1.30: Enantioselective synthesis using an *N*-acryloyl derivative of Oppolzer's sultam **103**.^{72,102}

Stereoselective induction in the acrylamide **103** has been demonstrated to rely on two factors: - i) preferential addition to the C_{α} *re*-face; and ii) the requirement of an “open” transition state. The *Z*-enolate intermediate, produced on the addition of catalyst, could exist in either of two rotameric forms **156I** or **156II** (Scheme 1.31). The rotamer **156II** has the carbonyl oxygen orientated *anti* to the sulfonyl group in order to minimize dipole interactions between the two groups and is favoured in non-chelated reactions. Conversely, in the presence of a Lewis acid co-catalyst, chelation of the carbonyl and sulfonyl groups occurs, resulting in arrangement of the carbonyl group *syn* to the sulfonyl group **157** (Figure 1.2). This should lead to the formation of enantiomeric products based on the presence, or lack thereof, of a Lewis acid. Furthermore, experimental evidence suggests that, in all reactions with acrylate **103**, addition to the *exo*-face is favoured, due to steric constraints imposed by the axial oxygen of the sulfonyl group, which effectively prevents addition from the *endo*-face.



Scheme 1.31: Arrangement of the acrylate zwitterion **156** ($R_3N = \text{DABCO}$) in the absence of chelation.^{72,102}

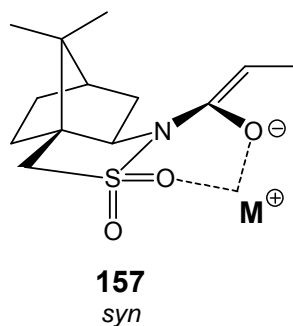
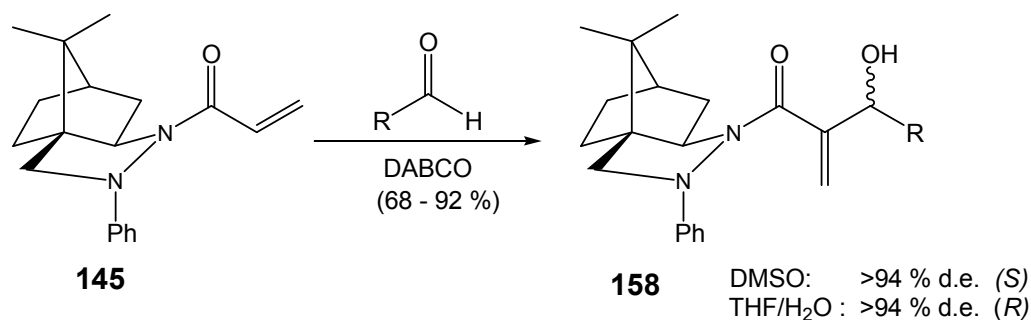


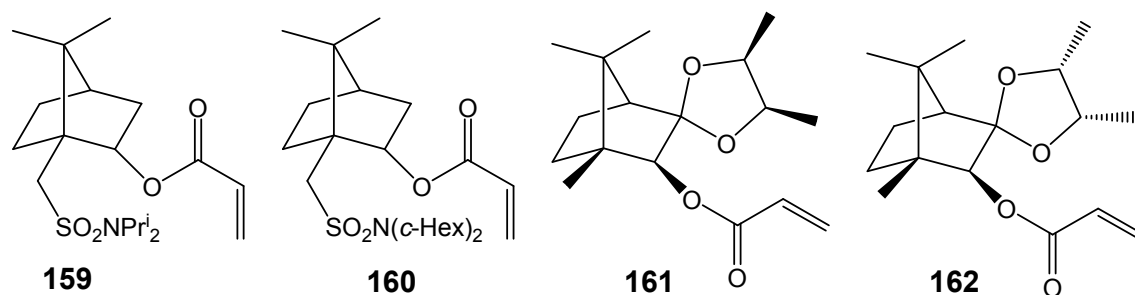
Figure 1.2: Arrangement of the acrylate anion **157** undergoing chelation with a Lewis acid.^{72,102}

Development of a highly efficient enantiopure acryloylhydrazide **145** was achieved by Yang and co-workers (**Scheme 1.32**).⁹⁵ The Baylis-Hillman adducts were produced in very high diastereoselectivities (>94 % d.e.) using this hydrazide, and reversal of stereoselectivity was found to be possible by changing the solvent from DMSO to THF-H₂O. It was assumed that the zwitterion intermediate in THF-H₂O is stabilized by intermolecular hydrogen bonding with solvent molecules, whereas destabilisation of the zwitterion occurs in DMSO.



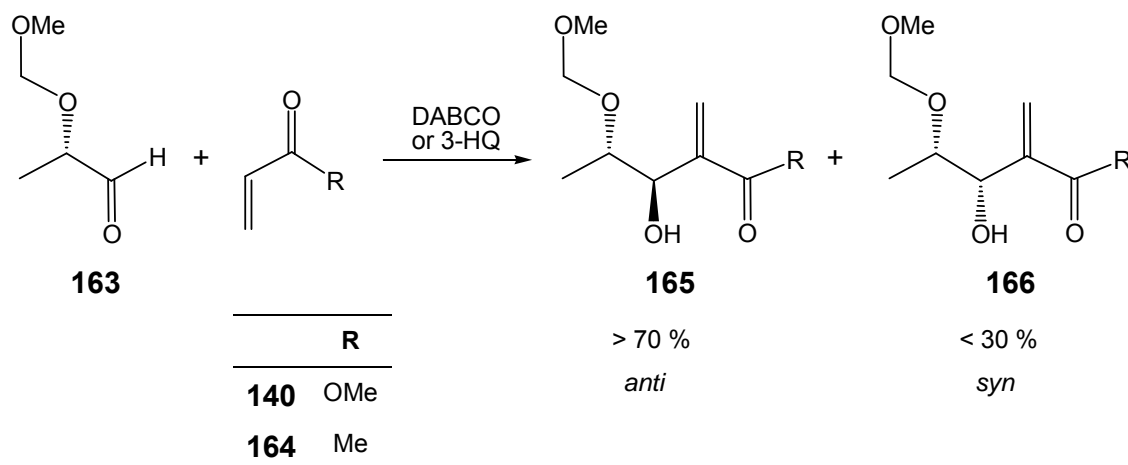
Scheme 1.32: The Morita-Baylis-Hillman reaction involving the camphor-derived acryloylhydrazide **145**.⁹⁵

Several other camphor-derived acrylic esters, such as **159**,¹⁰³ **160**,¹⁰³ **161**^{99,82} and **162**,^{99,82} have been explored as Baylis-Hillman substrates. However, none of these have been particularly successful in inducing stereoselectivity. Presumably the steric demands are not sufficient to favour addition to a particular face of the enolate intermediate.



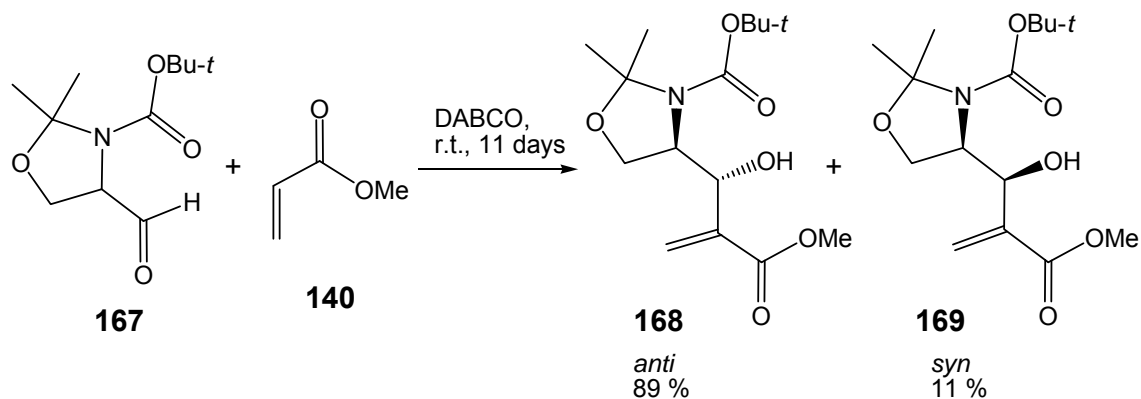
1.3.3.1.2 Chiral electrophiles

Research into the asymmetric version of the Morita-Baylis-Hillman reaction has been concentrated on the use of chiral Michael acceptors and little attention has been given to the use of chiral electrophiles.⁹² Most studies involving chiral electrophiles have focused on the addition of single enantiomers of α -branched aldehydes to acrylates and methyl vinyl ketone (MVK). Drewes *et al.*¹⁰⁴ reacted the (*S*)-(-)-2-(methoxymethoxy)propanal **163** with methyl acrylate **140** and methyl vinyl ketone (MVK) **164** in the presence of DABCO or 3-hydroxyquinuclidine (3-HQ) to obtain mixtures dominated by the *anti*-isomer **165** (Scheme 1.33).



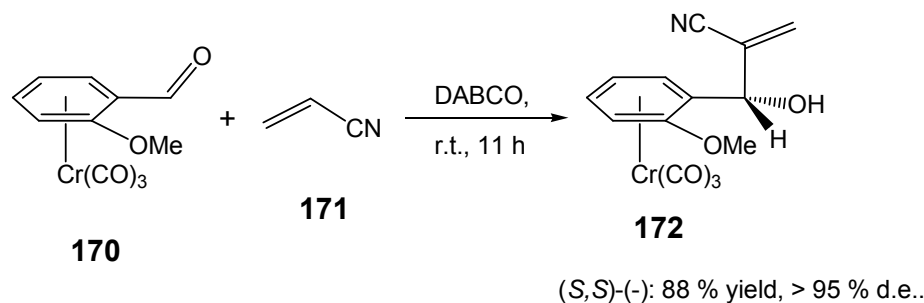
Scheme 1.33: Use of optically active aldehydes in the Morita-Baylis-Hillman reaction.¹⁰⁴

Manickum *et al.*¹⁰⁵ also found that use of the heterocyclic aldehyde **167** afforded the *anti*-product **168** with high stereoselectivity (78 % d.e.) (Scheme 1.34).



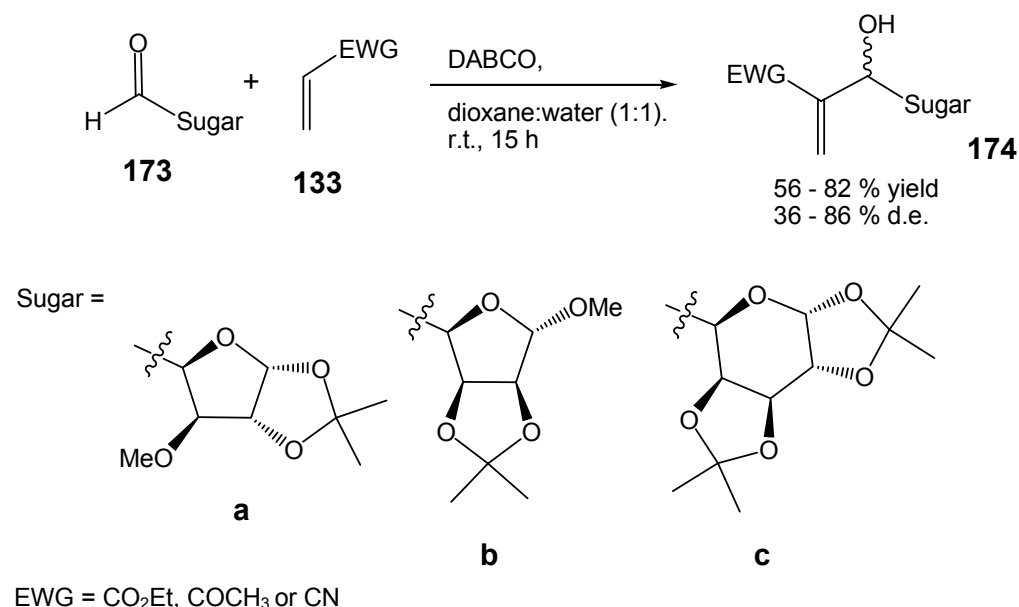
Scheme 1.34: Use of bulky aldehydes in the Morita-Baylis-Hillman reaction.¹⁰⁵

Kundig *et al.*^{106,107} have achieved good to excellent diastereoselectivity (68 - 95 % d.e.) with tricarbonylchromium complexes of *ortho*-substituted aromatic benzaldehydes, *e.g.* **170** (**Scheme 1.35**). The nature of the *ortho* substituent was found to be critical in achieving high levels of diastereoselectivity.



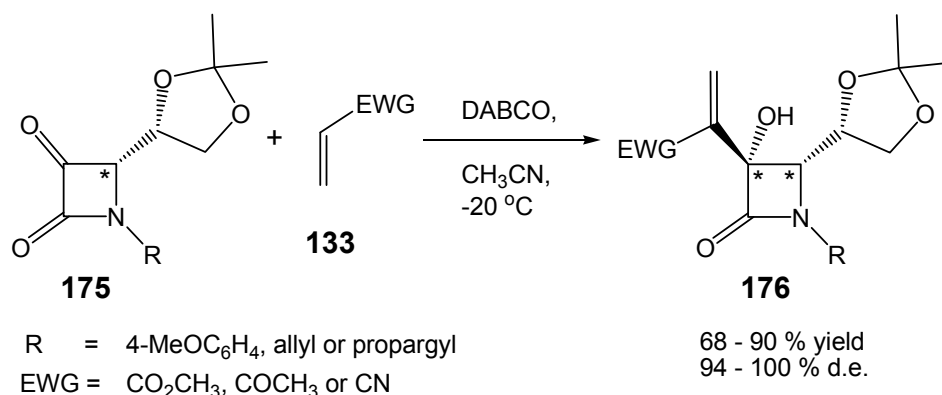
Scheme 1.35: Tricarbonylchromium complexes of *ortho*-substituted aromatic benzaldehydes.^{106,107}

Krishna *et al.*^{92,108} have investigated the use of sugar-derived aldehydes **173a-c** as chiral electrophiles with an activated alkene in dioxane/water (1:1) with low to high diastereoselectivity (36 – 86 % d.e.) and good yields (56 – 82 %) (**Scheme 1.36**). The observed stereoselectivity was explained by favoured attack of the zwitterion at the *si*-face of the aldehyde, resulting in a predominance of the *S*-isomer. The stereochemistry of the newly created centre accords with the non-chelation Felkin-Anh model.¹⁰⁹



Scheme 1.36: The use of sugar-derived aldehydes **173a-c** as chiral electrophiles.^{92,108}

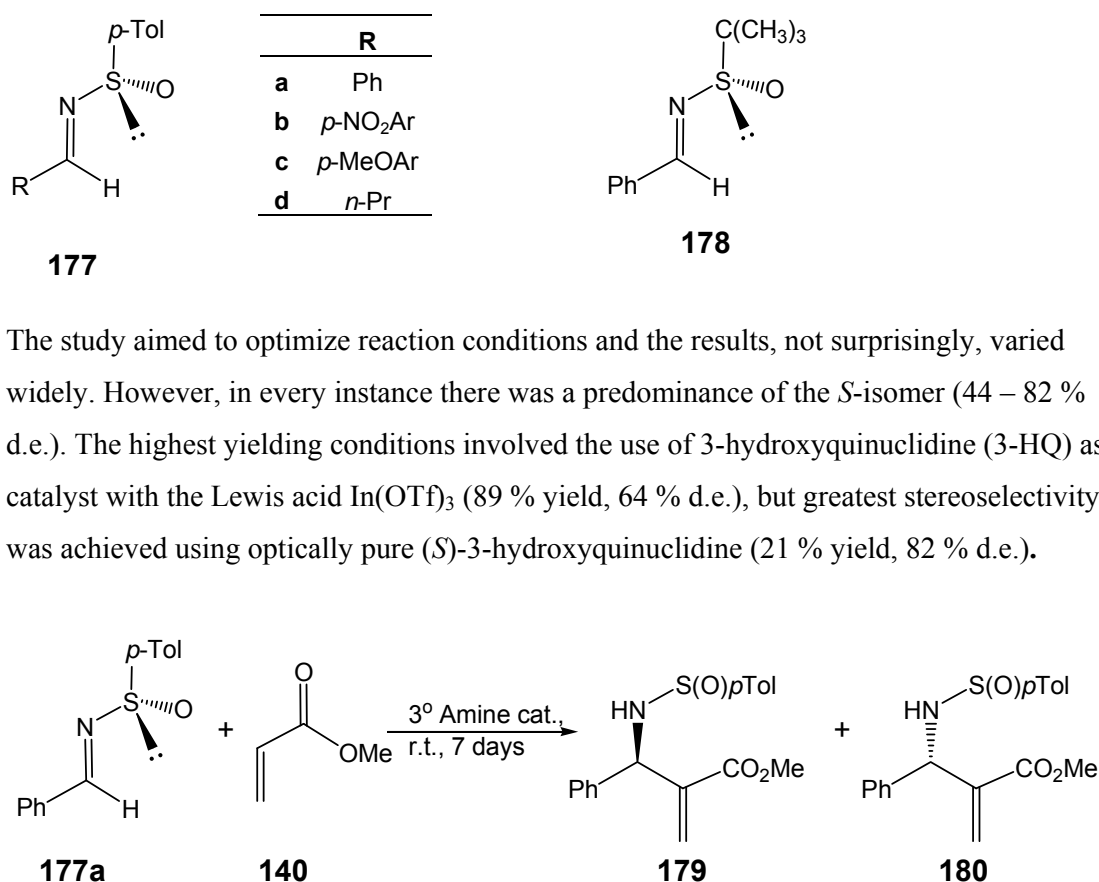
Alcaide *et al.*⁹¹ reported the synthesis of 3-oxo-2-azetidiones **175** from 2-hydroxy- β -lactams *via* Swern oxidation, and their use in the asymmetric Morita-Baylis-Hillman reaction with excellent diastereoselectivity (94 – 100 % d.e.), high yields (69 – 90 %) and fast rates of reaction (1 – 72 h) (**Scheme 1.37**).



Scheme 1.37: The use of 3-oxo-2-azetidiones in the asymmetric Morita-Baylis-Hillman reaction.⁹¹

In some rare instances, imines have been utilized as electrophiles in place of aldehydes in the Morita-Baylis-Hillman reaction, affording entry to the corresponding β -amino products;^{110,111} however, very few attempts have been made to render this process asymmetric. Recently Aggarwal *et al.*⁹³ investigated the effectiveness in this reaction of optically pure *N-p*-

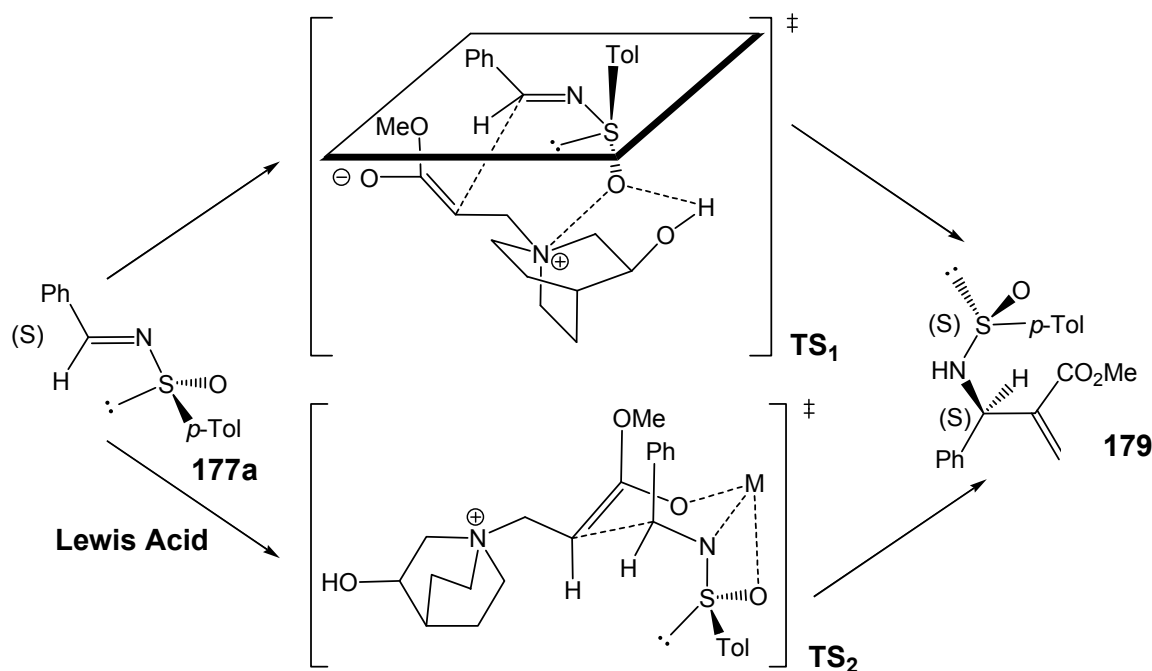
toluenesulfinimines **177a-d** and *N-tert*-butylsulfinimine **178** with methyl acrylate both in the presence and absence of Lewis acids (**Scheme 1.38**).



3° Amine cat. = 3-HQ or DABCO
 Lewis Acid = None, La(OTf)₃, Al(O*i*-Pr)₃, Zn(O*i*-Pr)₄,
 Zn(OTf)₂, Sc(OTf)₃, Yb(OTf)₃ or In(OTf)₃

Scheme 1.38: The Morita-Baylis-Hillman reaction utilizing imines as the electrophile.⁹³

In the preferred conformation of the imine the bulky sulfur substituents lie out of the plane of the double bond. Nucleophilic attack by the catalyst is considered to occur *anti* to the large *p*-tolyl substituent, resulting in the observed diastereoselectivity (**Scheme 1.39**), while coulombic attraction between the sulfinyl oxygen and the quaternary ammonium moiety coupled with hydrogen bonding to the 3-hydroxy group serve to stabilize the transition state **TS**₁. Alternatively, when a Lewis acid is present, the transition state **TS**₂ adopts a chair-like conformation in which the metal coordinates with the imine nitrogen, the sulfinyl oxygen and the acrylate oxygen, such that C-C bond formation takes place within a rigid coordinated species.



Scheme 1.39: Transition state conformations for stereoselective reactions of the imine electrophile **177a**.⁹³

1.3.3.1.3 Solvent Effects

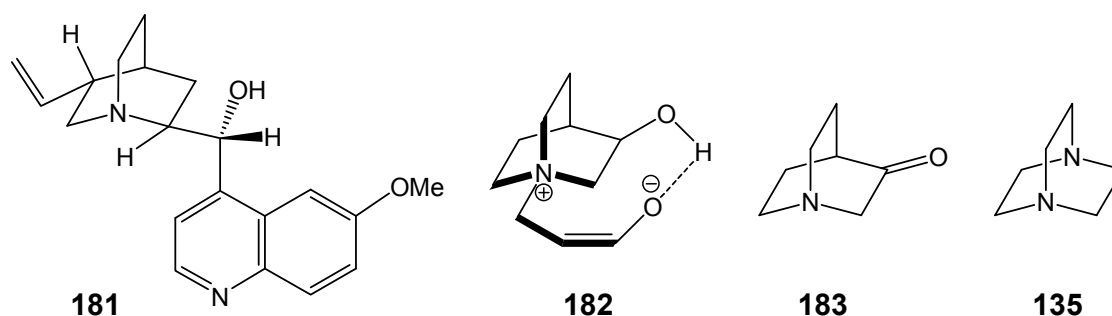
Perhaps the most interesting solvent effect was noted by Yang and co-workers as described earlier (**Scheme 1.32**, p. 35),⁹⁵ where the chiral acryloylhydrazide **145** was reacted with aldehydes in the presence of DABCO. Either diastereomeric product could be obtained in high optical purity by changing the solvent. When DMSO was used, the *S*-isomer predominated (94 – 98 % d.e.), whilst the *R*-isomer predominated (94 – 98 % d.e.) when the solvent system was changed to THF/H₂O (5:1). It seems that the transition state conformation is highly solvent-dependent. Cai *et al.*¹¹² also undertook an investigation of the rate acceleration in Morita-Baylis-Hillman reactions and noted excellent diastereoselectivity (83 – 99 % d.e.) on using 1,4-dioxane as solvent in the trimethylamine catalyzed reaction.

1.3.3.2 Enantioselectivity

1.3.3.2.1 Chiral catalysts

The use of chiral catalysts, usually tertiary amines, in the Morita-Baylis-Hillman reaction theoretically provides a means of effecting chiral discrimination, as the catalyst participates in the step in which the chiral centre is created. This method of achieving enantioselectivity has, however, only enjoyed limited success. It would appear that many catalysts fail to pass on steric information, even if the chiral centre is in close proximity to the nitrogen atom, and additionally, they often demonstrate low conversion efficacy and the use of high pressure is usually necessary.⁷¹

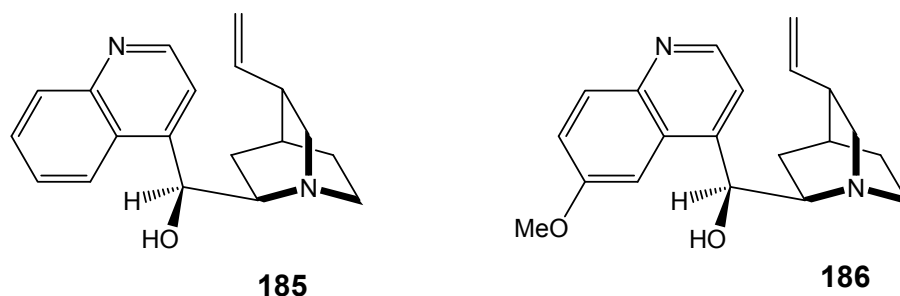
Wynberg has, however, successfully demonstrated the usefulness of chiral catalysts.¹¹³ Benzaldehyde was reacted with diethyl zinc in the presence of quinine **181** and afforded (*R*)-(+)-1-phenylpropanol with moderate stereoselectivity (68 % e.e.), while use of 2-ethoxybenzaldehyde as the substrate, afforded even better stereoselectivity (90 % e.e.). Motivated by these results, Drewes *et al.*⁸⁸ attempted to use quinine **181**, as well as several other tertiary amines (such as quinidone, retronecine, cinchonidine and brucine), in the Morita-Baylis-Hillman reaction with limited success (≤ 10 % e.e.).



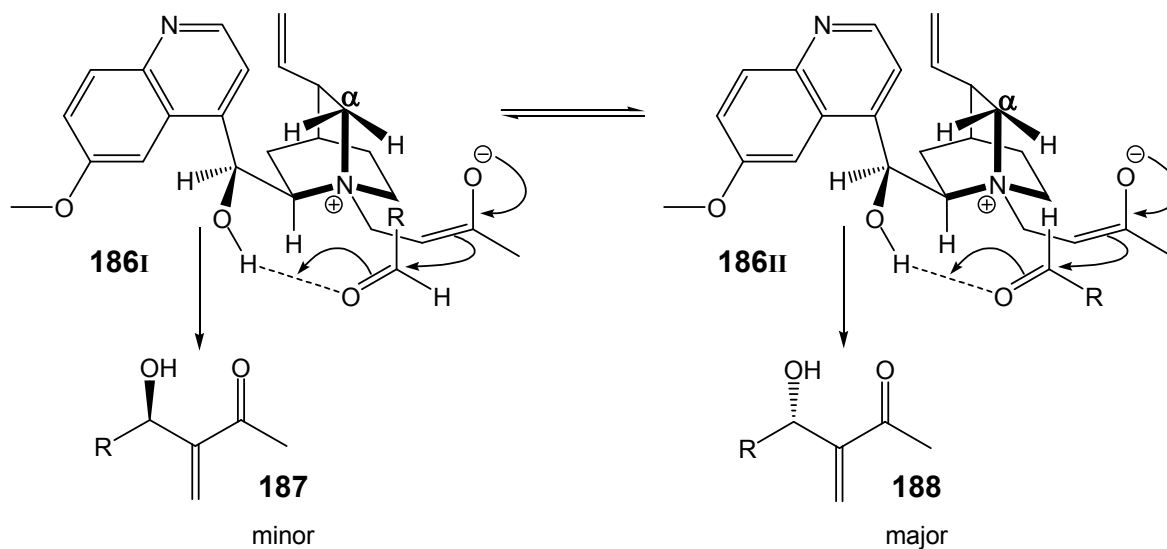
Drewes *et al.*⁸⁸ suggested the possibility of a protic species causing stabilization of a catalyst-acrylate system by hydrogen bonding interactions. These authors then reported enhancement of the rate of the reaction, as well as increased asymmetric induction when a hydroxy group was suitably disposed on the amine catalyst.⁹⁶ The reaction involved the use of methanol as the protic species and 3-hydroxyquinuclidine **139** as catalyst. Participation of a cyclically stabilized anion intermediate **182** appeared to be supported by the considerably longer

reaction times observed when the hydroxyl group in 3-hydroxyquinuclidine was blocked or when the non-hydroxylated 3-quinuclidinone **183** was used. As described earlier (Section 1.3.1, p. 28), Bode⁸³ also noted a significant increase in rate with the use of 3-hydroxyquinuclidine **139** as compared to DABCO **135**.

Marko⁹⁰ attempted to take advantage of the hydrogen bonding phenomenon by using a range of hydroxy-amine catalysts to effect enantioselective syntheses; however, the enantiomeric excesses achieved were poor (0-25 % e.e.). The two most selective compounds, cinchonine **185** and quinidine **186**, were subsequently used in a study to determine conditions for achieving high enantioselectivity.

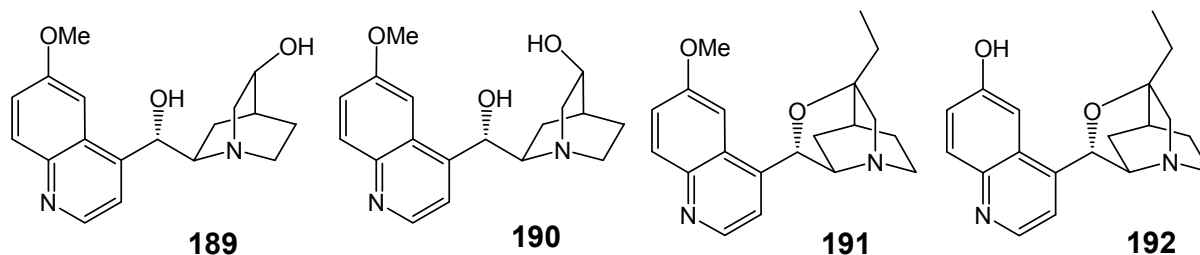


The suggestion, by Marko,⁹⁰ was that the role of the hydroxyl group is two-fold: - i) to lock the conformation of the ternary complex by hydrogen bonding to one of the lone pairs of the aldehyde carbonyl; and ii) to lower the energy of the transition state, by stabilizing the incipient negative charge developed on the oxygen atom during the aldol condensation, thus accelerating the reaction and providing an asymmetric environment (Scheme 1.40). Another important aspect of these results was the observation that the size of the aldehyde R-group relates directly to the observed enantioselectivity, the increased steric interactions between the R-group and the two hydrogens at C_α favouring intermediate **186II**.

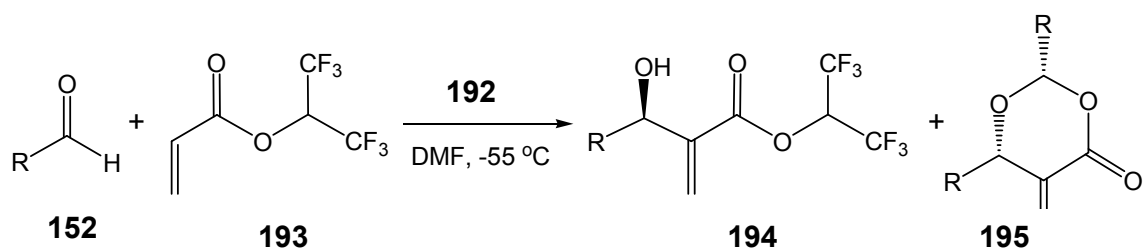


Scheme 1.40: Proposed mechanistic model of the interactions involving the intermediate species of quinidine **186**.⁹⁰

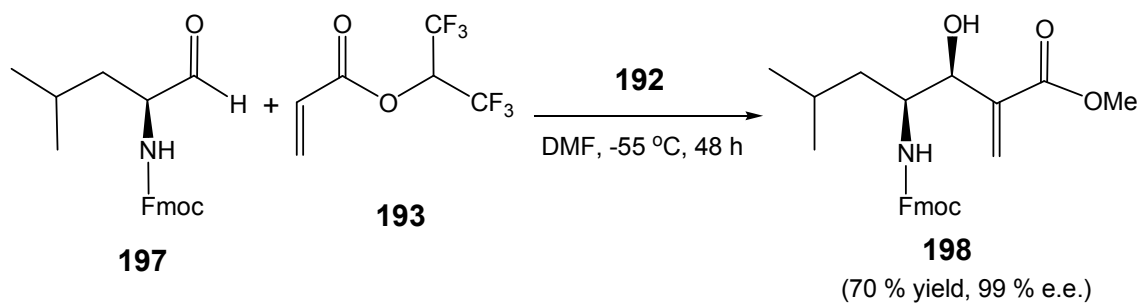
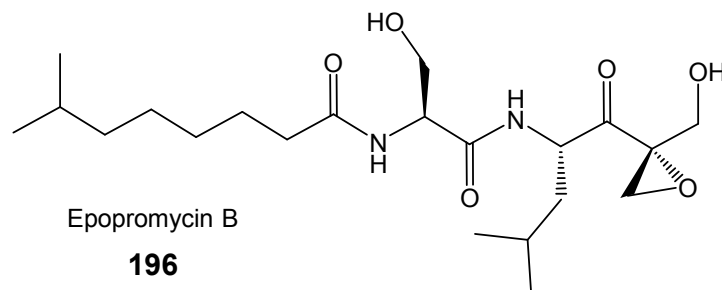
Iwabuchi *et al.*⁹⁸ furthered Marko's work by using several suitably modified hydroxyquinidine derivatives **189-192**⁹⁰ and achieved good yields and a wide range of enantioselectivities (10 - 91 % e.e.).



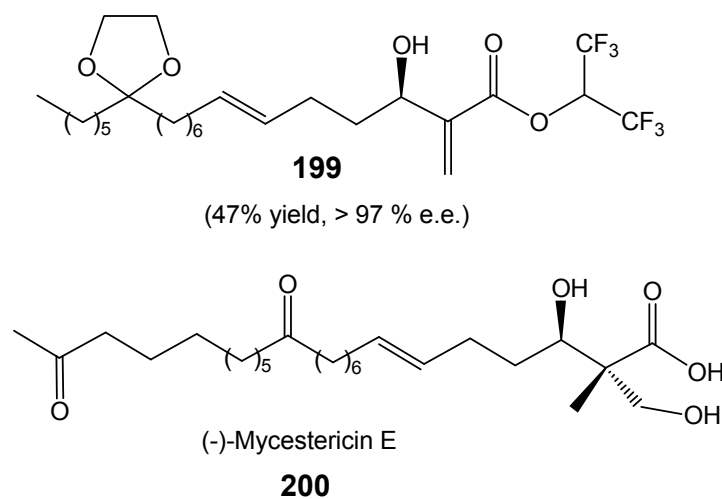
The cyclic ether **192** showed particular promise (64 – 91 % e.e.) and, upon optimization of the reaction conditions, reacted with a number of aldehydes at -55 °C in DMF to give the chiral alcohols **194** in good yield and excellent enantiomeric excess (91 – 99 % e.e.), the *R*-enantiomer predominating in each case (**Scheme 1.41**); the dioxanones **195** were isolated as side products. These authors subsequently used the hydroxyquinidine derivative **192** as a catalyst in a Morita-Baylis-Hillman reaction to synthesise the α -methylene-statine framework **198** as part of the overall synthesis of epopromycin B **196** (**Scheme 1.42**).⁹⁷ Iwabuchi *et al.*⁹⁴ successfully used the same hydroxyquinidine derivative **192** in the synthesis of the ester **199** as an intermediate in the complete synthesis of (-)-mycestercin E **200** (**Scheme 1.43**).



Scheme 1.41: Catalysis of the Morita-Baylis-Hillman reaction using the tertiary amine **192**.⁹⁸



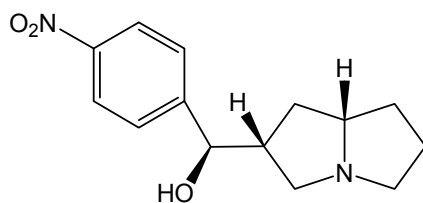
Scheme 1.42: Synthesis of the α -methylene-statine framework of epopromycin B **196**.⁹⁷



1.3.3.2.2 Chiral Co-Catalysts

The concept of using a Lewis acid-chiral ligand complex to catalyse the Morita-Baylis-Hillman transformation has been documented.¹¹⁴ The role of the chiral ligand is twofold: - i) to act as a chiral nucleophilic Morita-Baylis-Hillman catalyst, and; ii) to coordinate to the metal. The stereochemical elements for achieving enantioselective carbon-carbon formation with a Lewis acid co-catalyst rely on the correct choice of metal and chiral ligand for a particular substrate.¹¹⁴ The design and synthesis of a tuneable chiral ligand were clearly critical, since the Lewis acidity of the metal, and thus its potential for activation, is controlled by the donor atoms of a ligand.¹¹⁵ The donor group functionality is also important in directing enantioselectivity.¹¹⁴

Barrett *et al.*¹¹⁶ examined the use of the achiral Lewis acid $\text{BF}_3 \cdot \text{OEt}_2$ together with alkali metal salts in the synthesis of Morita-Baylis-Hillman products in the presence of the chiral ligand **201**. Initially the reactions were conducted in the absence of a Lewis acid, and the products were isolated in good yields and exhibited a range of enantiomeric excesses (21- 47 % e.e.).



201

Addition of a co-catalyst, however, was observed to increase the rate and, in most cases, more than double the enantioselectivity (up to 72 % e.e.). The stereocontrol was explained in terms of hydrogen bonding to the co-catalyst and a lowering of the energy of the transition state conformation **201II** relative to **201I** (Figure 1.3).

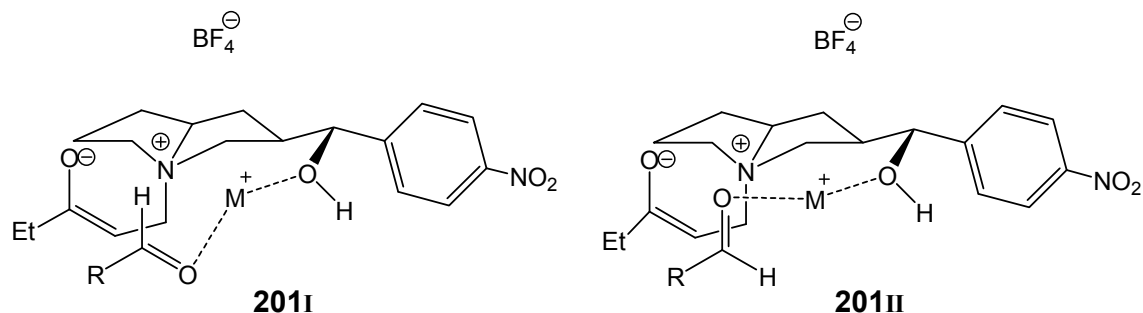


Figure 1.3: Mechanistic model of the interactions on use of the chiral co-catalyst **201** during Morita-Baylis-Hillman reactions.¹¹⁶

Aggarwal *et al*¹¹⁷ have also investigated the use of Lewis acid co-catalysts, including lanthanides and group III metal triflates, and have achieved significant rate acceleration. However, the authors were unable to achieve acceptable enantioselectivity (5 % e.e.). Yang *et al*.¹¹⁴ were far more successful in using Lewis acid co-catalysts; synthesizing and making use of camphor-derived dimerized amino ligands to achieve high enantioselectivity (up to 95 % e.e.). The authors then decided to incorporate carboxylic acid functionality into a number of ligands to take advantage of the oxophilic nature of the metal. The most successful ligand was found to be **202**, when used in conjunction with the Lewis acid La(OTf)₃. When this system was used with a range of acrylate esters and aldehydes, high to excellent enantioselectivity was achieved (65 – 95 % e.e.); with the *S*-isomer predominating in all cases and the products being obtained in moderate to excellent yields (35 – 89 %). The proposed coordinated complex is shown in **Figure 1.4**.

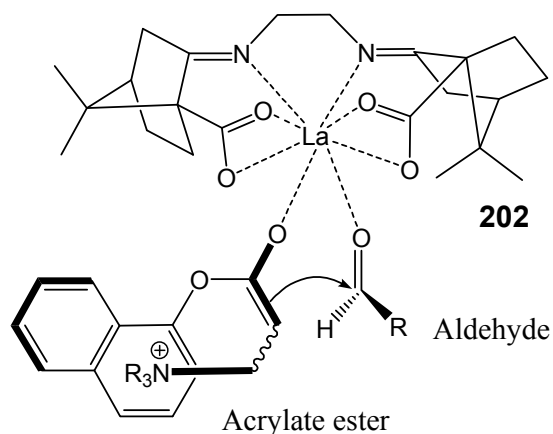
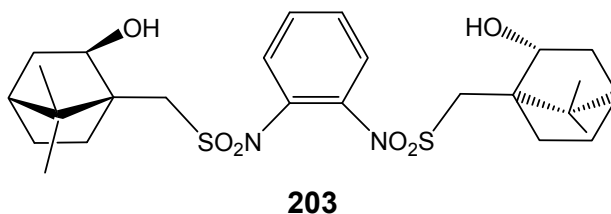


Figure 1.4: Proposed coordination of the reactants in the enantioselective Morita-Baylis-Hillman reaction in the presence of the lanthanum-dimer **202** complex.¹¹⁴

Bauer *et al.*¹¹⁸ achieved a wide range of enantioselectivities (2 -67 % e.e.) using bisulfonamide camphor-derived ligands, the metal complex, titanium tetraisopropoxide (Ti(O-iPr)₄), and the promoter diethylzinc (ZnEt₂). The greatest success was achieved with the ligand **203** (52 – 67 % e.e.). The authors concluded that C-2 symmetry was not always advantageous to stereoselectivity as both sides of the C-2 symmetric molecules they developed were able to act independently.



1.3.3.2.3 Chiral solvents

In most instances, it has been found that the presence of a solvent in the Morita-Baylis-Hillman reaction adversely affects the rate of the reaction.⁸⁴ However, it is not unreasonable to expect that a chiral solvent should induce some degree of enantioselectivity.⁷¹ Gilbert *et al.* were amongst the first to study solvent effects on enantioselectivity.⁸⁶ Acrylonitrile was reacted with acetaldehyde in the presence of 3-hydroxyquinuclidine in (+)-ethyl lactate but, unfortunately, exceedingly poor enantioselectivity was achieved (3 % e.e.).

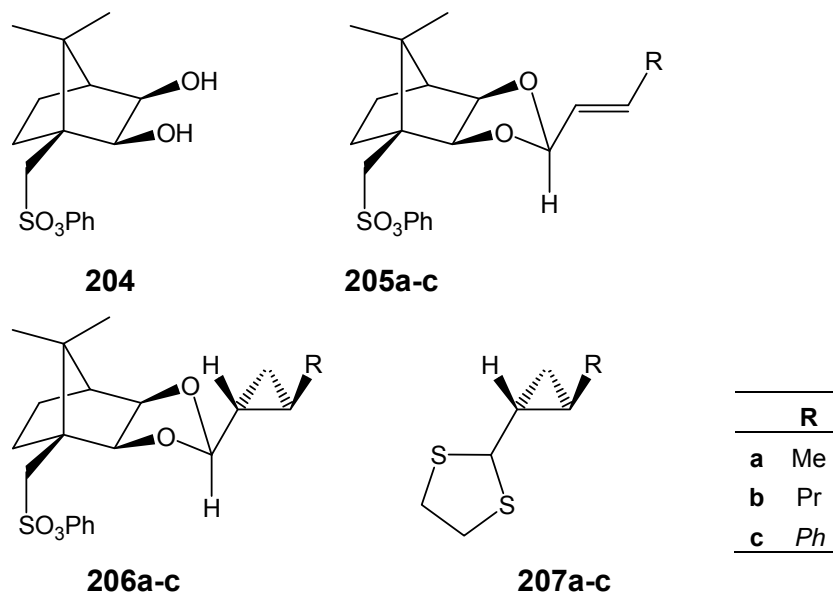
1.3.3.2.4 Resolution of Racemic Products

A popular method for obtaining Morita-Baylis-Hillman-derived products of high enantiomeric purity is through resolution. Brown *et al.*¹¹⁹ kinetically resolved α -methylene- β -hydroxyalkanoates, sulfones and α -methylene- β -aminoalkanoates *via* homogenous hydrogenation using chiral phosphines-rhodium catalysts. The recovered alcohols were obtained in high enantiomeric excess (>90 % e.e.). Kitamura *et al.*¹²⁰ obtained enantiomerically pure α -hydroxylalkyl acrylates through fractional crystallization of diastereomeric salt mixtures of the corresponding acids and by kinetic resolution involving hydrogenation with chiral rhodium biphosphine. Trost *et al.*¹²¹ were also able to achieve excellent resolution of enantiomers (85 – 96 % e.e.) through a dynamic kinetic asymmetric transformation process.

1.4 PREVIOUS WORK BY THE RHODES RESEARCH GROUP

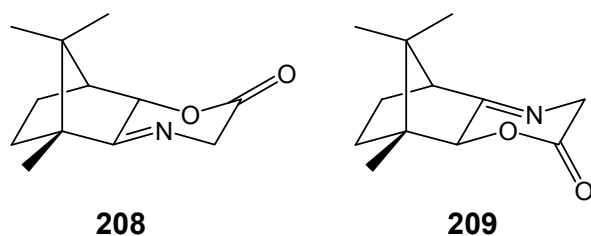
The ability of camphor and its derivatives to participate as auxiliaries with high chiral discriminatory properties is well established. The origin of the stereocontrol achieved by camphor derivatives arises from the overall rigidity of the bicyclic skeleton and the stereodirecting groups innately present or introduced. These properties combined with the numerous transformations that camphor is capable of undergoing have made it a significant focal point for various members of our group for a number of years.^{99,122-125} The most recent research has focused on the origin and optimization of stereocontrol in several reactions including the following.

- i) In a highly successful cyclopropanation study, Molema³⁷ developed the camphor-derived chiral auxiliary **204**. Cyclopropanation of acetal intermediates **205a-c** afforded the cyclopropyl derivatives **206a-c** in 76 – 95 % yield and in > 99 % d.e. The chiral auxiliary **204** was then released through transthioacetalisation and the corresponding dithiones **207a-c** were isolated in 87 – 92 % yield.

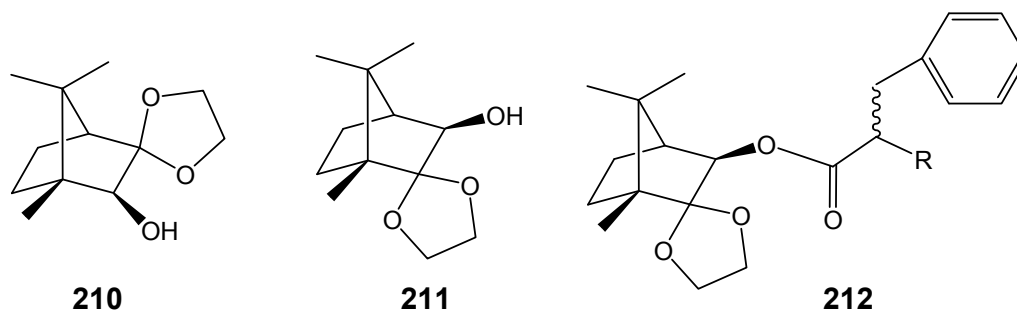


- ii) In a search for a synthetically viable route to α -alkylated α -amino acids, Ravindran¹²³ successfully developed the 2-iminolactone **208** and the regioisomeric 3-iminolactone **209**. Monoalkylation of the 3-iminolactone was successfully achieved by Matjila¹²²

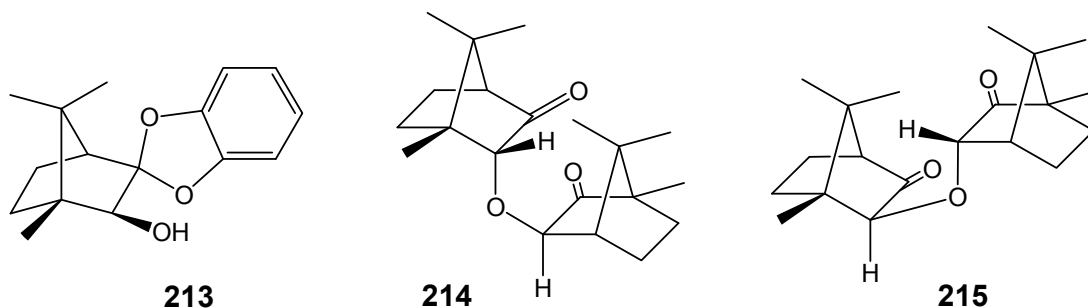
and Klein¹²⁴ in good yields (63 – 82 %) and in 43 - >99 % d.e. Dialkylation of the 2-iminolactone was also achieved but efforts to obtain monoalkylated products failed.¹²²



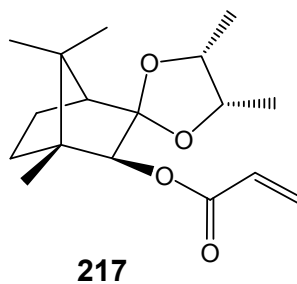
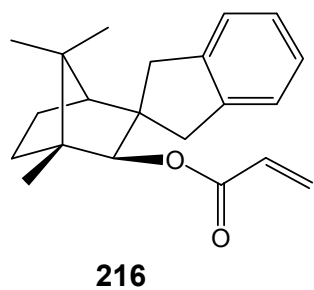
- iii) Bulky groups were introduced to the camphor moiety by Evans⁹⁹ and Ravindran¹²³ to afford, for example **210** and **211**, in an attempt to increase the stereodirecting ability. Klein¹²⁴ subsequently illustrated the potential of the alcohol **211** by achieving the α -benzylation of the ester-derivatives to produce the diastereomeric products **212** in 60 – 83 % d.e.



- iv) Ravindran's attempted synthesis of the borneol derivative **213**, containing a bulky 3-catechol blocking group,¹²³ led to the unexpected formation of camphor dibornyl ethers **214** and **215**. With a view to developing reagents analogous to the highly successful BINOL reagents, Matjila¹²² undertook preliminary studies on the reduction of the dimers and reported a monohydroxy and dihydroxy product.



- v) Evans⁹⁹ explored use of camphor-derived acrylate esters such as **216** and **217**, in Morita-Baylis-Hillman reactions. Application of the novel camphor-derived acrylate ester **216** resulted in high yields (71 – 91 %) but indifferent stereoselectivity (5 – 59 % d.e.), whereas use of the ester **217** failed to attain even moderate stereoselectivity (0 – 34 % d.e.).⁹⁹



1.5 AIMS OF THE PRESENT INVESTIGATION.

The development of camphor derivatives with the ability to enhance stereocontrol in various reactions remains a priority in our research programme. Throughout the investigation of numerous camphor derivatives, a primary objective has been to rationalize the interactions responsible for the observed stereocontrol. The present investigation represents a continuation of this programme and has focused on the following objectives.

- i) Extension of the earlier work done on camphor derived dibornyl ethers and their reduction to produce asymmetric hydroxy dimers.
- ii) Synthesis and stereoselective monoalkylation of the 2-iminolactone.
- iii) The development and evaluation of novel camphor-derived chiral auxiliaries for use in the Morita-Baylis-Hillman reaction.
- iv) Elucidation of an unexpected intramolecular transesterification of bornane-2,3-diol monoacrylate esters.
- v) Computational analysis at the density functional (DFT) level of the intramolecular transesterification.

2. DISCUSSION

This research has involved the modification of (1*R*)-(+)-camphor **16** (**Figure 2.1**) to yield a variety of novel chiral auxiliaries with potential for application in a range of asymmetric reactions. In the discussion which follows, attention will be given to: - the synthesis of *exo*-hydroxybornanones and an extension of earlier work involving their dimerisation (**Section 2.1**); further investigations into the preparation of chiral iminolactones and their use in the asymmetric synthesis of α -amino acids (**Section 2.2**); the development of chiral Morita-Baylis-Hillman substrates (**Section 2.3**); and kinetic-mechanistic and DFT computational studies of the intramolecular transesterification of bornane-2,3-diol monoacrylates (**Sections 2.33** and **2.34**, respectively).

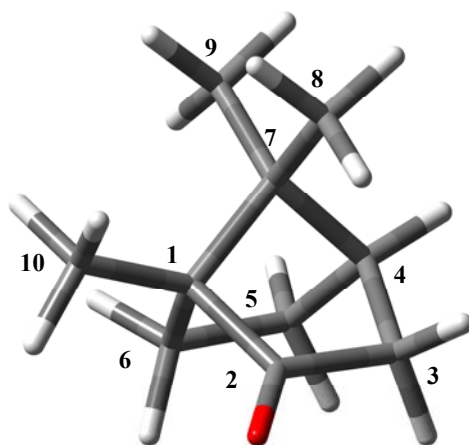
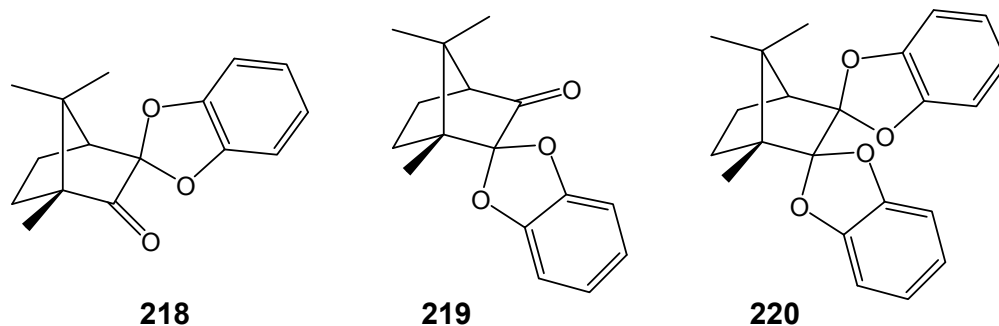


Figure 2.1: DFT Geometry optimized representation of (1*R*)-(+)-camphor **16**.

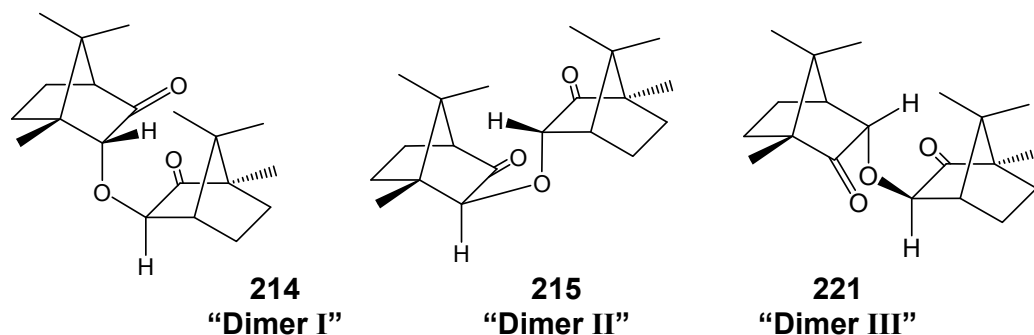
2.1 SYNTHESIS and DIMERISATION REACTIONS of *EXO*-HYDROXYBORNANONES

Stereo-directing groups have been the subject of numerous studies and have been found to influence the formation of specific diastereomers. The general synthetic principle involves the introduction of steric constraints into a relatively rigid substrate to promote stereofacial selectivity by an attacking species at a prochiral centre, resulting in the preferential, if not exclusive production of a single diastereomer.

The synthesis of sterically hindered camphor acetals as chiral auxiliaries has attracted considerable interest in our own laboratories.¹²³ Thus, Ravindran attempted to increase steric bulk at positions C-2 or C-3 of the camphor system by preparing the monocatechol acetals **218** and **219**.¹²³ However, monoketalisation of camphorquinone proved to be unexpectedly difficult and dicatechol **220** appeared to be formed exclusively. Various protection strategies were investigated to achieve the desired products, but without success.

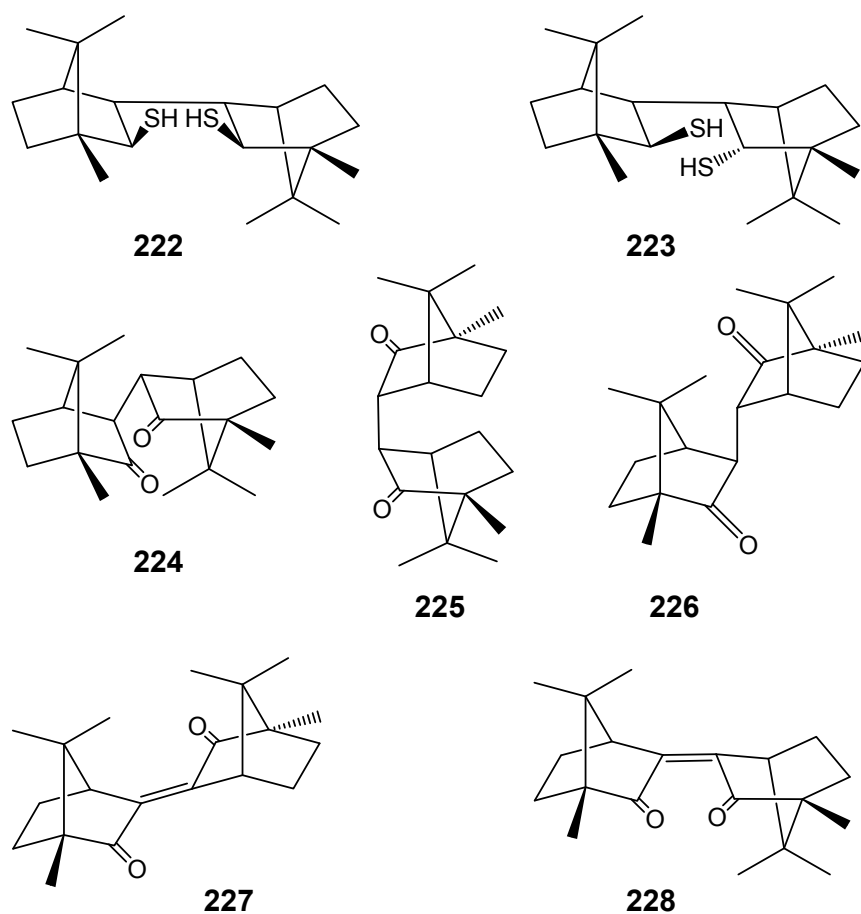


Ravindran¹²³ attempted to synthesise the 3-hydroxy derivative of the monoketal **219** by heating 3-*exo*-hydroxybornan-2-one **231** with catechol and *p*-TsOH. However, an unexpected product was obtained, ¹³C analysis of which indicated the presence of twenty *different* carbon atoms. Similar treatment of the 2-*exo*-hydroxybornan-3-one analogue afforded a second, isomeric compound. These two novel products were identified as the camphor dimers **214** and **215**, respectively. Matjila¹²² reproduced these results and in the course of his research, isolated a third isomer, formulated as **221**. The present study focused, initially, on confirming the earlier results, establishing the structural assignments by thorough 1- and 2-D NMR spectroscopy, furthering the reaction sequence and exploring the mechanistic implications.



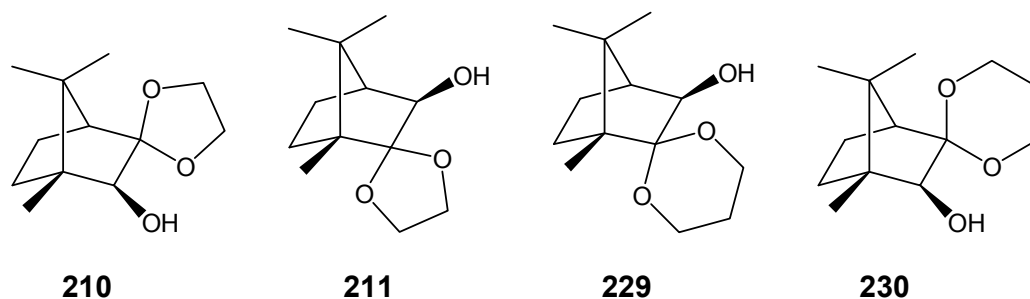
The synthesis of carbon-carbon linked camphor dimers has been achieved by several researchers. Manasse¹²⁶ reported the production of a 2-*endo*-hydroxyepicamphor dimer,

which later was identified by Banks *et al.*¹²⁷ as a bridged bis(methyl ketal). Rautenstrauch *et al.*,¹²⁸ followed by Pradhan *et al.*,¹²⁹ obtained several (C-2)–(C-2') linked pinacols by alkali metal-ammonia reduction of (+)-[3,3-D₂]camphor, while the synthesis of bithiocamphor derivatives **222** and **223**, with C–C linkages, was reported by Bonnat *et al.*¹³⁰ Ito *et al.*¹³¹ synthesised a mixture of bicamphor epimers, **224**, **225** and **226**, with C–C linkages. McNulty *et al.*¹³² repeated Ito's research but altered the conditions to stereoselectively synthesise 3-*exo*-3'-*exo*-bicamphor **224** and the dioxobisbornanylidenes **227** and **228**. An extensive literature search, however, has failed to reveal any syntheses of the ether dimers isolated in our laboratories.



The investigation necessitated the synthesis of the two distinct hydroxybornanone precursors **231** and **233** (Scheme 2.1) and the maintenance, through several steps, of their chiral information. Several methods of obtaining these α -ketols were considered, most of which: afforded little or no stereocontrol; involved many steps and poor yields; produced unwanted products¹³ or led to enantiomers of opposite configuration¹³ to our requirements. This last-

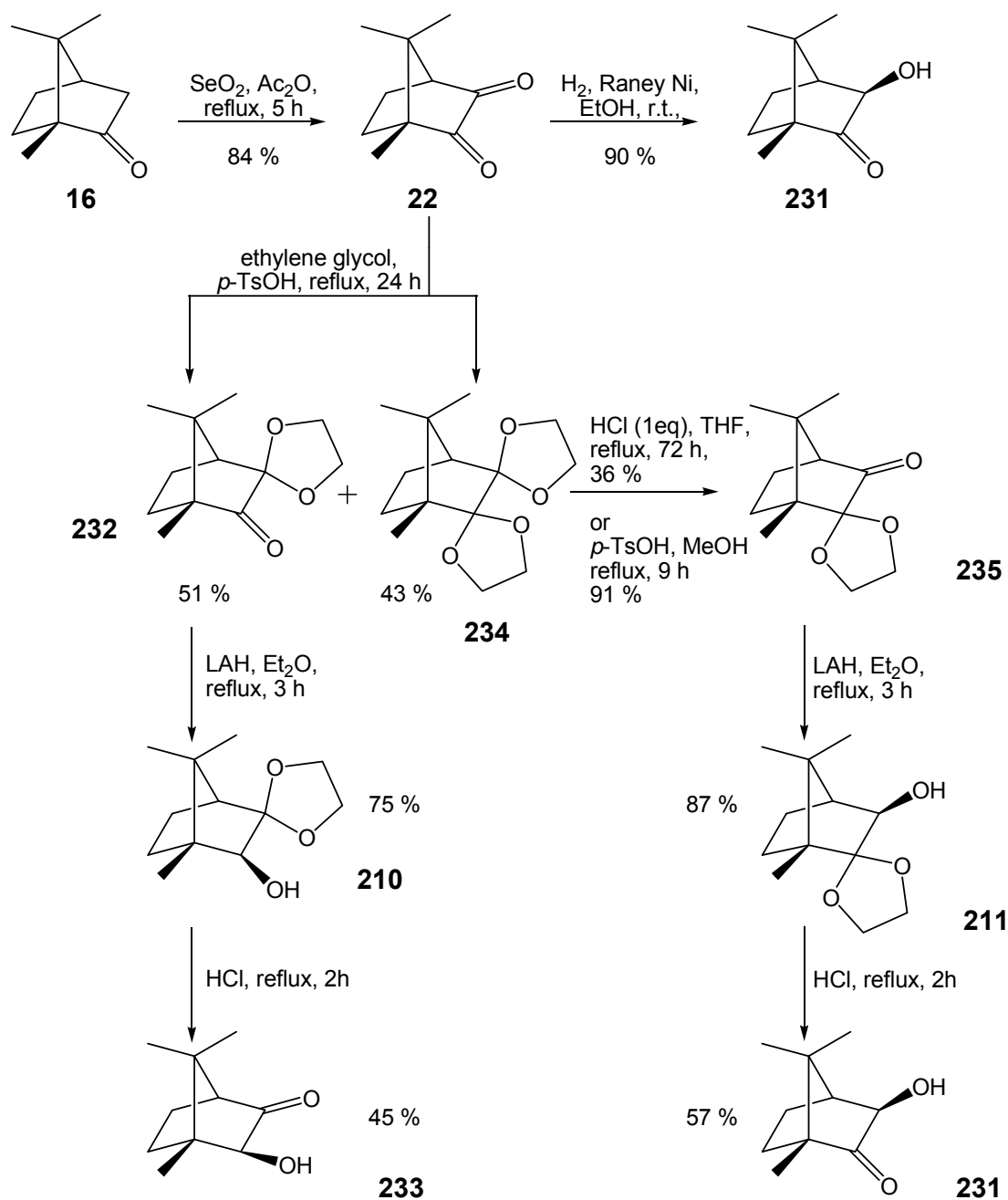
mentioned approach involved biological metabolism to afford the *endo*-hydroxy product and, moreover, it was not immediately obvious how it was extracted from the canine involved!¹³ Previous researchers in our laboratories had, however, introduced protecting groups in the form of ketals at either the C-2 or C-3 position.¹²²⁻¹²⁴ Reduction of these ketals gave the chiral auxiliaries **210**, **211**, **229** and **230**, which were subsequently used in the diastereoselective syntheses of alkylated esters with moderate¹²³ to high stereocontrol.¹²⁴ Of particular significance to the present study was the fact that deprotection of these auxiliaries provides access to the desired α -hydroxybornanones.¹²²



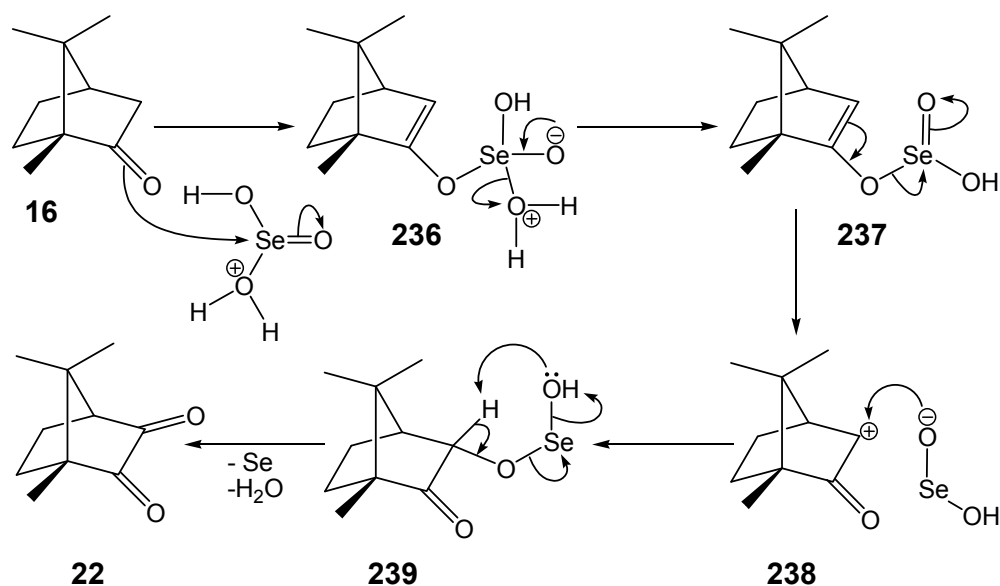
2.1.1 Synthesis of α -Ketols

The methodologies developed within our group were thus followed to access the required 2-*exo*-hydroxybornan-3-one **233** and the 3-*exo*-hydroxybornan-2-one **231** (**Scheme 2.1**). The basic rationale behind the synthesis was to protect either the C-2 or C-3 carbonyl group in camphorquinone as the corresponding ketal, then reduce the unprotected carbonyl group to give an alcohol functionality and, finally, remove the protecting group.

The first step was to produce camphorquinone **22** *via* selective oxidation of camphor. This is possible as the C-3 methylene group of (+)-camphor is adjacent to the carbonyl and is thus easily oxidized to an α -diketone using SeO_2 .^{133,134} A yield of 84 % was achieved for this reaction. The mechanism as initially proposed by Corey and Schaefer,¹³⁵ is mediated by a protonated selenic acid species generated *in situ*, and is shown in **Scheme 2.2**.



Scheme 2.1: Selective synthesis of 2-*exo*- and 3-*exo*-hydroxybornanones.



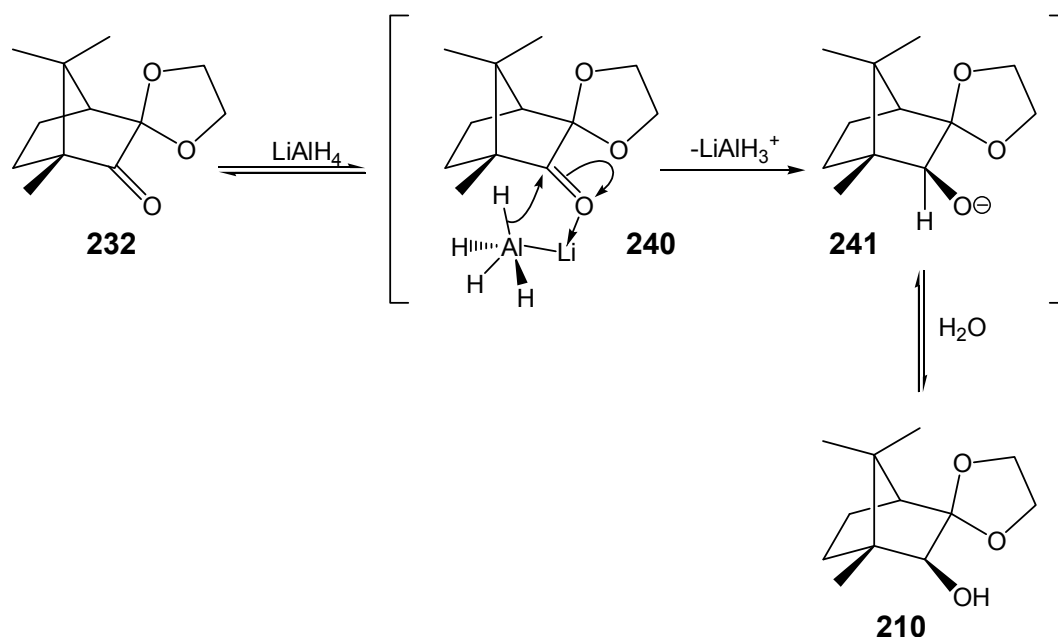
Scheme 2.2: Mechanism of (+)-camphor oxidation by selenium dioxide.¹³⁵

The subsequent protection of the C-3 carbonyl function was achieved by ketalisation with ethylene glycol, the resulting ketal being expected to be inert under the conditions required for the reduction of the C-2 carbonyl by LAH. The ketalisation procedure developed by Ravindran¹²³ was followed, affording the sterically favoured monoketal **232** in 51 % yield together with the diketal **234** in 43 % yield. The reversibility of the reaction necessitated the use of a Dean-Stark trap to collect azeotropically distilled H₂O, thus driving the equilibrium to favour the ketalisation products. Klein¹²⁴ found that diketal **234** could be obtained as the major product by increasing the reaction time to five days and increasing the amount of ethylene glycol ten-fold. It is noteworthy to mention that, while diketalisation occurs readily, formation of the monoketal **235** appears to be inhibited by the proximity of the 10-methyl group and was only found to be present in trace amounts in the crude reaction mixture. The diketal **234** was then selectively deprotected at the less hindered C-3 position by refluxing with aqueous HCl for 72 h to afford **235**, in 36 % yield.

In an alternative approach, refluxing the diketal **234** in a solution of *p*-toluenesulfonic acid in MeOH for 9 h resulted in a greatly improved yield of 91 %. **Scheme 2.1** illustrates the overall sequence of reactions for the interconversion between mono- and diketals, and it is apparent that either of the desired products are accessible by manipulation of the reaction conditions.

LAH was chosen to effect the reduction of monoketals **232** and **235** as it is known to reduce even sterically hindered ketones in excellent yield.¹³⁶ It is important to conduct the reaction in diethyl ether or THF to facilitate dissolution of the LAH.¹³⁶ The diastereoselectivity of the reduction is, of course, a major consideration. The rigidity of the camphor skeleton, together with the steric bulk of the 8-, 9- and 10-methyl groups, favour attack of the carbonyl oxygen by the complexed hydride ion from the *endo*-face of the molecule, resulting in the *exo*-hydroxy diastereomer¹²⁴ (**Scheme 2.3**). Simple attack by a free hydride ion would result in predominance, rather than exclusivity of one diastereomeric product. Stereoselective reduction of the monoketals **232** and **235** under the chosen conditions was achieved producing the respective *exo*-hydroxy ketals **210** and **211** in 75 % and 87 % yields (**Scheme 2.1**).

The mechanism for the LAH reduction (**Scheme 2.3**)¹³⁷ is believed to involve a dative covalent bond from the carbonyl oxygen to lithium. This brings a hydrogen, attached to the aluminum complex, within close proximity of the carbonyl carbon. Hydride ion transfer, loss of the LiAlH_3^+ complex and hydrolysis upon work-up results in the product **210**. Overall, the sp^2 hybridized C-2 is converted into a new sp^3 stereogenic centre with exclusive *S*-configuration. Significantly, attack of the hydride ion complex can only occur from the *endo*-face of the molecule due to the overall size of the LAH complex. This appears to be the most significant factor responsible for the production of only one diastereomeric product.

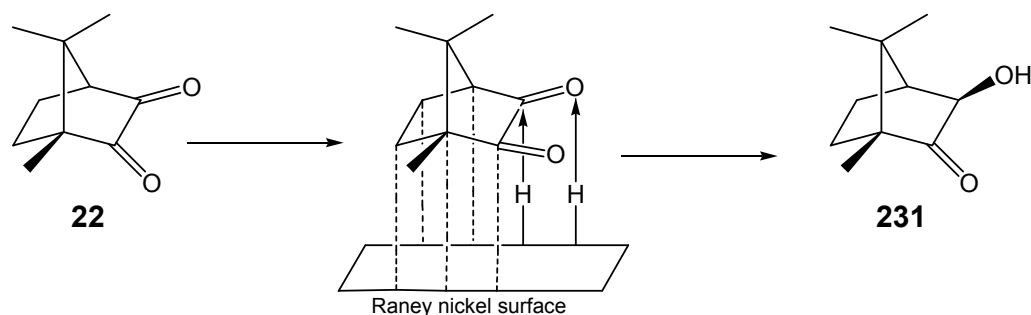


Scheme 2.3: Mechanism of LAH reduction of monoketal **232**.¹³⁷

The last step in this sequence of reactions was the deprotection of monoketals **210** and **211**, which was achieved by acid-catalysed hydrolysis in THF to afford **233** (45 %) and **231** (57 %), respectively. The yields were not optimized as this was felt to be unnecessary at this stage.

In an alternative approach to the α -ketol **231**, direct, regio- and stereoselective reduction of camphorquinone **22** with Raney nickel afforded the 3-*exo*-hydroxy isomer exclusively.¹³⁸ This well-known heterogeneous transition metal hydrogenation catalyst has found use in reduction of carboxylic esters to alcohols, hydrogenation of double and triple bonds in quantitative yields and desulfurization of thiols and thioethers. Diketones can be reduced stereoselectively to an intermediate ketol or to the diol depending on the catalyst and solvent system used.¹³⁹

Raney nickel catalyzed hydrogenation of camphorquinone **22** resulted in a high yield of 3-*exo*-hydroxybornan-2-one **231** (94 %). The mechanism of Raney nickel hydrogenation is not fully understood, but is considered to involve adsorption of the substrate onto the surface of the metal catalyst, followed by addition of adsorbed molecular hydrogen¹³⁹ (**Scheme 2.4**). The reaction is believed to involve free radicals with hydrogen transfer occurring at the relatively unhindered *endo*-face of the adsorbed substrate molecule. The absence of the 2-hydroxybornanone isomer may be attributed to the fact that access to the 2-carbonyl group is hindered by the close proximity of the 10-methyl group.

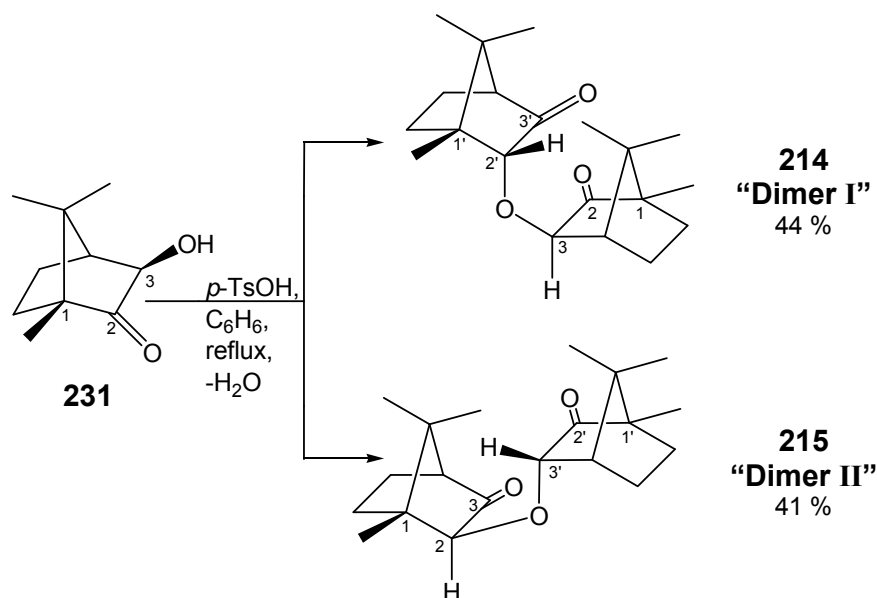


Scheme 2.4: Raney nickel reduction of camphor quinone.

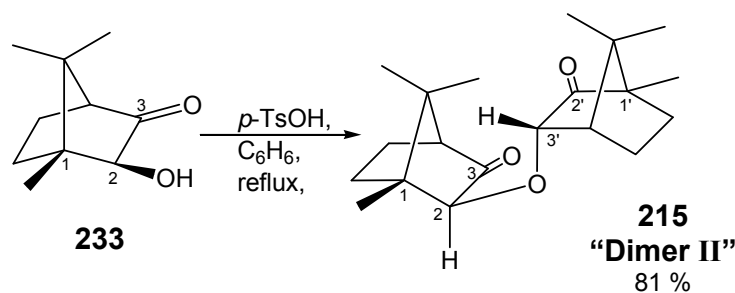
2.1.2 Rearrangement and Dimerization of α -Ketols

The current research was aimed at confirming the previous work and in particular: - verifying the selective synthesis of the dimers based on the 2- or 3-hydroxybornanone precursor; isolation of the third dimer **221** (and possibly a fourth); and clarifying the synthesis of the mono- and dihydroxy products.

The dimerization of the hydroxybornanones **231** and **233** was achieved using Ravinidran's revised methodology which excludes the unnecessary catechol (**Schemes 2.5** and **2.6**).¹²² The acid-catalysed condensation was effected by refluxing 3-*exo*-hydroxybornan-2-one **231** with *p*-toluenesulfonic acid in anhydrous benzene overnight, using a Dean-Stark trap to azeotropically remove the H₂O generated by the reaction. Two crystalline products "dimer I" (**214**; 44 %) and "dimer II" (**215**; 41 %) were obtained. Similar treatment of 2-*exo*-hydroxybornan-3-one **233** afforded "dimer II" **215** exclusively in 81 % yield.



Scheme 2.5: Dimerisation of 3-*exo*-hydroxybornan-2-one **231**.



Scheme 2.6: Dimerisation of 2-*exo*-hydroxybornan-3-one **233**.

The structures of “dimer I” and “dimer II” were confirmed through a thorough investigation of the 1-D and 2-D NMR spectroscopic and high resolution chemical ionisation mass spectrometric (HRCIMS) data. Assignment of spectral peaks to the corresponding ^1H and ^{13}C nuclei was relatively straightforward, being facilitated primarily by the HMQC spectra (**Figures 2.2 and 2.6**), which also allowed the deduction of the regiochemistry and *endo* or *exo* stereochemistry of the ether links through comparative analysis of chemical shifts and coupling constants. HMBC (**Figures 2.3 and 2.7**), COSY and NOESY spectra permitted confirmation of signal assignments to the nuclei in each case.

The HMQC spectrum of **214** (**Figure 2.2**) clearly shows the presence of 18 carbon signals (the two carbonyl signals are not included in the figure) and the corresponding signals for the 30 protons expected for this compound. In practically every instance there are two resonances for a particular type of proton or carbon, which indicates the presence of a dimeric compound that does not exhibit symmetry.

The HMBC spectrum of **214** (**Figure 2.3**), which shows all 20 carbon signals, illustrates some of the correlations that allowed assignment of regiochemistry to each monomeric unit. In the case of the first monomer: the 3-H nucleus (3.93 ppm) couples with C-1 (57.3 ppm), C-4 (49.3 ppm), C-5 (24.9 ppm), C-1' (50.3 ppm) and C-2' (85.5 ppm); 4-H couples with C-1 (57.3 ppm), C-2 (218.4 ppm), C-3 (84.2 ppm), and the 10-Me nuclei (0.87 ppm) couples with C-1 (57.3 ppm) and C-2 (218.4 ppm). The couplings observed with the second monomeric unit include: the 2'-H nucleus (3.97 ppm) with C-3' (217.3 ppm), C-6' (25.9 ppm), and C-10' (13.0 ppm); and the 4'-H nucleus (2.14 ppm) with C-3' (217.3 ppm) and C-7' (46.3 ppm).

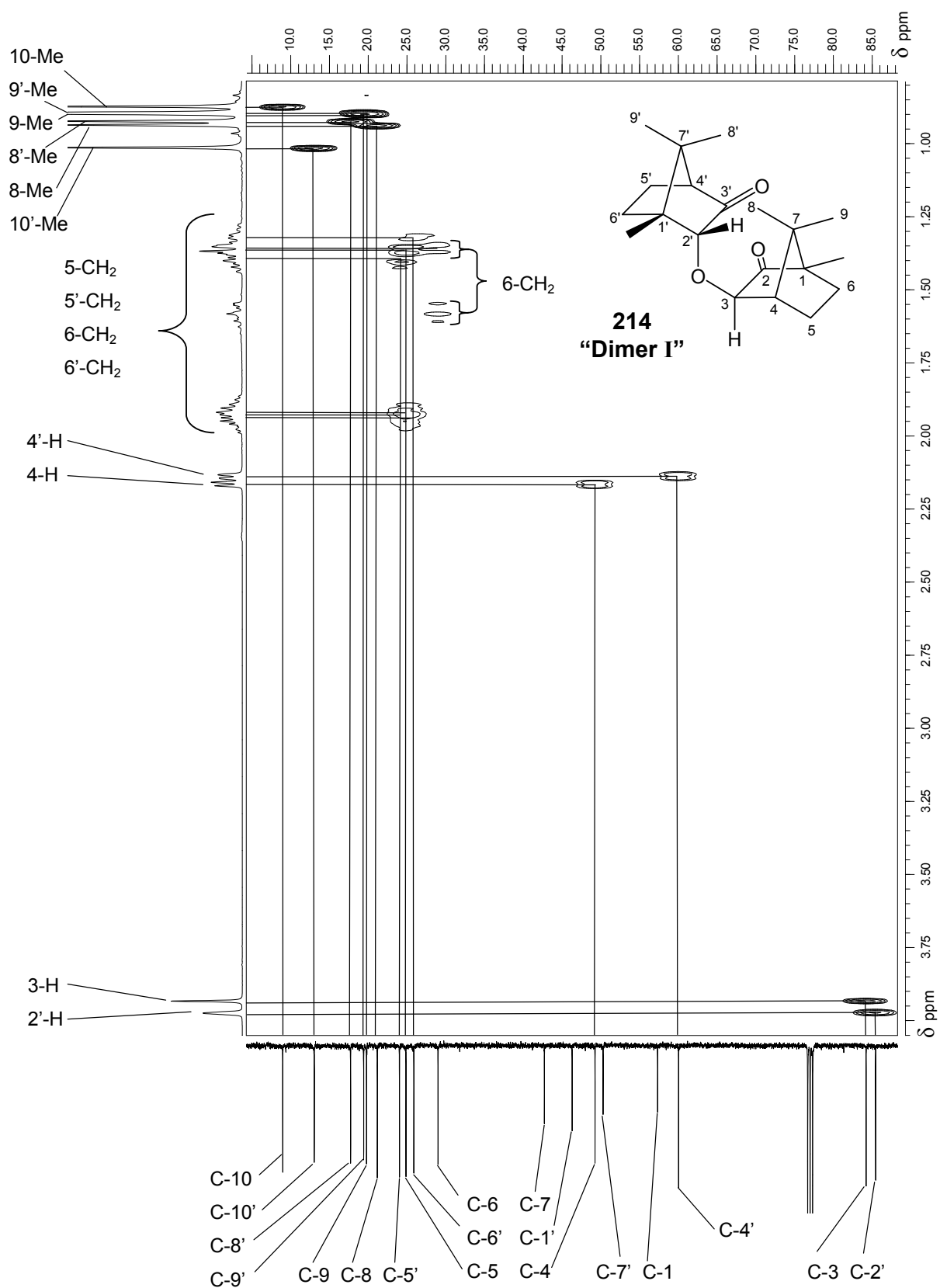


Figure 2.2: 400 MHz HMQC spectrum of **214** in CDCl₃.

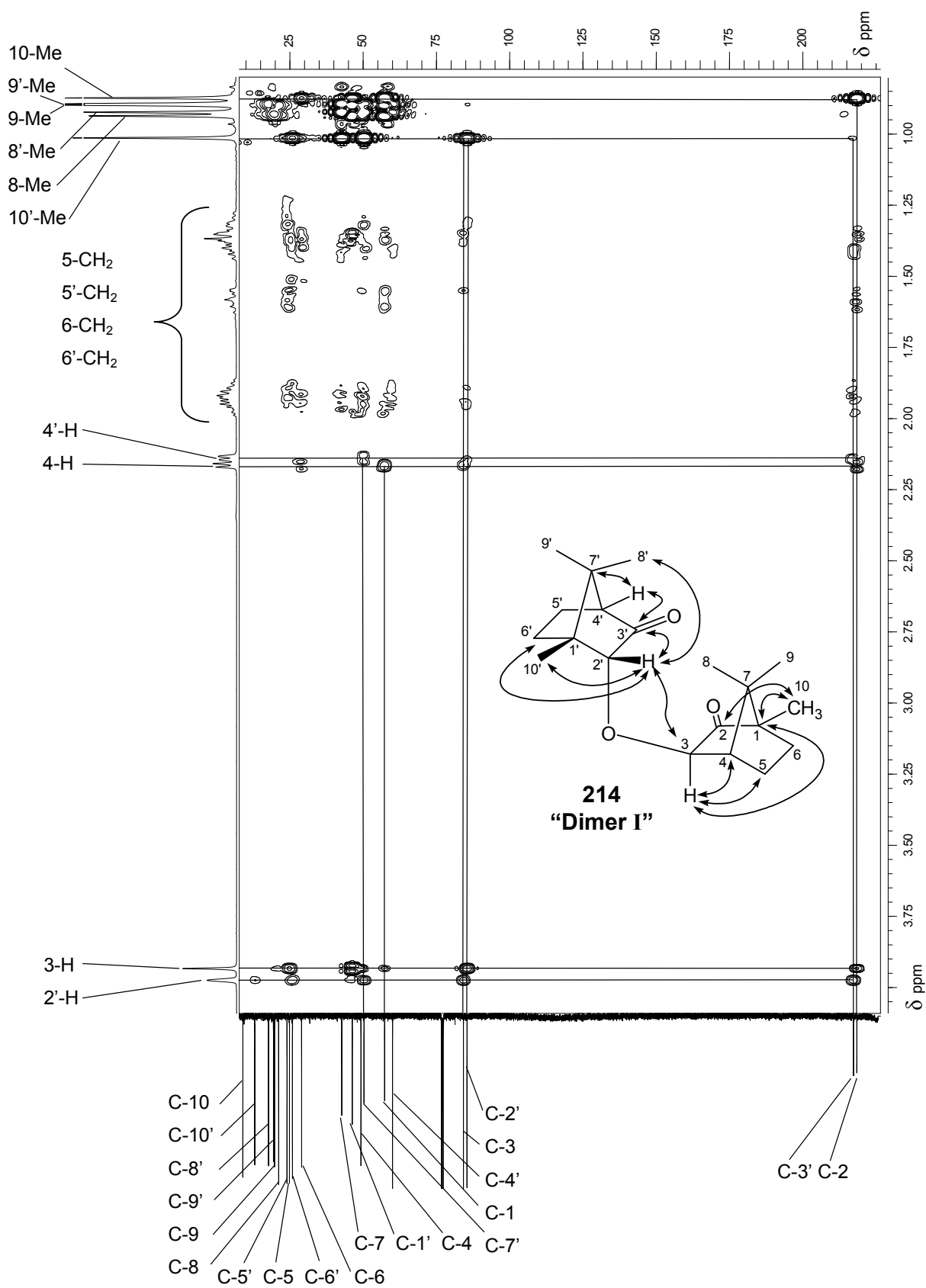
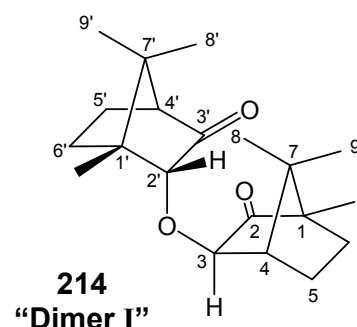


Figure 2.3: 400 MHz HMBC spectrum of **214** in CDCl_3 .

Assignment of the regiochemistry and stereochemistry of the ether linkage is based on an analysis of the multiplicities of the 2'-H, 3-H, 4-H and 4'-H signals and the C-1, C-1', C-4 and C-4' chemical shifts. The significant deshielding of the C-1 and C-4' nuclei, reflect their close proximity to the magnetically anisotropic carbonyl group on their respective monomeric units (**Table 2.1**), whereas the corresponding C-1' and C-4 nuclei resonate at higher fields, which is indicative of more shielded environments, further away from the carbonyl moieties.

Table 2.1: Summary of selected ^{13}C chemical shifts^a for **214** (“dimer I”) reflecting the increasing deshielding and its structural implications.

Nucleus	δ (ppm)	Environment	
(C-1')	quaternary	50.29	near ether link
(C-1)	quaternary	57.32	adjacent to carbonyl
(C-4)	CH	49.25	near ether
(C-4')	CH	60.03	adjacent to carbonyl
(C-3)	CH-O	84.22	ether carbon
(C-2')	CH-O	85.45	ether carbon
(C-3')	C=O	217.29	carbonyl
(C-2)	C=O	218.43	carbonyl



^a 100 MHz data in CDCl_3 .

In order to assign the *stereochemistry* of the ether link in the dimer, use was made of the ^1H signal multiplicities. The 3-H nucleus resonates at 3.93 ppm as a singlet, inferring the absence of vicinal coupling and implying its *endo*-orientation while the 4-H nucleus resonates as a doublet (J 4.8 Hz) at 2.17 ppm, showing coupling with 5- H_{exo} nucleus only. The lack of vicinal coupling between the 4-H and either the 3- H_{endo} or the 5- H_{endo} nuclei is consistent with torsion angles approaching 80° as determined by solving the Haasnoot-de-Leeuw-Altona equation,¹⁴⁰ which is a variation of the traditional Karplus relationship¹⁴¹ with β -substituent correction. The equation allows for a second solution, *i.e.* 260° , but this is an impossible angle given the structure of the molecule. The torsion angle between the 3-H and 4-H nuclei was also calculated using this equation with the aid of the Mestre-J¹⁴² software package and was found to be *ca.* 82.5° - a value which corresponds to the curve minimum. The calculated relationship between torsion angle and coupling constant is shown in **Figure 2.4**.

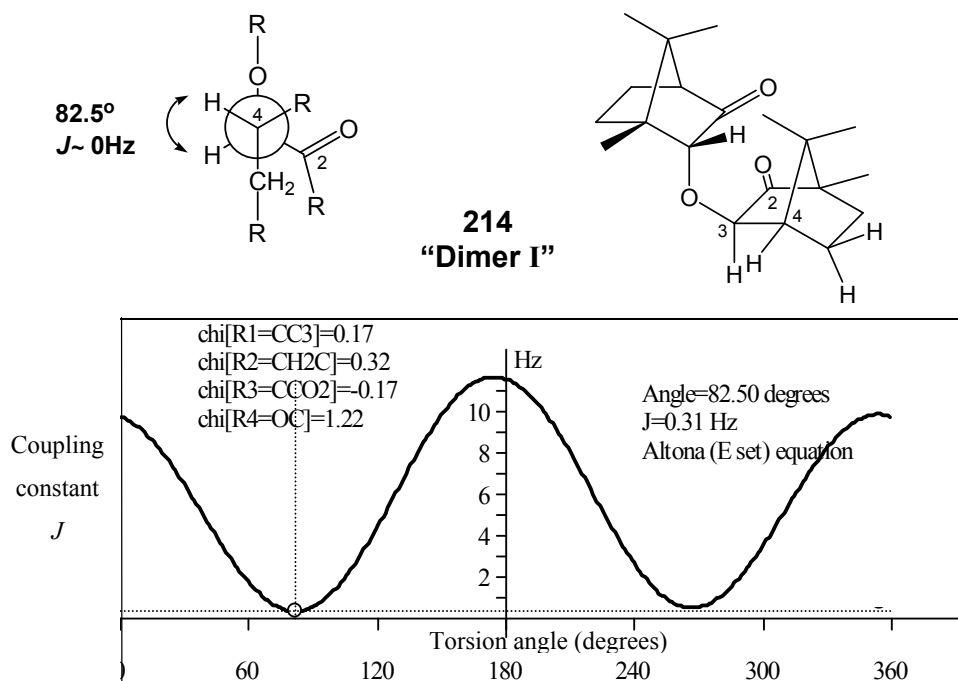


Figure 2.4: Prediction of 3-H and 4-H dihedral angle for "dimer I" 214.¹⁴²

Further support for the structural assignment was provided by the NOESY spectrum as illustrated by the observed interactions summarised in **Figure 2.5**. Significant NOE interactions between the 3-H, 4-H, 5- H_{endo} and 6- H_{endo} nuclei, suggest that they are all on the same (*endo*)-face of one monomeric unit. Additionally, interactions between the 2'-H and the 8'-methyl, the 9'-methyl and the 5'- H_{exo} nuclei and the 2'-H and 10'-methyl nuclei confirm the position of these groups on the *exo*-face of the second monomeric unit. No NOE interactions between the two monomeric units were obvious, presumably due to their distance from one another as a result of twisting about the ether linkage.

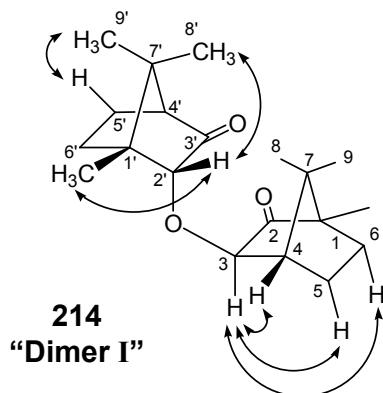
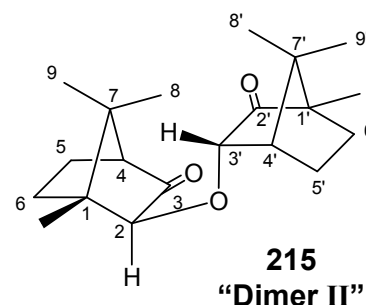


Figure 2.5: Structure showing selected NOE interactions observed for 214.

The second dimer to be isolated, “dimer II” **215**, was characterised using similar arguments. The HMQC spectrum (**Figure 2.8**) reveals the ^{13}C and ^1H signals expected for the $\text{C}_{20}\text{H}_{30}$ molecular composition and permits more definitive assignment of the methylene signals due to better resolution of the spectrum. Correlations provided by the HMBC spectrum are shown in **Figure 2.9** and were essential to the assignment of regiochemistry in the monomeric units. In the first monomeric unit, the 2-H nucleus (3.81 ppm) couples with C-1 (50.0 ppm), C-2 (85.6 ppm), C-3 (217.9 ppm), C-4 (59.2 ppm), C-6 (33.4 ppm) and C-3' (81.6 ppm), while the 4-H nucleus (2.05 ppm) couples with C-6 (33.4 ppm). Interactions in the second monomeric unit include: the 3'-H nucleus (4.25 ppm) with C-4' (48.3 ppm), C-2' (218.0 ppm) and C-8' (19.9 ppm); and the 4'-H nucleus (2.31 ppm) with C-5' (31.8 ppm). As for “dimer I” **214**, the 2'-H, 3-H, 4-H and 4'-H signal multiplicities and the C-1, C-1', C-4 and C-4' chemical shifts were vital in definitive identification of the isolated product as the 2-*exo*, 3'-*endo*-ether. The proximity of C-1' and C-4 to the magnetically anisotropic carbonyl group on their respective monomeric units resulted in their chemical shifts being significantly greater than their more shielded counterparts, C-1 and C-4' respectively. **Table 2.2** shows critical data used in the determination of the *regiochemistry* of the ether linkage.

Table 2.2: Summary of the ^{13}C chemical shifts^a for “dimer II” **215** reflecting the increasing deshielding and its structural implications.

Nucleus	δ (ppm)	Environment	
(C-1')	quaternary	58.36	adjacent to carbonyl
(C-1)	quaternary	49.96	near ether link
(C-4)	CH	59.20	adjacent to carbonyl
(C-4')	CH	48.27	near ether
(C-3')	CH-O	84.62	ether carbon
(C-2)	CH-O	85.57	ether carbon
(C-3)	C=O	217.88	carbonyl
(C-2')	C=O	218.99	carbonyl



^a 100 MHz data in CDCl_3 .

Consideration of the signal multiplicities of the vicinal 3'-H and 4'-H nuclei and their coupling (J 5.0 Hz) suggests that the 3'-H nucleus is *exo*-orientated and, hence, that the ether link is *endo*-orientated. Confirmation of the geometry is again provided by solving the Haasnoot-de-Leeuw-Altona equation, which indicates that the coupling constant of 5.0 Hz

corresponds to a dihedral angle of 49.9° , the other three possible solutions to the equation again being considered unlikely or impossible given the molecule's rigidity (**Figure 2.6**).

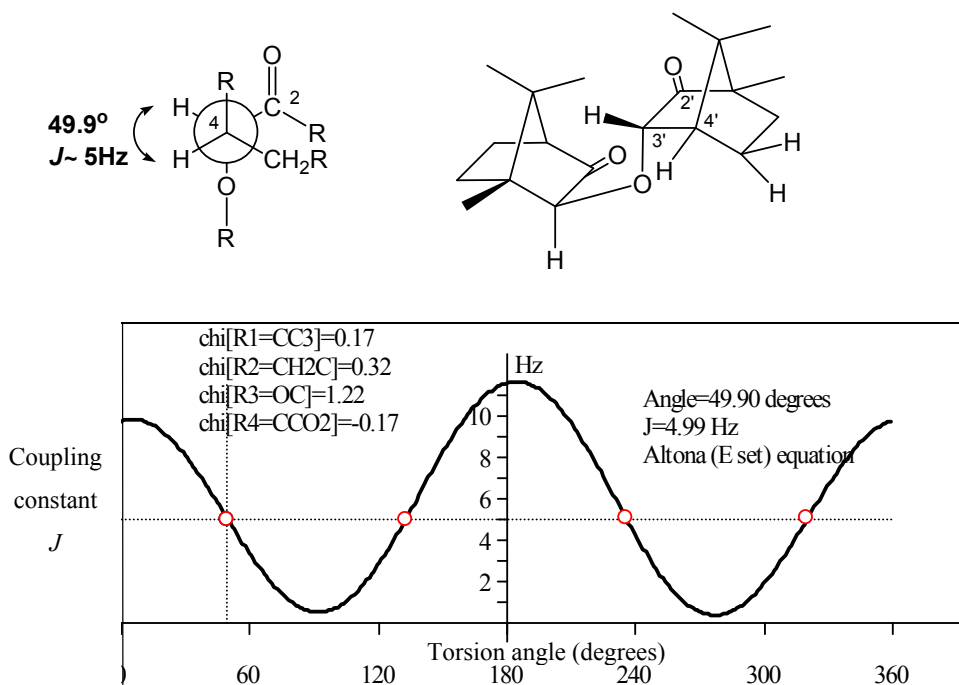


Figure 2.6: Prediction of the 3'-H and 4'-H torsion angle corresponding to a coupling of 5.0 Hz for "dimer II" **215**.¹⁴²

Further verification of the structure of "dimer II" is provided by the NOE interactions, which are illustrated in **Figure 2.7**.

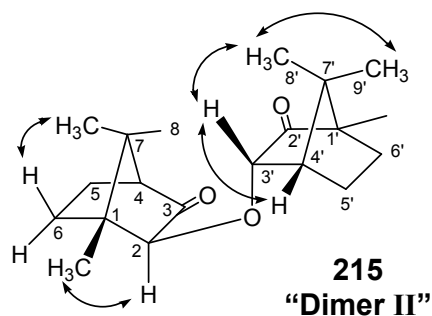


Figure 2.7: Selected NOE interactions observed for **215**.

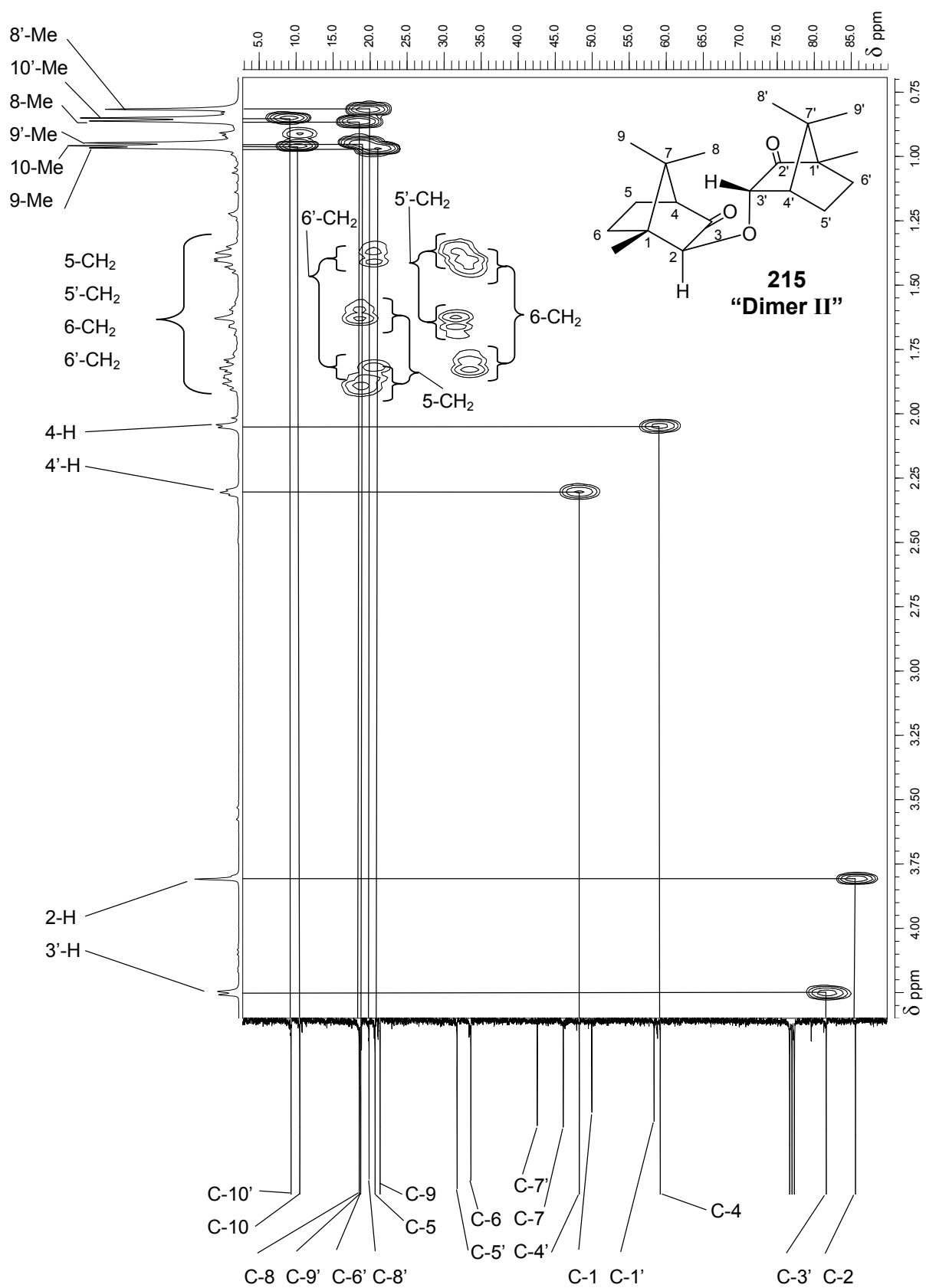
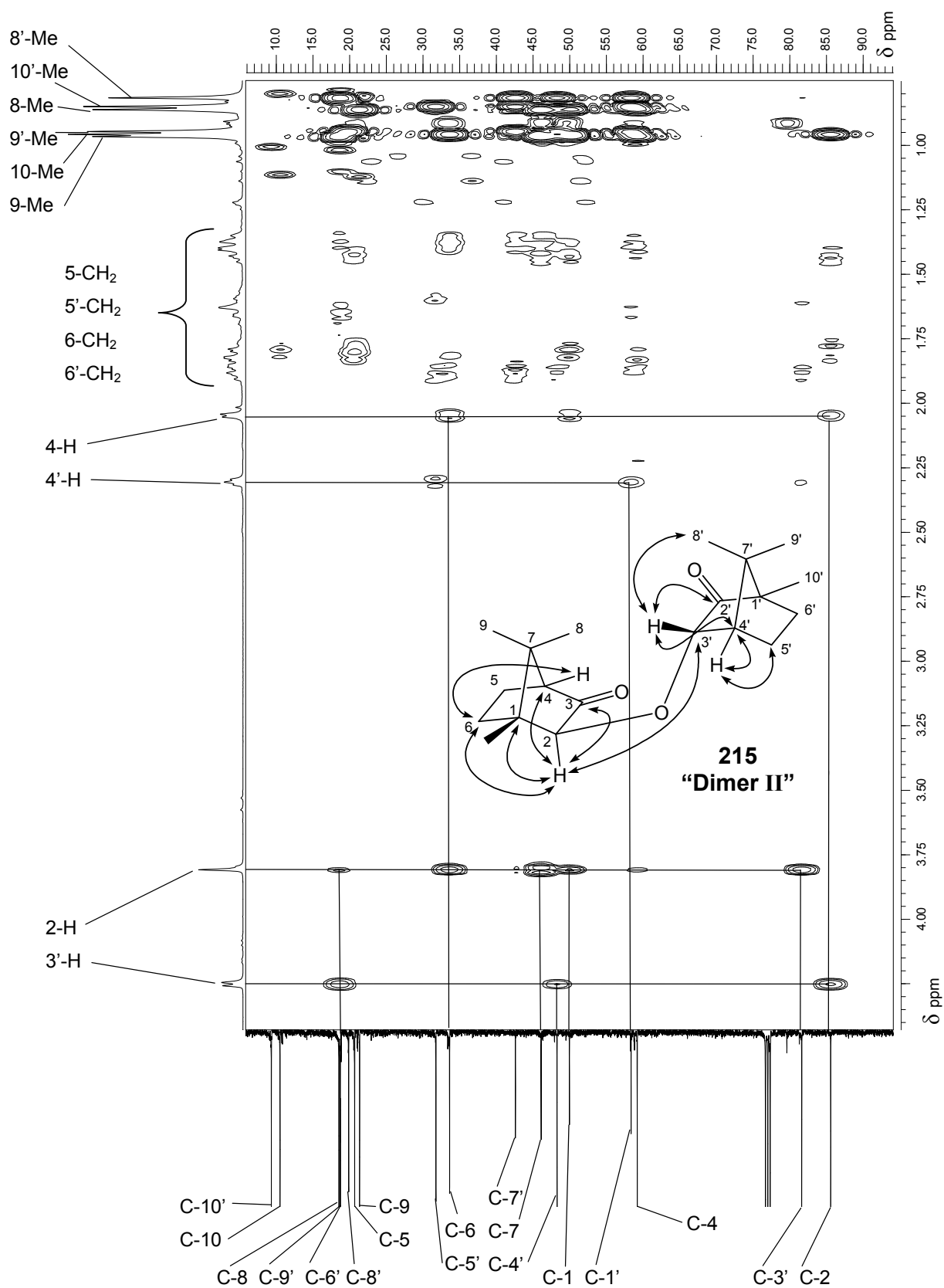
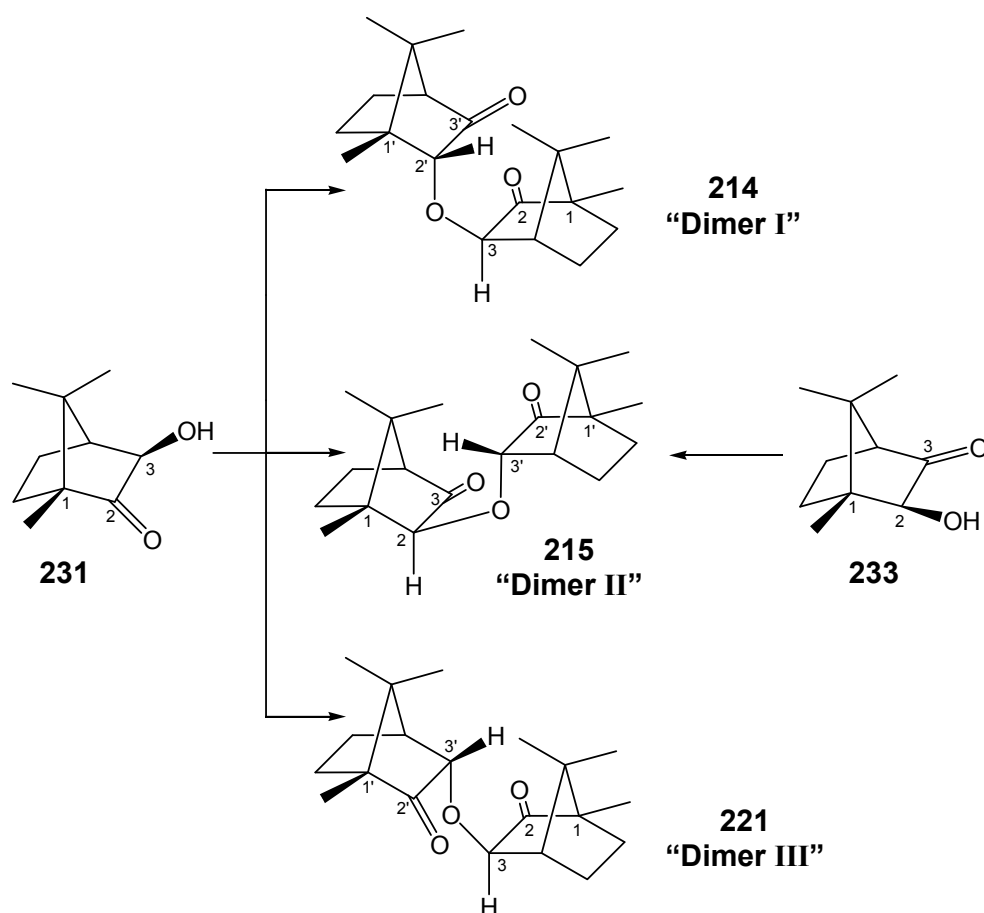


Figure 2.8: 400 MHz HMQC spectrum of **215** in CDCl_3 .

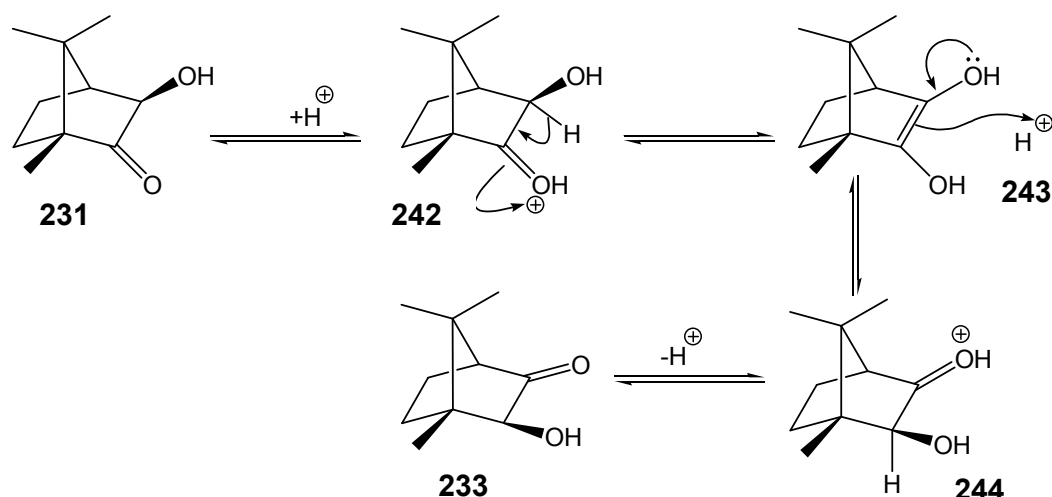


The study of these compounds has raised some interesting questions. Initially, it was assumed that one α -ketol precursor would result in the stereocontrolled synthesis of one dimer. From the experimental results, however, it became obvious that the mechanism was more complex than might have been anticipated. While the condensation of 2-*exo*-hydroxybornan-3-one **233** resulted in the exclusive formation of “dimer II”, the condensation of 3-*exo*-hydroxybornan-2-one **231** gave three products, “dimer I” (as the major product), dimer II and a third dimer isolated in trace quantities (**Scheme 2.7**).¹²²



Scheme 2.7: Overview of the acid-catalysed condensation of α -hydroxybornanones **231** and **233**.

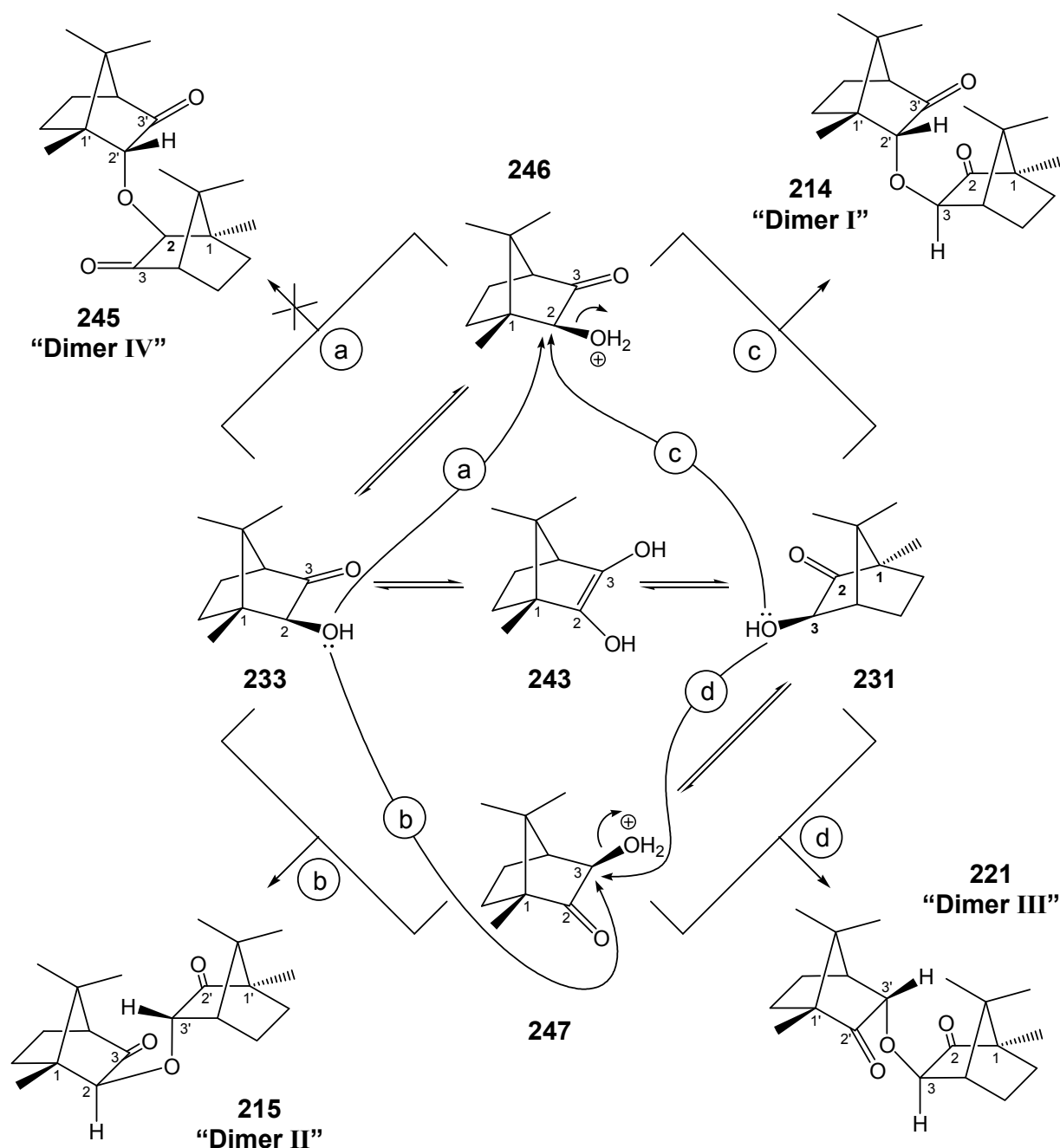
The mixture of dimers I – III obtained from the reaction of the 3-*exo*-hydroxy precursor **231** suggested the possibility of contamination of the reactant by the 2-*exo*-hydroxy analogue **233**. However, this was not the case as the α -ketols had been synthesised *via* different routes and were shown to be pure by NMR spectroscopy prior to the reaction. Another possibility is that α -ketol-enediol tautomerism results in a mixture of **231** and **233** under the reaction conditions, as illustrated in (**Scheme 2.8**).



Scheme 2.8: α -Ketol-enediol tautomerism of the 2-*exo*- (**233**) and 3-*exo*-hydroxybornanone **231**.

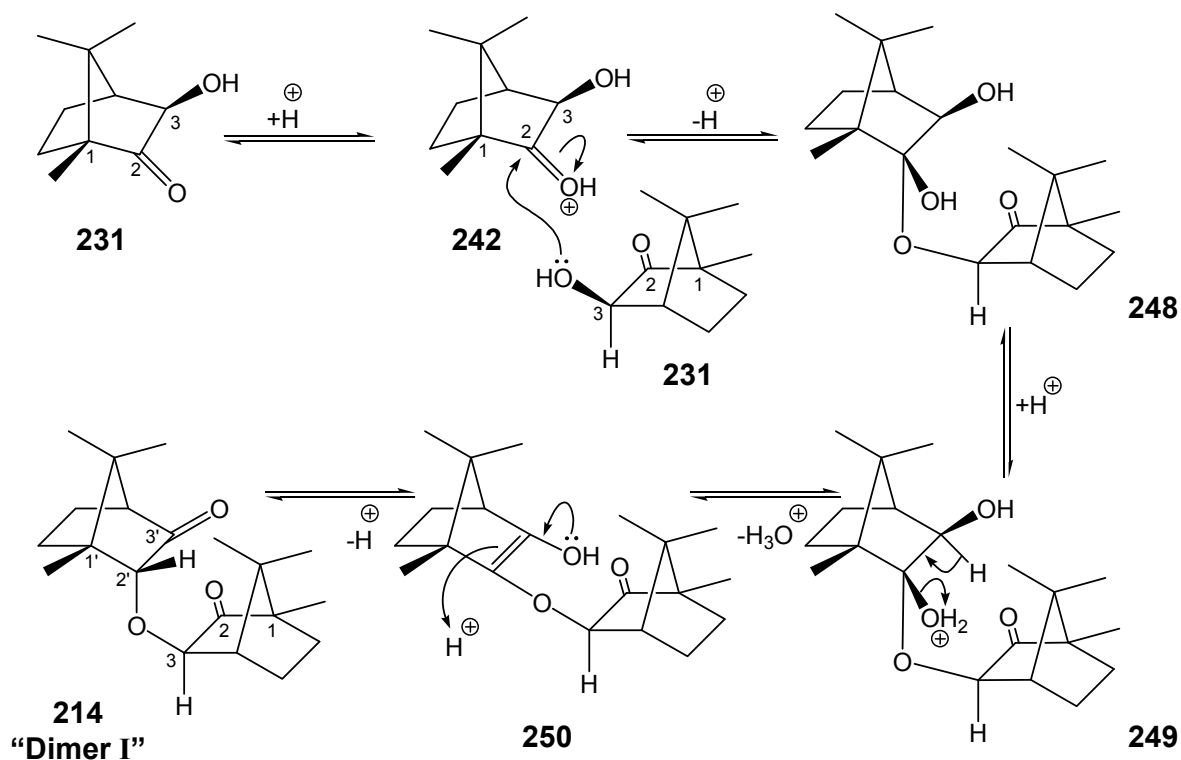
In the presence of *p*-toluenesulfonic acid these tautomers are likely to be rapidly interconvertible *via* the common enediol **243** with the α -ketol forms existing almost exclusively at equilibrium. It should be noted that the enediol moiety is planar, which raises the possibility of four diastereomeric α -ketol products. However, due to the steric bulk of the 8-methyl group, *endo* protonation should be favoured resulting in formation of the *exo*- α -ketols shown in **Scheme 2.8**. A further consideration is whether the equilibria between the two α -ketols and the enediol favour one α -ketol over the other. The fact that only one dimer is formed from the 2-*exo*-hydroxy precursor **233** may give substance to such a view.

While the *p*-toluenesulfonic acid could catalyze tautomerism of the α -ketols, it could also catalyze the etherification reaction leading to the dimerization. The mechanism for dimerization could be expected to involve S_N2 displacement of H_2O from the protonated alcohols **246** and **247** by the hydroxyl oxygen of a second alcohol (**Scheme 2.9**). The different directions of attack “**a**”-“**d**” could lead to the formation of the four isomeric dimers I-IV, three of which have been isolated – the fourth, as yet, unobserved. It is important to note that this mechanistic rationalisation (which is presented in our paper¹⁴³) relies implicitly on tautomerisation of the precursor α -ketols.



Scheme 2.9: Acid-catalysed etherification pathways involving α -ketol-enediol tautomerism and S_N2 displacement.

However, an alternative or parallel mechanistic pathway could be envisaged, involving the formation of hemiacetal and enol intermediates, which ultimately yield “dimer I” (Scheme 2.10) or similarly “dimer II”.



Scheme 2.10: Acid-catalysed mechanism involving hemiacetal and enol intermediates to yield "dimer I" **214**.

Considering the formation of "dimer I", initial protonation of the C-2 carbonyl oxygen strongly polarizes the carbonyl group, thus facilitating subsequent nucleophilic attack by a second 3-*exo*-hydroxybornan-2-one molecule **231**. Loss of a proton yields the neutral hemiacetal **248**, acid-catalyzed dehydration of which results in the formation of an enol intermediate **250**. Acid-catalyzed tautomerism then leads to "dimer I". An analogous mechanism would account for the formation of "dimer II" from two 2-*exo*-hydroxybornan-3-one molecules **233**.

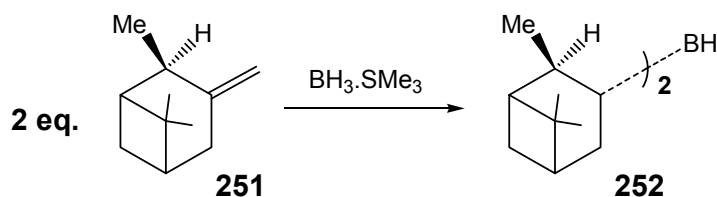
The crucial feature of this hemiacetal-enol pathway is that prior isomerization of the precursor is unnecessary for the production of the major dimeric products **214** and **215**, since they can be formed solely from the corresponding *exo*-hydroxybornanones **231** or **233**, respectively. However, the formation of dimers II and III (albeit in minor proportions) in the reaction of 3-*exo*-hydroxybornan-2-one **231** requires the presence of some 2-*exo*-hydroxybornan-3-one **233**. This leads to the conclusion that prior isomerization must contribute to the complex of reactions – at least in the formation of dimers II and III from **231** and **233**. The apparently exclusive formation of "dimer II" from the 2-*exo*-hydroxybornan-3-one **233** may reflect

dominance of the hemiacetal-enol pathway – a possibility which will form part of a future computational study.

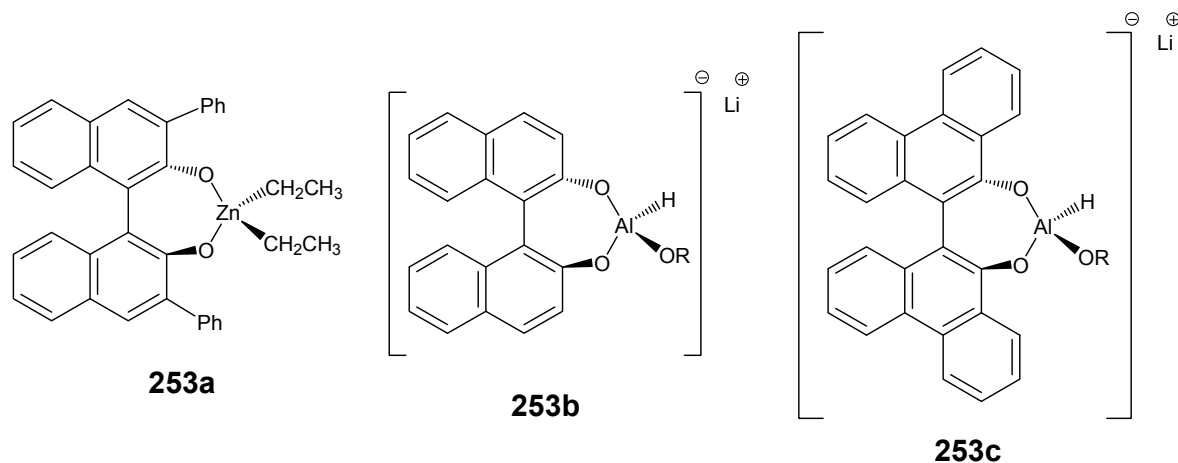
2.1.3 Reduction of the α -Ketol Dimers

Aldehydes can be reduced to primary alcohols and ketones to secondary alcohols by a number of reducing agents, of which metal hydrides, such as lithium aluminum hydride (LAH) and sodium borohydride (NaBH_4), are the most commonly used. The two most attractive qualities that hydrides have over other reducing agents are that they: - i) do not generally reduce carbon-carbon double or triple bonds; and ii) they generally provide a high proportion of active hydride. Reduction of specific functional groups can be controlled to some degree by selection of the reagent; however, regioselective and stereoselective reductions are far more difficult and require considerably more specialized reducing agents, such as the rhodium-phosphorus complexes DIPAMP^{144,145} or (*R*)-(*S*)-BPPFOH.¹⁴⁶ Lithium *N*-dihydropyridyl-aluminum hydride reduces diaryl ketones in preference to dialkyl or alkyl aryl ketones,¹⁴⁷ and zinc borohydride reduces saturated ketones in preference to α,β -unsaturated ketones.¹⁴⁸

Asymmetric reduction of ketones with high % e.e. values has been achieved using a variety of chiral reducing agents, each being more effective for certain types of ketones than for others. Such as chiral reducing agents including binaphthyl reagents and their derivatives, such as BINAP-ruthenium acetate,¹⁴⁹⁻¹⁵¹ BINOL-diethyl zinc **253a**,¹⁵⁵ BINOL-aluminum hydride **253b-c**¹⁵² and hydroborating reagents, such as Ipc_2BH **252** developed by H.C. Brown (**Scheme 2.11**).^{153,154} The chiral Ipc_2BH **252** is prepared by controlled hydroboration of the chiral alkene, α -pinene **251**,¹⁵³ while the binaphthyl derivative, BINOL aluminum hydride reagent **253b**, is prepared from lithium aluminum hydride, 2,2'-dihydroxy-1,1'-binaphthyl and an alcohol.¹⁵² **253b** has previously been shown to exhibit complete topological control in the reduction of carbonyl compounds.¹⁵²

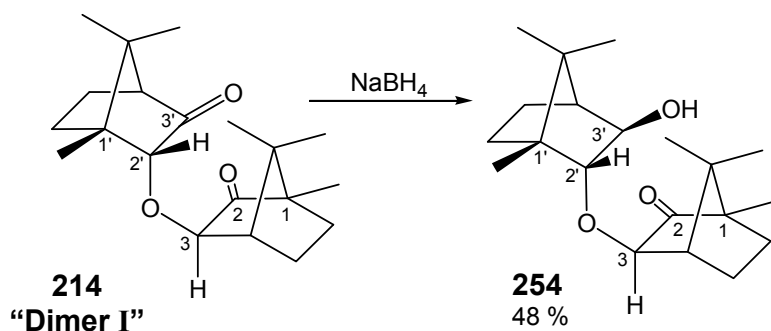


Scheme 2.11: Hydroboration of α -pinene **251**.¹⁵⁴

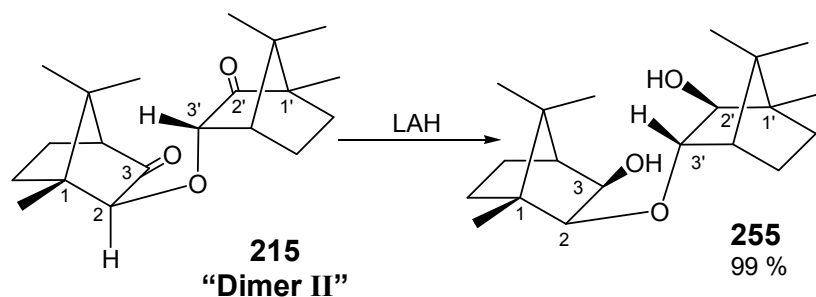


The restricted rotation about a single bond that causes chirality in the binaphthyl derivatives¹⁵² is also known as atropisomerism.¹⁵⁷ The potential of our dimers **214** and **215** to provide scaffolds for the construction of reagents analogous to the atropisomeric BINOL reagents (**253a-c**)^{151,152,155} prompted a study of their reduction to chiral diols.

Previous work in our laboratories was conducted by Matjila, who attempted the synthesis of the 2-*exo*-3'-*exo*-dihydroxy analogue of “dimer I” **214**,¹²² using NaBH_4 in ethanol; however, only the 3'-*exo*-monohydroxy compound **254** (Scheme 2.12) was obtained in low yield (48 %). In a second reaction, the reduction of “dimer II” with LAH afforded a dihydroxy compound, identified as the 3-*exo*-2'-*exo*-dihydroxy product **255** (Scheme 2.13), in excellent yield (99 %).

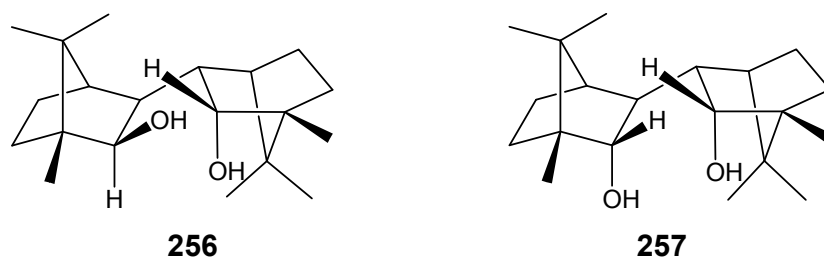


Scheme 2.12: Reduction of “dimer I” **214**.¹²²

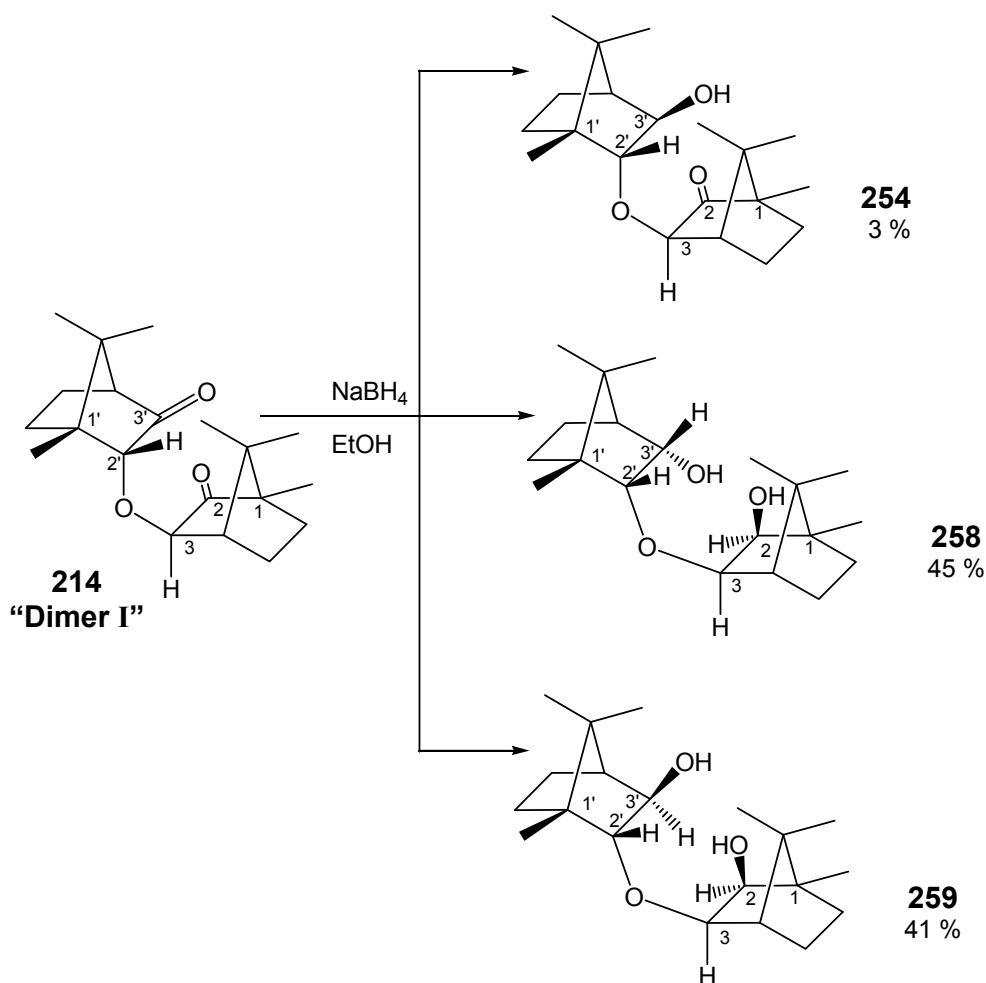


Scheme 2.13: Reduction of "dimer II" **215**.¹²²

In an extension of their work involving the dimerization of camphor enolates to give dioxobornanylidenes, McNulty *et al.*¹³² reported the reduction of their dimers with LAH to give the diols **256** and **257**. As expected for camphor systems, it was found that nucleophilic attack occurred mainly at the *endo*-face of each carbonyl group owing to steric hindrance by the 8-methyl group and the 3-*exo*-substituent. The authors did not attempt reduction with the more selective reducing agent, NaBH₄,¹³⁶ nor did they observe any monohydroxy products.¹³²



In our own investigation, reduction of the camphor ether dimers was, in fact, explored using NaBH₄. Two separate reactions were conducted in which "dimer I" **214** and "dimer II" **215** were treated with 2 equivalents of NaBH₄ in ethanol at 0 °C followed by stirring at room temperature for 12 h. Work-up and flash chromatography afforded the corresponding mono- and dihydroxy derivatives: **254**, **258** and **259** (Scheme 2.14); and **260** and **255** (Scheme 2.15, p. 82). 1-D and 2-D NMR spectroscopy and HRCIMS data were utilized to tentatively identify the three compounds as the 3'-*exo*-hydroxy product **254** (3.2 %), 2-*exo*-3'-*endo*-dihydroxy product **258** (45.3 %) and the 2-*exo*-3'-*exo*-dihydroxy **259** (41.2 %)



Scheme 2.14: Reduction of “dimer I” 214.

At this stage, no attempt was made to optimize yields or effect exclusive synthesis of any of the products, but it is expected that this could be achieved by increasing the ratio of NaBH₄ and fine tuning the reaction conditions. Consideration was first given to the dihydroxy derivatives, for which the ¹³C and ¹H NMR spectra showed the presence of the expected 20 carbons and 34 protons. Furthermore, the absence of carbonyl signals and the presence of two new methine signals confirmed that reduction of both carbonyls had occurred (**Figures 2.11, 2.12 and 2.13**). The realization that two isomers of the dihydroxy derivative had been synthesised necessitated careful analysis of the data in order to determine their stereochemistry. NaBH₄ is responsible for providing a source of hydride ions which, as indicated earlier, are expected to attack the carbonyl groups of “dimer I” 214 predominantly from the *endo*-face (path “a” or “b”; **Figure 2.10**). In the case of “dimer I”, however, monomeric unit **M1** is located on the *endo*-face of monomeric unit **M2**, partially blocking the

endo-face of **M2**. This arrangement would thus account for the observed *exo*-face attack (path “c”) of **M2** affording the 3’-*endo*-hydroxy product **258** together with the expected analogues **254** and **259** arising from “normal” *endo*-face hydride attack.

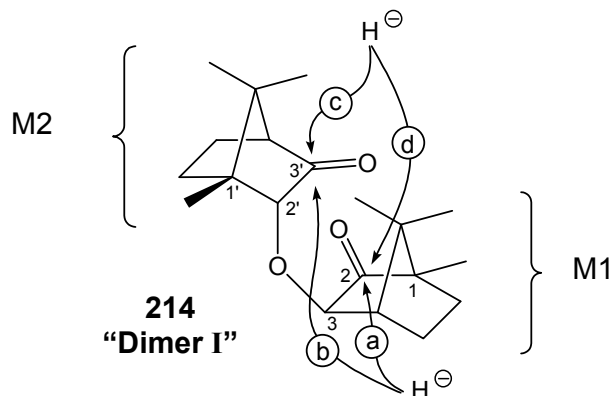


Figure 2.10: Possibilities for nucleophilic hydride attack on “dimer I” **214**.

The ^1H and ^{13}C NMR spectra of compounds **258** (Figures 2.11 and 2.12) and **259** (Figure 2.13), reveal that both molecules have two hydroxylic protons, and comparison of the spectra allowed the stereochemistry of the hydroxyl groups to be assigned.

The stereochemistry of the 3-*exo*-2’-*endo* ether linkage is established in the precursor **214**, while the *exo*-orientation of the 2-hydroxy group is based on the expectation of *endo*-hydride delivery at the 2-carbonyl carbon. The stereochemistry of the 3’-hydroxy group on monomeric unit **M2** was confirmed through analysis of the multiplicity of the 4’-H signal, which appears as a triplet (1.83 ppm) in compound **258** due to coupling with 5’- H_{exo} and 3’- H_{exo} , whereas in compound **259** it resonates as a doublet (1.64 ppm), as 4’-H only couples with the 5’- H_{exo} nucleus (3’- H_{endo} being at an angle of *ca.* 80° to 4’-H). The compounds were thus characterized as the 2-*exo*-3’-*endo*-dihydroxy derivative **258** and the 2-*exo*-3’-*exo*-dihydroxy derivative **259**.

More evidence for the formation of the dihydroxy derivatives **258** and **259** is provided by analysis of their HRCI mass spectra (illustrated for compound **258** in Figure 2.14), which reveal peaks at m/z 322.24999 and m/z 322.25012, respectively, which correspond to the expected molecular formula $\text{C}_{20}\text{H}_{34}\text{O}_3$ (calculated m/z 322.25080).

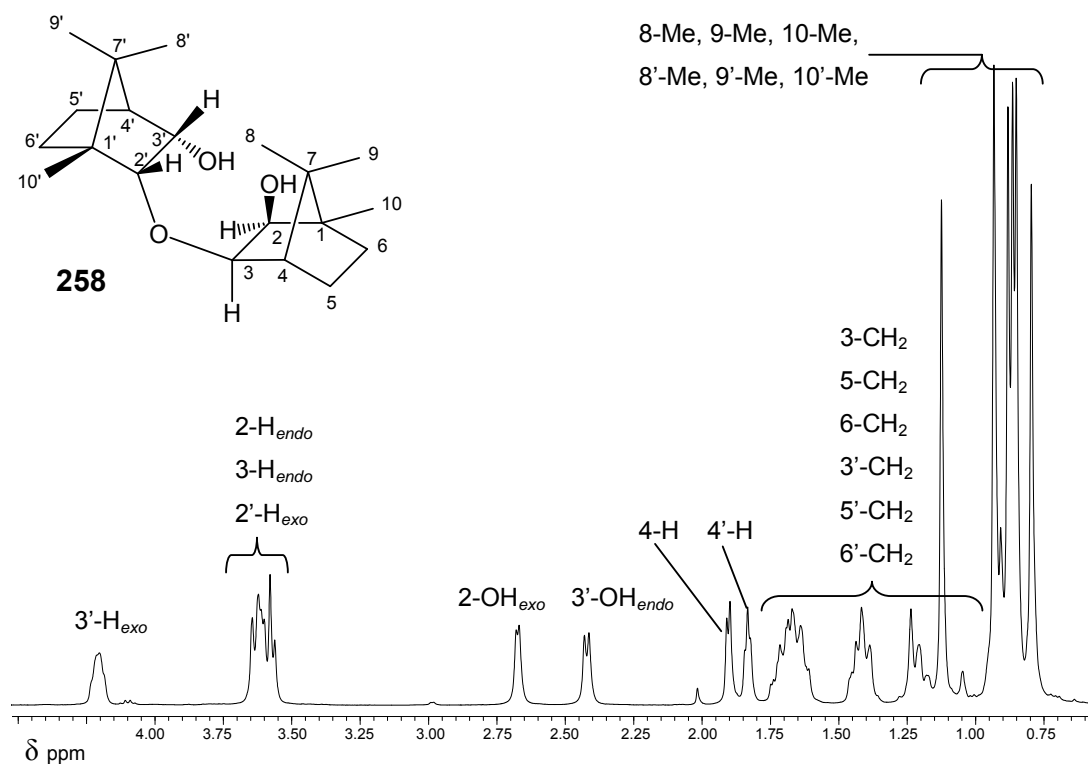


Figure 2.11: 400 MHz ¹H NMR spectrum of **258** in CDCl₃.

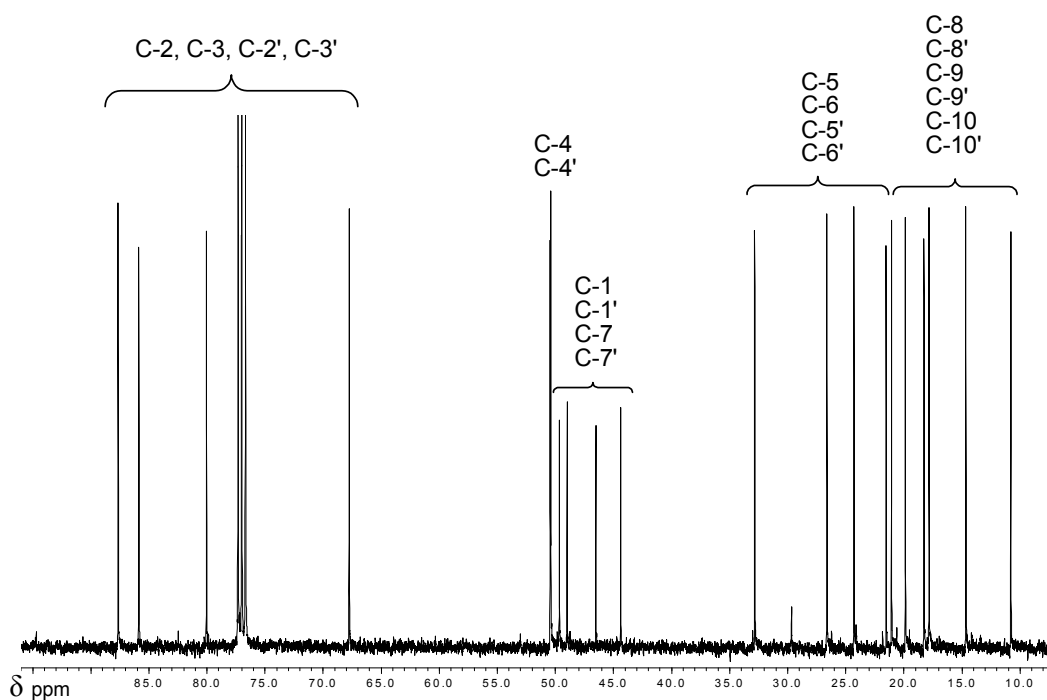


Figure 2.12: 100 MHz ¹³C NMR spectrum of **258** in CDCl₃.

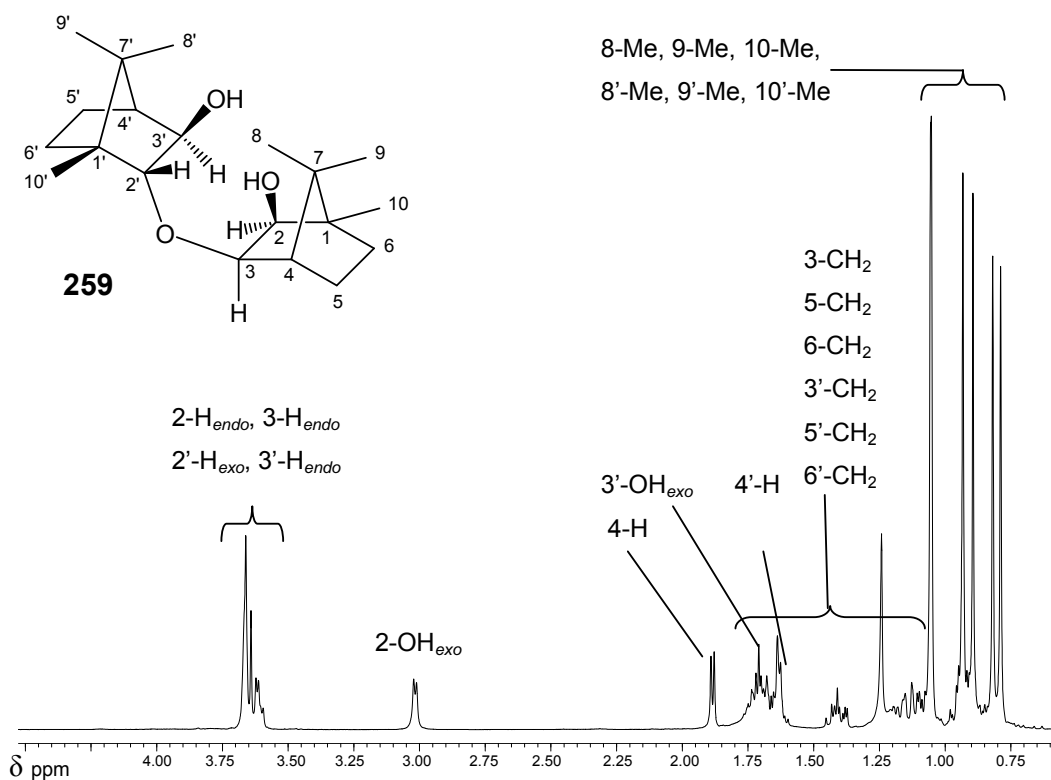


Figure 2.13: 400 MHz ^1H spectrum of **259** in CDCl_3 .

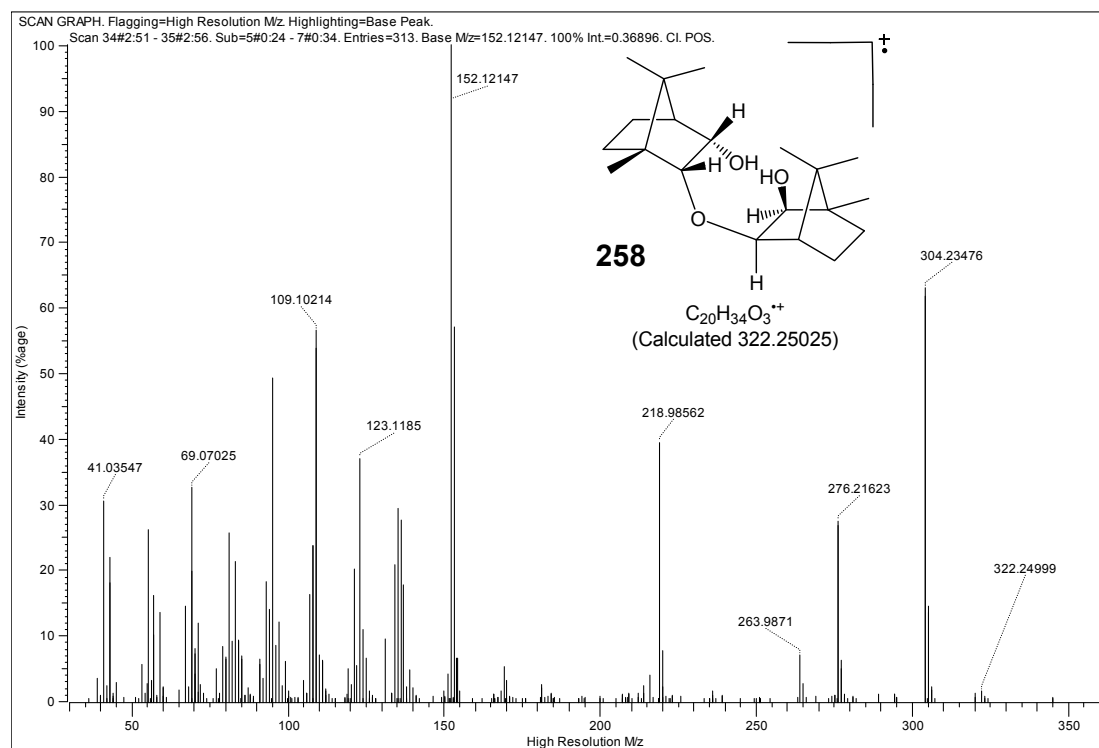


Figure 2.14: HRCI mass spectrum of the dihydroxy derivative **258**.

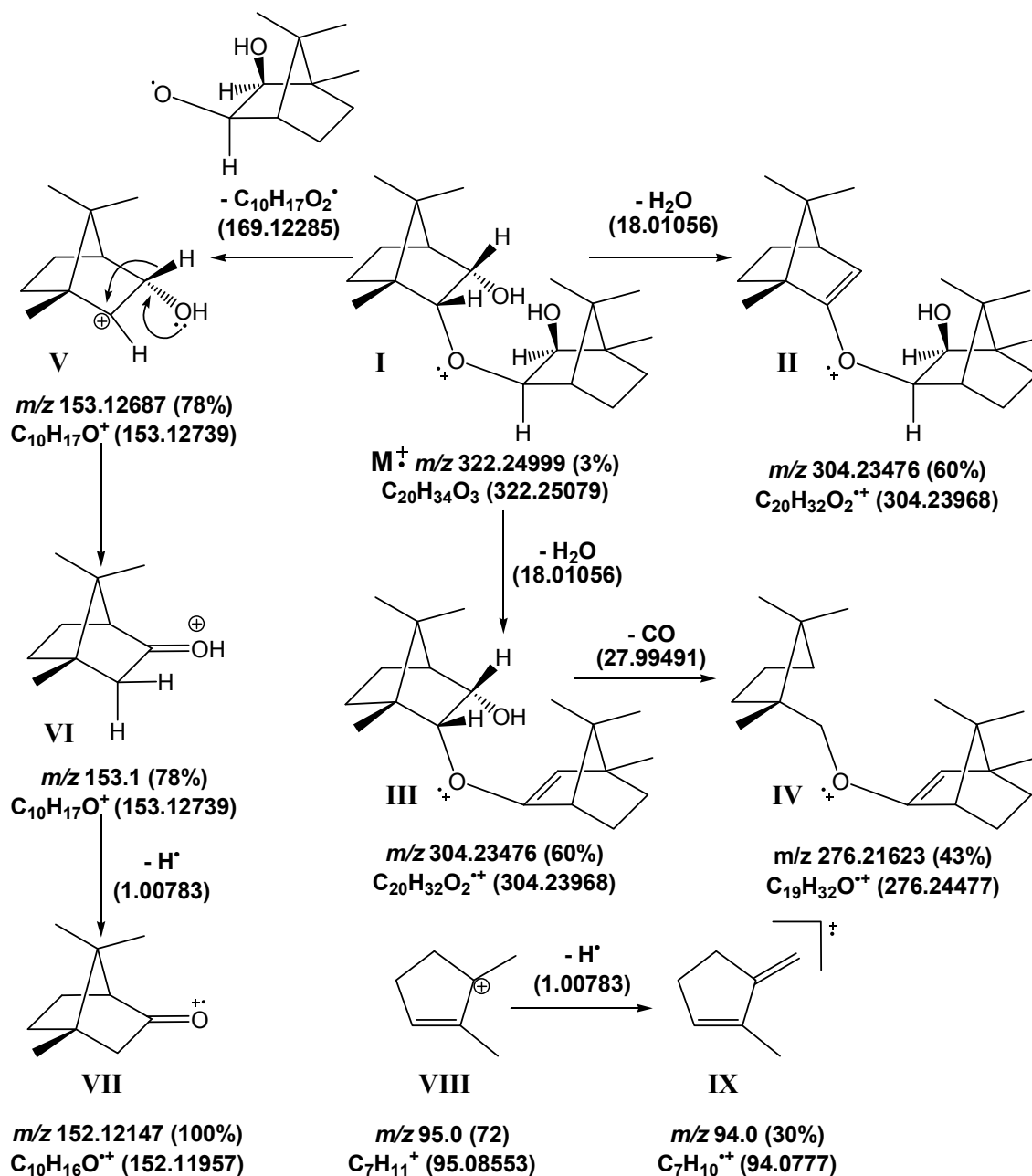


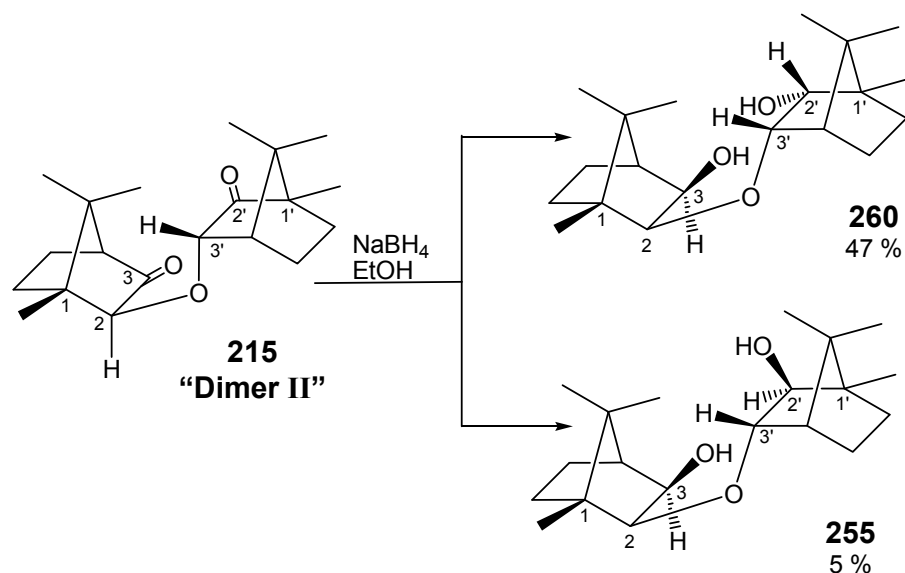
Figure 2.15: Mass Spectrometric fragmentation of compound **258**.

A fragmentation study of both dihydroxy products was carried out and several dominant peaks were accounted for as illustrated for compound **258** in **Figure 2.15**. The molecular ion **I** undergoes elimination of H_2O from either the *exo*-monomeric unit, forming the odd electron fragment **II**, or from the *endo*-monomeric unit giving the analogous fragment **III**. Elimination of the neutral CO molecule from fragment **III** gives the odd-electron species **IV**. Heterolytic cleavage at the ether linkage of the molecular ion **I** gives the carbocation **V** and/or the

rearranged even-electron fragment **VI**. Loss of an H atom from the latter affords the odd-electron species **VII**, which is responsible for the base peak in the spectrum. Lower m/z peaks indicate fragmentation of the camphor skeleton to afford, *inter alia*, the characteristic fragments **VIII** and **IX**.¹⁵⁶

The third compound to be isolated from the NaBH₄ reduction of “dimer I” **214** was characterised as the 3'-*exo*-hydroxy product **254**. A molecular formula of C₂₀H₃₂O₃ corresponds to the monohydroxy derivative (observed m/z 320.23498; calculated m/z 320.23513), while the NMR signal assignments were based on the arguments discussed above. The ¹H NMR spectrum indicates the presence of a broad 3'-hydroxylic signal at 2.20 ppm. The corresponding 3'-H nucleus resonates as a singlet at 2.59 ppm, the lack of coupling to either the 2'- or 4'-proton suggesting that it is *endo*-orientated, implying that the 3'-hydroxylic group is *exo*. The spectroscopic data for the monohydroxy product **254** indicated that it was, in fact, the same as the compound isolated by Matjila,¹²² X-ray analysis of which had confirmed the 3-*exo*-2'*endo*-orientation of the ether linkage and the *exo*-orientation of the hydroxy group at C-3'.

Similar reduction of “dimer II”, using NaBH₄, afforded two products (**Scheme 2.15**) that were tentatively identified through analysis of the 1-D and 2-D NMR spectroscopic and HRCIMS data as the 3-*exo*-2'*endo*-dihydroxy derivative **260** (47 %) and the 3-*exo*-2'-*exo*-dihydroxy derivative **255** (5 %).



Scheme 2.15: Reduction of “dimer II”.

Nucleophilic attack on the *endo*-face of each monomeric unit (paths “a” and “b”; **Figure 2.16**) should, in principle, be favoured and would result in the alcohol groups being *exo*-orientated. A blocking effect by monomer **M1** on the *endo*-face of monomer **M2**, however, could disfavour *endo* attack (path “b”; **Figure 2.16**) at C-2' thus permitting competitive 2'-*exo* attack (path “c”). The net result is the formation of the isomeric 3-*exo*-2'-*endo*- and the 3-*exo*-2'-*exo*-dihydroxy derivatives **260** and **255**, respectively.

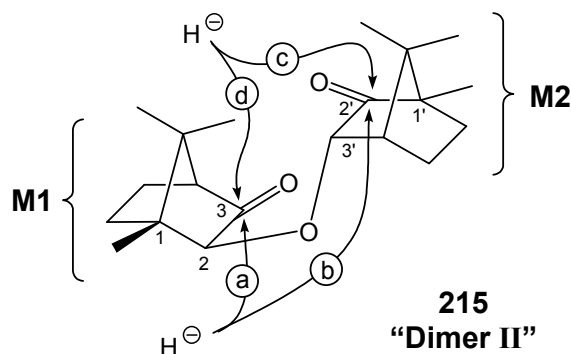


Figure 2.16: Possibilities for nucleophilic hydride attack on “dimer II” **215**.

The structure elucidation of the dihydroxy derivatives **260** and **255** was achieved by analysis of the NMR spectroscopic data (*e.g.* **Figures 2.17** and **2.18**) in a similar manner to the dihydroxy derivatives of “dimer I”, **258** and **259**.

It was evident that the stereochemistry of the **M1** monomeric unit of both compounds was identical, based on the multiplicity of the 4-H signal, which appears as a triplet due to coupling with 5-*H_{endo}* and 3-*H_{endo}*, thus the 3-OH is of *exo*-orientation. Comparison of the resonances for the 2'-H and 3'-H protons on the second monomeric unit **M2** of both compounds allowed for the determination of stereochemistry of the 2'-OH. The 3'-H of structure **255** resonates as a broad triplet due to coupling with 4'-H and a long-range interaction with 2'-OH. The 2'-H signal appears as a broad singlet due to its proximity to 2'-OH. The 3'-H proton of structure **260** resonates as a multiplet due to coupling with 4'-H and 2'-*H_{exo}* and, the 2'-*H_{exo}* resonates as a multiplet (unfortunately somewhat obscured by the 3-H resonance) due to coupling with 3'-H. Thus the compounds were assigned as the 3-*exo*-2'-*endo*-dihydroxy derivative **260** and the 3-*exo*-2'-*exo*-dihydroxy derivative **255**.

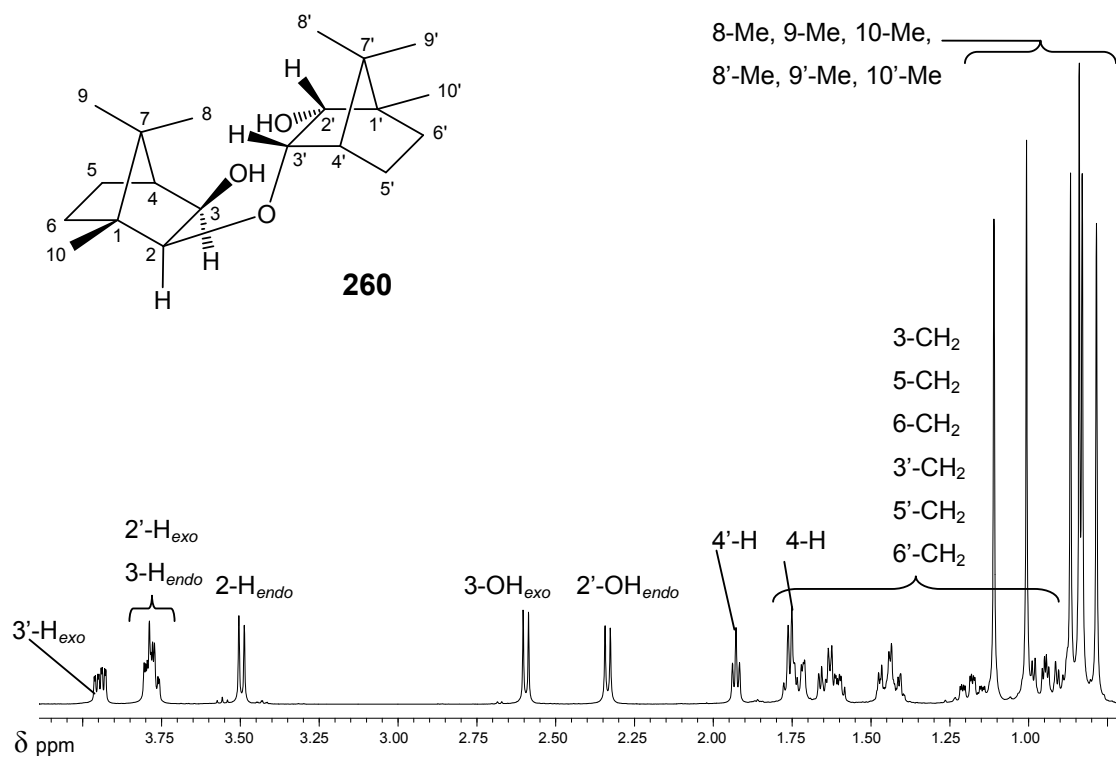


Figure 2.17: 400 MHz ¹H NMR spectrum of **260** in CDCl₃.

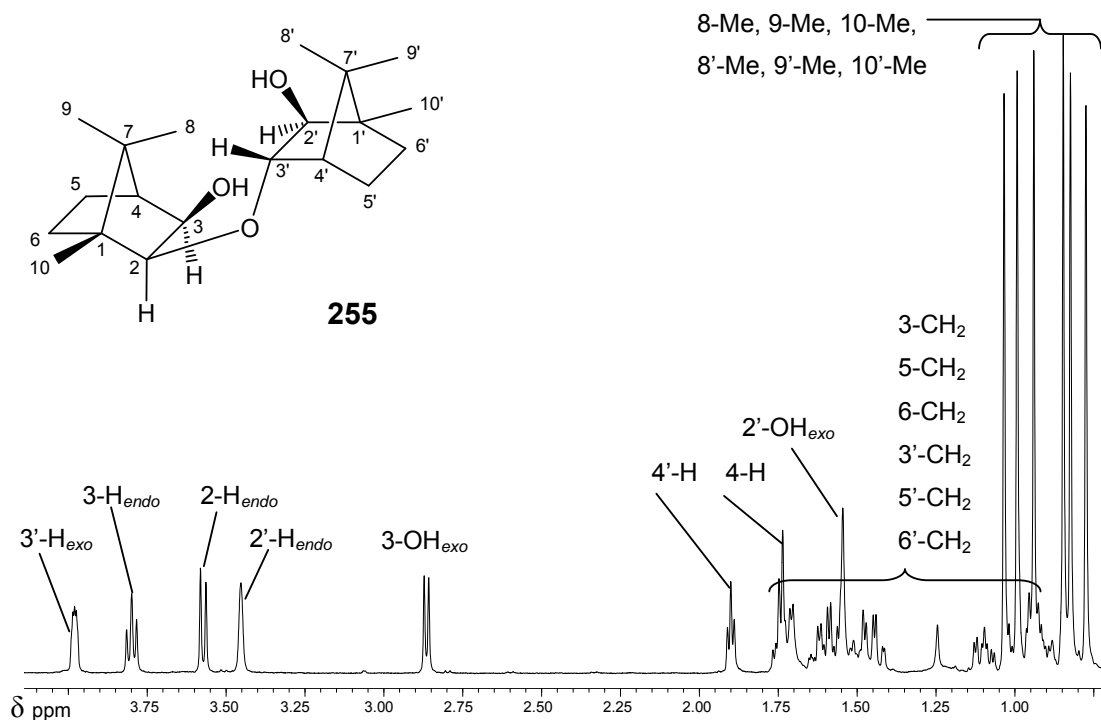


Figure 2.18: 400 MHz ¹H NMR spectrum of **255** in CDCl₃.

The reduction of “dimer I” and “dimer II” followed predictions for the directional attack of the hydride anion. In the case of both dimers, attack of the lower monomeric unit **M1** occurred exclusively from the *endo*-face, generating the *exo*-hydroxy monomer and furthermore attack of the second monomer **M2** occurred from either the *endo*- or *exo*-face. Attack of **M2** on “dimer I” showed no clear preference of either direction of attack, however, attack of “dimer II” was 90 % more likely from the *exo*-face generating the *endo*-hydroxy monomer. It is probable that with “dimer II” the combination of the blocking effect of **M1** and the 10'-methyl group highly disfavours approach from any position except the *exo*-face of **M2**, whereas the approach of “dimer I” is constrained to a similar degree by blocking from **M1** and the 8'- and 9'-methyls but does not have another vicinal methyl to further reduce attack from the *endo*-face. **Figure 2.19** illustrates the expected directions of nucleophilic hydride attack (bold arrows), lesser favoured (dashed arrows) and strongly disfavoured (red arrows) directions of attack of the dimers **214** and **215**.

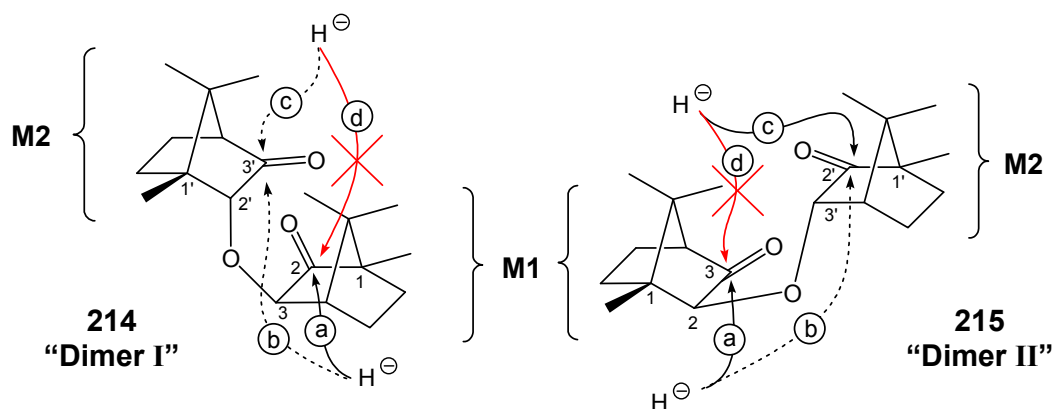


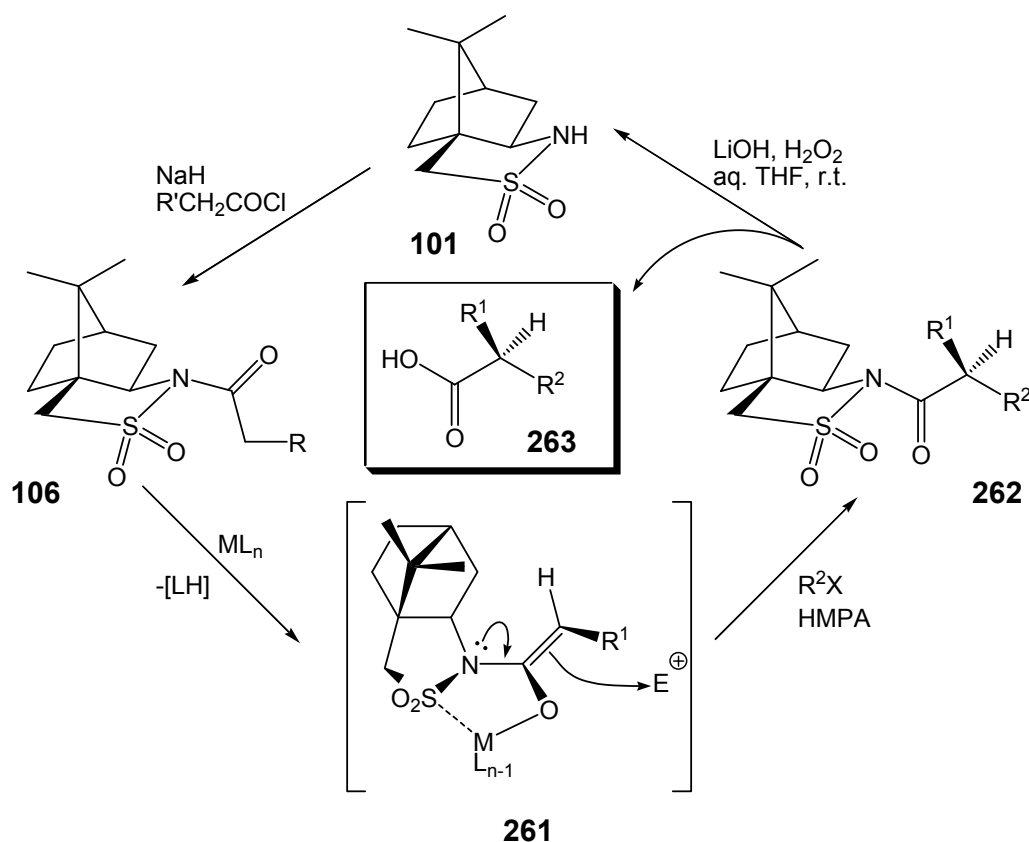
Figure 2.19: Direction of attack of the dimers.

In conclusion, a multi-step process has been developed which is able to supply a range of mono- and dihydroxy camphor ether dimers, which have potential as scaffolds for the construction of chiral reagents.

2.2 ASYMMETRIC SYNTHESIS OF α -ALKYLATED α -AMINO ACIDS

Given the importance of α -amino acids, the asymmetric synthesis of these vital biological building blocks is of considerable interest. Their inherent chirality is crucial to their function and is of primary concern in their synthesis.

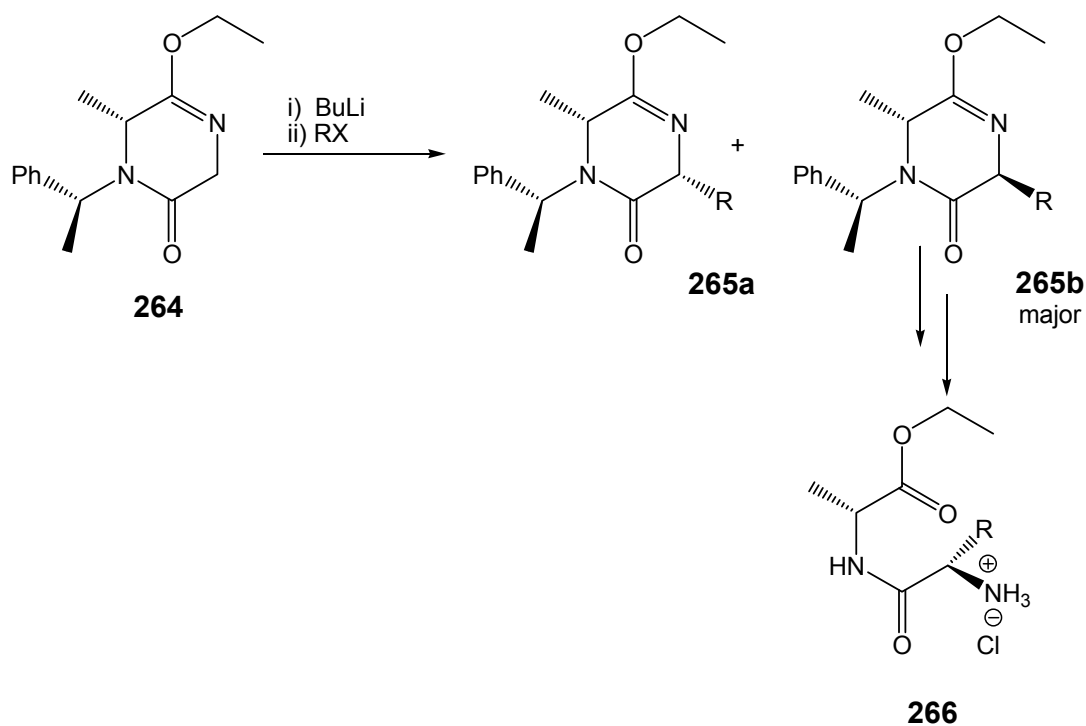
The alkylation of glycine enolate derivatives has been widely used in the synthesis of optically pure amino acids, the most well known example being that involving Oppolzer's sultam-derived glycine equivalent **106**^{158,52} (Scheme 2.16). This versatile auxiliary permits almost total stereocontrol and, due to its efficiency, has also found use in the synthesis of enantiopure deuterium labeled amino acids as precursors in peptide synthesis.¹⁵⁹



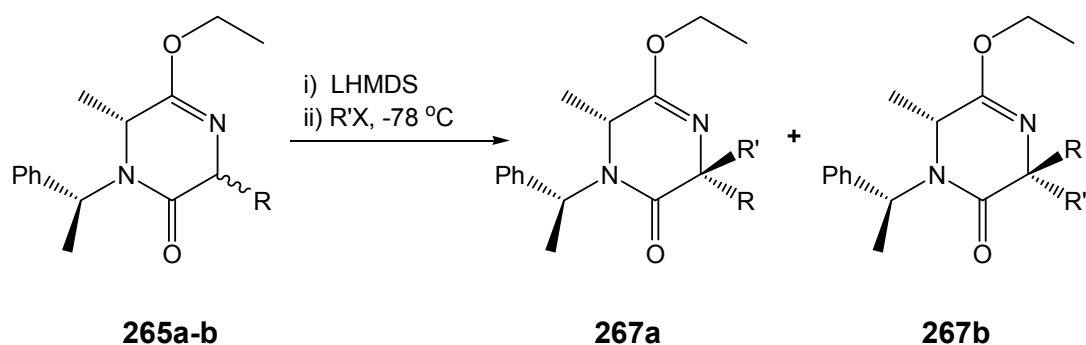
Scheme 2.16: Oppolzer's sultam as an auxiliary in α -alkylation reactions.

Porzi *et al.*¹⁶⁰ reported the use of Oppolzer's sultam in the synthesis of both natural and unnatural α -amino acids in good yield and with high enantiomeric purity. They have also

reported the alkylation of lactim auxiliaries *e.g.* **264** (Scheme 2.17) to form natural and unnatural dipeptides with moderate to good stereoselectivity.¹⁶¹ The most recent focus of Porzi's research¹⁶² has been the dialkylation of a mixture of the diastereomeric alkylated products **265a** and **265b**, to form uncommon C- α,α' dialkyl dipeptides **267a** and **267b** (Scheme 2.18). These examples merely touch the surface of diverse alkylation studies involving the synthesis of proteinogenic and non-proteinogenic α -alkylated amino acid derivatives.



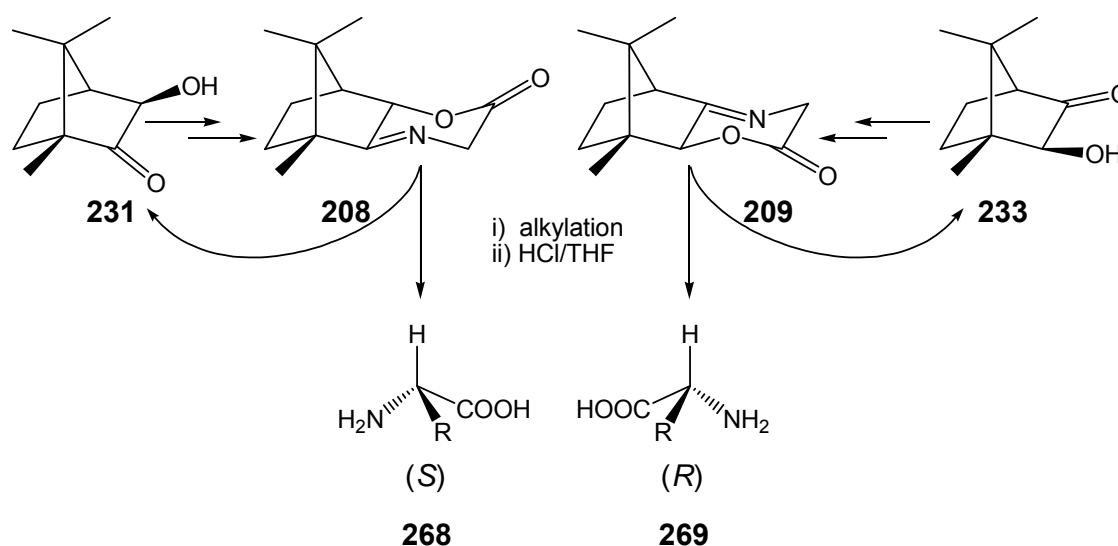
Scheme 2.17: Alkylation of lactims and cleavage of selected products.



Scheme 2.18: Dialkylation of a mixture of monoalkylated chiral synthons.

2.2.1 Synthetic Rationale

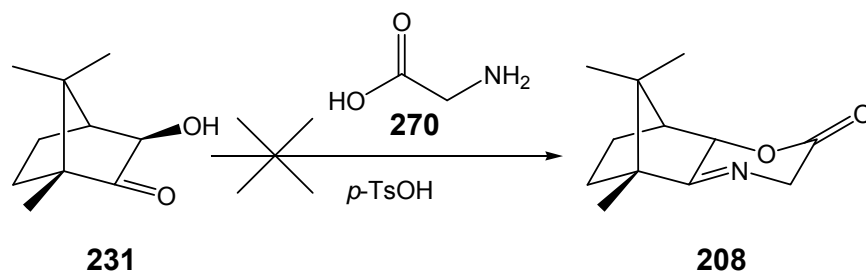
Research in our laboratory over the last few years has focused on the use of the regioisomeric camphor-derived iminolactones **208** and **209** as convenient scaffolds to provide access to chiral α -amino acids **268** and **269** (Scheme 2.19).



Scheme 2.19: Synthesis of enantiomeric α -amino acids.

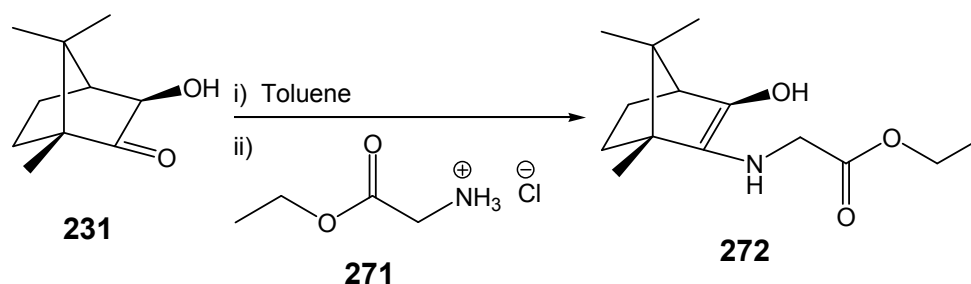
The conjugated enolates derived from the iminolactones **208** and **209** are expected to be conformationally rigid and the 8-methyl group should exert steric hindrance on the *exo*-face of both systems. These two factors should encourage preferential electrophilic alkylation from the less hindered *endo*-face. Mild hydrolysis should release both the alkylated α -amino acid and the chiral auxiliary. The configuration at the stereogenic centre in the α -amino acid could thus be controlled either by the regiochemistry of the iminolactone **208** or **209** or by the enantiomeric form of camphor used as a starting material.

The iminolactone work pioneered by Ravindran¹²³ initially met with little success. An early attempt was made to synthesise the 2-iminolactone **208** by a one-pot reaction of the α -ketol **231** with glycine **270** and a catalytic amount of *para*-toluenesulfonic acid (Scheme 2.20), in the hope that the hydroxyl and carbonyl groups of the α -ketol would react with glycine to give the iminolactone **208** directly. However, none of the desired product was obtained.

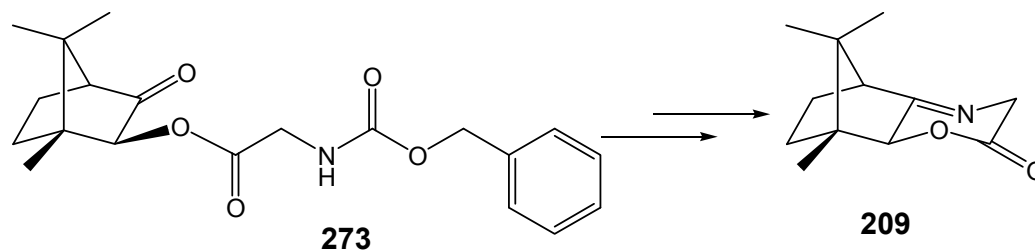


Scheme 2.20: Ravindran's attempt at direct synthesis of the 2-iminolactone **208**.¹²³

The next method attempted involved reacting ethyl glycine hydrochloride **271**, generated *in situ*, with the α -ketol **231** under reflux. This again failed to produce any lactone product but did afford the hydroxy enamine derivative **272** (**Scheme 2.21**) in low yield. Several other methods of synthesis were attempted without success until finally, using a carbonyl diimidazole coupling agent and CBZ-protected glycine, Ravindran¹²³ obtained **273** and its regioisomer **274** in good yields. Following deprotection and cyclization (**Scheme 2.22**), alkylation of the 3-iminolactone **209** was achieved by Matjila¹²² and Klein¹²⁴, but similar treatment of the 2-iminolactone analogue **208** failed to yield any of the monoalkylated product, affording dialkylated products instead.¹²² One of the aims of the present study was to confirm the reproducibility of these earlier results, and to achieve stereoselective *monoalkylation* of the 2-iminolactone **208**.



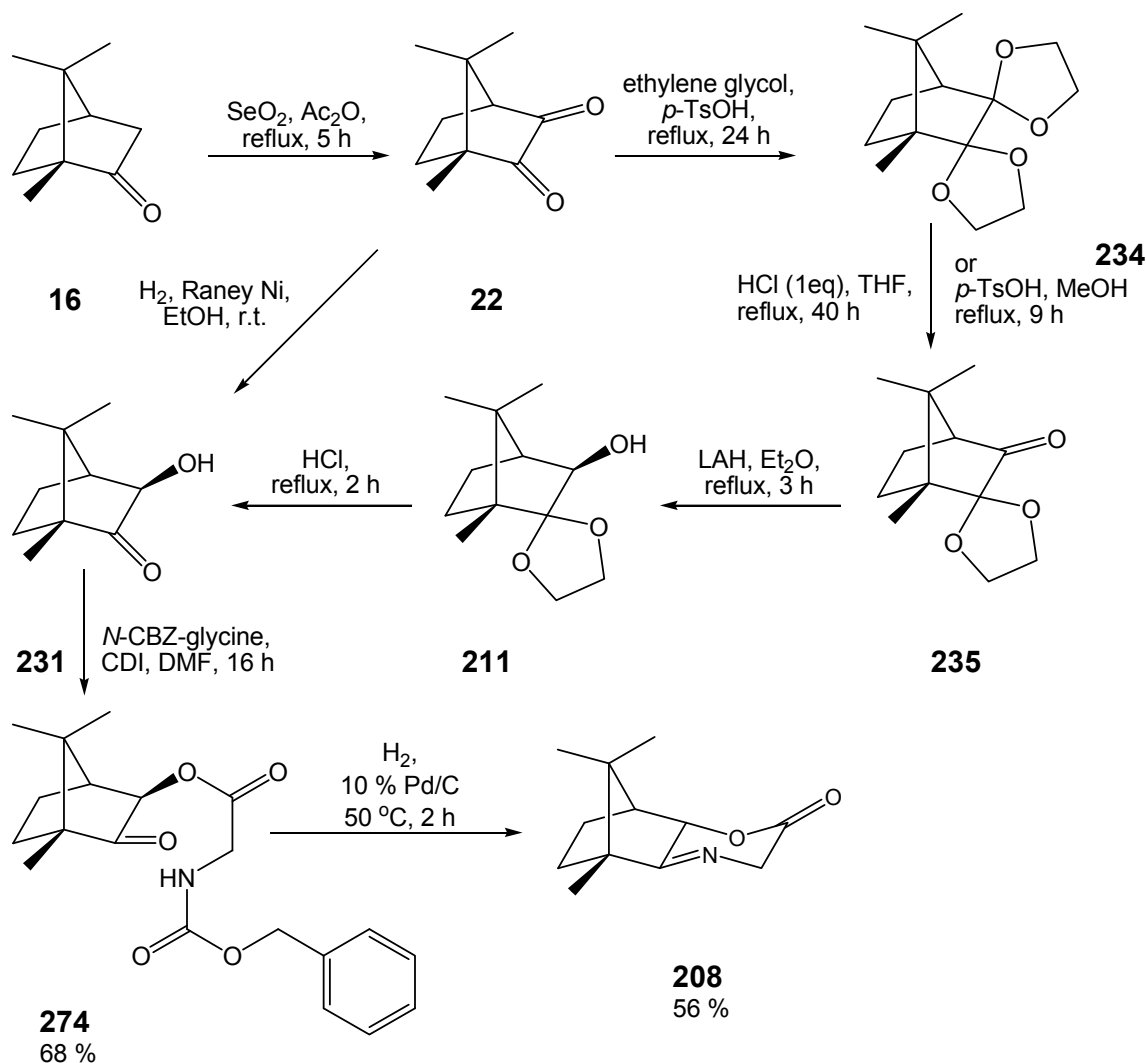
Scheme 2.21: Formation of enamine **272**.¹²³



Scheme 2.22: Deprotection and cyclization of the CBZ-protected compound **273**.

2.2.2 Synthesis of the 2-Iminolactone

The overall route to the tricyclic 2-iminolactone **208** is outlined in **Scheme 2.23**. Approaches to the α -ketol intermediate **231** have been discussed in detail in **Section 2.1**. Following the approach developed by Ravindran,¹²³ esterification of the α -ketol **231** was effected using *N*-carbobenzyloxyglycine (CBZ-gly)¹⁶³ in the presence of the coupling agent *N,N'*-carbonyl-diimidazole (CDI) to afford the ester **274** in 68 % yield.



Scheme 2.23: Synthetic pathway for the 2-iminolactone **208**.

The carbobenzyloxy group is widely used as a protecting group in organic synthesis^{164,165} and CBZ-protected amino acids are readily available. Many coupling reagents have been developed, the most well known probably being dicyclohexylcarbodiimide (DCC).¹³⁶ While

DCC has been used extensively,¹⁶⁶ it gives variable yields and *N*-acyl urea side products [e.g. dicyclohexylurea (DHU)]. The mode of action of *N,N'*-carbonyldiimidazole (CDI)¹⁶⁷ is similar to that of DCC and the only side product is imidazole, which is easily removed.

Ester **274** was fully characterised using 1- and 2-D NMR methods. The ¹H NMR spectrum of the purified sample (**Figure 2.20**) shows the diastereotopic 2'-methylene protons resonating as *multiplets* at 4.01 ppm, reflecting their magnetic non-equivalence in the chiral environment provided by the camphor moiety. The 4'-methylene protons, however, resonate as a *singlet* at 5.11 ppm, apparently unaffected by the chiral auxiliary due to their distance from it. The deshielded 3-H_{endo} nucleus resonates as a singlet at 4.82 ppm. This is characteristic of the camphor systems that have been studied previously where no coupling with the adjacent 4-methine proton is observed due to a torsion angle of *ca.* 80°. For the same reason the 4-methine proton exhibits no coupling with the 5-H_{endo} nucleus but resonates as a doublet at 2.10 ppm due to coupling with the 5-H_{exo} nucleus alone.

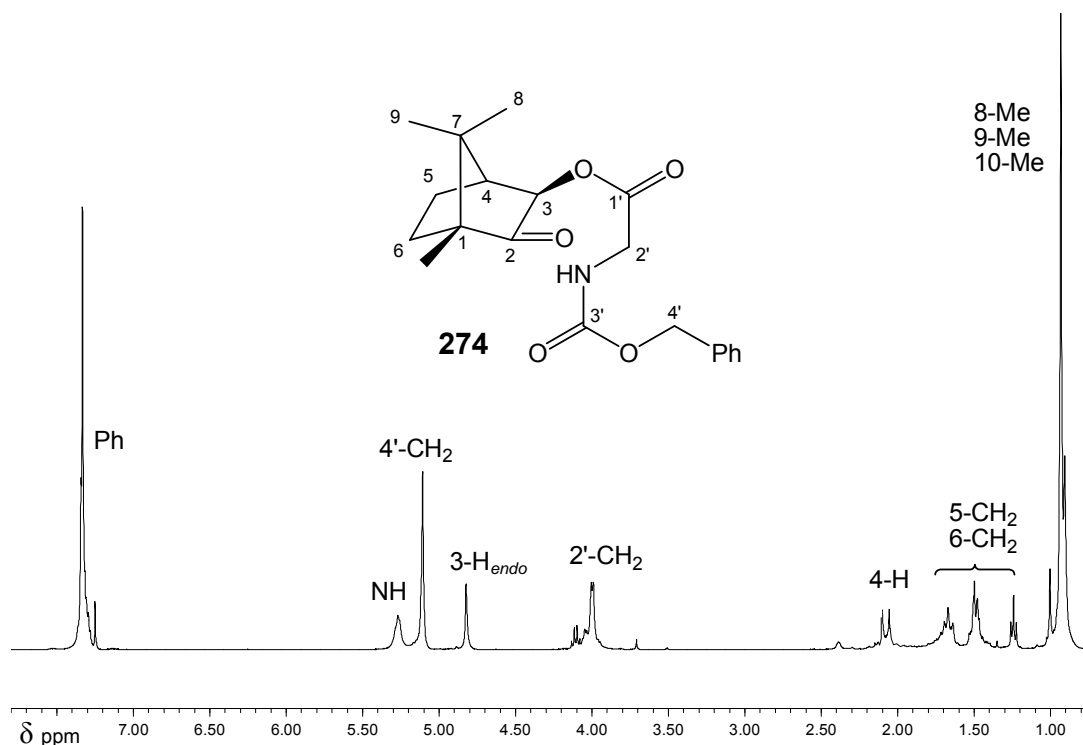
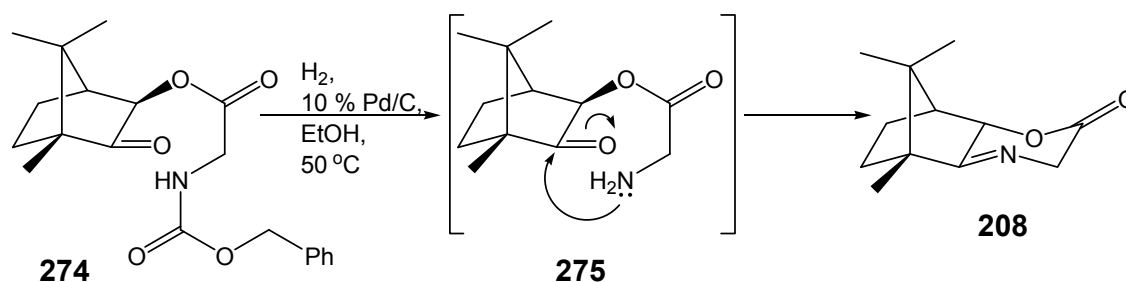


Figure 2.20: 400 MHz ¹H NMR spectrum of **274** in CDCl₃.

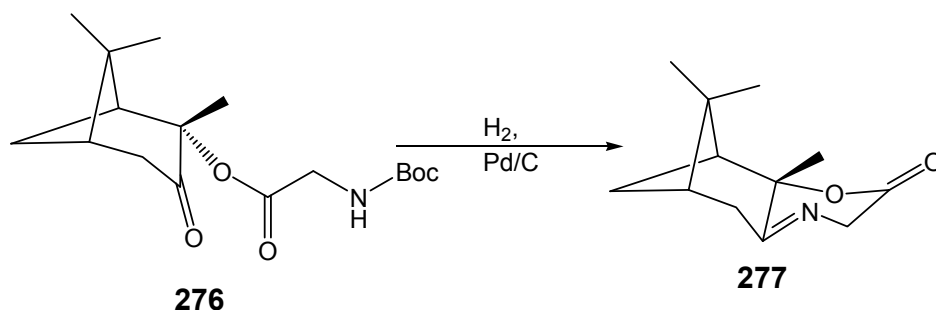
Removal of the CBZ-protecting group was readily achieved by palladium catalyzed hydrogenolysis^{166,168} following the methodology described by Bodansky *et al.*¹⁶³ Thus, a solution of the CBZ-protected system **274** in absolute ethanol was heated to 50 °C for 2 h

under a hydrogen atmosphere in the presence of 10 % palladium-on-carbon. Work-up and chromatography gave the 2-iminolactone **208** directly in 56 % yield, due to spontaneous cyclization *via* intramolecular nucleophilic attack at the electron-deficient carbonyl carbon by the amino lone pair electrons, following deprotection (Scheme 2.24).



Scheme 2.24: Deprotection and intramolecular cyclization of the intermediate ester **274**.

Interestingly El Achqar *et al.*¹⁶⁶ reported that analogous deprotection of the α -pinene-derived system **276** also proceeded with spontaneous ring closure, to afford the α -pinene-derived iminolactone **277** (Scheme 2.25).



Scheme 2.25: Deprotection and intramolecular cyclization of the α -pinene glycine ester **276**.¹⁶⁶

Confirmation of the structure of the 2-iminolactone **208** was provided by 1- and 2-D NMR analysis. The ^{13}C NMR spectrum shows 12 carbon resonances, including the characteristic ester carbonyl carbon at 183.7 ppm and an α carbon at 52.6 ppm. The ^1H NMR spectrum (Figure 2.21) shows the diastereotopic 2'-methylene protons resonating at significantly different chemical shifts (3.89 and 4.53 ppm) due to their different magnetic environments. The 2'- H_{endo} proton resonates at 3.89 ppm as a doublet of doublets due to geminal coupling with the 2'- H_{exo} -proton (4.53 ppm, J 17.9 Hz) and remarkably long-range homoallylic coupling to the 3- H_{endo} nucleus (4.49 ppm, J 1.6 Hz).

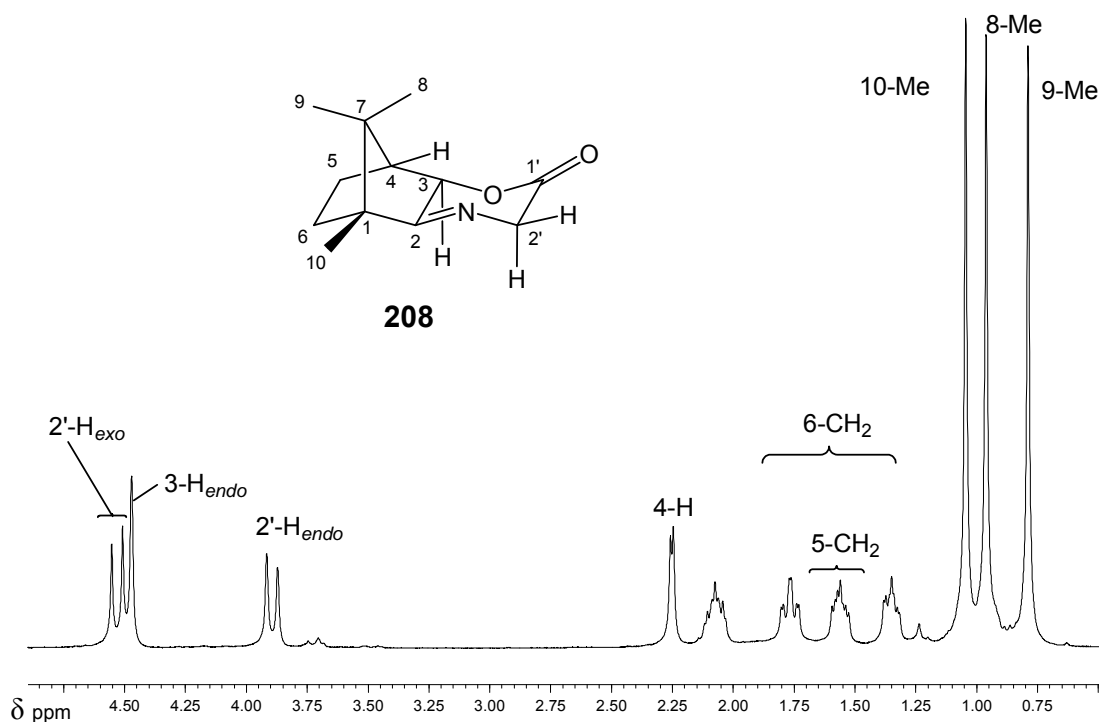


Figure 2.21: 400 MHz ¹H NMR spectrum of **208** in CDCl₃.

It is important to note that the relative instability of the 2-iminolactone **208** necessitates its use reasonably soon after synthesis, otherwise it undergoes degradation involving fission of the imine bond and consequent opening of the lactone ring. Klein¹²⁴ noted similar degradation of the 3-iminolactone **209**, and suggested that this property might be advantageous, as isolation of the subsequently α -alkylated amino acid and recovery of the auxiliary by hydrolysis might also be very easy.

2.2.3 Alkylation of the 2-Iminolactone

The presence of the two adjacent activating groups (imino and ester carbonyl) is expected to enhance the acidity of the 2'-methylene protons in the lactone **208**, hence facilitating formation of the corresponding enolate anion in the presence of a suitable base. Subsequent attack by alkyl halides is expected to be favoured at the less hindered face, resulting in *endo*-alkylation.¹⁶⁹ One point of concern, however, has been the uncontrolled dialkylation observed in earlier studies,¹²² and its minimization was of particular interest in the present investigation.

Lithium diisopropylamide (LDA) would seem to be an obvious choice as the base for the deprotonation of the iminolactone. However, problems experienced by other researchers^{122,166} in the group and the success achieved by El Achqar *et al.*¹⁶⁶ using potassium tert-butoxide (KOBU^t) in their work on the α -pinene-derived iminolactone **277** prompted us to use KOBU^t. Catievela *et al.*¹⁷⁰ also used KOBU^t in their synthesis of (*S*)-amino acids. Thus, treatment of the iminolactone **208** with KOBU^t in THF under anhydrous conditions at -78 °C led to the formation of the enolate **278** (Scheme 2.26). To ensure complete enolization, the mixture was stirred for a further 1 h before a solution of the alkyl halide in THF was added. The reaction mixture was maintained at -78 °C for a further 2 h before allowing it to warm to room temperature overnight. Work-up followed by ¹H NMR spectroscopic analysis of the crude reaction mixtures permitted the level of stereocontrol to be determined. The integrals of corresponding but unobscured signals (typically the 2'-H or 3-H signals) were used to determine the relative proportions of the *endo*- and *exo*-diastereomeric products in each instance, as illustrated for **279a** and **279b** (Figure 2.22).

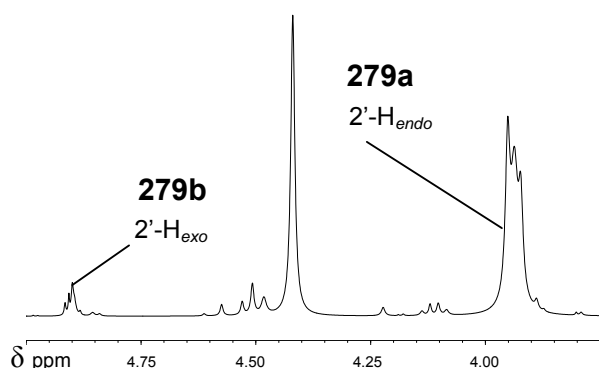
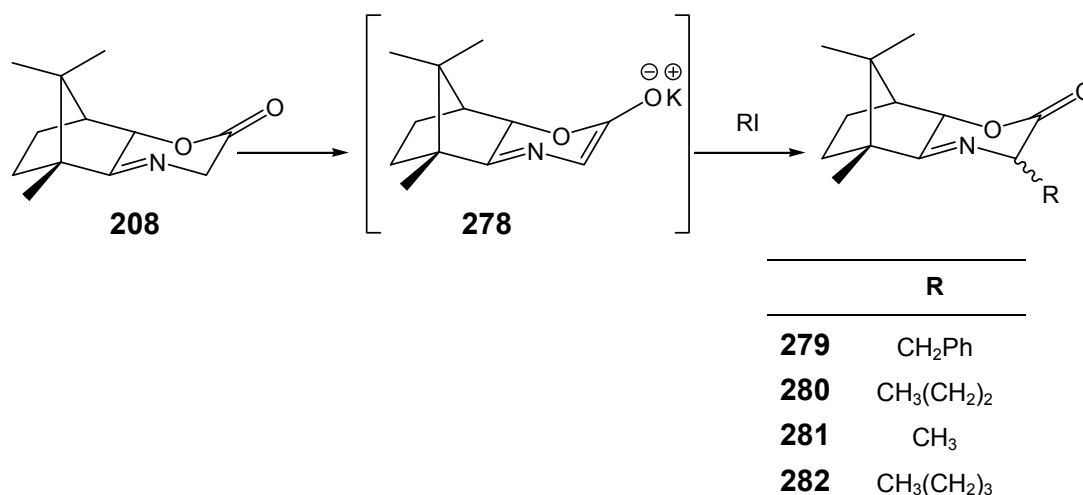


Figure 2.22: Partial ¹H NMR spectrum for determining stereoselectivityalkylation of **279**.

Purification of the crude reaction mixtures and separation of the diastereomers was achieved using a chromatotron. Each isolated diastereomer was then fully characterised by NMR spectroscopy; the ^1H NMR spectra of the benzylated diastereomers **279a** and **279b** are illustrated in **Figures 2.23** and **2.24**. The overall yields were typically moderate and, in all cases, the *exo* product predominated, in contradiction with initial predictions. The highest stereoselectivity (84.8 % d.e.) was found, as expected, in the benzyl product. This was attributed to the steric demands of the aromatic ring. The predominance of *exo* products in all cases was most likely a direct result of the use of KOBU^1 as the base (**Table 2.3**). It has previously been established that the mode of interaction of the base directly corresponds with the direction of alkylation at the activated centre and that substitution of the base could potentially reverse the facial selectivity.¹³⁶ It is important to note that ^1H NMR analysis of each reaction mixture showed the successful and exclusive synthesis of monoalkylated products and no trace of any dialkylated product.



Scheme 2.26: Alkylation of iminolactone **208**.

Table 2.3: Data for the alkylation of the iminolactone **208**.

Product	RX	Yield (%)	Endo: Exo	% d.e.
279	$\text{C}_6\text{H}_5\text{CH}_2\text{Br}$	64.9	7.6 : 92.4	84.8
280	$\text{CH}_3(\text{CH}_2)_2\text{I}$	52.1	25.4 : 74.6	49.2
281	CH_3I	53.2	38.5 : 61.5	23.5
282	$\text{CH}_3(\text{CH}_2)_3\text{I}$	56.9	25.8 : 74.2	48.4

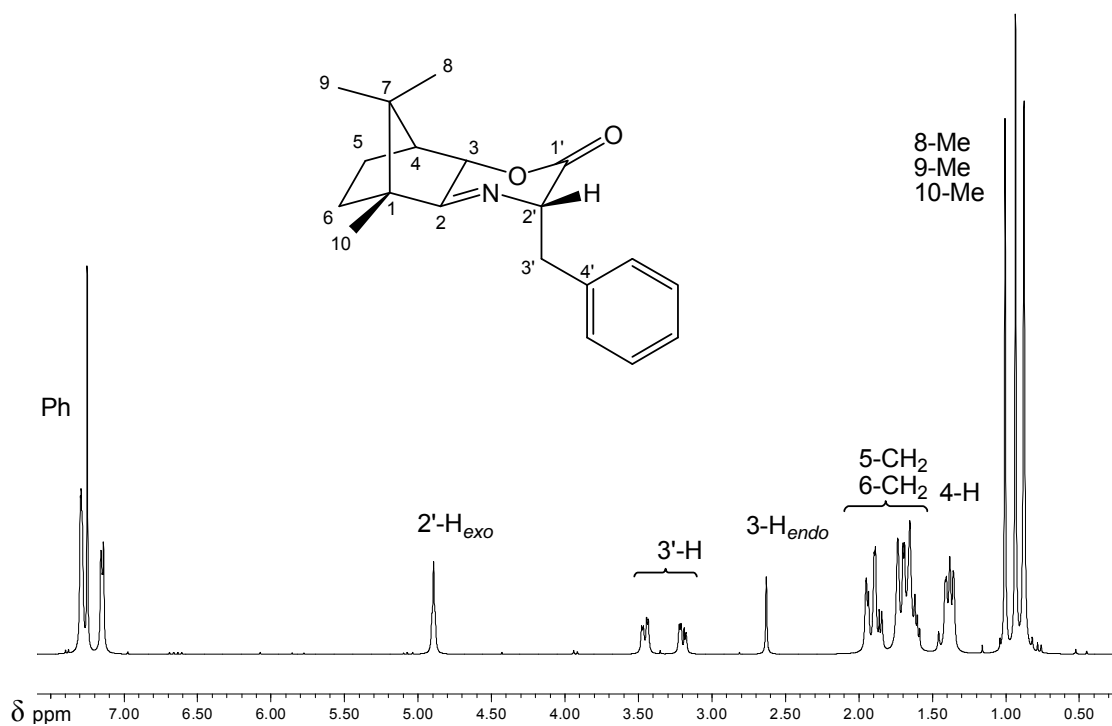


Figure 2.23: 400 MHz ^1H NMR spectrum of **279a** in CDCl_3 .

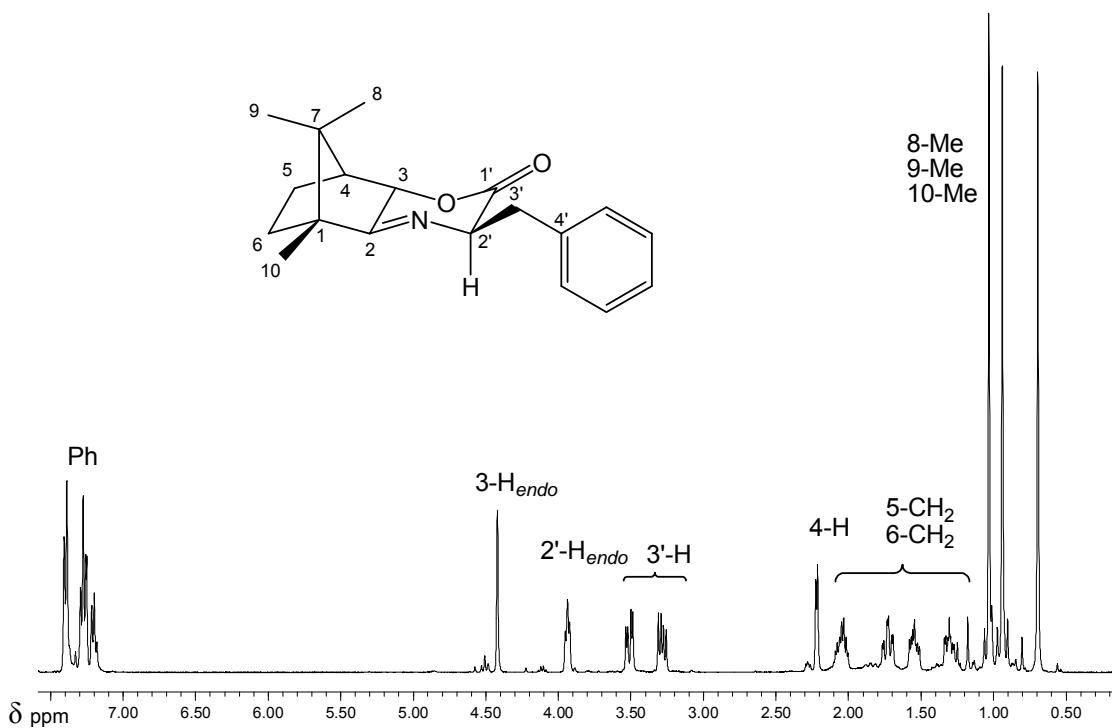


Figure 2.24: 400 MHz ^1H NMR spectrum of **279b** in CDCl_3 .

^1H - and ^{13}C NMR spectroscopy was used to confirm the structure of the alkylated products. Use was made of the 2-iminolactone **208** as a reference and signal assignments were carried out for all the alkylated products. The assignment of *exo*- or *endo*- stereochemistry was based predominantly on the positions and splitting patterns of the 2'-H and 3-H signals (**Figure 2.25**).

Generally, when the 2'-H is *endo* (and, hence the alkyl group is *exo*), long range homoallylic coupling with the 3-H nucleus is observed. This is unusual and only possible due to the degree of eclipsing of the two protons.¹⁷¹ The coupling was also noted to be very small (*ca.* 1.2 Hz). The chemical shifts of the 3-H and 2'-H nuclei of the *exo*- and *endo*-isomers were also observed to be significantly different. With the exception of the benzylated products, in which magnetic anisotropic effects are likely to be significant, it was found that deshielding of both the 3-H and the 2'-H protons occurs when they are on opposite faces of the molecule. For *exo*-alkylated products, 2'-H_{endo} is in a constrained position relatively close to 3-H_{endo} and, additionally, 2'-H_{endo} is within the shielding environment of the carbonyl π -bond, and both *endo*-protons are shielded. For *endo*-alkylated products, the 2'-H_{exo} and 3-H_{endo} protons do not experience mutual van der Waals shielding and, more importantly the 2'-*exo* proton lies in the deshielding zone of the lactone carbonyl group (**Figure 2.25**), and thus resonates at lower field. *Endo* alkyl groups appear to have little effect on the 3-H_{endo} chemical shift. The *endo*-benzyl group, however, appears to be responsible for significant shielding of the 3-H_{endo} nucleus due to the magnetic anisotropic effect illustrated in **Figure 2.26**. Assignment of signals for the ^1H NMR spectra of the mono-alkylated products **279** - **282** are shown in **Figures 2.26** - **2.29**.

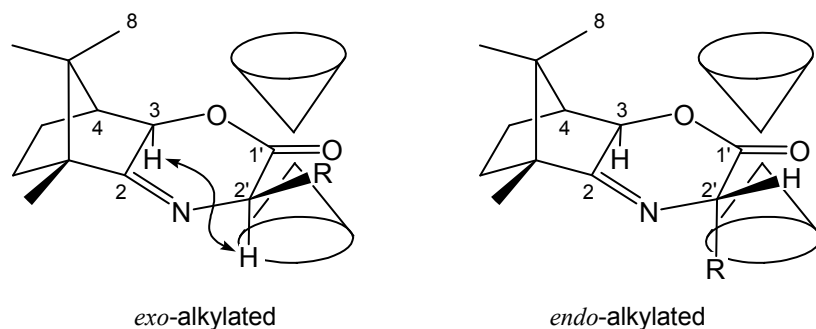


Figure 2.25: Putative 1,4-diaxial interactions of the 2'-H_{endo} and 3-H_{endo} protons in *exo*-alkylated products and the carbonyl anisotropic deshielding of the 2'-H_{exo} nucleus in *endo*-alkylated products.

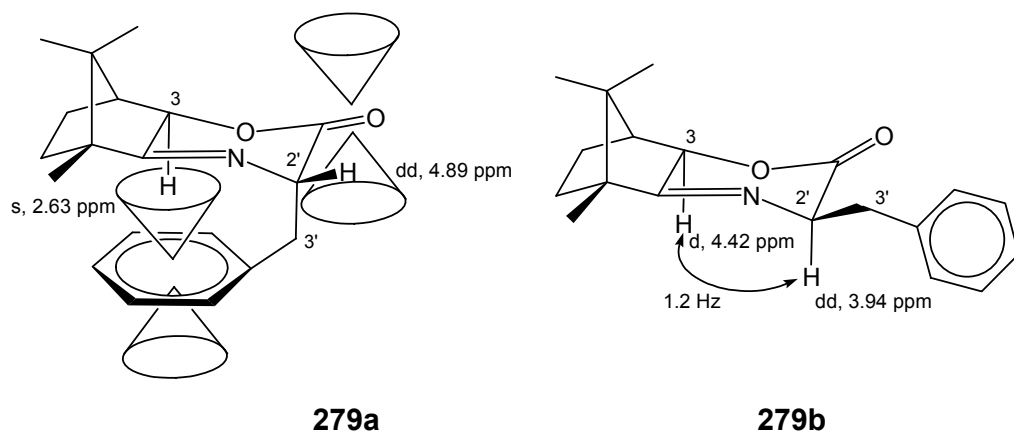


Figure 2.26: Specific ^1H NMR chemical shift and coupling data for 279a and 279b.

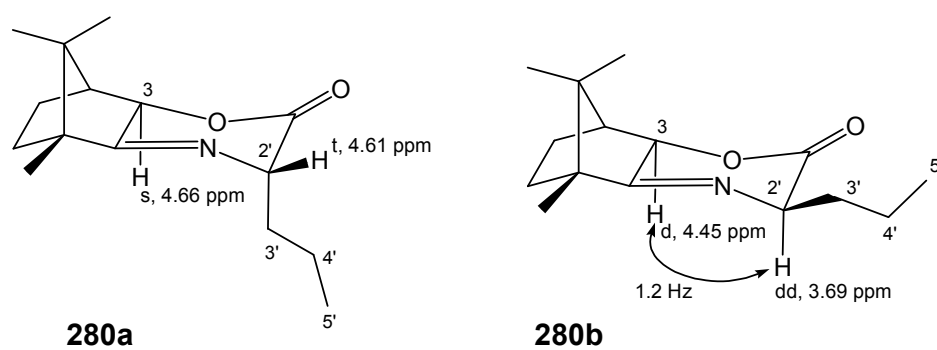


Figure 2.27: Specific ^1H NMR chemical shift and coupling data for 280a and 280b.

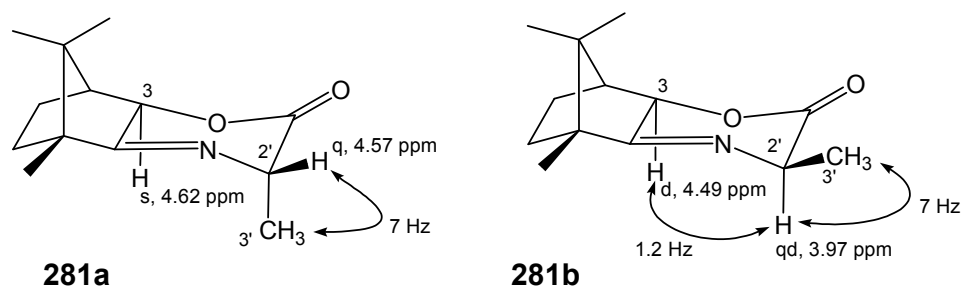


Figure 2.28: Specific ^1H NMR chemical shift and coupling data for 281a and 281b.

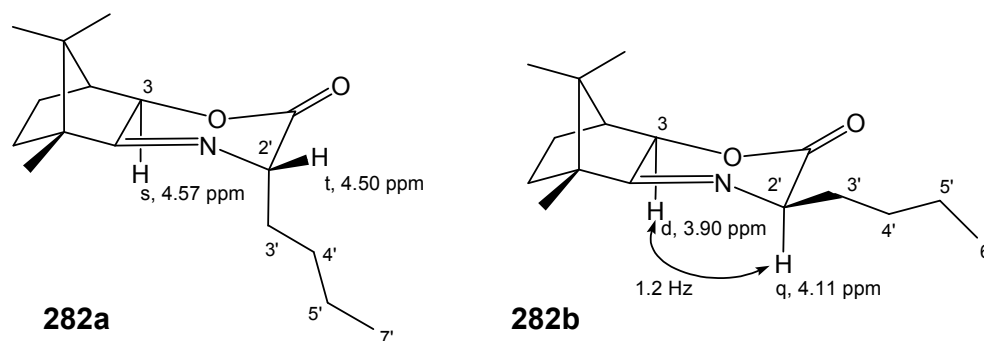


Figure 2.29: Specific ^1H NMR chemical shift and coupling data for **282a** and **282b**.

Hydrolysis of the corresponding alkylated iminolactone products was not attempted due to the paucity of material. Hydrolysis has, however, been carried out on the analogous alkylated α -pinene-derived iminolactone **277**¹⁶⁶ and also on the predominantly *endo*-alkylated 3-iminolactone product(s) to generate (*R*)-amino acids.¹²⁴ Hence it is expected that hydrolysis would likewise proceed smoothly with the 2-iminolactone analogues generating α -amino acids.

In summary, a route has been developed from (1*R*)-(+)-camphor to produce 3-*exo*-hydroxy bornanone, which undergoes condensation with CBZ-protected glycine, deprotection and cyclization giving the 2-iminolactone and then finally exclusive monoalkylation to give a range of predominantly *exo*-alkyl-2-iminolactones. In no instance was any dialkylated product observed for any of the alkylated iminolactones.

Unfortunately, subsequent to the completion of the iminolactone study and the earlier research, published in PhD theses from as far back as 1994, by Ravindran,¹²³ Matjila¹²² and Klein,¹²⁴ it was noted that Xu *et al.*^{172,173} had in 2002 published similar work to that done in our laboratories involving essentially identical pathways to the 2- and 3-iminolactones. Their results, however, confirmed our structure assignment through X-ray analysis and revealed that the sense of diastereoselectivity could be reversed by using LDA in place of KOBu^t (*endo*-isomer in up to 98 % d.e.).

2.3 SYNTHESIS OF CAMPHOR-DERIVED MORITA-BAYLIS-HILLMAN SUBSTRATES

2.3.1 Synthetic Rationale

The presence of a stereogenic centre in the activated alkene should induce asymmetry in the reaction intermediates and transition state complexes and, consequentially, cause the preferential formation of one diastereomer. However, this is not generally the case due to the distance between chiral and reacting centres.⁷¹ It has been theorized that the presence of a chiral hydroxyl moiety, with its associated hydrogen bonding potential, could increase the reaction rate, through stabilization of the reaction intermediates and, additionally, promote asymmetric induction.

Thus, our requirements for an effective auxiliary were that it should induce a high degree of stereoselectivity, promote the rate of the reaction as much as possible and be recyclable. It was determined that important structural criteria for an effective chiral auxiliary in the Baylis-Hillman reaction were: - i) a rigid scaffold to minimize conformational flexibility; ii) the presence of a proximate asymmetric moiety to induce asymmetry; iii) a hydroxylic group to facilitate intramolecular hydrogen bonding, thus increasing conformational rigidity in the transition state and increasing the rate of the reaction; and iv) an efficient “blocking group” to promote stereofacial attack.

The readily available chiral camphor system provides a rigid scaffold upon which sterically demanding and chemoselective groups can be attached, and two general approaches to the construction of chiral acrylic esters as Morita-Baylis-Hillman substrates were considered. In the first, the introduction of a hydroxyl group at C-2 with the potential for hydrogen bonding might be expected to stabilize both the intermediate Morita-Baylis-Hillman zwitterion and the developing negative charge on the aldehyde oxygen (**Figure 2.30**). In the second, introduction of a bulky substituent R at C-10, might be expected to favour an arrangement of the corresponding Morita-Baylis-Hillman zwitterion whereby attack by the electrophile would occur from the *endo*-face. Of course, in both approaches the preferred orientation of the aldehyde would be a major factor in determining overall stereocontrol. Thus the generalised model compound **283** was envisaged.

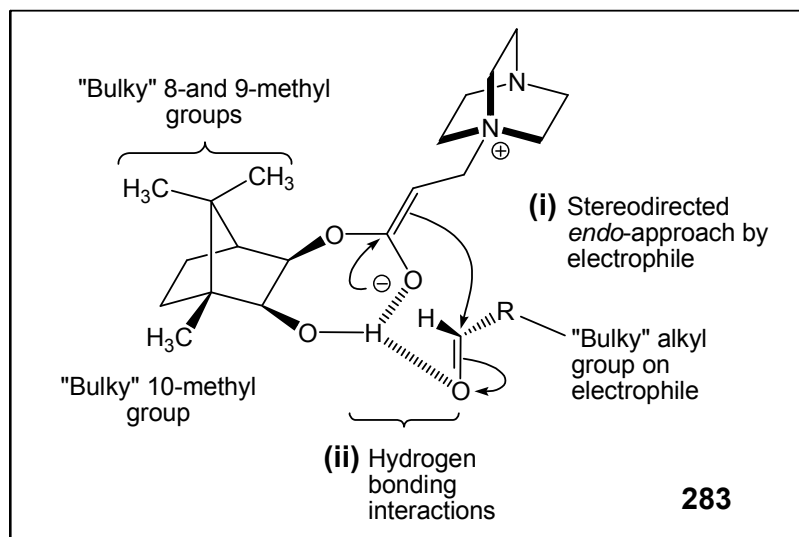
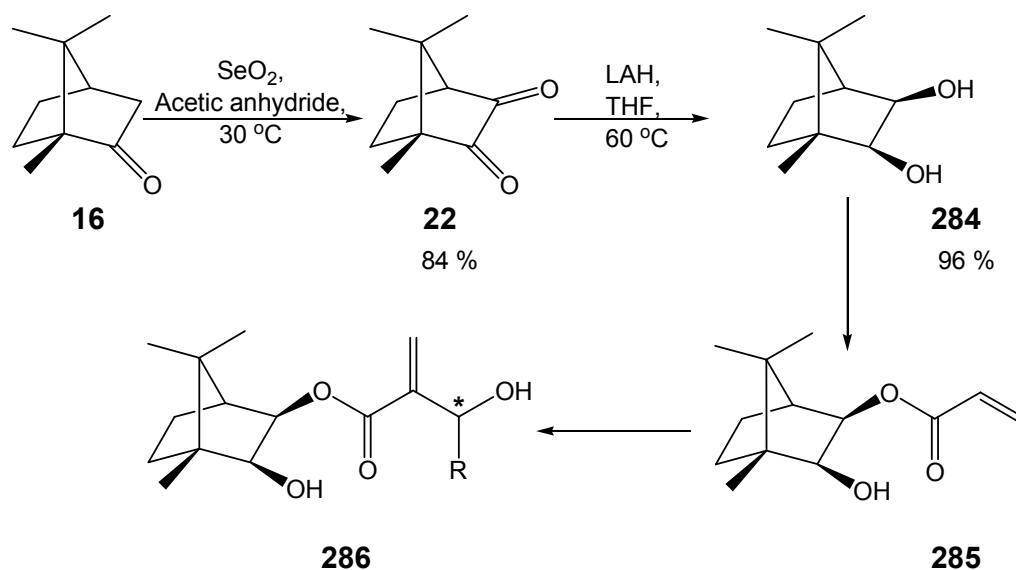


Figure 2.30: Expected transition state interactions involving the 2-*exo*-hydroxy-3-*exo*-bornyl enolate intermediate **283**.

The first compound to be targeted using this model was the hydroxy ester **285**, which contains the requisite hydroxyl group and a 10-methyl group.

2.3.2 Monoacrylate Esters of Dihydroxybornane

Several possible routes were considered to access the chiral Morita-Baylis-Hillman substrate **285**. These included the use of protecting groups to direct the acrylate moiety to the desired 3-hydroxy group. This, however, seemed an over-complication as the camphor moiety is known to react preferentially at the less hindered C-3 position first. Selective acylation of the diol **284** was thus a reasonable expectation; and the route outlined in **Scheme 2.27** was explored. The oxidation of camphor **16** was followed by reduction of both carbonyl groups in the resulting camphorquinone **22**. Regioselective esterification at C-3 of **284** with one equivalent of acryloyl chloride was expected to afford the substrate **285**, which could then be reacted with a range of aldehydes to afford chiral Morita-Baylis-Hillman products **286**.



Scheme 2.27: Proposed synthetic route to the 2-*exo*-hydroxy Baylis-Hillman products **286**.

2.3.2.1 Synthesis of the Acrylate Esters.

The oxidation of camphor **16** was achieved using SeO_2 in acetic anhydride to produce camphorquinone **22** in high yield (84 %) (**Scheme 2.27**).^{133,134} The choice of reducing agent was then considered. NaBH_4 has been used previously for the reduction of camphor derivatives,¹⁷⁴ as has hydrogenation in the presence of nickel catalysts.¹⁷⁵ However, previous success with LiAlH_4 in the synthesis of the alcohols **210** and **211** and its reported ability to readily reduce even hindered ketones^{99,134}, or diketones¹⁷⁵ to secondary alcohols prompted its selection as the reducing agent. LiAlH_4 is a powerful reducing agent requiring anhydrous conditions. Diethyl ether or THF are generally the solvents of choice for such reductions,¹³⁶ and the latter was chosen, so as to maximize the reaction temperature and thus increase the rate of reduction. Due to the steric bulk of the 8-methyl group, *endo* attack by the hydride ion is expected. The reduction of both carbonyl groups was readily achieved with this reducing agent and 2-*exo*-3-*exo*-dihydroxybornane **284** was obtained in excellent yield (96 %). ^{13}C NMR and DEPT analyses confirmed the presence of the requisite 10 carbons, while the ^1H NMR spectrum was used to assign the stereochemistry at the new chiral centres (**Figure 2.31**). The coupled 2-H (3.58 ppm) and the 3-H (3.81 ppm) nuclei resonate as doublets, the 2-H nucleus being more shielded due to its proximity to the 10-methyl group. The lack of vicinal coupling between the 3-H and 4-H nuclei is consistent with a torsion angle

approaching 80° and confirms the *endo*-orientation of the 3-H proton, while the vicinal coupling constant $J_{2,3} = 7.0$ Hz is consistent with eclipsing of the 2-H and 3-H nuclei. Since the 2-H and 3-H nuclei are thus both *endo*-orientated, the attached 2- and 3-hydroxy groups must both be *exo*-orientated. This conclusion is consistent with preferential delivery of hydride ion by LiAlH_4 at the *endo*-face. In fact, there was no evidence of the formation of the other possible stereoisomers.

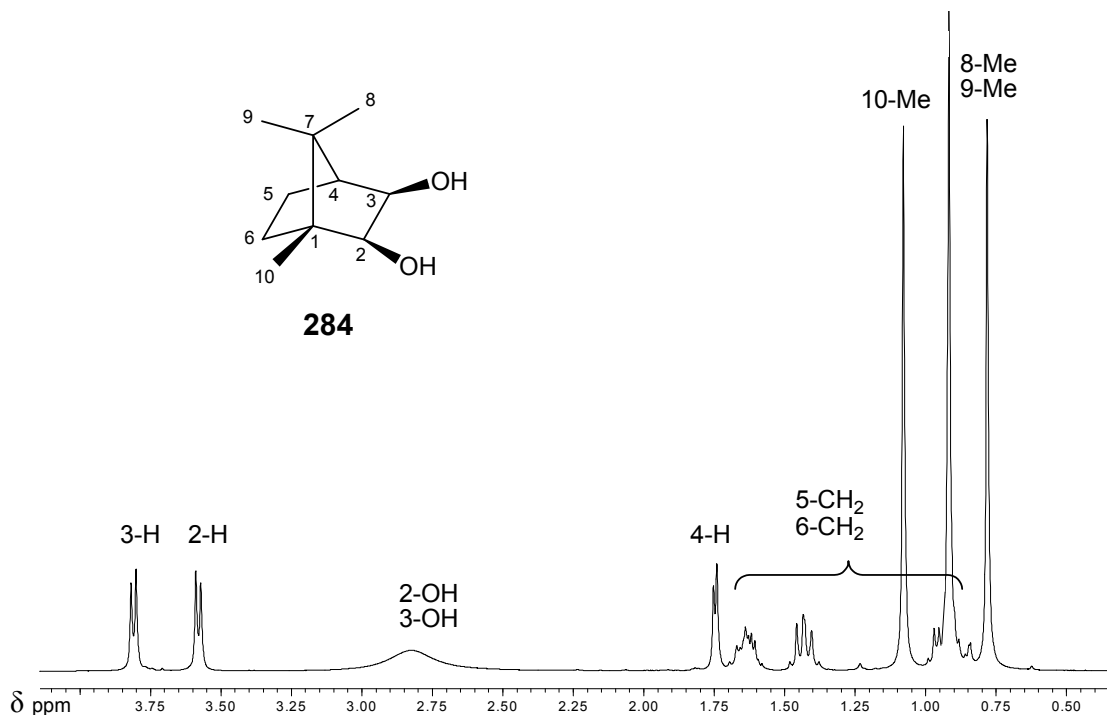
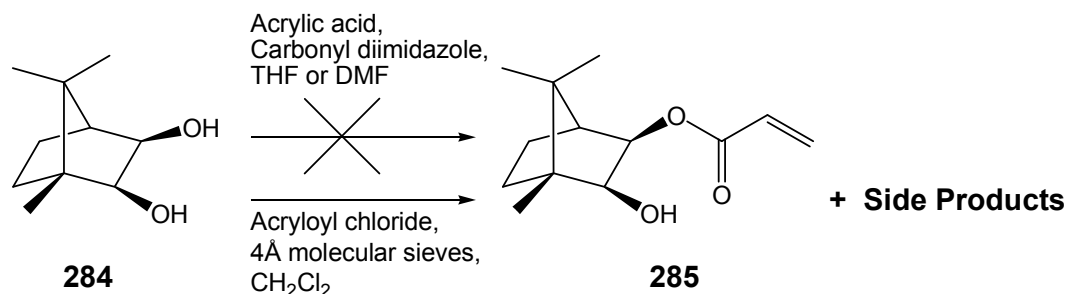


Figure 2.31: ^1H NMR spectrum of **284** (400 MHz, CDCl_3).

Following the synthesis of the diol **284**, regioselective esterification of the 3-hydroxy group was required. The acid catalyzed reaction of carboxylic acids with alcohols to form esters is a well established equilibrium process.^{176,177} However, the reactions can be slow and generally require a significant excess of the alcohol to ensure complete esterification.¹⁷⁸ Various coupling reagents have been developed to facilitate esterification^{176,179} and, in previous studies in our laboratories (**Section 2.2.2**), carbonyldiimidazole (CDI) has been used for this purpose with considerable success; hence it was decided to use this reagent.

Esterification of 2,3-dihydroxybornane **284** was attempted using acrylic acid in the presence of CDI in both anhydrous THF and anhydrous DMF (**Scheme 2.28**), as it has been suggested

that the choice of solvent can influence the yield.¹³⁶ After work-up, ¹H NMR spectra were obtained for the crude reaction mixtures and it was observed that, in both cases, the acrylic acid signals were weak and that new signals were present, indicating the formation of products. However, the lack of any vinylic proton signals ruled out the possibility of the desired acrylic ester **285**. Subsequently, a ¹H NMR spectrum was obtained for the commercial acrylic acid, which indicated a high degree of polymerization. The use of acryloyl chloride in the esterification of **284** was then explored under various reaction conditions. The first method to be attempted involved the use of 4Å molecular sieves as they are known to scavenge small molecules such as H₂O or HCl,^{99,122,134,180} thus preventing acid catalyzed polymerization.^{99,122,180}



Scheme 2.28: Esterification of dihydroxybornane **284**.

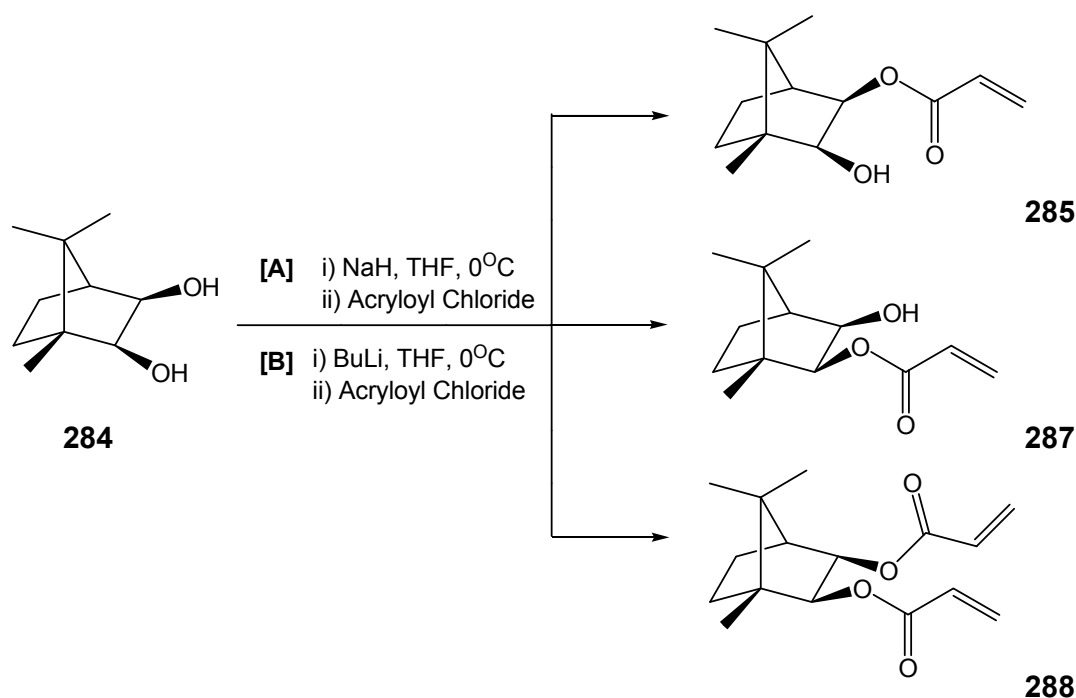
Dihydroxybornane **284** was therefore reacted with acryloyl chloride in dichloromethane in the presence of 4 Å molecular sieves, at 40°C for 17 h (**Scheme 2.28**). ¹H NMR analysis of the crude reaction mixture indicated the successful synthesis of one or more esterified products. Thin layer chromatography (TLC) of the crude sample showed the presence of at least eight compounds, and separation on a chromatotron was attempted. However, since effective separation proved difficult and it was apparent that this method was not sufficiently selective, other methods of esterification were considered.

The use of strong bases to deprotonate the alcohol, followed by reaction of the resulting alkoxide with an acid chloride, is a well established method for obtaining esters from alcohols.¹³⁶ The base of choice is often NaH,^{124, 181,182} and this was consequently used in the present study. The diol **284** was added to a pre-washed suspension of NaH in anhydrous THF and the resulting mixture was boiled under reflux to generate a monoalkoxide. Acryloyl

chloride was then introduced and the mixture again boiled under reflux. The diol **284** was used as the limiting reagent, due primarily to its economic value but also as excess acrylic acid (produced by hydrolysis of the acid chloride during work-up) is more easily removed from the crude reaction mixture (by washing with aqueous NaHCO₃) than excess auxiliary would have been.¹²⁴ ¹H NMR analysis indicated the crude product to be significantly cleaner than the product obtained in the previous reaction with 4Å molecular sieves. Purification on a chromatotron gave four fractions, which were unambiguously characterised as 2-*exo*-3-*exo*-bornanyl diacrylate **288**, 2-*exo*-hydroxy-3-*exo*-bornanyl acrylate **285**, 3-*exo*-hydroxy-2-*exo*-bornanyl acrylate **287** (Scheme 2.29) and starting material **284**.

The reaction was repeated several times in attempts to increase the yields of the three new compounds **285**, **287** and **288**. However, it was noted that increasing the reflux period resulted in the formation of numerous side products and eventual generation of insoluble polymeric material. Polymerization of reactive α,β -unsaturated systems is catalyzed by traces of free acid, which are inevitably present during such reactions and which have been found to be the cause of low yields.¹³⁶ The maximum yield obtained after five reactions were: **288**; 2.3 %; **285**; 13.2 %; and **287**; 15.3 %.

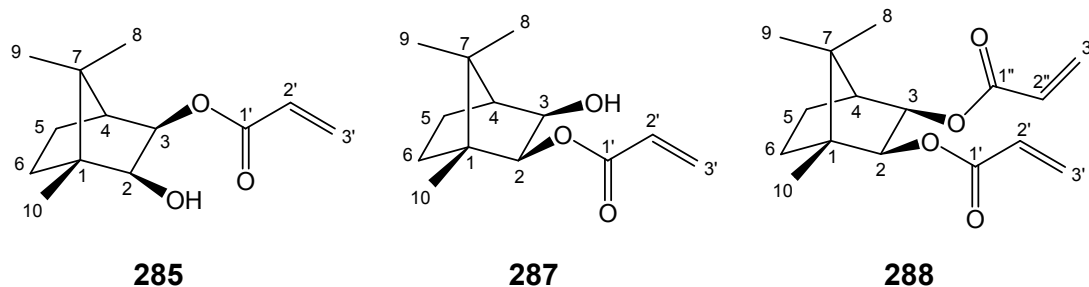
Given the low yields obtained for the acrylate esters it was decided to abandon the use of NaH in favour of the stronger base BuLi.⁹⁹ The addition of BuLi to the diol **284** was done over 20 min at 0 °C and was followed by the addition of acryloyl chloride also at 0 °C. This mixture was stirred for 2 h and then warmed to room temperature overnight. ¹H NMR spectroscopy was used to monitor the formation of products, and confirm that the reaction was complete. After purification of the crude mixture on the chromatotron, the pure esters **285**, **287** and **288** were obtained in moderate yield (overall < 50 %). Although the yield was lower than desired, it was significantly better than the best yield using NaH as base. Optimization studies resulted in the complete disappearance of starting material and an excellent overall yield of 93 % (**285**; 34 %; **287**; 47.8 %; **288**; 10.8 %).



Entry	285	287	288
[A]	13 %	15 %	2 %
[B]	34 %	48 %	11 %

Scheme 2.29: Esterification of **284** producing monoesters **285** and **287** and diester **288**.

Unambiguous characterization of the esters **285**, **287** and **288** was achieved using 1-D and 2-D NMR spectroscopic (**Figures 2.32 – 2.36**) and HRCIMS data (**Figures 2.37** and **2.38**). The spectroscopic data indicated that compound **288** has the molecular formula $\text{C}_{16}\text{H}_{22}\text{O}_4$ (Found M^+ 278.15199, calculated m/z 278.15181) and that compounds **285** and **287** both have the same molecular formula, $\text{C}_{13}\text{H}_{20}\text{O}_3$ (Found M^+ 224.14161, $\text{C}_{13}\text{H}_{20}\text{O}_3$ requires m/z 224.14124). The two latter compounds were found to be regioisomers differing only in the position of the ester and alcohol functional groups.



Both sets of ^1H NMR data for the isomeric compounds **285** and **287** were remarkably similar (**Figures 2.32** and **2.33**). The COSY, HMQC and HMBC data were consistent with the expected monoesters but the relative positions of the acrylate and alcohol groups could not, initially, be deduced. Careful examination of the ^1H NMR spectra was critical in the final characterisation of the compounds as 2-*exo*-hydroxy-3-*exo*-bornanyl acrylate **285** and 3-*exo*-hydroxy-2-*exo*-bornanyl acrylate **287**. NOESY experiments were also run in the hope that they would be of use in establishing the relative positions of the acrylate and alcohol groups but, in the event, they were of no assistance.

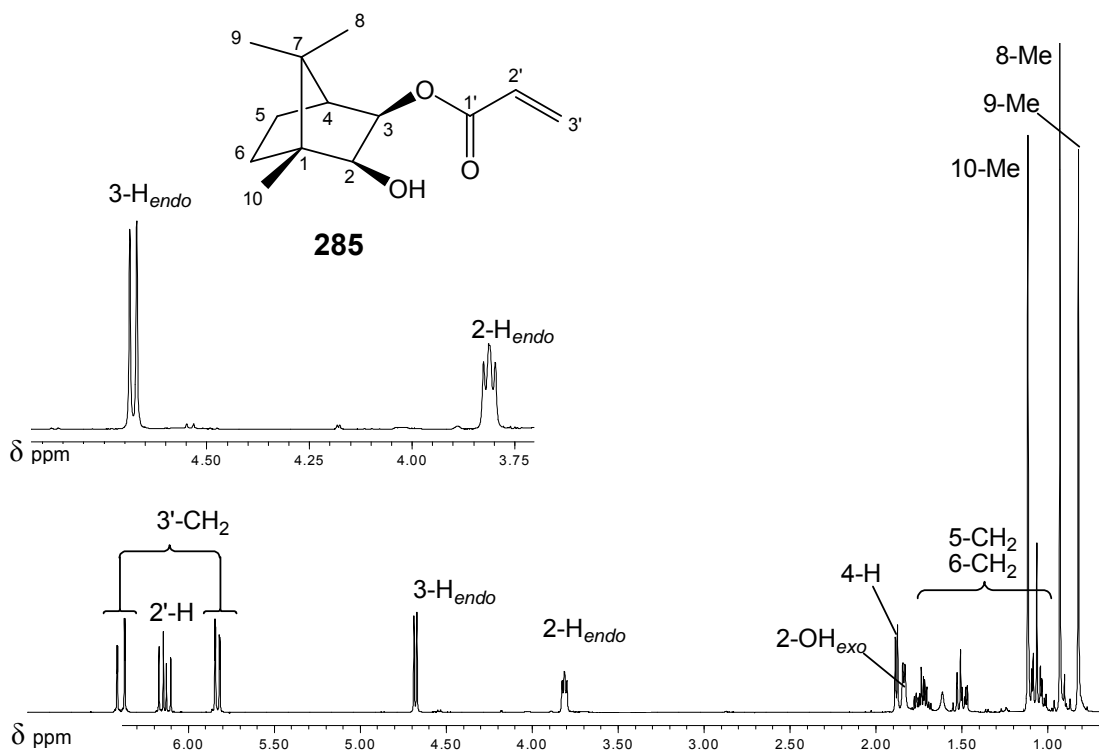


Figure 2.32: 400 MHz ^1H NMR spectrum, with expansion, of the monoester **285** in purified[§] CDCl_3 .

The 2-H, 2-OH and 3-H signals of the monoester **285** (**Figure 2.32**) were instrumental in characterizing its structure. The primary aspects to be explored were the multiplicities and coupling constants; the 2-hydroxyl proton (1.84 ppm) resonates as a doublet and only couples (J ca. 5.2 Hz)[‡] with the 2-H nucleus (3.81 ppm) which, in turn, resonates as a doublet of doublets due to further coupling (J ca. 6.8 Hz) with the 3-H nucleus (4.68 ppm, doublet).

[§] The reason for specifying *purified* chloroform, will be made clear in section 2.3.3.2

[‡] The value is approximate due to the labile nature of the hydroxylic proton, see section 2.3.3.2

Additionally, the 4-H nucleus (1.88 ppm) resonates as a doublet (J 4.9 Hz) due to coupling with the 5-*exo*-proton. The lack of vicinal coupling between the 4-H and the *endo*-3- and *endo*-5-proton is characteristic of the camphor derivatives examined in this research and clearly locates both the 3-H and 2-H nuclei on the *endo*-face of the molecule.

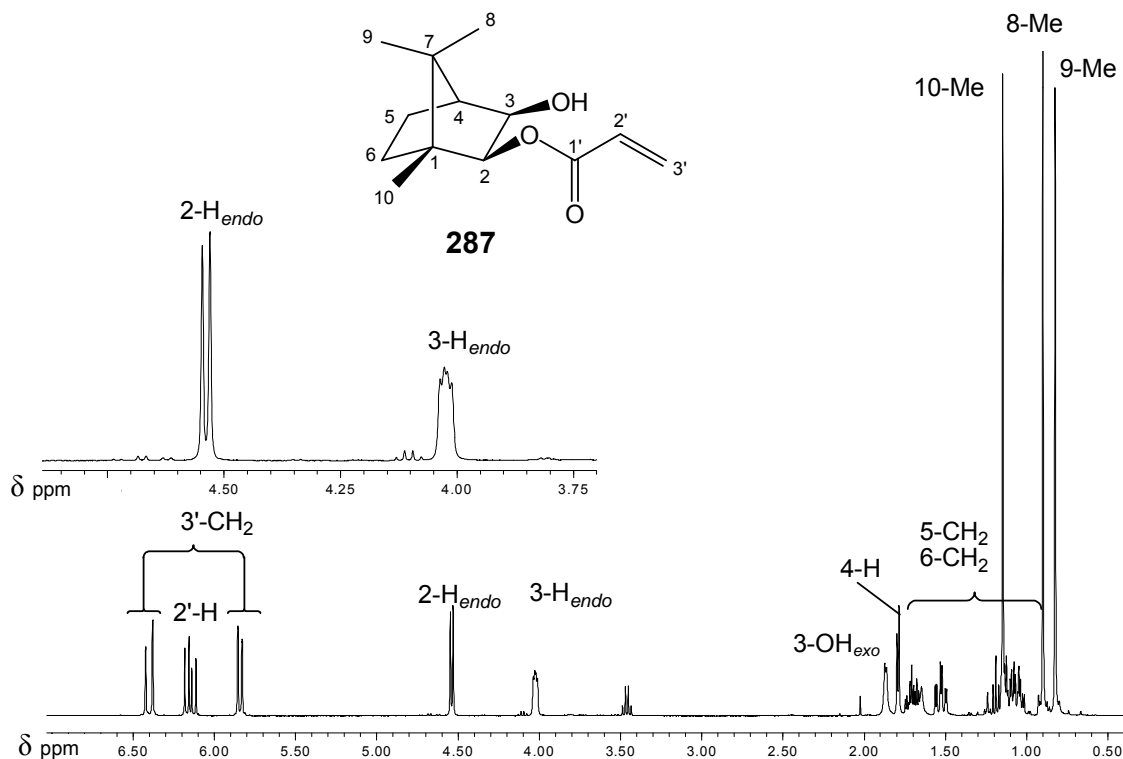


Figure 2.33: 400 MHz ^1H NMR spectrum, with expansion, of the monoester **287** in purified CDCl_3 .

Similar arguments can be used in the assignment of the ^1H NMR signals for the monoester **287** (Figure 2.33). The 3-OH proton (1.87 ppm) resonates as a doublet (J ca. 4.2 Hz), coupling with the 3-H nucleus (doublet of doublets at 4.02 ppm), which also couples (J ca. 6.7 Hz) with the 2-H nucleus (doublet at 4.54 ppm). The 4-H nucleus resonates as a doublet at 1.79 ppm due to coupling (J 4.8 Hz) to the 5-*exo*-proton. The crucial difference between the two compounds **285** and **287** is the position of their acrylate and alcohol groups relative to the 10-methyl group. This group causes shielding of nuclei in close proximity (*i.e.* at C-2) and, thus, an upfield shift of their proton resonances. Conversely nuclei further away from the 10-methyl group (*i.e.* at C-3) are somewhat deshielded and thus resonate further downfield. Thus, comparison of the relative chemical shifts for the 3-*endo*, 2-*endo* and 2-hydroxyl protons in monoester **285** with the 2-*endo*, 3-*endo* and 3-hydroxyl protons in monoester **287** confirms the indicated assignments. The HMBC spectrum of the monoester **285** confirmed the relative

positions of the acrylate and alcohol groups. Thus, the *2-endo* proton, is seen to be close to C-6 and the *3-endo* proton, adjacent to the acrylate moiety, is seen to be close to C-5. The spectrum of **287**, on the other hand, shows the reverse relationships: *i.e.* the *2-endo* proton, adjacent to the acrylate moiety, is close to C-6, while the *3-endo* proton is close to C-5.

Examination of 1-D and 2-D NMR spectra, including HMQC, HMBC and COSY methods, confirmed the structure of the diester **288**. Specifically, the ^{13}C spectrum (**Figure 2.34**) indicates the presence of 16 carbon atoms, with two quaternary carbon signals at 47.5 and 48.8 ppm (C-1 and C-7); three tertiary at 49.6 ppm (C-4), 77.1 ppm (C-2) and 79.8 ppm (C-3); two secondary at 23.8 ppm (C-6) and 32.9 ppm (C-5), three primary at 10.9 ppm, 20.4 ppm and 20.9 ppm (C-8, C-9 and C-10), and two pairs of acrylate sp^2 carbon signals at 128.4 ppm (C-2'), 128.5 ppm (C-2''), 130.47 ppm (C-3'), 130.54 ppm (C-3'') and two ester carbonyl signals at 164.89 ppm (C-1') and 165.00 ppm (C-1''). Analysis of the corresponding ^1H spectrum (**Figure 2.35**) showed: one methine (4-CH); two methylene (5- and 6- CH_2); three methyl (8-, 9- and 10-Me); and two sets of acrylate resonances (C-1', C-1'', C-2', C-2'', C-3' and C-3'') and, significantly no OH signal. Somewhat surprisingly, the singlet at 4.91 ppm, which integrates for two protons, must then be assigned to the *2-* and *3-endo* protons. These protons might well have been expected to resonate as doublets at different frequencies but, with the assistance of the HMQC spectrum (**Figure 2.36**), it was established that the observed singlet actually arises from the fortuitous coincidence of two signals corresponding to two protons attached to two different carbon nuclei. The absence of visible coupling between these nuclei is a result of their isochronous nature.

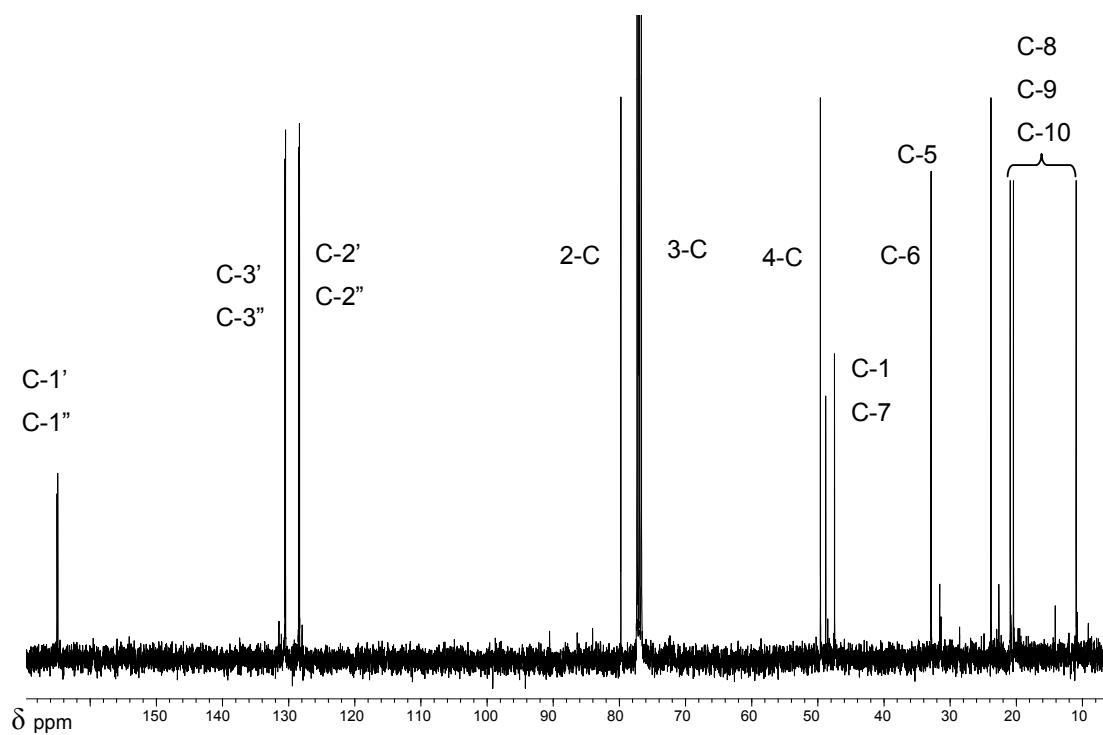


Figure 2.34: 100 MHz ^{13}C NMR spectrum of the diester **288** in CDCl_3 .

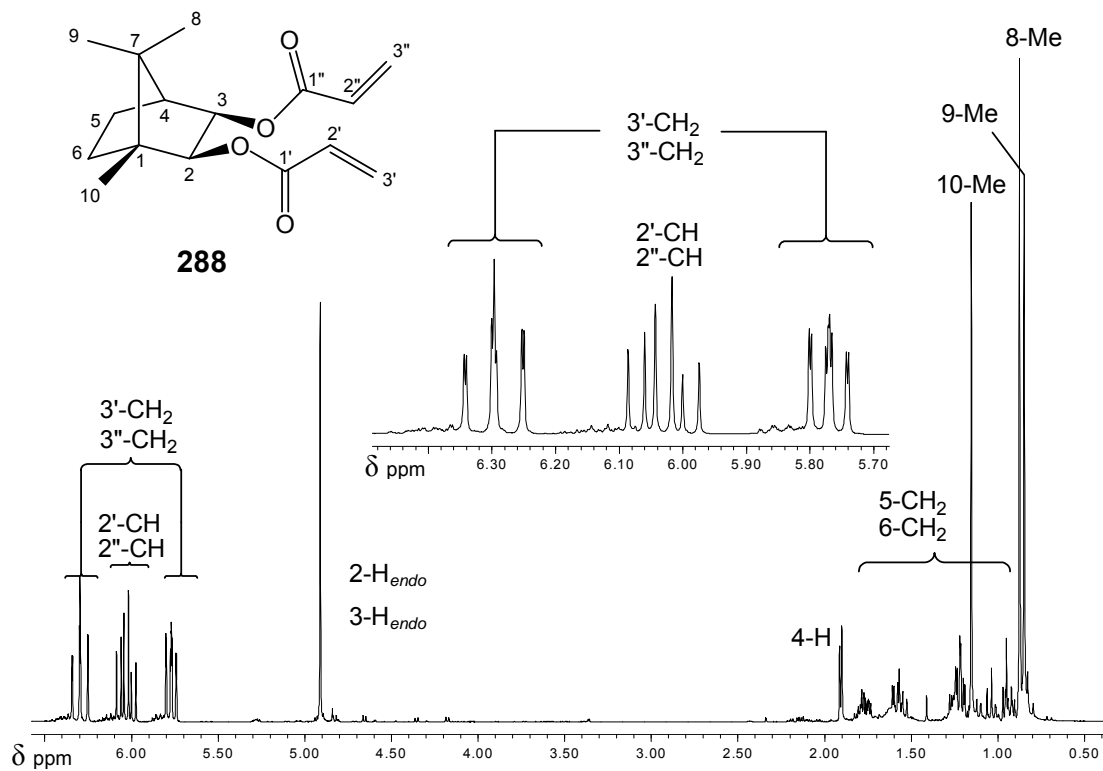


Figure 2.35: 400 MHz ^1H NMR spectrum, with expansion, of the diester **288** in purified CDCl_3 .

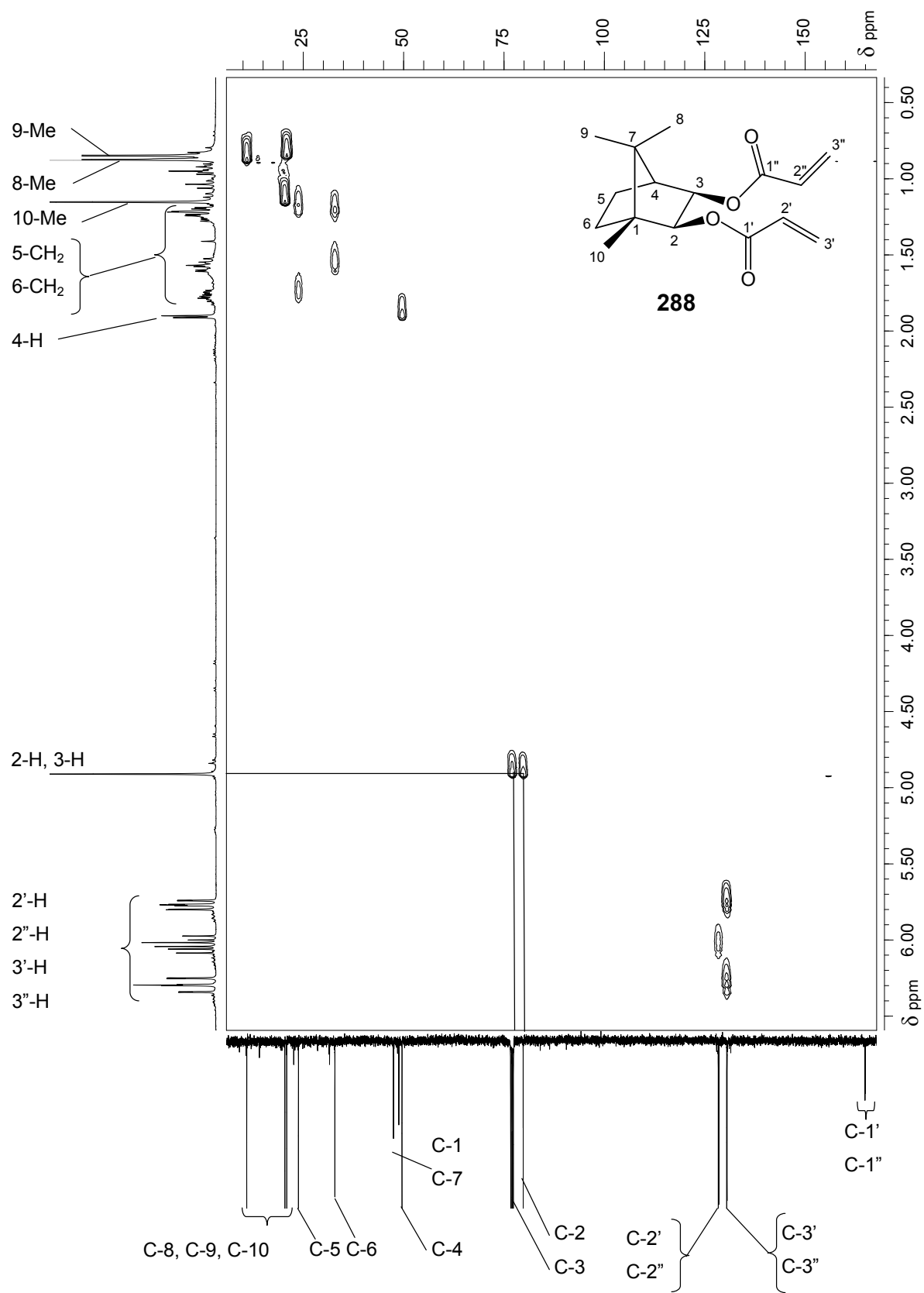


Figure 2.36: 400 MHz HMQC spectrum of the diester **288** in CDCl_3 .

Confirmation of the molecular composition was provided by HRCI mass spectrum analysis (**Figure 2.37**) which revealed a molecular ion at m/z 278.15199 corresponding to the molecular formula $C_{16}H_{22}O_4$ (calculated m/z 278.15181). The proposed fragmentation pathways are illustrated in **Figure 2.38**. Although fragmentation is described for the 3-acrylate ester moiety, analogous fragmentation of the 2-acrylate ester group is likely. Elimination of an acyl radical from the molecular ion affords the even-electron species **II**, which undergoes elimination of an H atom to form the odd-electron fragment **III** (or its keto tautomer). Correspondingly, homolytic fission α to the carbonyl of the molecular ion **I** results in the acylium ion **IX** with elimination of a 13-carbon radical. Fission of the *O*-alkyl-ester linkage eliminates an acrylate radical and affords the 2° carbocation **IV**, which may undergo a 1,2-hydride shift to give the resonance stabilized carbocation **V**. Elimination of an H atom from **V** then affords the odd electron species **VI**. Also shown in **Figure 2.38** are the fragments **VII** and **VIII**, which are characteristic of bornane systems,¹⁵⁶ together with structures **IX** and **X**, which have been tentatively assigned to the fragments responsible for peaks at m/z 152 and 123, respectively.

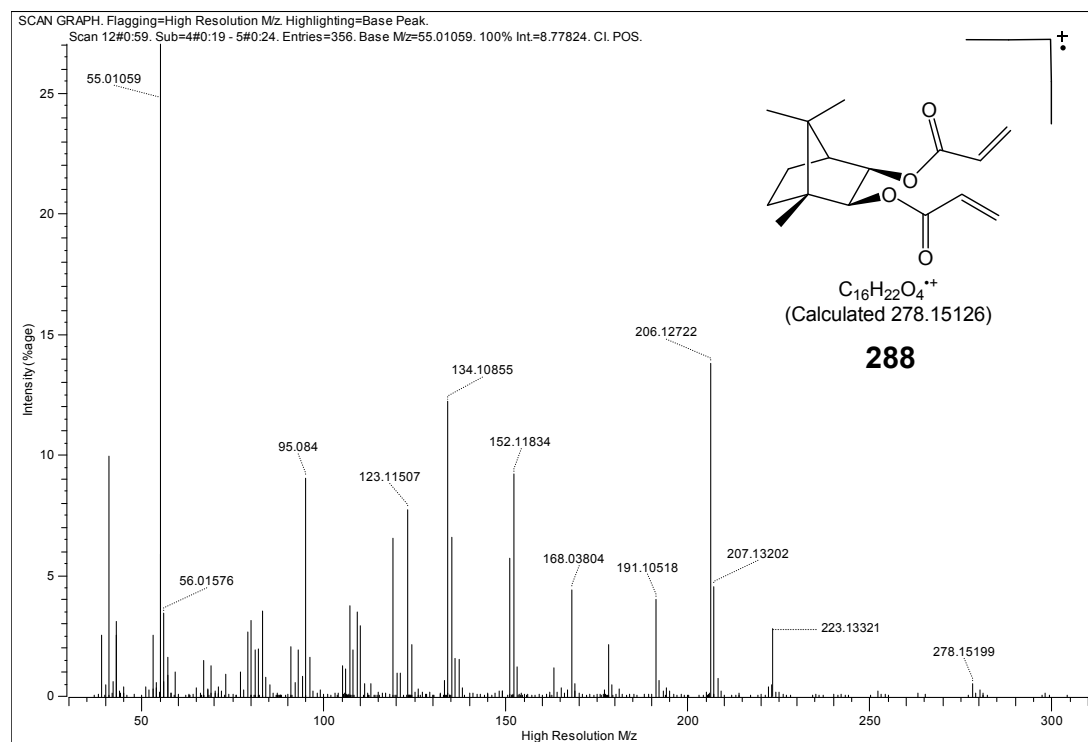


Figure 2.37: HRCI mass spectrum of the diester **288**.

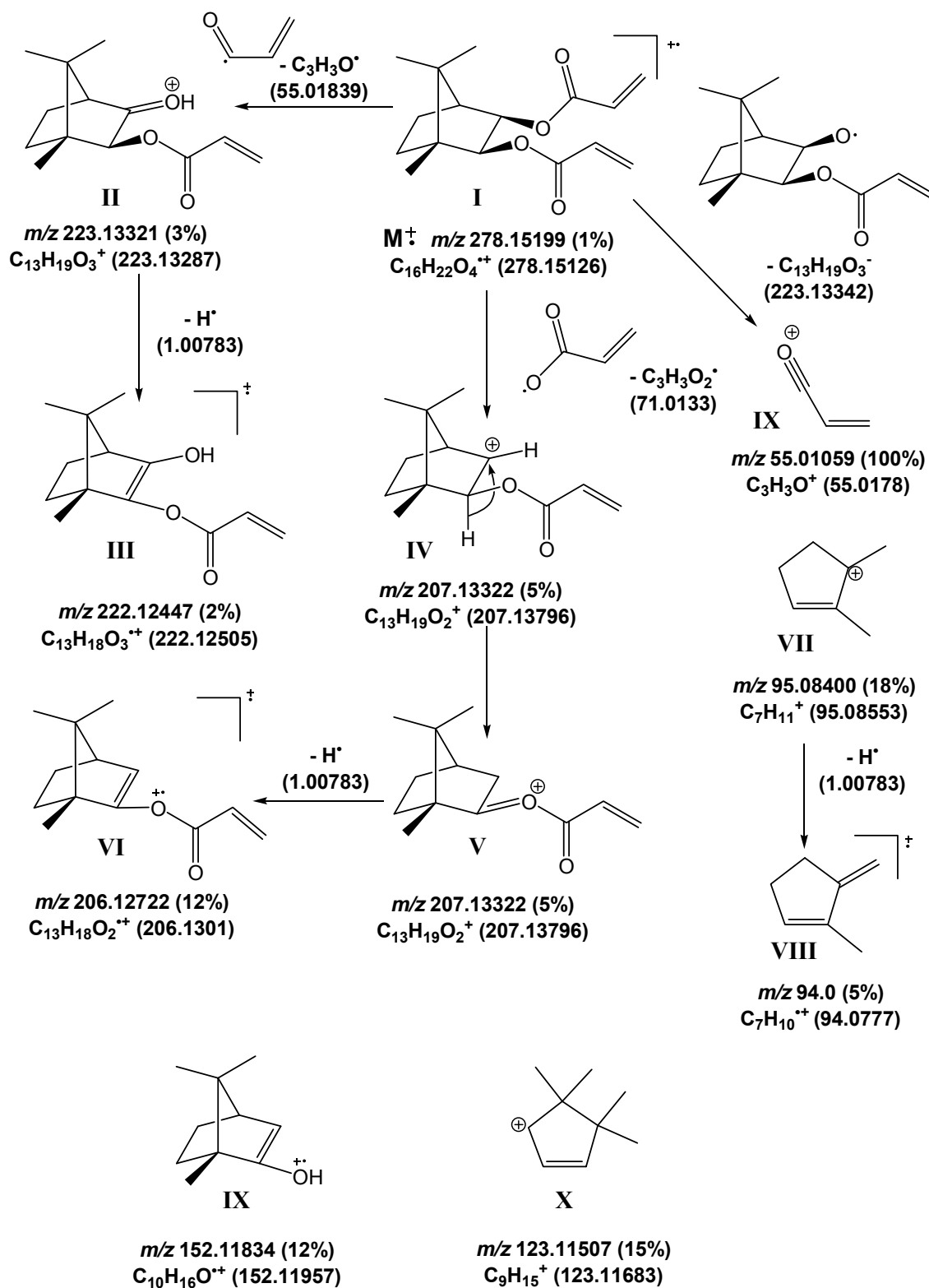
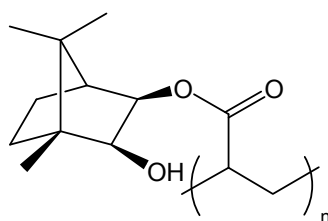


Figure 2.38: Mass spectrometric pathways for the fragmentation of diacrylate ester 288.

Mono-acylation of the diol **284** was expected to occur mainly, if not exclusively, at C-3, the steric effects of the 10-methyl group typically disfavoring reaction at C-2. Thus while formation of the 2-acylated analogue **287** seemed to provide an additional substrate for exploring asymmetric Morita-Baylis-Hillman products, its isolation as the *major* product was, initially, very surprising. During the optimization studies, it was observed that prolonged exposure of *purified* monoester fractions to heat, or high vacuum drying resulted in polymerization, whereas *impure* samples appeared far less likely to undergo polymerization. Incidentally, it was also noticed that the *pure* monoesters **285** or **287** were isolated as oils, whereas a *mixture* of the two compounds crystallised!

Polymerization of alkenes is known to occur by three mechanisms: radical, cationic and anionic.¹⁸³ The presence of the electron-withdrawing, anion-stabilizing ester groups, as well as the presence during the acylation reaction of a strong base (NaH or BuLi) suggested that polymerization follows the anionic pathway to products such as **289**. Consequently, hydroquinone was added as a polymerization inhibitor during the purification and storage of products. However, while the hydroquinone was found to minimize polymerization, removal of the black competitive oxidation products proved tedious, and it was found that, provided extreme care was taken to exclude heat, EtOAc (which was found to exacerbate polymerization) and prolonged drying, the polymerization was not a major problem.

**289**

Purification of crude reaction mixtures was effected on a chromatotron plate. The resolution was generally good (**Figure 2.39**), but NMR analysis revealed that “purified” fractions of monoester **285** inevitably contained significant quantities of the isomer **287**. This observation was paralleled in purified fractions of the monoester **287**, which were shown to contain the isomer **285**.

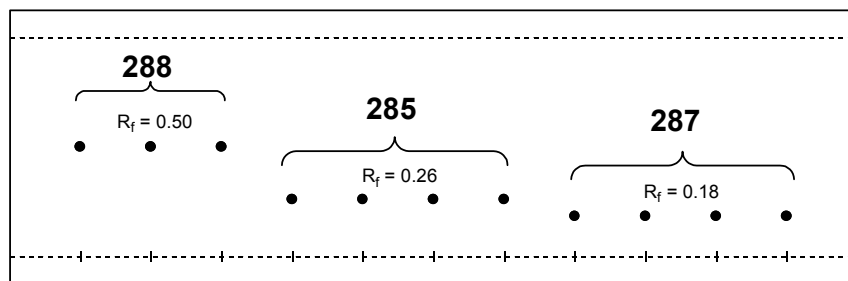
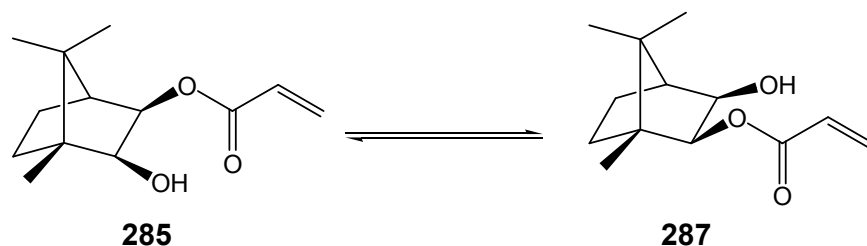


Figure 2.39: Representation of the TLC analysis following chromatotron separation of the acylation products **288**, **285** and **287** [hexane-EtOAc (7:3)].

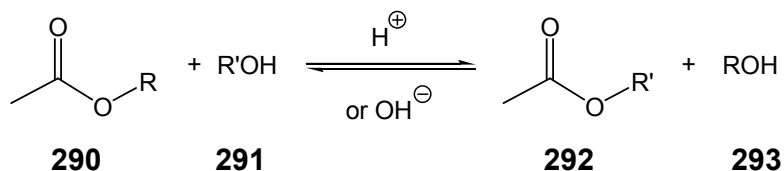
Initially, it was assumed that tailing or, perhaps, inadvertent errors were responsible for the contaminating ester in each case. However, ^1H NMR analysis of a sample of purified monoester **285** in CDCl_3 at 12 h intervals for 4 days revealed that the concentration of the monoester **285** decreased while the concentration of the isomer **287** increased until virtually equal amounts of the two isomers were present. It was thus concluded that transesterification was occurring between the isomeric esters **285** and **287** (Scheme 2.30)!



Scheme 2.30: Transesterification of monoesters **285** and **287**.

2.3.3 Kinetic Study of the Monoacrylate Ester Rearrangements.

Transesterification, a well known equilibrium reaction, which the chemical and pharmaceutical industries use in the production of organic ester intermediates,¹⁸⁴⁻¹⁸⁶ is achieved most frequently by acid or base catalysis (Scheme 2.31),^{136,187} although it has been known to occur under neutral conditions.¹⁸⁸ Acid catalysis involves protonation of the carbonyl oxygen, which results in a significantly more positive carbonyl carbon making it more susceptible to nucleophilic attack. Ester hydrolysis, and therefore transesterification, is also known to be catalyzed by metal ions.¹⁸⁶ The detailed transesterification mechanism was investigated by means of NMR-based kinetic¹⁸⁹⁻¹⁹⁹ and quantum mechanical computational studies.



Scheme 2.31: Transesterification Reaction.

Understanding the mechanism by which a reaction occurs involves, *inter alia*, knowledge of which bonds are broken, in what order, the number of steps involved and the relative rate of each step.¹³⁶ Although no mechanism can be considered to be known completely and absolutely, it is possible to determine, with reasonable accuracy, much of the information about a reaction sequence. Kinetic studies allow insight into the mechanism by which chemical change occurs and reveal details of the interaction of the reactant molecules. The reaction mechanism is validated only where experimentally determined data correspond to theoretical treatments of the reaction kinetics. The rate law of a reaction is a mathematical expression that is unique to that reaction and describes the dependence of the rate of reaction on the concentration of reactants and defines the number of steps of the reaction.²⁰⁰

In the present studies, preliminary investigations involved HPLC purification of a small quantity of each of the acrylates **285** and **287**, followed by NMR analysis of solutions in CDCl₃ over a period of time. The data so obtained showed that the acrylate esters were indeed undergoing transesterification and that complete equilibration was achieved after approximately five days.

It was also noted that although HPLC separation of the two compounds was virtually absolute, the compound ratio changed to *ca.* 80:20 within the time taken to remove solvent and set up the NMR experiment (*ca.* 2 h). This led to the obvious conclusion that the time delay between purification and analysis would have to be minimized. It was found, however, that on lowering the temperature of the pure compounds, to -78 °C (195 K), equilibration could be slowed to such an extent that the pure compounds could be stored for a number of days with only minimal change in composition. The only serious disadvantage of storing the pure compounds at reduced temperature became evident later, in that polymerization appeared to occur without warning. It has in fact been suggested that low temperature could be a contributing factor in initiating polymerization.²⁰¹ Consequently the experimental

methodology was fine-tuned to minimize equilibration prior to sample analysis, and initial compound ratios of $\geq 95:5$ were generally achieved at the beginning of the NMR analysis.

In order to obtain data that would permit elucidation of the mechanistic details, it was necessary to measure the rate at different temperatures and concentrations, with different solvents and in the presence or absence of a catalyst. **Figure 2.40** illustrates the flow diagram of the steps taken to purify the compounds and obtain the necessary data. While representative calculations, data and graphs are presented throughout this section, full details are to be found in the **Experimental Section 3.3** and **Appendix II (CD)**

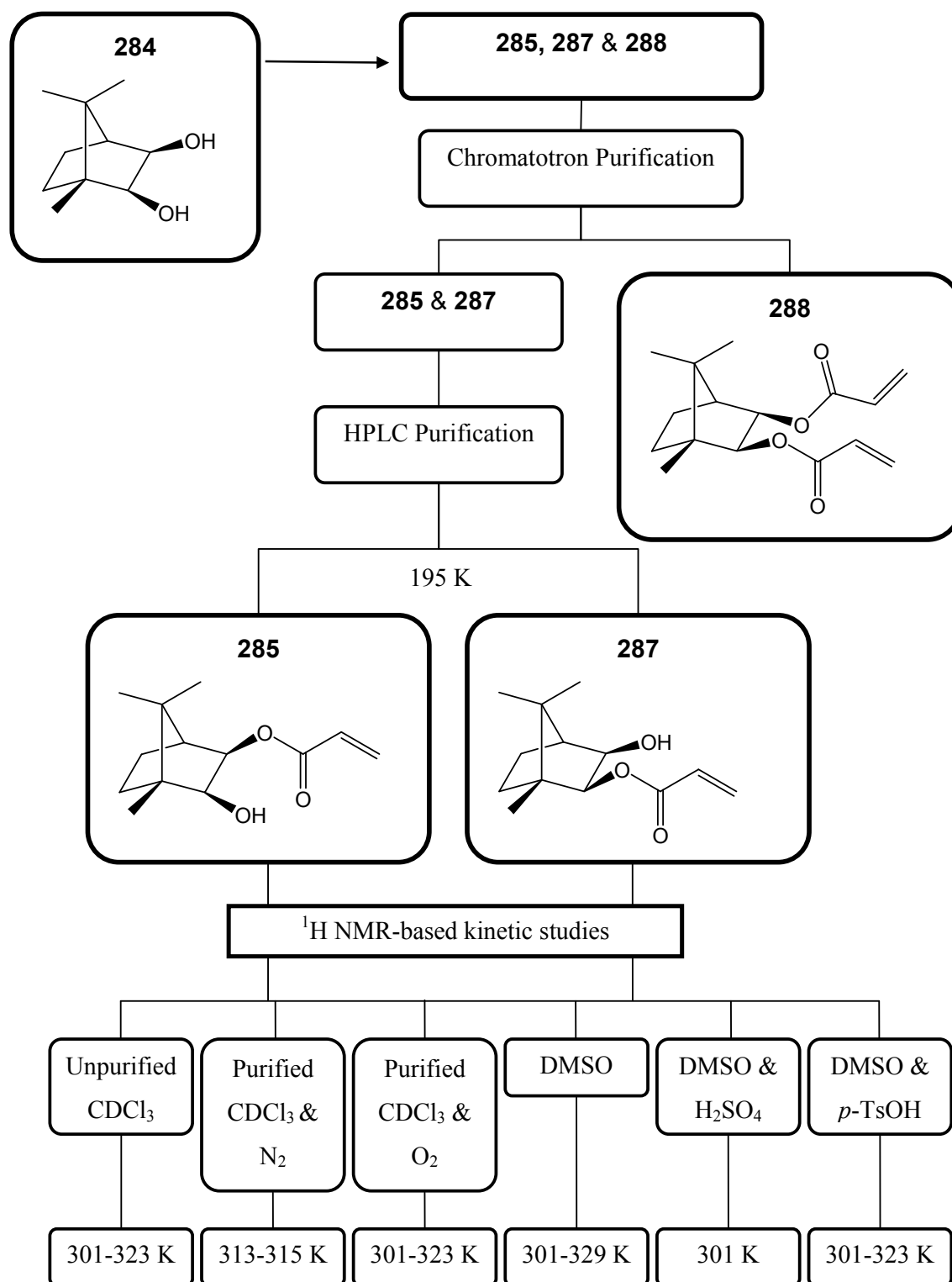


Figure 2.40: Flow diagram of the processes involved in the synthesis, purification and, where relevant, acquisition of kinetic data for the transesterification of the acrylate esters **285** and **287**.

2.3.3.1 Reaction of Acrylate Esters in Unpurified CDCl_3

One of the first complete kinetic experiments was performed on the monoester **285** in unpurified CDCl_3 at 323 K over a period of *ca.* 42 h, affording a total of 60 sequential ^1H NMR data sets. Analogous kinetic experiments were conducted, in the same unpurified CDCl_3 , using samples of the pure isomeric ester **287**, at temperatures ranging from 301 – 323 K, to obtain data for the calculation of kinetic and thermodynamic properties. Experiments in which CDCl_3 was used as solvent were conducted at temperatures which did not exceed 323 K as the solvent boils at 334 K. **Figure 2.41** illustrates the ^1H NMR spectrum of an equilibrium mixture of **285** and **287**.

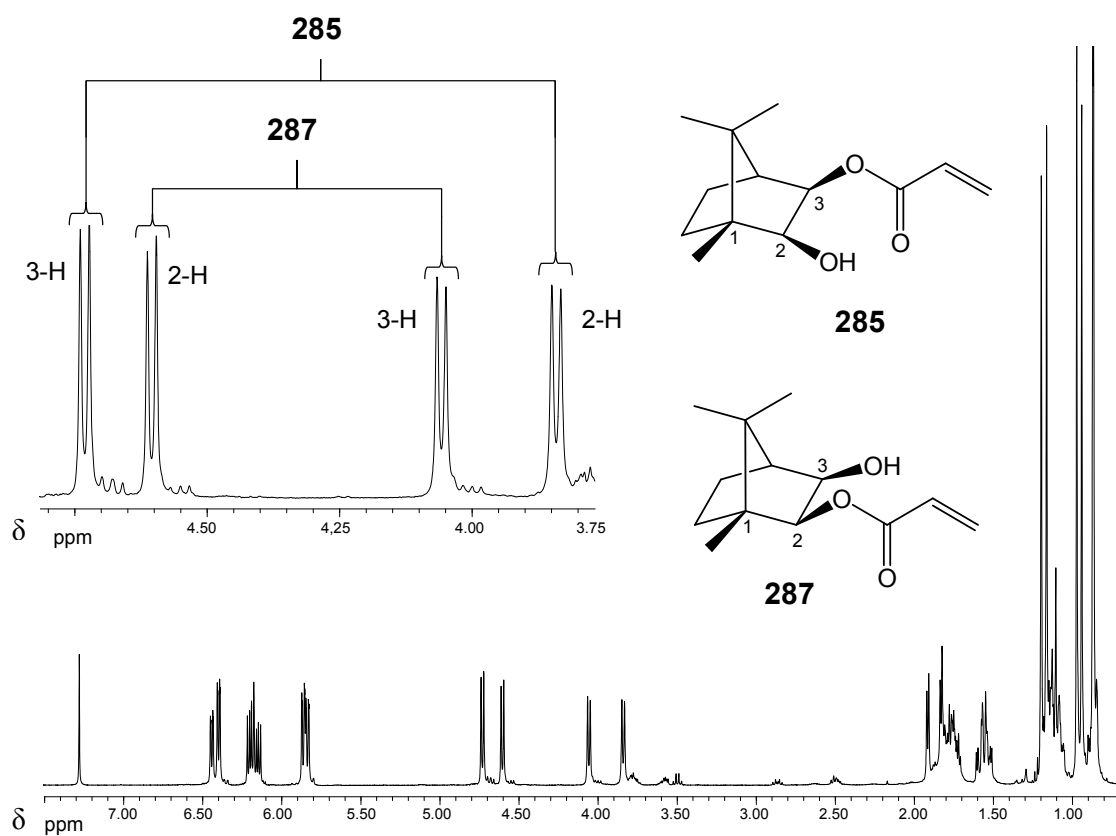


Figure 2.41: ^1H NMR spectrum at equilibrium, with expansion to show relevant peaks used to calculate the integral ratios of **285** and **287** (323 K; 400 MHz; unpurified CDCl_3).

The 2-H and 3-H signals of both compounds are well resolved and, in most instances, sufficiently distant from other signals, such that they proved to be excellent probes to monitor

the transesterification. The sum of the integral values of these two signals, in each compound, was used in all kinetic experiments, unless otherwise stated, for the determination of the ratios of the acrylates **285** and **287**.

The full ^1H NMR data sets obtained for each experiment were analyzed, using a specially developed automated programme²⁰² to process the F.I.D. data and to integrate the selected signals. A representative selection of the ^1H NMR data, for the equilibration from pure **285** at 323 K, is reproduced as a stack-plot in **Figure 2.42**. For the sake of clarity and due to the importance of these specific signals, only the 2-H and 3-H signals are shown. Although the data is perhaps not the most aesthetically pleasing of all the experiments completed, *i.e.* having only 90.4 % pure starting material, **285**, it was selected as the majority of the data was obtained in one unbroken kinetic run, only final equilibrium values being determined after several days. This was possible as the rate was the greatest of all the reactions examined, having been conducted at elevated temperature (323 K).

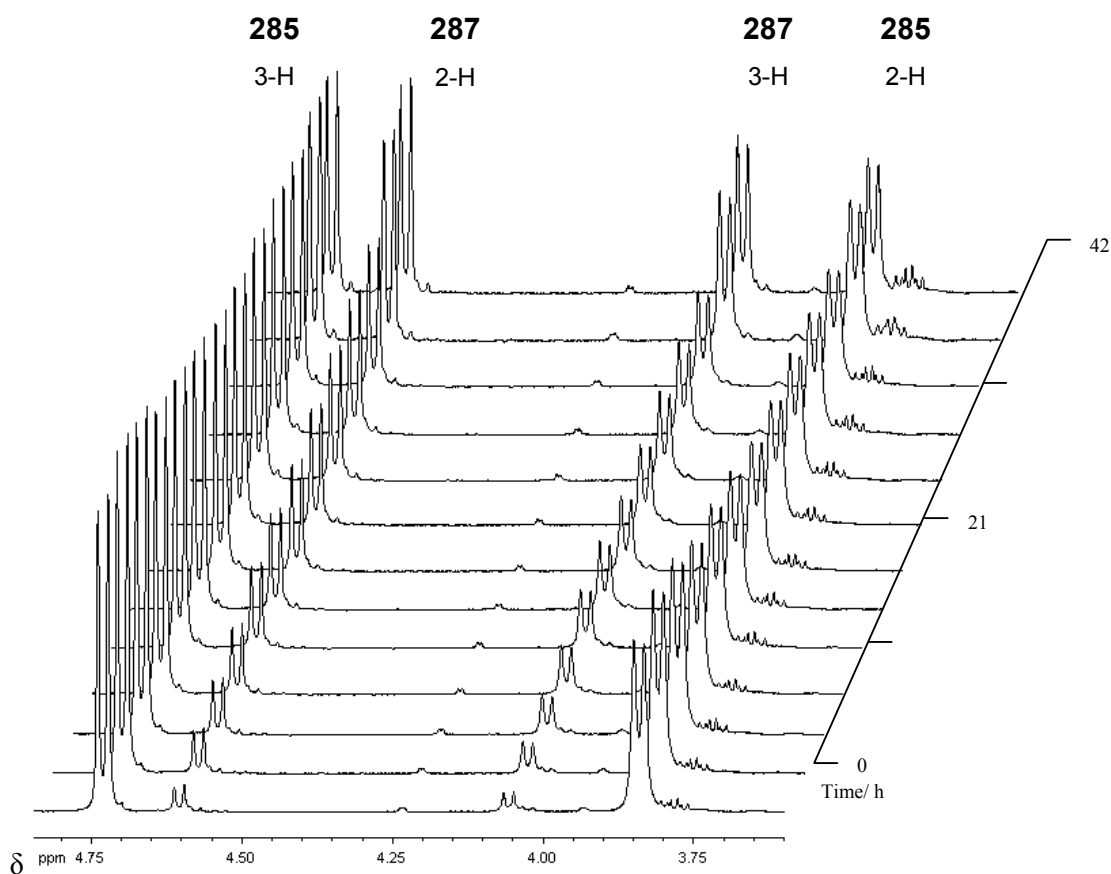


Figure 2.42: Stack-plot of partial 400 MHz ^1H NMR spectra recorded over 42 h, showing equilibration commencing with **285** at 323 K in unpurified CDCl_3 .

The integral ratios were then plotted against time to illustrate graphically the change in relative concentration of the two acrylate esters (**Figure 2.43**).

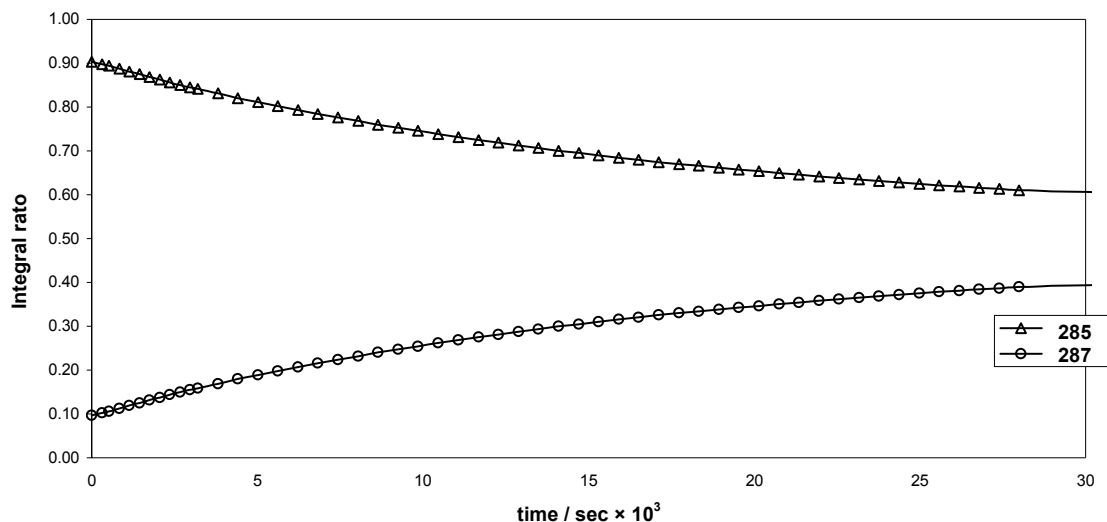
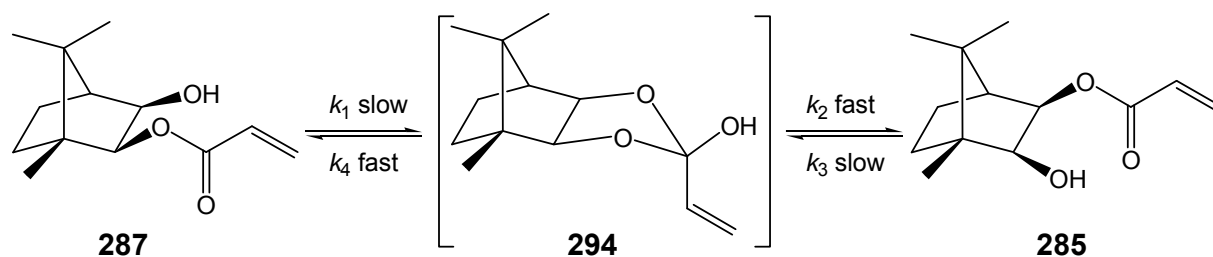


Figure 2.43: Plot of the integral ratios of the 2-H and 3-H signals of the corresponding acrylate esters **285** and **287** at 323 K in unpurified CDCl_3 .

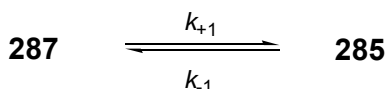
The graph demonstrates a smooth decline in the concentration of **285** and a correspondingly smooth increase in concentration of **287** to a point where there is no significant observable change in the relative concentrations of the isomeric esters. Additional data were obtained to determine the exact concentration ratios at equilibrium. This was achieved by placing the NMR tube, containing the reaction mixture, in a constant temperature water bath, at 323 K, immediately on termination of the kinetic run; ^1H NMR spectra were then recorded at regular intervals over a period of fourteen days. Once the integral ratio for the selected signals was relatively constant for a sustained time period (*ca.* 12h), equilibrium was deemed to have been established, and the equilibrium ratio was used to calculate the equilibrium constant K , as described below. The experimental data were found to fit a first-order reversible kinetic model,^{199,200,203,204} in which the forward and reverse reactions occur simultaneously. The rate of the reaction will change with time as it is proportional to the reactant concentration which decreases with time. The initial rate, which corresponds to the highest ratio of reactant to product, approximates to the rate of the forward reaction alone. However, in view of the great difficulty in obtaining *ca.* 95 % pure starting material (and the virtual impossibility of obtaining > 99 % pure material), the method of initial rates was not considered to be a satisfactory option.

The monoester **287** was arbitrarily defined as the starting material, as most of the reactions initially involved use of **287** as a starting compound; however, as the species are in dynamic equilibrium, either acrylate could have been defined as such. Assuming the intermediacy of a transient tricyclic species **294**, the overall process can be summarized as indicated in **Scheme 2.32**.



Scheme 2.32: Transesterification of monoesters **285** and **287**.

Since there was no *experimental* evidence for the presence of the intermediate **294**, it was assumed that, if involved at all, its existence was transient, *i.e.* once formed it would transform rapidly to **285** or **287**. Thus, while the formation of the intermediate **294** might be rate determining in the forward reaction ($k_1 \ll k_2$) and the reverse reaction ($k_3 \ll k_4$), its contribution to the rate equation can be ignored. Such assumptions are common in similar cases.¹³⁶ The reversible first order reaction can thus be represented by:



Where k_{+1} and k_{-1} are the rate constants for the forward and reverse reactions respectively, and the overall rate coefficient is the sum of the rate constants for the opposing reactions.

The rate of disappearance of **287** thus equals the rate of formation of **285** (**Equation 2.1**), while the equilibrium constant (K) is the quotient of the rate constants for the forward and reverse reactions (**Equation 2.2**). Algebraic combination of these equations, followed by integration affords the integrated rate equation for a reversible first order reaction (**Equation 2.3**), where $[\mathbf{287}]_0$ is initial concentration of **287** and $[\mathbf{287}]_{\text{eqm}}$ is the equilibrium concentration. This equation can then be expressed in the form, “ $y = mx + c$ ” (*i.e.* the equation for a straight line; **Equation 2.4**). This useful relationship permits the plotting of

graphs of $\ln ([287] - [287]_{\text{eqm}})$ versus t to give a straight line of slope $-(k_{+1} + k_{-1})$. **Equations 2.5 and 2.6** can then be used to determine the individual rate constants.

$$-\frac{d[287]}{dt} = \frac{d[285]}{dt} = k_{+1}[287] - k_{-1}[285] \quad (2.1)$$

$$K = \frac{[285]_{\text{eqm}}}{[287]_{\text{eqm}}} = \frac{k_{+1}}{k_{-1}} \quad (2.2)$$

$$\ln \frac{[287] - [287]_{\text{eqm}}}{[287]_0 - [287]_{\text{eqm}}} = -(k_{+1} + k_{-1})t \quad (2.3)$$

$$\ln ([287] - [287]_{\text{eqm}}) = -(k_{+1} + k_{-1})t + \ln ([287]_0 - [287]_{\text{eqm}}) \quad (2.4)$$

$$k_{+1} = \frac{k_{+1} - k_{-1}}{(1 + [287]/[285])} \quad (2.5)$$

$$k_{-1} = k_{+1} \left(\frac{[287]}{[285]} \right) \quad (2.6)$$

Of course, the same holds true for data in which **285** is the starting compound and the resulting graph for the equilibration of **285** at 323 K is shown in **Figure 2.44**. Following established methodology described by March¹³⁶ and Jordan,¹⁹⁹ as outlined above, the calculation of kinetic and thermodynamic data was undertaken.

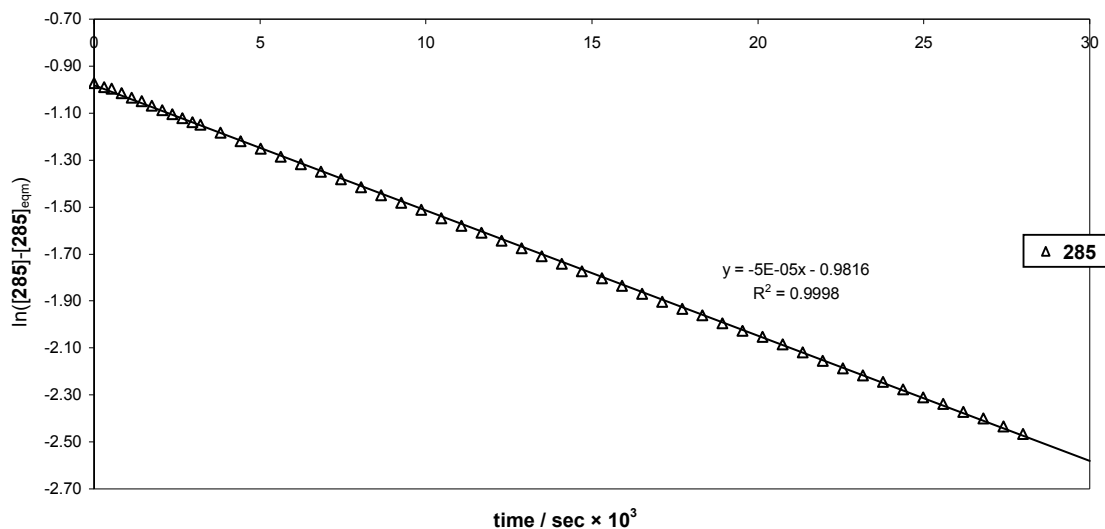


Figure 2.44: Plot of $\ln ([285]-[285]_{\text{eqm}})$ against time for the equilibration of acrylate esters **285** and **287** at 323 K in unpurified CDCl_3 .

The linear relationship ($r^2 = 0.9998$) clearly confirms the operation of a first order reversible reaction. Regression analysis of the data afforded the slope (-4.91×10^{-5}) and, hence from **Equation 2.4**, the sum of the forward and reverse rate constants, *i.e.*

$$k_{+1} + k_{-1} = 4.91 (\pm 0.07) \times 10^{-5}$$

Application of **Equations 2.5** and **2.6** permitted the determination of values for k_{+1} and k_{-1} .

$$k_{+1} = 2.58 (\pm 0.08) \times 10^{-5}$$

$$k_{-1} = 2.33 (\pm 0.05) \times 10^{-5}$$

Due to the nature of an equilibrium reaction, the respective rate constants (k_{+1} and k_{-1}) obtained from data using *either* starting material should be the same. To demonstrate this, the kinetic study at 323 K was repeated using pure **287** instead of **285** (**Table 2.4**). The data varied by $< 1\%$ from the mean of the experimentally determined values of k_{+1} and of k_{-1} confirming the validity of subsequent comparisons.

Table 2.4: Summary and comparison of kinetic data for the equilibration of the acrylate esters **285** and **287** in unpurified CDCl_3 at 323 K.

Expt.	Starting Compound	T/K	[287] _{eqm}	[285] _{eqm}	k_{+1}/k_{-1}	$k_{+1}+k_{-1}$ (s^{-1})	k_{-1} (s^{-1})	k_{+1} (s^{-1})
A8	287	323	0.47	0.53	1.11 (± 0.01)	5.00 (± 0.08) $\times 10^{-5}$	2.37 (± 0.02) $\times 10^{-5}$	2.63 (± 0.04) $\times 10^{-5}$
A9	285	323	0.47	0.53	0.90 (± 0.01)	4.91 (± 0.08) $\times 10^{-5}$	2.33 (± 0.05) $\times 10^{-5}$	2.58 (± 0.08) $\times 10^{-5}$

Information about the energetics of a reaction requires that the temperature dependence of the rate constant be determined.¹⁹⁹ Consequently, starting with “pure” **287**, the same general approach was followed to obtain kinetic data for the equilibration at different temperatures. The data obtained at 8 different temperatures, in the range, 301 – 323 K, are summarized in **Table 2.5**. Once kinetic experiments had been completed on several samples of **287**, determination of the activation energy (E_a) of the equilibrium reaction was possible by applying the Arrhenius equation (**Equation 2.7**) or its logarithmic form (**Equation 2.8**). The activation energy of a reaction is the energy in excess of that possessed by ground state molecules that is required for the reaction to proceed and is independent of temperature.

$$k = Ae^{E_a/RT} \quad (2.7)$$

$$\ln k = \frac{-E_a}{RT} + \ln A \quad (2.8)$$

In the equations, A is the frequency factor (a constant for a given reaction which relates to the relative orientation of the reactants and the rate of interaction of the reactive centres), R is the gas constant ($8.314 \times 10^{-3} \text{ kJ}^{-1} \text{ mol}^{-1}$) and T is the temperature (K). This relationship was used to plot graphs of $\ln k_{+1}$ and $\ln k_{-1}$ versus $1/T$, and the gradient E_a was obtained by linear regression analysis. A summary of the data for reactions using the monoester **287** is presented in **Table 2.5** and graphically illustrated for the forward and reverse reactions in **Figures 2.45** and **2.46**, respectively; the complete data sets can be found in the experimental (**Section 3.3.2**) and **Appendix II** (CD).

Table 2.5: Summary of the kinetic data for equilibration of the acrylate esters **285** and **287**, in unpurified CDCl_3 from pure **287** at different temperatures.

Expt.	T (K)	[287] _{eqm}	[285] _{eqm}	k_{+1}/k_1	$k_{+1}+k_1$ (s^{-1})	k_1 (s^{-1})	k_{+1} (s^{-1})	$\ln k_1$	$\ln k_{+1}$	1/T (K^{-1})
A1	301	0.47	0.53	1.15 (± 0.01)	$5.68 (\pm 0.03) \times 10^{-6}$	$2.64 (\pm 0.02) \times 10^{-6}$	$3.04 (\pm 0.05) \times 10^{-6}$	-12.8 (± 0.1)	-12.7 (± 0.2)	$3.32 (\pm 0.01) \times 10^{-3}$
A2	307	0.48	0.52	1.08 (± 0.01)	$9.96 (\pm 0.02) \times 10^{-6}$	$4.80 (\pm 0.04) \times 10^{-6}$	$5.16 (\pm 0.08) \times 10^{-6}$	-12.2 (± 0.1)	-12.2 (± 0.2)	$3.26 (\pm 0.01) \times 10^{-3}$
A3	313	0.49	0.51	1.04 (± 0.01)	$1.41 (\pm 0.01) \times 10^{-5}$	$6.92 (\pm 0.06) \times 10^{-6}$	$7.18 (\pm 0.10) \times 10^{-6}$	-11.9 (± 0.1)	-11.8 (± 0.2)	$3.19 (\pm 0.01) \times 10^{-3}$
A4	315	0.48	0.52	1.08 (± 0.01)	$2.27 (\pm 0.01) \times 10^{-5}$	$1.09 (\pm 0.01) \times 10^{-5}$	$1.18 (\pm 0.02) \times 10^{-5}$	-11.4 (± 0.1)	-11.3 (± 0.2)	$3.17 (\pm 0.01) \times 10^{-3}$
A5	317	0.47	0.53	1.11 (± 0.01)	$2.18 (\pm 0.01) \times 10^{-5}$	$1.03 (\pm 0.01) \times 10^{-5}$	$1.15 (\pm 0.02) \times 10^{-5}$	-11.5 (± 0.1)	-11.4 (± 0.2)	$3.15 (\pm 0.01) \times 10^{-3}$
A6	319	0.49	0.51	1.05 (± 0.01)	$3.75 (\pm 0.02) \times 10^{-5}$	$1.83 (\pm 0.01) \times 10^{-5}$	$1.92 (\pm 0.03) \times 10^{-5}$	-10.9 (± 0.1)	-10.9 (± 0.2)	$3.13 (\pm 0.01) \times 10^{-3}$
A7	321	0.48	0.52	1.09 (± 0.01)	$2.72 (\pm 0.01) \times 10^{-5}$	$1.30 (\pm 0.01) \times 10^{-5}$	$1.42 (\pm 0.01) \times 10^{-5}$	-11.3 (± 0.1)	-11.2 (± 0.1)	$3.12 (\pm 0.01) \times 10^{-3}$
A8	323	0.47	0.53	1.11 (± 0.01)	$5.00 (\pm 0.08) \times 10^{-5}$	$2.37 (\pm 0.02) \times 10^{-5}$	$2.63 (\pm 0.04) \times 10^{-5}$	-10.6 (± 0.1)	-10.5 (± 0.2)	$3.10 (\pm 0.01) \times 10^{-3}$

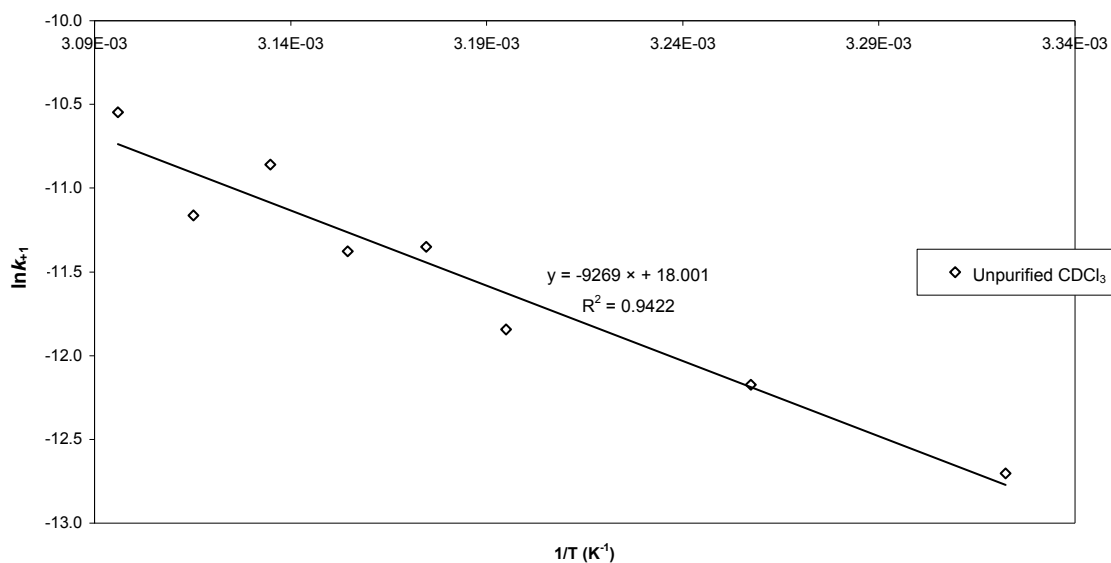


Figure 2.45: Plot of $\ln k_{+1}$ against $1/T$ for the forward reaction of the acrylate ester **287** in unpurified CDCl_3 .

Regression analysis of the data (**Table 2.5; Figure 2.45**) for the forward reaction gave:

$$E_{a287}/R = 9269 (\pm 868) \text{ K}$$

∴

$$E_{a287} = 77 (\pm 7) \text{ kJmol}^{-1}$$

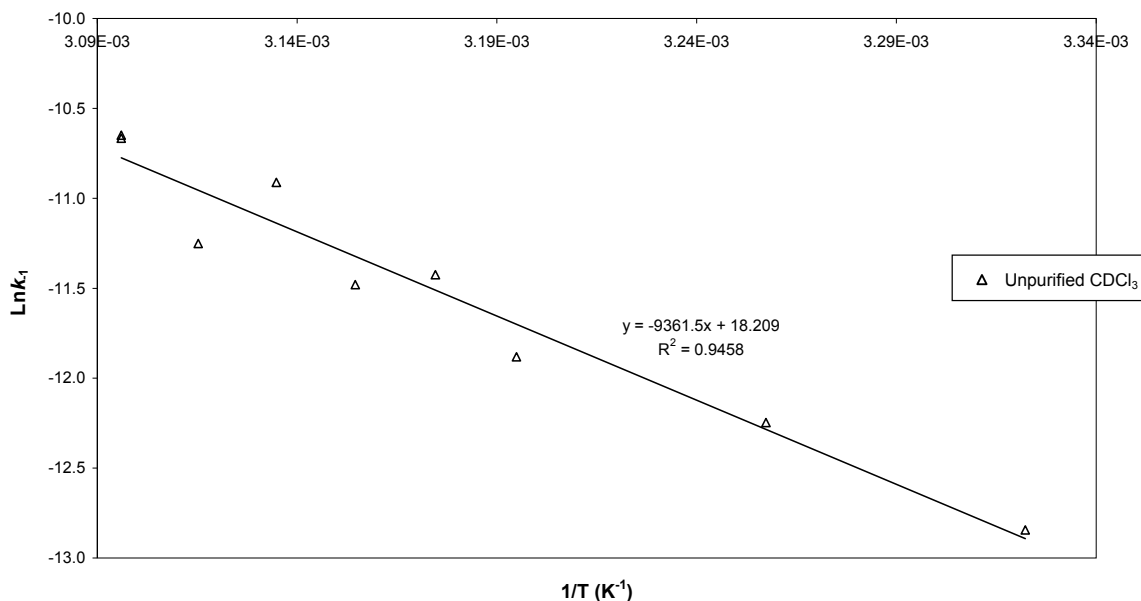


Figure 2.46: Plot of $\ln k_{-1}$ against $1/T$ for the reverse reaction of the acrylate ester **287** in unpurified CDCl_3 .

Similar treatment of the data (**Table 2.5; Figure 2.46**) for the reverse reaction, gave:

$$E_{a285}/R = 9361 (\pm 847) \text{ K}$$

∴

$$E_{a285} = 78 (\pm 7) \text{ kJmol}^{-1}$$

The enthalpy (ΔH^\ddagger), entropy (ΔS^\ddagger) and Gibbs free energy (ΔG^\ddagger) of activation for the formation of the activated (or transition state) complex in the forward and reverse reactions at 298 K were calculated using **Equations 2.9 – 2.12** and the results are summarized in **Tables 2.6 and 2.7**:

$$E_a = \Delta H^\ddagger + RT \quad (2.9)$$

$$\Delta H^\ddagger = E_a - RT \quad (2.10)$$

$$\frac{\Delta S^\ddagger}{19.15} = \log k - 10.753 - \log T + \frac{E_a}{19.15T} \quad (2.11)$$

$$\Delta G^\ddagger = \Delta H^\ddagger - T\Delta S^\ddagger \quad (2.12)$$

Table 2.6: Summary of kinetic and thermodynamic data for the activated complex of the reverse reaction, in unpurified CDCl₃, (298 K, 1 atm).

$-E_{a285}/R$ (K)	E_{a285} (kJmol ⁻¹)	ΔH^\ddagger_{285} (kJ)	k_{-1} (s ⁻¹)	ΔS^\ddagger_{285} (Jmol ⁻¹)	ΔG^\ddagger_{285} (kJmol ⁻¹)
-9361 (± 847)	78 (± 7)	76 (± 7)	$1.84 (\pm 0.11) \times 10^{-6}$	-363 (± 12.1)	183 (± 23)

Table 2.7: Summary of kinetic and thermodynamic data for the activated complex of the forward reaction, in unpurified CDCl₃, (298 K, 1 atm).

$-E_{a287}/R$ (K)	E_{a287} (kJmol ⁻¹)	ΔH^\ddagger_{287} (kJ)	k_{+1} (s ⁻¹)	ΔS^\ddagger_{287} (Jmol ⁻¹)	ΔG^\ddagger_{287} (kJmol ⁻¹)
-9269 (± 963)	77 (± 7)	75 (± 7)	$2.04 (\pm 0.12) \times 10^{-6}$	-362 (± 12)	182 (± 23)

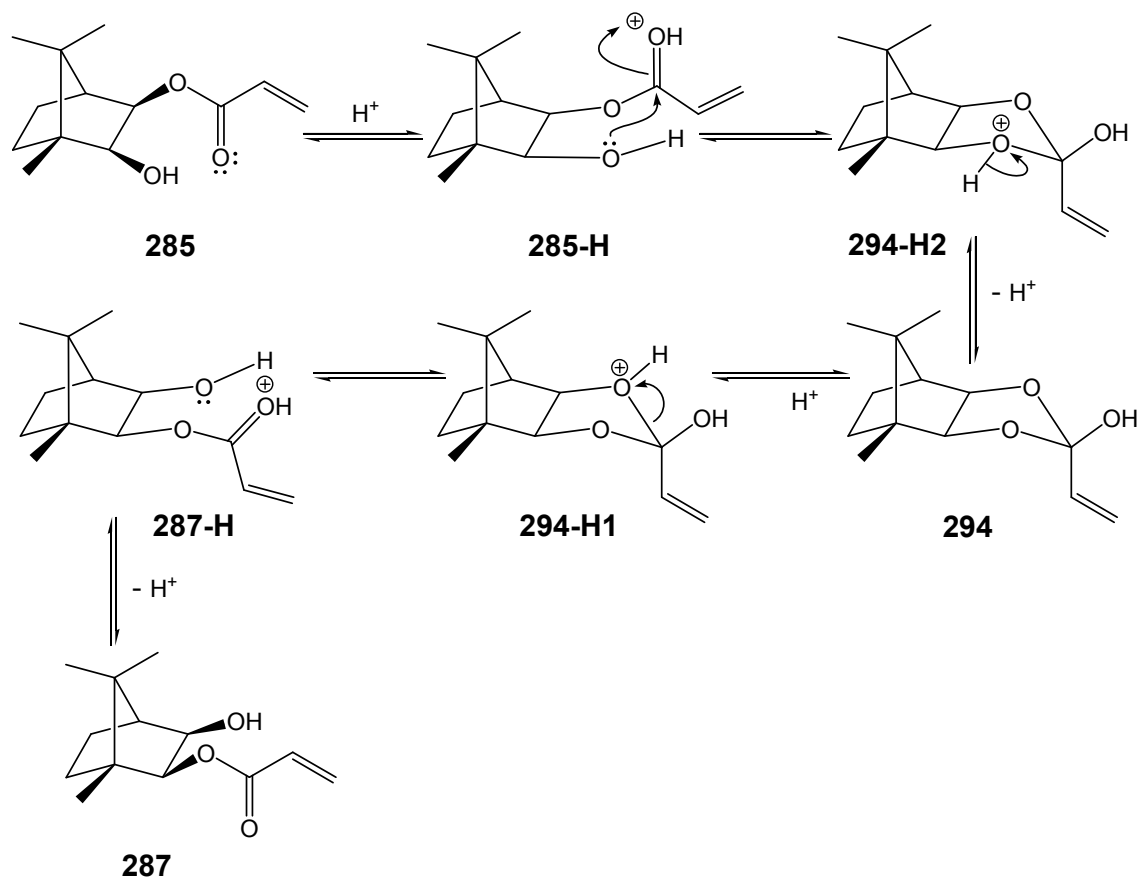
The results are consistent with first order reversible kinetics for which:

$$\text{rate} = k_{+1}[\mathbf{287}] = k_{-1}[\mathbf{285}]$$

At all temperatures, the rate of the forward reaction is slightly faster than the rate of the reverse reaction – a result consistent with the observed equilibrium concentrations and, hence, for values of the chemical equilibrium constant *K*. The large negative entropy changes for the formation of the activated complex (ΔS^\ddagger_{287} : -362 Jmol⁻¹; ΔS^\ddagger_{285} : -363 Jmol⁻¹) imply a decrease in entropy and, thus, an increase in order consistent with the formation of the transient cyclic intermediate **294** (Scheme 2.32). The activation energies for the forward and reverse reactions are very similar (E_{a287} , 77 kJmol⁻¹, E_{a285} , 78 kJmol⁻¹).

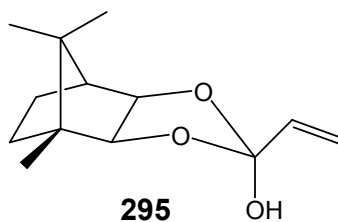
2.3.3.2 Reaction of the Acrylate Esters in Purified CDCl_3 under N_2

During the course of the foregoing experiments, it became apparent that DCl or HCl present in the CDCl_3 solution was probably responsible for catalyzing the reaction. Acidic impurities are known to develop on exposure of CDCl_3 to atmospheric conditions, such as air, light and water vapour.¹⁷¹ The possible role of an acid catalyst in the transesterification reactions was then investigated and a pathway was envisaged for the interconversion of the acrylate esters **285** and **287** (Scheme 2.33).^{136,205,206} Initially, the carbonyl oxygen of **285** is protonated by the acid catalyst giving **285-H**. This is followed by intramolecular attack at the electron-deficient carbonyl carbon affording intermediate **294-H2**. Proton loss results in the cyclized intermediate **294** which then gains a proton affording **294-H1**. Cleavage of the cyclic intermediate **294-H1** followed by deprotonation then affords the isomeric product **287**.



Scheme 2.33: Proposed acid-catalyzed transesterification of the acrylate esters **285** and **287**.

The possible involvement of diastereomeric cyclic intermediates **294** and **295** (in which the hydroxyl and vinyl groups are interchanged) was considered in the subsequent theoretical study (Section 2.3.2.3).



A preliminary study was conducted on a sample of the monoester **285**, in which the CDCl_3 had been purified by passing it through activated alumina and crushed 4 Å molecular sieves to remove practically all traces of HCl and H_2O .¹⁷¹ A solution of the sample in the purified CDCl_3 was prepared immediately and placed in a dry NMR tube under dry N_2 . The differences in the resulting ^1H NMR spectrum, as compared to that of the acrylate ester in unpurified CDCl_3 , were immediately apparent. The most significant signal changes for acrylate **285** are shown in **Figure 2.47** and summarized in **Table 2.8**. A similar procedure was employed using the isomeric ester **287** and the corresponding ^1H NMR spectra are shown in **Figure 2.48** and the data summarized in **Table 2.9**.

In the purified CDCl_3 additional coupling interactions became apparent in the ^1H NMR spectra of both monoesters. The hydroxylic and vicinal proton signals are slightly broadened due to an intermediate rate of exchange of the hydroxylic protons with free protons in the medium; the associated coupling constants are consequently somewhat inaccurate (**Tables 2.8** and **2.9**). Since the “purified” CDCl_3 was not *completely* free of acid impurities, exchange of the labile proton was still possible, although at a slower rate. The assumption throughout subsequent experiments was that slow exchange of labile protons is characterised by sharp hydroxylic signals and, conversely, that broad signals indicate the presence of free acid and the consequent rapid exchange of labile protons.¹⁷¹ The purification of CDCl_3 could thus be monitored and experiments were terminated or results disregarded if the line-shape of signals in the primary spectra was found to be significantly broadened. Slight modifications were made to improve the purification of the CDCl_3 . Small quantities were purified under a stream of N_2 by passage through neutral alumina and crushed 4Å molecular sieves in a dry Pasteur pipette directly into the NMR tubes, which had been pre-filled with N_2 . The modifications may seem minor, but excluding contact of the purified CDCl_3 with air resulted in far superior NMR spectra and the minimization of acid catalysis.

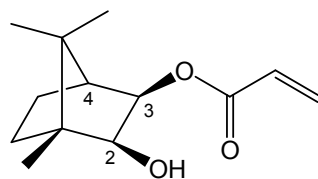
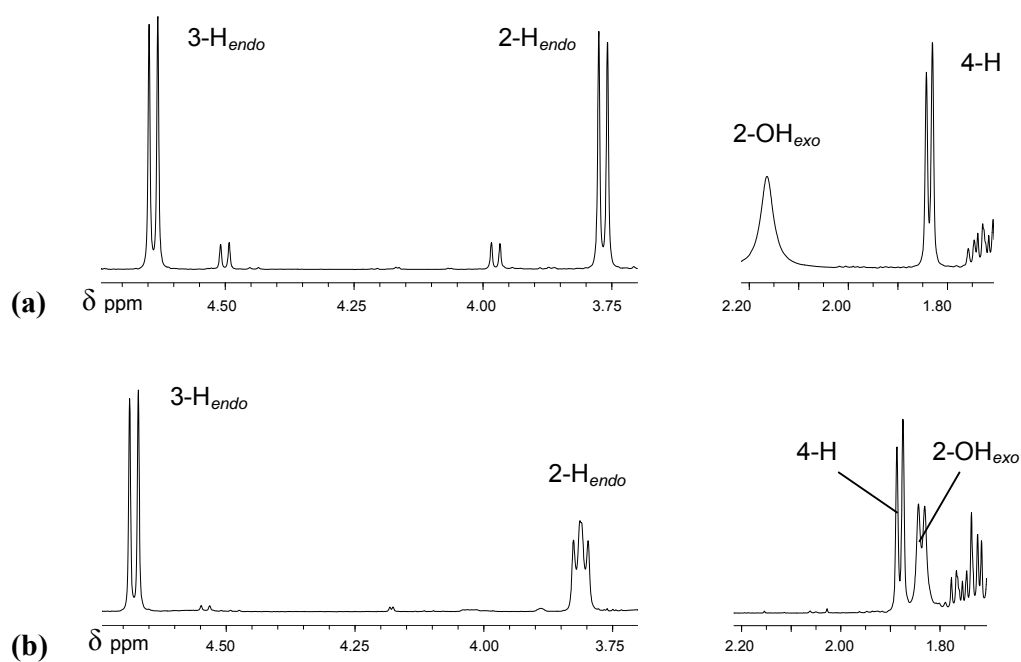
**285**

Figure 2.47: Comparison of selected signals in the 400 MHz ^1H NMR spectra of the monoester **285** at 301K in (a) unpurified CDCl_3 and (b) purified CDCl_3 .

Table 2.8: Comparison of 400 MHz ^1H NMR data for the monoester **285** at 301 K in unpurified and purified CDCl_3 .

285	Unpurified CDCl_3			Purified CDCl_3		
	2-OH	2- H_{endo}	3- H_{endo}	2-OH	2- H_{endo}	3- H_{endo}
Proton assignment	2-OH	2- H_{endo}	3- H_{endo}	2-OH	2- H_{endo}	3- H_{endo}
Chemical shift, δ_{H} (ppm)	2.16	3.76	4.64	1.84	3.81	4.68
Multiplicity	br s	d	d	d	dd ^a	d
Coupling Constants, J (Hz)	---	6.8	6.8	5.0 [†]	5.2 ^b ; 6.2 ^b	6.8

^a Incompletely resolved.

^b Values for coupling constants are approximate due to the lability of the hydroxide proton.

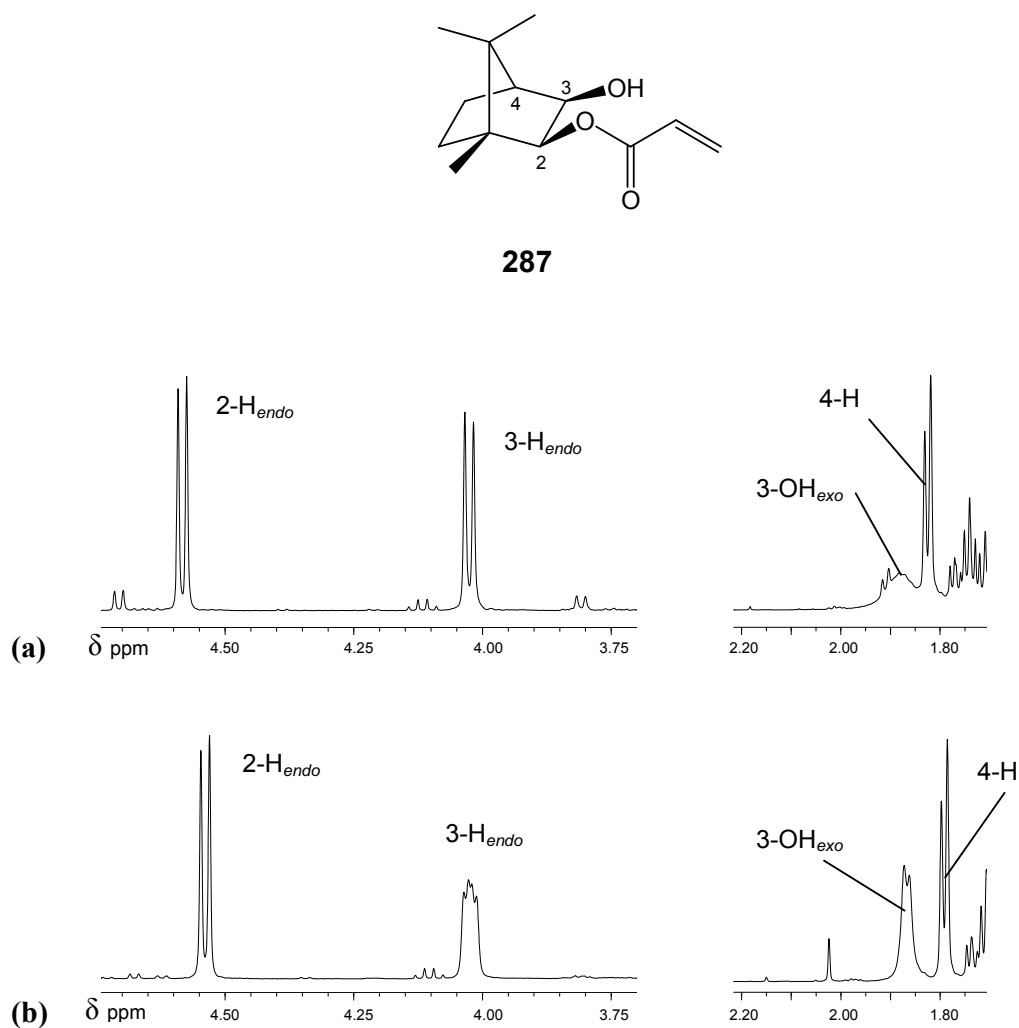


Figure 2.48: Comparison of selected signals in the 400 MHz ¹H NMR spectra of the monoester **287** at 301 K in (a) unpurified and (b) purified CDCl₃.

Table 2.9: Comparison of 400 MHz ¹H NMR data of the monoester **287** at 301 K in unpurified and purified CDCl₃.

287	Unpurified CDCl₃			Purified CDCl₃		
	3-OH	3-H _{endo}	2-H _{endo}	3-OH	3-H _{endo}	2-H _{endo}
Proton assignment	3-OH	3-H _{endo}	2-H _{endo}	3-OH	3-H _{endo}	2-H _{endo}
Chemical shift, δ_H (ppm)	1.88	4.02	4.58	1.87	4.02	4.54
Multiplicity	br s	d	d	d	dd ^a	d
Coupling Constants, J (Hz)	---	6.7	6.7	4.1 [†]	3.7 ^b ; 6.2 ^b	6.7

^a Incompletely resolved

^b Values for coupling constants are approximate due to the lability of the hydroxide proton.

A study was then conducted to determine the stability of the purified CDCl_3 under N_2 . The first part to the study related to the stability of the CDCl_3 in a sealed NMR tube over a period of 72 h at 301 K. A sample of the monoester **287** was then added and the ^1H spectrum was immediately recorded. The CDCl_3 was found to have remained relatively pure, as the line-shape of the hydroxylic proton was as sharp as or better than similar samples described previously. The second part of the study was to determine the stability of CDCl_3 at elevated temperature. Purified CDCl_3 was added to a sample of **287** in an NMR tube under N_2 . A ^1H NMR spectrum of the acrylate ester was immediately recorded at 305 K; the temperature was then raised in increments of 2 K and, following optimization of the shimming at each temperature, a further spectrum was obtained. This proceeded to a maximum temperature of 323 K over a period of 30 min. The sample was then allowed to cool to 301 K and a final spectrum was recorded. The resulting spectra are illustrated in **Figures 2.49** and **2.50**.

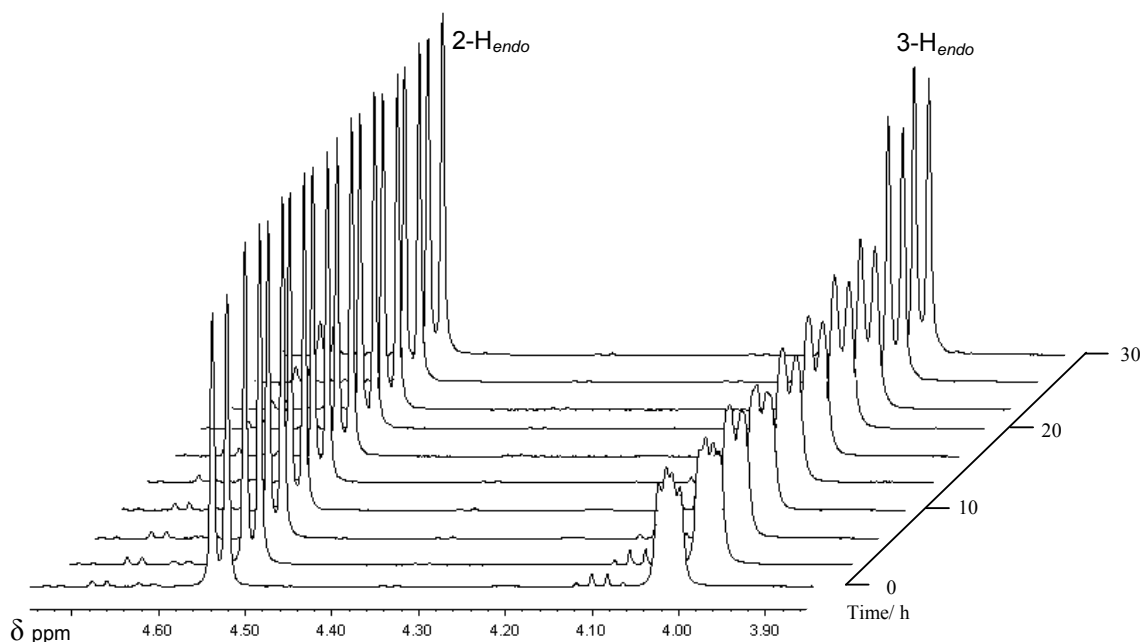


Figure 2.49: Partial 400 MHz ^1H NMR spectra showing the change in the 3- H_{endo} signal (δ 4.02 ppm) relative to the 2- H_{endo} (δ 4.53 ppm) signal of the acrylate ester **287** on warming (305 – 323 K; over 30 min) in purified CDCl_3 .

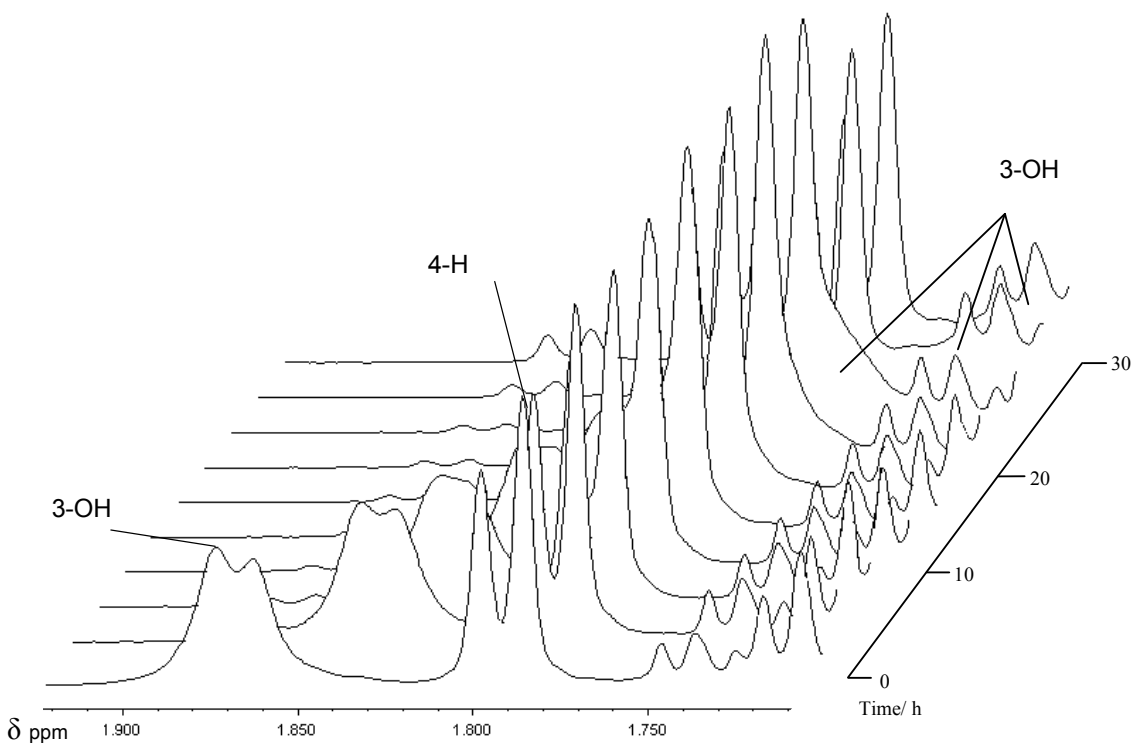


Figure 2.50: Partial 400 MHz ^1H NMR spectra showing coalescence and migration of the 3-OH signal (4.53 ppm) relative to the 4-H signal (1.79 ppm) of the acrylate ester **287** on warming (305 – 323 K; over 30 min) in purified CDCl_3 .

Thus on warming the solution of the acrylate ester **287** in purified CDCl_3 , the corresponding ^1H NMR spectra showed coalescence of the 3-H and 3-OH signals and a significant upfield shift of the 3-OH signal, the latter effect presumably indicating a reduction in intramolecular hydrogen bonding interactions at the higher temperatures. The concern was that, on warming, HCl would be generated, but on cooling the spectrum returned to its former sharp line-shape implying that HCl was not being generated to any great extent and that heating the solution was unlikely to induce acid catalysis.

In order to observe the effect of the acid catalysis and to obtain data for the transesterification under “neutral” conditions, the equilibration of **285** and **287** was repeated in “purified” CDCl_3 under N_2 at a range of temperatures (301 – 315 K). The treatment of the data was identical to that for the reactions in unpurified CDCl_3 , and the results are presented in **Tables 2.10** and **2.11**. The Arrhenius plot to determine E_a is illustrated in **Figure 2.51**.

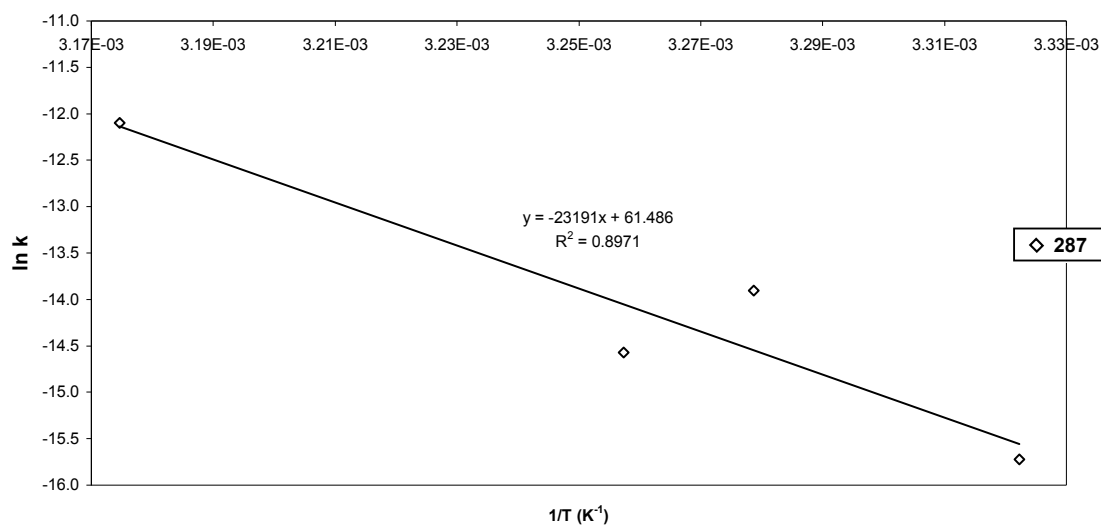


Figure 2.51: Plot of the Arrhenius relationship for the forward reaction of the monoester **287** in purified CDCl_3 .

Table 2.10: Summary of kinetic and thermodynamic data for the reverse reaction from the monoester **285**, in purified CDCl_3 , (298 K, 1 atm).

$-E_{a285}/R$ (K)	E_{a285} (kJmol^{-1})	ΔH^\ddagger_{285} (kJ)	k_{-1} (s^{-1})	ΔS^\ddagger_{285} (Jmol^{-1})	ΔG^\ddagger_{285} (kJmol^{-1})
- 23089 (± 5430)	192 (± 45)	189 (± 45)	7.2×10^{-8} ($\pm 0.4 \times 10^{-8}$)	-389 (± 70)	306 (± 127)

Table 2.11: Summary of kinetic and thermodynamic data for the forward reaction from the monoester **287**, in purified CDCl_3 , (298 K, 1 atm).

$-E_{a287}/R$ (K)	E_{a287} (kJmol^{-1})	ΔH^\ddagger_{287} (kJ)	k_{+1} (s^{-1})	ΔS^\ddagger_{287} (Jmol^{-1})	ΔG^\ddagger_{287} (kJmol^{-1})
- 23191 (± 5555)	193 (± 46)	190 (± 46)	8.0×10^{-8} ($\pm 0.4 \times 10^{-8}$)	-389 (± 72)	306 (± 130)

The values obtained for the rates of the forward and reverse reactions proved interesting. The forward rate constant, k_{+1} ($8.0 \times 10^{-8} \text{ s}^{-1}$), was again *ca.* 10 % greater than the rate constant for the reverse reaction, k_{-1} ($7.2 \times 10^{-8} \text{ s}^{-1}$). However, the rates of equilibration in unpurified CDCl_3 , k_{+1} ($2.04 \times 10^{-6} \text{ s}^{-1}$) and k_{-1} ($1.84 \times 10^{-6} \text{ s}^{-1}$) are of the order of 25 times greater than those in purified CDCl_3 . While fewer points and greater scatter ($R^2 = 0.8971$) in the Arrhenius

plot (**Figure 2.51**) mean increased uncertainty in the absolute values of the kinetic parameters, the overall patterns are clearly discernable. Thus, the activation energies [E_{a285} (192 kJmol⁻¹) and E_{a287} (193 kJmol⁻¹)] were basically the same for both compounds **285** and **287** and were significantly higher than for equilibration in unpurified CDCl₃ [E_{a285} (78 kJmol⁻¹) and E_{a287} (77 kJmol⁻¹)]. The enthalpies of activation in purified CDCl₃ [ΔH^\ddagger_{285} (189 kJ) and ΔH^\ddagger_{287} (190 kJ)] were also significantly greater than for the reaction in unpurified CDCl₃ [ΔH^\ddagger_{285} (76 kJ) and ΔH^\ddagger_{287} (75 kJ)] – a pattern repeated for the calculated free energies of activation [ΔG^\ddagger_{285} (306 kJmol⁻¹) and ΔG^\ddagger_{287} (306 kJmol⁻¹)] compared to those in unpurified CDCl₃ [ΔG^\ddagger_{285} (184 kJmol⁻¹) and ΔG^\ddagger_{287} (183 kJmol⁻¹)]. The observed increases in E_a , ΔH^\ddagger and ΔG^\ddagger clearly reflect the absence of acid catalysis in the reaction conducted in purified CDCl₃. Interestingly, the entropies of activation for both sets of reactions are comparable [ΔS^\ddagger_{285} (-389 Jmol⁻¹) and ΔS^\ddagger_{287} (-389 Jmol⁻¹)] compared to [ΔS^\ddagger_{285} (-363 Jmol⁻¹) and ΔS^\ddagger_{287} (-362 Jmol⁻¹)] in unpurified CDCl₃. This suggests that even in the absence of the acid catalyst, the activated complex for the transesterification possesses a similar degree of order.

These results show conclusively that the acidic impurity in unpurified CDCl₃ is responsible for catalyzing the reaction and increasing the rate of the reaction 25 fold, since the protonated species is far more likely to undergo intramolecular nucleophilic addition than the neutral substrate.

2.3.3.3 Reaction of Acrylate Esters in Purified CDCl₃ in Air

Several similar experiments were then performed between 313 and 323 K, using purified CDCl₃ in air to test the validity of running the experiments in purified CDCl₃ under N₂. Initially the reactions proceeded slowly, with rates similar to those observed using *purified* CDCl₃ under N₂. The rates then gradually increased over time (*e.g.* see **Figures 2.52** and **2.53**), becoming comparable to those in the reactions in *unpurified* CDCl₃, the general trend being the higher the temperature, the sooner the increase in the rate. The obvious conclusion is that catalytic, acidic impurities were being generated over time due to the degeneration of CDCl₃ in air, the higher the temperature the faster the generation of the acid. At higher temperatures (321 and 323 K; see experimental section), further rate acceleration was observed in the later stages of the reaction.

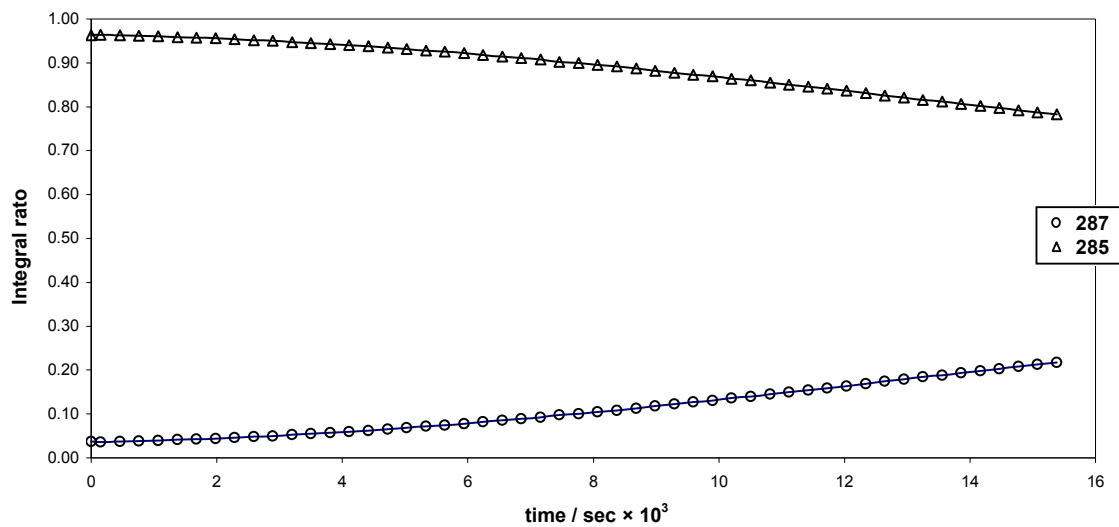


Figure 2.52: The ratio of the sum of the 2-H and the 3-H integrals of the acrylate esters **285** and **287** at 313 K in purified CDCl_3 in air.

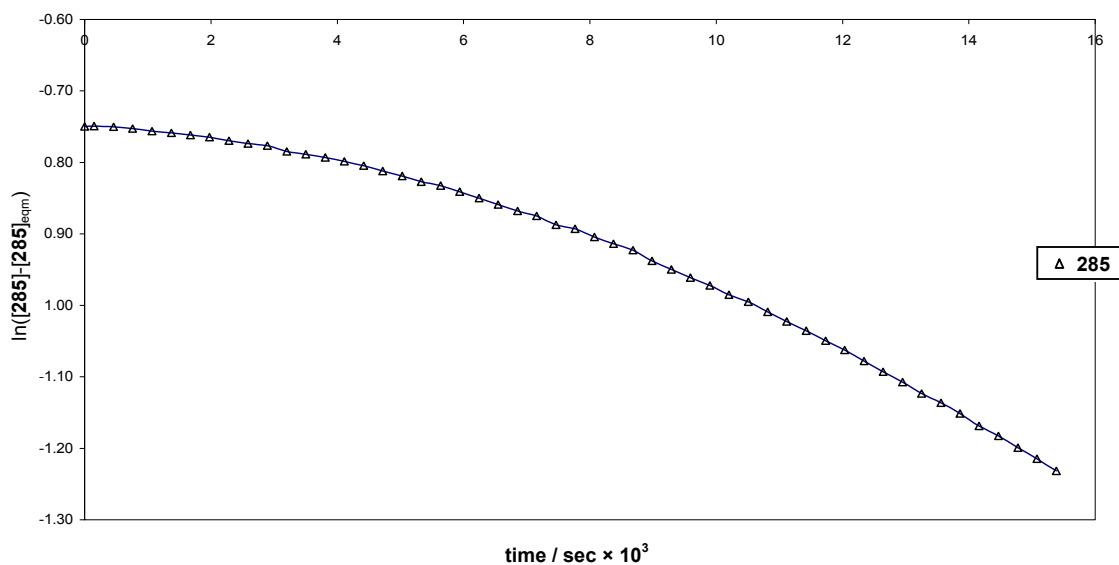


Figure 2.53: The logarithmic function of the integral ratio of the acrylate ester **285** at 313 K in purified CDCl_3 in air.

2.3.3.4 Reaction of Acrylate Esters in Purified DMSO- d_6

In further consideration of the effect of the solvent on the transesterification, it was decided to explore the use of DMSO- d_6 . This was expected to obviate the acidic complications observed with $CDCl_3$.¹⁸³

The DMSO- d_6 was purified by passage through neutral alumina and crushed 4 Å molecular sieves (to remove the H_2O invariably present) directly into a dry NMR tube containing the acrylate ester (**285** or **287**) which was then flushed with nitrogen. The methodology as described previously was followed and reactions were conducted at various temperatures in the range 301 – 329 K. Not surprisingly, chemical shifts for the compounds **285** and **287** in DMSO- d_6 were observed at somewhat different values from those in $CDCl_3$ (**Table 2.12**). In fact the 2-H, 3-H and 3-OH signals are all shifted downfield. Furthermore, the 2- and 3-H signals for the equilibrating esters are well resolved (**Figures 2.54** and **2.55**), permitting the course of the reaction to be readily monitored through comparison of the integrals of these signals (**Figure 2.56**) and, thus, the rate of reaction as well (**Figure 2.57**). The protons geminal to hydroxyl groups resonate as doublets of doublets in the DMSO- d_6 spectra of the two compounds, reflecting coupling in each case with the proton on the adjacent carbon as well as the hydroxyl proton.

Table 2.12: 400 MHz 1H NMR data of the isomeric acrylate esters **285** and **287** in DMSO- d_6 at 301 K.

	285			287		
Proton assignment	2- H_{endo}	3- H_{endo}	2-OH	3- H_{endo}	2- H_{endo}	3-OH
Chemical shift, δ_H (ppm)	3.59	4.65	4.97	3.79	4.53	4.87
Multiplicity	dd	d	d	dd	d	d
Coupling Constants,^a J (Hz)	2.2; 6.4	6.8	6.0	5.1; 6.6	6.7	5.0

^a Values are approximate.

The rate of equilibration was markedly slower than any of the previous experiments. In fact, no noticeable change was observed at lower temperatures; at 315 K the integral ratio change was less than 1 % over 12 h and less than 5 % over 11 h at 329 K. Consequentially, equilibrium was not achieved in any of the experiments over a three week period, precluding

estimation of the equilibrium integral ratios and, hence, calculation of reaction rates. It was observed that the samples, although stored under dry nitrogen in sealed NMR tubes, developed signals characteristic of H₂O over the three week period. This is attributed to the highly hygroscopic property of DMSO and imperfect sealing of the NMR tubes.

The slowness of equilibration in pure DMSO-*d*₆ is attributed to the absence of the acid impurities needed to catalyze the reaction and, possibly, solvation and hydrogen-bonding stabilization of the substrate.¹⁷¹

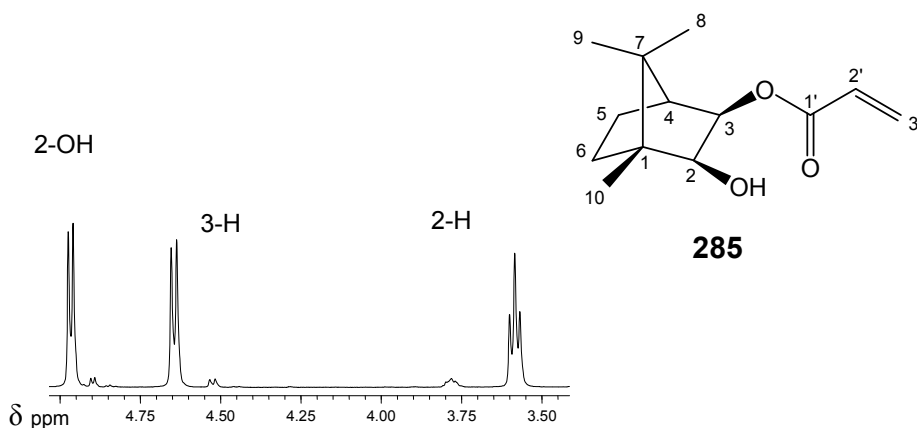


Figure 2.54: Partial 400 MHz ¹H NMR spectrum of the monoester **285** (301 K, purified DMSO-*d*₆).

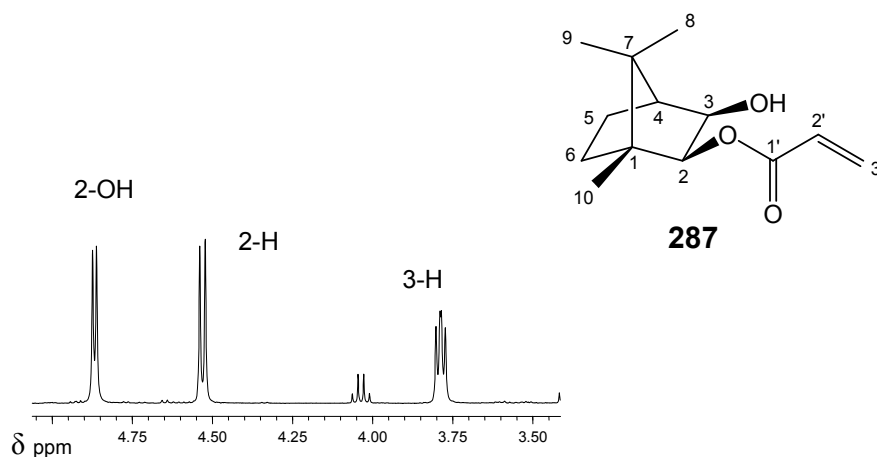


Figure 2.55: Partial 400 MHz ¹H NMR spectrum of the monoester **287** (301 K, purified DMSO-*d*₆).

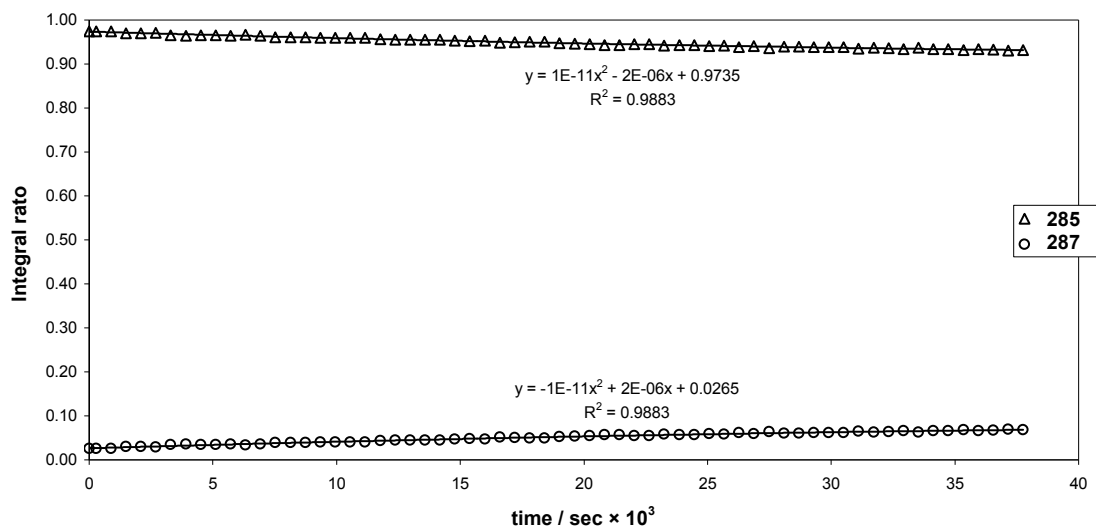


Figure 2.56: The ratio of the sum of the 2-H and the 3-H integrals for the acrylate esters **285** and **287** at 329 K in purified DMSO- d_6 .

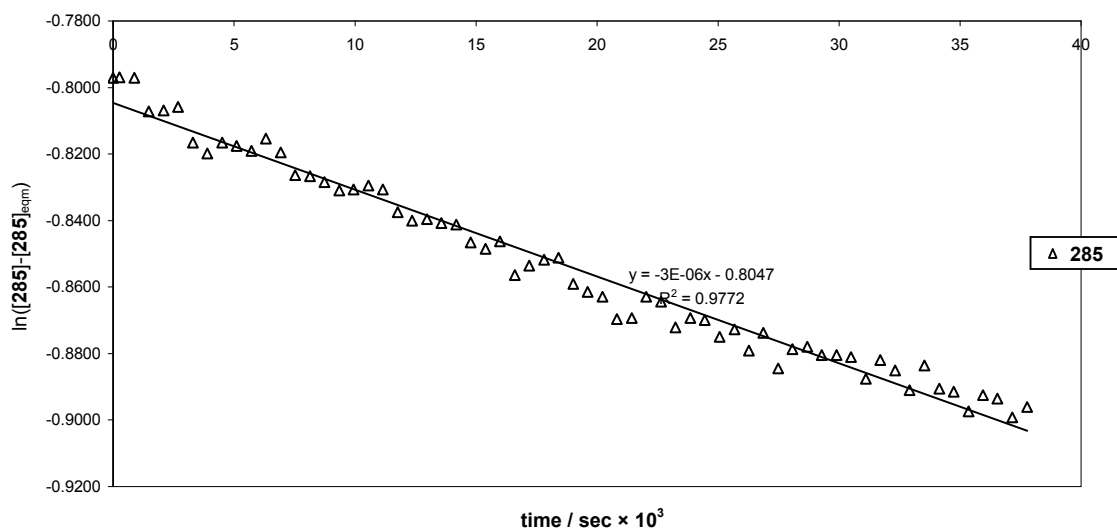


Figure 2.57: The logarithmic function of the integral ratio of the acrylate ester **285** at 329 K in purified DMSO- d_6 .

2.3.3.5 Reaction of Acrylate Esters in Purified DMSO- d_6 in the presence of H_2SO_4

Finally, based on the assumption that the transesterification is subject to acid catalysis, a preliminary reaction was carried out in DMSO- d_6 in the presence of a catalytic amount of concentrated H_2SO_4 (in place of the HCl/DCI present in $CDCl_3$). The 1H NMR spectrum of the mixture, at the beginning of a reaction, is shown in **Figure 2.58**.

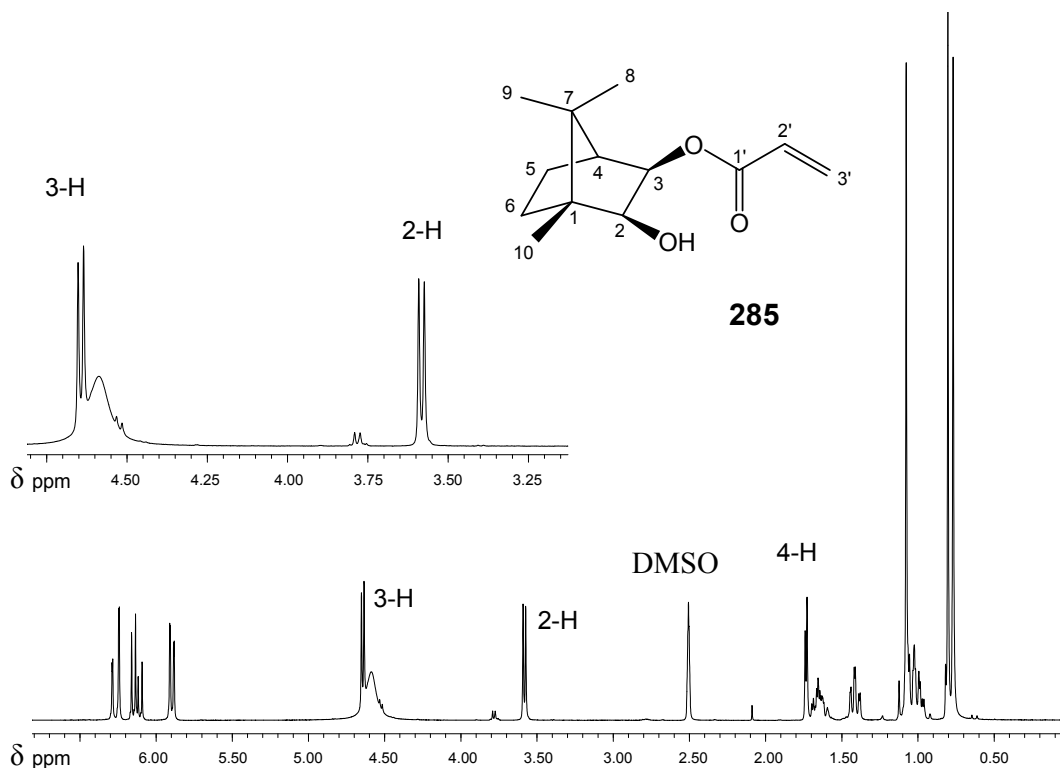


Figure 2.58: Initial 400 MHz 1H NMR spectrum, at 301 K, for the acrylate ester **285** in the presence of H_2SO_4 in purified DMSO- d_6 .

The introduction of H_2SO_4 causes the discrete hydroxylic proton signal to disappear, while a new, broad signal appears under the 3-H signal. The resulting overlap made it impossible to use the 3-H integral in the calculation of the integral ratios; instead integrals for the 2-H signal of **285** and the 3-H signal of **287** were used to calculate the integral ratios. The forward and reverse rates [$k_{+1} = 3.6 \times 10^{-6} s^{-1}$ and $k_{-1} = 3.1 \times 10^{-6} s^{-1}$; **Table 2.13**] for the reaction of the acrylate ester **285** at 301 K are approximately 15 % faster than results obtained at the same temperature in unpurified $CDCl_3$ [$k_{+1} = 3.04 \times 10^{-6} s^{-1}$ and $k_{-1} = 2.64 \times 10^{-6} s^{-1}$; **Table 2.5**, p. 126]. Clearly the H_2SO_4 accelerates the reaction and confirms that protonation is critical in the transesterification process. However, further investigations with concentrated H_2SO_4 were not attempted as significant degradation of the organic material was apparent.

Table 2.13: Rates of the equilibration of the acrylate esters **285** and **287**, in purified DMSO- d_6 in the presence of H₂SO₄ at 301 K.

k_{+1} (s ⁻¹)	k_{-1} (s ⁻¹)
$3.6 (\pm 0.3) \times 10^{-6}$	$3.1 (\pm 0.3) \times 10^{-6}$

2.3.3.6 Reaction of Acrylate Esters in Purified DMSO- d_6 in the presence of *p*-TsOH

An alternate acid catalyst to H₂SO₄ was consequently explored, *viz.*, *para*-toluenesulfonic acid (*p*-TsOH), as it is a milder acid than H₂SO₄, a solid (and thus easier to work with) and soluble in organic solvents. The *p*-TsOH was added to the sample in the NMR tube immediately after introduction of the purified DMSO- d_6 , and data acquisition was then commenced. The kinetic experiments were repeated at temperatures ranging from 302 – 323 K, and the initial ¹H NMR spectrum for the reaction at 301 K is presented in **Figure 2.59**.

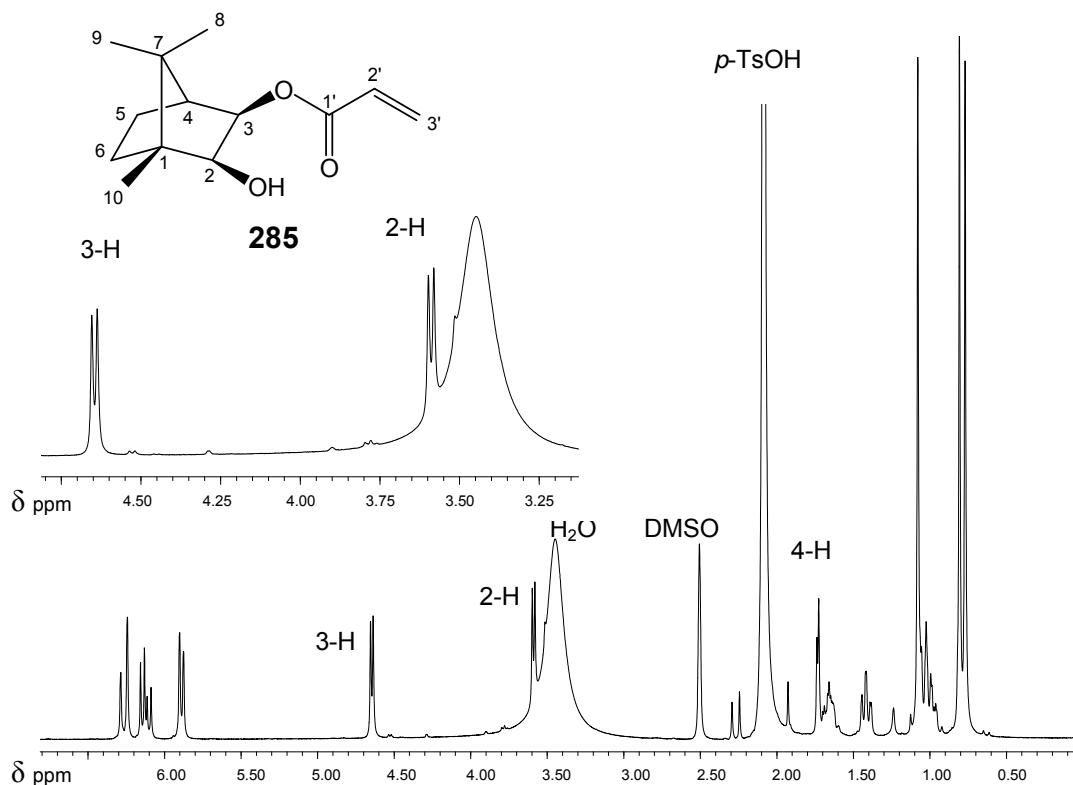


Figure 2.59: Partial initial 400 MHz ¹H NMR spectrum, at 301 K, of the acrylate ester **285** in the presence of *p*-TsOH in purified DMSO- d_6 .

Due to the overlap of a broad residual H₂O signal (from new commercially supplied *p*-TsOH and/or the highly hygroscopic DMSO-*d*₆) with the 2-H signal of **285**, the integral ratios, for all experiments, had to be calculated using the 3-H (for **285**) and the 2-H (for **287**) signals. Kinetic and thermodynamic parameters were calculated using data collected at different temperatures and are presented in **Tables 2.14** and **2.15**.

Table 2.14: Summary of kinetic and thermodynamic data for the “reverse” reaction from **285** in the presence of *p*-TsOH in DMSO-*d*₆ (298 K, 1 atm).

$-E_{a285}/R$ (K)	E_{a285} (kJmol ⁻¹)	ΔH^\ddagger_{285} (kJ)	k_{-1} (s ⁻¹)	ΔS^\ddagger_{285} (Jmol ⁻¹)	ΔG^\ddagger_{285} (kJmol ⁻¹)
- 13182 (± 2442)	110 (±20)	107 (± 20)	1.2×10^{-6} (± 0.1 × 10 ⁻⁶)	-367 (± 42)	216 (± 65)

Table 2.15: Summary of kinetic and thermodynamic data for the “forward” reaction from **287** in the presence of *p*-TsOH-DMSO-*d*₆ (298 K, 1 atm).

$-E_{a287}/R$ (K)	E_{a287} (kJmol ⁻¹)	ΔH^\ddagger_{287} (kJ)	k_{+1} (s ⁻¹)	ΔS^\ddagger_{287} (Jmol ⁻¹)	ΔG^\ddagger_{287} (kJmol ⁻¹)
- 13182 (± 2620)	109 (± 22)	107 (±21)	1.3×10^{-6} (± 0.1 × 10 ⁻⁶)	-365 (± 45)	216 (± 70)

The rate of the forward reaction, k_{+1} (1.3×10^{-6} s⁻¹) was *ca.* 8 % faster than the rate of the reverse reaction, k_{-1} (1.2×10^{-8} s⁻¹). The activation energies, E_{a285} (110 kJmol⁻¹) and E_{a287} (109 kJmol⁻¹), were the same within the limits of error for both compounds as were the free energies of activation [ΔG^\ddagger_{285} (306.3 kJmol⁻¹) and ΔG^\ddagger_{287} (305.8 kJmol⁻¹)]. Entropies and enthalpies of activation for the acrylate esters were indistinguishable [ΔS^\ddagger_{285} (-367 Jmol⁻¹) and ΔS^\ddagger_{287} (-365 Jmol⁻¹); ΔH^\ddagger_{285} (107.1 kJ) and ΔH^\ddagger_{287} (106.9 kJ)].

2.3.3.7 Comparison of Kinetic Data for Transesterification in Different Media

Arrhenius plots and the comparative kinetic data obtained for the forward and reverse reactions of the acrylate ester **287** in different media are summarized in **Tables 2.16** and **2.17**, respectively, and illustrated in **Figure 2.60**.

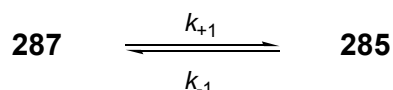
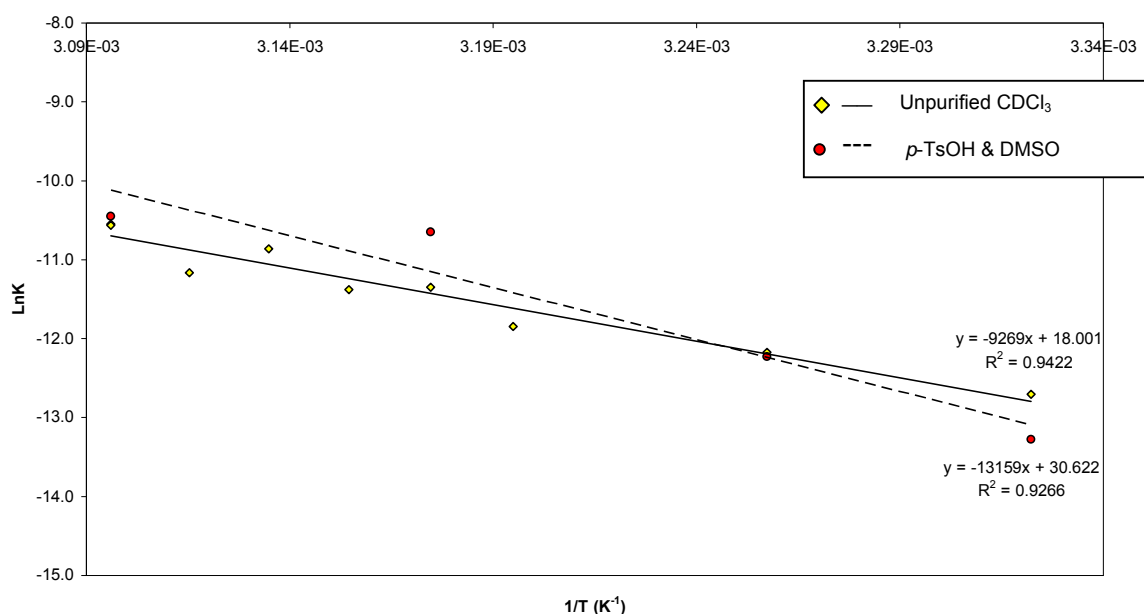


Table 2.16: Comparative kinetic and thermodynamic data for the forward reaction of the acrylate ester **287** (298 K, 1 atm).

	$-E_{a287}/R$ (K)	E_{a287} (kJmol ⁻¹)	ΔH^\ddagger_{287} (kJ)	k_{+1} (s ⁻¹)	ΔS^\ddagger_{287} (Jmol ⁻¹)	ΔG^\ddagger_{287} (kJmol ⁻¹)
Unpurified CDCl ₃	-9361 (± 868)	77 (± 7)	75 (± 7)	$2.0 (\pm 0.1) \times 10^{-6}$	-362 (± 12)	182 (± 23)
Purified CDCl ₃	-23191 (± 5555)	193 (± 46)	190 (± 46)	$8.0 (\pm 0.4) \times 10^{-8}$	-389 (± 72)	306 (± 130)
DMSO- <i>d</i> ₆ & <i>p</i> -TsOH	-13159 (± 2620)	109 (± 22)	107 (± 21)	$1.3 (\pm 0.1) \times 10^{-6}$	-365 (± 45)	216 (± 70)

Table 2.17: Comparative kinetic and thermodynamic data for the reverse reaction of the acrylate ester **285** (298 K, 1 atm).

	$-E_{a285}/R$ (K)	E_{a285} (kJmol ⁻¹)	ΔH^\ddagger_{285} (kJ)	k_{-1} (s ⁻¹)	ΔS^\ddagger_{285} (Jmol ⁻¹)	ΔG^\ddagger_{285} (kJmol ⁻¹)
Unpurified CDCl ₃	-9361 (± 847)	78 (± 7)	75 (± 7)	$1.8 (\pm 0.1) \times 10^{-6}$	-363 (± 12)	183 (± 23)
Purified CDCl ₃	-23089 (± 5430)	192 (± 45)	189 (± 45)	$7.2 (\pm 0.4) \times 10^{-8}$	-389 (± 70)	306 (± 127)
DMSO- <i>d</i> ₆ & <i>p</i> -TsOH	-13182 (± 2442)	110 (± 20)	107 (± 20)	$1.2 (\pm 0.1) \times 10^{-6}$	-367 (± 42)	216 (± 65)

**Figure 2.60:** Arrhenius plots for the forward reaction of acrylate ester **287** in different media.

In all cases, the rate of the forward reaction, k_{+1} , is *ca.* 10 % faster than that for the reverse reaction, k_{-1} . The rate of the reaction is influenced by the medium, increasing in the order: - DMSO- d_6 § < purified CDCl₃ < DMSO- d_6 with *p*-TsOH < unpurified CDCl₃ < DMSO- d_6 with H₂SO₄ ‡. The activation energies, E_a , for both compounds, in a given medium, are very similar as are the activation parameters ΔH^\ddagger , ΔG^\ddagger and ΔS^\ddagger . The entropy of activation, ΔS^\ddagger , was negative in all instances and comparable in magnitude.

In summary it is evident that the experimentally determined kinetic data is consistent with:

- i) first order forward and reverse reactions occurring concurrently;
- ii) acid catalysis of the process;
- iii) marginal dominance of the forward reaction (*i.e.* $k_{+1} > k_{-1}$); and
- iv) the mechanistic sequence outlined in **Scheme 2.32** (p. 122).

In the next phase of the investigation, a computational study was undertaken to examine the mechanistic details concerning the existence of suspected intermediates and thus the most likely pathway for the transesterification process.

§ Although rate constants could not be obtained in DMSO- d_6 alone, the comparison is based on the extreme slowness of the observed reactions.

‡ The rate was the fastest, but decomposition of the monoesters precluded accurate data acquisition for the equilibrium reaction.

2.3.4 Computational Study of the Transesterification of the Acrylate Esters.

The NMR studies of the transesterification of the acrylate esters **285** and **287** provided kinetic and thermodynamic data for the reaction and, in an attempt to obtain further insights into the mechanism, a computational study of the reaction was undertaken.

The experimental data had indicated that transesterification may occur under both neutral (albeit very slowly) and acid-catalyzed conditions. Pathways involving the likely intermediates were explored using Gaussian-03²²³ at the density functional theory (DFT) level with the basis set, B3LYP/6-311+G(d). This particular approach is considered to be one of the more accurate and, additionally, is fairly cost effective, time-wise.²⁰⁷

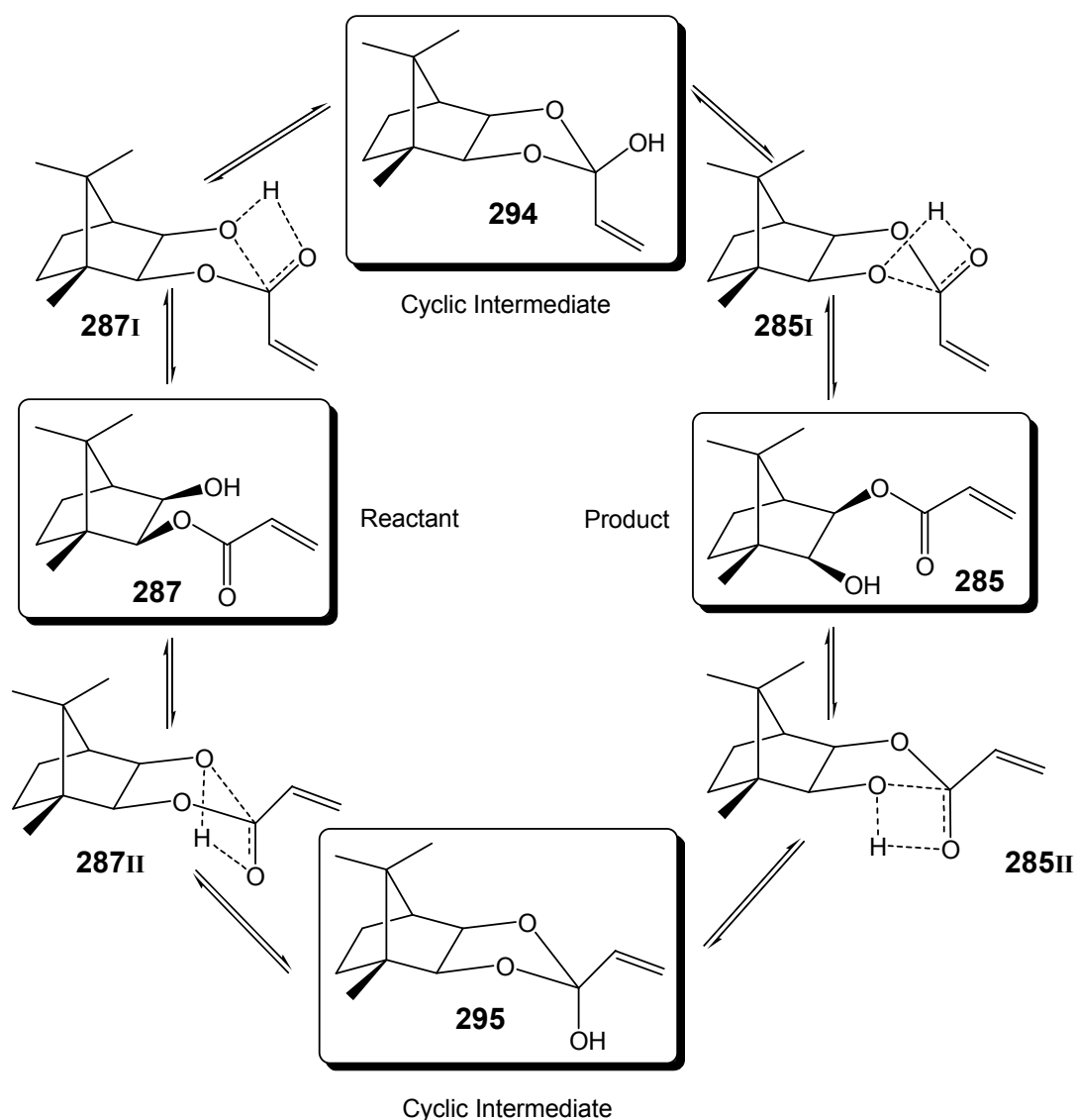
The aim was to locate and determine the relative energies of the significant stationary points on the free energy surface. To this end, the following computational steps were performed.

- i) Geometry optimization of the “reactant” and “product” and the putative intermediates;
- ii) verification of the various minima through frequency calculations (the requirement being zero imaginary frequencies);
- iii) location of transition state structures by exploring the potential energy surfaces between the minima;
- iv) optimization of the transition states and confirmation of their nature through frequency calculations (one imaginary frequency required)
- v) calculation of the thermodynamic and kinetic parameters, ΔE , E_a , ΔG_{298} , ΔG_{298}^\ddagger ; and
- vi) intrinsic reaction coordinate (IRC) calculations to validate the reaction pathways.

Possible mechanistic pathways for the neutral and acid-catalysed processes are illustrated in **Schemes 2.34** and **2.35** (p. 154) respectively. Similar calculations were performed on all structures present in each pathway. These and other structures, even unlikely ones, were included to assess the likelihood of their involvement in the reaction pathway.

2.3.4.1 Uncatalysed Transesterification

The NMR-based kinetic study had confirmed that the acrylate ester **287** rearranges *via* migration of the acryloyl moiety to form the isomeric acrylate **285**, and *vice versa*. It seemed likely that rearrangement in both directions involved the transient, cyclic, isomeric intermediates **294** and/or **295** and, consequently, the transition states **287I**, **285I**, **287II** and **285II** connecting the intermediates to the “reactant” and “product” (**Scheme 2.34**).



Scheme 2.34: Possible pathways for transesterification under neutral conditions.

Once the “reactant” **287**, “product” **285** and intermediate **294** and **295** structures had met the minimum requirements of the convergence criteria for geometry optimization, frequency calculations showed that all four structures were indeed minima on the potential energy surface with zero imaginary frequencies. Three distinct approaches for scanning the reaction trajectories were explored.

- i) Utilising the intermediates **294** and **295** as starting points, each of the O–C bonds, was stretched, in anticipation that the hydroxyl proton would spontaneously attach to the developing alkoxide oxygen. In the case of intermediate **294** (paths “a” and “b”; **Figure 2.61**), the respective O–C bond broke and a zwitterion was formed without any proton shift occurring. These results suggested that, for this route to proceed, collapse of the cyclic intermediates is not initiated by cleavage of an O–C bond, but rather by a shift of the hydroxyl proton to one of the ester oxygens, followed by cleavage of an adjacent O–C bond. Of course, once formed, the zwitterionic species could readily undergo proton transfer to afford the respective monoesters.

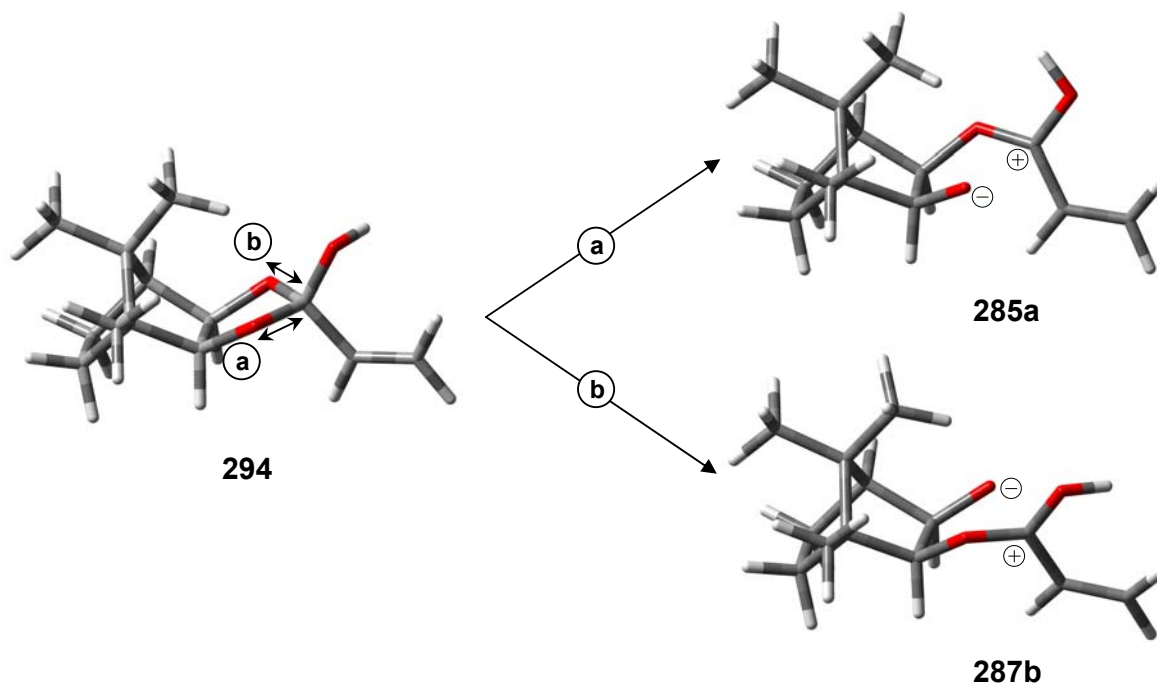


Figure 2.61: First approach in the search for transition states, illustrating the formation of the zwitterionic species from intermediate **294**.

Similar fission of intermediate **295** (paths “c” and “d”; **Figure 2.62**) resulted in the corresponding zwitterionic species and spontaneous proton shifts to the expected products.

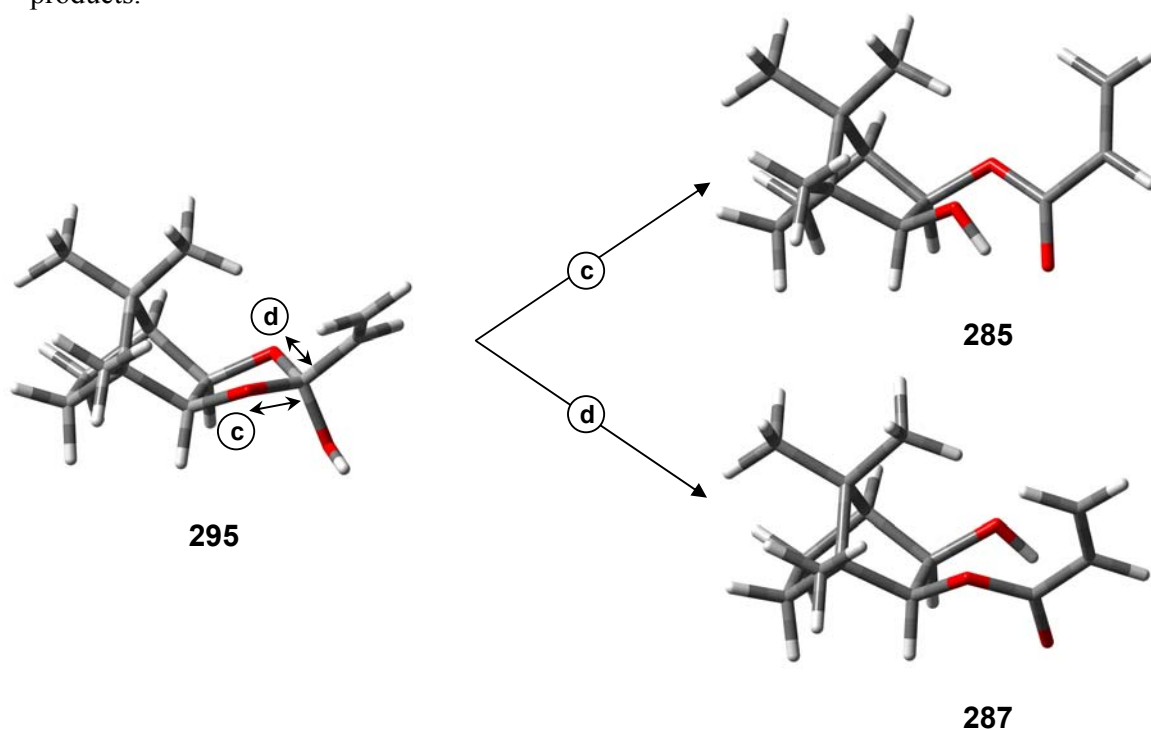


Figure 2.62: First approach in the search for transition states from intermediate **295**.

No transition structures or the corresponding thermodynamic parameters were able to be obtained as the potential energy scans failed to provide stationary points.

- ii) In the second approach, the interatomic distance between the hydroxylic oxygen and carbonyl carbon was gradually decreased to $< 1 \text{ \AA}$, in both the “reactant” **287** and “product” **285** (**Figure 2.63**), in an attempt to locate the putative transition state complexes **287I**, **287II**, **285I** and/ or **285II**, respectively (from **Scheme 2.34**). One to two steps forward from either transition state gives the corresponding isomeric esters.

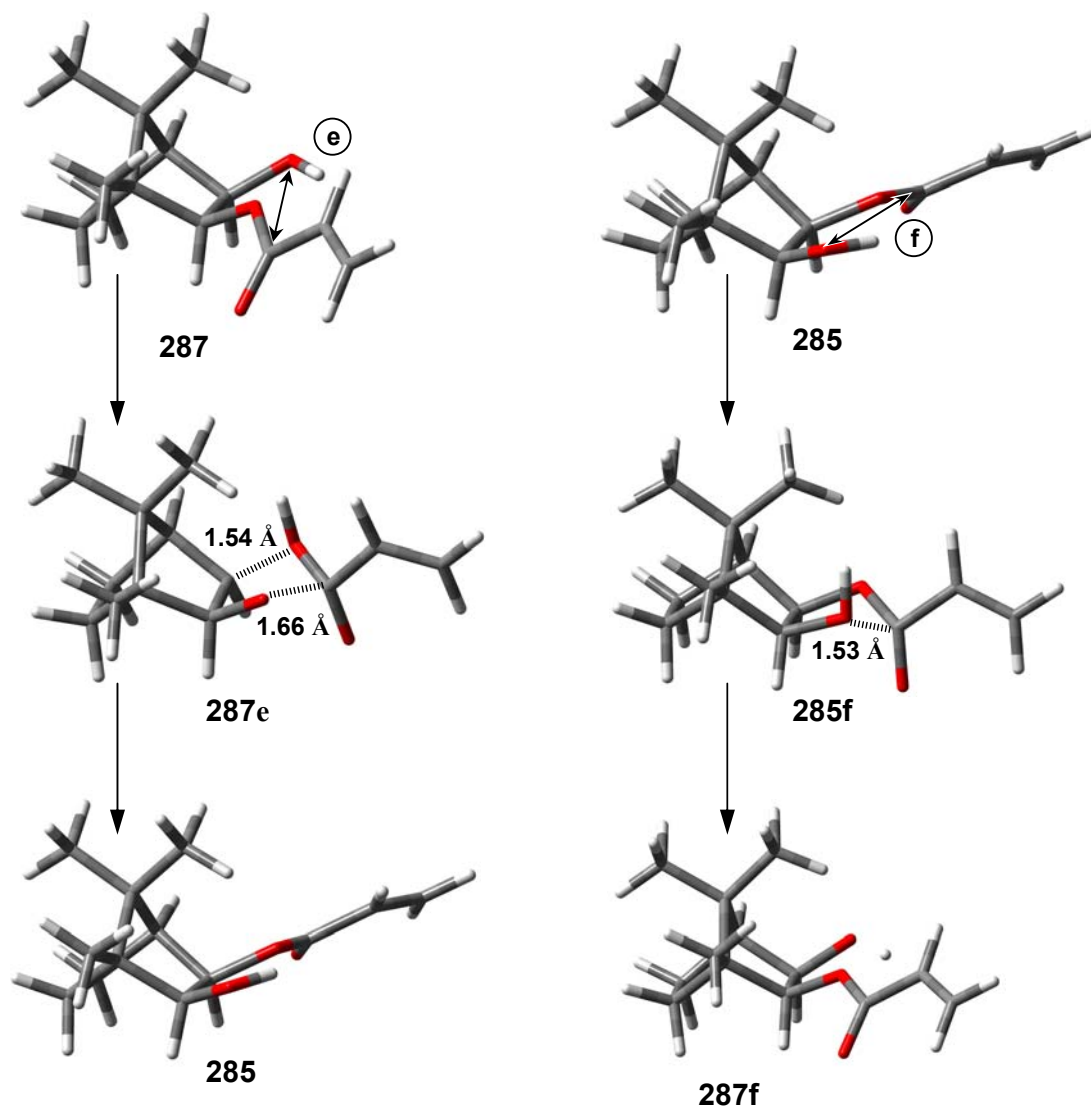


Figure 2.63: Second approach in the search for transition states.

iii) The third approach was based on the assumption that migration of the proton is a critical factor. Use was again made of the intermediates **295** and **294**, but in this approach, the reaction pathway was investigated by decreasing the interatomic distance between the hydroxyl proton and one or other of the ester oxygens (paths “g”–“j”) to $< 1 \text{ \AA}$ (**Figure 2.64**). Transition states were identified, geometry optimized and their nature verified through frequency calculations. A complete investigation of the potential energy surfaces, together with intrinsic reaction coordinate calculations, allowed the reaction pathways to be plotted (**Figures 2.65** and **2.66**) and the corresponding kinetic and thermodynamic parameters to be calculated (**Tables 2.18** and **2.19**).

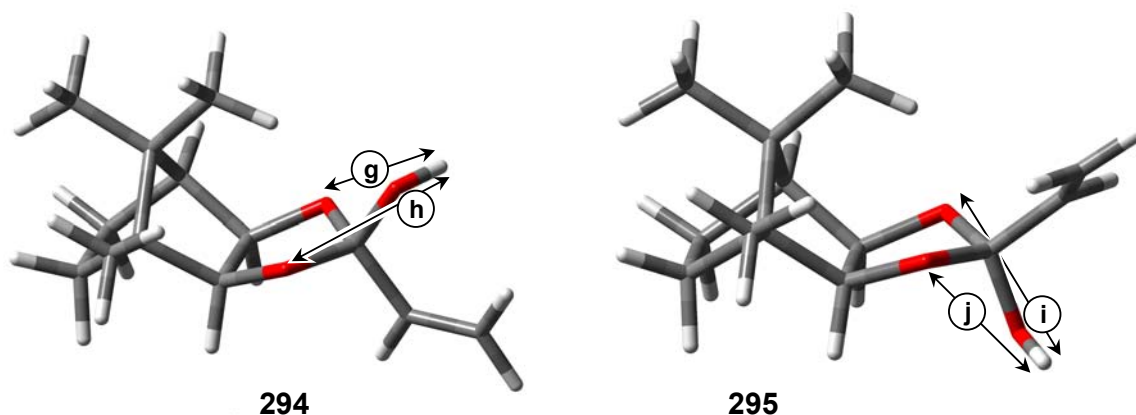


Figure 2.64: Third approach in the search for transition states.

Geometry optimization and frequency analysis of all structures illustrated in **Figures 2.65** and **2.66** confirmed their identity as stationary points. Thus: -i) the geometry optimisations converged; and ii) a single imaginary frequency was exhibited by each transition state and no negative frequencies were exhibited by the “reactant”, intermediate and “product” structures. Furthermore, IRC calculations verified that the transition states connect the respective “reactants” and “products”. The theoretical data thus support the mechanism illustrated in **Scheme 2.34**, and indicate that **pathway 1** (via the “*exo*-hydroxy” intermediate **294**) involves significantly higher activation barriers, in both directions, than **pathway 2** (via the “*endo*-hydroxy” intermediate **295**); the “*endo*-hydroxy” intermediate **295** also appears to be 3 kcal mol⁻¹ more stable than the isomeric “*exo*-hydroxy” analogue **294**. However, both pathways exhibit large activation energy barriers.

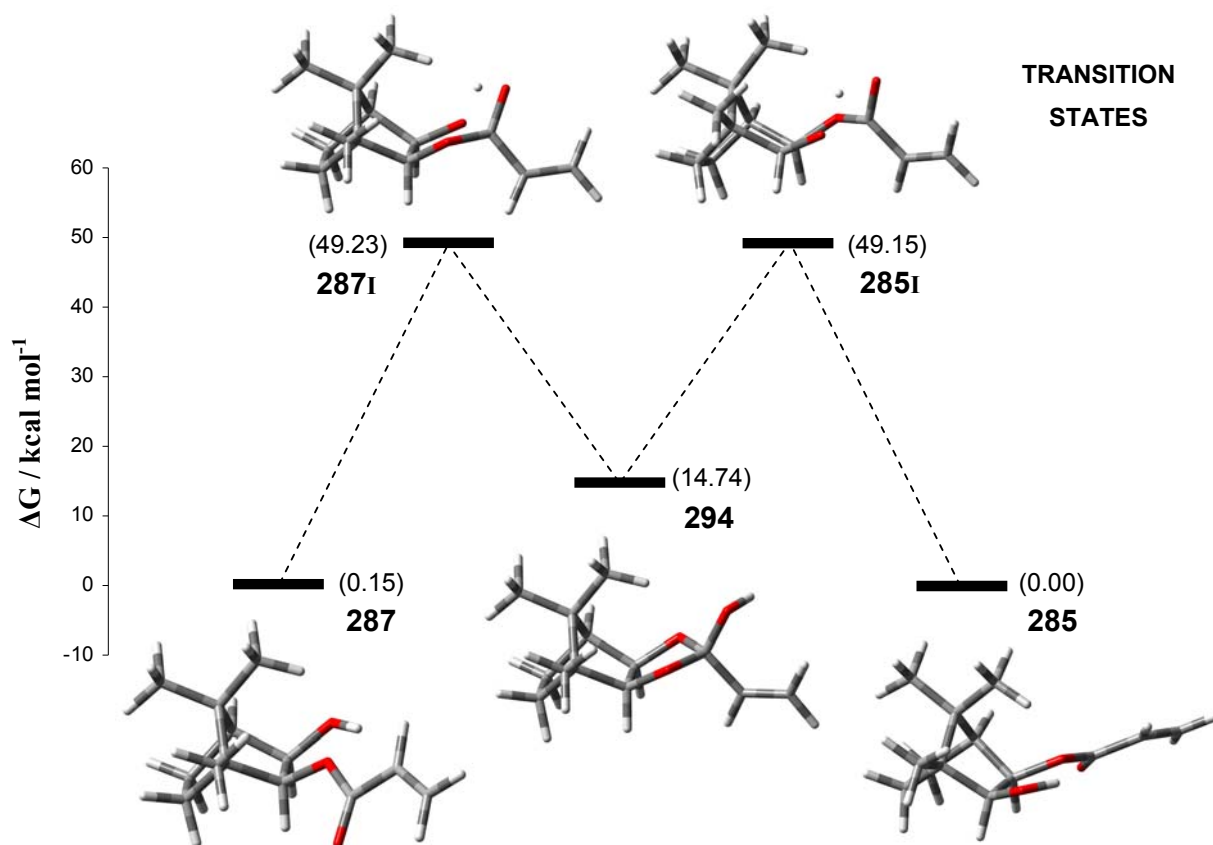


Figure 2.65: Uncatalysed “exo-hydroxy” transesterification route, pathway 1.

Table 2.18: Uncatalysed “exo-hydroxy” transesterification route, pathway 1.

Reaction Step	ΔG_{298} (kcal mol ⁻¹)	ΔG_{298}^\ddagger (kcal mol ⁻¹)	ΔE_{298} (kcal mol ⁻¹)	E_{a298} (kcal mol ⁻¹)	E_{a298} (kJ mol ⁻¹)
287 → 294	14.59	49.08	13.29	51.00	213.39
294 → 285	-14.74	34.41	-13.68	37.72	157.81
285 → 294	14.74	49.15	13.68	51.39	215.03
294 → 287	-14.59	34.50	-13.29	37.71	157.78

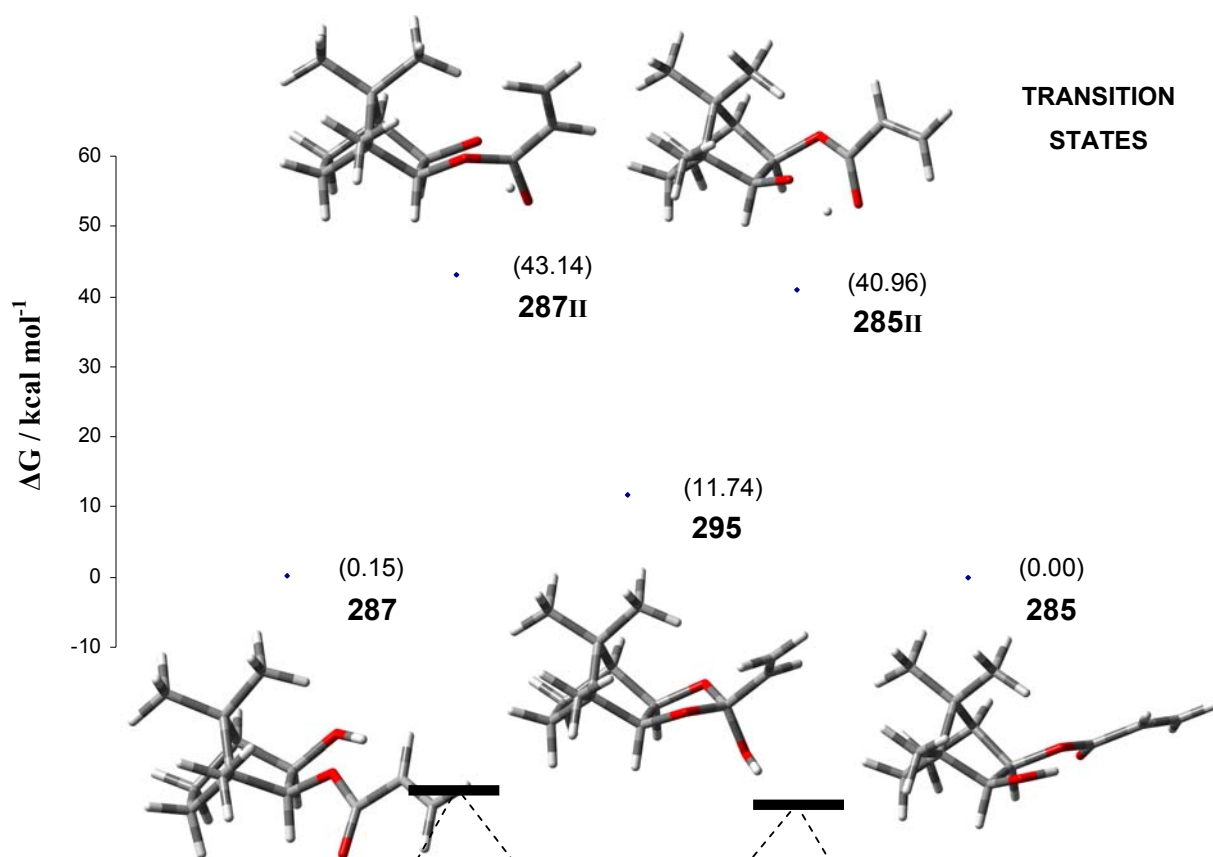


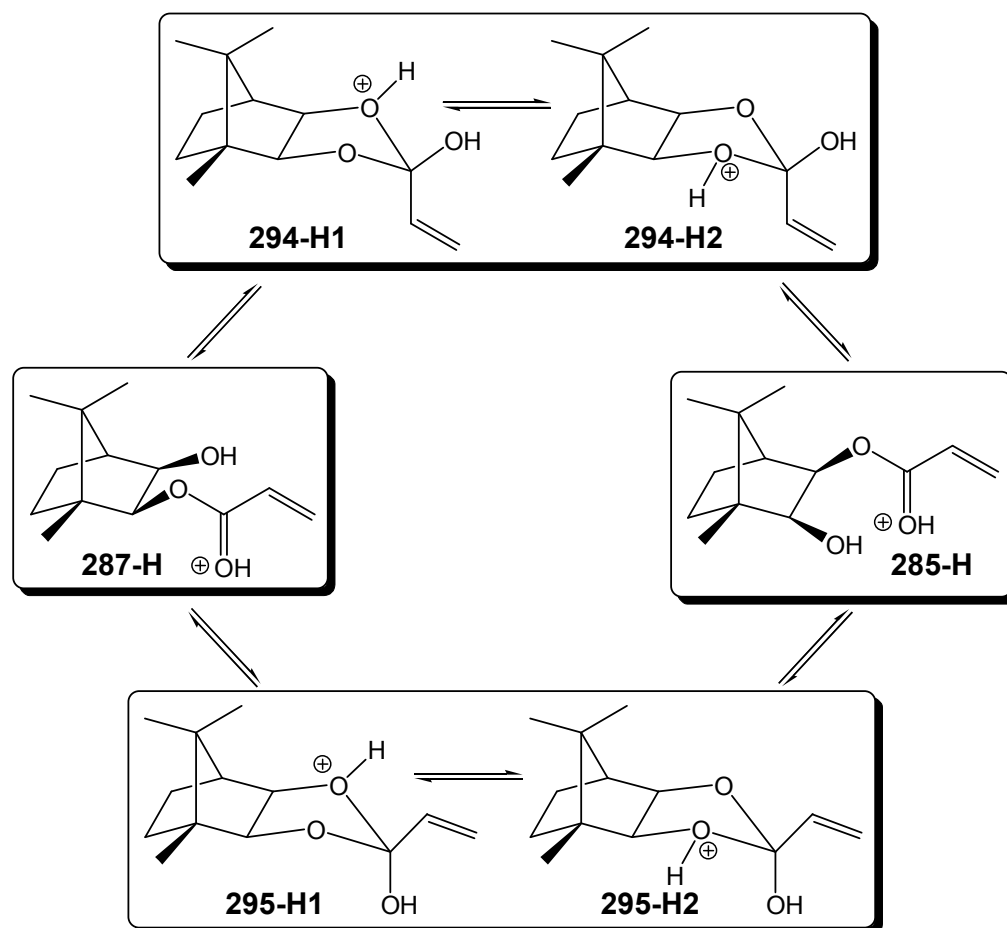
Figure 2.66: Uncatalysed “endo-hydroxy” transesterification route, **pathway 2**.

Table 2.19: Uncatalysed “endo-hydroxy” transesterification route, **pathway 2**.

Reaction Step	ΔG_{298} (kcal mol ⁻¹)	$\Delta G^{\ddagger}_{298}$ (kcal mol ⁻¹)	ΔE_{298} (kcal mol ⁻¹)	E_{a298} (kcal mol ⁻¹)	E_{a298} (kJ mol ⁻¹)
287 → 295	11.59	42.99	9.23	44.16	184.78
295 → 285	-11.74	29.23	-10.11	32.06	134.12
285 → 295	11.74	40.96	10.11	42.16	176.42
295 → 287	-11.59	31.40	-9.23	34.44	144.08

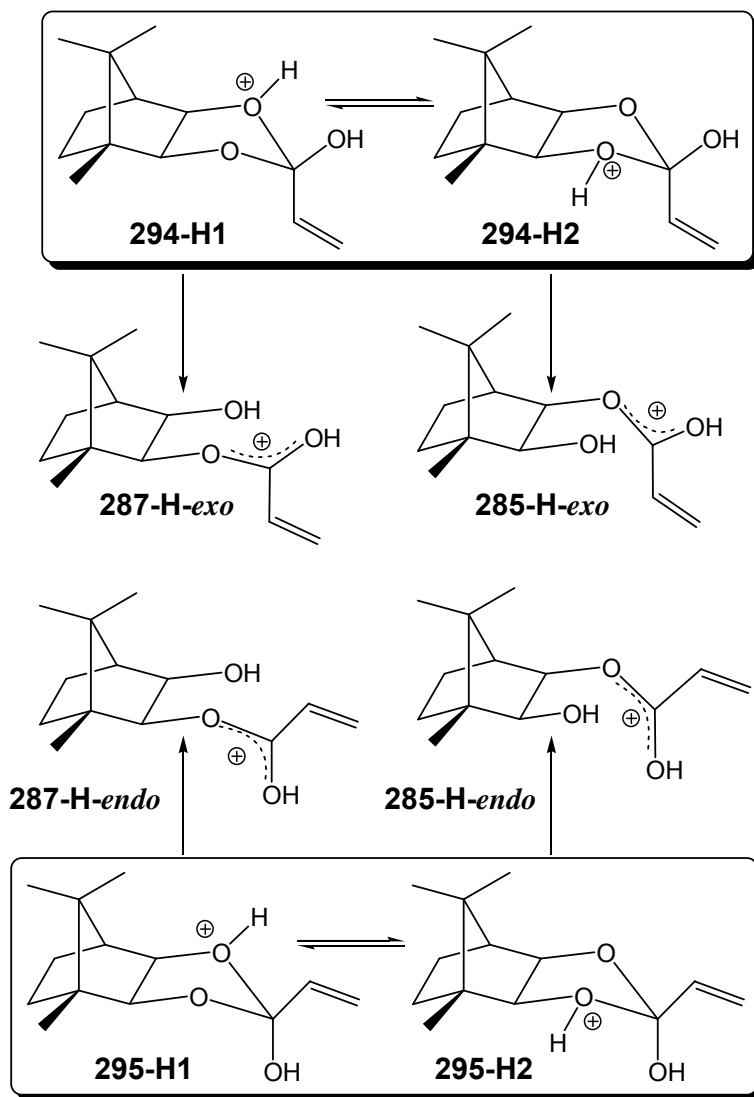
2.3.4.2 Catalysed Transesterification

The NMR-based kinetic experiments (**Section 2.3.3**) clearly indicated the importance of acid catalysis in the transesterification reactions. In light of these results, the mechanism illustrated in **Scheme 2.35** was considered.



Scheme 2.35: Possible pathways for transesterification under acidic conditions.

Geometry optimisations for protonated “reactants”, “products” and intermediates were performed. Successful convergence of the protonated “reactant” and “product” structures were achieved; however, initial attempts to optimise the geometry of the protonated cyclic intermediates resulted in dissociation to the corresponding non-cyclic cationic species **287-H-endo**, **287-H-exo**, **285-H-endo** or **285-H-exo** (**Scheme 2.36**), and it became apparent that the potential energy surface was more complex than anticipated. Frequency calculations on the geometry optimized structures showed that all four non-cyclic structures were indeed minima on the potential energy surface with zero imaginary frequencies.



Scheme 2.36: Possible pathways for transesterification under acidic conditions.

Two approaches were then followed in an attempt to map the reaction pathways for the catalysed reaction:

- i) The first approach involved decreasing the interatomic distance between the hydroxylic oxygen and protonated carbonyl carbon to $< 1 \text{ \AA}$, commencing with the geometry optimized structures **285-H-endo**, **285-H-exo**, **287-H-endo** and **287-H-exo** (**Figure 2.67**). In each case, the expected transition state could not be located. Instead fission of the C(2)–O or C(3)–O bond and migration of a hydroxyl anion from the camphor skeleton to the acrylate moiety was observed, followed by further dissociation.

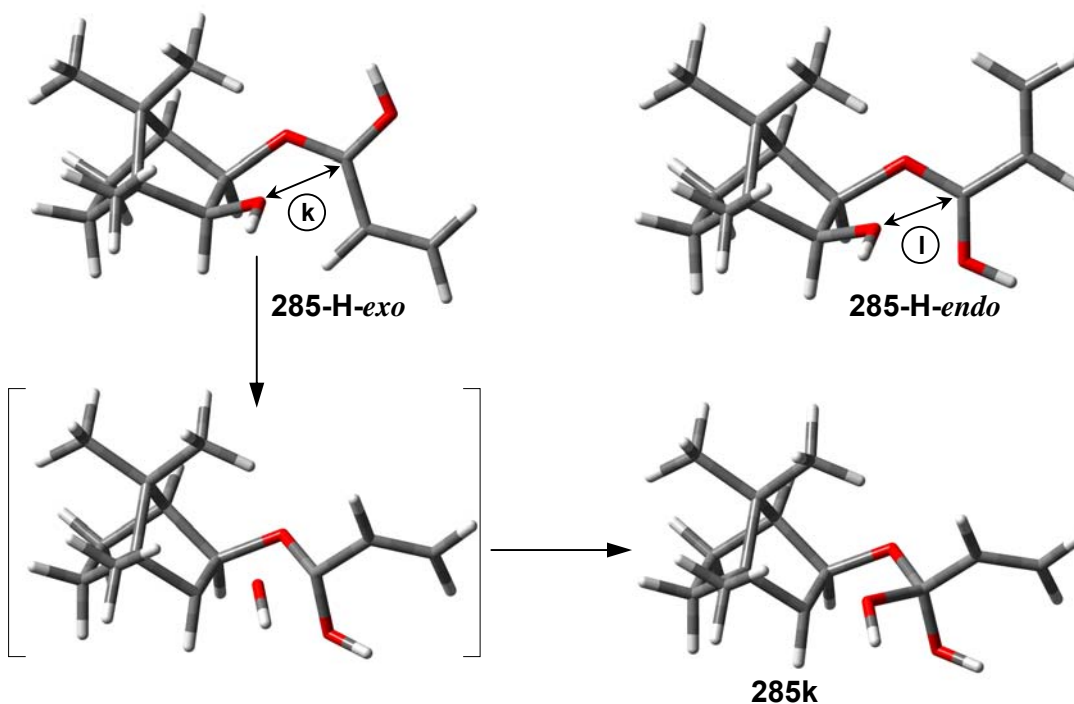


Figure 2.67: First approach in the search for transition states arising from “*exo*-hydroxy” acrylate **285-H-*exo*** and “*endo*-hydroxy” acrylate **285-H-*endo*** in the acid-catalysed reaction.

- ii) Initial attempts to optimise the geometry of the protonated putative cyclic intermediates (**Scheme 2.36**) had shown that localising the proton on either ether oxygen in the cyclic system raised the free energy to such a point that fission of the ring occurred. Consequently, in an alternative approach, it was decided to observe what would happen if a proton was brought towards the cyclic system from a non-bonding position to the point where an O–H bond formed (paths “**m**” and “**n**”), and beyond (**Figure 2.68**).

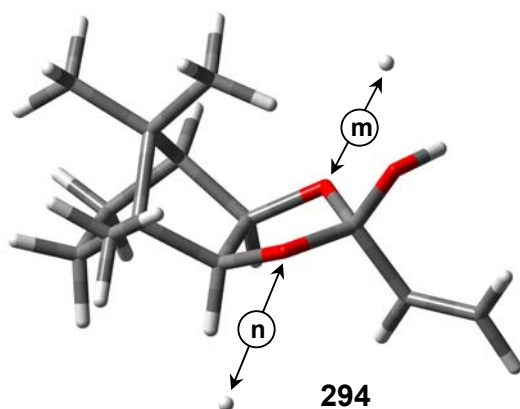


Figure 2.68: Second approach in the search for transition states in the acid-catalysed transesterification *via* the “*exo*-hydroxy” intermediate **294**.

In the case of the “*exo*-hydroxy” systems, the transition states **287III** and **285III** (**Figure 2.69**) were located, geometry optimized and single imaginary frequencies were obtained. Furthermore, the data obtained in the search gave more accurate representations of the structures on either side of the transition states, and these were used to obtain geometry-optimized minima corresponding to structures **294-H1**, **294-H2**, **287-H-*exo*** and **285-H-*exo*** (**Figure 2.69**). IRC calculations verified that the transition state structures connected the reactants and products. The kinetic and thermodynamic parameters for the acid-catalysed transesterification *via* the “*exo*-hydroxy” intermediates **294-H1** and **294-H2** are summarised in **Table 2.20**.

The results indicate that the ground state monoesters are protonated at the carbonyl oxygen. The hydroxyl oxygen is then able to attack the electron deficient carbonyl carbon and in so doing forms a transient cyclic structure (**294-H1** or **294-H2**), with loss of the hydroxyl proton. In the acidic medium protonation of an ether oxygen in the cyclic intermediates is able to occur from either the front or back face, leading to the isomeric monoester or returning to the starting structure.

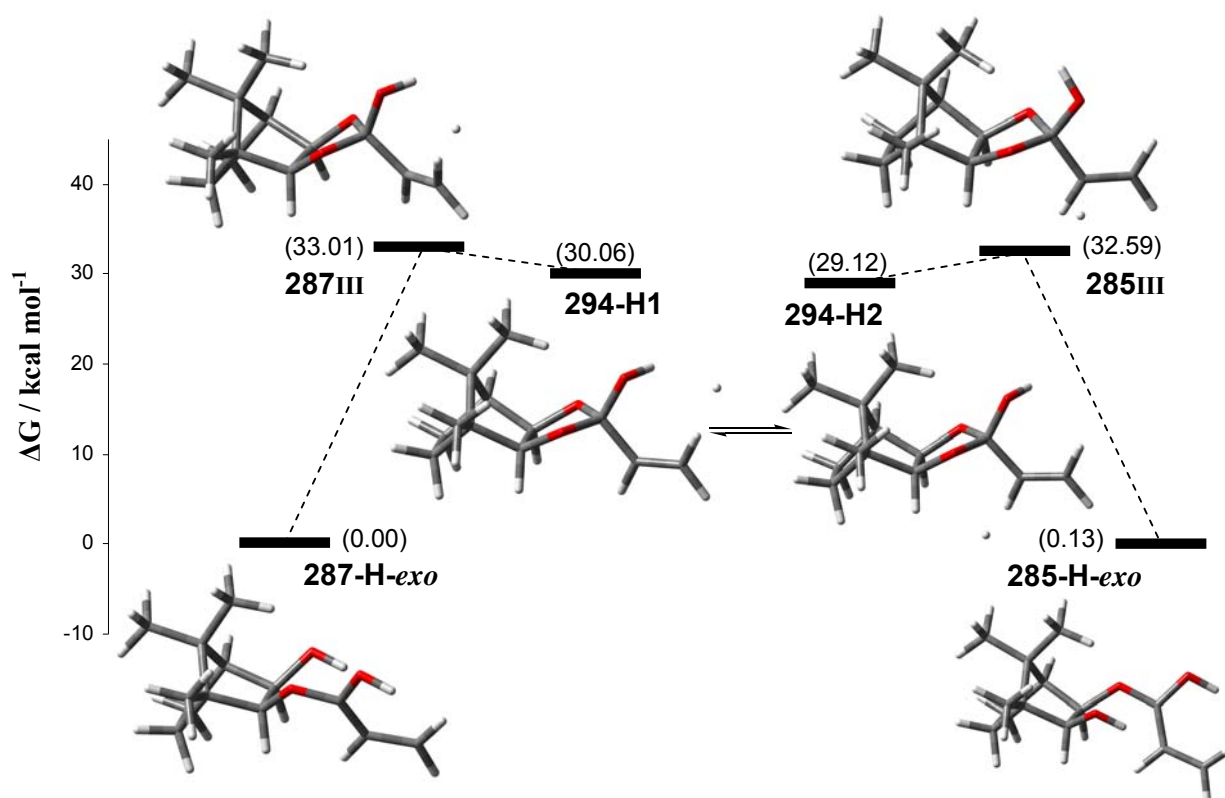


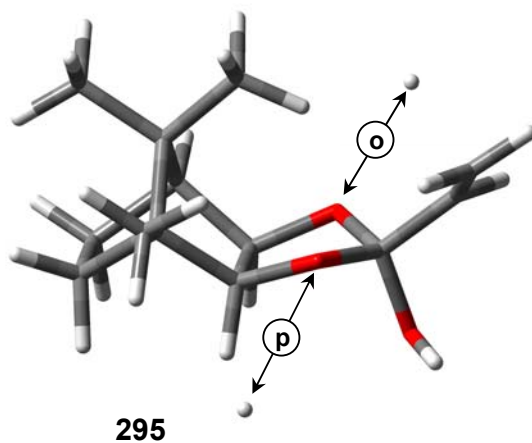
Figure 2.69: Acid-catalysed “*endo*-hydroxy” transesterification route, **pathway 1**.

Table 2.20: Acid-catalysed “*endo*-hydroxy” transesterification route, **pathway 1**.

Reaction Step	ΔG_{298} (kcal mol ⁻¹)	$\Delta G^{\ddagger}_{298}$ (kcal mol ⁻¹)	ΔE_{298} (kcal mol ⁻¹)	E_{a298} (kcal mol ⁻¹)	E_{a298} (kJ mol ⁻¹)
287-H-<i>exo</i> → 294-H1	30.06	33.01	35.78	36.96	154.64
294-H2 → 285-H-<i>exo</i>	-28.98	3.48	-36.07	0.10	0.4
285-H-<i>exo</i> → 294-H2	28.98	32.46	36.07	35.97	150.93
294-H1 → 287-H-<i>exo</i>	-30.06	2.96	-35.78	1.18	4.95

Comparison of the results for the acid-catalysed “*exo*-hydroxy” route with those of the corresponding uncatalysed transesterification, clearly show significant differences in the free energy of activation for each step of the reaction, particularly those involving collapse of the cyclic intermediates. The significantly lower free energies of activation calculated for the former are clearly consistent with the experimentally observed acid-catalysis.

Surprisingly, similar computational treatment of the corresponding *endo*-hydroxy intermediate species **295-H1** and **295-H2** (paths “**o**” and “**p**”) (**Figure 2.70**) and the related protonated species **287o**, **287IV**, **285p** and **285IV** gave very different results! Tentative transition state structures (**285IV** and **287IV**) were located, exhibiting single imaginary frequencies (**Figure 2.71**) and the corresponding kinetic and thermodynamic parameters are presented in **Table 2.21**.

**Figure 2.70:** Second approach in the search for transition states in the acid-catalysed transesterification *via* the “*endo*-hydroxy” intermediate **295**.

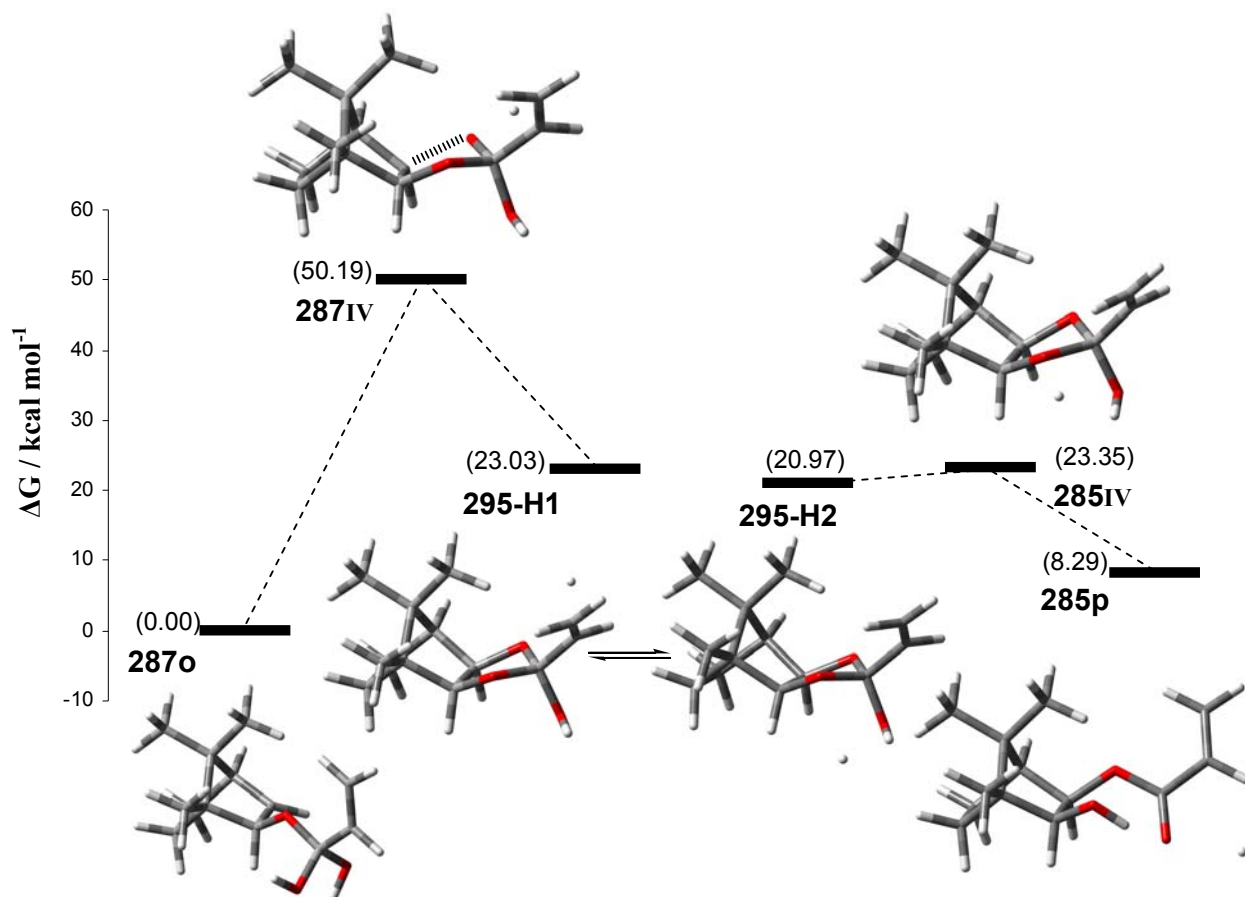


Figure 2.71: Acid-catalysed “endo-hydroxy” transesterification route, pathway 2.

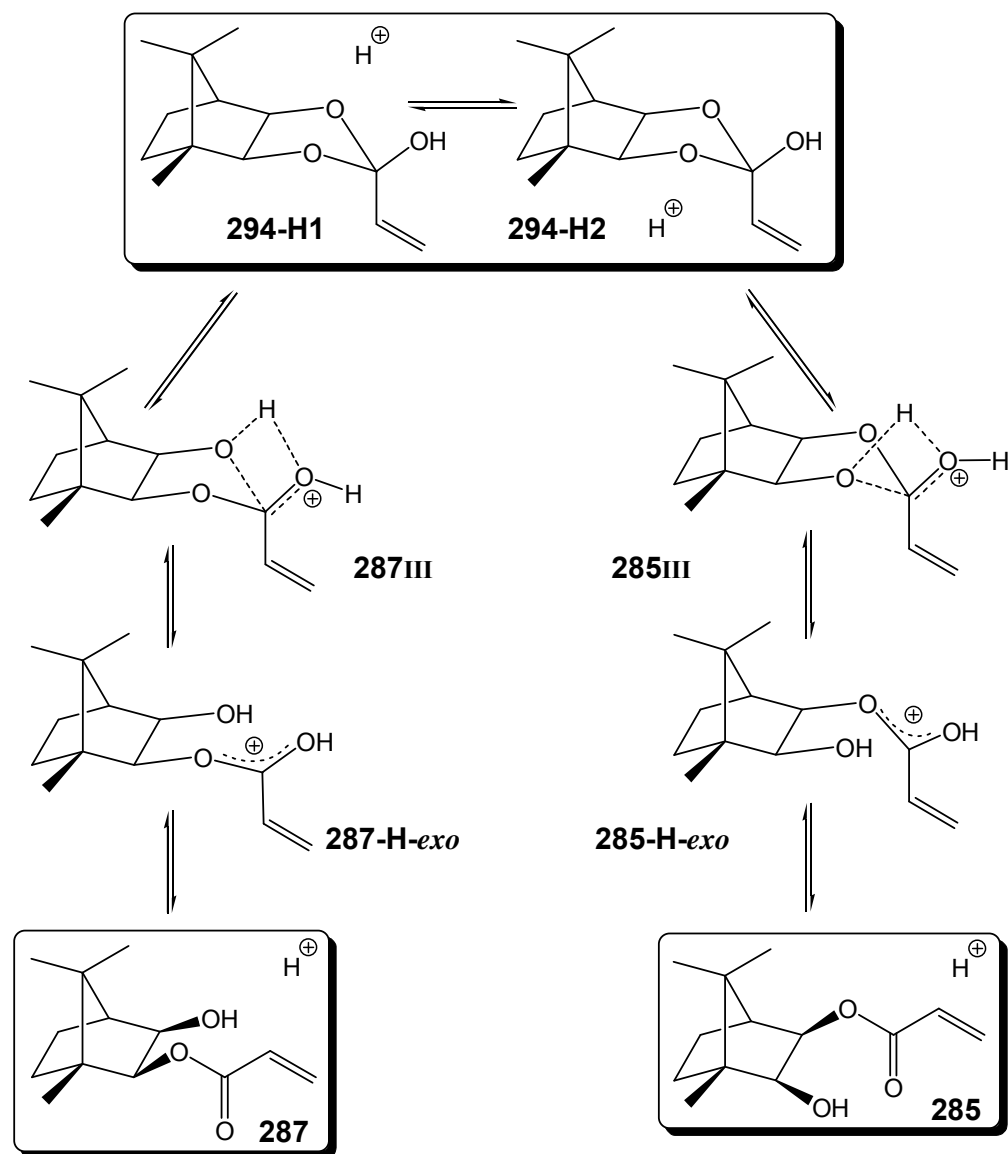
Table 2.21: Acid-catalysed “endo-hydroxy” transesterification route, pathway 2.

Reaction Step	ΔG_{298} (kcal mol ⁻¹)	ΔG_{298}^\ddagger (kcal mol ⁻¹)	ΔE_{298} (kcal mol ⁻¹)	E_{a298} (kcal mol ⁻¹)	E_{a298} (kJ mol ⁻¹)
287o → 295-H1	23.03	50.19	24.78	51.79	216.69
295-H2 → 285p	-12.68	2.38	-11.44	1.62	6.77
285p → 295-H2	12.68	15.06	11.44	13.06	54.62
295-H1 → 287o	-23.03	27.16	24.78	26.99	112.93

However, the high energy transition state **287IV** exhibits cleavage of the C(3)–O ether bond, and unconstrained geometry optimisation leads to the isomeric gem-diol **287o**. The free-energy of activation for this step (**295-H1** → **287o**; $\Delta G^\ddagger = 27.16 \text{ kcal mol}^{-1}$) is significantly larger than any of the other acid-catalysed ring-opening pathways examined. The surprising structures of the transition state **287IV** and the corresponding gem-diol moiety **287o** were investigated further, and the calculations were modified to allow approach of the proton along different trajectories and re-run numerous times. Each result was analogous to the data presented above. Thus, in the absence of an appropriate low energy transition state connecting the cyclic intermediate **295-H1** and the protonated monoacrylate ester **287o**, we conclude that the transesterification cannot proceed *via* the “*endo*-hydroxy” route.

2.3.4.3 Mechanistic Conclusions.

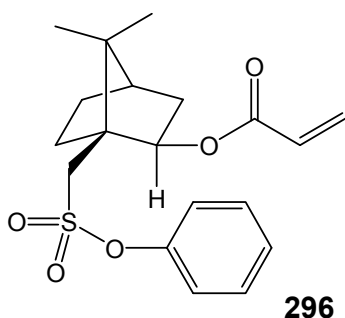
It must be recognised, of course, that the theoretical data have not been solvent-corrected, and gas-phase structures may differ from the corresponding solvated structures. However, based on both the experimental kinetic and theoretical data, it seems that the favoured pathway for the transesterification involves the protonated “*exo*-hydroxy” intermediates **294-H1** and **294-H2** (Scheme 2.37). The involvement of these cyclic intermediates appears to be beyond doubt.^{205,206} However, at no point has it been possible to detect these elusive structures by spectroscopic means as their lifetime and concentration are likely to render them incapable of detection within the NMR timescale.²⁰⁸



Scheme 2.37: Favoured pathway for transesterification under acidic conditions.

2.3.5 Acrylate Esters of Phenyl 2-Hydroxybornane-10-Sulfonate

In view of the transesterification problems encountered with the bornandiol monoacrylates, the search for a suitable camphor scaffold to act as a chiral auxiliary in Morita-Baylis-Hillman reactions was then steered in the direction of the phenyl 10-sulfonate system **296**.



It was suspected that the steric bulk of the 8-methyl group and the phenyl sulfonate group at C-10 would induce preferential approach of the attacking electrophile from a single face, resulting in a predominance of one enantiomeric Morita-Baylis-Hillman product. Additionally, the electron-deficient sulfur and the delocalized electron cloud of the phenyl group could stabilize the neighbouring enolate species **297** present during the course of the reaction, thus increasing enolate rigidity (**Figure 2.72**).

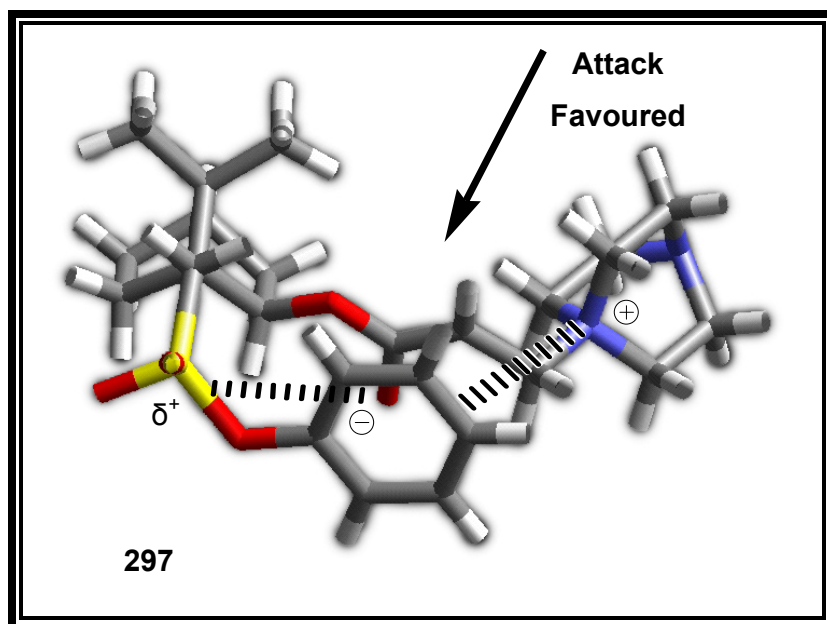
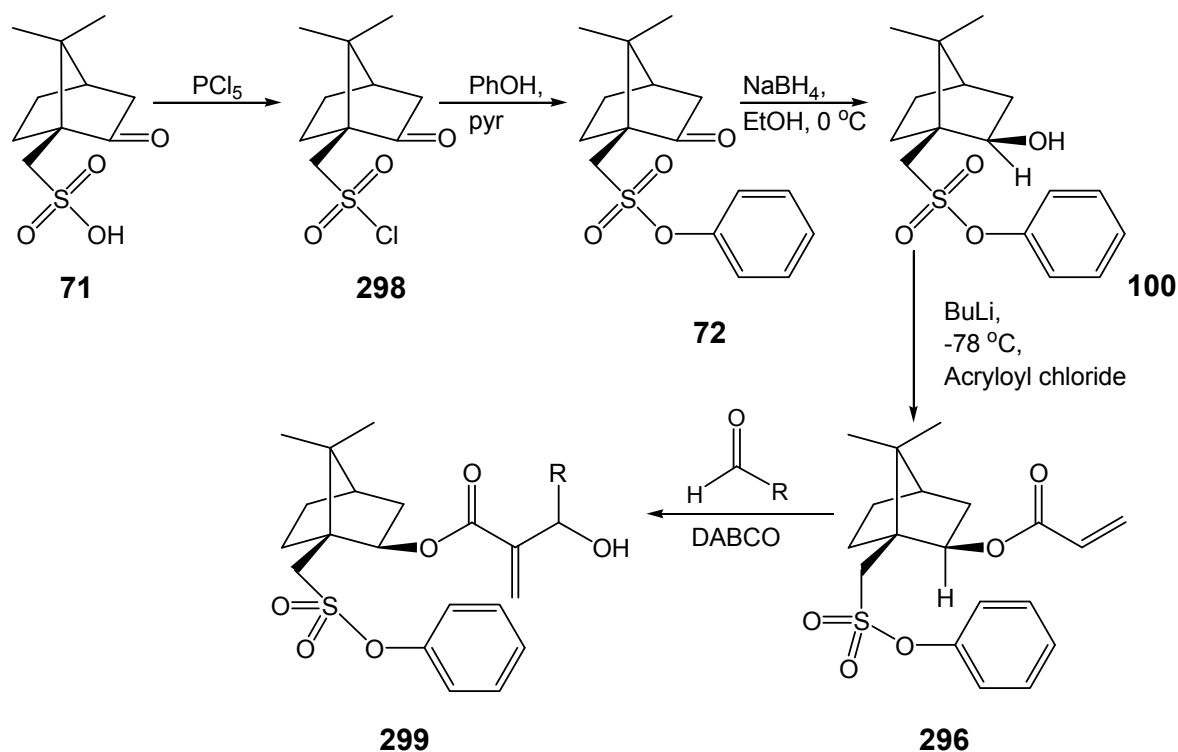


Figure 2.72: Expected interactions of the reactive enolate species **297** undergoing a Morita-Baylis-Hillman reaction.

The anticipated route to the phenyl 10-sulfonate substrate **296** and the associated Morita-Baylis-Hillman product **299** is shown in **Scheme 2.38**.



Scheme 2.38: Proposed route to phenyl 2-*exo*-acryloyloxybornane-10-sulfonate **296** and the Morita-Baylis-Hillman product **299**.

2.3.5.1 Synthesis of Phenyl Camphor-10-sulfonate

The proposed esterification to produce the phenyl 10-sulfonate **72** (**Scheme 2.38**) required the starting material to have a good leaving group; hence, commercially available camphor sulfonic acid **71** was chlorinated with phosphorus pentachloride (PCl_5),^{136,211} giving camphorsulfonyl chloride **298**. However, yields of the recrystallised product proved to be lower than reported,²¹¹ with a maximum of only 59 %. Synthesis of the phenyl 10-sulfonate **72** was achieved by addition of phenol to the sulfonyl chloride **298** in pyridine. Nucleophilic substitution of the sulfonyl chloride **298** by the nucleophilic phenoxide anion resulted in phenyl camphor-10-sulfonate **72** in good yield (78 %).^{212,213}

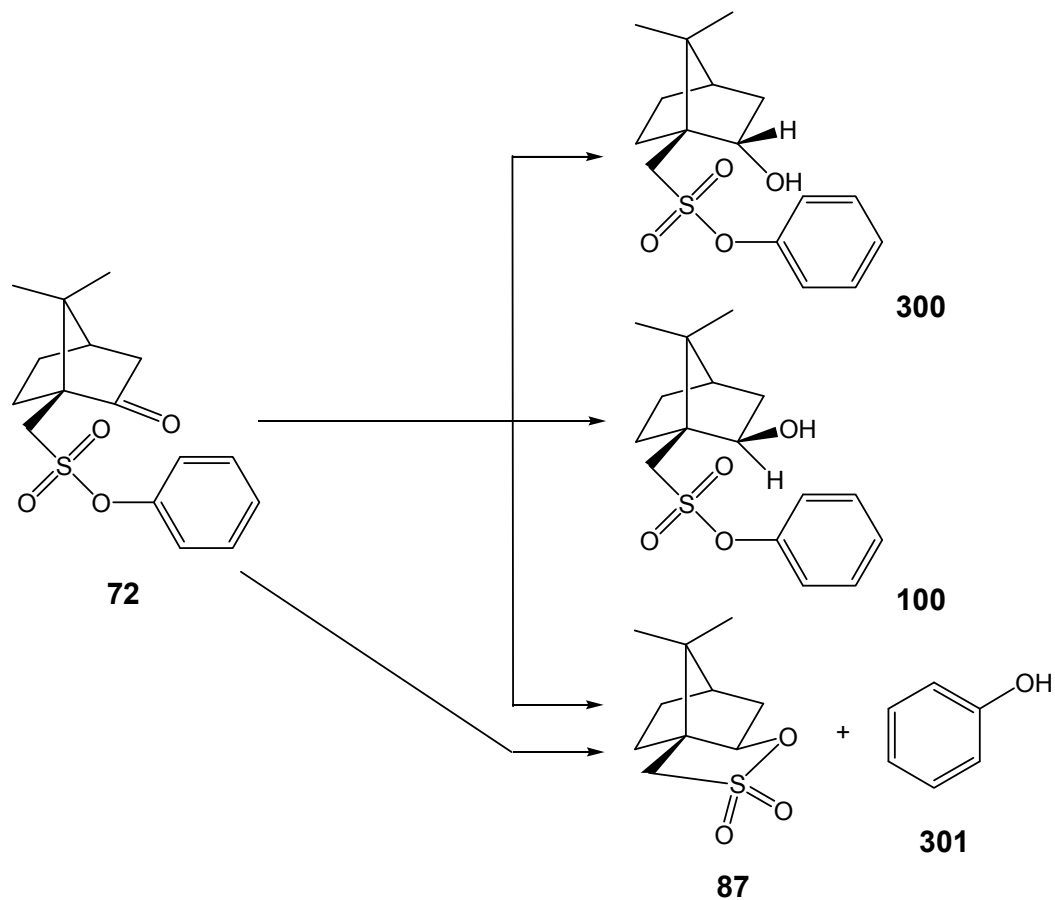
2.3.5.2 Reduction of Phenyl Camphor-10-sulfonate

Careful consideration of the structure and reactivity of phenyl camphor-10-sulfonate **72** led to the concern that reduction or hydrolysis of the sulfonate might be possible even under mild conditions.¹³⁶ Therefore, reaction conditions had to ensure reduction of the hindered ketone and, at the same time, be mild enough not to effect reduction of the sulfonate ester.

Reductions are most often achieved using metal hydrides or through metal-catalysed hydrogenation. However, carbon-sulfur single bonds are known to be susceptible to metal-catalyzed hydrogenolysis,¹⁶⁹ a characteristic used to bring about the desulfurisation of thioacetal protecting groups in the presence of Raney nickel.¹⁶⁹ Hydride-transfer reagents,^{136,169} such as lithium aluminium hydride (LAH) and sodium borohydride (NaBH₄), are advantageous in that they contain a large amount of hydrogen for a small quantity of reagent,¹³⁶ but LAH was considered too powerful a reducing agent for use in this reaction as it is not particularly selective.¹⁶⁹ NaBH₄ is significantly milder than LAH¹³⁴ and in hydroxylic solvents reduces aldehydes and ketones rapidly at room temperature, while remaining essentially inert to other functional groups.¹³⁸ It has also been found to reduce aldehydes faster than ketones whilst in isopropanol,²¹⁴ reducing ketones first in aqueous ethanol at -15 °C in the presence of cerium trichloride,^{215,216} and reducing the more hindered ketone in a mixture of two ketones.²¹⁷ NaBH₄ has been found to be very soluble in methanol, less soluble in ethanol and even less soluble in 2-propanol.^{138,153} However, Brown *et al.*²¹⁸ observed that NaBH₄ reacts readily to produce hydrogen with methanol, less readily with ethanol and not at all with 2-propanol over a 24 h period.

In an attempt to selectively reduce the ketone function, phenyl camphor-10-sulfonate **72** was treated with NaBH₄ in ethanol and in 2-propanol at 0 °C (**Scheme 2.39**). In both cases the synthesis of the novel products phenyl 2-*exo*-hydroxybornane-10-sulfonate **100** and phenyl 2-*endo*-hydroxybornane-10-sulfonate **300** were achieved in very low yields (see **Table 2.22**). The dominant product, however, was found to be 10-isobornyl sulfone **87**, which is well known and has been the subject of numerous studies,^{44,45,47,219-222} and a large quantity of phenol **301** was also present. Removal of phenol from the reaction mixture was achieved with a basic wash, and subsequent purification of the remaining compounds was easily achieved by radial chromatography. Structure elucidation of compounds **100** and **300** was achieved by analysis of the 1-D and 2-D NMR spectroscopic data (**Figures 2.73** and **2.74**), which showed characteristic signals for all expected protons; of particular importance was the presence of

new methine and hydroxylic signals corresponding to the C-2 secondary alcohol moiety, confirming that the reduction of **72** had occurred.



Scheme 2.39: Synthesis of phenyl 2-*exo*-hydroxybornane-10-sulfonate **100**, phenyl 2-*endo*-hydroxybornane-10-sulfonate **300** and 10-isobornyl sultone **87**.

Table 2.22: Data for the reduction of phenyl camphor-10-sulfonate.

Compound	Reaction Conditions			
	1 eq. NaBH ₄ , EtOH, 0 °C, 12 h	1 eq. NaBH ₄ , Isopropanol, 0 °C, 12 h	10 eq. NaBH ₄ , EtOH/ H ₂ O (2:1), -8 °C, 8 h	10 eq. NaBH ₄ , abs. EtOH, 25 °C, 12 h
	Yield (%)	Yield (%)	Yield (%)	Yield (%)
100	11.2	10.7	81	0
300	1.3	1.0	12	0
87	23.1	22.3	4	94

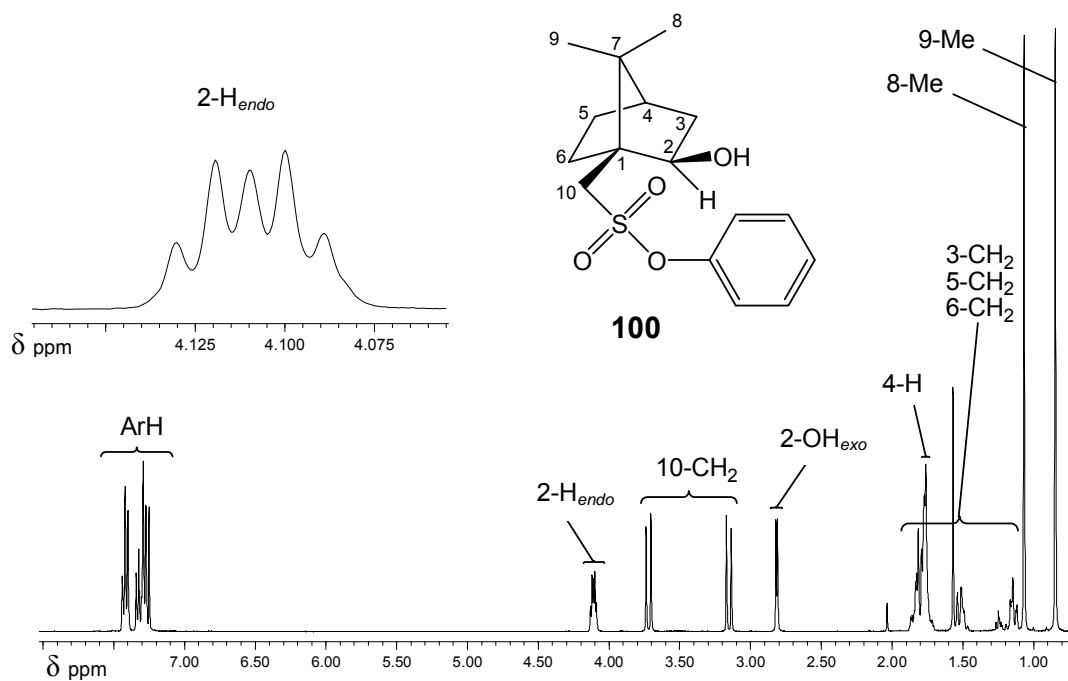


Figure 2.73: 400 MHz ^1H NMR spectrum of phenyl 2-*exo*-hydroxybornane-10-sulfonate **100** in CDCl_3 .

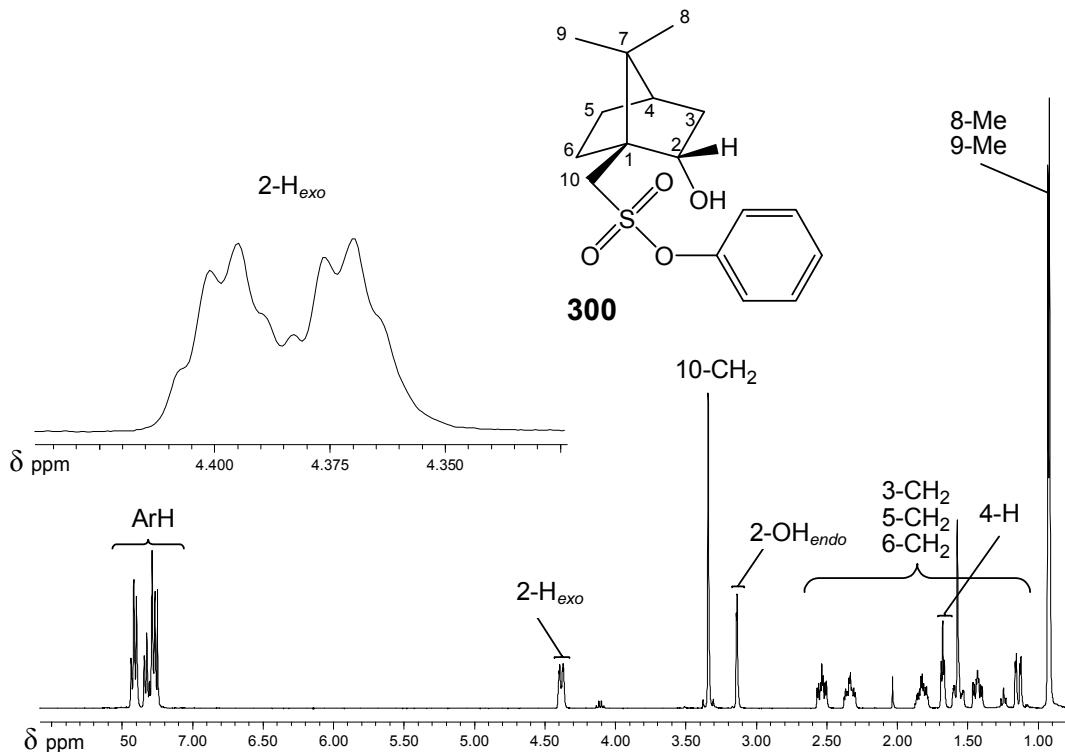


Figure 2.74: 400 MHz ^1H NMR spectrum of phenyl 2-*endo*-hydroxybornane-10-sulfonate **300** in CDCl_3 .

Assignment of the stereochemistry was based on the analysis of the C-2 proton signals and their correlation with protons at C-5, C-6, C-8 and C-10. As is characteristic of camphor structures similar to the 2-*exo*-hydroxy compound **100**, where 2-H is *endo*-orientated, shielding between 2-H_{endo} and all *endo* protons results in the 2-H signal (4.11 ppm) and all the *endo* proton signals being shifted upfield relative to the corresponding signals in the isomeric ester **300**. The 2-hydroxylic group, being *exo*-orientated, causes deshielding of the 8-methyl group, and the 8- and 9-methyl signals are thus significantly separated (1.07 and 0.85 ppm, respectively), whereas in the 2-*endo*-hydroxy analogue **300**, where the 2-H is *exo*-orientated, the 2-OH_{endo} deshields the *endo*-orientated protons, the 2-H_{exo} proton experiences less shielding (4.30 ppm) and the 8- and 9-methyl signals resonate closer together (0.92 and 0.93 ppm) as the methyl groups are in a similar chemical environment.

Finally, the 10-CH₂ nuclei of **100** resonate as two doublets (3.15 and 3.73 ppm) and experience geminal coupling (13.7 Hz) characteristic of magnetically non-equivalent nuclei; the 10-CH₂ nuclei of **300**, however, resonate as a singlet (3.34 ppm) indicating chemical shift equivalence. Computational analysis, performed with Gaussian-03,²²³ afforded stable hydrogen-bonded conformers (**Figures 2.75** and **2.76**), the structures of which provide a possible explanation. The hydroxylic oxygen in **100** is relatively close to H-10_a (3.63 Å) but distant to H-10_b (4.16 Å), whilst the corresponding 10-CH₂ nuclei in **300** are both distant from the hydroxylic oxygen. Thus H-10_a in **100** is deshielded relative to the other 10-CH₂ nuclei and resonates further downfield at δ 3.72 ppm .

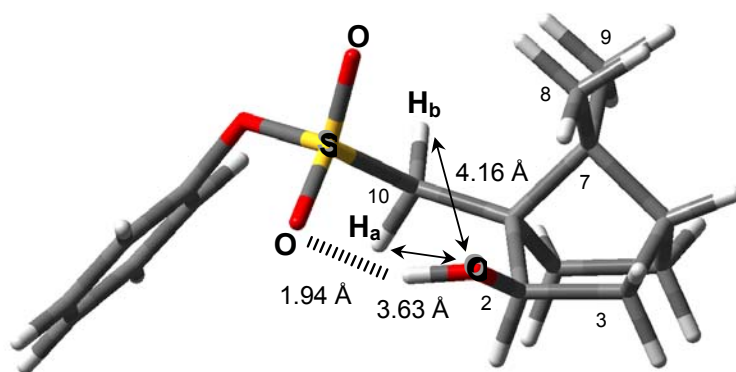


Figure 2.75: Computer-modelled representation of a stable conformation of phenyl 2-*exo*-hydroxybornane-10-sulfonate **100**, showing distances between the 10-CH₂ nuclei and the hydroxylic oxygen.

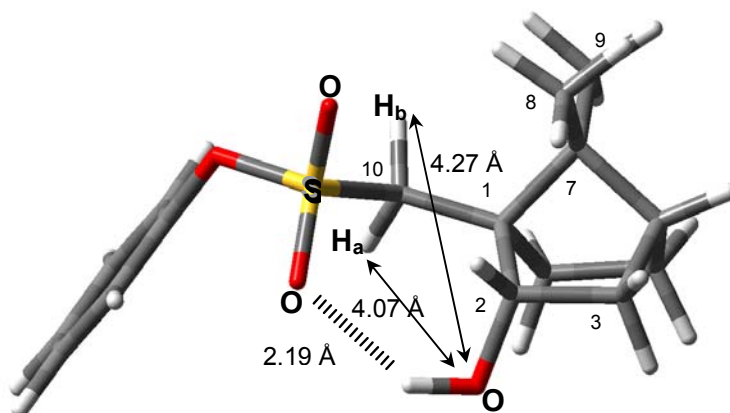
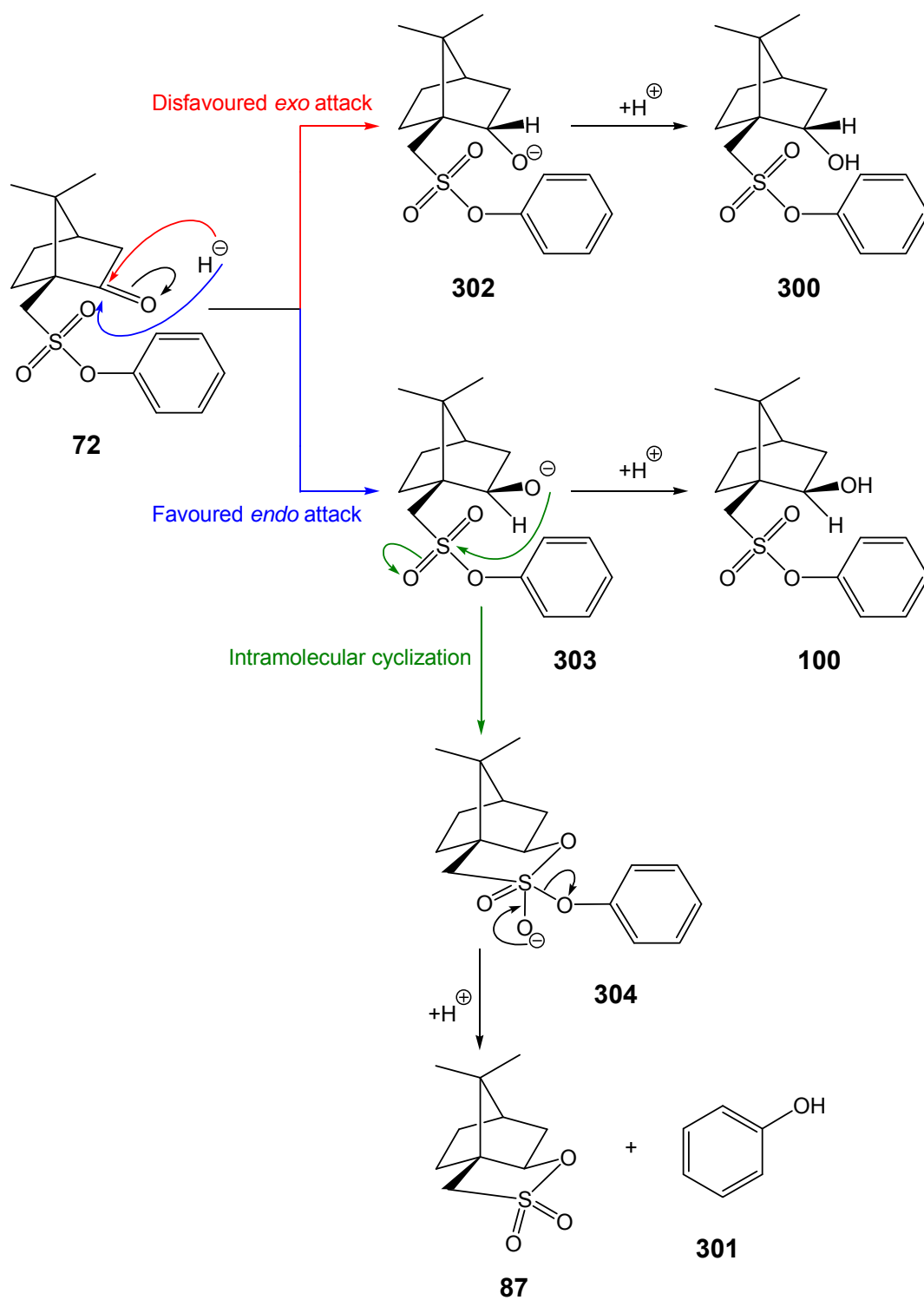


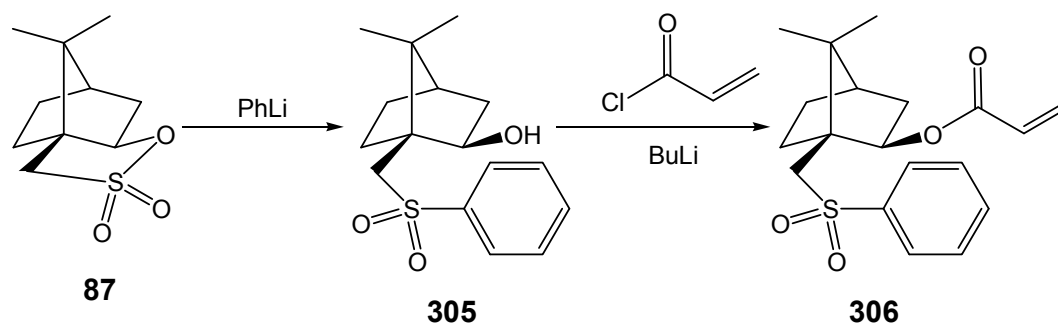
Figure 2.76: Computer-modelled representation of a stable conformation of phenyl 2-*endo*-hydroxybornane-10-sulfonate **300** showing distances between the 10-CH₂ nuclei and the hydroxylic oxygen.

Consideration of the mechanism of the reaction (**Scheme 2.40**) was necessary to account for the observed products. As indicated earlier the carbonyl group at C-2 of the substrate **72**, is sterically hindered on the *exo*-face by the bulky 8-methyl group. Thus, nucleophilic attack is expected to be favoured at the *endo*-face, generating the *exo*-hydroxy compound **100** as the dominant ester product. The major reaction product, however, was the 10-isobornyl sultone **87**, formed by intramolecular nucleophilic attack on the sulfonate ester by the highly reactive alkoxide species,²²⁴ (the liberated phenoxide is neutralized on work-up to give phenol). Limited attack at the *exo*-face by the metal hydride accounts for the minor ester product, the *endo*-hydroxy isomer **300**. It is interesting to note that no trace of an analogous *endo*-cyclized sultone was observed, presumably due to unfavourable orientation of the reactive centres.



Scheme 2.40: Mechanistic pathways for the reduction of phenyl camphor-10-sulfonate **72**.

Analysis of the reaction mechanism suggested that if the concentration and reactivity of the alkoxide intermediate **303** could be reduced, cyclization might be minimized. This was achieved by reducing the temperature, and by adding H₂O to permit early protonation of the alkoxide species **303**. The amount of water was carefully monitored, as was the overall progress of the reaction, and the quantity of NaBH₄ was increased to account for any that might be rendered inactive by hydrolysis. A vigorous reaction was observed during final acid quenching of the reaction, signifying that active NaBH₄ was still present. Fine tuning of the reaction conditions [NaBH₄ (10 eq.), EtOH/H₂O (2:1), -8 °C, 8 h], followed by purification on the chromatotron or by HPLC, led to a huge improvement in the yield of phenyl 2-*exo*-hydroxybornane-10-sulfonate **100** (81 %) and phenyl 2-*endo*-hydroxybornane-10-sulfonate **300** (12 %), and a concomitant decrease in the production of 10-isobornyl sultone **87** (4 %) (**Scheme 2.39**; **Table 2.22**; **p. 165**). A further variation in reaction conditions [NaBH₄ (10 eq.), absolute EtOH, room temperature, 12 h], however, afforded the sultone **87** in excellent yield (94 %) with no trace of either hydroxy compound! This is a somewhat different synthetic method for the production of the sultone **87** than those reported in the literature,^{44,45,47,212,220} primarily as phenoxide is a better leaving group than the alkoxides involved in the reported methods; the reaction conditions are thus far milder, the product cleaner and the yield generally equivalent or higher. Cleavage of **87**^{46,219,222} and the subsequent synthesis of the Morita-Baylis-Hillman auxiliary **306** may be attempted in the future (**Scheme 2.41**).



Scheme 2.41: Proposed route to the Morita-Baylis-Hillman auxiliary 2-acryloyloxy-10-phenylsulfonylbornane **306**.

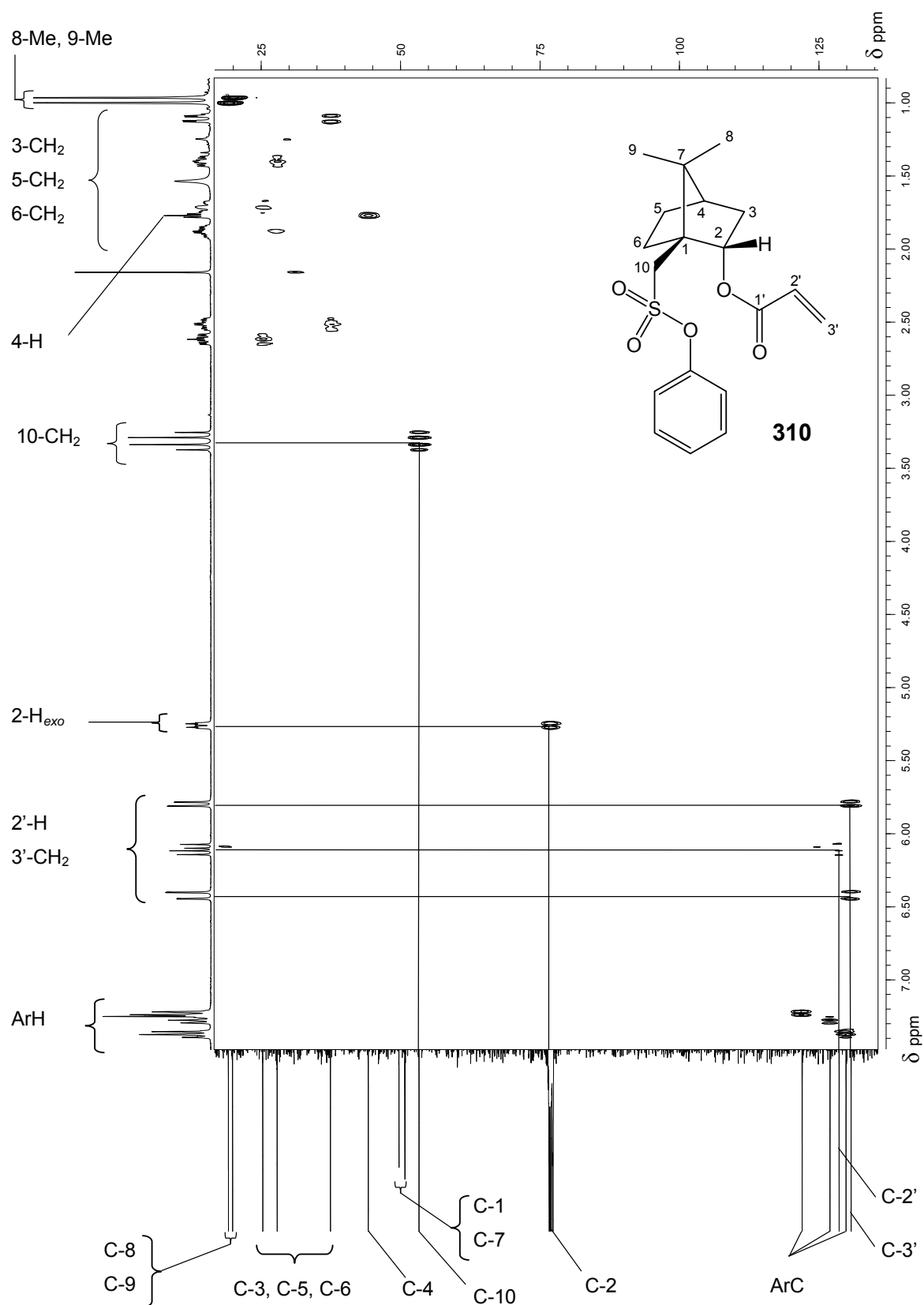


Figure 2.77: 400 MHz HSQC spectrum of phenyl 2-endo-acryloyloxybornane-10-sulfonate **310** in CDCl₃.

Computational analysis of the conformation of the 2-*endo*-acrylate **310** (Figure 2.78) suggests that the phenyl and acrylate groups could favour alignment parallel to one another at a distance of between 5 and 6 Å, supporting the idea that the phenyl ring might block access to one face (approach “a”) of the acrylate moiety in a Morita-Baylis-Hillman reaction. Similar analysis of the 2-*exo*-acrylate **296** (Figure 2.79) suggests that the phenyl group is disposed some distance from the acrylate moiety. While this might raise concern about the stereodirecting potential of the phenyl group, internal rotation about the C(1)–C(10) and C(10)–S bonds could still provide effective shielding of one face of the acrylate group (approach “a”). Perhaps of more significance is the relative orientation of the acrylate groups of the isomeric esters **310** and **296**, which clearly shows the acrylate carbonyl groups pointing in opposite directions, thus exposing different faces to attack by an electrophile and raising the possibility of generating enantiomeric products by choosing one isomeric substrate or the other.

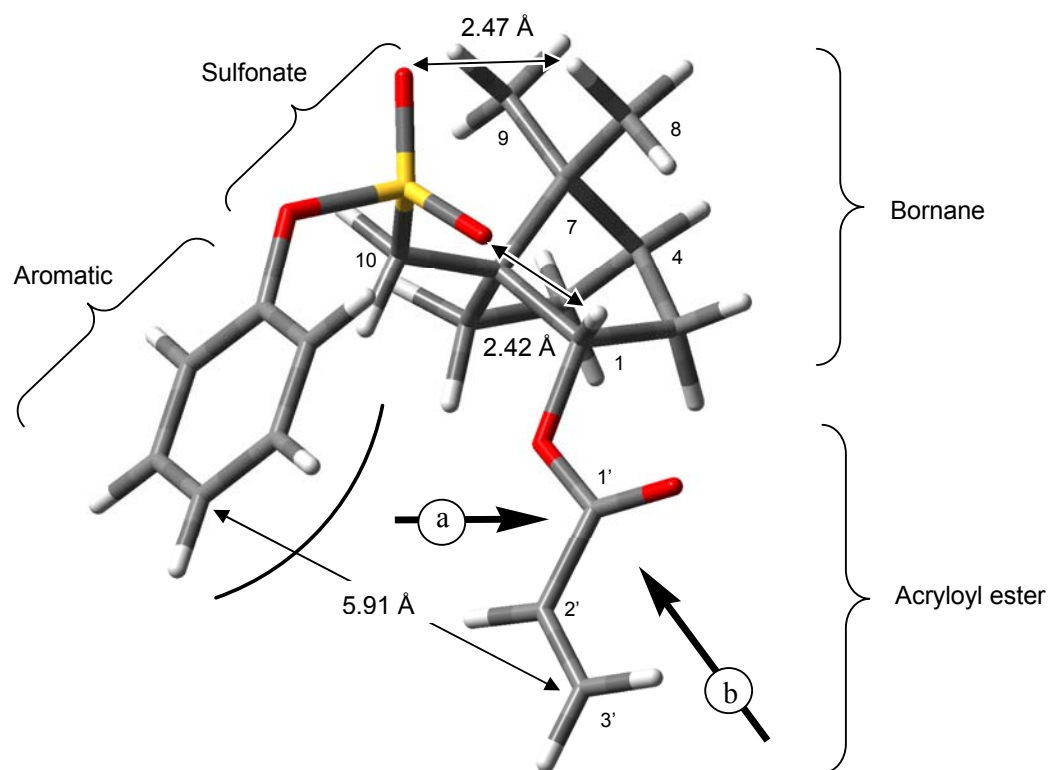


Figure 2.78: Computer-modelled representation of a stable conformation of phenyl 2-*endo*-acryloyloxybornane-10-sulfonate **310**.

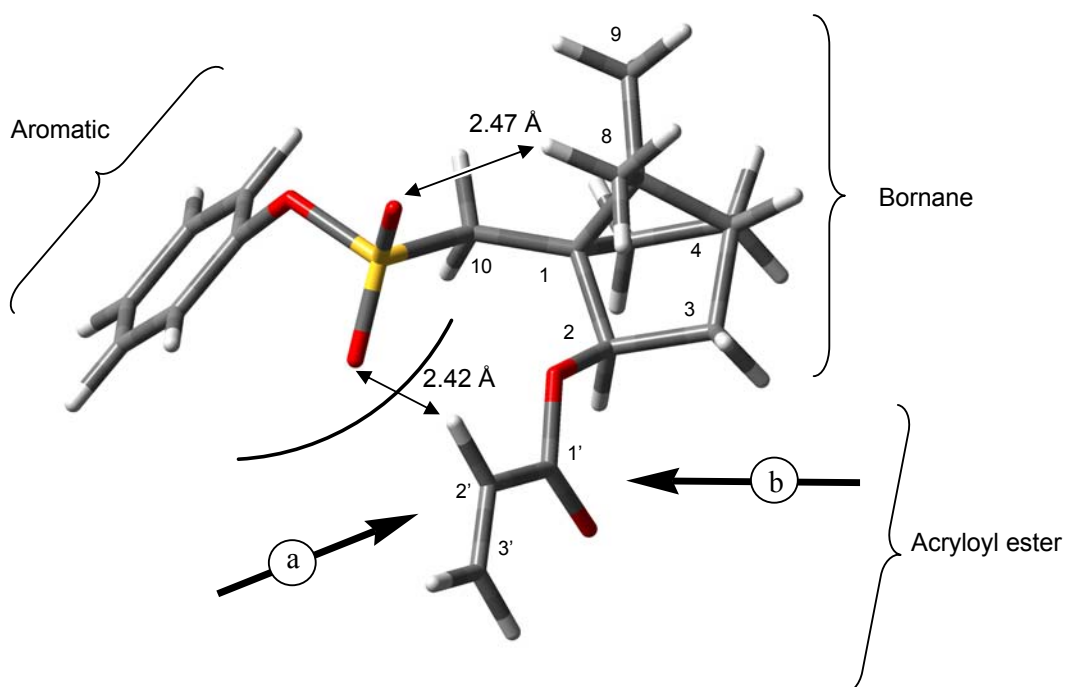


Figure 2.79: Computer-modelled representation of a stable conformation of phenyl 2-*exo*-acryloyloxybornane-10-sulfonate **296**.

The successful synthesis of the *endo*-acrylate **310** coupled with the tendency of the *exo*-isomer to form the sultone **87** added weight to the earlier suspicion that cyclization of the *endo*-alkoxide is sterically unfavourable. Further attempts to produce the 2-*exo*-acrylate ester **296** necessitated a search for other possible methods. The problem of cyclization arises from the reactivity of the alkoxide species and a possible solution lay in by-passing alkoxide formation entirely. While most methods appear to proceed *via* the alkoxide, a notable exception involved the use of tertiary amines to catalyze the reaction.^{122,225,226} The presence of these catalysts is known to increase the rate of acylation of alcohols by a factor of up to 10^4 ,²²⁷ and to result in high yielding reactions.^{227,228} 4-(Dimethylamino)pyridine (DMAP)²²⁹ functions as a nucleophilic catalyst enhancing the electrophilicity of the acyl carbon, as a neutral leaving group during acyl substitution and, as a base, neutralising the HCl generated in the process (although Et₃N can be used for this purpose). Unfortunately, treatment of the 2-*exo*-alcohol **100** with DMAP, Et₃N and acryloyl chloride in dichloromethane failed to produce the required ester **296**.

Attention was turned to the literature²³⁰⁻²³³ in an attempt to find more suitable reaction conditions for the required acylation and two particularly interesting methods were identified. The first method involved the highly efficient direct condensation of carboxylic acids with alcohols in the presence of Hf(IV) or Zr(IV) salts.²³² Unfortunately, the unavailability of the catalysts and concerns about the possibility of generating an alkoxide intermediate eventually ruled this method out. The second and more recent method,²³³ however, seemed remarkably straightforward and is reported to give excellent yields (90 - 100 %). Yadev and co-workers²³³ described the simple and effective acylation of alcohols and amines through the use of acylating reagents on an aluminium oxide (Al₂O₃) solid support. The acylation of alcohols was found to occur most readily with acid chlorides and primary alcohols, less readily with secondary alcohols and not at all with tertiary alcohols.

The acylation of both alcohols, **100** and **300**, was therefore attempted under identical conditions. In each reaction the alcohol, Al₂O₃ and acryloyl chloride were mixed together without solvent and left to stand overnight (**Scheme 2.43**, p. 179). ¹H NMR analysis of a sample of the reaction mixture showed the decrease of the alcohol signals and the appearance of acrylate ester signals. However, the reaction had not yet gone to completion and the mixture was left to stand for a total of 72 h. ¹H NMR data for the crude reaction mixture showed almost complete disappearance of signals for the starting material (**100** or **300**) and an anomalous “doubling” of practically all product signals. The preliminary thought was that hindered rotation might afford rotamers.¹³⁶ However, before any conclusions could be drawn it was necessary to purify the crude reaction mixture. This was initially attempted by radial chromatography, but separation was exceedingly poor and final purification was achieved by semi-preparative HPLC. Several fractions were isolated and subjected to ¹H NMR analysis. Surprisingly, two products were evident from each of the starting materials **100** and **300**, and full 1-D and 2-D NMR data sets were obtained. HSQC spectra of the products **296** and **308** are presented in **Figures 2.81** and **2.82**. The first product was identified as the *exo*-acrylate **296**. Comparison with the spectrum of the *endo*-acrylate **310** (**Figure 2.77**) revealed that the 2-H_{endo} signal is shifted upfield, relative to the 2-H_{exo} signal in the spectrum of the *endo*-acrylate **310**.

The HSQC spectrum of the second product **308** (**Figure 2.82**) isolated from the acylation of the 2-*exo*-alcohol **100** showed many similarities to the spectrum of the acrylate ester **296** (**Figure 2.81**). However, no characteristic acrylate peaks were visible and this, together with

the presence of two new methylene signals (2.58 and 3.60 ppm), suggested loss of the π -bond between C-2' and C-3' to form a saturated alkyl chain. The spectra, however, gave very little indication as to exactly what was present on the end of the alkyl chain. The IR spectrum suggested the presence of a halogen. Confirmation of the molecular composition was provided by the HRCI mass spectrum which revealed a peak at m/z 400.10598 which corresponds to the molecular formula $C_{19}H_{25}O_5SCl$ (calculated m/z 400.11112) and which permitted identification of the second product as the 2-*exo*-(3-chloropropanoyloxy) derivative **308**.

An X-ray diffraction analysis supported the presence of chlorine, and confirmed the stereochemical orientation of the 3-chloropropanoyloxy moiety as *exo*- and thus the complete structure of **308** (Figure 2.80).

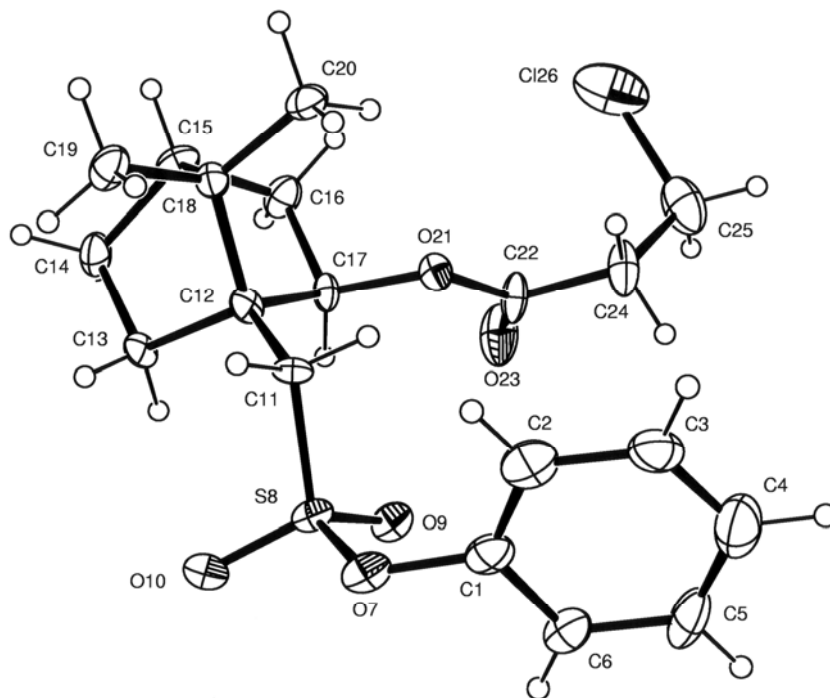


Figure 2.80: X-ray crystallographic structure of phenyl 2-*exo*-(3-chloropropanoyloxy)-bornane-10-sulfonate **308**, showing the crystallographic numbering.

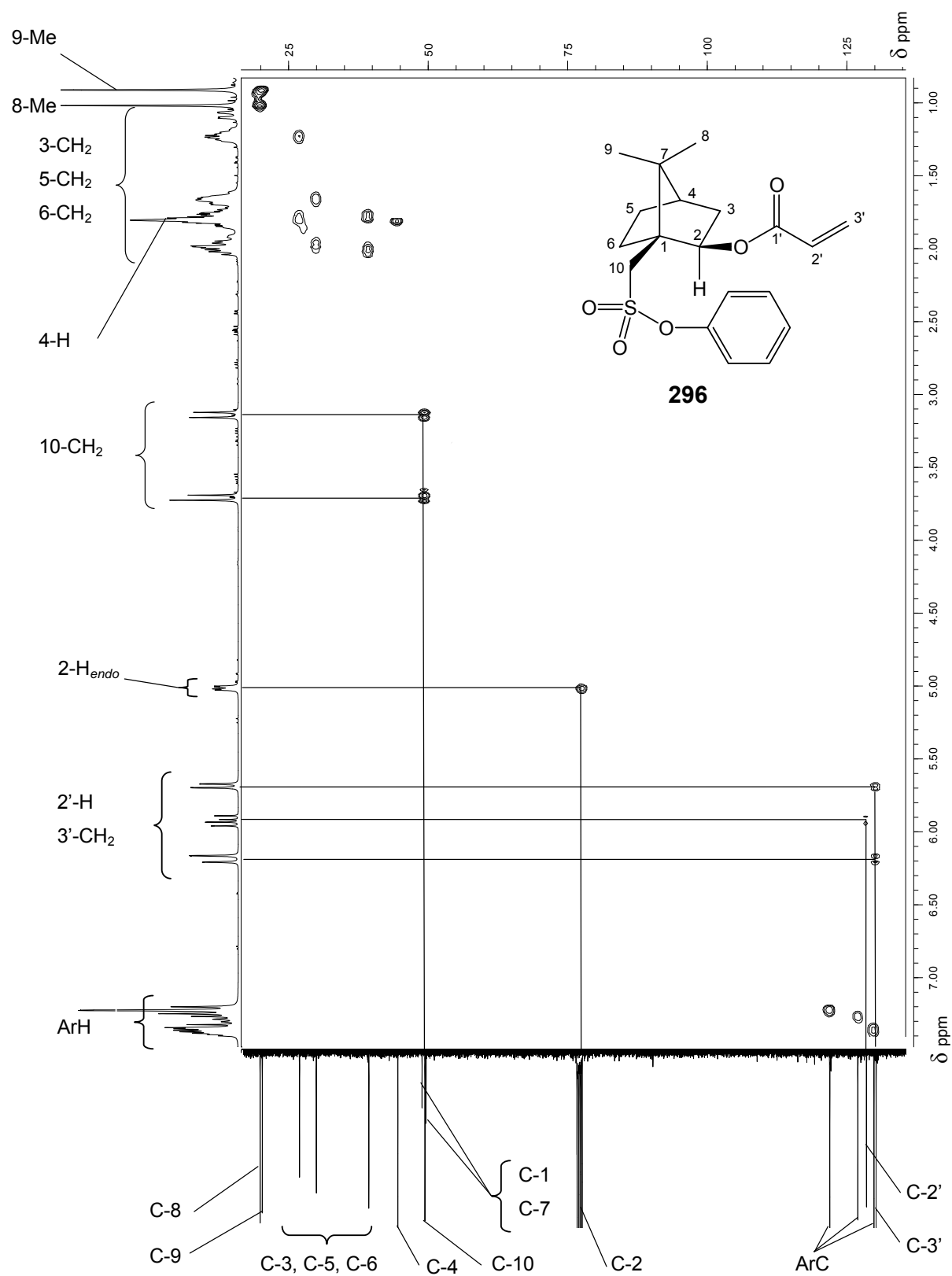


Figure 2.81: 400 MHz HSQC spectrum of phenyl 2-*exo*-acryloyloxybornane-10-sulfonate **296** in CDCl₃.

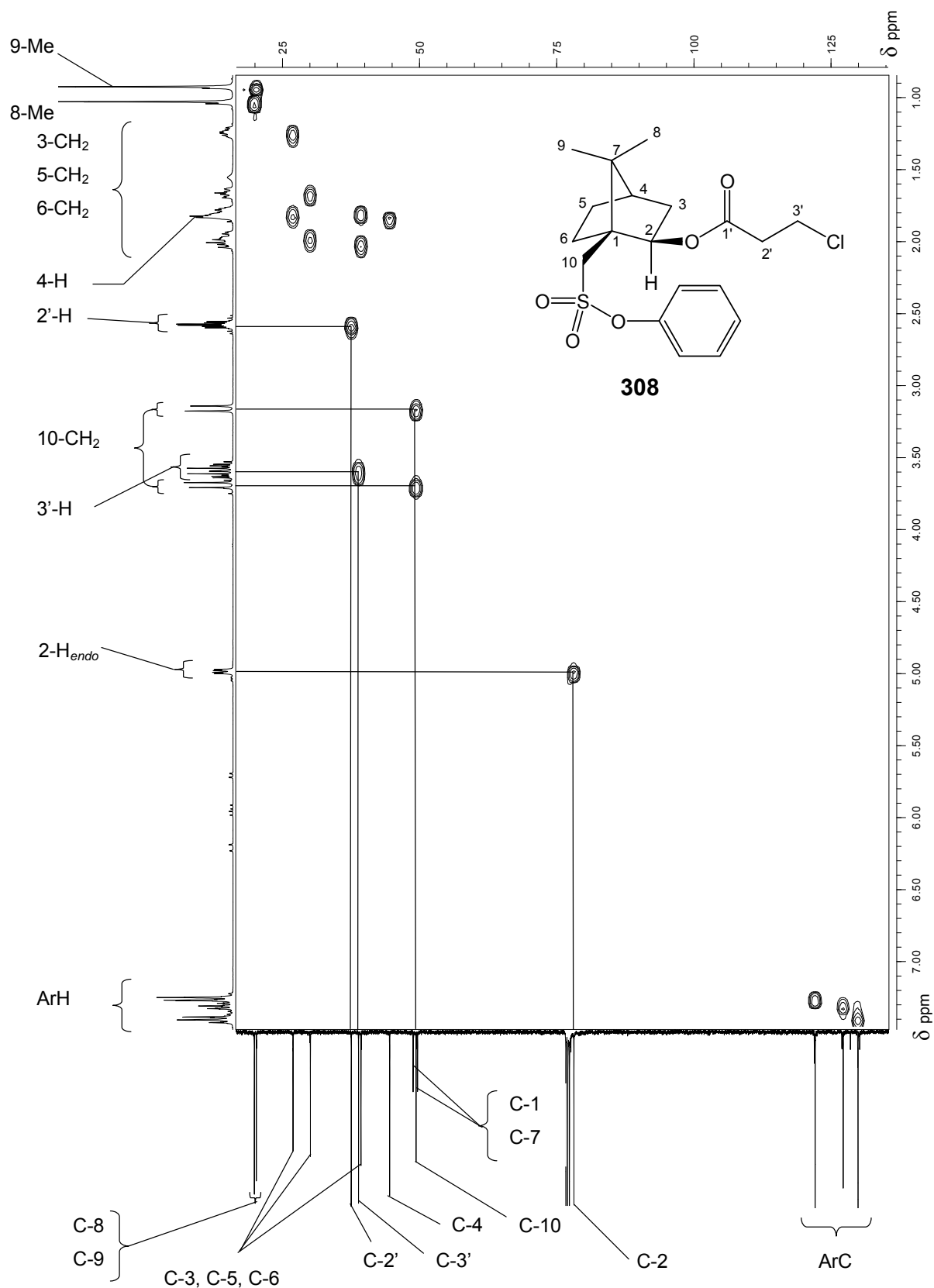
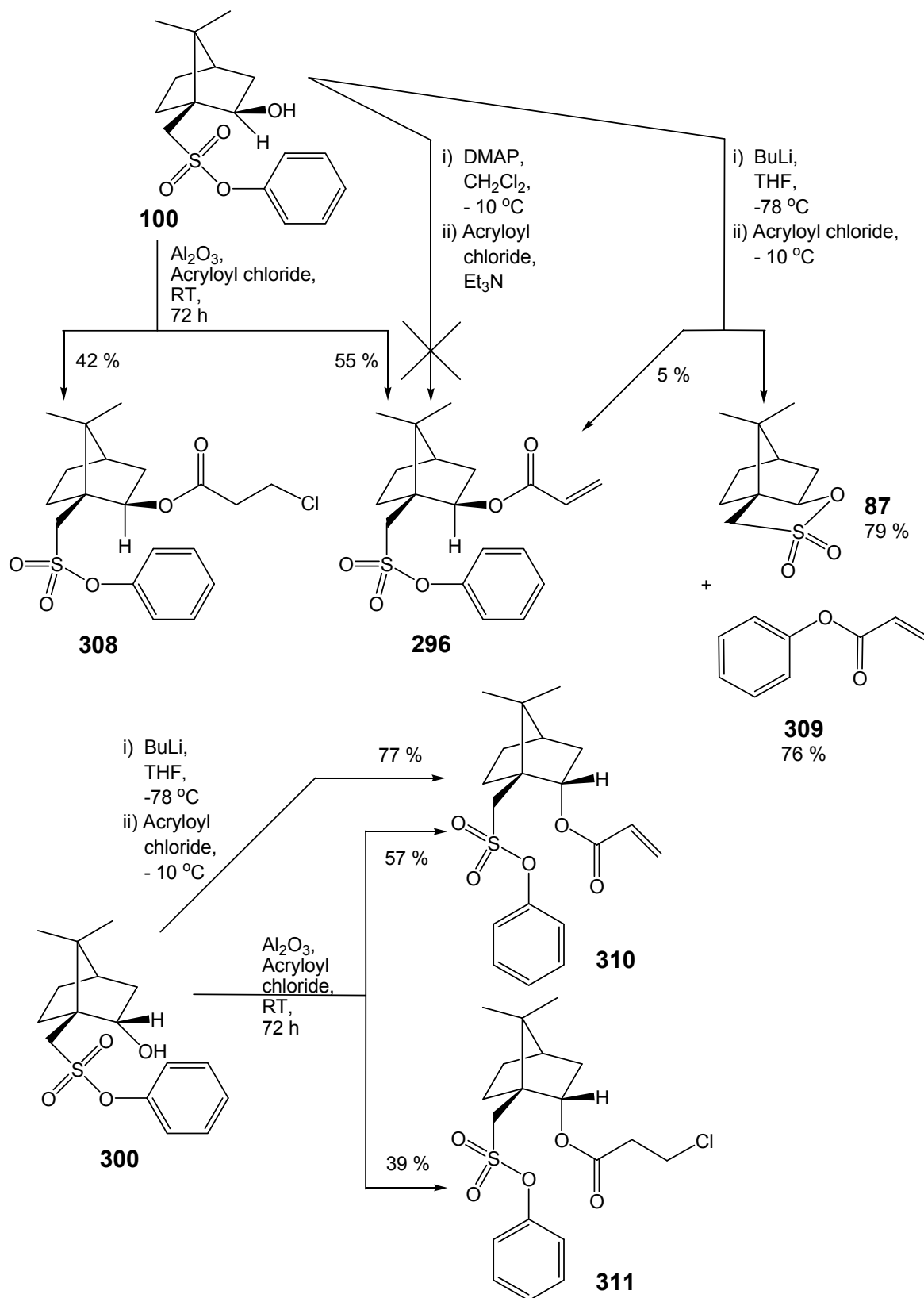


Figure 2.82: 400 MHz HSQC spectrum of phenyl 2-*exo*-(3-chloropropanoyloxy)bornane-10-sulfonate **308** in CDCl₃.



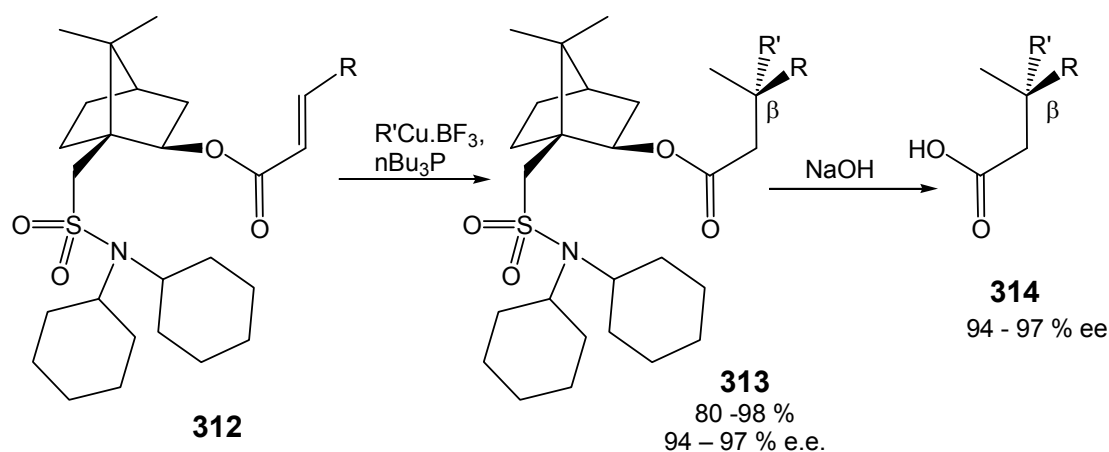
Scheme 2.43: Acylation reactions of phenyl 2-*exo*-hydroxybornane-10-sulfonate **100** and phenyl 2-*endo*-hydroxybornane-10-sulfonate **300**.

The Al_2O_3 -catalysed reaction of the 2-*endo*-alcohol **300** also afforded two products, the expected 2-*endo*-acrylate ester **310** (57 %) and the 2-*endo*-(3-chloropropanoyloxy) derivative **311** (39 %) (**Scheme 2.43**). The formation of the chlorinated products **308** and **311** under these conditions is attributed to addition of the liberated HCl to the acrylate double bond.

Although the synthesis of the phenyl sulfonate acrylates **310** and **296** was successfully achieved, their use in the Morita-Baylis-Hillman reaction was not attempted. The difficulty associated with their synthesis and, more importantly, the difficulty in separating the final products led to the decision to explore an analogous route employing an adamantyl blocking group.

2.3.6 Acrylate Esters of *N*-(1-adamantyl)-2-hydroxybornane-10-sulfonamide

Oppolzer and co-workers studied the potential of the camphor-10-sulfonamide **312** as a chiral substrate in the synthesis of β -substituted carboxylic acids **314**.²¹⁹ Yields were good to excellent, as were the enantiomeric excesses of the final products (**Scheme 2.44**).



Scheme 2.44: The synthesis of β -substituted carboxylic acids.²¹⁹

Sulfonamides tend to be more stable than their sulfonate ester equivalents,¹³⁶ and a range of these compounds has been investigated. In addition, adamantane and its derivatives have attracted considerable interest in the recent past,^{227,234-236} and the potential for the bulky adamantyl group²³⁵ to effectively block electrophilic attack at one face of an acrylate system

was attractive. The expected mode of attack by aldehydes on the Morita-Baylis-Hillman intermediate **315** is illustrated in **Figure 2.83**.^{237,238}

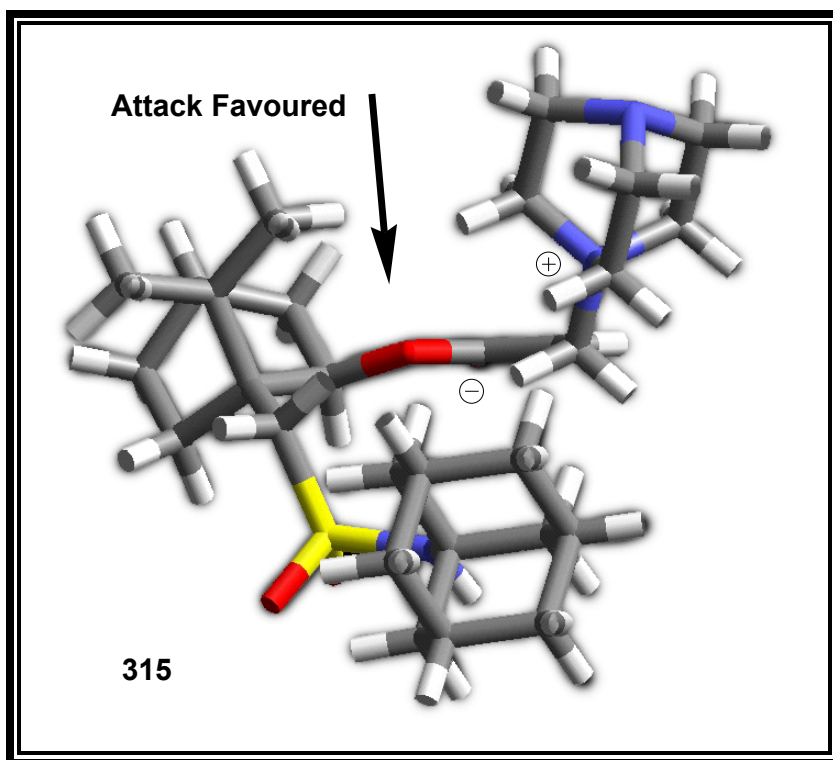


Figure 2.83: Expected direction of electrophilic attack on the reactive species **315** undergoing a Morita-Baylis-Hillman reaction.

It was anticipated that, as a result of the effective delocalisation of the nitrogen lone-pair electrons (**Figure 2.84**), the adamantylsulfonamide linkage should be considerably more stable than the phenyl sulfonate link had been found to be and, consequently, that formation of the sultone **87** (*via* an intermediate alkoxide) would be less likely.¹³⁶

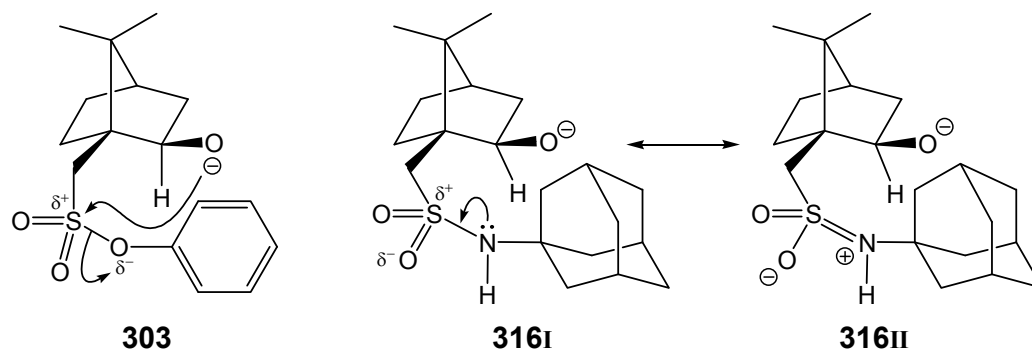


Figure 2.84: Comparison of alkoxide intermediates of the phenyl sulfonate **303** and the *N*-adamantylsulfonamide **316**.

2.3.6.1 Preparation of N-(1-adamantyl)camphor-10-sulfonamide

Alkyl amines are known to be excellent nucleophiles in S_N2 reactions,¹⁸³ and acylation of adamantylamine to form the corresponding sulfonamide **318** (Scheme 2.45, p. 194) was expected to occur easily; however, the addition of a catalytic amount of the tertiary amine, DMAP, was determined to be useful for its rate enhancing ability.²³¹

A concern was that adamantylamine, as a primary amine, had the potential to be diacylated, but this was suspected to be unlikely due to the bulk of the camphorsulfonyl chloride. In an analogous acylation of benzylamine, Ramon *et al.*²³⁹⁻²⁴¹ obtained only the corresponding monoacylated product. Nevertheless, the sulfonyl chloride **298** was used as a limiting reagent as a pre-emptive measure. Thus, sulfonyl chloride **298** (1 eq.), adamantylamine **317** (2 eq.) and DMAP (0.2 eq.) in acetonitrile were allowed to react at 0 °C for one hour before quenching by the successive addition of H₂O and 10 % HCl. Separation and purification of the reaction mixture was readily achieved by sequential acid and base extractions to obtain the sulfonamide **318** in excellent yield (92 %). Analysis of 1-D and 2-D NMR spectra, particularly the HSQC spectrum (Figure 2.85), as well as HRCI mass spectrum analysis (Figure 2.87), permitted unambiguous characterization of the sulfonamide **318**. Examination of the ¹³C and DEPT 135 spectra suggested that compound **318** contained a total of 20 carbon nuclei with 3 intense signals (43.2, 36.0 and 29.7 ppm) each representing 3 magnetically equivalent carbon nuclei (one methine and two methylene signals) and the characteristic bornane signals evidenced previously. The ¹H NMR spectrum contained several signals expected for the bornane skeleton; however, several new, broad resonances were evident. Attention was focused on the HSQC spectrum (Figure 2.85), and the two intense methylene signals (43.2 and 36.0 ppm) in the ¹³C spectrum were found to correlate directly with two of the broad signals in the ¹H spectrum (1.66 and 2.99 ppm), which integrated for 6 protons each and which were assigned to the adamantyl methylene groups. The final intense signal (29.7 ppm) correlated with another broad signal (2.09 ppm) in the ¹H spectrum, which integrated for 3 protons and was identified as the adamantyl methine resonance. The 4-H signal at 2.08 ppm, almost obscured by the adamantyl methine signal, may be assigned by its correlation to C-4 (42.8 ppm) in the HSQC spectrum. The broad singlet in the ¹H spectrum at 4.95 ppm was noted to have no correlations in the ¹³C spectrum and was assigned to the amide proton. A computer-modelled structure of a stable conformation of the sulfonamide **318** is illustrated in Figure 2.86.

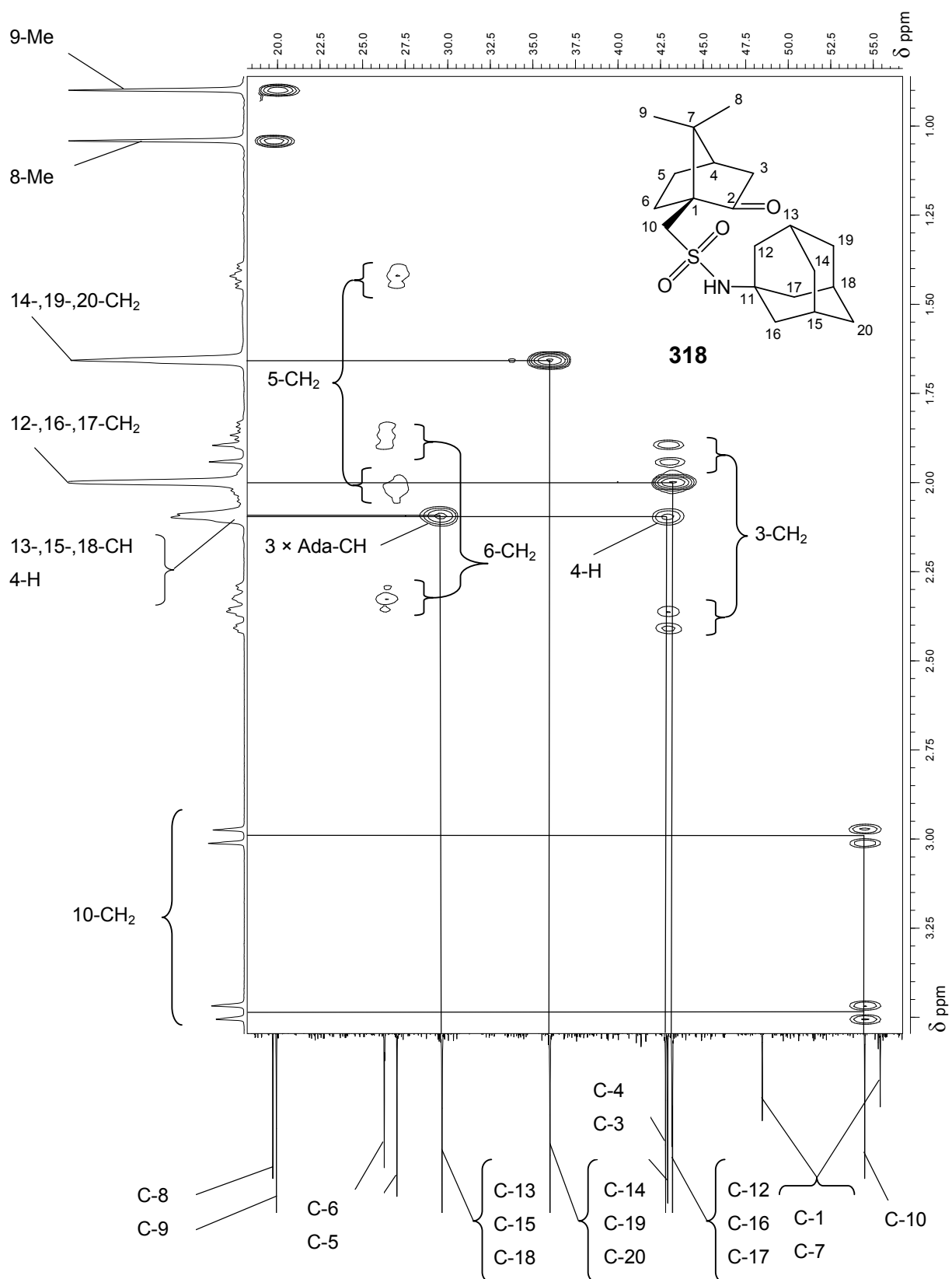


Figure 2.85: 400 MHz HSQC spectrum of *N*-(1-adamantyl)-2-oxo-bornane-10-sulfonamide **318** in CDCl₃.

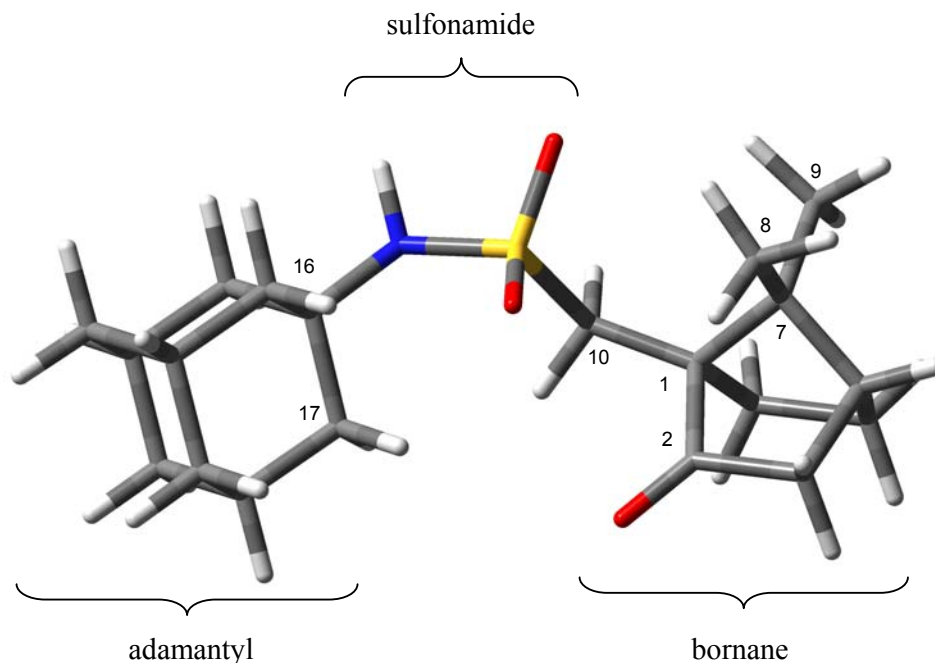


Figure 2.86: Computer-modelled representation of a stable conformation of *N*-(1-adamantyl)-2-oxo-bornane-10-sulfonamide **318**.

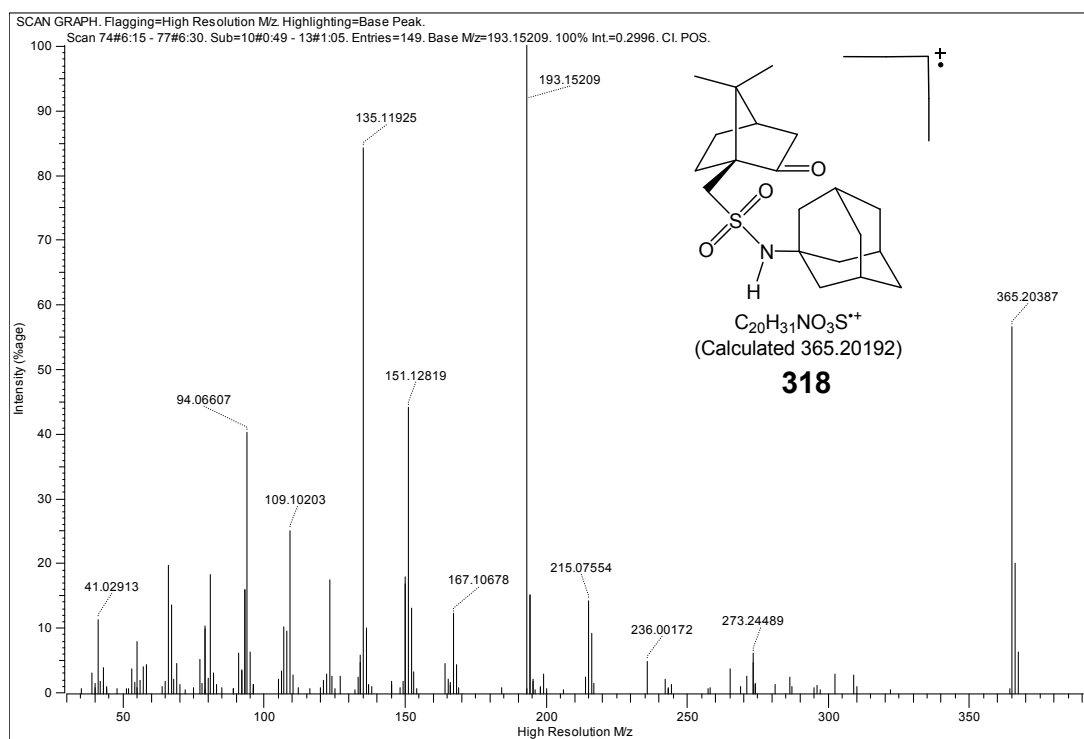


Figure 2.87: HRCI mass spectrum, with selected fragments, of *N*-(1-adamantyl)-2-oxo-bornane-10-sulfonamide **318**.

The HRCI mass spectrum of **318** (Figure 2.87) reveals a peak at m/z 365.20387, the odd mass being characteristic of a compound containing an odd number of nitrogen atoms; this corresponds to the expected molecular formula $C_{20}H_{31}NO_3S$ (calculated m/z 365.20247).

Complete characterization of *N*-(1-adamantyl)-2-oxo-bornane-10-sulfonamide **318** was thus completed, and the excellent yield and easy separation of product were most encouraging.

2.3.6.2 Reduction of *N*-(1-adamantyl)camphor-10-sulfonamide

The reduction of *N*-(1-adamantyl)-2-oxo-bornane-10-sulfonamide **318** was expected to occur in much the same way as phenyl camphor-10-sulfonate **72**, but without the problem of sulfone formation. *Endo* attack was again expected to favour production of the *exo*-alcohol.

The stereoselective reduction of analogous phenyl sulfonamides by Ramon *et al.*²⁴¹ was conducted in EtOH under various conditions. At 0 °C, an *exo*: *endo* ratio of 86:12 was observed, while the use of bulky reducing agents, such as *N*- or *L*-selectride, improved the ratio marginally (88 % *exo*: 10 % *endo*). The reduction of the adamantyl analogue **318** was carried out with $NaBH_4$ in EtOH/H₂O (5:1) at room temperature overnight. Purification by radial chromatography afforded the isomeric *exo*- and *endo*-alcohols (**319** and **328**) in excellent yield (99 %) with a higher diastereomeric ratio (94 % *exo*: 6 % *endo*) than Ramon *et al.*²⁴¹ had achieved with the phenyl sulfonamides. No trace of any side products was evident, confirming that cyclization was unfeasible under these conditions.

Structure elucidation of the isomeric alcohols **319** and **328** was achieved through detailed analysis of the ¹H, ¹³C, DEPT 135 and HSQC NMR data (Figures 2.88 - 2.91) and by comparison with data for similar systems, in particular the ketone precursor **318** and the phenyl sulfonates **100** and **300**.

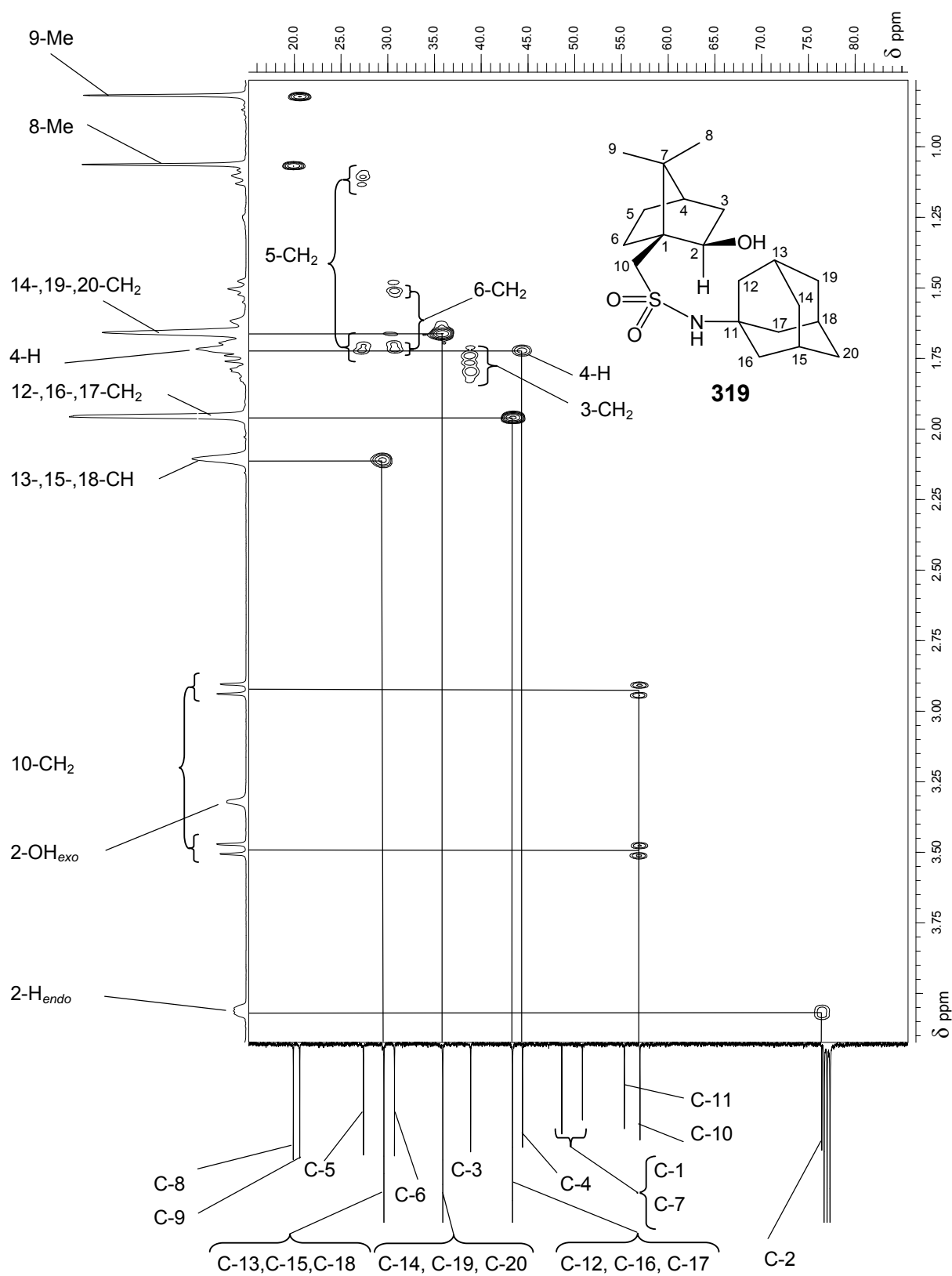


Figure 2.88: 400 MHz HSQC spectrum of *N*-(1-adamantyl)-2-*exo*-hydroxybornane-10-sulfonamide **319** in CDCl₃.

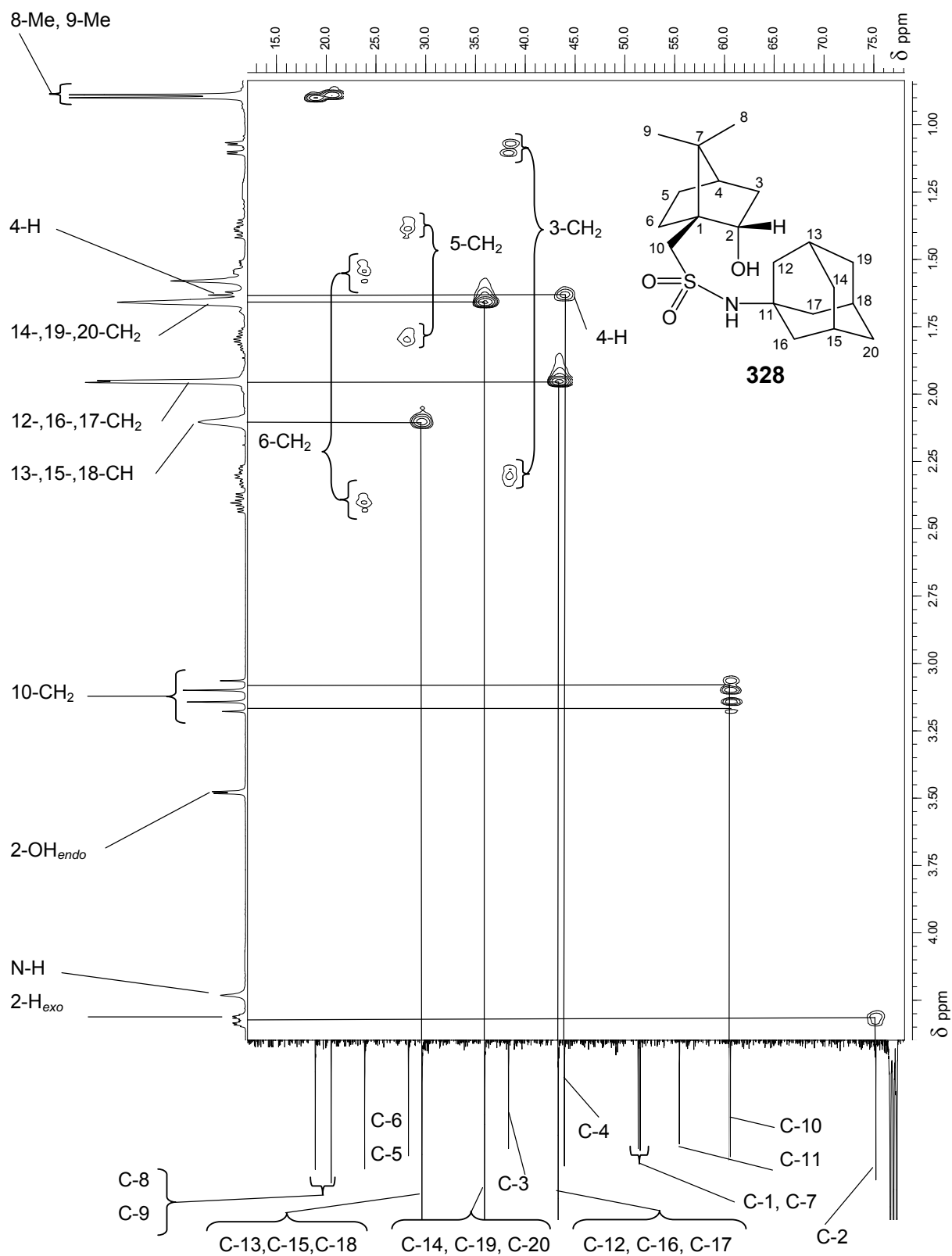


Figure 2.89: 400 MHz HSQC spectrum of *N*-(1-adamantyl)-2-*endo*-hydroxybornane-10-sulfonamide **328** in CDCl₃.

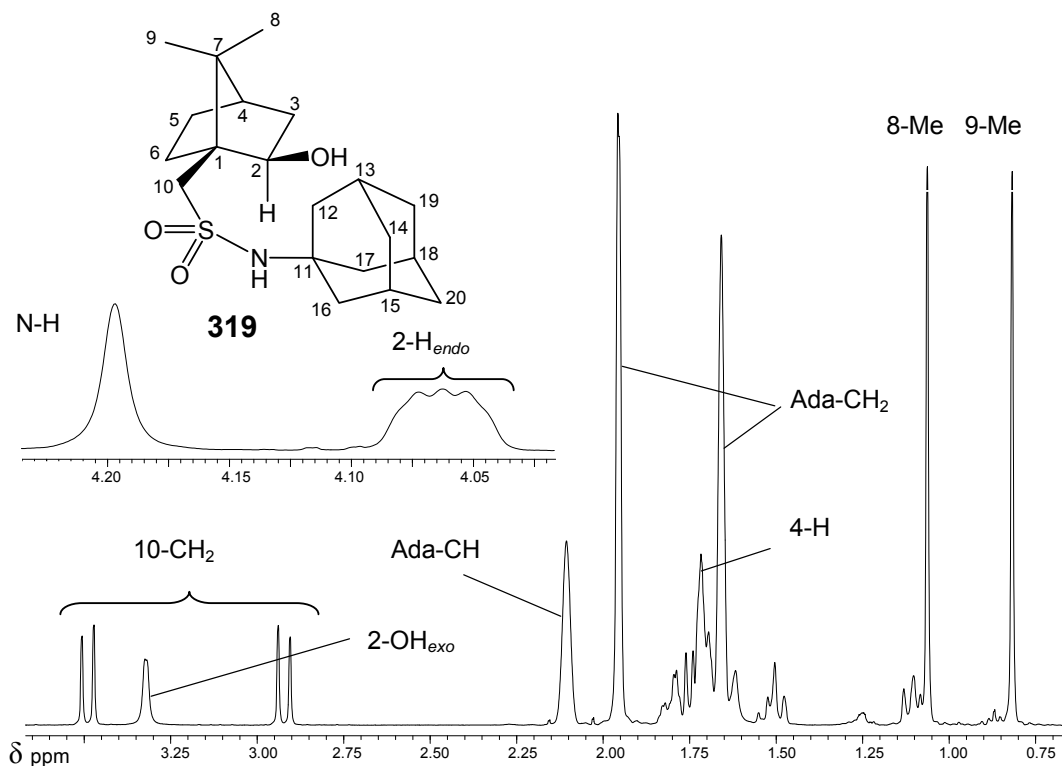


Figure 2.90: 400 MHz ^1H NMR spectrum, with an expansion showing 2- H_{endo} and N-H, of *N*-(1-adamantyl)-2-*exo*-hydroxybornane-10-sulfonamide **319**.

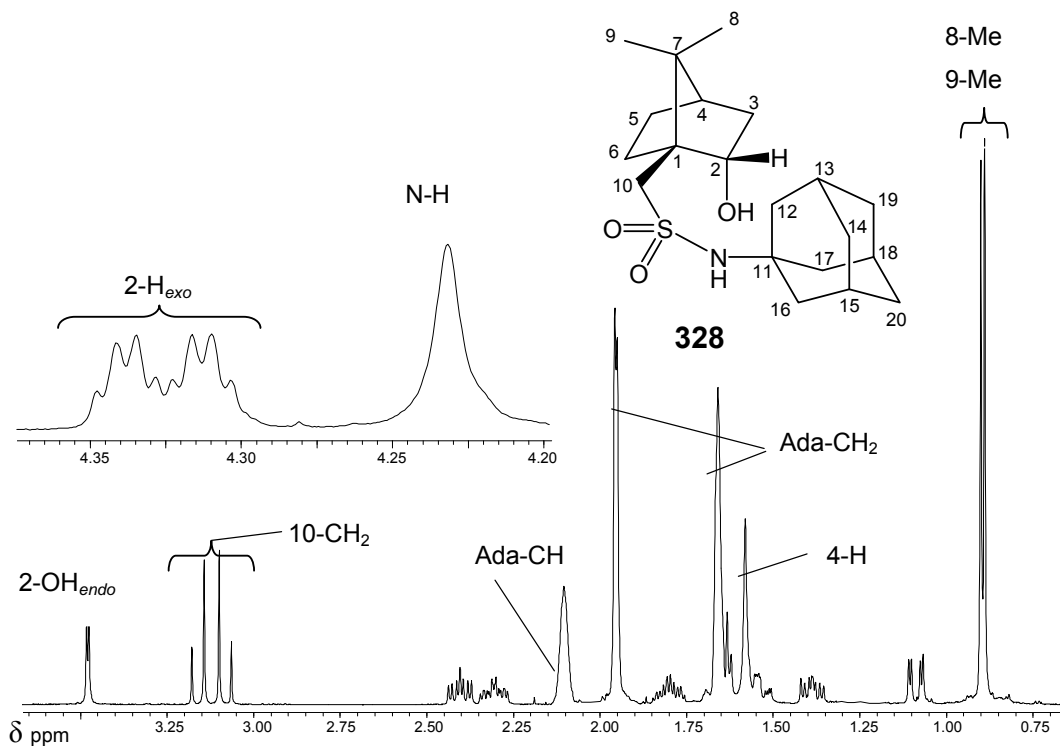


Figure 2.91: 400 MHz ^1H NMR spectrum, with an expansion showing 2- H_{exo} and N-H, of *N*-(1-adamantyl)-2-*endo*-hydroxybornane-10-sulfonamide **328**.

The HSQC spectra (**Figures 2.88** and **2.89**) show proton-carbon correlations for **319** and **328** that allow the identification of nuclei whose signals are obscured in the ^1H spectra. Both compounds show the presence of new hydroxyl signals and the associated 2-H signals. The deshielding effect of the hydroxyl group on nearby nuclei facilitated the assignment of stereochemistry. The *exo*-hydroxylic group of **319** causes deshielding of the nearby 8-Me group (1.06 ppm) relative to the 9-Me group (0.82 ppm); hence the signals are widely separated. The *endo*-hydroxylic group of the isomeric system **328** exerts minimal effect on the 8- and 9-Me nuclei and the signals are close together (**Figures 2.90** and **2.91**).

The complexity of the ^1H NMR signals for the 2- H_{endo} nucleus of **319** and the 2- H_{exo} nucleus of **328** makes detailed coupling analysis impossible (**Figures 2.90** and **2.91**); however, the 2- H_{endo} nucleus (4.06 ppm) is in a more shielded environment than the 2- H_{exo} nucleus (4.33 ppm) and, consequentially the signal for the former is found further upfield. The 3- H_{endo} (1.79 ppm), 5- H_{endo} (1.72 ppm) and 6- H_{endo} (1.69 ppm) signals for the *exo*-alcohol **319** are found further upfield than in the isomeric sulfonamide system **328**, in which the 2-*endo*-hydroxyl group causes deshielding of the *endo* protons, 3- H_{endo} (2.33 ppm), 5- H_{endo} (1.82 ppm) and 6- H_{endo} (2.41 ppm). The 10- CH_2 nuclei of **319** resonate at widely separated shifts (2.92 and 3.49 ppm) compared to the corresponding signals in the *endo*-alcohol **328** - a phenomenon attributed to the relative proximity of the 2-*exo*-hydroxyl group in the former isomer (as illustrated in **Figures 2.92** and **2.93**). Computer-modelling also illustrates the close proximity of the 2- OH_{exo} proton to the sulfonyl oxygen of the *exo*-hydroxy-alcohol **319**, suggesting the possibility of hydrogen bonding, whereas the significant distance between the corresponding groups in the *endo*-hydroxy epimer **328** would suggest the absence of such hydrogen bonding. It is, of course, likely that other conformers contribute to the conformational equilibrium.

The HRCI mass spectrum of the 2-*exo*-alcohol **319** revealed a peak at m/z 367.21993 corresponding to a compound containing an odd number of nitrogen atoms and to the expected molecular formula $\text{C}_{20}\text{H}_{33}\text{NO}_3\text{S}$ (calculated m/z 367.21812). Similarly the HRCIMS analysis of the *endo*-isomer **328** revealed a peak at m/z 367.21706, which corresponds to the same expected molecular formula.

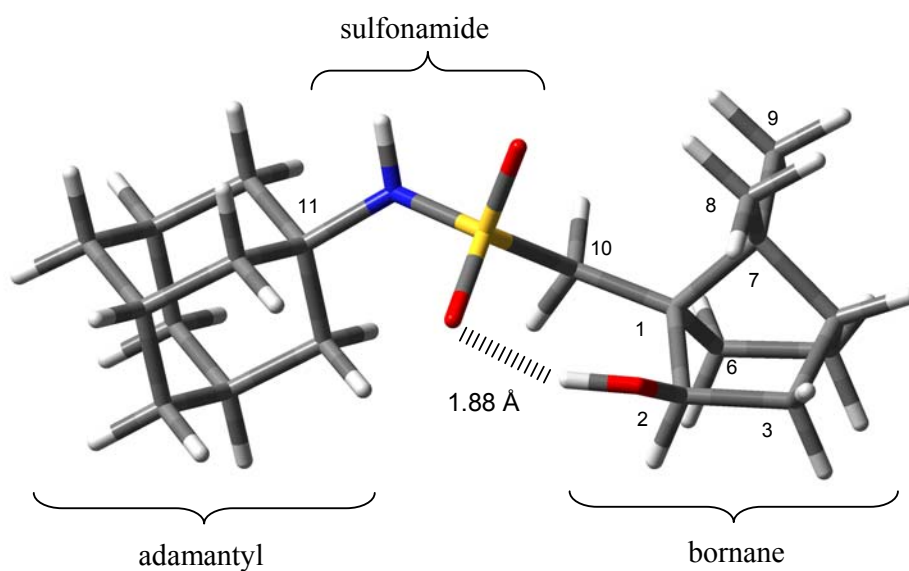


Figure 2.92: Computer-modelled representation of a stable conformation of *N*-(1-adamantyl)-2-*exo*-hydroxybornane-10-sulfonamide **319**.

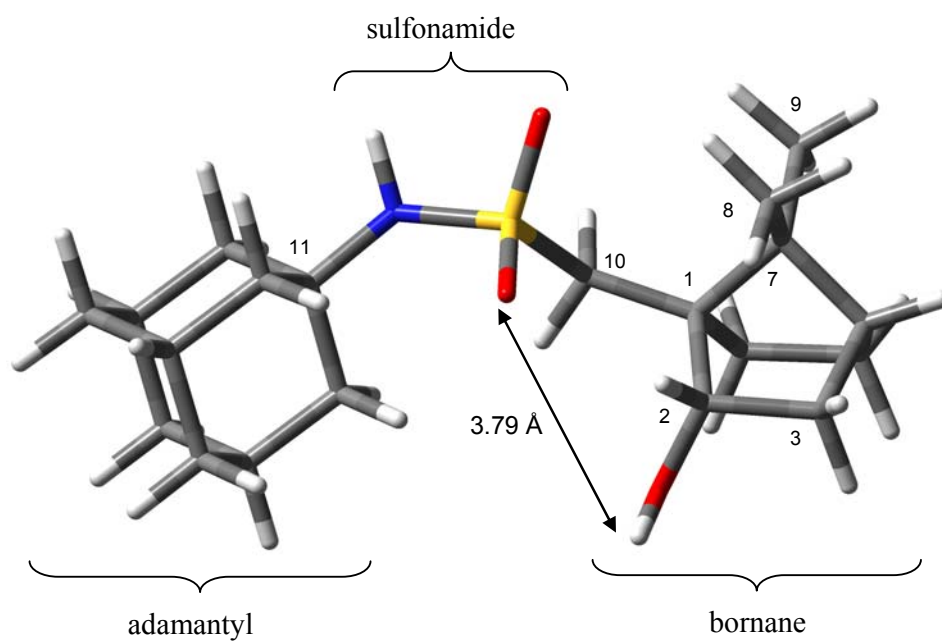


Figure 2.93: Computer-modelled representation of a stable conformation of *N*-(1-adamantyl)-2-*endo*-hydroxybornane-10-sulfonamide **328**.

2.3.6.3 Acylation of the N-(1-adamantyl)-2-hydroxybornane-10-sulfonamides

The problems encountered with the acylation of the *exo*-hydroxy sulfonate **100** were in a large part due to the reactive alkoxide and the availability of the phenyl sulfonate moiety to undergo nucleophilic substitution. In the case of the acylation of the *endo*-hydroxy sulfonate **300**, the *endo*-orientation of the hydroxyl group prevented the alkoxide from attacking the sulfonate. The relative stability of the adamantyl sulfonamides **319** and **328** suggested that the use of a strong base, such as NaH or BuLi, would be appropriate. The acylation was attempted by the addition of BuLi at -78 °C and the addition of acryloyl chloride at -10 °C. The reaction mixture was allowed to warm to room temperature overnight, but ¹H NMR analysis showed no sign of any acrylate signals. This was very surprising considering the strength of the base and the fact that the vigorous reaction on quenching meant that the BuLi was indeed very active. Attention was then turned to the use of Al₂O₃ as a catalyst.²³³ The epimeric alcohols **319** and **328** were reacted under identical conditions, *viz.*, addition of the alcohol to neutral Al₂O₃ (1.5 eq.) followed by the addition of acryloyl chloride (2 eq.) and stirring at room temperature for 96 h. Purification of the crude reaction mixtures proved difficult, but use of semi-preparative HPLC permitted the isolation of four novel compounds, **321** and **320** (**Figures 2.94** and **2.95**) and **330** and **329** (**Figures 2.96** and **2.97**). Assignment of the stereochemistry was achieved in a similar manner to that used for the acrylate esters **310** and **296** and the chloroalkyl derivatives **311** and **308**. Confirmation of the molecular composition of the acrylate esters **321** and **330** was provided by the HRCIMS analysis which revealed peaks at *m/z* 421.22844 and 421.22485, respectively, which correspond to the expected molecular formula, C₂₃H₃₅O₄NS (calculated *m/z* 421.22868). Confirmation of the molecular composition of the chloroalkyl derivatives **320** and **329** was also provided by the HRCIMS data which revealed peaks at *m/z* 457.21058 and 457.21295, respectively, which correspond to the expected molecular formula C₂₃H₃₆O₄NS³⁵Cl (calculated *m/z* 457.20536). The complete pathway to the acrylate esters is illustrated in **Scheme 2.45** (p. 194).

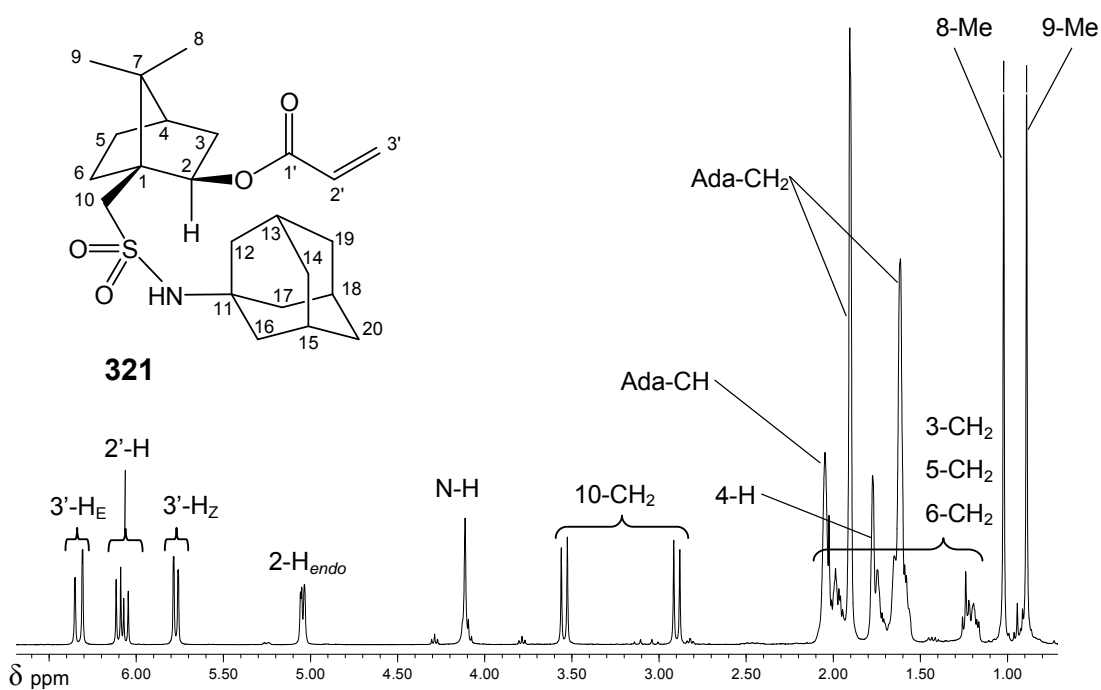


Figure 2.94: 400 MHz ^1H NMR spectrum for 2-*exo*-acryloyloxy-*N*-(1-adamantyl)bornane-10-sulfonamide **321** in CDCl_3 .

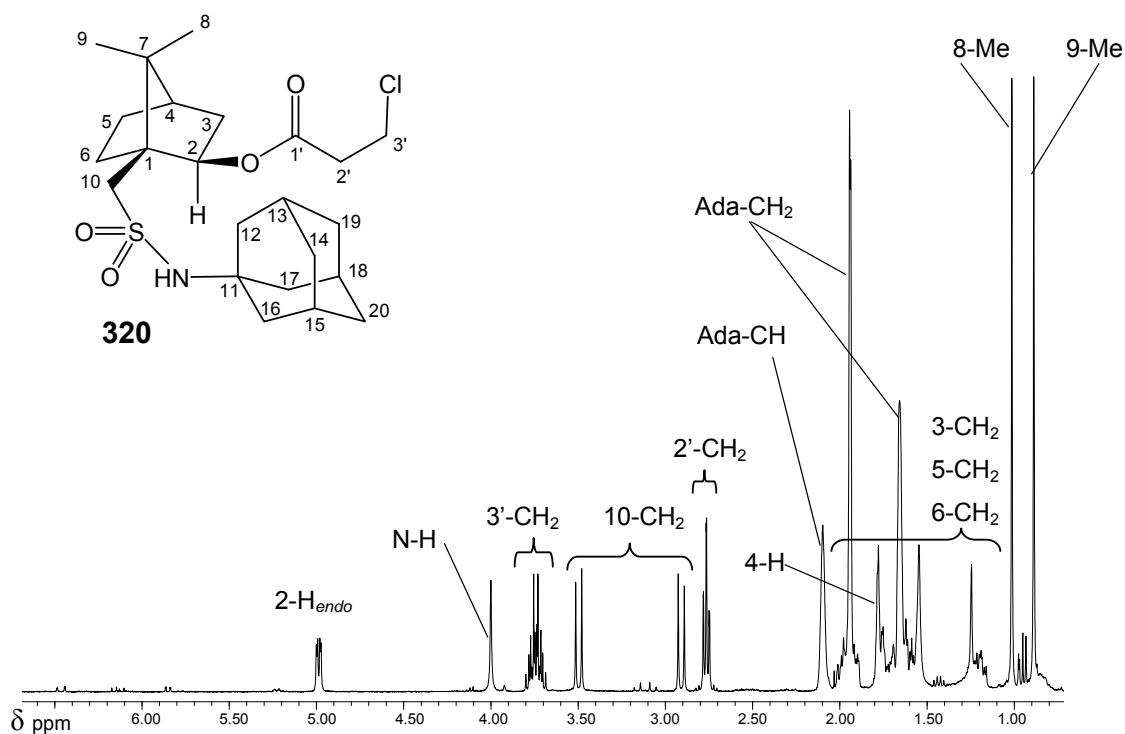


Figure 2.95: 400 MHz ^1H NMR spectrum for *N*-(1-adamantyl)-2-*exo*-(3-chloropropanoyloxy)bornane-10-sulfonamide **320** in CDCl_3 .

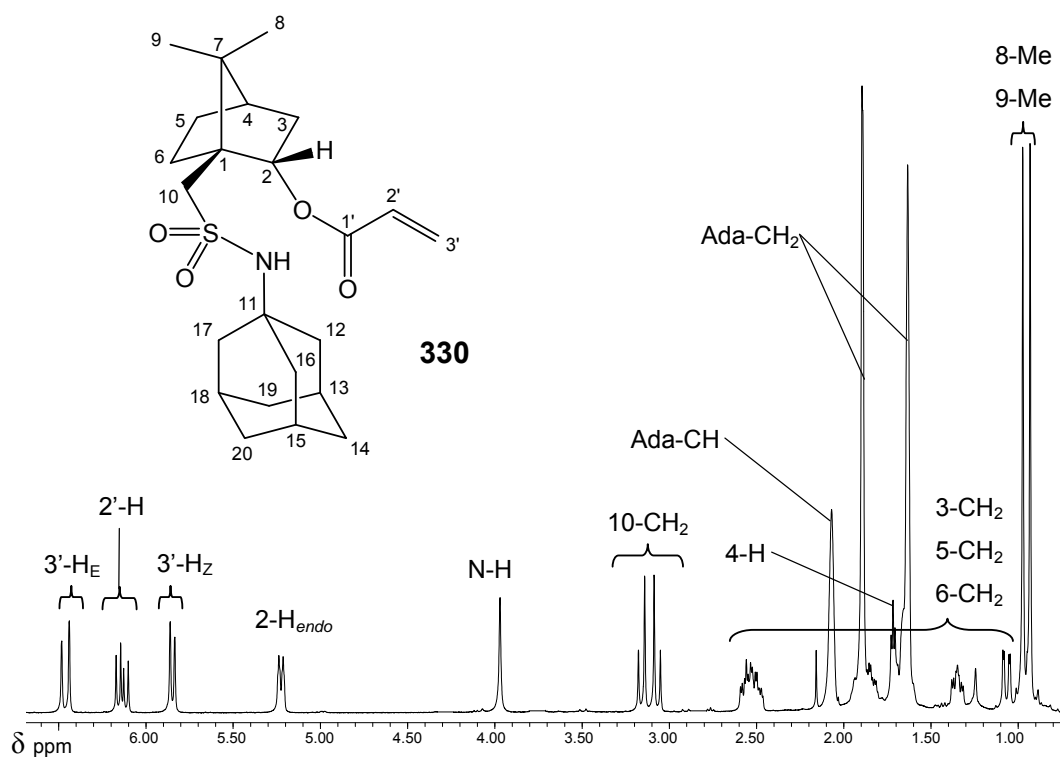


Figure 2.96: 400 MHz ¹H NMR spectrum for 2-endo-acryloyloxy-N-(1-adamantyl)bornane-10-sulfonamide **330** in CDCl₃.

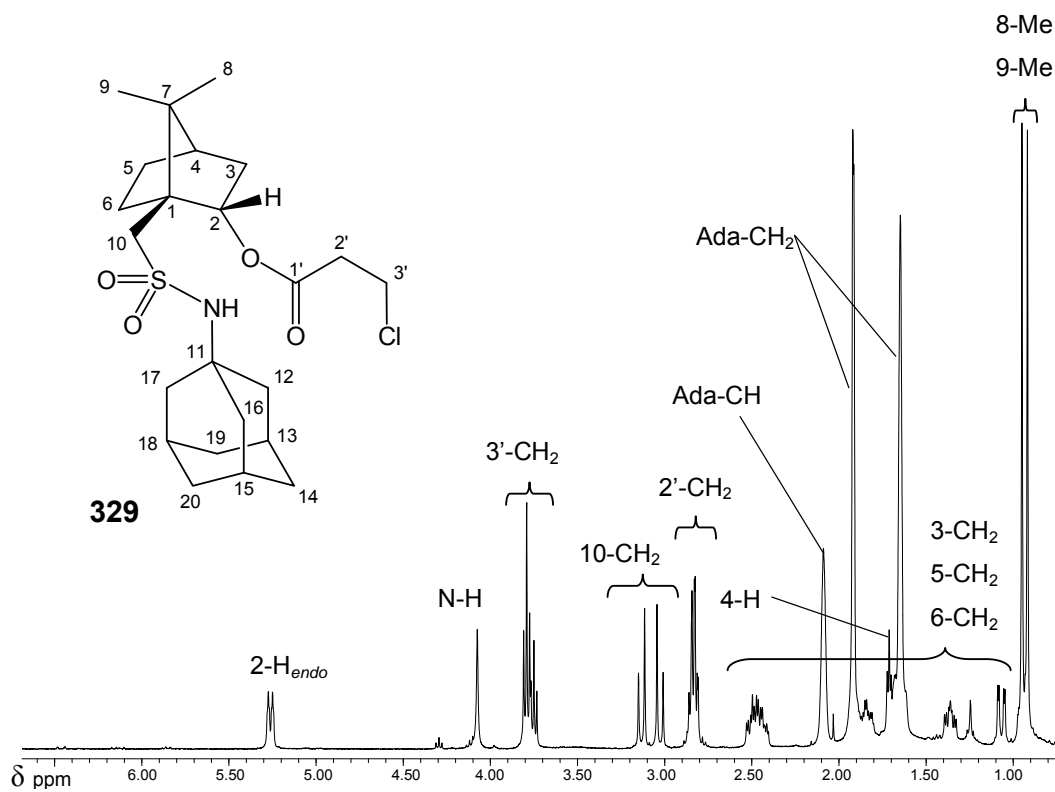
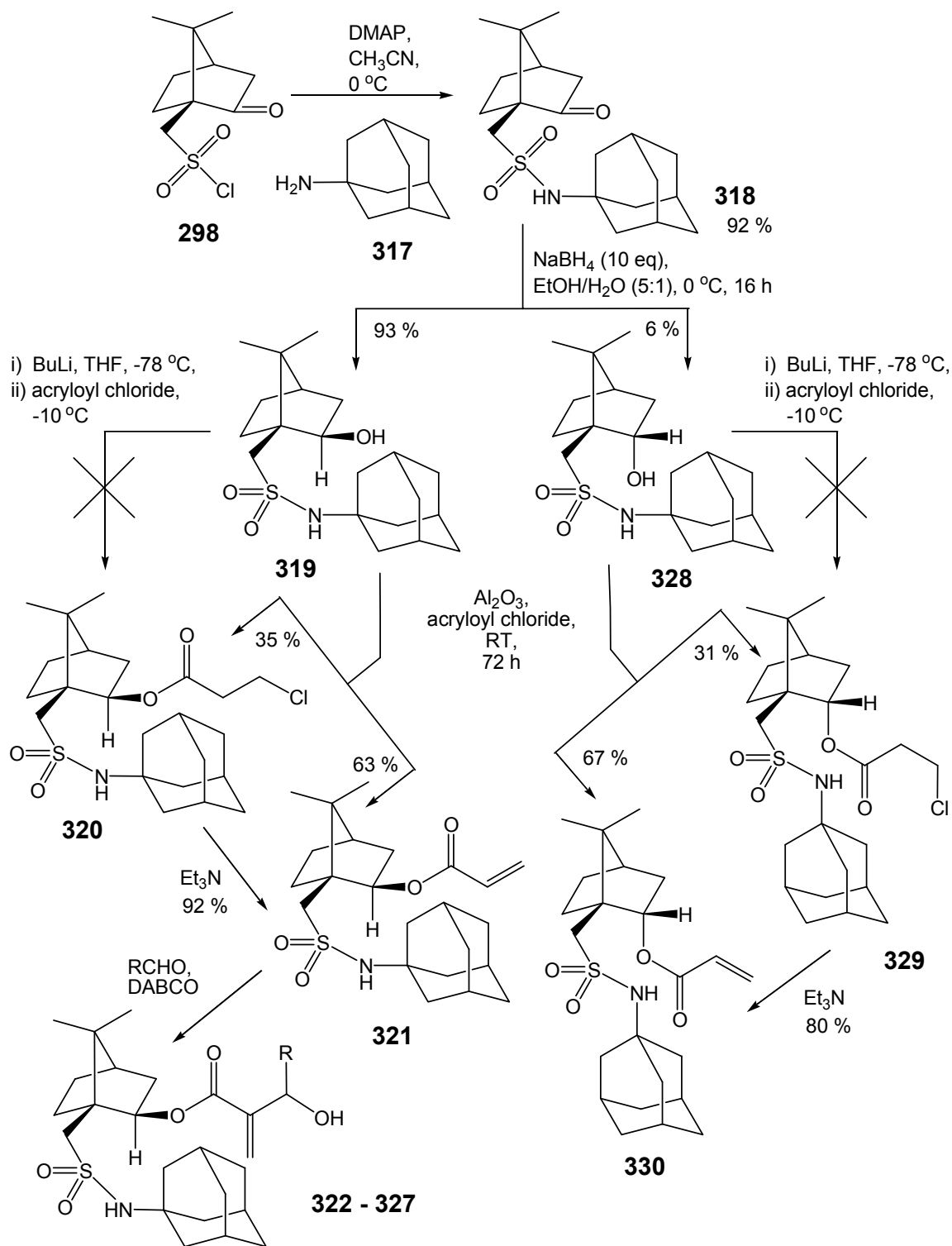


Figure 2.97: 400 MHz ¹H NMR spectrum for N-(1-adamantyl)-2-endo-(3-chloropropanoyloxy)bornane-10-sulfonamide **329** in CDCl₃.



Scheme 2.45: Synthetic routes to the chiral Morita-Baylis-Hillman substrates **321** and **330** and the products **322 - 327**.

2.3.6.4 Use of the 2-Exo-acryloyloxy-N-(1-adamantyl)bornane-10-sulfonamide auxiliary in the Morita-Baylis-Hillman reaction

Computer-modelling was used to visualize possible intramolecular interactions in the 2-*exo*- and 2-*endo*-acrylate esters **321** and **330**, respectively (**Figures 2.98** and **2.99**). Potential approaches of the aldehyde in a Morita-Baylis-Hillman reaction are labelled “**a**” and “**b**”. In both instances approach “**b**” seems to be the more likely direction of attack as the large adamantyl moiety may be expected to block approach “**a**” to some degree. In the Morita-Baylis-Hillman reaction, tertiary amine-catalyzed addition of a zwitterionic enolate intermediate to an aldehyde results in the formation of a carbon-carbon bond at the α -position of the enolate.¹⁰² Following the successful synthesis and encouraging computer-modelling analysis of the acrylates **321** and **330**, ample motivation was provided for their use in this reaction. As the *endo*-acrylate **330** is by far the minor product, it was necessary to use the *exo*-acrylate **321** for subsequent reactions. A range of six structurally varied aldehydes and the tertiary amine catalyst DABCO were chosen to effect this transformation with the *exo*-acrylate **321** (**Scheme 2.46**).

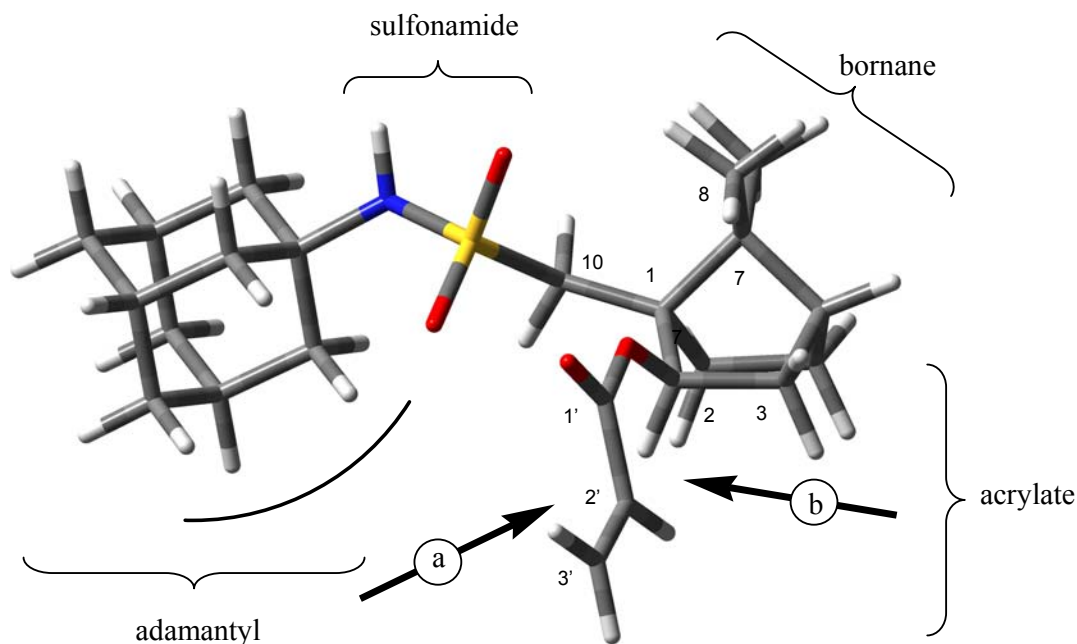


Figure 2.98: Computer-modelled representation of a stable conformation of 2-*exo*-acryloyloxy-*N*-(1-adamantyl)bornane-10-sulfonamide **321**.

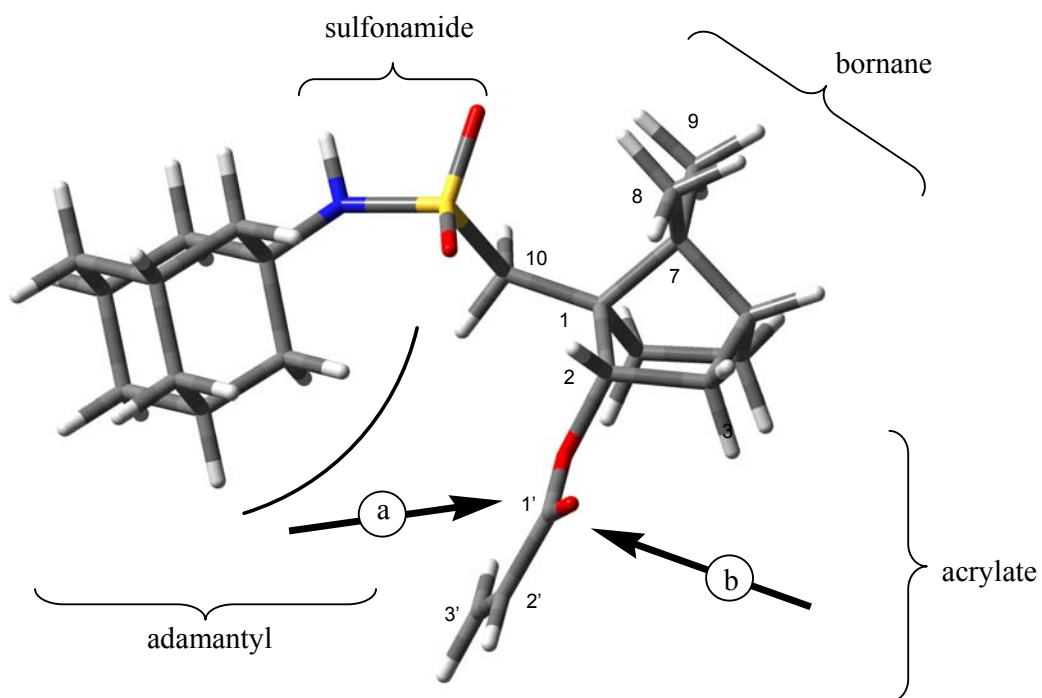
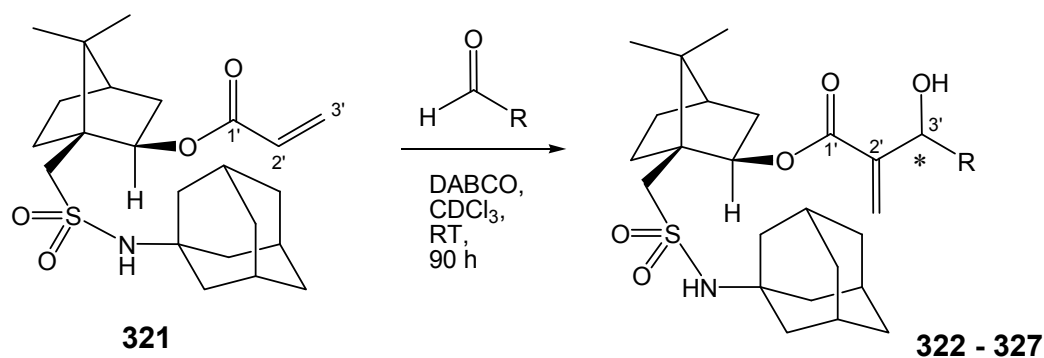


Figure 2.99: Computer-modelled representation of a stable conformation of 2-*endo*-acryloyloxy-*N*-(1-adamantyl)bornane-10-sulfonamide **330**.



RCHO	Product
4-Pyridinecarbaldehyde	322
2-Pyridinecarbaldehyde	323
3-Pyridinecarbaldehyde	324
6-Methyl-2-pyridinecarbaldehyde	325
2-Nitrobenzaldehyde	326
Pivaldehyde	327

Scheme 2.46: Morita-Baylis-Hillman reactions of 2-*exo*-acryloyloxy-*N*-(1-adamantyl)-bornane-10-sulfonamide **321**.

The reactions were conducted in NMR tubes and progress was monitored by ^1H NMR spectroscopy. The disappearance of the 2'-H and 3'-CH₂ vinylic signals of the acrylate **321** was accompanied by the appearance of the 3'-H, 3'-OH and vinylic methylene signals of the new Morita-Baylis-Hillman products **322** - **327**. Structure elucidation was achieved through the use of 1-D and 2D-NMR analysis and the HSQC spectrum for the product **325** is illustrated in **Figure 2.100**. The remaining products in the series were characterized similarly.

The ^{13}C and DEPT spectra of **325** showed the presence of 30 carbons including: - three methyl signals at 20.0, 20.4 and 27.1 ppm (C-8, C-9 and C-9'); three intense signals at 29.5, 35.8 and 43.2 ppm (adamantyl); four downfield quaternary signals at 143.2, 156.6, 157.9 and 165.1 ppm (C-1', C-2', C-4' and C-8'); characteristic pyridine signals at 118.6, 122.1 and 137.4 ppm (C-5', C-6' and C-7'); and a methylene signal at 125.4 ppm (C-10'). The HSQC spectrum indicated the correlations detailed in **Figure 2.100**. Crucial observations from the spectroscopic data include the absence of the 2'-H and 3'-CH₂ acrylate precursor signals and the presence of the 3'-H methine signal (5.68 ppm) and the broad 3'-OH signal (5.49 ppm). The corresponding acrylate precursor carbon signals (129.0, 130.0 and 164.6 ppm) are absent and new product signals are evident at 70.2 ppm (C-3'), 125.4 (C-10'), 143.2 ppm (C-2') and 165.1 (C-1'). The stereoselectivity exhibited in these reactions was determined by comparing the 10-CH₂, 2-H_{endo}, 3'-H, 8- and/or 9-Me signal integrals of the purified diastereomeric mixture (*e.g.* **Figure 2.101**) (The signals in the ^1H NMR spectra of the crude reaction mixture are, in most instances, broad and overlap considerably, thus precluding their use).

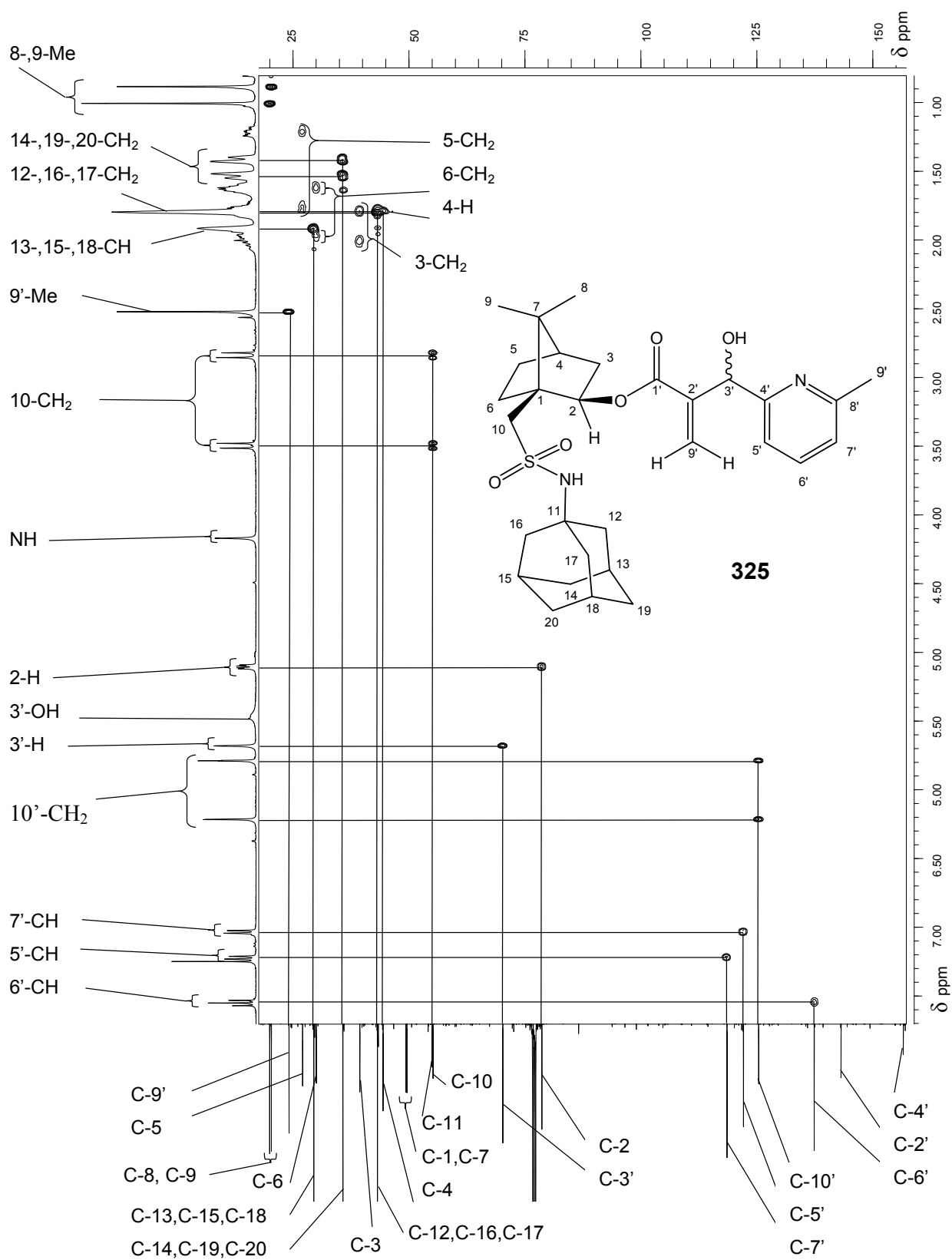


Figure 2.100: 400 MHz HSQC spectrum of the Morita-Baylis-Hillman product **325** in CDCl₃.

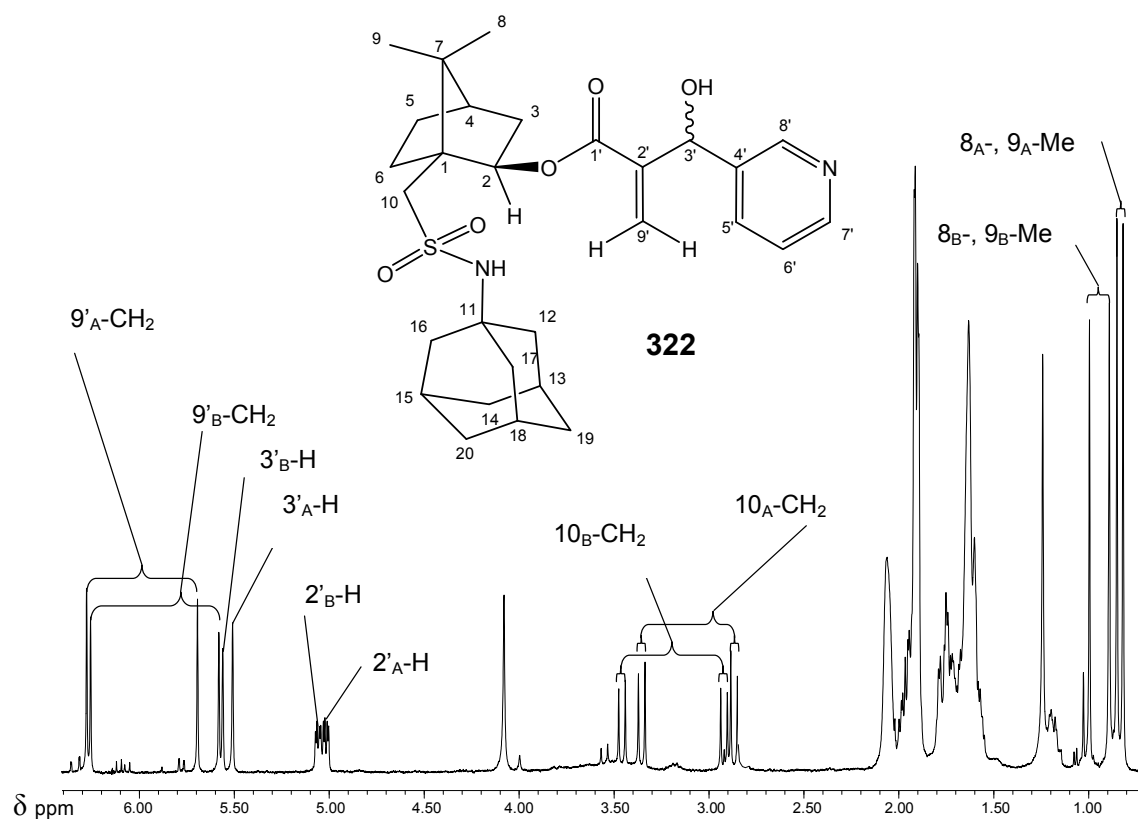
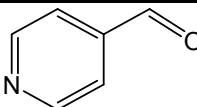
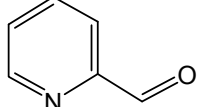
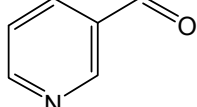
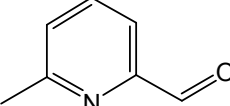
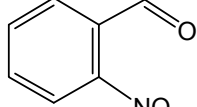


Figure 2.101: Diastereoselectivity determination of the Morita-Baylis-Hillman product **322**.

Yields of the various Morita-Baylis-Hillman reactions were obtained from a comparison of the relative integrals of product and reactant signals in the ¹H NMR spectra of the crude reaction mixtures after work-up. The overall results are summarized in **Table 2.23**.

Table 2.23: Stereoselectivity data for the Morita-Baylis-Hillman reaction of the chiral acrylate ester **321** with selected aldehydes (**Scheme 2.46**).

Entry	Aldehyde	Structure	Product	Yield ^a (%)	% d.e. ^b
1	4-Pyridinecarbaldehyde		322	93	38
2	2-Pyridinecarbaldehyde		323	99	22
3	3-Pyridinecarbaldehyde		324	98	60
4	6-Methyl-2-pyridinecarbaldehyde		325	95	95
5	2-Nitrobenzaldehyde		326	89	52
6	Pivaldehyde		327	0	---

^aYields determined from ¹H NMR spectroscopic data of crude reaction mixtures.

^bDiastereomeric excesses determined from the purified reaction mixtures.

Based on the experimental data, the following conclusions can be drawn:

- i) Stereoselectivity varies widely (22 – 95 % d.e.).
- ii) 6-Methyl-2-pyridinecarbaldehyde afforded the corresponding product in good yield and with significantly higher diastereomeric excess.
- iii) All the reactions proceeded relatively quickly (90 h) for typical Morita-Baylis-Hillman reactions.
- iv) In general, very good yields were obtained (89 – 99 %) with the exception of pivaldehyde, where no reaction was observed. The carbonyl moiety of this aldehyde may be too sterically hindered to allow approach of the Morita-Baylis-Hillman zwitterion.

2.4 CONCLUSIONS

This project has involved an integrated approach to:- the synthesis of a range of camphor-derived scaffolds for use in asymmetric synthesis; an investigation of their configurational and conformational features; and NMR-based kinetic-mechanistic and computational studies of an unexpected intramolecular transesterification.

More specifically, spectroscopic (1- and 2-D NMR) methods have been used to establish, unambiguously, the structures of two camphor ketols, and their reduction to mono- and dihydroxy derivatives has been explored. “Dimer I” has been shown to afford a 3'-*exo*-hydroxy derivative, a 2-*exo*-3'-*endo*-dihydroxy derivative and a 2-*exo*-3'-*exo*-dihydroxy derivative, while “dimer II” gave a 3-*exo*-2'-*endo*-dihydroxy derivative as the major product, together with a small amount of a 3-*exo*-2'-*exo*-dihydroxy derivative. Not unexpectedly, the reduction of both dimers involved preferential hydride delivery from the less sterically-hindered *endo*-face – an observation attributed to substantial blocking of the *endo*-face of the *endo*-orientated monomeric units.

In contrast to earlier results,¹²² alkylation of a specially prepared camphor-derived iminolactone was found to afford monoalkylated rather than dialkylated products. Alkylation yields of 52 – 65 % were obtained with diastereoselectivities of up to 85 % d.e – results consistent with those reported by Xu *et al.*^{172,173} and with our original expectation¹²³ that the iminolactone scaffold could be used to construct chiral α -amino acids.

The search for novel substrates for use in the chiral Morita-Baylis-Hillman reaction led to the identification of a monoacylated camphor-derived molecule with potential for participating in hydrogen bonding in the transition state complex. Synthesis afforded the 2-*exo*- and 3-*exo*-acrylate esters together with the diacrylate ester. The observation of an unexpected transesterification equilibrium between the monoacrylate esters led to a detailed ¹H NMR kinetic study of the reaction in various media and at different temperatures. The results indicated that first-order forward and reverse reactions were occurring concurrently and, in all instances, the rate constant of the forward reaction, (k_{+1}), was found to be *ca.* 10 % faster than that for the reverse reaction (k_{-1}). Acid-catalysis was found to be of great significance, if not imperative, in catalysing the process. The catalysed and uncatalysed reactions were further

explored in detail through calculations at the DFT level, and a thorough potential energy surface scan confirmed the probability of both reactions occurring, although the catalysed pathway is favoured.

Continued design and synthesis of suitable substrates for use in the chiral Morita-Baylis-Hillman reaction, led to several potential candidates with bulky moieties at the C-10 position. Several synthetic steps afforded phenyl 2-*exo*-acryloyloxybornane-10-sulfonate and the *endo*-isomer, each step giving excellent yields of 92 – 98 %. These compounds were then acylated to give acryloyloxy derivatives together with the related chlorinated competition products in excellent yields of up to 97 %. However, the route was plagued by problems related to the ready cyclization to afford Oppolzer's sultone. An alternative approach to a bulky C-10 moiety involved the use of adamantylamine. Yields of the acrylate esters were again excellent, and the use of 2-*exo*-acryloyloxy-*N*-(1-adamantyl)bornane-10-sulfonamide as a Morita-Baylis-Hillman substrate was explored. Analysis of the results showed that yields were high (89 – 99 %) and that stereoselectivity varied widely (22 – 95 % d.e.) with 6-methyl-2-pyridinecarbaldehyde affording the corresponding product in good yield and with the highest diastereomeric excess. Furthermore, all the reactions proceeded relatively quickly (90 h) for typical Morita-Baylis-Hillman reactions.

Future research is expected to focus on:

- i) The use of the dimeric camphor-derived ethers in the construction of chiral reagents, such as chirally modified lithium aluminium hydride.
- ii) Fission of Oppolzer's sultone to afford the phenyl sulfonyl ester, and use of this and the phenyl sulfonate esters in the Morita-Baylis-Hillman reaction.
- iii) Exploration of the stereoselectivity afforded by the *endo*-adamantylamine sulfonamide in the Morita-Baylis-Hillman reaction.

3. EXPERIMENTAL

3.1. GENERAL

3.1.1 Analysis

All melting points were determined using a Kofler hot-stage apparatus and are uncorrected. NMR spectra were obtained on a Bruker AMX400 spectrometer at 303 K in CDCl₃ unless otherwise stated. Spectra were calibrated using the residual protonated solvent signals in CDCl₃ (7.25 ppm for ¹H and 77.0 for ¹³C) or in DMSO-*d*₆ (2.5 ppm for ¹H and 39.7 ppm for ¹³C). Coupling constants are given in hertz (Hz). Infra-red spectra were obtained for samples analysed as KBr discs on a Perkin Elmer FT-IR Spectrum 2000 spectrophotometer. Low-resolution mass spectrometry was carried out on a Finnigan GCQ mass spectrometer using the electron impact (EI) mode, whilst HRCI mass spectra were obtained on a double focusing Kratos MS 80RF mass spectrometer (Cape Technikon Mass Spectrometry Unit). Optical rotations were measured on a Perkin Elmer 141 polarimeter using a 1 dm cell, with concentrations cited in g / 100 mL. Optically pure compounds were derived from commercially available, homochiral, (1*R*)-(+)-camphor.

The atom numbering used in quoting NMR data generally follows systematic nomenclature. However, given the complexity of certain systems, trivial names are sometimes used to facilitate recognition and the numbering follows accordingly. Where necessary, the numbering is illustrated by appropriate examples.

3.1.2 Chromatography

Semi-preparative HPLC separations were achieved on a Whatman Partisil 10 Magnum 6 normal phase column using a Spectra-Physics P100 isocratic pump and a Waters RI410 differential refractometer detector. Flash chromatography was conducted using Merck silica gel 60 PF₂₅₄. Chromatotron plates were prepared using silica gel 60 PF₂₅₄ containing CaSO₄. Routine thin layer chromatography (TLC) was carried out on pre-coated Merck silica gel PF₂₅₄ plates, which were visualised using UV light (254 nm) or I₂ vapour.

3.1.3 Solvents

Solvents were dried using conventional methods as described by Perrin and Armarego.²⁴² Thus: - THF was pre-dried over CaH₂ and then distilled from Na wire and benzophenone under dry N₂. Et₂O was pre-washed with aq. ferrous sulfate and with water, to remove peroxides, and then pre-dried over CaH₂; this was followed by distillation from Na wire and benzophenone under dry N₂. EtOH was dried by reaction with Mg turnings and iodine and then distilled from the resulting Mg(OEt)₂ under dry N₂. DMF was refluxed over 4Å molecular sieves, distilled under reduced pressure and stored over 4Å molecular sieves, all under dry N₂. Acetonitrile was stored for several hours over 4Å molecular sieves. All reactions requiring anhydrous conditions were conducted in heat-gun or flame-dried glassware under an inert atmosphere of dried spectroscopic grade nitrogen or argon. NaH was washed free of oil prior to use, with dry hexane (3 aliquots) and then with the dry solvent to be used in the subsequent reaction.

3.1.4 Computational Methods

3.1.4.1 *Molecular mechanics calculations*

The Accelrys Cerius² software package,²⁴³ and running on an SGI O² unix-based platform, was used exclusively to perform molecular mechanics calculations. The Universal Force Field was used as the default setting, as it is a general-purpose force-field, parameterised and validated for the complete periodic table. Structures were drawn, cleaned and minimized before running isothermal molecular dynamics routines in order to locate the lowest energy conformers.

3.1.4.2 *Density functional theory calculations*

All calculations for the determination of thermodynamic parameters were performed on Pentium 4 PCs at the density functional theory (DFT) level, using the Gaussian-03²²³ computational package and the Becke-three-parameter, Lee-Yang-Parr (B3LYP) method, with a middle-high basis set. The preferred level of theory for calculations involving general structures being B3LYP/6-311++G(d,p) but, where extended mechanistic calculations were

necessary, the B3LYP/6-31+G(d) method was used throughout (a requirement for accurate comparison of data).

Mechanistic studies required geometry optimization of ground state and putative intermediate molecules, followed by potential energy scans to determine transition state structures. All the structures identified as stationary points were subjected to frequency analysis to confirm their identities as either equilibrium geometries (zero imaginary frequencies) or as transition states (one imaginary frequency) and, additionally, to obtain thermodynamic parameters for the structures. The energies of the structures are reported as Gibbs free energies at 298.15 K. Intrinsic reaction coordinate (IRC) calculations were performed to verify that a given transition structure actually connects the starting material and product structures, and the activation energies were calculated by comparison of zero-point corrected energies of the reactants and transition states.

3.2 SYNTHETIC PROCEDURES

3.2.1 Dibornyl Ethers

Camphorquinone 22

Selenium dioxide (100.89 g, 909 mmol) was added to a stirred solution of (1*R*)-(+)-camphor **16** (81.25 g, 534 mmol) in acetic anhydride (80 mL). The resulting suspension was boiled under reflux for 5 h and thereafter stirred vigorously at 30 °C overnight. The black selenium powder was filtered off and washed with a minimal volume of glacial acetic acid to remove the yellow crystals. The filtrate was then neutralized with 10 % aqueous NaOH at 0 °C, and the resulting yellow precipitate was filtered off and washed with a minimum amount of water and suction-dried. The yellow solid was then dissolved in petroleum ether (80 – 100 °C) and the residual aqueous layer removed. The organic layer was concentrated *in vacuo* until crystallization began, and then heated to boiling to redissolve the crystals. Initial slow crystallization occurred on cooling to room temperature and further crystallization was induced by storing overnight at 10 °C. Filtration afforded bright yellow crystals of: camphorquinone **22** (74.59 g, 84.1 %); mp. 189-194 °C (lit.,²⁴⁴ 198 – 201 °C); $\nu_{\max} / \text{cm}^{-1}$ (CHCl₃) 1770 and 1750 (C=O); δ_{H} (400 MHz; CDCl₃) 0.92, 1.05 and 1.09 (9H, 3 × s, 8-, 9- and 10-Me), 1.58 - 2.21 (4H, complex of multiplets, 5- and 6-CH₂) and 2.61 (1H, d, *J* 5.2 Hz, 4-H); δ_{C} (100 MHz; CDCl₃) 8.8, 17.4 and 21.1 (C-8, C-9 and C-10), 22.3 and 29.9 (5-C and 6-C), 42.6 and 58.0 (C-1 and C-7), 58.7 (C-4) and 202.8 and 204.7 (C-2 and C-3).

3,3-(Ethylenedioxy)-2-exo-hydroxybornane 210

Method 1

A solution of 3,3-(ethylenedioxy)-2-bornanone **232** (2.01 g, 9.6 mmol) in dry Et₂O (50 mL) was added under N₂ to a stirred slurry of LiAlH₄ (0.52 g, 14 mmol) in dry Et₂O at 0 °C. The mixture was allowed to warm to room temperature and then boiled under reflux for 3 h. The reaction was then quenched with moist ether and the resulting precipitate removed by filtration. The organic layer was subsequently dried over anhydrous MgSO₄ and concentrated *in vacuo* to give an oil, which was chromatographed [using silica gel on a chromatotron, 4 mm plate; elution with hexane-EtOAc (9:1)] to afford:

3,3-(ethylenedioxy)-2-*exo*-hydroxybornane **210** as an oil (1.42 g, 69.9 %) (Found: M^+ , 212.14216. C₁₂H₂₉O₃ requires *M*, 212.14124); $\nu_{\max} / \text{cm}^{-1}$ (CHCl₃) 3020 (OH); δ_{H} (400 MHz; CDCl₃) 0.82, 0.89 and 1.08 (9H, 3 × s, 8-, 9- and 10-Me), 1.47 - 1.75 (5H, complex of

multiplets, 4-CH, 5- and 6-CH₂), 2.35 (1H, br s, OH), 3.27 (1H, s, 2-H) and 3.80 - 4.03 (4H, complex of multiplets, OCH₂CH₂O); δ_C (100 MHz; CDCl₃) 10.9, 20.8 and 21.1 (C-8, C-9 and C-10), 21.4 (C-5), 33.5 (C-6), 47.6 and 49.7 (C-1 and C-7), 52.8 (C-4), 63.6 and 65.7 (OCH₂CH₂O), 85.6 (C-2) and 115.3 (C-3); m/z 212 (M⁺, 15.65 %) and 127 (100).

Method 2

A suspension of LiAlH₄ (0.86 g, 23 mmol) in dry Et₂O (100 mL) was boiled under reflux in an atmosphere of dry N₂ for 1 h. A solution of 3,3-(ethylenedioxy)-2-bornanone **232** (4.52 g, 21.5 mmol) in Et₂O was added drop-wise, and the resulting mixture boiled under reflux for 3 h and then stirred overnight. The reaction was quenched by the sequential addition of 3M NaOH (3 mL) and H₂O (3 mL). The resulting white precipitate was filtered off and washed by boiling in EtOAc for 1 h. The combined filtrates were then extracted with EtOAc (3 × 20 mL), and the combined extracts dried over anhydrous MgSO₄ and concentrated *in vacuo*. The crude residue was chromatographed [flash chromatography on silica gel; elution with hexane-EtOAc (19:1)] to afford:

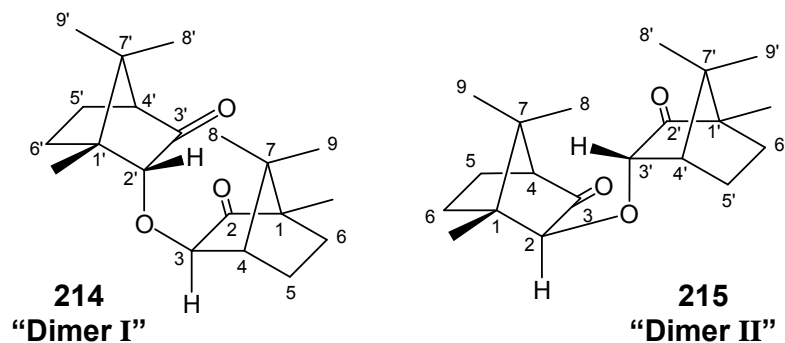
3,3-(ethylenedioxy)-2-*exo*-hydroxybornane **210** (3.41 g, 74.7 %).

2,2-(Ethylenedioxy)-3-*exo*-hydroxybornane **211**

The experimental procedure (**Method 2**) described for the synthesis of 3,3-(ethylenedioxy)-2-*exo*-hydroxybornane **210** was followed, using 2,2-(ethylenedioxy)-3-bornanone **235** (2.02 g, 9.6 mmol) and LiAlH₄ (0.14 g, 3.7 mmol). Work-up and flash chromatography [elution with hexane-ethyl acetate (9:1)] afforded, as white crystals:

2,2-(ethylenedioxy)-3-*exo*-hydroxybornane **211** (1.78 g, 87.3 %) (Found: M⁺, 212.14206. C₁₂H₂₀O₃ requires *M*, 212.14124); $[\alpha]_D^{23} = -26.1^\circ$; $\nu_{\max} / \text{cm}^{-1}$ (CHCl₃) 3045 (OH); δ_H (400 MHz; CDCl₃) 0.80, 0.81 and 1.07 (9H, 3 × s, 8-, 9- and 10-Me), 1.06 - 1.83 (5H, series of multiplets, 4-CH, 5- and 6-CH₂), 2.54 (1H, br s, OH), 3.43 (1H, s, 3-H) and 3.72 - 4.07 (4H, m, OCH₂CH₂O); δ_C (100 MHz; CDCl₃) 9.3, 21.2 and 21.7 (C-8, C-9 and C-10), 24.6 (C-5), 29.1 (C-6), 47.8 and 51.8 (C-1 and C-7), 51.6 (C-4), 63.9 and 66.6 (OCH₂CH₂O), 83.0 (C-3) and 116.9 (C-2); m/z 212 (25 %) and 162 (100).

2'-endo-3-exo-dibornyl ether **214** ("dimer I") and 2-endo-3'-exo-dibornyl ether **215** ("dimer II")



A solution of 3-*exo*-hydroxybornan-2-one **231** (0.53 g, 3.2 mmol) and *p*-toluenesulfonic acid (0.04 g, 0.2 mmol) in dry benzene (12 mL) was boiled under reflux for 14 h using a Dean-Stark trap to remove water. The reaction mixture was then cooled and quenched with water (5 mL). The resulting mixture was extracted with EtOAc (4 × 5 mL) and the organic layers were combined and dried over anhydrous MgSO₄. The solvent was removed *in vacuo* to give an oil, which was chromatographed [flash chromatography on silica gel; elution with hexane-EtOAc (9:1)] to afford two colourless crystalline products:

2'-*endo*-3-*exo*-dibornyl ether **214** ("dimer I") (0.22 g, 44.4 %); m.p. 106 - 108 °C (lit.,¹²³ 104 °C) (Found: M⁺, 318.22067. C₂₀H₃₀O₃ requires M, 318.21950); ν_{max} / cm⁻¹ (CHCl₃) 1730 (C=O); δ_H (400 MHz; CDCl₃) 0.87 (1H, s, 10-Me), 0.89 (1H, s, 8'-Me), 0.90 (1H, s, 9-Me), 0.92 (1H, s, 9'-Me), 0.94 (1H, s, 8-Me), 1.01 (1H, s, 10'-Me), 1.28 - 1.44, 1.546 - 1.65 and 1.86 - 1.99 (8H, complex of multiplets, 5-, 5'-, 6- and 6'CH₂), 2.14 (1H, d, *J* 4.4 Hz, 4'-H), 2.16 (1H, d, *J* 4.8 Hz, 4H), 3.93 (1H, s, 3-H) and 3.98 (1H, s, 2'-H); δ_C (100 MHz; CDCl₃) 9.0 (C-10), 13.0 (C-10'), 17.7 (C-8'), 19.4 (C-9'), 19.8 (C-9), 21.2 (C-8), 24.0 (C-5'), 24.9 (C-5), 25.9 (C-6'), 29.0 (C-6), 42.7 (C-7), 46.3 (C-1'), 49.3 (C-4), 50.3 (C-7'), 57.3 (C-1), 60.0 (C-4'), 84.2 (C-3), 85.5 (C-2'), 217.3 (C-3'), 218.4 (C-2); *m/z* 318.1(M⁺, 18.1 %) and 123 (100); and

2-*endo*-3'-*exo*-dibornyl ether **215** ("dimer II") (0.21 g, 41.3 %); m.p. 98-102 °C (lit.,¹²³ 102 °C) (Found: M⁺, 318.21969. C₂₀H₃₀O₃ requires M, 318.21950); ν_{max} / cm⁻¹ (CHCl₃) 1730; δ_H (400 MHz; CDCl₃) 0.82 (1H, s, 8'-Me), 0.85 (1H, s, 10'Me), 0.86 (1H, s, 8-Me), 0.95 (1H, s, 9'-Me), 0.96 (1H, s, 10-Me), 0.97 (1H, s, 9-Me), 1.35 - 1.45, 1.57 - 1.70 and 1.76 - 1.91 (8H, complex of multiplets, 5-, 5'-, 6- and 6'CH₂), 2.05 (1H, d, *J* 4.3 Hz, 4-H), 2.31 (1H, t, *J* 4.3 Hz, 4'H), 3.81 (1H, s, 2-H_{endo}), 4.25 (1H, s, *J* 5.0 Hz, 3'-H_{exo}); δ_C (100 MHz; CDCl₃) 9.3 (C-10'), 10.5 (C-10), 18.5 (C-8), 18.70 (C-9'), 18.74 (C-6'), 19.9 (C-8'), 20.7 (C-5), 21.4 (C-9),

31.8 (C-5'), 33.4 (C-6), 42.6 (C-7'), 46.1 (C-7), 48.3 (C-4'), 50.0 (C-1), 58.4 (C-1'), 59.2 (C-4), 81.6 (C-3'), 85.6 (C-2), 217.9 (C-3) and 218.0 (C-2'); m/z 318 (M^+ , 35.5 %) and 123 (100).

2-endo-3'-exo-dibornyl ether 215 ("dimer II")

The experimental procedure employed for the synthesis of "dimers I and II", **214** and **215** was followed, using *2-exo*-hydroxybornan-3-one **233** (0.80 g, 4.8 mmol) and *p*-toluenesulfonic acid (0.06 g, 0.3 mmol) in dry benzene (7 mL) and refluxing for 23 h to afford the crystalline product:

2-endo-3'-exo-dibornyl ether 215 ("dimer II") (1.23 g, 81.3 %).

3-Exo-hydroxybornan-2-one 231

Method 1

1M-HCl (7 mL) was added to a solution of 2,2-(ethylenedioxy)-3-*exo*-hydroxybornane **211** (1.53 g, 7.21 mmol) in THF (4 mL). The resulting mixture was gently boiled under reflux for 2.5 h. The HCl was then neutralised with 3 **M**-NaOH (2.5 mL). The organic solvent was removed *in vacuo* and the residue extracted with EtOAc (4 × 5 mL). The organic layers were combined and dried with anhydrous MgSO₄, then concentrated *in vacuo* to give an oil, which was chromatographed [flash chromatography on silica gel; elution with hexane-ethyl acetate (9:1)] to afford, as white crystals:

3-exo-hydroxybornan-2-one **231** (0.69 g, 57 %); m.p. 164 -166 °C (lit., ¹⁷³ 166 - 168 °C); ν_{\max} / cm^{-1} (CHCl₃) 3560 (OH) and 1340 (C=O); δ_{H} (400 MHz; CDCl₃) 0.90, 0.92 and 0.97 (9H, 3 × s, 8-, 9- and 10-Me), 1.30 - 2.22 (4H, complex of multiplets, 5- and 6-CH₂), 2.07 (1H, d, *J* 4.6 Hz, 4-H), 2.95 (1H, br s, OH) and 3.72 (1H, s, 3-H); δ_{C} (100 MHz; CDCl₃) 9.0, 20.1 and 21.0 (C-8, C-9 and C-10), 25.2 and 28.6 (C-5 and C-6), 48.7 (C-1), 49.3 (C-7), 57.1 (C-4), 77.4 (C-3) and 220.2 (C-2); m/z 168.

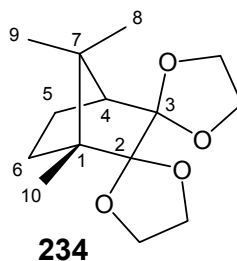
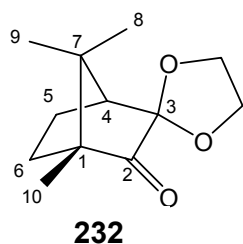
Method 2

Activated Raney nickel (3.50 g) was added to a solution of camphorquinone **22** (6.22 g, 37.4 mmol) in absolute ethanol under N₂. H₂ was then allowed to flood the system and the solution was stirred under H₂ (1 atm) overnight. Approximately 1.2 L of H₂ was taken up by the reaction. Removal of the Raney nickel was achieved by filtering the reaction mixture through celite under a blanket of N₂. The filtrate was concentrated *in vacuo*, recrystallised from

petroleum ether (80 – 100 °C) and washed with hexane {or, alternatively, chromatographed [flash chromatography on silica gel; elution with hexane-ethyl acetate (7:3)]} to afford:

3-*exo*-hydroxybornan-2-one **231** (5.69 g, 90.4 %)

3,3-(Ethylenedioxy)-2-bornanone **232** and 2,2;3,3-bis(ethylenedioxy)bornane **234**



Ethylene glycol (50 mL, 720 mmol) and *p*-toluenesulfonic acid (1.56 g, 8.2 mmol) were added to a solution of camphorquinone **22** (25.08 g, 150.9 mmol) in dry benzene (120 mL). The solution was then refluxed in a flask equipped with a Dean-Stark trap for 24 h. The cool reaction mixture was washed with 1M-NaOH (100 mL) and H₂O (100 mL). The organic layer was separated, dried over anhydrous MgSO₄ and concentrated *in vacuo*. The oil obtained was stored for seven days at 10 °C to allow crystallization to take place. Filtration of the mixture gave a solid which was recrystallised from hot EtOH to afford transparent needles of:

3,3-(ethylenedioxy)-2-bornanone **232** (16.24 g, 51.2 %); m.p. 86 – 88 °C (lit.,¹²⁴ 88 °C); ν_{\max} / cm⁻¹ (CHCl₃) 1740 (C=O); δ_{H} (400 MHz; CDCl₃) 0.89, 0.96 and 1.00 (9H, 3 × s, 8-, 9- and 10-Me), 1.52 - 2.01 (4H, complex of multiplets, 5- and 6-CH₂), 1.94 - 1.95 (1H, m, 4-H) and 3.93 - 4.30 (4H, complex of multiplets, OCH₂CH₂O); δ_{C} (100 MHz; CDCl₃) 9.2 (C-10), 19.0 (C-9), 21.4 (C-5), 21.5 (C-8), 30.9 (C-6), 43.6 (C-7), 51.5 (C-1), 58.2 (C-4), 64.5 and 66.1 (C-1' and C-2'), 106.9 (C-3) and 217.4 (C-2); *m/z* 210 (M⁺, 11 %) and 162 (100).

The mother liquor was further concentrated and then chromatographed [flash chromatography on silica gel; elution with hexane-ethyl acetate (9:1)] to afford more **232** and, as transparent needles:

2,2;3,3-bis(ethylenedioxy)bornane **234** (16.49 g, 43.0 %); m.p. 58 °C (lit.,¹²⁴ 59 - 60 °C) (Found: M⁺, 254.15222. C₁₄H₂₂O₄ requires *M*, 254.15181); ν_{\max} / cm⁻¹ (KBr) 1240 (C-O) δ_{H} (400 MHz; CDCl₃) 0.78, 0.85 and 1.16 (9H, 3 × s, 8-, 9- and 10-Me), 1.29 - 1.97 (4H, m, 5- and 6-CH₂) and 3.72 - 3.96 (8H, complex of multiplets, 2 × OCH₂CH₂O), 1.67 (1H, d, 4-H); δ_{C} (100 MHz; CDCl₃) 9.9 (C-10), 20.7 (C-9), 21.0 (C-5), 21.1 (C-8), 29.3 (C-6), 44.5 (C-

7), 52.7 (C-1), 53.3 (C-4), 64.2, 64.5, 65.0, 65.9 (OCH₂CH₂O), 113.8 (C3) and 114.7 (C-2); *m/z* 254 (M⁺, 26.8 %) and 113 (100).

2-Exo-hydroxybornan-3-one **233**

The experimental procedure described for the synthesis of 3-*exo*-hydroxybornan-2-one **231** (**Method 1**) was followed, using 3,3-(ethylenedioxy)-2-*exo*-hydroxybornane **210** (1.22 g; 5.7 mmol) and 1-**M** HCl (5.8 mL). Work-up and flash chromatography [elution with hexane-ethyl acetate (9:1)] afforded, as white crystals:

2-*exo*-hydroxybornan-3-one **233** (0.43 g, 45.0 %); m.p. 223 - 224 °C (lit.,¹³⁴ 228 - 230 °C) (Found: M⁺, 168.1143. C₁₀H₁₆O₂ requires *M*, 168.11503); ν_{\max} / cm⁻¹ (CHCl₃) 3550 and (OH) 1750 (C=O); δ_{H} (400 MHz; CDCl₃) 0.91, 1.00 and 1.02 (9H, 3 × s, 8-, 9- and 10-Me), 1.33 - 1.95 (4H, complex of multiplets, 5- and 6-CH₂), 2.15 (1H, d, 4-H), 2.78 (1H, br s, OH) and 3.51 (1H, s, 2-H); δ_{C} (100 MHz; CDCl₃) 10.3 (C-10), 18.9 (C-9), 20.3 (C-5), 21.1 (C-8), 33.9 (C-6), 46.6 (C-1), 49.2 (C-7), 58.7 (C-4), 79.5 (C-2) and 218.7 (C-3); *m/z* 168 (M⁺, 58.5 %) and 71 (100).

2,2-(Ethylenedioxy)-3-bornanone **235**

Method 1

1**M**-Hydrochloric acid (4 mL) was added to a stirred solution of 2,2;3,3-bis(ethylenedioxy)-bornane **234** (0.23 g, 0.9 mmol) in THF (15 mL) and the resulting solution was stirred for 40 h at room temperature. The reaction mixture was concentrated *in vacuo*, washed with brine (3 × 3 mL) then extracted into EtOAc (3 × 10 mL). The organic layers were combined, and dried over anhydrous MgSO₄. The solvent was removed *in vacuo* to give an oil, which was chromatographed [using silica gel on a chromatotron, 1 mm plate; elution with hexane-EtOAc (9:1)] yielding:

2,2-(ethylenedioxy)-3-bornanone **235** as a colourless crystalline solid (0.081 g, 35.8 %); m.p. 43 - 44 °C (lit.,¹²⁴ 42 - 44 °C); ν_{\max} / cm⁻¹ (CHCl₃) 1756 (C=O); δ_{H} (400 MHz; CDCl₃) 0.87, 0.92 and 1.01 (9H, 3 × s, 8-, 9- and 10-Me), 1.49 - 2.06 (4H, complex of multiplets, 5- and 6-CH₂), 2.13 (1H, d, *J* 5.4 Hz, 4-H) and 3.91 - 4.29 (4H, complex of multiplets, OCH₂CH₂O); δ_{C} (100 MHz; CDCl₃) 8.7, 18.2 and 21.5 (C-8, C-9 and C-10), 22.7 (C-5), 29.2 (C-6), 43.7 and 51.3 (C-1 and C-7), 59.2 (C-4), 64.8 and 66.3 (OCH₂CH₂O), 107.4 (C-2) and 216.6 (C-3); *m/z* 210 (14 %) and 162 (100).

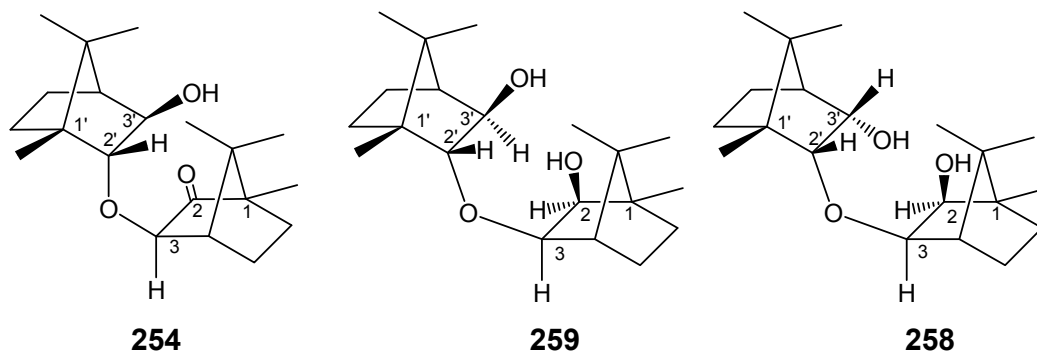
Method 2

p-Toluenesulfonic acid (1.80 g, 9.5 mmol) was added to a stirred solution of 2,2;3,3-

bis(ethylenedioxy)bornane **234** (3.05 g, 12.0 mmol) in aqueous methanol (1:1; 40 mL) and the resulting solution was boiled under reflux for 9 h. The reaction mixture was neutralised with 1M-NaOH (15 mL) and concentrated *in vacuo*. The residual aqueous layer was extracted with EtOAc (3 × 20 mL). The organic layers were combined, washed with brine and dried over anhydrous MgSO₄. The solvent was removed *in vacuo* to give, as a colourless crystalline solid:

2,2-(ethylenedioxy)-3-bornanone **235** (2.30 g, 91.4 %).

3'-Exo-hydroxy-2'-endo-(2-oxo-3-exo-bornyl)bornane **254**, 3'-exo-hydroxy-2'-endo-(2-exo-hydroxy-3-exo-bornyl)bornane **259** and 3'-endo-hydroxy-2'-endo-(2-exo-hydroxy-3-exo-bornyl)bornane **258**



Sodium borohydride (0.05 g, 1.4 mmol) was slowly added to a stirred solution of, 2'-endo-3-exo-dibornyl ether **214** ("dimer P") (0.10 g, 0.3 mmol) in ethanol (2 mL) at -10 °C. The solution was stirred at 0 °C for 2 h and then at room temperature for a further 14 h. The reaction was then quenched by the addition of H₂O and the solvent evaporated *in vacuo* to give an oil, which was chromatographed [using silica gel on a chromatotron, 1mm plate; elution with hexane-EtOAc (6:1)] to afford three white crystalline products:

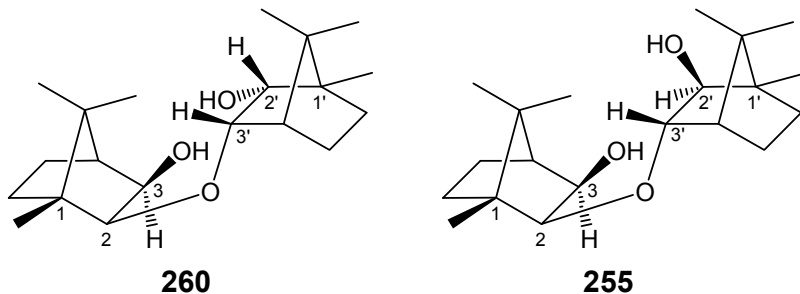
3'-exo-hydroxy-2'-endo-(2-oxo-3-exo-bornyl)bornane **254** (0.003 g, 3.2 %); m.p. 194-196°C (lit.,¹²² 196 °C) (Found: M⁺, 320.2332. C₂₀H₃₂O₃ requires M, 320.2351); ν_{\max} / cm⁻¹ (CHCl₃) 3320 (OH) and 1680 (C=O); δ_{H} (400 MHz; CDCl₃) 0.84, 0.86, 0.87, 0.89, 0.90 and 0.98 (18H, 6 × s, 8-, 8'-, 9-, 9'-, 10- and 10'-Me), 1.24 – 2.08 (8H, complex of multiplets, 5-, 5'-, 6- and 6'-CH₂), 2.12 and 2.23 (2H, 2 × d, 4- and 4'-H), 2.20 (1H, br s, 3'-OH), 2.59 (1H, s, 3'-H) and 3.91 and 4.11 (2H, 2 × s, 2'-H and 3-H); δ_{C} (100 MHz; CDCl₃) 8.8, 12.8, 16.7, 19.3, 20.3 and 22.1, (C-8, C-8', C-9, C-9', C-10 and C-10'), 24.1 and 24.6 (C-6 and C-6'), 25.9 and 28.8 (C-5 and C-5'), 42.4 and 47.5 (C-7 and C-7'), 48.9 and 51.9 (C-1 and C-1'),

49.2 and 60.1 (C-4 and C-4'), 66.8 (C-3'), 84.9 and 85.6 (C-2' and C-3) and 210.0 (C-2); m/z 320 (18 %);

3'-exo-hydroxy-2'-endo-(2-exo-hydroxy-3-exo-bornyl)bornane 259 (0.041 g, 41.1 %)(Found: M^+ , 322.25012. $C_{20}H_{34}O_3$ requires M , 322.25080); δ_H (400 MHz; $CDCl_3$) 0.79, 0.82, 0.89, 0.93, 0.97 and 1.05 (18H, $6 \times s$, 8-, 8'-, 9-, 9'-, 10- and 10'-Me), 0.81 – 1.75 (8H, complex of multiplets, 5-, 5'-, 6- and 6'- CH_2), 1.64 (1H, m, 4'-H), 1.70 (1H, m, 3'- OH_{exo}), 1.88 (1H, d, J 4.9 Hz, 4-H), 3.02 (1H, d, 4.2 Hz, 2- OH_{exo}) and 3.56 – 3.66 (4H, complex of multiplets, 2- H_{endo} , 3- H_{endo} , 2'- H_{exo} , 3'- H_{endo}); δ_C (100 MHz; $CDCl_3$) 13.4, 19.5, 10.9, 20.6, 21.1 and 21.8 (C-8, C-8', C-9, C-9', C-10 and C-10'), 24.1, 25.5, 26.2 and 33.0 (C-5, C-6, C-5' and C-6'), 29.7, 46.6, 48.7, 50.3 (C-1, C-7, C-1' and C-7'), 49.8 and 53.0 (C-4 and C4') and 79.9, 82.5, 84.2 and 94.7 (C-2, C-3, C-2' and C-3'); m/z 322 (M^+ , 1.2 %) and 95 (100); and

3'-endo-hydroxy-2'-endo-(2-exo-hydroxy-3-exo-bornyl)bornane 258 (0.045 g, 45.3 %) (Found: M^+ , 322.24999. $C_{20}H_{34}O_3$ requires M , 322.25080); δ_H (400 MHz; $CDCl_3$) 0.80, 0.85, 0.86, 0.88, 0.93 and 1.12 (18H, $6 \times s$, 8-, 8'-, 9-, 9'-, 10- and 10'-Me), 1.12 - 1.75 (8H, complex of multiplets, 5-, 5'-, 6- and 6'- CH_2), 1.83 (1H, t, J 4.0 Hz, 4'-H), 1.90 (1H, d, J 4.7 Hz, 4-H), 2.42 (1H, d, J 6.6 Hz, 3'- OH_{endo}), 2.67 (1H, d, J 4.1 Hz, 2- OH_{exo}), 3.56 - 3.64 (3H, complex of multiplets, 2'-H, 3-H, 2-H) and 4.20 (1H, s, 3'-H); δ_C (100 MHz; $CDCl_3$) 10.8, 14.7, 17.8, 18.3, 19.9 and 21.1, (C-8, C-8', C-9, C-9', C-10 and C-10'), 21.5 (C-5), 24.3 (C-5'), 26.6 (C-6), 32.8 (C-6'), 44.4 and 46.5 (C-1 and C-1'), 49.0, 49.7, 50.4 and 50.5 (C-4, C4', C-7 and C-7'), 67.8 (C-3'), 80.0 (C-2) and 85.9 and 87.6 (C-2' and C-3); m/z 322 (M^+ , 2.2 %) and 95 (100).

2'-Endo-hydroxy-3'-endo-(3-exo-hydroxy-2-exo-bornyl)bornane 260 and *2'-exo-hydroxy-3'-endo-(3-exo-hydroxy-2-exo-bornyl)bornane 255*



The experimental procedure employed for the synthesis of *3-exo-hydroxy-2-endo-(2-oxo-3-endo-bornyl) 254* was followed, using *2-endo-3'-exo-dibornyl ether 215* (“dimer II”) (0.24 g, 0.8 mmol), $NaBH_4$ (0.05 g, 1.4 mmol), and ethanol (3 mL). Work-up and purification

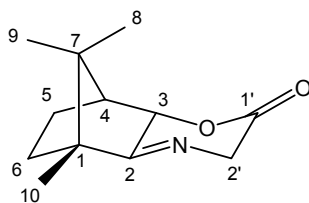
[chromatography on silica gel on a chromatotron, 1 mm plate; elution with hexane-EtOAc (9:1)] afforded two white crystalline products:

2'-endo-hydroxy-3'-endo-(3-exo-hydroxy-2-exo-bornyl)bornane **260** (0.11 g, 46.8 %)(Found: M^+ , 322.48198. $C_{20}H_{34}O_3$ requires M , 322.48216); $\nu_{\max} / \text{cm}^{-1}$ (CHCl_3) 3310 (OH); δ_{H} (400 MHz; CDCl_3) 0.78, 0.83, 0.84, 0.87, 1.01 and 1.11 (18H, 6 \times s, 8-, 8'-, 9-, 9'-, 10- and 10'-Me), 1.14 - 1.94 (8H, complex of multiplets (5-, 5'-, 6- and 6'- CH_2), 2.33 and 2.59 (2H, 2 \times s, 4 and 4'-H), 3.50 (1H, d, J 6.8 Hz, 2-H) and 3.76 - 3.96 (3H, 2 \times m, 2'-H, 3-H and 3'-H); δ_{C} (100 MHz; CDCl_3) 11.7, 14.1, 18.3, 18.8, 19.7 and 21.4. (C-8, C-8', C-9, C-9', C-10 and C-10'), 21.5 and 23.8 (C-6 and C-6'), 25.4 and 33.5 (C-5 and C-5'), 44.2 and 46.5 (C-7 and C-7'), 49.5 and 49.6 (C-4 and C-4'), 49.1 and 51.7 (C-1 and C-1'), 76.5 and 73.2 (C-3 and C-2') and 78.5 and 89.2 (C-2 and C-3'); m/z 322 (M^+ , 0.74 %) and 41 (100); and

2'-exo-hydroxy-3'-endo-(3-exo-hydroxy-2-exo-bornyl)bornane **255** (0.01 g, 5.4 %); m.p. 208 - 210 °C (lit.,¹²² 212 °C) (Found: M^+ , 322.48210. $C_{20}H_{34}O_3$ requires M , 322.48216); $\nu_{\max} / \text{cm}^{-1}$ (KBr) 3310 (OH); δ_{H} (400 MHz; CDCl_3) 0.77, 0.82, 0.85, 0.94, 0.99 and 1.03 (18H, 6 \times s, 8-, 8'-, 9-, 9'-, 10- and 10'-Me), 0.85 - 1.77 (8H, complex of multiplets (5-, 5'-, 6- and 6'- CH_2), 1.55 (1H, s, 2'-OH), 1.75 and 1.90 (2H, 2 \times m, 4- and 4'-H, 2.86 (1H, d, J 5.8 Hz, 3-OH), 3.45 (1H, br s, 2'-H), 3.57 (1H, d, J 6.9 Hz, 2-H), 3.80 (1H, t, J 6.3 Hz, 3-H) and 1.90 (1H, t, J 4.2 Hz, 3'-H); δ_{C} (100 MHz; CDCl_3) 11.2, 12.1, 19.9, 20.5, 21.3 and 21.7 (C-8, C-8', C-9, C-9', C-10 and C-10'), 18.8, 23.9, 33.4 and 34.4 (C-5, C-6, C-5' and C-6'), 46.5, 46.7, 49.0 and 49.9 (C-1, C-7, C-1' and C-7'), 49.1 and 51.6 (C-4 and C-4'), 75.8 (C-2'), 85.6 (C-3), 86.9 (C-2) and 89.5 (C-3'); m/z 322 (M^+ , 0.8 %) and 152 (100).

3.2.2 Iminolactones

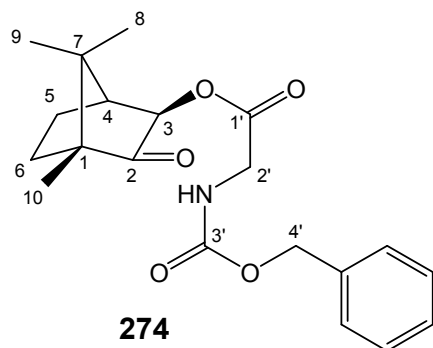
The 2-iminolactone **208**



208

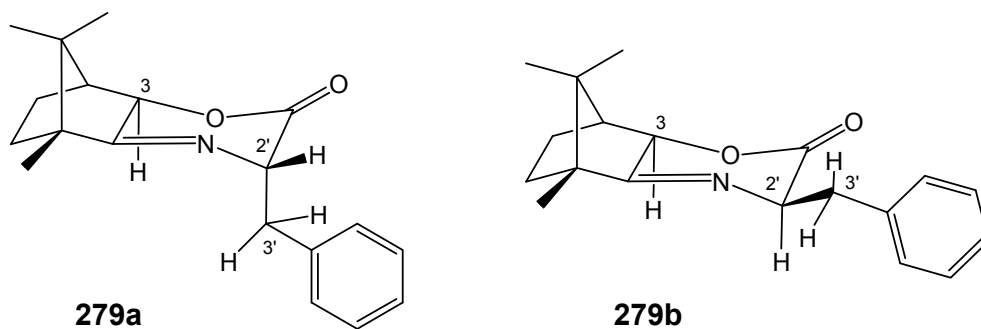
10 % Pd on C catalyst (0.07 g, 0.007 g Pd metal) was added under a blanket of N₂ to a stirred solution of *N*-(carbobenzyloxy)glycine 2-oxo-3-*exo*-bornyl ester **274** (0.50 g, 1.4 mmol) in absolute ethanol (4 mL). The catalyst was kept in suspension by vigorous stirring. N₂ was allowed to flow for a further 5 min, followed by the introduction of a slow stream of H₂. Escaping gas was bubbled through a saturated solution of aqueous Ba(OH)₂. Once the evolution of CO₂ had ceased (as evidenced by the cessation of BaCO₃ formation), the mixture was heated to *ca.* 50 °C until no further evolution of CO₂ was observed. The reaction mixture was cooled to room temperature, the flow of H₂ halted and the system then flushed with N₂. The suspension was filtered through celite and the solid was washed with ethanol. The filtrate and washings were combined and the solvent removed *in vacuo* to give a yellow oil, which was chromatographed [flash chromatography on silica gel; elution with hexane-EtOAc (1:1)] to afford a white crystalline solid:

The 2-iminolactone **208** (0.16 g, 56.2 %); m.p. 101 – 103 °C (lit.¹⁷³ 103 - 104 °C); $[\alpha]_D^{23} = +263.2^\circ$; $\nu_{\max} / \text{cm}^{-1}$ (CHCl₃) 1745 (C=O); δ_{H} (400 MHz; CDCl₃) 0.79, 0.96 and 1.05 (9H, 3 × s, 8-, 9- and 10-Me), 1.32 - 2.14 (4H, complex of multiplets, 5- and 6-CH₂), 2.25 (1H, d, *J* 4.5, 4-H), 3.89 (1H, dd, *J* 17.8 and 1.6 Hz, 2'-H_{endo}), 4.49 (1H, d, 1.6 Hz, 3-H_{endo}) and 4.53 (1H, d, *J* 17.9 Hz, 2'-H_{exo}); δ_{C} (100 MHz; CDCl₃) 9.9, 19.7 and 20.0 (C-8, C-9 and C-10), 25.4 and 29.5 (C-5 and C-6), 47.5 (C-4), 49.1 and 52.6 (C-1 and C-7), 52.6 (C-2'), 79.7 (C-3), 168.9 (C-2) and 183.7 (C-1'); *m/z* 207 (M⁺, 3.8 %).

N-(Carbobenzyloxy)glycine 2-oxo-3-exo-bornanyl ester **274**

To a solution of *N*-(carbobenzyloxy)glycine (1.26 g, 6 mmol) in dry DMF (6 mL) was added carbonyldiimidazole (0.98 g, 6 mmol) and the resulting solution was stirred for 30 min. 3-*exo*-hydroxybornan-2-one **231** (1.01 g, 6 mmol) was then added and the reaction mixture was stirred at room temperature for 16 h. The solvent was removed *in vacuo* to give an oil, which was chromatographed [flash chromatography on silica gel; elution with hexane-EtOAc (1:1)] to afford:

N-(carbobenzyloxy)glycine 2-oxo-3-*exo*-bornyl ester **274** as a clear oil (1.46 g, 67.2 %) (Found: M^+ , 359.17342. $C_{20}H_{25}NO_5$ requires M , 359.17327); $[\alpha]_D^{23} = +45.2^\circ$; $\nu_{\max} / \text{cm}^{-1}$ (CHCl_3) 1750 (C=O); δ_{H} (400 MHz; CDCl_3) 0.91, 0.93 and 0.94 (9H, 3 \times s, 8-, 9- and 10-Me), 1.40 - 1.80 (4H, series of multiplets, 5- and 6- CH_2), 2.10 (1H, d, 4-H), 3.95 - 4.06 (2H, series of multiplets, 2'- CH_2), 4.82 (1H, s, 3- H_{endo}), 5.11 (2H, s, 4'- CH_2), 5.27 (1H, br s, NH) and 7.25 - 7.36 (5H, m, ArH); δ_{C} (100 MHz; CDCl_3) 9.0 (C-10), 19.6 (C-9), 20.7 (C-8), 24.8 (C-5), 28.5 (C-6), 42.8 (C-2'), 48.3 (C-1), 57.2 (C-7), 59.8 (C-4), 67.1 (C-4'), 77.5 (C-3), 128.1, 128.2, 128.5 and 136.2 (ArC), 156.2 (C-1'), 169.3 (C-3') and 213.7 (C-2); m/z 359 (M^+ , 23.85 %) and 91 (100).

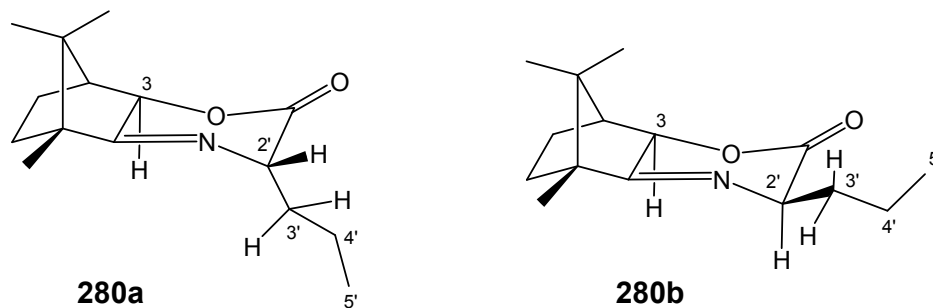
The α -endo-benzyl 2-iminolactone **279a** and α -exo-benzyl 2-iminolactone **279b**

A solution of the 2-iminolactone **208** (0.05 g, 0.2 mmol) in dry THF (3 mL) was added dropwise under N_2 to a stirred solution of *t*-BuOK (0.03 g, 0.2 mmol) in dry THF (3 mL) at $-78\text{ }^\circ\text{C}$ and the solution stirred for 1 h to ensure complete enolization. Benzyl bromide (0.04 g, 0.2 mmol) in dry THF (3 mL) was then added slowly to the enolate solution and the resulting mixture stirred at $-78\text{ }^\circ\text{C}$ for 3 h. The mixture was allowed to warm to room temperature and stirring continued overnight. The solvent was removed *in vacuo* and purification [chromatography on silica gel on a chromatotron, 1 mm plate; elution with hexane-EtOAc (9:1)] afforded, as light brown oils, two products:[†]

the α -endo-benzyl 2-iminolactone **279a** (0.004 g, 4.9 %); $\nu_{\text{max}} / \text{cm}^{-1}$ (CHCl_3) 1745 (C=O); δ_{H} (400 MHz; CDCl_3) 0.88, 0.93 and 1.01 (9H, 3 \times s, 8-, 9- and 10-Me), 1.35 - 1.41 (1H, complex of multiplets, 4-H), 1.63 - 1.95 (4H, complex of multiplets, 5- and 6- CH_2), 2.63 (1H, s, 3- H_{endo}), 3.20 (1H, dd, J 5.1 Hz, J 13.8 Hz, 3'- H_{A}), 3.46 (1H, dd, J 4.7 Hz, J 13.7 Hz, 3'- H_{B}), 4.89 (1H, t, J 4.7 Hz, 2'- H_{exo}) and 7.14 - 7.30 (5H, complex of multiplets, Ar-H); δ_{C} (100 MHz; CDCl_3) 9.9, 19.6 and 19.9 (C-8, C-9 and C-10), 25.8 and 29.5 (C-5 and C-6), 47.1 (C-4), 37.9 and 49.1 (C-2' and C-7), 52.4 (C-1), 62.9 (C-3'), 79.1 (C-3), 127.5, 128.6, 131.4 and 137.8 (Ar-C), 170.9 (C-2) and 181.7 (C-1');

the α -exo-benzyl 2-iminolactone **279b** (0.043 g, 60.2 %); $\nu_{\text{max}} / \text{cm}^{-1}$ (CHCl_3) 1740 (C=O); δ_{H} (400 MHz; CDCl_3) 0.70, 0.94 and 1.03 (9H, 3 \times s, 8-, 9- and 10-Me), 1.27 - 1.34, 1.51 - 1.58, 1.69 - 1.77 and 2.00 - 2.09 (4H, series of multiplets, 5- and 6- CH_2), 2.22 (1H, d, J 4.7 Hz, 4-H), 3.28 (1H, dd, J 7.5 Hz, J 14.1 Hz, 3'- H_{B}), 3.51 (1H, dd, J 5.1 Hz, J 14.1 Hz, 3'- H_{A}), 3.94 (1H, dd, J 4.8 Hz, J 1.2 Hz, 2'- H_{endo}), 4.42 (1H, d, J 1.2 Hz, 3- H_{endo}) and 7.18 - 7.41 (5H, complex of multiplets, Ar-H); δ_{C} (400 MHz; CDCl_3) 9.9, 19.6 and 20.0 (C-8, C-9 and C-10), 25.3 and 29.4 (C-5 and C-6), 37.4 and 49.1 (2'-C and C-7), 47.4 (C-4), 52.5 (C-1), 62.5 (C-3'), 79.6 (C-3), 126.3, 128.1, 130.0, and 138.8 (Ar-C), 170.7 (C-2) and 182.8 (C-1').

[†] ^1H NMR analysis of the crude mixture indicated 84.9 % d.e. where the *exo*-isomer predominated.

The α -endo-propyl 2-iminolactone **280a** and α -exo-propyl 2-iminolactone **280b**

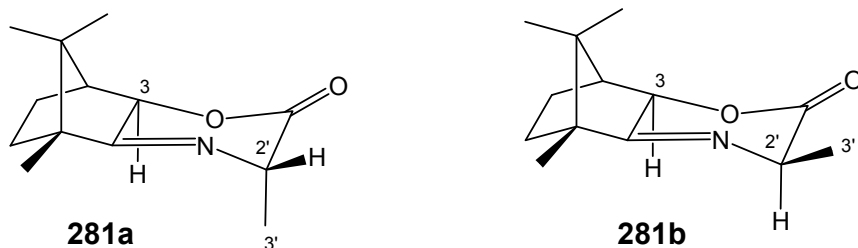
The experimental procedure employed for the synthesis of **279** was followed, using the 2-iminolactone **208** (0.05 g, 0.2 mmol) in THF (3 mL), *t*-BuOK (0.03g, 0.3 mmol) in THF (3 mL) and propyl iodide in THF (3 mL). Work-up and chromatography [using silica gel on a chromatotron, 1 mm plate; elution with hexane-EtOAc (9:1)] afforded, as light brown oils, two products:[†]

the α -endo-propyl 2-iminolactone **280a** (0.008 g, 13 %); ν_{\max} / cm^{-1} (CHCl_3) 1745 (C=O); δ_{H} (400 MHz; CDCl_3) 0.84, 0.99 and 1.17 (9H, 3 \times s, 8-, 9- and 10-Me), 0.93 - 1.03, 1.37 - 1.45, 1.53-1.61, 1.74-1.90 and 2.06-2.17 (11H, series of multiplets, 3'-, 4'-, 5- and 6- CH_2 and 5'- CH_3), 2.25 (1H, d, *J* 4.8 Hz, 4-H), 4.61 (1H, t, *J* 7.0 Hz, 2'-H) and 4.66 (1H, s, 3-H); δ_{C} (100 MHz; CDCl_3) 10.0, 13.9, 19.5, 19.8 (C-5'-, C-8, C-9 and C-10), 20.1, 25.7, 29.3 and 33.3 (C-3', C-4', C-5 and C-6), 47.9 (C-4), 48.1, 52.6, 62.2 (C-1, C-2' and C-7), 78.6 (C-3), 171.0 (C-2) and 180.4 (C-1');

the α -exo-propyl 2-iminolactone **280b** (0.024 g, 38.88 %); ν_{\max} / cm^{-1} (CHCl_3) 1740 (C=O); δ_{H} (400 MHz; CDCl_3) 0.96 - 1.08, 1.31 - 1.39, 1.53 - 1.61, 1.72 - 1.80 and 1.92 - 2.12 (11H, series of multiplets, 3'-, 4'-, 5- and 6- CH_2 and 5'- CH_3), 0.75, 0.95 and 1.04 (9H, 3 \times s, 8-, 9- and 10-Me), 2.24 (1H, d, *J* 4.9 Hz, 4-H), 3.69 (1H, dd, *J* 1.2, *J* 5.8 Hz, 2'-H) and 4.45 (1H, d, *J* 1.2, 3-H); δ_{C} (100 MHz; CDCl_3) 10.0 14.0, 19.0, 19.7 (C-5', C-8, C-9 and C-10), 20.1, 25.3, 29.6 and 33.3 (C-3', C-4', C-5 and C-6), 47.4 (C-4), 49.6, 52.5, 60.7 (C-1, C-2' and C-7), 79.5 (C-3), 169.0 (C-2) and 181.4 (C-1').

[†] ¹H NMR analysis of the crude mixture indicated 49.2 % d.e. where the *exo*-isomer predominated.

The α -endo-methyl 2-iminolactone **281a** and α -exo-methyl 2-iminolactone **281b**

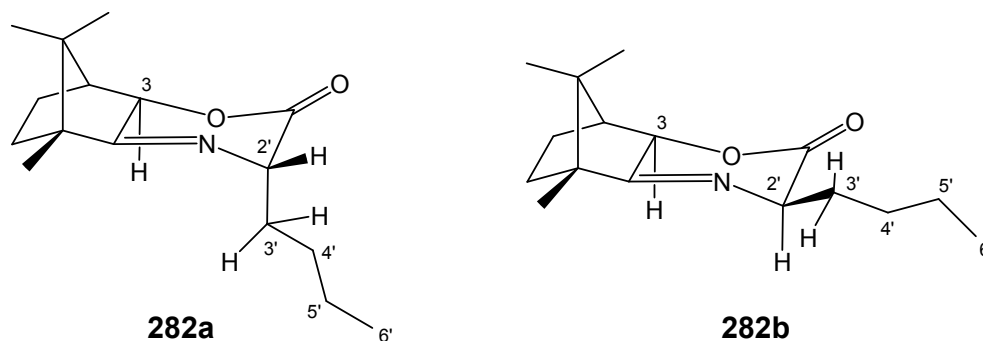


The experimental procedure employed for the synthesis of **279** was followed, using the 2-iminolactone **208** (0.05 g, 0.3 mmol) in THF (3 mL), *t*-BuOK (0.03g, 0.3 mmol) in THF (3 mL) and methyl iodide in THF (3 mL). Work-up and chromatography [using silica gel on a chromatotron, 1 mm plate; elution with hexane-EtOAc (9:1)] afforded, as light brown oils, two products:[†]

the α -endo-methyl 2-iminolactone **281a** (0.012 g, 21 %); ν_{\max} / cm^{-1} (CHCl_3) 1740 (C=O); δ_{H} (400 MHz; CDCl_3) 0.80, 0.97 and 1.05 (9H, 3 \times s, 8-, 9- and 10-Me), 1.34 - 1.36, 1.60 - 1.63, 1.73 - 1.80 and 2.05 - 2.11 (4H, series of multiplets, 5- and 6- CH_2), 1.67 (3H, d, *J* 7.0 Hz, 2'- CH_3), 2.25 (1H, d, *J* 4.8 Hz, 4-H), 4.57 (1H, s, 3-H) and 4.58 (1H, q, *J* 7.3 Hz, 2'-H); δ_{C} (100 MHz; CDCl_3) 10.0, 19.5 and 20.1 (8-, 9- and 10-Me), 16.3 (C-2'), 25.8 and 29.1 (C-5 and C-6), 47.8 (C-4), 48.4 and 52.5 (C-1 and C-7), 57.7 (C-2'), 78.5 (C-3), 172.0 (C-2) and 181.2 (C-1'), and

the α -exo-methyl 2-iminolactone **281b** (0.018 g, 32.7 %); ν_{\max} / cm^{-1} (CHCl_3) 1745 (C=O); δ_{H} (400 MHz; CDCl_3) 0.77, 0.96 and 1.05 (9H, 3 \times s, 8-, 9- and 10-Me), 1.32 - 1.43, 1.54 - 1.59, 1.73 - 1.81 and 2.05 - 2.12 (4H, series of multiplets, 5- and 6- CH_2), 1.67 (3H, d, *J* 7.0 Hz, 2'-Me), 2.25 (1H, d, *J* 4.8 Hz, 4-H), 3.97 (1H, qd, *J* 7.1 Hz, *J* 1.2 Hz, 2'-H) and 4.49 (1H, d, *J* 1.2 Hz 3-H); δ_{C} (100 MHz; CDCl_3) 10.0, 19.7 and 20.0 (8-, 9- and 10-Me), 17.3 (C-2'), 25.1 and 29.5 (C-5 and C-6), 47.4 (C-4), 49.0 and 52.4 (C-1 and C-7), 56.7 (C-2'), 79.7 (C-3), 172.0 (C-2) and 183.7 (C-1').

[†] ¹H NMR analysis of the crude mixture indicated 23.5 % d.e. where the *exo*-isomer predominated.

The α -endo-butyl 2-iminolactone **282a** and α -exo-butyl 2-iminolactone **282b**

The experimental procedure employed for the synthesis of **279** was followed, using the 2-iminolactone **208** (0.05 g, 0.3 mmol) in THF (3 mL), *t*-BuOK (0.03g, 0.3 mmol) in THF (3 mL) and butyl iodide in THF (3 mL). Work-up and chromatography [using silica gel on a chromatotron, 1mm plate; elution with hexane-EtOAc (9:1)] afforded, as light brown oils, two products:[†]

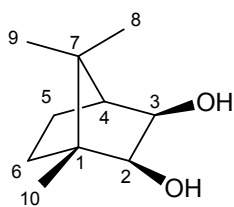
the α -endo-butyl 2-iminolactone **282a** (0.010 g, 14 %); ν_{\max} / cm^{-1} (CHCl_3) 1745 (C=O); δ_{H} (400 MHz; CDCl_3) 0.75, 0.95 and 1.04 (9H, 3 \times s, 8-, 9- and 10-Me), 0.93 - 0.94, 1.33 - 1.44, 1.46 - 1.53, 1.72 - 1.80, 2.07 - 2.13 and 2.18 - 2.19 (13H, series of multiplets, 3'-, 4'-, 5- and 6- CH_2 and 5'- CH_3), 2.25 (1H, m, 4-H), 4.50 (1H, t, *J* 7.9 Hz, 2'-H) and 4.57 (1H, s, 3-H); δ_{C} (100 MHz; CDCl_3) 10.1, 19.5 and 20.1 (C-8, C-9 and C-10), 13.8 (C-6'), 22.3, 25.8, 28.6, 29.3 and 31.0 (C-5, C-6, C-3', C-4' and C-5'), 47.8 (C-4), 48.3 and 56.6 (C-1 and C-7), 62.5 (C-2'), 78.6 (C-3), 171.3 (C-2) and 180.9 (C-1'); and

the α -exo-butyl 2-iminolactone **282b** (0.029 g, 42 %); ν_{\max} / cm^{-1} (CHCl_3) 1745 (C=O); δ_{H} (400 MHz; CDCl_3) 0.89, 0.97 and 1.03 (9H, 3 \times s, 8-, 9- and 10-Me), 0.94 - 2.01 (13H, complex of multiplets, 3'-, 4'-, 5- and 6- CH_2 and 5'- CH_3), 2.34 (1H, d, *J* 5.3 Hz, 4-H), 3.90 (1H, d, *J* 1.2 Hz, 3-H) and 4.11 (1H, q, *J* 1.2, *J* 7.1 Hz, 2'-H); δ_{C} (100 MHz; CDCl_3) 10.0, 19.0 and 20.0 (C-8, C-9 and C-10), 14.0 (C-6'), 22.4, 26.2, 28.8, 29.3 and 31.3 (C-5, C-6, C-3', C-4' and C-5'), 47.7 (C-4), 49.4 and 56.9 (C-1 and C-7), 61.4 (C-2'), 79.5 (C-3), 169.3 (C-2) and 180.9 (C-1').

[†] ^1H NMR analysis of the crude mixture indicated 48.4 % d.e. where the *exo*-isomer predominated.

3.2.3 Acrylate Esters of 2,3-Dihydroxybornane

2,3-Dihydroxybornane **284**

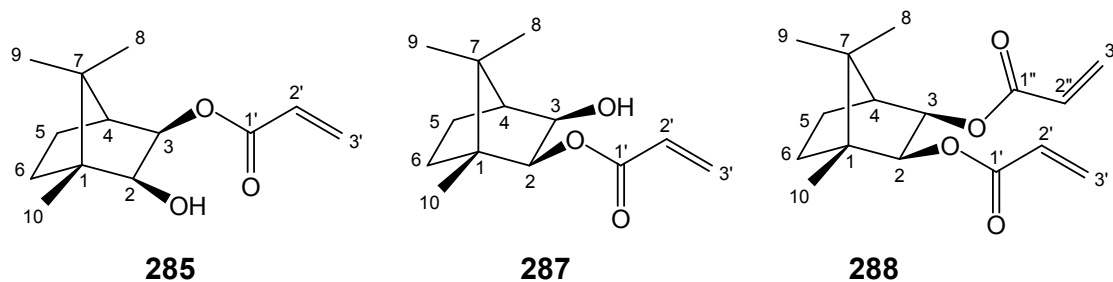


284

LiAlH₄ (5.73 g, 151 mmol) was added to dry THF (100 mL) under N₂ and the resulting mixture stirred for 2 h at 0 °C. Camphorquinone **22** (10.00 g, 60 mmol) in dry THF (10 mL) was then added drop-wise under N₂ and the mixture allowed to warm to room temperature overnight. The reaction mixture was then heated to, and maintained at, 60 °C for 2 h. The reaction was then quenched under N₂ by the successive addition of 3 M-NaOH (5 mL) and water (2.5 mL). The resulting precipitate was filtered off, collected and extracted by boiling with Et₂O (4 × 50 mL). The filtrate and extracts were subsequently combined, washed with saturated aqueous NaHCO₃ (3 × 20 mL) and dried over anhydrous MgSO₄. Concentration of the mixture *in vacuo* afforded, without need for further purification, as a white crystalline solid:

2,3-dihydroxybornane **284** (9.83 g, 96.1 %); m.p. 253-257 (lit.,¹⁷⁴ 230-231 °C) (Found: M⁺, 170.13050. C₁₀H₁₈O₂ requires M, 170.13068); ν_{max} / cm⁻¹ (CHCl₃) 3550 (OH); δ_H (400 MHz; CDCl₃) 0.78 (3H, s, 10-CH₃), 0.88 - 0.99, 1.38 - 1.48 and 1.58 - 1.70 (4H, series of multiplets, 5- and 6-CH₂) 0.92 and 1.08 (6H, 2 × s, 8- and 9-CH₃), 1.75 (1H, d, *J* 4.7 Hz, 4-H), 2.54 - 3.09 (2H, br signal, 2 × OH), 3.58 (1H, d, *J* 7.0 Hz, 2-H) and 3.81 (1H, d, *J* 7.0 Hz, 3-H); δ_C (100 MHz; CDCl₃) 11.1, 21.0 and 21.8 (C-8, C-9 and C-10), 24.0 (C-6), 33.1 (C-5), 46.4 and 48.7 (C1 and C-7), 51.4 (C-4), 76.1 (C-2) and 79.9 (C-3); *m/z* 170 (M⁺, 4.2 %) and 95 (100).

2-Exo-3-exo-bornanyl diacrylate **288**, 2-exo-hydroxy-3-exo-bornanyl acrylate **285** and 3-exo-hydroxy-2-exo-bornanyl acrylate **287**.



Method 1

Bornane-2,3-diol **284** (1.01 g, 5.9 mmol) was dissolved in dichloromethane (20 mL) and 4 Å molecular sieves were added. Acryloyl chloride (0.56 g, 6.2 mmol) was introduced and the reaction mixture was boiled under reflux overnight. The molecular sieves were filtered off and the filtrate was washed with saturated aqueous NaHCO₃ (3 × 20 mL) to neutralize any acid and then dried over anhydrous MgSO₄. Removal of the solvent was achieved under reduced pressure and the residue was chromatographed [using silica gel on a chromatotron, 1 mm plate; elution with hexane-EtOAc (19:1)] to afford three products:

2-exo-3-exo-bornanyl diacrylate **288**, as white crystals, (0.19 g, 12 %) (Found: M⁺, 278.15199. C₁₆H₂₂O₄ requires M, 278.15181); δ_H (400 MHz; CDCl₃) 0.85, 0.88 and 1.15 (9H, 3 × s, 8-, 9- and 10-Me), 1.19 - 1.83 (4H, complex of multiplets, 5- and 6-CH₂), 1.91 (1H, d, J 4.9 Hz, 4-H), 4.91 (2H, s, 2-H and 3-H), 5.77 (2H, ddd, J 1.4 Hz, 10.4 and 12.7 Hz, 3'- and 3''-H), 6.03 (2H, dt, J 10.4 and 17.1 Hz, 3'- and 3''-H) and 6.30 (2H, ddd, J 1.4 and 17.4 Hz, J 18.9 Hz, 2' and 2''-H); δ_C (100 MHz; CDCl₃) 10.9, 20.4 and 20.9 (C-8, C-9 and C-10), 23.8 (C-6), 32.9 (C-5), 47.5 and 48.8 (C-1 and C-7), 49.6 (C-4), 77.1 (C-2), 79.8 (C-3), 128.4 (C-2'), 128.5 (C-2''), 130.47 (C-3'), 130.54 (C-3''), 164.89 (C-1') and 165.00 (C-1''); m/z 278 (M⁺, 0.4 %) and 206 (100);

2-exo-hydroxy-3-exo-bornanyl acrylate **285**, as an oil, (0.10 g, 7 %) (Found: M⁺, 224.14161. C₁₃H₂₀O₃ requires M, 224.14124); δ_H (400 MHz; CDCl₃) 0.82 (3H, s, 9-Me), 0.93 (3H, s, 8-Me), 1.02 - 1.84 (4H, complex of multiplets, 5- and 6-CH₂), 1.12 (3H, s, 10-Me), 1.84 (1H, d, J 5.0 Hz, 2-OH), 1.88 (1H, d, J 4.9 Hz, 4-H), 3.81 (1H, dd, J 5.2 and 6.2 Hz, 2-H_{endo}), 4.68 (1H, d, J 6.8 Hz, 3-H_{endo}), 5.83 (1H, dd, J 1.4 and 10.4 Hz, 3'-H_Z), 6.13 (1H, dd, J 10.4 and 17.3 Hz, 2'-H) and 6.39 (1H, dd, J 1.4 and 17.3 Hz, 3-H_E); δ_C (100 MHz; CDCl₃) 11.0 (C-8), 20.7 (C-10), 21.1 (C-9), 23.9 (C-5), 33.2 (C-6), 46.9 (C-7), 49.0 (C-1), 49.2 (C-4), 79.6 (C-2), 80.0 (C-3), 128.4 (C-2'), 130.7 (C-3') and 166.2 (C-1'); m/z 224 (M⁺, 0.8 %) and 66 (100); and

3-exo-hydroxy-2-exo-bornanyl acrylate **287**, as an oil, (0.16 g, 12 %)(Found: M^+ , 224.14161. $C_{13}H_{20}O_3$ requires M , 224.14124); δ_H (400 MHz; $CDCl_3$) 0.82 (3H, s, 9-Me), 0.90 (3H, s, 8-Me), 1.01 - 1.75 (4H, complex of multiplets, 5- and 6- CH_2), 1.15 (3H, s, 10-Me), 1.79 (1H, d, J 4.8 Hz, 4-H), 1.87 (1H, d, J 4.1 Hz, 3-OH), 4.02 (1H, dd, J 3.7 Hz, 6.2 Hz, 3- H_{endo}), 4.54 (1H, d, J 6.7 Hz, 2- H_{endo}), 5.84 (1H, dd, J 0.9 and 10.4 Hz, 3'- H_Z), 6.15 (1H, dd, J 10.4 and 17.3 Hz, 2'-H) and 6.40 (1H, dd, J 1.4 and 17.3 Hz, 3- H_E); δ_C (100 MHz; $CDCl_3$) 11.2 (C-8), 20.6 (C-10), 21.1 (C-9), 24.1 (C-5), 33.1 (C-6), 47.0 (C-7), 48.3 (C-1), 51.6 (C-4), 76.7 (C-3), 82.9 (C-2), 128.4 (C-3'), 130.7 (C-2') and 166.4 (C-1'); m/z 224 (M^+ , 0.8 %) and 66 (100).

Method 2

A solution of bornane-2,3-diol **284** (0.50 g, 2.9 mmol) in dry THF (7.5 mL) was added drop-wise under N_2 to a stirred solution of pre-washed NaH (0.14 g, 5.6 mmol) in dry THF (25 mL). The mixture was stirred for 2 h and then refluxed for approximately 2 h until the orange colour of the alkoxide was observed. The reaction mixture was cooled, acryloyl chloride (0.34 g, 3.8 mmol) was added drop-wise and the mixture stirred for 12 h at room temperature and then refluxed for 1 h. The THF was removed *in vacuo* and the residue was partitioned between saturated aqueous $NaHCO_3$ (10 mL) and EtOAc (3×10 mL). The organic layers were combined, dried over anhydrous $MgSO_4$ and concentrated under reduced pressure to give an oil, which was chromatographed [using silica gel on a chromatotron, 2 mm plate; elution with hexane-EtOAc (5:1)] to afford three products;

2-exo-3-exo-bornanyl diacrylate **288** (0.019 g, 2.3 %);

2-exo-hydroxy-3-exo-bornanyl acrylate **285** (0.087 g, 11 %); and

3-exo-hydroxy-2-exo-bornanyl acrylate **287** (0.101 g, 15 %).

Method 3

Butyllithium (1.6 M solution in hexane; 9.62 mL, 15.4 mmol) was added drop-wise over 20 min, under dry N_2 to a stirred solution of bornane-2,3-diol **284** (2.02 g, 11.8 mmol) in dry THF (25 mL) at -5 °C. After 1.5 h acryloyl chloride (1.41 g, 15.6 mmol) was added drop-wise, the mixture was stirred at 0 °C for 1 h and then allowed to warm to room temperature over 14 h. The THF was removed *in vacuo* and the residue was treated with saturated aqueous $NaHCO_3$ (10 mL), extracted with Et_2O (3×10 mL) and dried over anhydrous $MgSO_4$.

Concentration under reduced pressure gave an oil, which was chromatographed [using silica gel on a chromatotron, 4 mm plate; elution with hexane-EtOAc (9:1)] to afford three products;

2-exo-3-exo-bornanyl diacrylate **288** (0.36 g, 11 %);

2-exo-hydroxy-3-exo-bornanyl acrylate **285** (0.90 g, 34 %); and

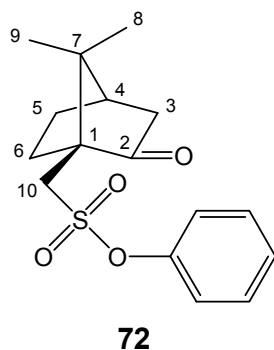
3-exo-hydroxy-2-exo-bornanyl acrylate **287** (1.27 g, 48 %).

Attempted synthesis

Carbonyldiimidazole (0.96 g, 5.9 mmol) was added to a stirred solution of acrylic acid (0.42 g, 5.9 mmol) in dry DMF (2 mL) at room temperature. After stirring for 30 minutes, this solution was then added drop-wise to a solution of 2,3-dihydroxybornane **284** (1.00 g, 5.9 mmol) in dry DMF (2.5 mL). The reaction mixture was stirred for 14 h. Removal of the DMF was achieved under reduced pressure and the residue was washed with saturated aqueous NaHCO₃ and then dried with anhydrous MgSO₄. ¹H NMR spectroscopy showed no sign of the expected acrylate ester.

3.2.4 Acrylate Esters of Phenyl 2-Hydroxybornane-10-sulfonate

Phenyl (+)-camphor-10-sulfonate **72**

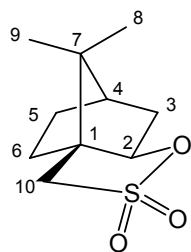


Camphor-10-sulfonyl chloride **298** (10.07 g, 40.2 mmol) was added to a stirred solution of phenol (3.78 g, 40.2 mmol) in pyridine (13 mL) at 0 °C over 20 min. The solution was stirred at this temperature for a further 2.5 h and then at room temperature for 1 h. The reaction was quenched by diluting with water and the resulting mixture was shaken with 10 % aqueous HCl (20 mL) to remove pyridine as the hydrochloride salt. Extraction was achieved with Et₂O (4 × 50 mL) and the combined organic layers were washed sequentially with H₂O (50 mL), 10 % aqueous HCl (20 mL) and H₂O (50 mL). The ether was then washed sequentially with 10 % aqueous NaOH (10 mL), brine (10 mL), 10 % aqueous NaOH (5 mL) and brine (10 mL) to remove excess phenol by generating the water soluble sodium phenoxide salt. The organic layer was then dried over anhydrous MgSO₄. The solvent was removed *in vacuo* to give a colourless oil:

phenyl (+)-camphor-10-sulfonate **72** (9.63 g, 77.7 %)(Found: M⁺, 308.10846. C₁₆H₂₀O₄S requires M, 308.10822); ν_{max} / cm⁻¹ (CHCl₃) 1640 (C=O), 1490, 1380 and 1100 (SO₂-OPh); δ_H (400 MHz; CDCl₃) 0.90 and 1.16 (6H, 2 × s, 8- and 9-Me), 1.45, 1.71, 2.08 and 2.56 (4H,

4 × m, 5-CH₂ and 6-CH₂), 1.96 (1H, d, J_{gem} 18.5 Hz, 3-H_{endo}), 2.13 (1H, m, 4-H), 2.41 (1H, m, 3-H_{exo}), 3.18 and 3.81 (1H, 2 × d, J 15.0 Hz, 10-CH₂) and 7.25 - 7.43 (5H, complex of multiplets, Ar-H); δ_{C} (400 MHz; CDCl₃) 19.7 and 20.0 (C-8 and C-9), 25.1 and 26.9 (C-5 and C-6), 42.5 (C-3), 42.9 (C-4), 47.6 and 58.2 (C-1 and C-7), 47.9 (C-10), 120.7, 127.2, 129.9 and 149.3 (Ar-C) and 214.1 (C-2); m/z 308 (M⁺, 1 %) and 215 (100).

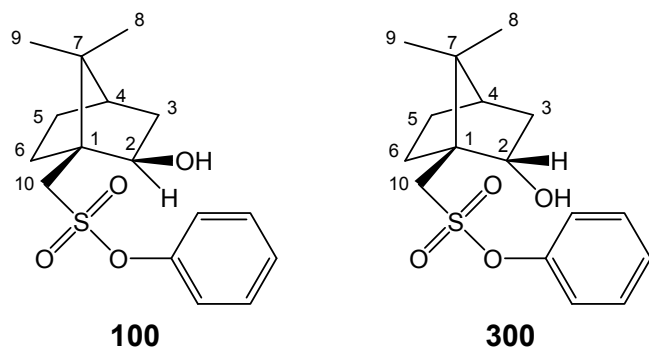
10-Isobornyl sultone **87**



87

A solution of phenyl (+)-camphor-10-sulfonate **72** (0.50 g, 1.6 mmol) in ethanol (2 mL) was added drop-wise to a stirred solution of NaBH₄ (0.10 g, 2.7 mmol) in ethanol (4 mL) at 0 °C over 20 min. The solution was allowed to warm to room temperature and stirred for 8 h. The reaction was quenched by the drop-wise addition of 5 % HCl. The resulting mixture was extracted with Et₂O (3 × 2 mL) and the combined organic layers were washed with brine (3 × 1 mL). The Et₂O solution was then washed sequentially with 10 % aqueous NaOH (1 ml), brine (1 mL), 10 % aqueous NaOH (1 mL) and brine (1 mL) to remove phenol and then dried over anhydrous MgSO₄. The solvent was removed *in vacuo* to give white crystals of: 10-isobornyl sultone **87** (0.33 g, 93.7 %); m.p. 109-112 °C (lit.⁴⁶ 114-116 °C) (Found: M⁺, 216.08158. C₁₀H₁₆O₃S requires M , 216.08202); ν_{max} / cm⁻¹ (CHCl₃) 1175 (SO₂); δ_{H} (400 MHz; CDCl₃) 0.94 and 1.11 (6H, 2 × s, 8- and 9-Me), 1.25, 1.40 and 1.88 - 1.96 (6H, series of multiplets, 3-, 5- and 6-CH₂), 2.22 - 2.32 (1H, m, 4-H), 3.22 (2H, 2 × d, J 13.7 and 10-CH₂) and 4.37 (1H, dd, J 3.5 and 7.9 Hz, 2-H); δ_{C} (100 MHz; CDCl₃) 19.7 and 19.8 (C-8 and C-9), 26.6 and 28.9 (C-5 and C-6), 35.7 (C-3), 44.2 (C-4), 47.3 and 55.4 (C-1 and C-7), 48.9 (C-10) and 87.8 (C-2); m/z 216 (M⁺, 1.5 %) and 93 (100).

Phenyl (+)-2-exo-hydroxybornane-10-sulfonate **100**, *phenyl (+)-2-endo-hydroxybornane-10-sulfonate* **300** and *10-isobornyl sultone* **87**.

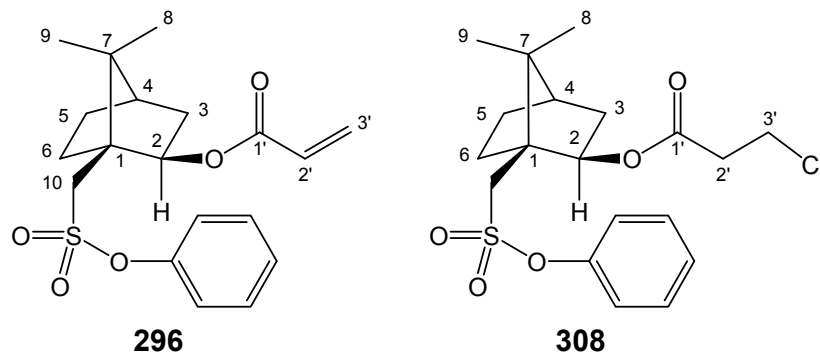


A solution of phenyl (+)-camphor-10-sulfonate **72** (2.37 g, 7.7 mmol) in ethanol (5 mL) was added to a stirred solution of NaBH₄ (0.10 g, 2.7 mmol) in EtOH-H₂O (10 mL: 5 mL) at -15 °C over 20 min. The solution was stirred vigorously for 16 h at -8 °C. 5 % aq. HCl was added drop-wise to quench excess NaBH₄. Solvent was removed under reduced pressure, and the residue was dissolved in Et₂O (8 mL), washed with brine (3 × 3 mL) and then dried over anhydrous MgSO₄. The solvent was removed *in vacuo* to give an oil, which was purified [flash chromatography on silica gel; hexane-EtOAc (8:2)] to afford three products:

phenyl (+)-2-exo-hydroxybornane-10-sulfonate **100**, as an oil (1.94 g, 81.0 %) (Found: M⁺, 310.12333. C₁₆H₂₂O₄S requires M, 310.12388); [α]_D²⁰ = -35.16° (c 4.42, CHCl₃); δ_H (400 MHz; CDCl₃) 0.85 (3H, s, 9-Me), 1.07 (3H, s, 8-Me), 1.12 - 1.87 (7H, complex of multiplets, 4-H and 3-, 5- and 6-CH₂), 2.82 (1H, d, J 4.4 Hz, 2-OH), 3.15 and 3.73 (2H, 2 × d, J 13.67 Hz, 10-CH₂), 4.11 (1H, m, 2-CH) and 7.25 - 7.44 (5H, complex of multiplets, Ar-H); δ_C (100 MHz; CDCl₃) 19.8 (C-8), 20.5 (C-9), 27.3 (C-5), 30.2 (C-6), 39.2 (C-3), 44.4 (C-4), 49.0 (C-7), 50.0 (C-1), 50.3 (C-10), 76.1 (C-2) and 122.0, 127.3, 130.0 and 149.0 (Ar-C); m/z 310 (M⁺, 0.3 %) and 94 (100);

phenyl (+)-2-endo-hydroxybornane-10-sulfonate **300**, as an oil (0.28 g, 11.5 %) (Found: M⁺, 310.12645. C₁₆H₂₂O₄S requires M, 310.12388); [α]_D²⁰ = +17.95° (c 0.44, CHCl₃); δ_H (400 MHz; CDCl₃) 0.92 (3H, s, 9-Me), 0.93 (3H, s, 8-Me), 1.14, 1.43, 1.57, 1.83, 2.34 and 2.53 (6H, complex of multiplets, 3-,5- and 6-CH₂), 1.68 (1H, t, J 4.5 Hz, 4-CH), 3.14 (1H, d, J 2.2 Hz, 2-OH_{endo}), 3.34 (2H, s, 10-CH₂), 4.39 (1H, dd, J 2.5 and 10.0 Hz, 2-H_{exo}) and 7.28, 7.32, 7.42 (5H, complex of multiplets, Ar-H); δ_C (100 MHz; CDCl₃) 18.9 (C-8), 20.5 (C-9), 23.8 (C-6), 28.1 (C-5), 38.2 (C-3), 44.0 (C-4), 51.0 (C-7), 51.9 (C-1), 54.3 (C-10), 75.1 (C-2) and 122.0, 127.4, 130.0 and 148.7 (Ar-C); m/z 310 (M⁺, 0.5 %) and 94 (100); and *10-isobornyl sultone* **87** (0.058 g, 3.5 %).

Phenyl 2-exo-acryloyloxybornane-10-sulfonate **296** and *phenyl 2-exo-(3-chloropropanoyloxy)bornane-10-sulfonate* **308**



Method 1

Neutral Al_2O_3 (0.32 g, 3.1 mmol) was added to the alcohol **100** (0.61 g, 2.0 mmol) and acryloyl chloride (0.39 g, 4.3 mmol) was then added. The resulting dispersion was sealed and kept unstirred at 25 °C for 72 h. The residue was taken up in EtOAc (3 × 1 mL), filtered and dried over anhydrous MgSO_4 . Solvent was removed *in vacuo* to give an oil, which was chromatographed [HPLC; elution with hexane-EtOAc (8:2)] to afford two products, as transparent crystals:

phenyl 2-exo-acryloyloxybornane-10-sulfonate **296** (0.40 g, 55 %) (Found: M^+ , 364.13395. $\text{C}_{19}\text{H}_{24}\text{O}_5\text{S}$ requires M , 364.13445); $[\alpha]_D^{20} = -30.52^\circ$ (c 2.90, CHCl_3); δ_{H} (400 MHz; CDCl_3) 0.91 and 1.02 (6H, 2 × s, 8- and 9-Me), 1.22, 1.79, 1.64, 1.79, 1.97 and 1.98 (6H, series of multiplets, 3-,5- and 6- CH_2), 1.81 (1H, m, 4-H), 3.14 and 3.67 (2H, 2 × d, J 13.9 Hz and 10- CH_2), 5.01 (1H, dd, J 3.1 and 7.9 Hz, 2-CH), 5.68 (1H, dd, J 1.4 and 10.4 Hz, 3'- H_Z), 5.92 (1H, dd, J 10.4 and 17.3 Hz, 2'-H), 6.19 (1H, dd, J 1.4 and 17.3 Hz, 3'- H_E) and 7.18 – 7.41 (5H, complex of multiplets, Ar-H); δ_{C} (100 MHz; CDCl_3) 19.9 and 20.3 (C-8 and C-9), 26.9, 29.9 and 39.3 (C-3, C-5 and C-6), 44.5 (C-4), 48.8 and 49.5 (C-1 and C-7), 49.3 (C-10), 77.5 (C-2), 121.9, 127.0, 129.8 and 149.0 (Ar-C), 128.5 (C-2'), 130.3 (C-3') and 164.6 (C-1'); m/z 364 (M^+ , 0.8 %) and 55 (100); and

phenyl 2-exo-(3-chloropropanoyloxy)bornane-10-sulfonate **308** (0.33 g, 42 %) (Found: M^+ , 400.10707. $\text{C}_{19}\text{H}_{25}\text{O}_5\text{SCl}$ requires M , 400.11112); $[\alpha]_D^{20} = -70.51^\circ$ (c 2.14, CHCl_3); δ_{H} (400 MHz; CDCl_3) 0.92 and 1.03 (6H, 2 × s, 8- and 9-Me), 1.24, 1.67, 1.78, 1.82 and 1.99 (6H, series of multiplets, 3-,5- and 6- CH_2), 1.83 (1H, m, 4-CH), 2.58 (2H, m, 2'- CH_2), 3.17 and 3.69 (2H, 2 × d, J 13.9 Hz, 10- CH_2), 3.60 (2H, m, 3'- CH_2), 4.99 (1H, dd, J 3.2 and 8.0 Hz, 2-CH) and 7.21 – 7.44 (5H, complex of multiplets, Ar-H); δ_{C} (100 MHz; CDCl_3) 19.9 and 20.3 (C-8 and C-9), 26.9, 30.1 and 39.3 (C-3, C-5 and C-6), 37.6 (C-2'), 38.9 (C-3'), 44.6 (C-4),

48.8 and 49.6 (C-1 and C-7), 49.4 (C-10), 78.1 (C-2), 122.1, 127.2, 129.9 and 149.1 (Ar-C) and 168.7 (C-1'); m/z 400 (M^+ , 2.0 %) and 94 (100).

Method 2

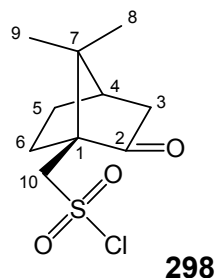
Butyllithium (1.6 M solution in hexane; 0.28 mL, 0.5 mmol) was added drop-wise over 20 min, under dry N_2 , to a stirred solution of phenyl (+)-2-*exo*-hydroxybornane-10-sulfonate **100** (0.13 g, 0.4 mmol) in dry THF (2 mL) at -78 °C. After 1 h, acryloyl chloride (0.04 g, 0.5 mmol) was added drop-wise, the mixture was stirred at -10 °C for 1 h and then allowed to warm to room temperature over 12 h. The THF was removed *in vacuo* and the residue was quenched with saturated aqueous $NaHCO_3$ (1 mL), extracted with Et_2O (3×1 mL) and dried over anhydrous $MgSO_4$. Concentration under reduced pressure gave an oil, which was chromatographed [HPLC; elution with hexane-EtOAc (9:1)] to afford three products:

phenyl 2-*exo*-acryloyloxybornane-10-sulfonate **296** (0.15 g, 5 %)

10-isobornyl sultone **87** (0.09 g, 79 %); and

phenyl acrylate **309** (0.05 g, 82 %)

10-Camphorsulfonyl chloride **298**

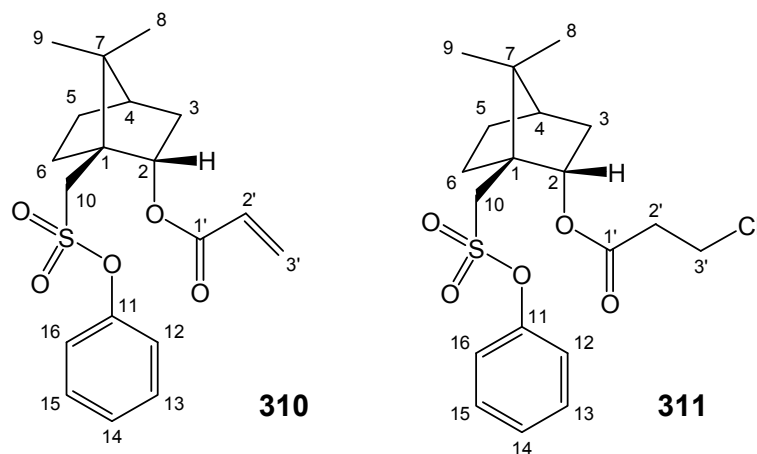


Camphorsulfonic acid **71** (50.17 g, 0.216 mol) was mixed with phosphorus pentachloride (44.85 g, 0.215 mol) in a flask connected to an HCl trap at 0 °C. Once the violently exothermic reaction had subsided, the solution was allowed to warm to room temperature and stirred for an additional 4 h. The solution was then poured over crushed ice (50 g) and the resulting mixture immediately poured over more ice (50 g) and mixed until the reaction had been quenched. The reaction mixture was filtered under vacuum and the residue washed with cold water before freeze-drying and recrystallisation from petroleum ether ($30 - 60$ °C) to yield white crystals of:

10-camphorsulfonyl chloride **298** (32.17 g, 59.4 %). δ_H (400 MHz; $CDCl_3$) 0.92 and 1.14 (6H, $2 \times s$, 8- and 9-Me), 1.45, 1.48, 1.77, 2.09 and 2.44 (6H, series of multiplets, 3-, 5- and 6-

CH₂), 1.98 (1H, d, *J* 18.6 Hz, 4-H) and 3.72 and 4.30 (2H, 2 × d, *J* 14.6 Hz, 10-CH₂); *m/z* 266 (M⁺, 12.3 %).

Phenyl 2-endo-acryloyloxybornane-10-sulfonate 310 and *phenyl 2-endo-(3-chloropropanoyloxy)bornane-10-sulfonate 311*



Method 1

The experimental procedure employed for the synthesis of phenyl 2-*exo*-acryloyloxybornane-10-sulfonate **296** and phenyl 2-*exo*-(3-chloropropanoyloxy)bornane-10-sulfonate **308**

(Method 1)

was followed, using neutral Al₂O₃ (0.14 g, 1.4 mmol), phenyl (+)-2-*endo*-hydroxybornane-10-sulfonate **300** (0.27 g, 0.9 mmol) and acryloyl chloride (0.18 g, 2.0 mmol). Work-up and chromatography [using silica gel on a chromatotron, 1 mm plate; elution with hexane-EtOAc (8:2)] afforded two products as transparent crystals:

phenyl 2-endo-acryloyloxybornane-10-sulfonate 310 (0.18 g, 57 %) (Found: M⁺, 364.13465. C₁₉H₂₄O₅S requires *M*, 364.13445); [α]²⁰_D = -61.03° (*c* 2.04, CHCl₃); δ_H (400 MHz; CDCl₃) 0.96 and 1.00 (6H, 2 × s, 8- and 9-Me), 1.09- 1.13 and 2.47- 2.55 (2H, 2 × m, 3-CH₂), 1.37 - 1.43, 1.70 - 1.73, 1.84 - 1.93, 2.58 - 2.651 (4H, series of multiplets, 5- and 6-CH₂), 1.77 (1H, t, *J* 4.6 Hz, 4-H), 3.26 and 3.35 (2H, 2 × d, *J* 14.1 Hz, 10-CH₂), 5.26 (1H, dt, *J* 2.6 and 9.8 Hz, 2-H), 5.80 (1H, dd, *J* 1.3 and 10.5 Hz, 3'-H_Z), 6.11 (1H, dd, *J* 10.5 and 17.4 Hz, 2'-H), 6.43 (1H, dd, *J* 1.3 and 17.4 Hz, 3'-H_E), 7.22 - 7.39 (5H, complex of multiplets, Ar-H); δ_C (400 MHz; CDCl₃) 19.1 and 19.9 (C-8 and C-9), 25.3, 27.9 and 37.4 (C-3, C-5 and C-6), 44.2 (C-4), 49.7 and 50.8 (C-1 and C-7), 53.3 (C-10), 76.8 (C-2), 122.0 (C-13 and C-15), 127.0 (C-14), 128.6 (C-2'), 129.9 (C-12 and C-16), 130.8 (C-3'), 149.3 (C-2) and 166.0 (C-1'); *m/z* 364 (M⁺, 0.1 %) and 55 (100); and

phenyl 2-endo-(3-chloropropanoyloxy)bornane -10-sulfonate **311** (0.14 g, 39 %) (Found: M^+ , 400.10875. $C_{19}H_{25}O_5SCl$ requires M , 400.11112); δ_H (400 MHz; $CDCl_3$) 0.96 and 0.99 (6H, $2 \times s$, 8- and 9-Me), 1.12, 1.40, 1.68, 1.89, 2.49 and 2.57 (6H, series of multiplets, 3-, 5- and 6- CH_2), 1.79 (1H, m, 4-H), 2.81 (2H, t, J 6.9 Hz, 2'- CH_2), 3.26 and 3.32 (2H, $2 \times d$, J 13.9 Hz, 10- CH_2), 3.76 (2H, dt, J 1.1 and 7.0 Hz, 3'- CH_2), 5.26 (1H, dd, J 9.8 Hz, 2-CH), 7.21 – 7.44 (5H, complex of multiplets, Ar-H); δ_C (100 MHz; $CDCl_3$) 19.1 and 19.8 (C-8 and C-9), 25.3, 27.9 and 37.3 (C-3, C-5 and C-6), 37.7 (C-2'), 39.1 (C-3'), 44.1 (C-4), 49.6 and 50.9 (C-1 and C-7), 53.3 (C-10), 77.1 (C-2), 122.0, 127.1, 129.9, 149.2 (Ar-C) and 170.1 (C-1'); m/z 400 (M^+ , 0.3 %) and 135 (100).

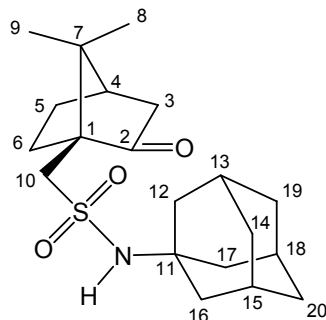
Method 2

The experimental procedure employed for the synthesis of phenyl 2-*exo*-acryloyloxybornane-10-sulfonate **296** (Method 2) was followed, using butyllithium (1.6 M solution in hexane; 0.28 mL, 0.5 mmol), phenyl (+)-2-*endo*-hydroxybornane-10-sulfonate **300** (0.10 g, 0.3 mmol) and acryloyl chloride (0.033 g, 0.4 mmol) in dry THF (2 mL). Work-up and chromatography [using silica gel on a chromatotron, 1mm plate; elution with hexane-EtOAc (8:2)] afforded transparent crystals of:

phenyl 2-endo-acryloyloxybornane-10-sulfonate **310** (0.09 g, 76.5 %)

3.2.5 Acrylate Esters of *N*-(1-adamantyl)-2-hydroxybornane-10-sulfonamide

N-(1-Adamantyl)-2-oxo-bornane-10-sulfonamide **318**

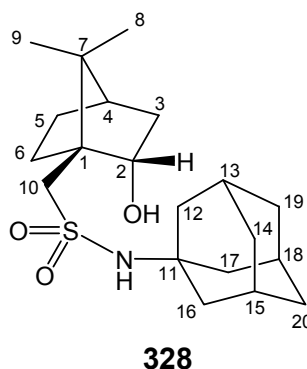
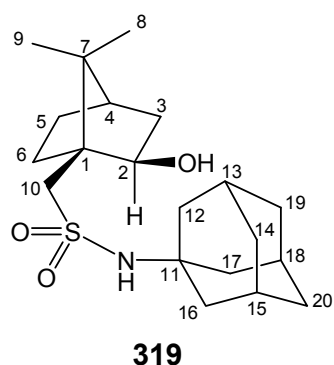


318

A solution of 10-camphor sulfonyl chloride **298** (2.52 g, 10.0 mmol) in acetonitrile (20 mL) was added drop-wise under N₂ to a stirred solution of adamantylamine **317** (3.22 g, 21.3 mmol) and dimethylaminopyridine (0.26 g, 2.1 mmol) in acetonitrile (10 mL) at 0 °C, and the solution was stirred for 1 h. The reaction mixture was then hydrolysed with water (10 mL) followed by 10 % aqueous HCl (2 mL) and the resulting mixture was extracted into EtOAc (3 × 25 mL). The organic layers were combined, washed with 5 % aqueous NaOH (5 mL) and dried over anhydrous MgSO₄. The solvent was removed *in vacuo* affording:

N-(1-adamantyl)-2-oxo-bornane-10-sulfonamide **318** as white crystals (3.51 g, 92.2 %) (Found: M⁺, 365.20387. C₂₀H₃₁NO₃S requires *M*, 365.20247); δ_H (400 MHz; CDCl₃) 0.90 (3H, s, 9-Me), 1.04 (3H, s, 8-Me), 1.41, 1.86, 2.02 and 2.32 (4H, series of multiplets, 5- and 6-CH₂), 1.66 (6H, m, 14-,19- and 20-CH₂), 1.92 and 2.38 (2H, 2 × m, 3-CH₂), 2.00 (6H, m, 12-, 16- and 17-CH₂), 2.09 (3H, m, 13-,15- and 18-CH), 2.10 (1H, m, 4-H), 2.99 and 3.49 (2H, 2 × d, *J* 15.0 Hz, 10-CH₂) and 4.953 (1H, s, NH); δ_C (100 MHz; CDCl₃) 19.7 (C-8), 19.9 (C-9), 26.3 and 27.0 (C-5 and C-6), 29.7 (C-13, C-15 and C-18), 36.0 (C-14, C-19 and C-20), 42.8 (C-4), 42.9 (C-3), 43.2 (12-C, 16-C and 17-C), 48.5 and 55.4 (C-1 and C-7), 54.5 (C-10), 59.4 (C-11) and 216.7 (C-2); *m/z* 365 (M⁺, 30.0 %) and 135 (100).

N-(1-Adamantyl)-2-exo-hydroxybornane-10-sulfonamide **319** and *N*-(1-adamantyl)-2-endo-hydroxybornane-10-sulfonamide **328**



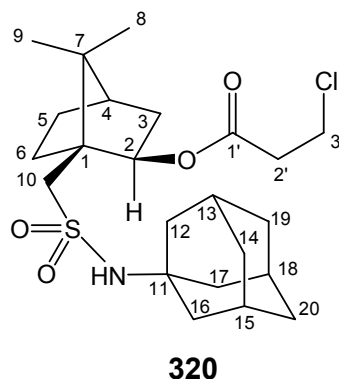
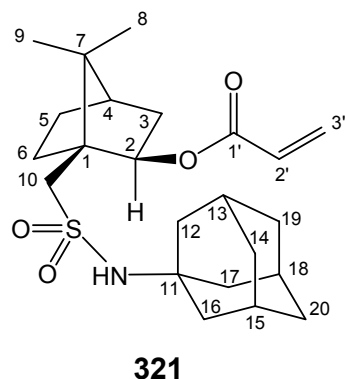
A solution of *N*-(1-adamantyl)-2-oxo-bornane-10-sulfonamide **318** (3.07 g, 8.4 mmol) in THF-H₂O (2 mL: 1 mL) was added drop-wise to a stirred solution of NaBH₄ (3.27 g, 86.3 mmol) in a solution of THF-H₂O (2 mL: 1 mL) at -15 °C over 20 min. The solution was stirred vigorously and allowed to warm to room temperature overnight. The reaction was then quenched with 5 % HCl (2 mL) and the resulting mixture extracted into EtOAc (3 × 1 mL). The organic layers were combined, washed with 5 % brine (3 mL) and dried over anhydrous MgSO₄. Solvent was removed *in vacuo* to give an oil, which was chromatographed [using silica gel on a chromatotron, 1mm plate; elution with hexane-EtOAc (8:2)] to afford two products:

N-(1-adamantyl)-2-exo-hydroxybornane-10-sulfonamide **319**, as transparent crystals (2.87 g, 92.8 %) (Found: M^+ , 367.21993. C₂₀H₃₃NO₃S requires M , 367.21812); $[\alpha]_D^{20} = -40.98^\circ$ (c 2.45, CHCl₃); δ_H (400 MHz; CDCl₃) 0.82 and 1.06 (6H, 2 × s, 8- and 9-Me), 1.12, 1.49, 1.68, 1.71 and 1.76 (6H, series of multiplets, 3-, 5- and 6-CH₂), 1.66 and 1.96 (12H, 2 × m, 12-, 14-, 16-, 17-, 19- and 20-CH₂), 1.72 (1H, m, 4-H), 2.11 (3H, m, 13-, 15- and 18-CH), 2.92 and 3.49 (2H, 2 × d, J 13.8 Hz, 10-CH₂), 3.32 (1H, d, J 2.1 Hz, 2-OH), 4.06 (1H, m, 2-H) and 4.20 (1H, br s, NH); δ_C (400 MHz; CDCl₃) 19.9 and 20.6 (C-8 and C-9), 27.4, 30.7 and 38.9 (C-3, C-5 and C-6), 29.6 (C-13, C-15 and C-18), 35.9 and 43.3 (C-12, C-14, C-16, C-17, C-19 and C-20), 44.4 (C-4), 48.6 and 50.8 (C-1 and C-7), 55.3 (C-11), 57.0 (C-10) and 76.4 (C-2); m/z 367 (M^+ , 0.6 %) and 151 (100); and

N-(1-adamantyl)-2-endo-hydroxybornane-10-sulfonamide **328**, as transparent crystals (0.17 g, 5.6 %) (Found: M^+ , 367.21706. C₂₀H₃₃NO₃S requires M , 367.21812); $[\alpha]_D^{20} = +4.64^\circ$ (c 0.56, CHCl₃); δ_H (400 MHz; CDCl₃) 0.89 and 0.90 (6H, 2 × s, 8- and 9-Me), 1.08, 1.38, 1.54, 1.79, 2.30 and 2.40 (6H, series of multiplets, 3-, 5- and 6-CH₂), 1.63 (1H, t, 4.5 Hz, 4-H), 1.66 and

1.95 (12H, 2 × m, 12-,14-,16-,17-,19- and 20-CH₂), 2.10 (3H, m, 13-,15- and 18-CH), 3.09 and 3.15 (2H, 2 × d, , *J* 14.1 Hz, 10-CH₂), 3.48 (1H, d, *J* 2.5 Hz, 2-OH), 4.23 (1H, br s, NH) and 4.33 (1H, ddd, *J* 2.6, 5.2 and 10.0 Hz, 2-H); δ_C (100 MHz; CDCl₃) 18.9 and 20.5 (C-8 and C-9), 23.9, 28.3 and 38.3 (C-3, C-5 and C-6), 29.6 (C-13, C-15 and C-18), 35.9 and 43.3 (C-12, C-14, C-16, C-17, C-19 and C-20), 43.9 (C-4), 51.3 and 51.5 (C-1 and C-7), 55.5 (C-11), 60.6 (C-10) and 75.2 (C-2); *m/z* 367 (M⁺, 0.5 %) and 151 (100).

N-(1-Adamantyl)-2-*exo*-acryloyloxybornane-10-sulfonamide **321** and *N*-(1-adamantyl)-2-*exo*-(3-chloropropanoyloxy)bornane-10-sulfonamide **320**



Method 1:

The experimental procedure employed for the synthesis of phenyl 2-*exo*-acryloyloxybornane-10-sulfonate **296** and phenyl 2-*exo*-(3-chloropropanoyloxy)bornane-10-sulfonate **308** (**Method 1**) was followed, using neutral Al₂O₃ (0.47 g, 4.6 mmol), *N*-(1-adamantyl)-2-*exo*-hydroxybornane-10-sulfonamide **319** (1.10 g, 3.0 mmol) and acryloyl chloride (0.56 g, 6.2 mmol). Work-up and purification [HPLC; elution with hexane-EtOAc (8:2)] afforded two products:

N-(1-adamantyl)-2-*exo*-acryloyloxybornane-10-sulfonamide **321**, as transparent crystals, (0.80 g, 63.2 %) (Found: M⁺, 421.22844. C₂₃H₃₅NO₄S requires *M*, 421.22868); [α]_D²⁰ = -51.26° (*c* 4.06, CHCl₃); δ_H (400 MHz; CDCl₃) 0.89 and 1.02 (6H, 2 × s, 8- and 9-Me), 1.18, 1.59, 1.75, 1.99 (6H, series of multiplets, 3-, 5- and 6-CH₂), 1.61 and 1.90 (12H, 2 × m, 12-,14-, 16-, 17-, 19- and 20-CH₂), 1.77 (1H, m, 4-H), 2.05 (3H, m,13-, 15- and 18-CH), 2.90 and 3.54 (2H, 2 × d, *J* 13.9 Hz, 10-CH₂), 4.11 (1H, s, NH), 5.03 (1H, m, 2-CH), 5.77 (1H, dd, *J* 1.0 and 10.4 Hz, 3'-H_E), 6.08 (1H, dd, *J* 10.4 and 17.3 Hz, 2'-H) and 6.33 (1H, dd, *J* 1.0 and 17.3 Hz, 3'-H_E); δ_C (100 MHz; CDCl₃) 20.0 and 20.4 (C-8 and C-9), 27.0, 29.9 and 39.5 (C-3, C-5 and C-6), 29.6 (C-13, C-15 and C-18), 35.9 (C-14, C-19 and C-20), 43.2 (C-12, C-16 and C-17), 44.4 (C-4), 49.3 and 49.5 (C-1 and C-7), 55.1 (C-11), 55.3 (C-10), 78.0 (C-2), 129.0

(C-2'), 130.0 (C-3') and 164.6 (C-1'); m/z 421 (M^+ , 2.8 %) and 135 (100); and *N*-(1-adamantyl)-2-*exo*-(3-chloropropanoyloxy)bornane-10-sulfonamide **320**, as transparent crystals, (0.48 g, 35.0 %) (Found: M^+ , 457.21058. $C_{23}H_{36}NO_4S$ requires M , 457.20536); $[\alpha]_D^{20} = -13.64^\circ$ (c 0.22, $CHCl_3$); δ_H (400 MHz; $CDCl_3$) 0.89 and 1.01 (6H, $2 \times s$, 8- and 9-Me), 1.16 -2.02 (6H, series of multiplets, 3-,5- and 6- CH_2), 1.66 and 1.94 (12H, $2 \times m$, 12-, 14-, 16-, 17-, 19- and 20- CH_2), 1.78 (1H, m, 4-H), 2.10 (3H, m, 13-, 15- and 18-CH), 2.77 (2H, t, J 6.8 Hz, 2'- CH_2), 3.21 (2H, $2 \times d$, J 13.9 Hz, 10- CH_2), 3.74 (2H, m, J 6.9 and 16.5 Hz, 3'- CH_2), 4.00 (1H, s, NH) and 4.99 (1H, dd, J 2.4 and 7.8 Hz, 2-CH); δ_C (100 MHz; $CDCl_3$) 20.0 and 20.4 (C-8 and C-9), 27.1, 30.1 and 39.5 (C-3, C-5 and C-6), 29.6 (C-13, C-15 and C-18), 35.9 and 43.4 (C-12, C-14, C-16, C-17, C-19 and C-20), 37.9 (C-2'), 39.2 (C-3'), 44.4 (C-4), 49.3 and 49.4 (C-1 and C-7), 55.1 (C-11), 55.5 (C-10), 78.7 (C-2) and 168.8 (C-1'); m/z 457 (M^+ , 3.3 %) and 135 (100).

Method 2:

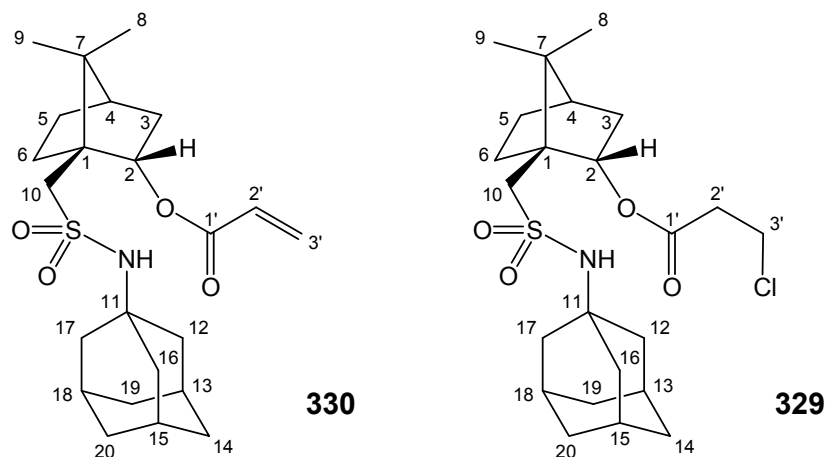
Triethylamine (0.32 g, 3.1 mmol) was added to a mixture of *N*-(1-adamantyl)-2-*exo*-acryloyloxybornane-10-sulfonamide **321** and *N*-(1-adamantyl)-2-*exo*-(3-chloropropanoyloxy)bornane-10-sulfonamide **320** [1.68 g (0.80 g, 1.7 mmol of **320**)]. The reaction mixture was stored under N_2 and stirred at 25 °C for 1 h and then taken up in EtOAc (5 mL), washed with brine and dried over anhydrous $MgSO_4$. Solvent was removed *in vacuo* to give transparent crystals of:

N-(1-adamantyl)-2-*exo*-acryloyloxybornane-10-sulfonamide **321** (0.67 g, 92.1 %).

Attempted Synthesis:

The experimental procedure employed for the synthesis of phenyl 2-*exo*-acryloyloxybornane-10-sulfonate **296** (Method 2) was followed, using *N*-(1-adamantyl)-2-*exo*-hydroxybornane-10-sulfonamide **319** (0.21 g, 0.6 mmol) in dry THF (8 mL) at -78 °C, butyllithium (1.6 M solution in hexane; 0.43 mL, 0.7 mmol) and acryloyl chloride (0.11 g, 1.2 mmol). Work-up was followed by 1H NMR analysis which failed to show any change in the starting material.

N-(1-Adamantyl)-2-endo-acryloyloxybornane-10-sulfonamide **330** and *N*-(1-adamantyl)-2-endo-(3-chloropropanoyloxy)bornane-10-sulfonamide **329**



Method 1:

The experimental procedure employed for the synthesis of phenyl 2-*exo*-acryloyloxybornane-10-sulfonate **296** and phenyl 2-*exo*-(3-chloropropanoyloxy)bornane-10-sulfonate **308** (**Method 1**) was followed, using neutral Al₂O₃ (0.08 g, 0.8 mmol), *N*-(1-adamantyl)-2-*endo*-hydroxybornane-10-sulfonamide **328** (0.19 g, 0.5 mmol) and acryloyl chloride (0.16 g, 1.8 mmol). Work-up and purification [HPLC; elution with hexane-EtOAc (8:2)] afforded two products, as white crystals:

N-(1-adamantyl)-2-*endo*-acryloyloxybornane-10-sulfonamide **330** (0.15 g, 67.1 %) (Found: M^+ , 421.22485. C₂₃H₃₅NO₄S requires M , 421.22868); $[\alpha]_D^{20} = -32.50^\circ$ (c 1.24, CHCl₃); δ_H (400 MHz; CDCl₃) 0.93 and 0.97 (6H, 2 × s, 8- and 9-Me), 1.08, 1.36, 1.68, 1.84, 2.49 and 2.57 (6H, series of multiplets, 3-, 5- and 6-CH₂), 1.63 and 1.90 (12H, 2 × m, 12-, 14-, 16-, 17-, 19- and 20-CH₂), 1.72 (1H, m, 4-H), 2.07 (3H, m, 13-, 15- and 18-CH), 3.10 and 3.14 (2H, 2 × d, J 14.3 Hz, 10-CH₂), 3.97 (1H, s, NH), 5.23 (1H, d, J 9.6 Hz, 2-H), 5.85 (1H, dd, J 1.0 and 10.4 Hz, 3'-H_Z), 6.14 (1H, dd, J 10.5 and 17.4 Hz, 2'-H) and 6.46 (1H, dd, J 1.0 and 17.3 Hz, 3'-H_E); δ_C (100 MHz; CDCl₃) 19.2 and 19.9 (C-8 and C-9), 25.6, 28.0 and 37.7 (C-3, C-5 and C-6), 29.6 (C-13, C-15 and C-18), 35.9 (C-14, C-19 and C-20), 43.3 (C-12, C-16 and C-17), 44.0 (C-4), 50.2 and 50.6 (C-1 and C-7), 55.0 (C-11), 59.6 (C-10), 77.3 (C-2), 128.9 (C-2'), 130.9 (C-3') and 165.9 (C-1'); m/z 421 (M^+ , 4.2 %) and 135 (100); and

N-(1-adamantyl)-2-*endo*-(3-chloropropanoyloxy)bornane-10-sulfonamide **329** (0.07 g, 30.7%) (Found: M^+ , 457.21295. C₂₃H₃₆NO₄Cl requires M , 457.20536); $[\alpha]_D^{20} = +24.52^\circ$ (c 0.42, CHCl₃); δ_H (400 MHz; CDCl₃) 0.92 and 0.95 (6H, 2 × s, 8- and 9-Me), 1.08, 1.36, 1.65, 1.85, 2.45 and 2.49 (6H, series of multiplets, 3-, 5- and 6-CH₂), 1.65 and 1.92 (12H, 2 × m,

12-, 14-, 16-, 17-, 19- and 20-CH₂), 1.73 (1H, m, 4-H), 2.10 (3H, m, 13-, 15- and 18-CH), 2.84 (2H, dd, *J* 6.8 and 12.3 Hz, 2'-CH₂), 3.06 and 3.14 (2H, 2 × d, *J* 14.0 Hz, 10-CH₂), 3.79 (2H, t, *J* 6.9 Hz, 3'-CH₂), 4.07 (1H, s, NH) and 5.26 (1H, d, *J* 9.7 Hz, 2-CH); δ_C (100 MHz; CDCl₃) 19.2 and 19.9 (C-8 and C-9), 25.5, 28.0 and 37.5 (C-3, C-5 and C-6), 29.6 (C-13, C-15 and C-18), 35.9 and 43.3 (C-12, C-14, C-16, C-17, C-19 and C-20), 37.9 (C-2'), 39.3 (C-3'), 43.9 (C-4), 50.3 and 50.7 (C-1 and C-7), 55.0 (C-11), 59.9 (C-10), 77.2 (C-2) and 170.2 (C-1'); *m/z* 457 (M⁺, 3.68 %) and 135 (100).

Method 2:

The experimental procedure employed for the synthesis of *N*-(1-adamantyl)-2-*exo*-acryloyloxybornane-10-sulfonamide **321** (Method 2) was followed, using triethylamine (0.01 g, 0.1 mmol) and a mixture of *N*-(1-adamantyl)-2-*endo*-acryloyloxybornane-10-sulfonamide **330** and *N*-(1-adamantyl)-2-*endo*-(3-chloropropanoyloxy)bornane-10-sulfonamide **329** [0.50 g (0.04g, 0.08 mmol of **329**)]. Workup afforded *N*-(1-adamantyl)-2-*endo*-acryloyloxybornane-10-sulfonamide **330** (0.03 g, 79.7 %).

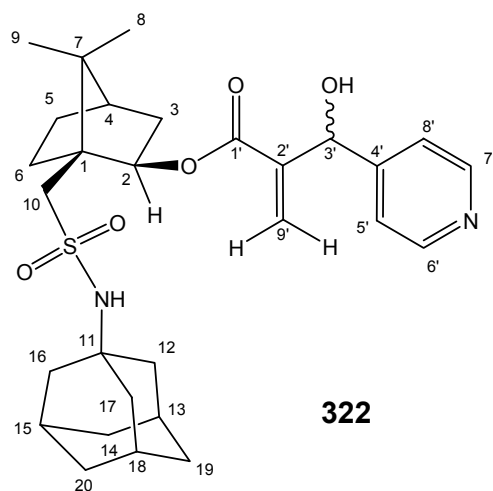
Attempted Synthesis:

The experimental procedure employed for the synthesis of phenyl 2-*exo*-acryloyloxybornane-10-sulfonate **296** (Method 2) was followed, using *N*-(1-adamantyl)-2-*endo*-hydroxybornane-10-sulfonamide **328** (0.15 g, 0.4 mmol) in dry THF (6 mL) at -78 °C, butyllithium (1.6 M solution in hexane; 0.30 mL, 0.5 mmol) and acryloyl chloride (0.07 g, 0.8 mmol). Work-up was followed by ¹H NMR analysis which failed to show any change in the starting material.

3.2.6 Morita-Baylis-Hillman Products from *N*-(1-adamantyl)-2-*exo*-acryloyloxybornane-10-sulfonamide

The reactions in this series were essentially complete; thus, the crude yield as determined from NMR analysis was considered an adequate assessment of the chemical transformation in each reaction. The diastereomeric excess (% d.e.) was determined from the integral ratios of several signals (typically 3'-H, 9'-CH₂ and 8- and 9-Me) for the diastereomeric components. Separation of diastereomeric products was not attempted thus NMR data for both isomers are reported together.

Morita-Baylis-Hillman products 322A and 322B

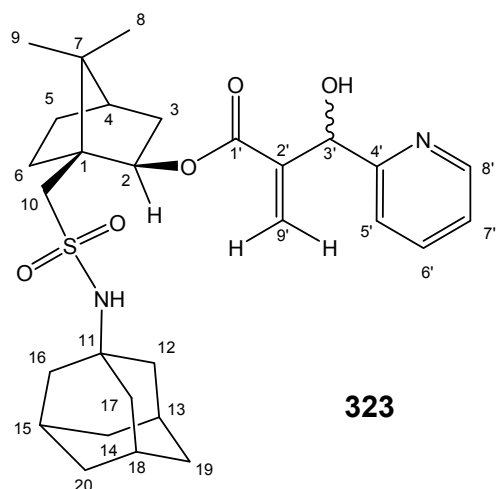


To a solution of *N*-(1-adamantyl)-2-*exo*-acryloyloxybornane-10-sulfonamide **321** (0.10 g, 0.24 mmol) in CDCl₃ (0.40 mL) was added pyridine-4-carbaldehyde (0.03 g, 0.27 mmol), and DABCO (0.003 g, 0.02 mmol). The solution was stirred at room temperature for 90 h then concentrated *in vacuo*. The residue was purified by washing with a minimal amount of cold Et₂O to afford a mixture of the diastereomeric compounds:

Morita-Baylis-Hillman products 322A and 322B (93 %, 38 % d.e.); δ_{H} (400 MHz; CDCl₃) 0.80/0.88 and 0.84/0.97 (6H, 2 \times s, 8- and 9-Me), 1.14 – 1.232 and 1.68 – 1.79 (2H, complex of multiplets, 5-CH₂), 1.52 – 1.65 and 1.92 – 1.99 (2H, complex of multiplets, 6-CH₂), 1.57 – 1.67 (6H, complex of multiplets, 14-, 19- and 20-CH₂), 1.62 – 1.69 and 1.93 – 1.99 (2H, complexes of multiplets, 3-CH₂), 1.73 – 1.78 (1H, m, 4-H), 1.86 – 1.94 (6H, complexes of multiplets, 12-, 16- and 17-CH₂), 2.05 (3H, br m, 13-, 15- and 18-H), 2.87 and 3.35/2.92 and 3.46 (2H, 2 \times d, *J* 13.9 Hz, 10-CH₂), 4.27 (1H, s, NH), 5.01/5.05 (1H, dd, *J* 3.2 and 7.9 Hz, 2-H), 5.02 (1H, br s, 3'-OH), 5.52/5.57 (1H, s, 3'-H), 5.93/5.99 (2H, 2 \times s, 9'-CH₂), 7.33 (2H, t,

J 6.3 Hz, 5'- and 8'-H), 8.54/8.55 (2H, s, 6'- and 7'-H); δ_C (100 MHz; $CDCl_3$) 19.6/19.9 and 20.2/20.3 (C-8 and C-9), 27.1/27.0 (C-5), 29.57/29.58 (C-13, C-15 and C-18), 30.2/30.8 (C-6), 35.88/35.90 (C-14, C-19 and 20), 39.4/39.6 (C-3), 43.3/43.4 (C-12, C-16 and C-17), 44.3/44.9 (C-4), 49.2/49.3 and 49.6/49.7 (C-1 and C-7), 55.2/55.7 (C-10), 55.7/55.7 (C-11), 71.6/72.4 (C-3'), 79.07/79.19 (C-2), 121.33/121.55 (C-5' and C-8'), 127.14/127.42 (C-9'), 141.70/142.19 (C-2'), 149.69/149.70 (C-6' and C-7'), 150.35/150.67 (C-4') and 164.78/164.81 (C-1');

Morita-Baylis-Hillman products 323A and 323B

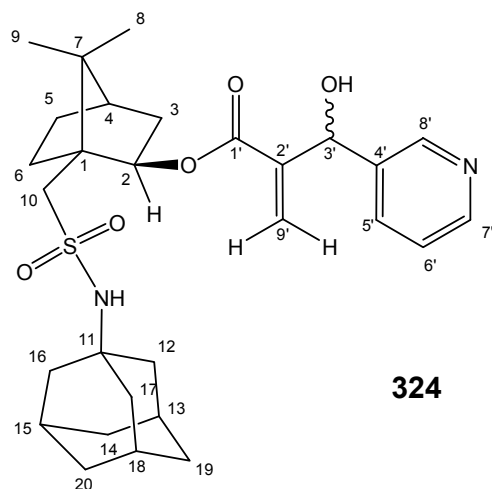


The experimental procedure employed for the synthesis of the Morita-Baylis-Hillman products **322A** and **322B** was followed, using *N*-(1-adamantyl)-2-*exo*-acryloyloxybornane-10-sulfonamide **321** (0.10 g, 0.24 mmol) in $CDCl_3$ (0.40 mL), pyridine-2-carbaldehyde (0.03 g, 0.26 mmol), and DABCO (0.003 g, 0.02 mmol). Work-up afforded the diastereomeric compounds:

Morita-Baylis-Hillman products 323A and 323B (99 %; 22 % d.e.); δ_H (400 MHz; $CDCl_3$) 0.66/0.88 and 0.82/1.01 (6H, 2 \times s, 8- and 9-Me), 1.13 – 1.26 and 1.40 – 2.12 (22H, complexes of multiplets, 3-, 5-, 6-, 13-, 14-, 15-, 18-, 19- and 20- CH_2 , 4-, 12-, 16- and 17-CH), 1.59 (1H, m, 4-H), 2.82/2.85 and 3.46/3.49 (2H, 2 \times d, J 14.1/13.8 Hz, 10- CH_2), 4.44/4.13 (1H, s, NH), 4.98/5.07 (1H, br s, 3'-OH), 5.02/ 5.10 (1H, dd, J 3.5/2.9 and 7.9/7.9 Hz, 2-H), 5.54/5.71 (1H, s, 3'-H), 5.90 and 6.36/5.80 and 6.23 (2H, 2 \times s, 9'- CH_2), 7.17 - 7.23 (1H, m, 7'-H), 7.41 /7.47 (1H, d, J 7.8/8.0 Hz, 5'-H), 7.65 - 7.70 (1H, complex of multiplets, 6'-H), 8.55 /8.50 (1H, d, J 4.7 Hz, 8'H); δ_C (100 MHz; $CDCl_3$) 19.5/20.0 and 20.4/20.3 (C-8 and C-9), 27.0/27.1 (C-5), 29.5/29.7 (C-13, C-15 and C-18), 35.7/35.8 (C-6), 35.8/36.0 (C-14, C-19 and C-20), 39.3/39.41 (C-3), 43.3/43.4 (C-12, C-16 and C-17), 44.3/44.5 (C-4),

49.2/49.5 and 49.3/49.6 (C-1 and C-7), 55.0/55.3 (C-10), 55.1/55.3 (C-11), 70.9/73.0 (C-3'), 79.0/78.7 (C-2), 120.9/121.7 (C-5'), 122.65/122.68 (C-7'), 125.6/128.0 (C-9'), 137.0/137.1 (C-6'), 142.9/143.1 (C-2'), 147.8/148.2 (C-8'), 151.8/152.0 (C-4'), 169.3/169.9 (C-1');

Morita-Baylis-Hillman products 324A and 324B

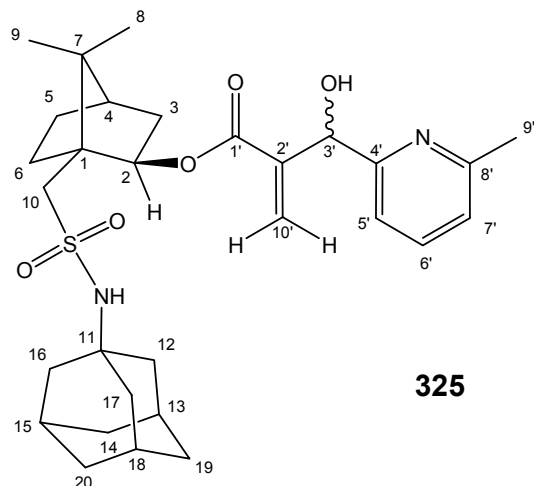


The experimental procedure employed for the synthesis of the Morita-Baylis-Hillman products **322A** and **322B** was followed, using *N*-(1-adamantyl)-2-*exo*-acryloyloxybornane-10-sulfonamide **321** (0.10 g, 0.24 mmol) in CDCl₃ (0.40 mL), pyridine-3-carbaldehyde (0.03 g, 0.26 mmol), and DABCO (0.003 g, 0.03 mmol). Work-up afforded the diastereomeric compounds:

Morita-Baylis-Hillman products 324A and 324B (93 %, 60 % d.e.); δ_{H} (400 MHz; CDCl₃) 0.86/0.88 and 0.89/0.96 (6H, 2 × s, 8- and 9-Me), 1.14 – 1.25 and 1.70 – 1.78 (2H, complex of multiplets, 5-CH₂), 1.56 -1.64 and 1.90 – 1.97 (2H, complex of multiplets, 6-CH₂), 1.64 (6H, br s, 14-, 19- and 20 CH₂), 1.67 – 1.75 (2H, complex of multiplets, 3-CH₂), 1.75/1.77 (1H, d, *J* 3.3/3.9 Hz, 4-H), 1.91/1.92 (6H, br s, 13-, 15- and 18-CH₂), 2.06 (3H, br s, 12- 16- and 17-CH), 2.85/2.90 and 3.30/3.41 (2H, 2 × d, *J* 13.8/13.8 Hz, 10-CH₂), 4.31/4.45 (1H, s, NH), 5.04 - 5.08 (1H, m, 2-H), 5.05 (br s, 3'-OH), 5.57/5.63 (1H, s, 3'-H), 5.75/5.63 and 6.27/6.27 (2H, 2 × s, 9'-CH₂), 7.27/7.29 (1H, d, *J* 4.8/4.8 Hz, 6'-CH), 7.73 - 7.77 (1H, m, 5'-CH), 8.50 - 8.53 (1H, m, 7'-CH), 8.59/ 8.58 (1H, d, *J* 2.1/1.9 Hz, 8'-CH); δ_{C} (100 MHz; CDCl₃) 19.9/20.0 and 20.3/20.3 (C-8 and C-9), 26.99/27.03 (C-5), 29.6 (C-14, C-19 and C-20), 30.1/30.2 (C-6), 35.9 (C-13, C-15 and C-18), 39.36/39.42 (C-3), 43.4 (C-12, C-16 and C-17), 44.3/44.4 (C-4), 49.25/49.32 and 49.6/49.7 (C-1 and C-7), 54.87/54.89 (C-11), 55.2/55.7 (C-10), 71.0/71.7 (C-3'), 78.9/79.0 (C-2), 123.38/123.42 (C-6'), 126.3/126.4 (C-9'),

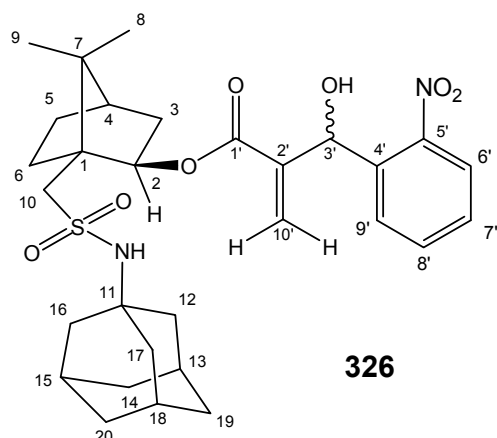
134.3/134.5 (C-5'), 142.9/142.5 (C-2'), 148.3/148.5 (C-8'), 148.9/149.1 (C-7'), 1.49.2/150.0 (C-4') and 164.8/164.9 (C-1');

Morita-Baylis-Hillman products 325A and 325B



The experimental procedure employed for the synthesis of the Morita-Baylis-Hillman products **322A** and **322B** was followed, using *N*-(1-adamantyl)-2-*exo*-acryloyloxybornane-10-sulfonamide **321** (0.10 g, 0.25 mmol) in CDCl₃ (0.40 mL), 6-methylpyridine-2-carbaldehyde (0.03 g, 0.27 mmol), and DABCO (0.004 g, 0.03 mmol). Work-up afforded the diastereomeric compounds:

Morita-Baylis-Hillman products 325A and 325B (98 %, 95 % d.e.); δ_{H} (400 MHz; CDCl₃) 0.88 and 1.01 (6H, 2 × s, 8- and 9-Me), 1.20 - 1.24 and 1.72 - 1.80 (2H, multiplet of multiplets, 5-CH₂), 1.41 and 1.53 (6H, 2 × d, *J* 12.1 Hz, 14-, 19- and 20-CH₂), 1.58 - 1.66 and 1.95 - 2.01 (2H, multiplet of multiplets, 6-CH₂), 1.76 - 1.92 and 1.97 - 2.05 (2H, complex of multiplets, 3-CH₂), 1.79 (1H, m, 4-H), 1.80 (6H, br s, 12-, 16- and 17-CH₂), 1.92 (3H, br s, 13-, 15- 18-CH), 2.52 (3H, s, 9'-Me), 2.84 and 3.50 (2H, 2 × d, *J* 13.9 Hz, 10-CH₂), 4.17 (1H, s, NH), 5.11 (1H, dd, *J* 3.0 Hz, *J* 7.9 Hz, 2-H), 5.49 (1H, br s, OH), 5.68 (1H, s, 3'-H), 5.79 and 6.22 (2H, 2 × s, 10'-CH₂), 7.03 (1H, d, *J* 7.6 Hz, 7'-H), 7.22 (1H, d, *J* 7.8 Hz, 5'-H) and 7.55 (1H, t, *J* 7.7 Hz, 6'-H); δ_{C} (100 MHz; CDCl₃) 20.0 and 20.4 (C-8 and C-9), 24.2 (C-9'), 27.1 (C-5), 29.5 (C-13, C-15 and C-18), 30.0 (C-6), 35.8 (C-14, C-19 and C-20), 39.4 (C-3), 43.2 (C-12, C-16 and C-17), 44.4 (C-4), 49.3 and 49.6 (C-1 and C-7), 55.0 (C-11), 55.2 (C-10), 70.2 (C-3'), 78.7 (C-2), 118.6 (C-7'), 122.1 (C-5'), 125.4 (C-10'), 137.4 (C-6'), 143.2 (C-2'), 156.6 (C-4'), 157.9 (C-8') and 165.1 (C-1');

Morita-Baylis-Hillman products 326A and 326B

The experimental procedure employed for the synthesis of the Morita-Baylis-Hillman products **322A** and **322B** was followed, using *N*-(1-adamantyl)-2-*exo*-acryloyloxybornane-10-sulfonamide **321** (0.10 g, 0.24 mmol) in CDCl₃ (0.40 mL), 2-nitrobenzaldehyde (0.04 g, 0.27 mmol), and DABCO (0.003 g, 0.03 mmol). Work-up afforded the diastereomeric compounds: *Morita-Baylis-Hillman* products **326A** and **326B**; (89 %, 52 % d.e.); δ_{H} (400 MHz; CDCl₃) 0.87/0.88 and 0.91/1.00 (6H, 2 × s, 8- and 9-Me), 1.14 – 1.28 and 1.55 – 2.12 (6H, complex of multiplets, 3-, 5- and 6-CH₂), 1.65/1.64 (6H, br s, 14-, 19- and 20-CH₂), 1.91/1.92 (1H, m, 4-H), 1.96/1.95 (6H, br s, 12-, 16- and 17-CH₂), 2.09 (3H, br s, 13-, 15- and 18-CH), 2.94/2.86 and 3.36/3.47 (2H, 2 × d, *J* 13.9/13.9 Hz, 10-CH₂), 4.31/4.20 (1H, s, NH), 4.99 - 5.04/5.09 – 5.13 (1H, m, 2-H), 5.05 (1H, br s, 3'-OH), 5.47/5.48 and 6.28/6.22 (2H, 2 × s, 10'-CH₂), 6.22/6.19 (1H, s, 3'-H), 7.43 – 7.49 (1H, m, 7'-H), 7.63 - 7.69 (1H, m, 9'-H), 7.72 - 7.96 (1H, m, 8'-H) and 8.00/8.11 (1H, dd, *J* 1.2/1.4 Hz, *J* 8.2/7.9 Hz, 6'-H); δ_{C} (100 MHz; CDCl₃) 19.7/19.9 and 20.29/20.31 (C-8 and C-9), 27.04/26.97 (C-6), 29.64/29.61 (C-13, C-15 and C-18), 30.3/30.0 (C-5), 35.9 (C-14, C-19 and C-20), 39.4/39.3 (C-3), 43.33/43.25 (C-12, C-16 and C-17), 44.37/44.41 (C-4), 49.29/49.19 and 49.31/49.78 (C-1 and C-7), 55.27/56.13 (C-10), 55.27/56.08 (C-11), 67.7/68.5 (C-3'), 79.1/78.7 (C-2), 124.9/126.0 (C-6'), 128.7/128.6 (C-10'), 129.0/128.9 (C-9'), 133.8/133.6 (C-7'), 134.0/134.1 (C-8'), 136.5/136.3 (C-4'), 142.0/141.5 (C-2'), 164.7/164.4 (C-5') and 171.5/171.6 (C-1');

Attempted Synthesis of Morita-Baylis-Hillman products 327A and 327B

The experimental procedure employed for the synthesis of the Morita-Baylis-Hillman products **322A** and **322B** was followed, using *N*-(1-adamantyl)-2-*exo*-acryloyloxybornane-10-sulfonamide **321** (0.10 g, 0.24 mmol) in CDCl₃ (0.40 mL), pivaldehyde (0.02 g, 0.26 mmol), and DABCO (0.003 g, 0.03 mmol). Work-up afforded the starting material **321**.

3.3 NMR KINETIC STUDY

This study focused on the transesterification of the hydroxybornanyl acrylates **285** and **287** in various media and under different reaction conditions. Complete data sets, together with graphical charts, can be found in **Appendix II** on CD. In the following section, the experimental details, plots of the integral ratios and the natural logarithm of the integral ratios as a function of time are presented for each of the reactions **A1 – G4**.

3.3.1. General Purification, Spectroscopic Techniques and Calculations

A mixture (*ca.* 1g) of the hydroxybornanyl acrylates, 2-*exo*-hydroxy-3-*exo*-bornanyl acrylate **285** and 3-*exo*-hydroxy-2-*exo*-bornanyl acrylate **287** was subjected to HPLC separation [staggered multiple injections at 10 min intervals, each injection consisting of *ca.* 30 mg sample in 200 μ L of solvent; elution with hexane-EtOAc (7:3); approximate retention times: **285**: 12.5 min and **287**: 16.5 min]. The solutions of the pure compounds were immediately stored at -78 °C (dry ice-acetone mixture) to minimize the possibility of transesterification. The solvent was removed from each fraction under reduced pressure and the pure compounds were stored under N₂ at -78 °C. Aliquots (0.5 mL) of solutions of **285** or **287** in deuterated solvent were used for NMR spectroscopic analysis. Each aliquot was injected into a clean, dry, N₂-flushed NMR tube. The NMR tube was inserted into the NMR spectrometer, its temperature was allowed to warm to that of the probe (*ca.* 5 min) and the instrument was then shimmed. Data acquisition was achieved using an automated programme to obtain individual spectra at regular time intervals. After a suitable number of data sets had been collected, the kinetic run was terminated and the data analyzed. Reactions were monitored over a range of temperatures in order to obtain data for the calculation of kinetic and thermodynamic parameters. The precision and accuracy of the spectrometer temperature setting was judged to be ± 0.5 K. In order to obtain the final equilibrium concentrations, the samples, in sealed NMR tubes, were placed in constant temperature (± 0.5 K) water baths for periods of seven to thirty days, and monitored by NMR spectroscopy at random time intervals until the product ratios were constant. Ratios of the hydroxybornanyl acrylates were obtained by comparing the integrals of selected signals. For convenience and accuracy, the 2-H_{endo} and 3-H_{endo} signals of both compounds were chosen for comparison, as they are characteristic for each isomer and are completely unobscured by other proton signals (**Tables 3.1, 3.2 and 3.3**).

Table 3.1: 400 MHz ^1H NMR data for comparison of the isomeric esters, 2-*exo*-hydroxy-3-*exo*-bornanyl acrylate **285** and 3-*exo*-hydroxy-2-*exo*-bornanyl acrylate **287**, in unpurified CDCl_3 at 303 K.

	285		287	
Proton assignment	2- H_{endo}	3- H_{endo}	3- H_{endo}	2- H_{endo}
Chemical shift, δ_{H} (ppm)	3.76	4.64	4.02	4.58
Multiplicity	d	d	d	d
Coupling Constants, J (Hz)	6.8	6.8	6.7	6.7

Table 3.2: 400 MHz ^1H NMR data for comparison of the isomeric esters, 2-*exo*-hydroxy-3-*exo*-bornanyl acrylate **285** and 3-*exo*-hydroxy-2-*exo*-bornanyl acrylate **287**, in purified CDCl_3 at 303 K.

	285		287	
Proton assignment	2- H_{endo}	3- H_{endo}	3- H_{endo}	2- H_{endo}
Chemical shift, δ_{H} (ppm)	3.81	4.68	4.02	4.54
Multiplicity	dd	d	dd	d
Coupling Constants, J (Hz)	5.2; 6.2	6.8	3.7; 6.2	6.7

Table 3.3: 400 MHz ^1H NMR data for comparison of the isomeric esters, 2-*exo*-hydroxy-3-*exo*-bornanyl acrylate **285** and 3-*exo*-hydroxy-2-*exo*-bornanyl acrylate **287**, in purified $\text{DMSO}-d_6$ at 303 K.

	285			287		
Proton assignment	2- H_{endo}	3- H_{endo}	2-OH	3- H_{endo}	2- H_{endo}	3-OH
Chemical shift, δ_{H} (ppm)	3.59	4.65	4.97	3.79	4.53	4.87
Multiplicity	dd	d	d	dd	d	d
Coupling Constants, J (Hz)	2.2; 6.4	6.8	6.0	5.1; 6.6	6.7	5.0

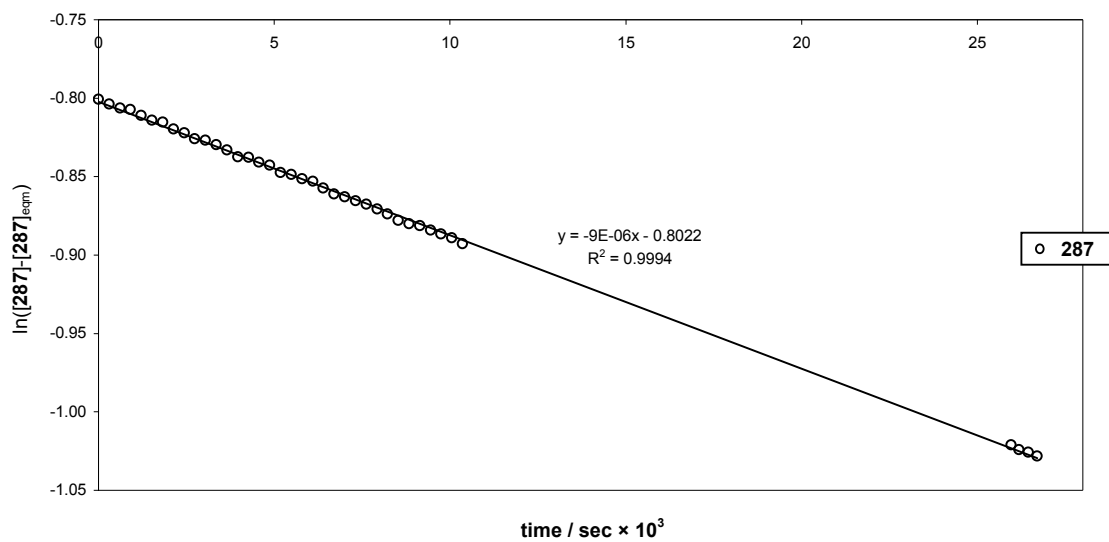
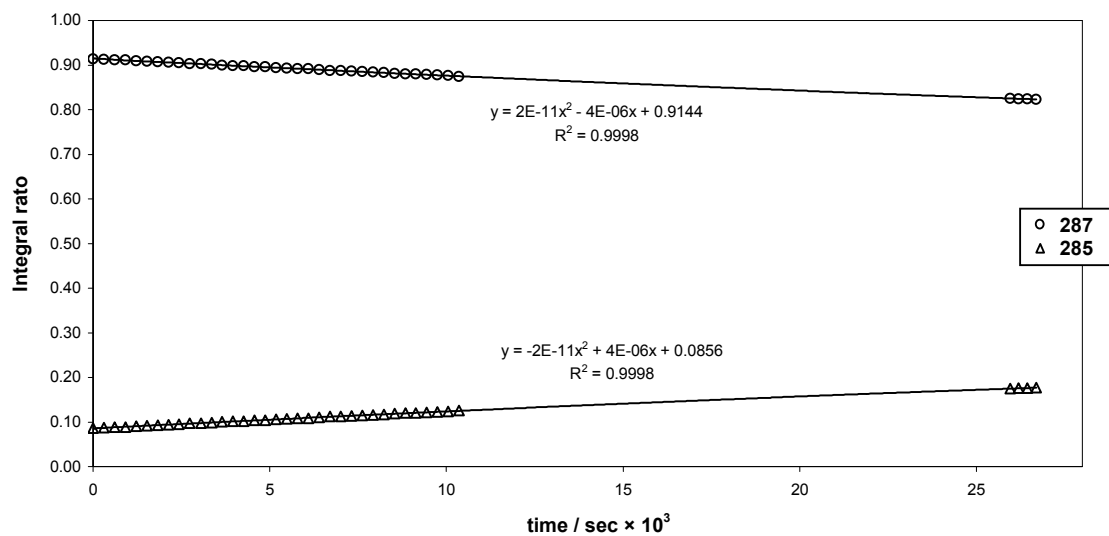
Following the automated processing of the integrals of the 2- H_{endo} and 3- H_{endo} signals for both compounds, the data were used to determine the relative concentrations. In each set of experiments, the mathematical relationships described in detail in the Discussion (**Section 2.3.2.1**) were used to calculate kinetic and thermodynamic parameters for both forward and reverse reactions.

3.3.2 Reactions in Unpurified CDCl₃

The acrylate ester, 3-*exo*-hydroxy-2-*exo*-bornanyl acrylate **287** (0.1316 g, 0.59 mmol) was transferred to a dry 5 mL volumetric flask. Unpurified CDCl₃ was added and the volume made up to 5 mL to give a concentration of 0.117 mol L⁻¹. Aliquots of 0.50 mL were removed from the flask and immediately used for NMR spectroscopic analyses at temperatures ranging from 301 to 323 K. A solution of the isomeric ester, 2-*exo*-hydroxy-3-*exo*-bornanyl acrylate **285** (0.0153 g, 0.068 mmol) in 0.50 mL of unpurified CDCl₃ was used similarly.

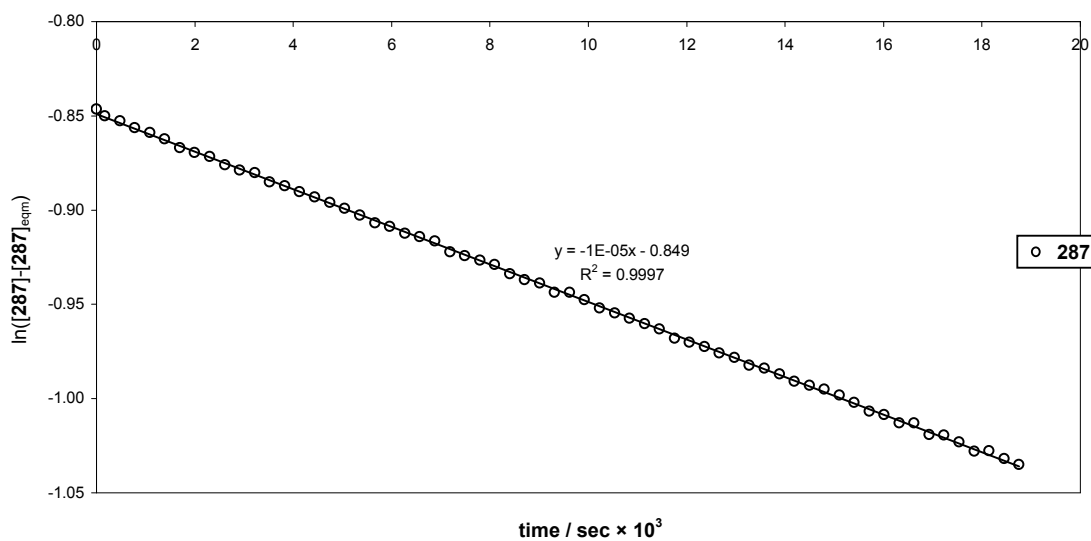
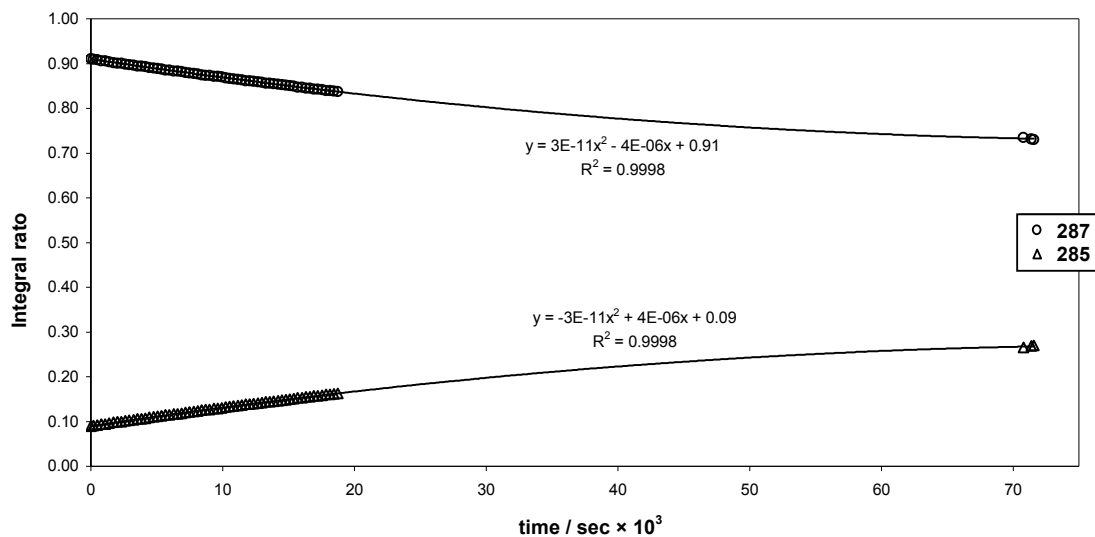
Experiment A1: Equilibration of 3-*exo*-hydroxy-2-*exo*-bornanyl acrylate **287** in unpurified CDCl_3 at **301 K**.

T/K	Mass/g	Conc. /mol L ⁻¹	[287] _{eqm}	[285] _{eqm}	k_{-1}/k_{+1}	$k_{+1}+k_{-1}$	k_{-1}	k_{+1}
301	0.0132	0.117	0.465	0.535	1.15	5.68E-06	2.64E-06	3.04E-06



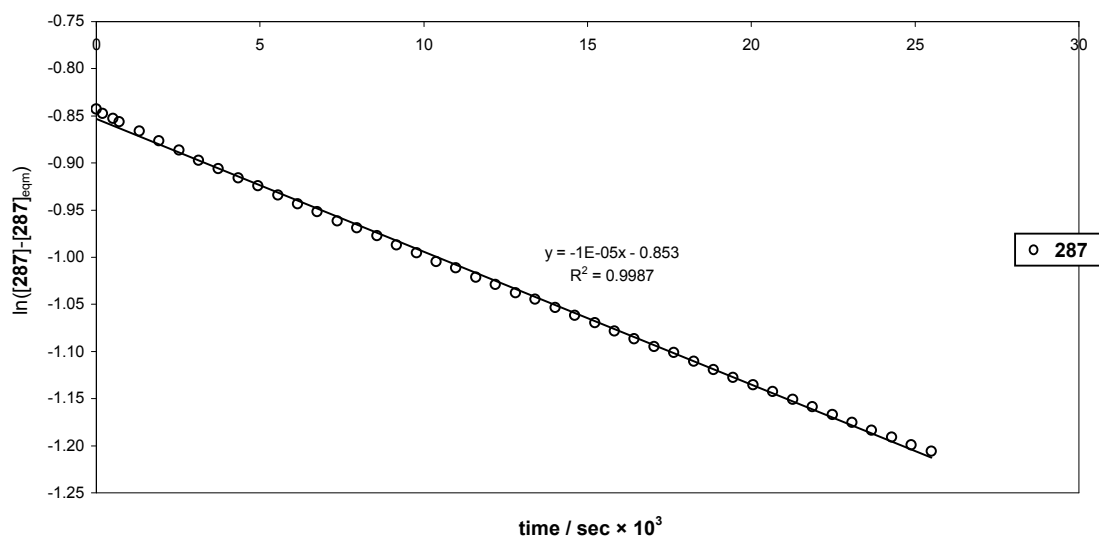
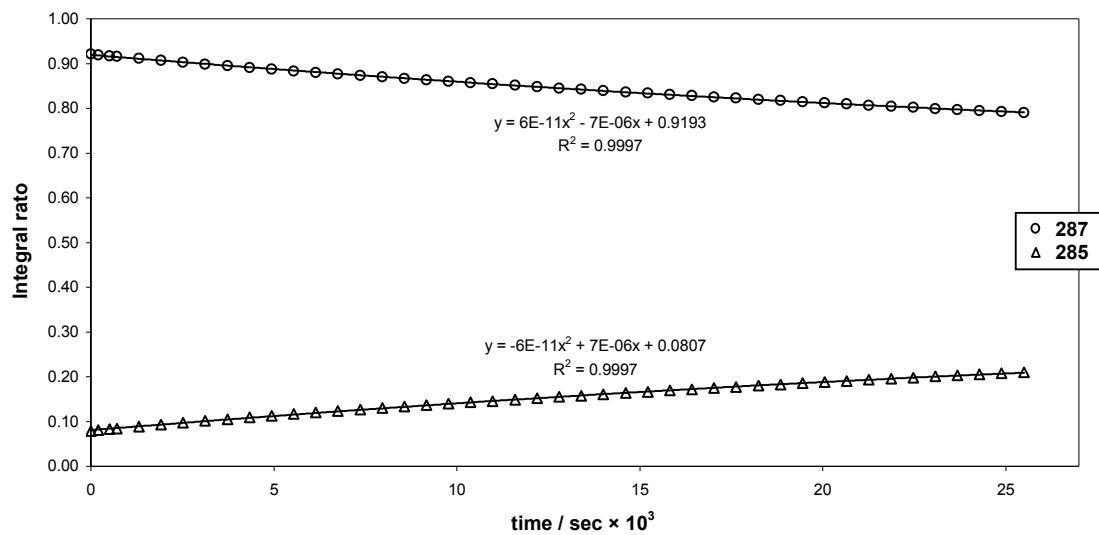
Experiment A2: Equilibration of 3-*exo*-hydroxy-2-*exo*-bornanyl acrylate **287** in unpurified CDCl_3 at **307 K**.

T/K	Mass/g	Conc. /mol L ⁻¹	[287] _{eqm}	[285] _{eqm}	k_1/k_{+1}	$k_{+1}+k_1$	k_1	k_{+1}
307	0.0132	0.117	0.482	0.518	1.08	9.96E-06	4.80E-06	5.16E-06



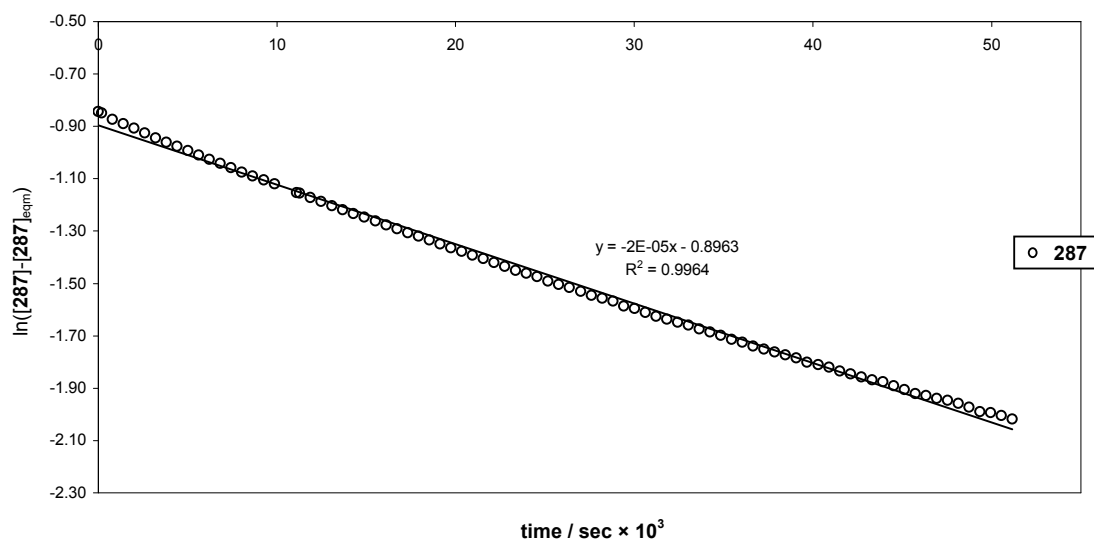
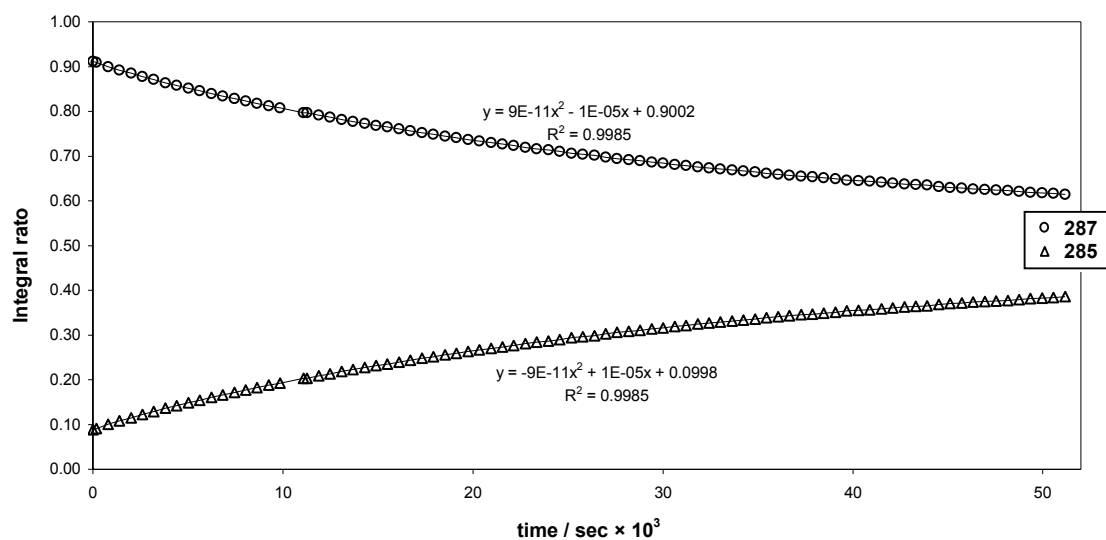
Experiment A3: Equilibration of 3-*exo*-hydroxy-2-*exo*-bornanyl acrylate **287** in unpurified CDCl₃ at 313 K.

T/K	Mass/g	Conc./mol L ⁻¹	[287] _{eqm}	[285] _{eqm}	k_{-1}/k_{+1}	$k_{+1}+k_{-1}$	k_{-1}	k_{+1}
313	0.0132	0.117	0.491	0.509	1.04	1.41E-05	6.92E-06	7.18E-06



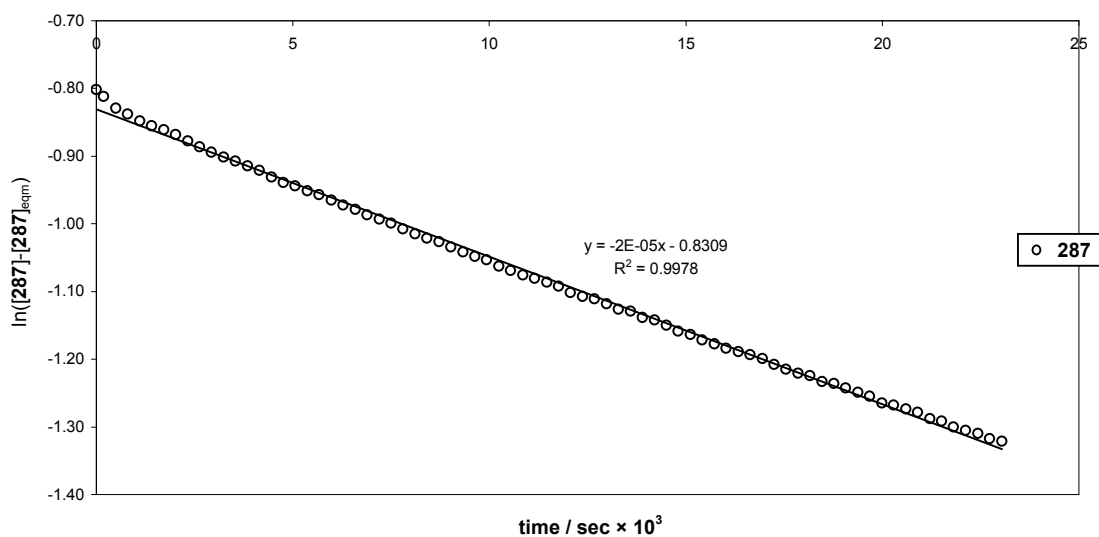
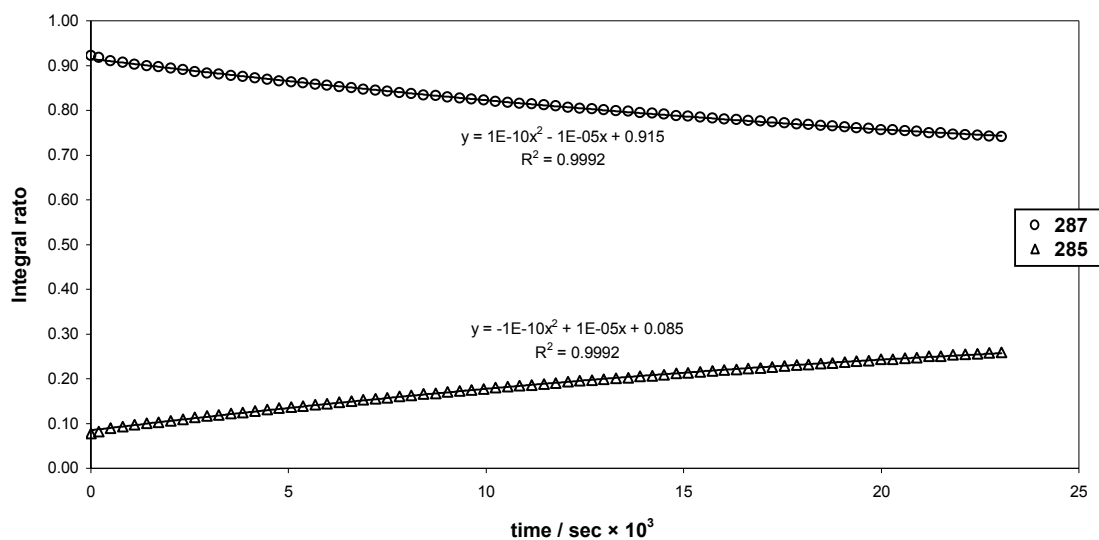
Experiment A4: Equilibration of 3-*exo*-hydroxy-2-*exo*-bornanyl acrylate **287** in unpurified CDCl₃ at **315 K**.

T/K	Mass/g	Conc./mol L ⁻¹	[287] _{eqm}	[285] _{eqm}	k_{-1}/k_{+1}	$k_{+1}+k_{-1}$	k_{-1}	k_{+1}
315	0.0132	0.117	0.481	0.519	1.08	2.27E-05	1.09E-05	1.18E-05



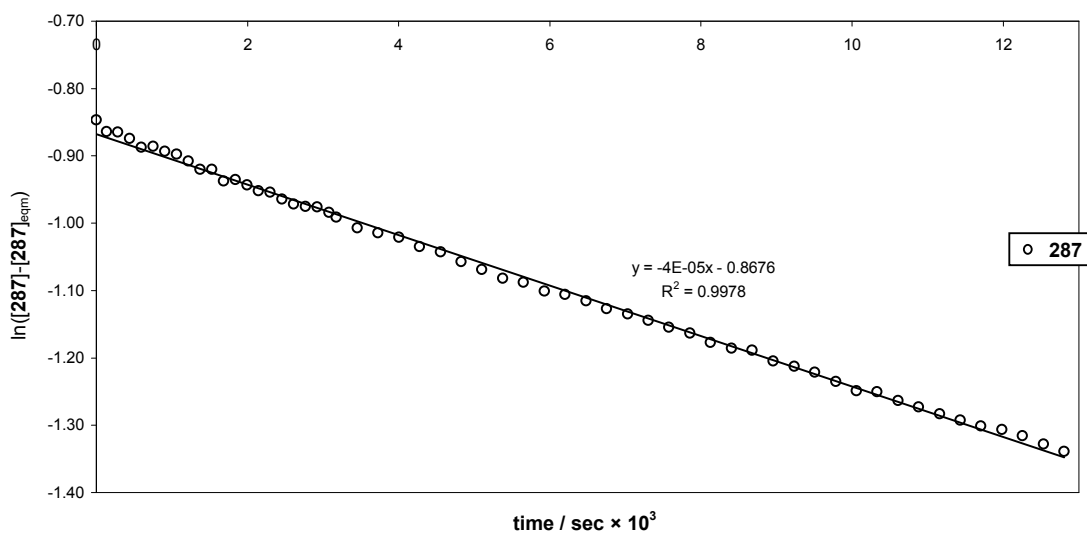
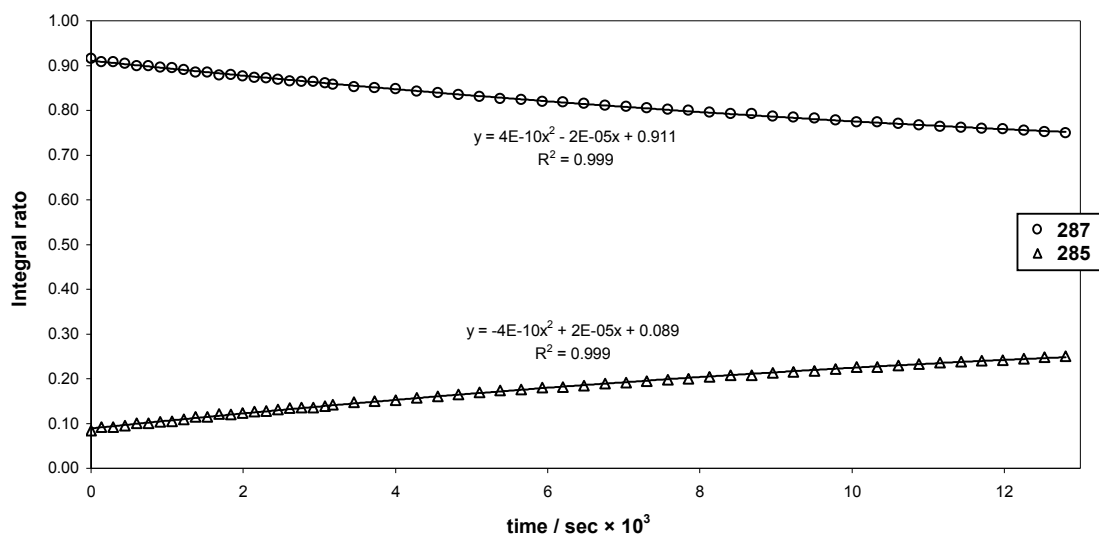
Experiment A5: Equilibration of 3-*exo*-hydroxy-2-*exo*-bornanyl acrylate **287** in unpurified CDCl₃ at **317 K**.

T/K	Mass/g	Conc./mol L ⁻¹	[287] _{eqm}	[285] _{eqm}	k ₁ /k ₊₁	k ₊₁ +k ₁	k ₁	k ₊₁
317	0.0132	0.117	0.474	0.526	1.11	2.18E-05	1.03E-05	1.15E-05



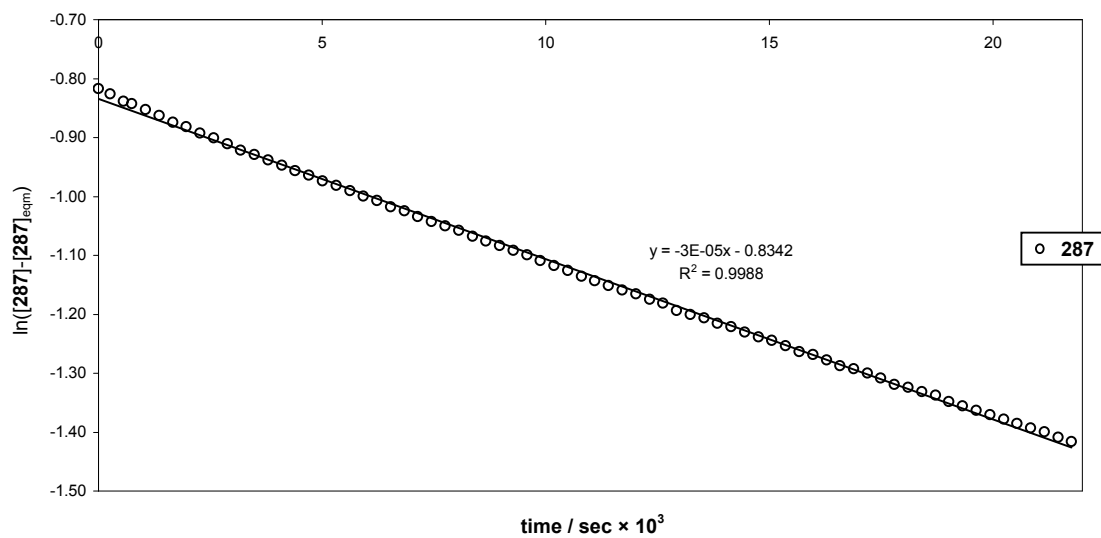
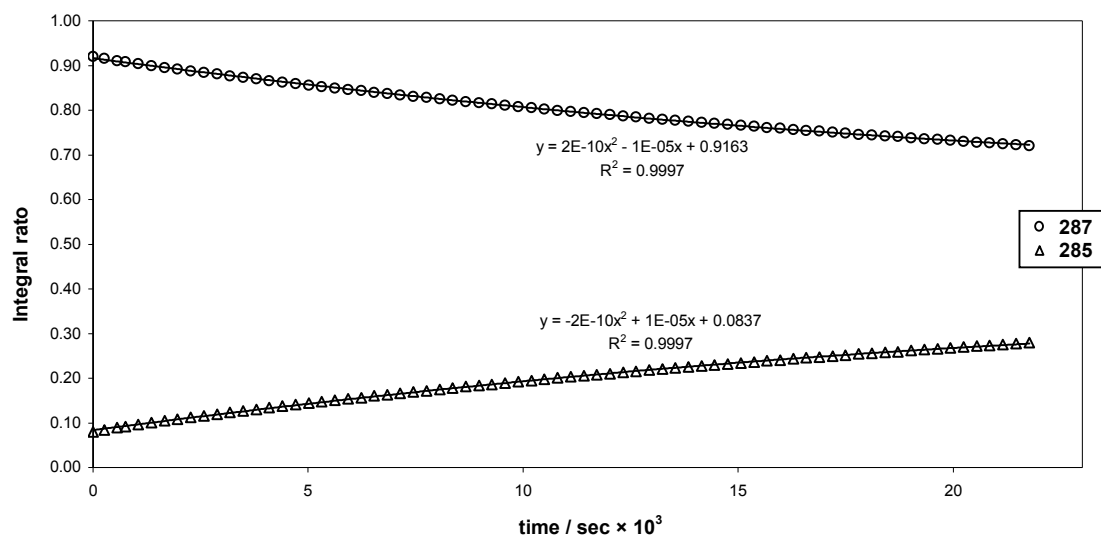
Experiment A6: Equilibration of 3-*exo*-hydroxy-2-*exo*-bornanyl acrylate **287** in unpurified CDCl₃ at **319 K**.

T/K	Mass/g	Conc./mol L ⁻¹	[287] _{eqm}	[285] _{eqm}	k ₁ /k ₊₁	k ₊₁ +k ₁	k ₁	k ₊₁
319	0.0132	0.117	0.487	0.513	1.05	3.75E-05	1.83E-05	1.92E-05



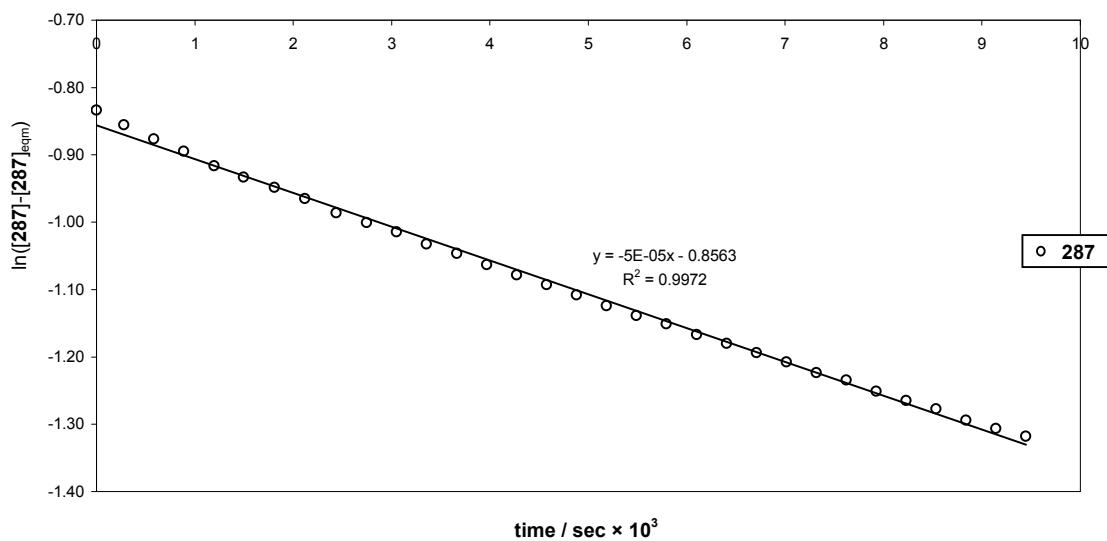
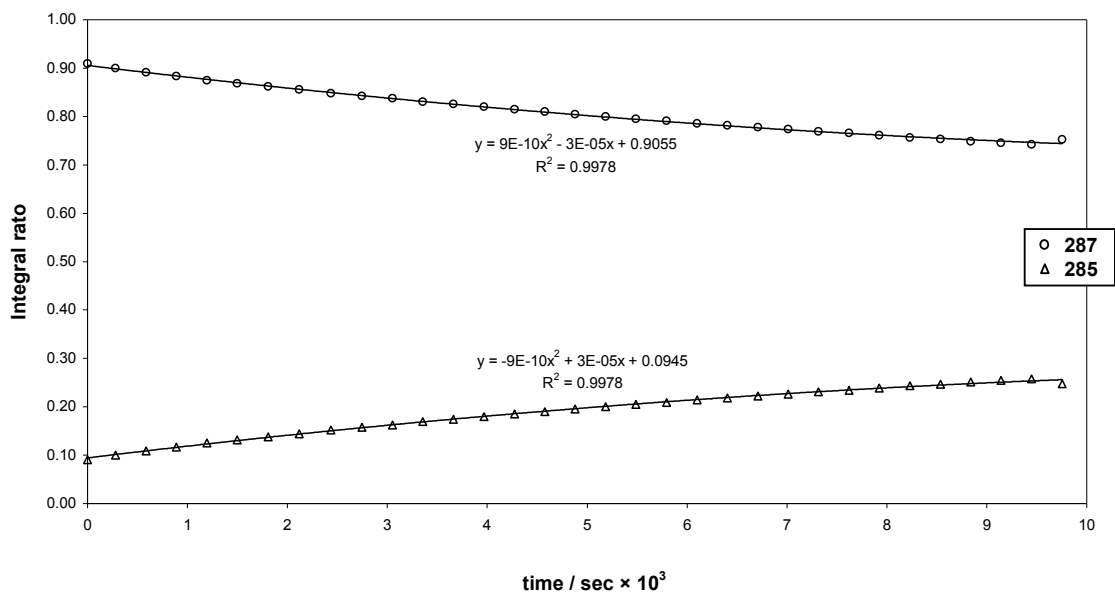
Experiment A7: Equilibration of 3-*exo*-hydroxy-2-*exo*-bornanyl acrylate **287** in unpurified CDCl₃ at **321 K**.

T/K	Mass/g	Conc./mol L ⁻¹	[287] _{eqm}	[285] _{eqm}	k_{-1}/k_{+1}	$k_{+1}+k_{-1}$	k_{-1}	k_{+1}
321	0.0132	0.117	0.478	0.522	1.09	2.72E-05	1.30E-05	1.42E-05



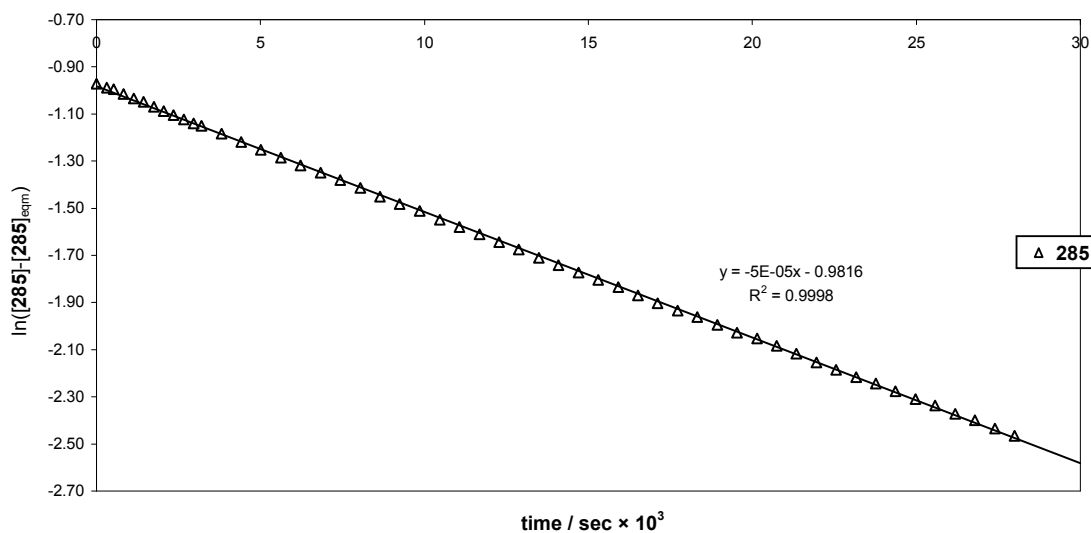
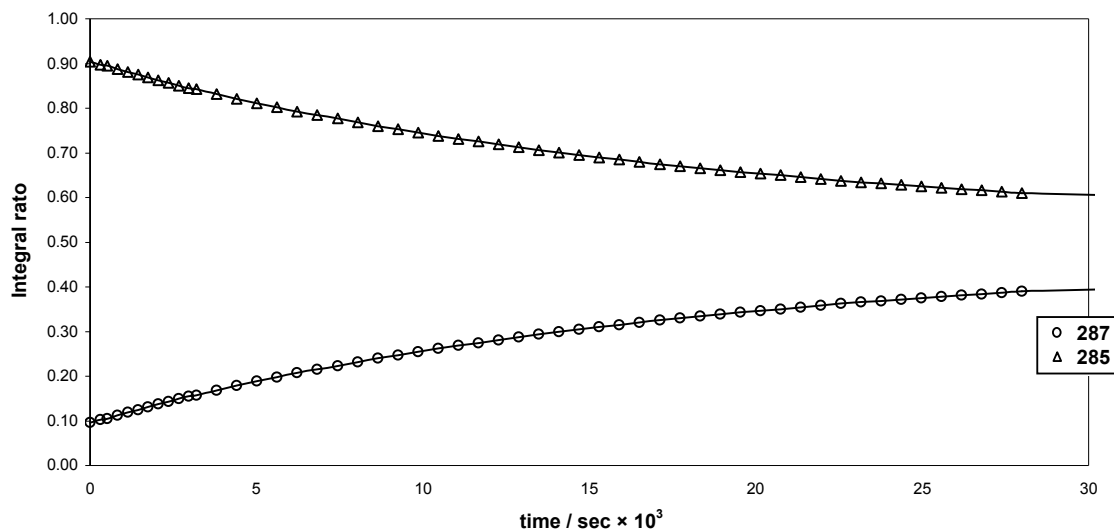
Experiment A8: Equilibration of 3-*exo*-hydroxy-2-*exo*-bornanyl acrylate **287** in unpurified CDCl₃ at **323 K**.

T/K	Mass/g	Conc./mol L ⁻¹	[287] _{eqm}	[285] _{eqm}	k_{-1}/k_{+1}	$k_{+1}+k_{-1}$	k_{-1}	k_{+1}
323	0.0132	0.117	0.475	0.525	1.11	5.00E-05	2.37E-05	2.63E-05



Experiment A9: Equilibration of 2-*exo*-hydroxy-3-*exo*-bornanyl acrylate **285** in unpurified CDCl_3 at **323 K**.

T/K	Mass/g	Conc./mol L ⁻¹	[287] _{eqm}	[285] _{eqm}	k_{-1}/k_{+1}	$k_{+1}+k_{-1}$	k_{-1}	k_{+1}
323	0.0153	0.136	0.475	0.525	0.90	4.91E-05	2.33E-05	2.58E-05

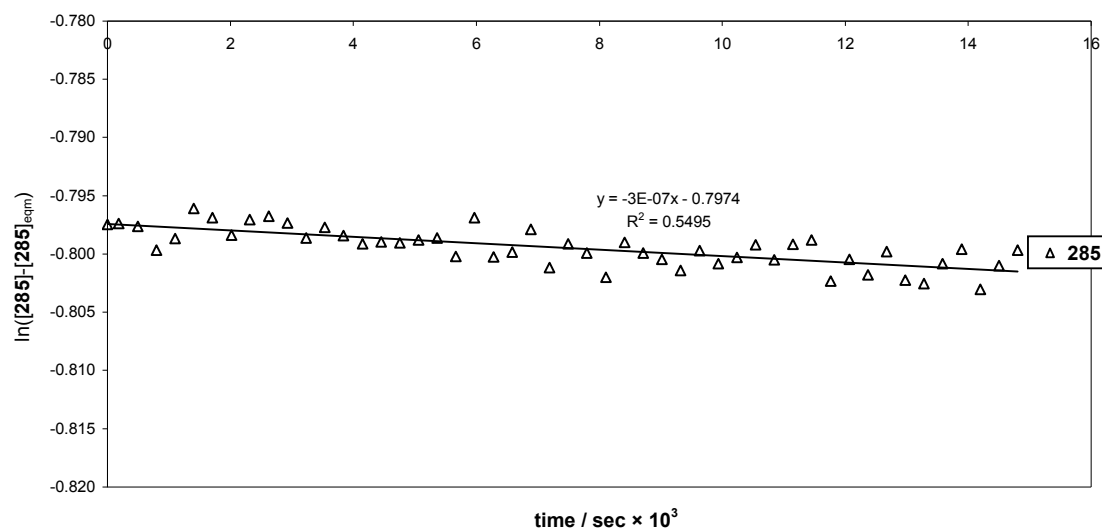
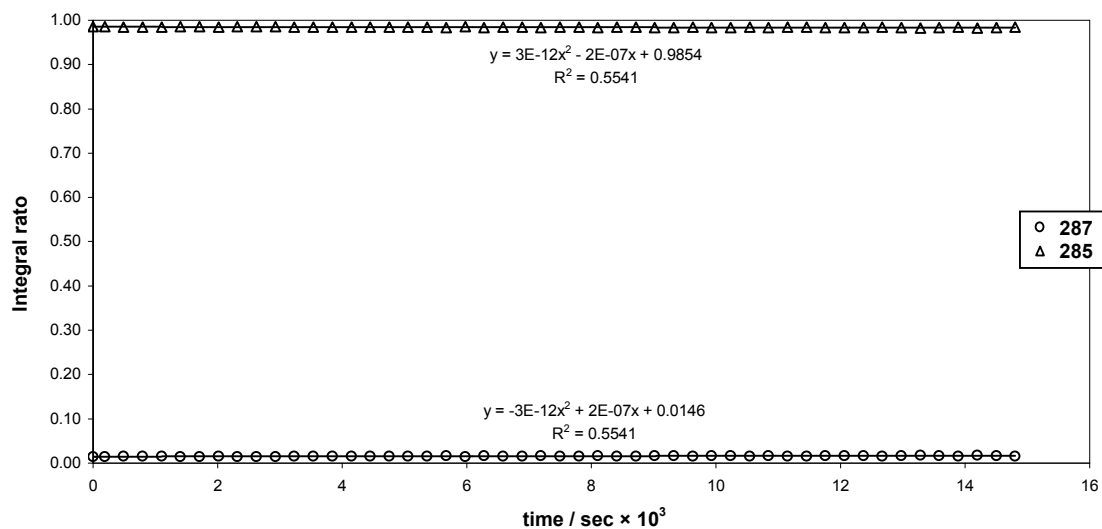


3.3.3 Reactions in Purified CDCl_3 under N_2

The acrylate ester 2-*exo*-hydroxy-3-*exo*-bornanyl acrylate **285** (0.010 – 0.021g) was accurately weighed into dry NMR tubes, which had been pre-filled with N_2 . CDCl_3 (0.5 mL) was then purified, under a stream of N_2 , by passage through neutral alumina and crushed 4Å molecular sieves in a dry Pasteur pipette directly into the NMR tubes, which were then flushed with N_2 before sealing. The samples were used immediately for NMR spectroscopic analysis and experiments were conducted at various temperatures (301 to 315 K) following the method described previously (**Section 3.3.1**).

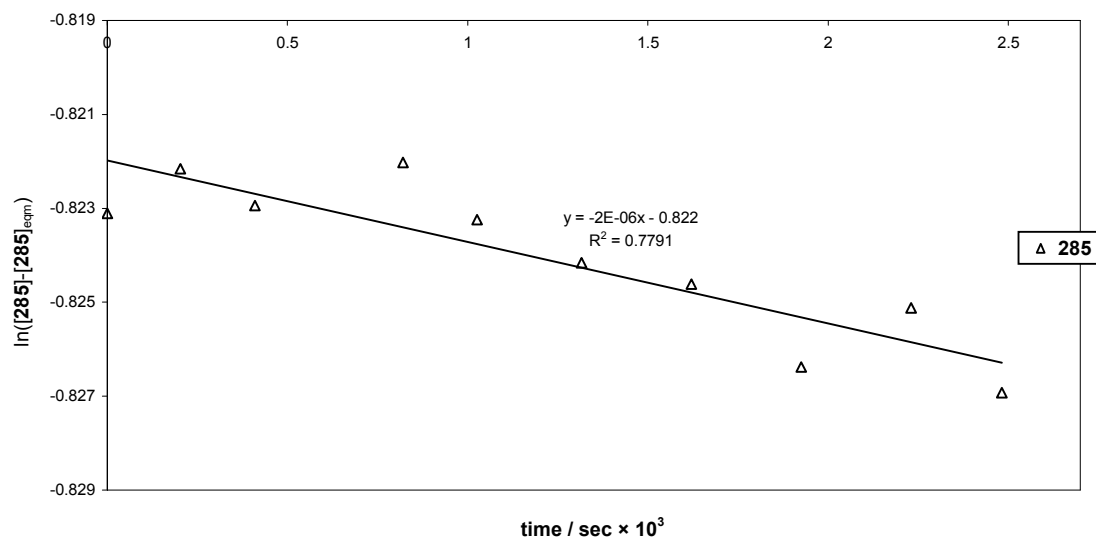
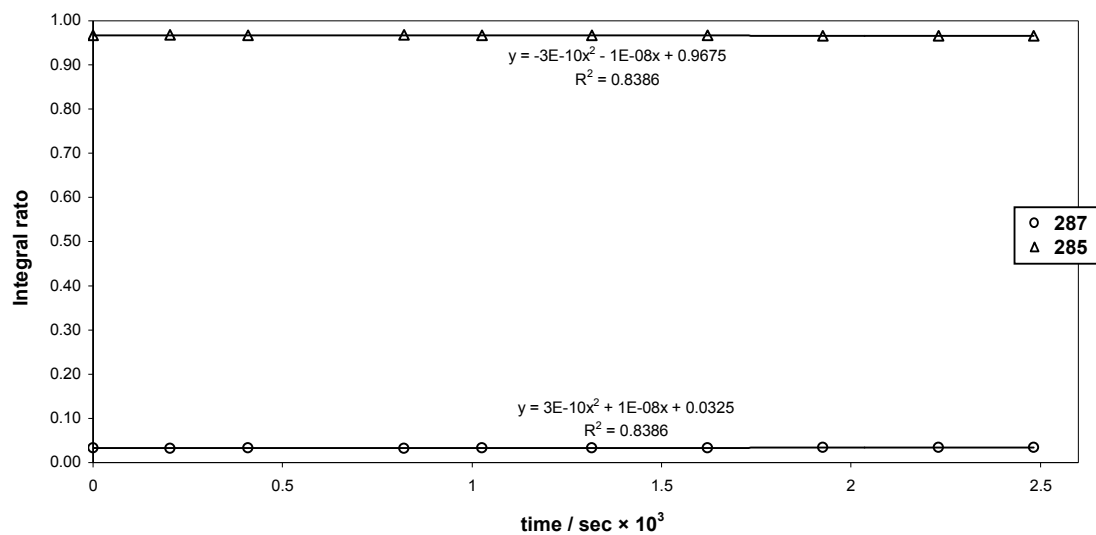
Experiment B1: Equilibration of 2-*exo*-hydroxy-3-*exo*-bornanyl acrylate **285** in purified CDCl₃ under N₂ at **301 K**.

T/K	Mass/g	Conc./mol L ⁻¹	[287] _{eqm}	[285] _{eqm}	k ₁ /k ₊₁	k ₊₁ +k ₁	k ₁	k ₊₁
301	0.0104	0.093	0.465	0.535	0.87	2.77E-07	1.29E-07	1.48E-07



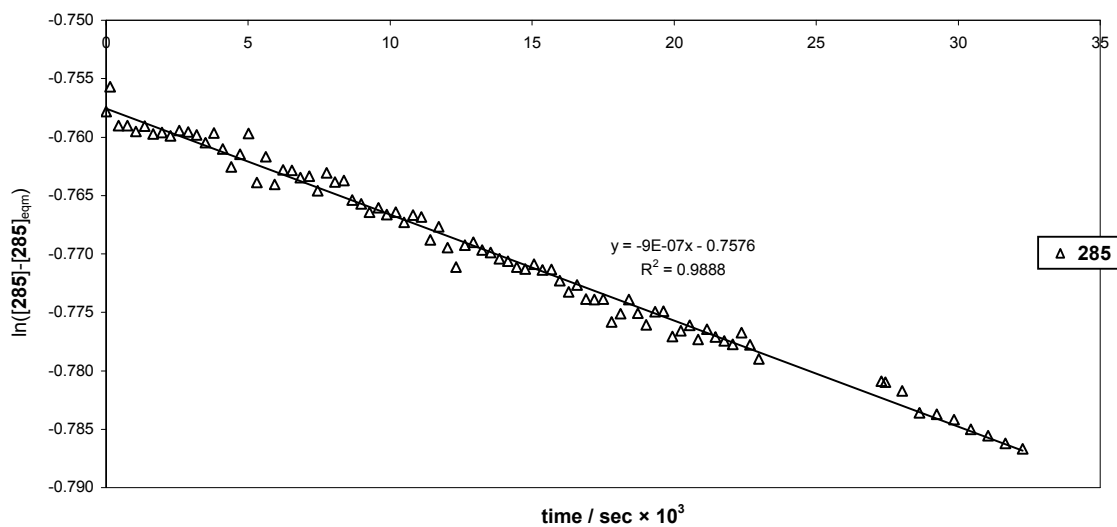
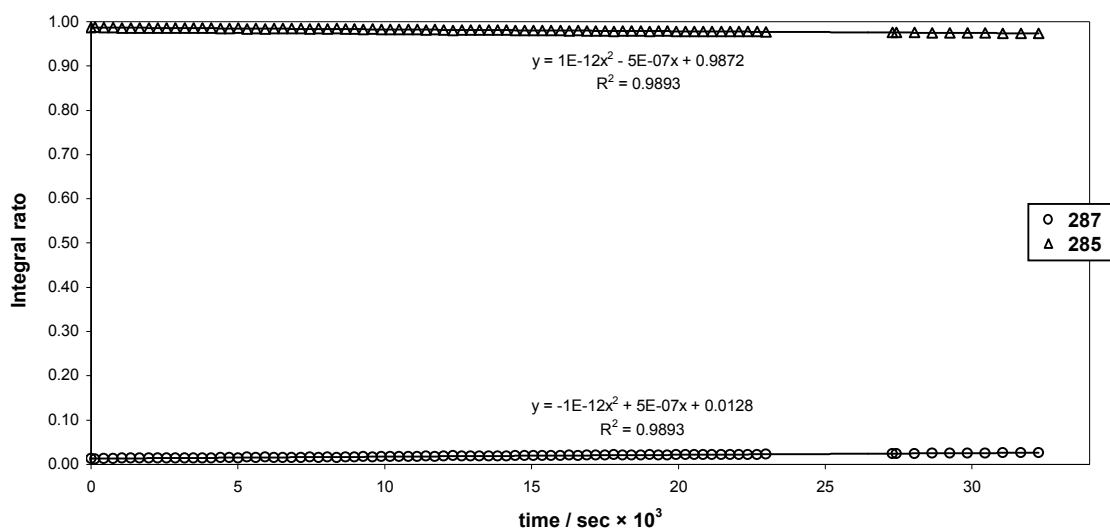
Experiment B2: Equilibration of 2-*exo*-hydroxy-3-*exo*-bornanyl acrylate **285** in purified CDCl₃ under N₂ at **305 K**.

T/K	Mass/g	Conc./mol L ⁻¹	[287] _{eqm}	[285] _{eqm}	k ₁ /k ₊₁	k ₊₁ +k ₁	k ₁	k ₊₁
305	0.0101	0.090	0.472	0.528	0.89	1.73E-06	8.17E-07	9.14E-07



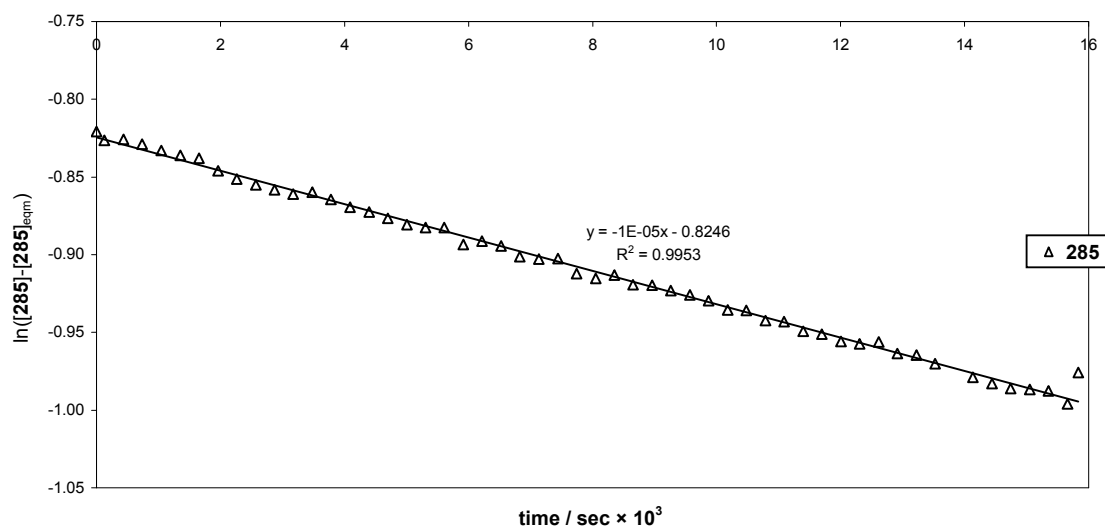
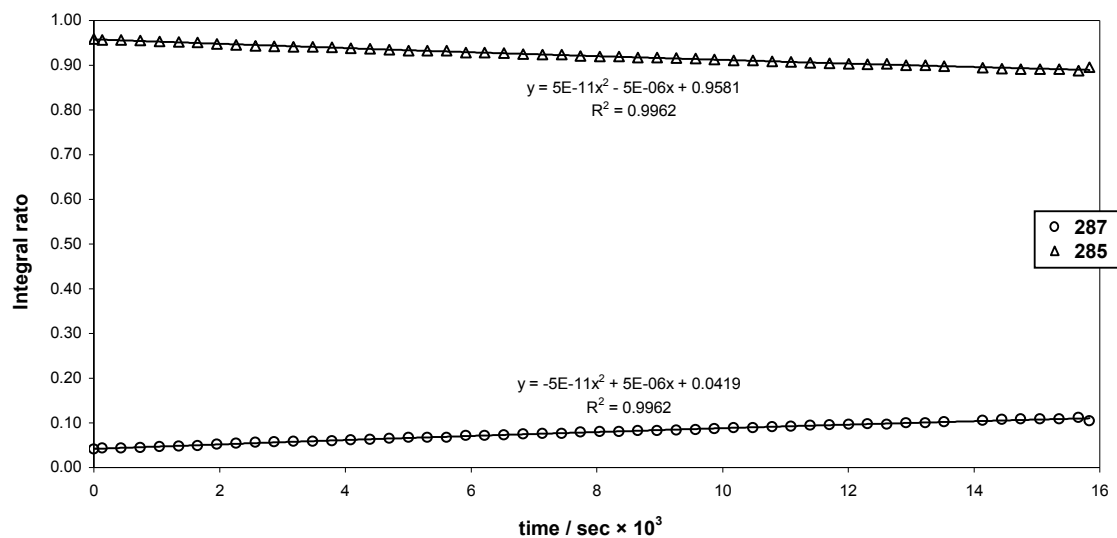
Experiment B3: Equilibration of 2-*exo*-hydroxy-3-*exo*-bornanyl acrylate **285** in purified CDCl₃ under N₂ at **307 K**.

T/K	Mass/g	Conc./mol L ⁻¹	[287] _{eqm}	[285] _{eqm}	k ₁ /k ₊₁	k ₊₁ +k ₁	k ₁	k ₊₁
307	0.0095	0.085	0.482	0.518	0.93	9.07E-07	4.37E-07	4.70E-07



Experiment B4: Equilibration of 2-*exo*-hydroxy-3-*exo*-bornanyl acrylate **285** in purified CDCl₃ under N₂ at 315 K.

T/K	Mass/g	Conc./mol L ⁻¹	[287] _{eqm}	[285] _{eqm}	k_{-1}/k_{+1}	$k_{+1}+k_{-1}$	k_{-1}	k_{+1}
315	0.0210	0.187	0.481	0.519	0.93	1.07E-05	4.80E-06	5.56E-06



3.3.4 Temperature Effect on Acrylate data in CDCl₃ under N₂

Purified CDCl₃ (0.5 mL) was added to 3-*exo*-hydroxy-2-*exo*-bornanyl acrylate **287** (0.014 g) in a dry NMR tube. The tube was flushed with nitrogen prior to sealing. Spectra were recorded over 1 h at temperatures in the range 305 to 323 K. ¹H NMR Spectra were obtained at various temperatures and their line-shape was compared at each temperature and again on cooling. The spectra are presented in **Section 2.3.2.2.2**.

Experiment C1: Data for the thermal stability study of purified CDCl₃ with 3-*exo*-hydroxy-2-*exo*-bornanyl acrylate **287**

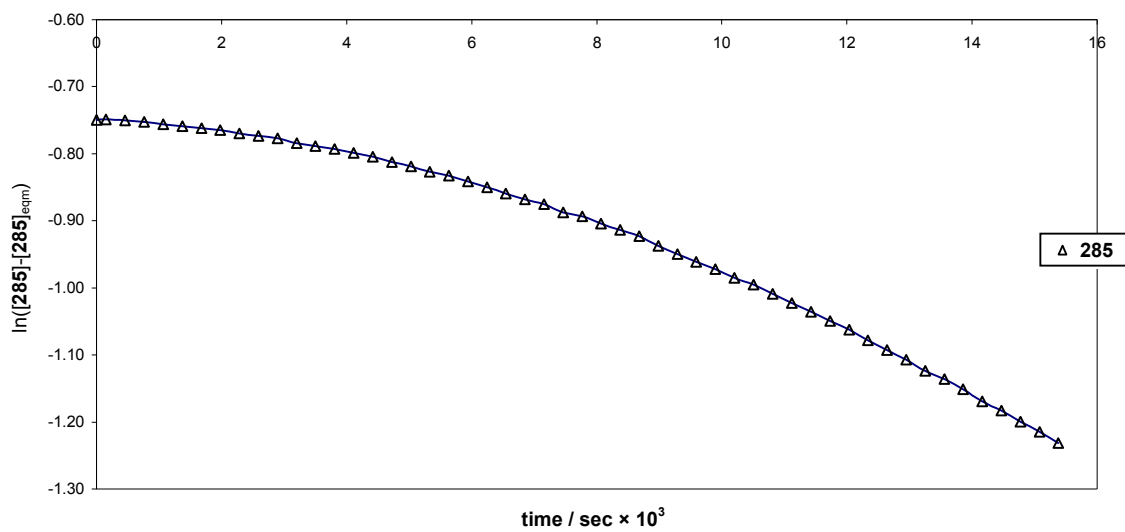
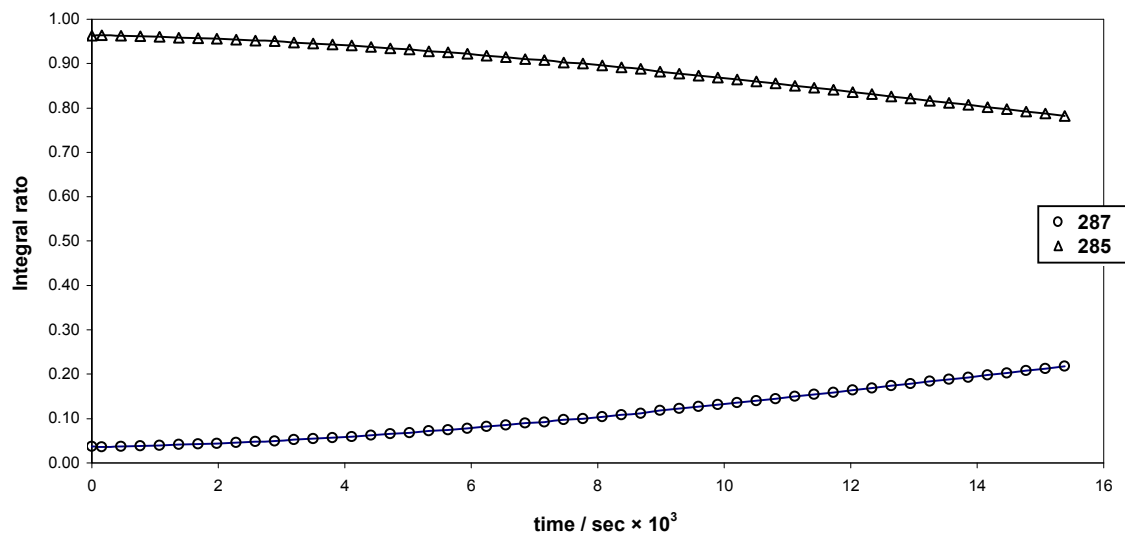
T/K	Mass/g	Conc./mol L ⁻¹
305 - 323	0.0140	0.125

3.3.5 Thermal Stability Study of Purified CDCl_3 in Air

Purified CDCl_3 (0.5 mL) was added to the acrylate esters 2-*exo*-hydroxy-3-*exo*-bornanyl acrylate **285** (0.010 g) or 3-*exo*-hydroxy-2-*exo*-bornanyl acrylate **287** (0.014 g) in dry NMR tubes. The tubes were *not* flushed with N_2 before sealing and the samples were used immediately for NMR spectroscopic analysis. Experiments were conducted at various temperatures (313 to 323 K) following the method described previously (**Section 3.3.1**).

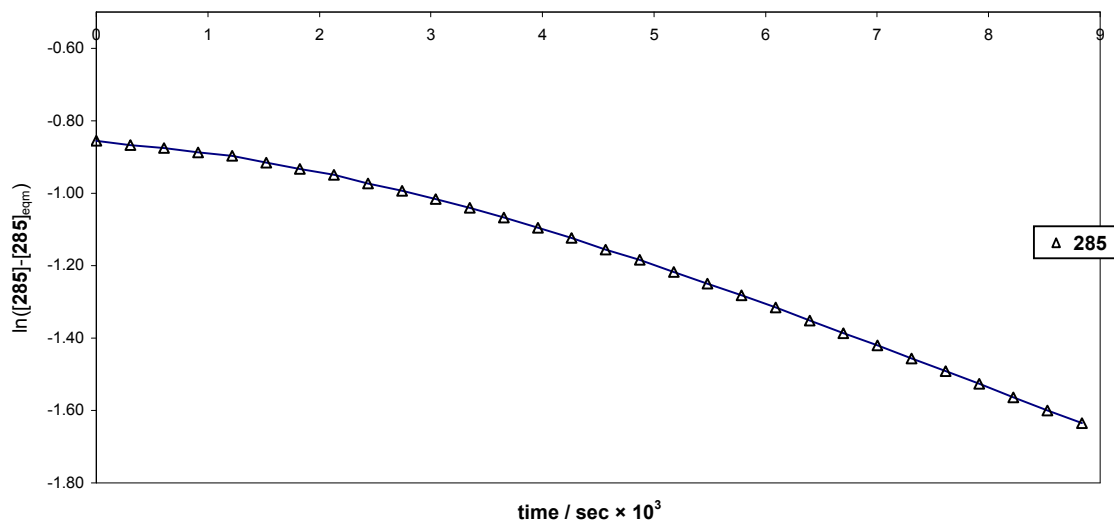
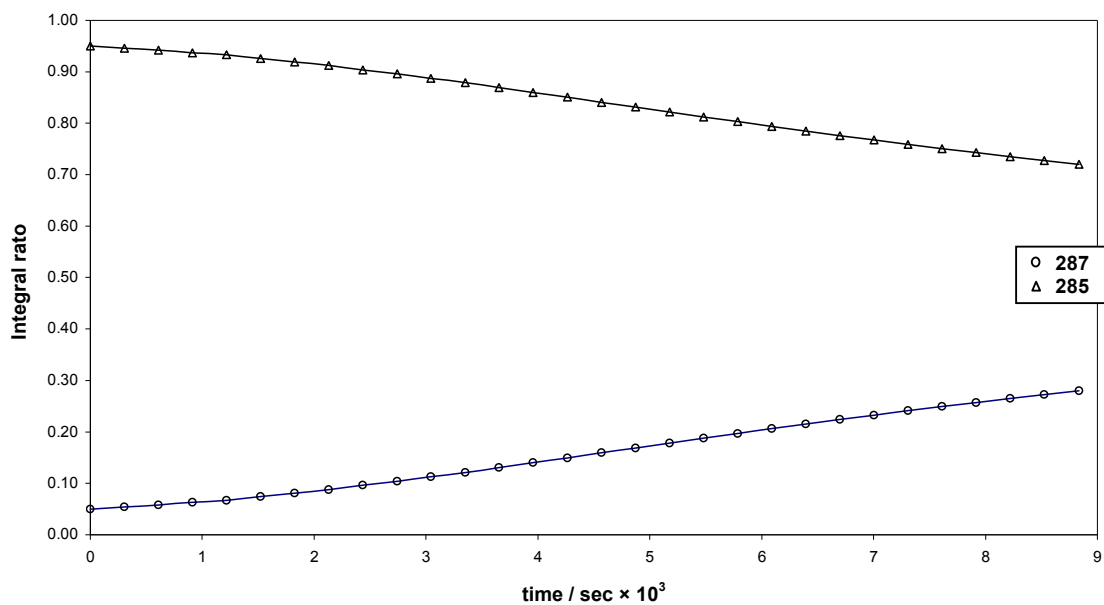
Experiment D1: Equilibration of 2-*exo*-hydroxy-3-*exo*-bornanyl acrylate **285** in purified CDCl_3 under air at **313 K**.

T/K	Mass/g	Conc./mol L ⁻¹	[287] _{eqm}	[285] _{eqm}	k_1/k_{+1}	$k_{+1}+k_1$	k_1	k_{+1}
313	0.0101	0.090	0.509	0.491	0.96	3.15E-05	1.55E-05	1.61E-05



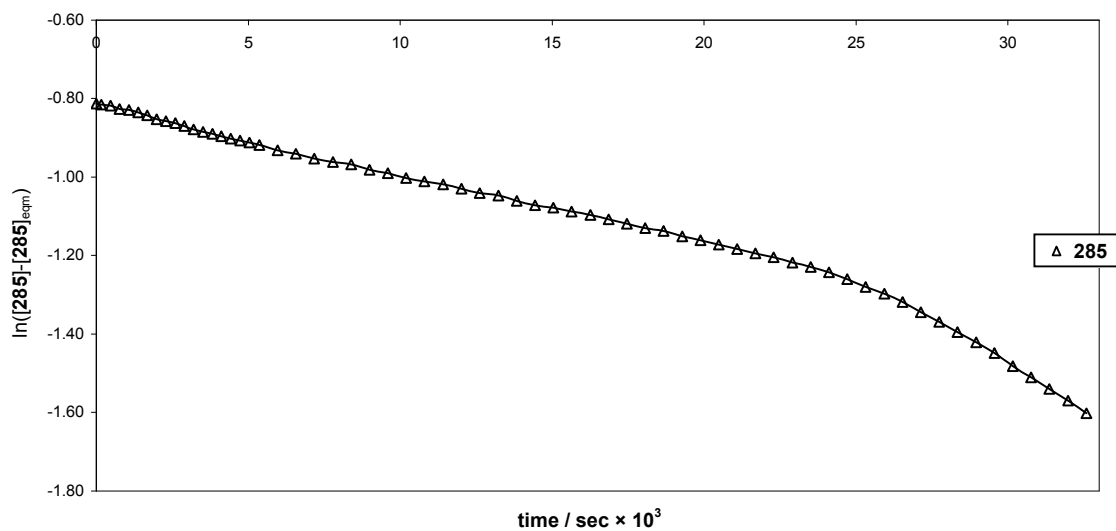
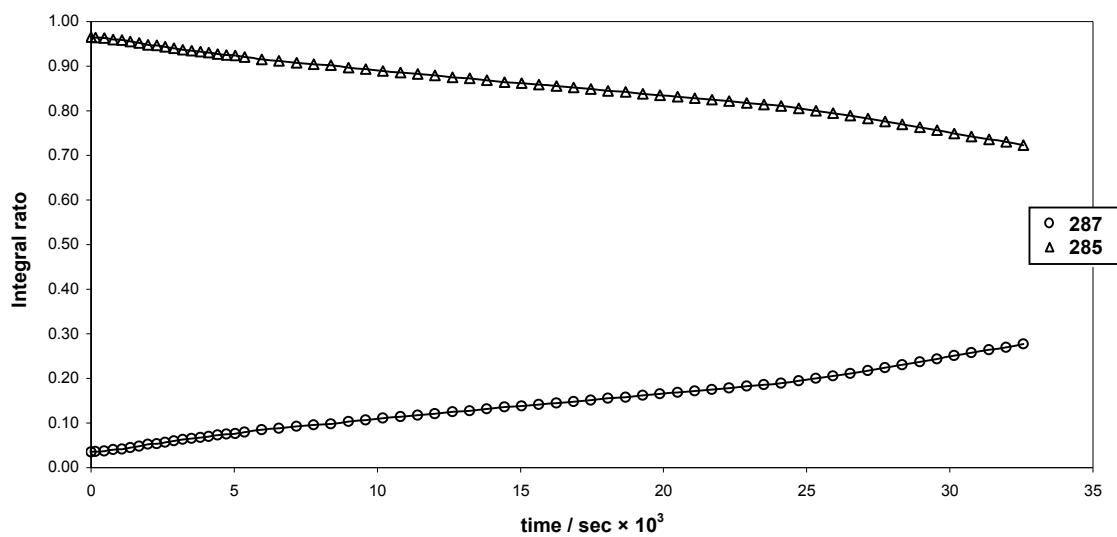
Experiment D2: Equilibration of 2-*exo*-hydroxy-3-*exo*-bornanyl acrylate **285** in purified CDCl_3 under air at **317 K**.

T/K	Mass/g	Conc./mol L ⁻¹	[287] _{eqm}	[285] _{eqm}	k_{-1}/k_{+1}	$k_{+1}+k_{-1}$	k_{-1}	k_{+1}
317	0.0101	0.090	0.474	0.526	0.89	9.15E-05	4.34E-05	4.81E-05



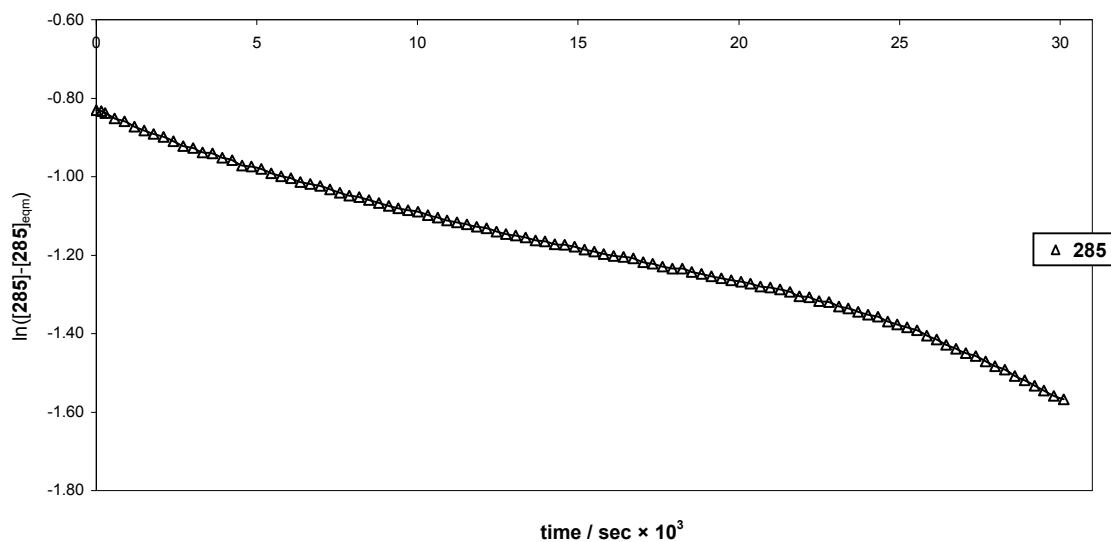
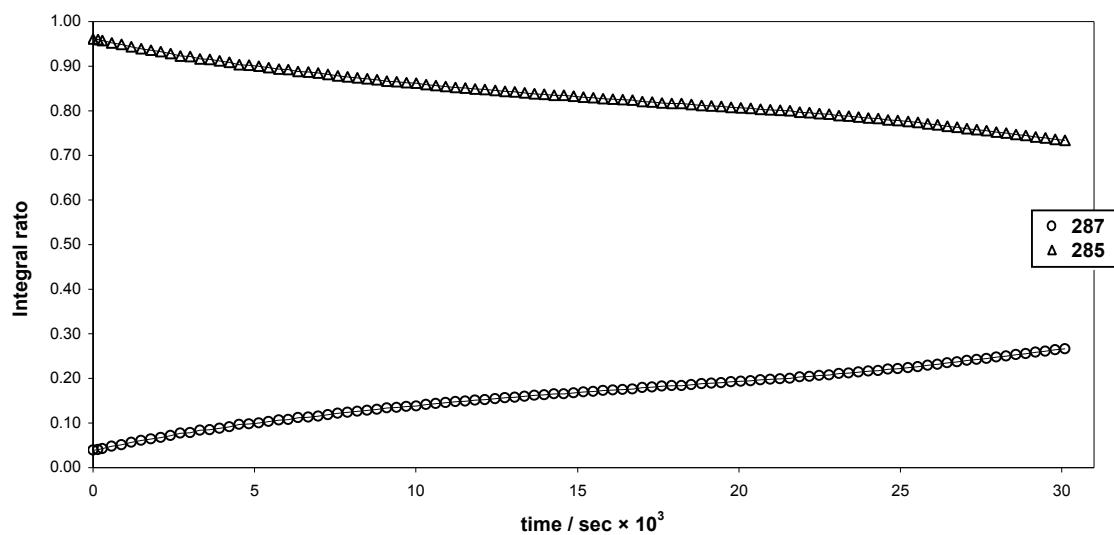
Experiment D3: Equilibration of 2-*exo*-hydroxy-3-*exo*-bornanyl acrylate **285** in purified CDCl_3 under air at **321 K**.

T/K	Mass/g	Conc./mol L ⁻¹	[287] _{eqm}	[285] _{eqm}	k_{-1}/k_{+1}	$k_{+1}+k_{-1}$	k_{-1}	k_{+1}
321	0.0101	0.090	0.478	0.522	0.92	2.08E-05	9.92E-06	1.08E-05



Experiment D4: Equilibration of 2-*exo*-hydroxy-3-*exo*-bornanyl acrylate **285** in purified CDCl₃ under air at 323 K.

T/K	Mass/g	Conc./mol L ⁻¹	[287] _{eqm}	[285] _{eqm}	k_{-1}/k_{+1}	$k_{+1}+k_{-1}$	k_{-1}	k_{+1}
323	0.0101	0.093	0.475	0.525	0.90	2.15E-05	1.02E-05	1.13E-05

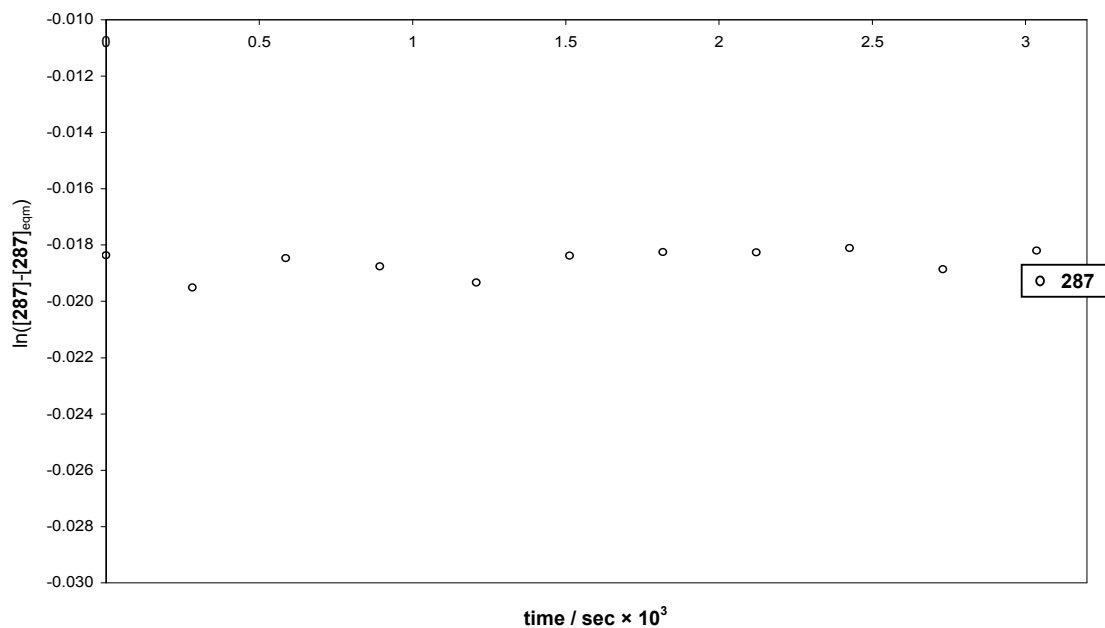
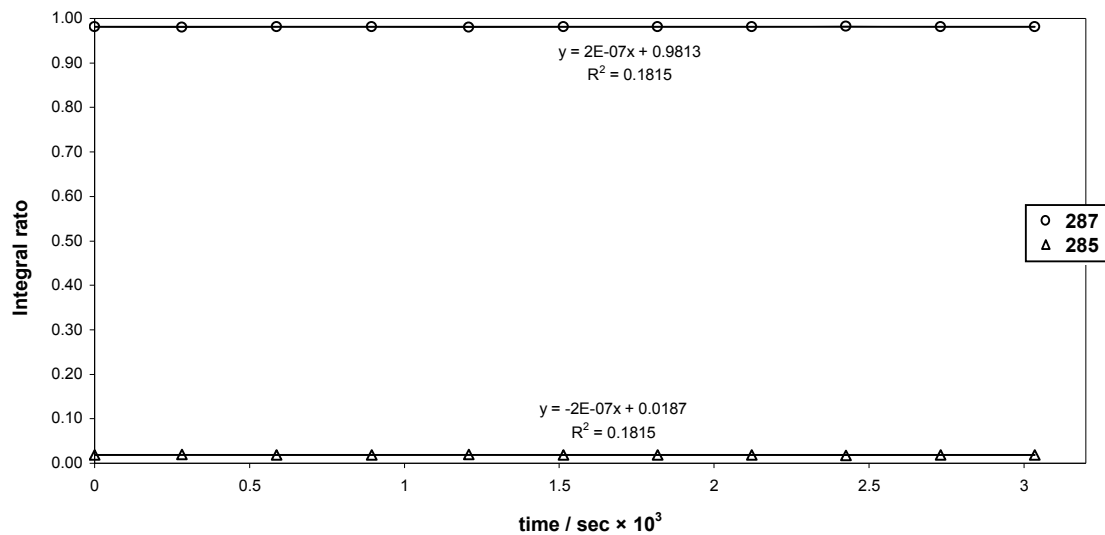


3.3.6 Reactions in Purified DMSO-*d*₆ under N₂

Purified DMSO-*d*₆ (0.5 mL) was added to the acrylate esters 2-*exo*-hydroxy-3-*exo*-bornanyl acrylate **285** (0.083 g) or 3-*exo*-hydroxy-2-*exo*-bornanyl acrylate **287** (0.164 g) in dry NMR tubes. The tubes were flushed with N₂ before sealing and the samples were used immediately for NMR spectroscopic analysis. Experiments were conducted at various temperatures (301 to 329 K) following the method described previously (**Section 3.3.1**).

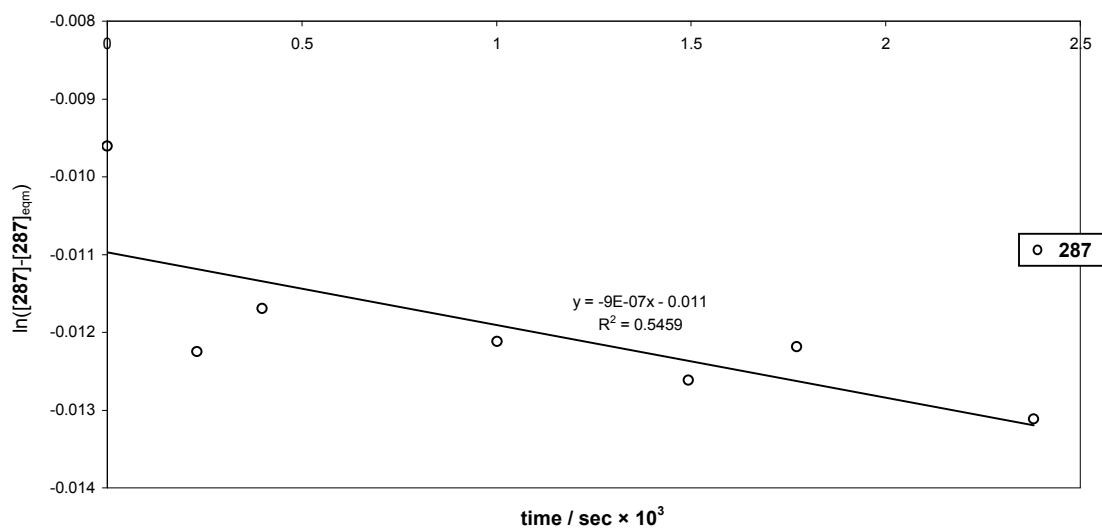
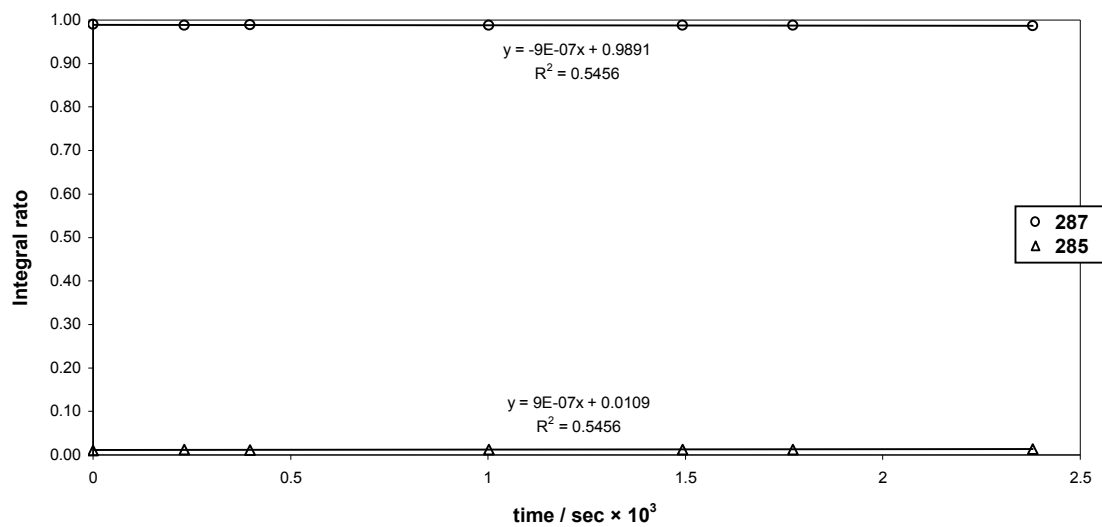
Experiment E1: Equilibration of 3-*exo*-hydroxy-2-*exo*-bornanyl acrylate **287** in purified DMSO-*d*₆ under N₂ at **301 K**.

T/K	Mass/g	Conc./mol L ⁻¹
301	0.0164	0.146



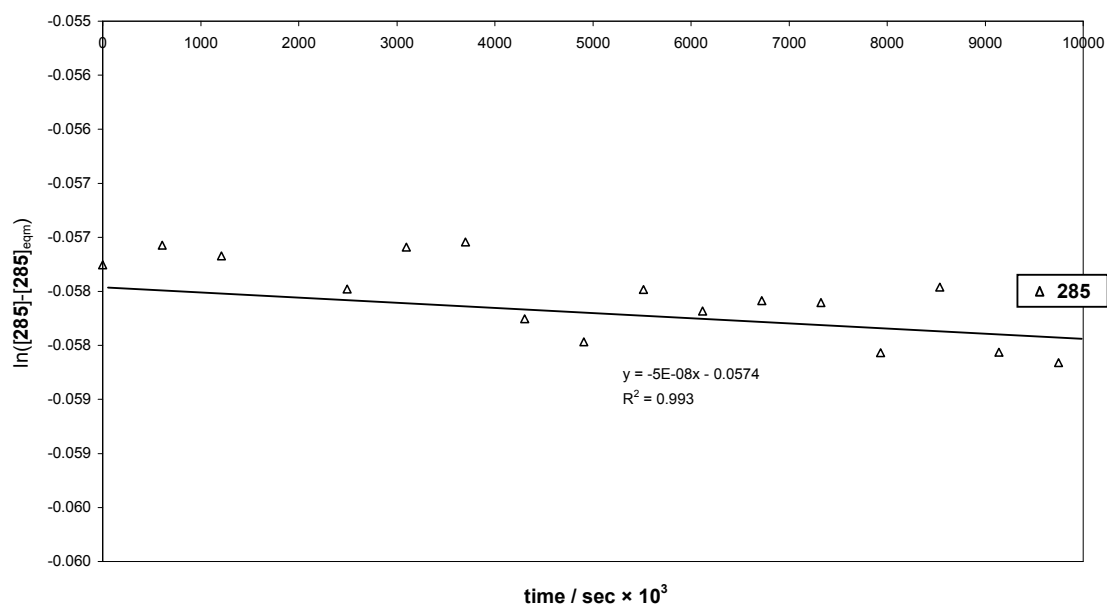
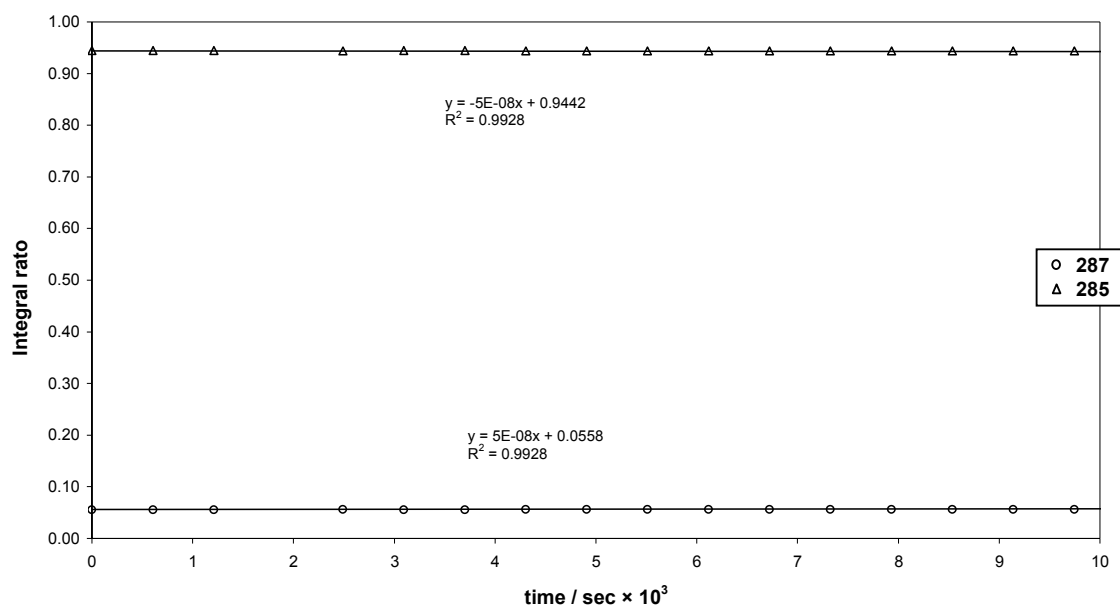
Experiment E2: Equilibration of 3-*exo*-hydroxy-2-*exo*-bornanyl acrylate **287** in purified DMSO-*d*₆ under N₂ at **305 K**.

T/K	Mass/g	Conc./mol L ⁻¹
305	0.0164	0.146



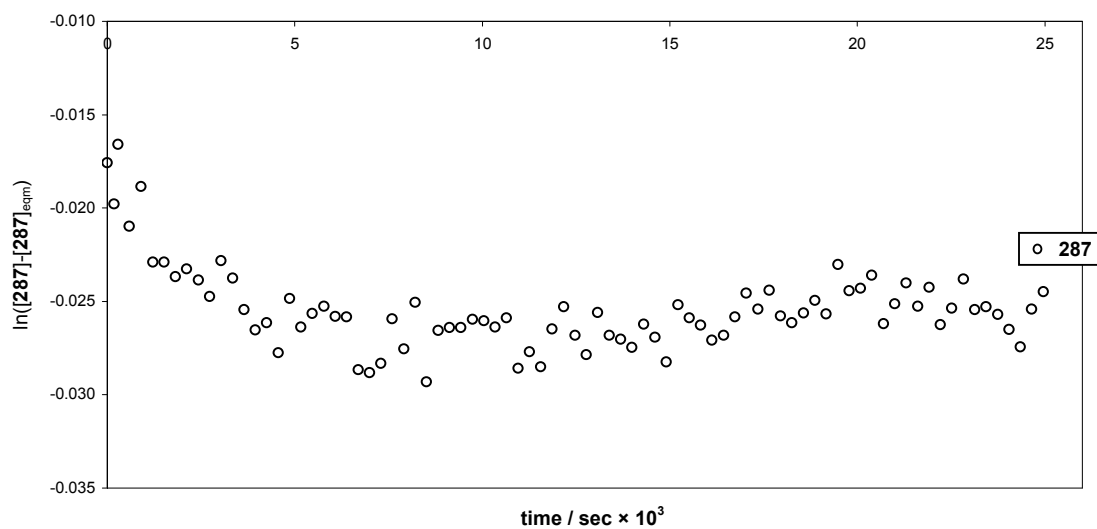
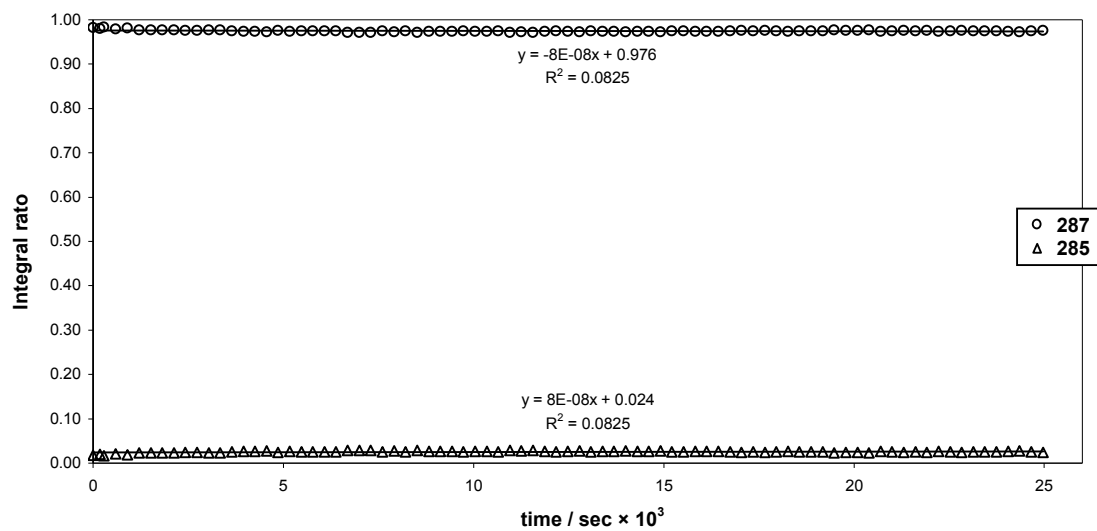
Experiment E3: Equilibration of 2-*exo*-hydroxy-3-*exo*-bornanyl acrylate **285** in purified DMSO-*d*₆ under N₂ at **315 K**.

T/K	Mass/g	Conc./mol L ⁻¹
315	0.0083	0.074



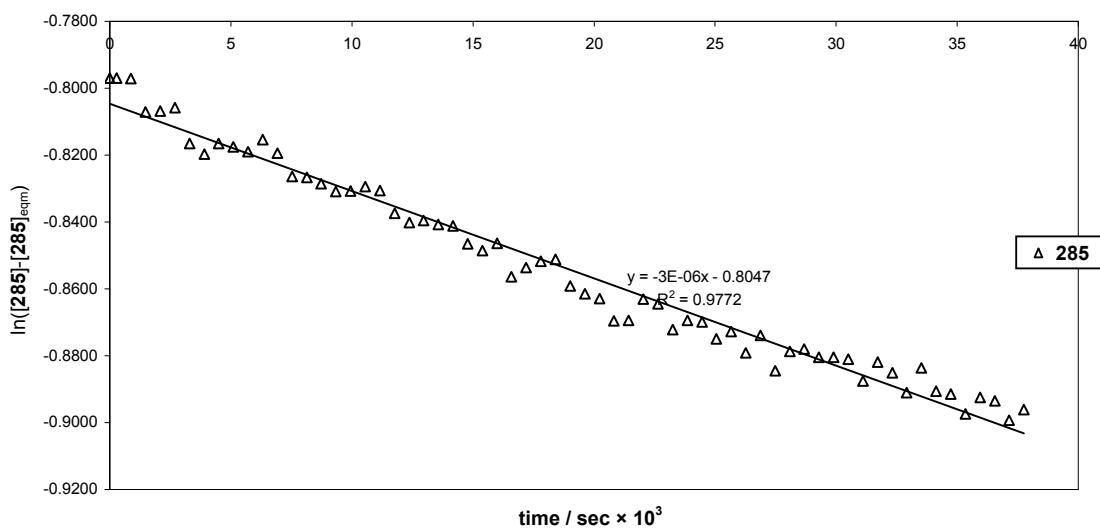
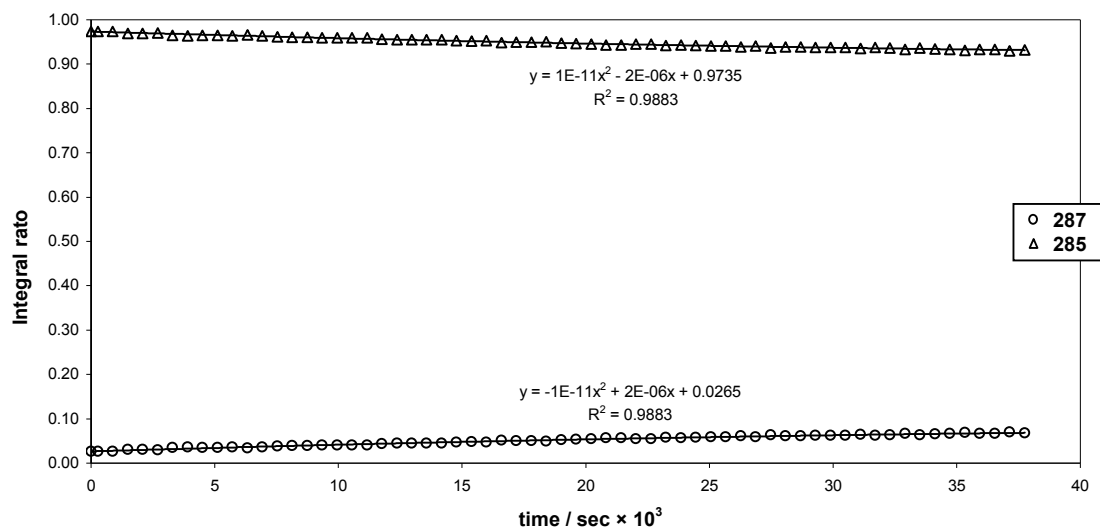
Experiment E4: Equilibration of 3-*exo*-hydroxy-2-*exo*-bornanyl acrylate **287** in purified DMSO-*d*₆ under N₂ at **315 K**.

T/K	Mass/g	Conc./mol L ⁻¹
315	0.0164	0.146



Experiment E5: Equilibration of 2-*exo*-hydroxy-3-*exo*-bornanyl acrylate **285** in purified DMSO-*d*₆ under N₂ at **329 K**.

T/K	Mass/g	Conc./mol L ⁻¹
329	0.0083	0.074

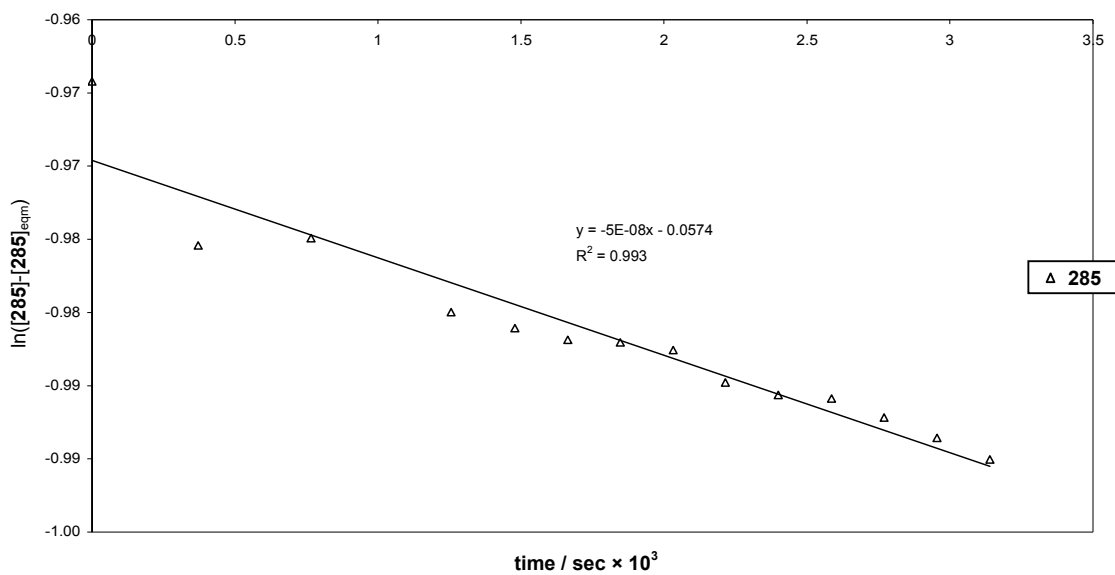
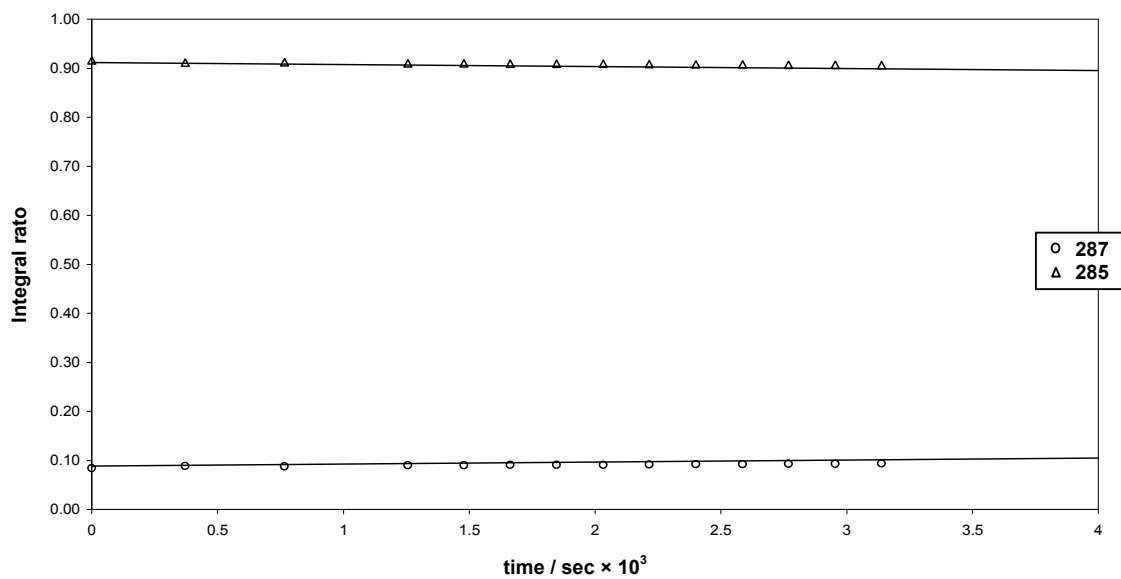


3.3.7 Reactions in Purified DMSO-*d*₆ with H₂SO₄ under N₂

Purified DMSO-*d*₆ (0.5 mL) was added to the acrylate ester 2-*exo*-hydroxy-3-*exo*-bornanyl acrylate **285** (0.0083 g) in a dry NMR tube. A catalytic amount (1 drop) of H₂SO₄ was added and the tube was flushed with N₂ before sealing. The sample was used immediately for NMR spectroscopic analysis (301 K) following the method described previously (**Section 3.3.1**).

Experiment F1: Equilibration of 2-*exo*-hydroxy-3-*exo*-bornanyl acrylate **285** in purified DMSO-*d*₆ with H₂SO₄ under N₂ at **301 K**.

T/K	Mass/g	Conc./mol L ⁻¹
301	0.0083	0.093

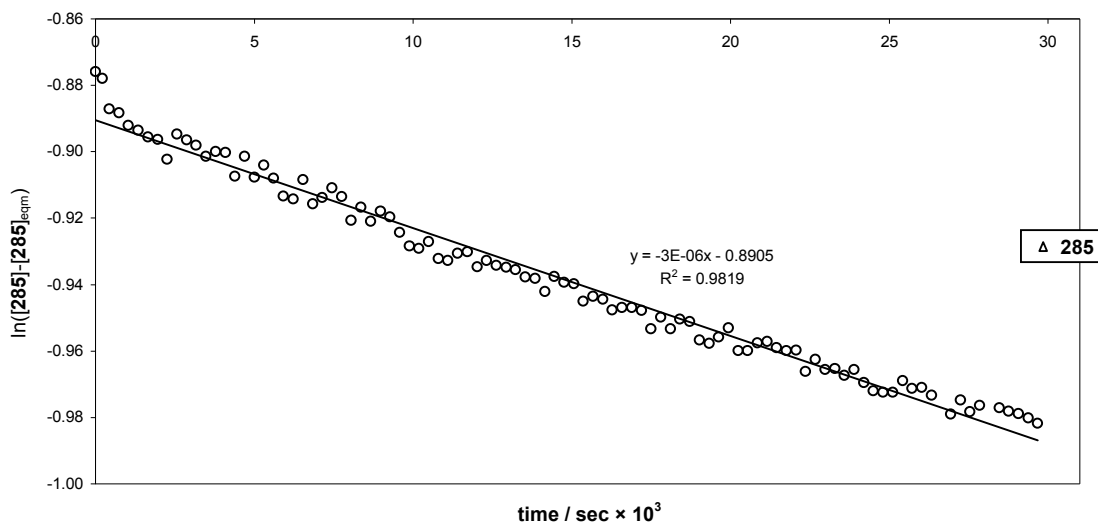
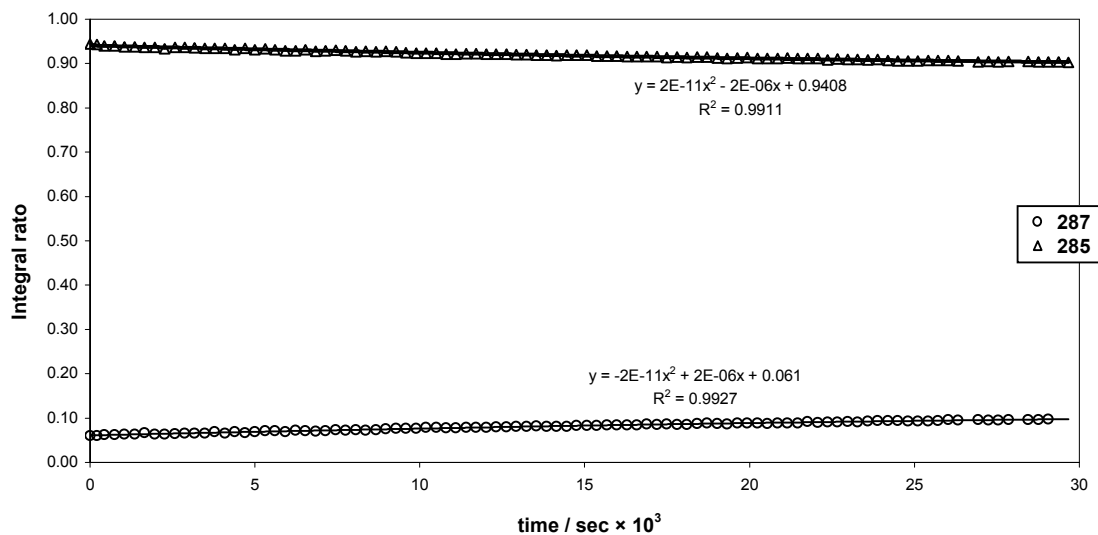


3.3.8 Reactions in Purified DMSO-*d*₆ with *p*-TsOH under N₂

Purified DMSO-*d*₆ (0.5 mL) was added to the acrylate ester 2-*exo*-hydroxy-3-*exo*-bornanyl acrylate **285** (0.0096 – 0.0135 g) in a dry NMR tube. A catalytic amount of *p*-TsOH was added and the tube was flushed with N₂ before sealing. The sample was used immediately for NMR spectroscopic analysis (301 – 323 K) following the method described previously (**Section 3.3.1**).

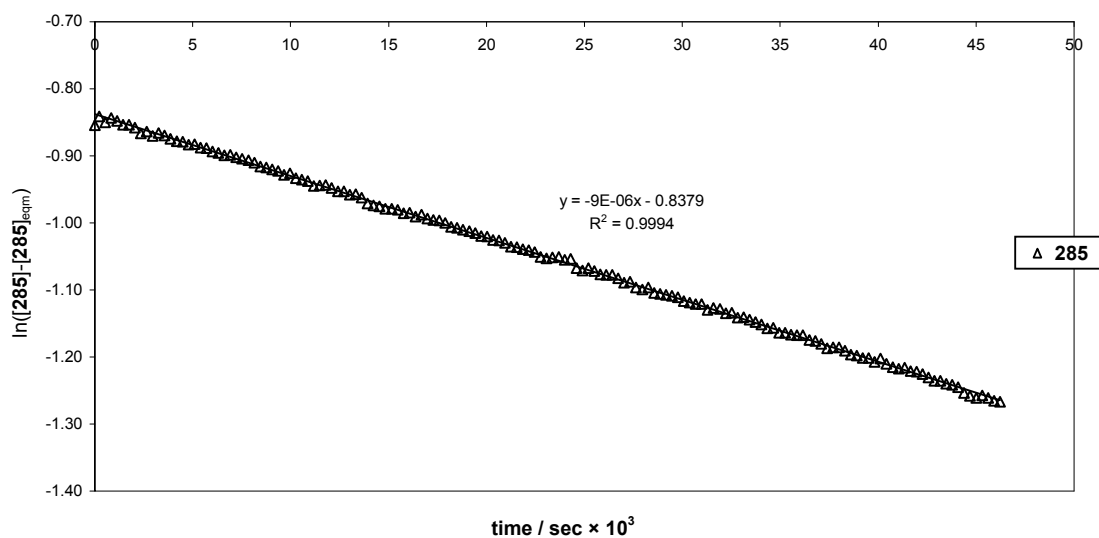
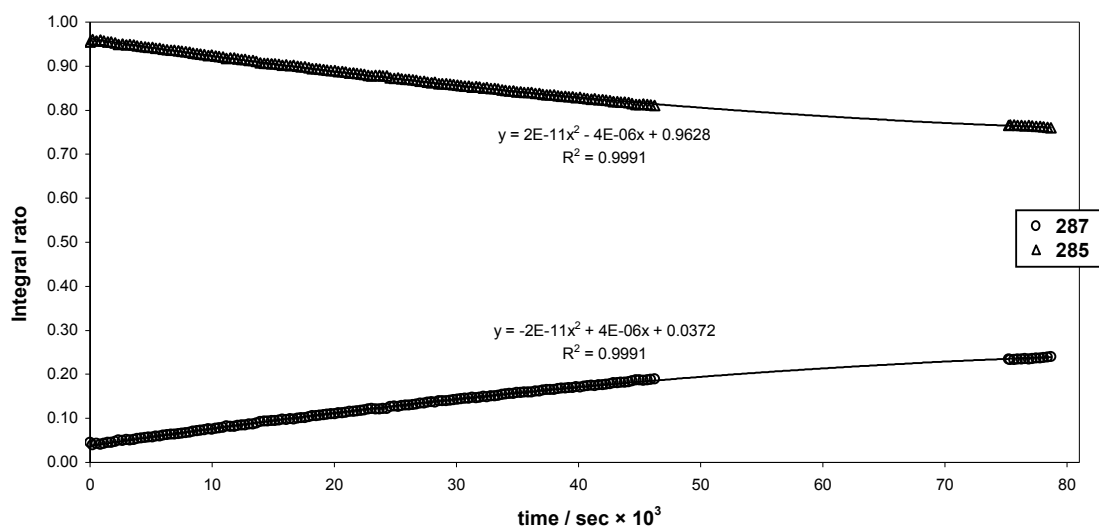
Experiment G1: Equilibration of 2-*exo*-hydroxy-3-*exo*-bornanyl acrylate **285** in purified DMSO-*d*₆ with *p*-TsOH under N₂ at **301 K**.

T/K	Mass/g	Conc./mol L ⁻¹	[287] _{eqm}	[285] _{eqm}	k_{-1}/k_{+1}	$k_{+1}+k_{-1}$	k_{-1}	k_{+1}
301	0.0135	0.120	0.472	0.528	0.89	3.25E-06	1.53E-06	1.71E-06



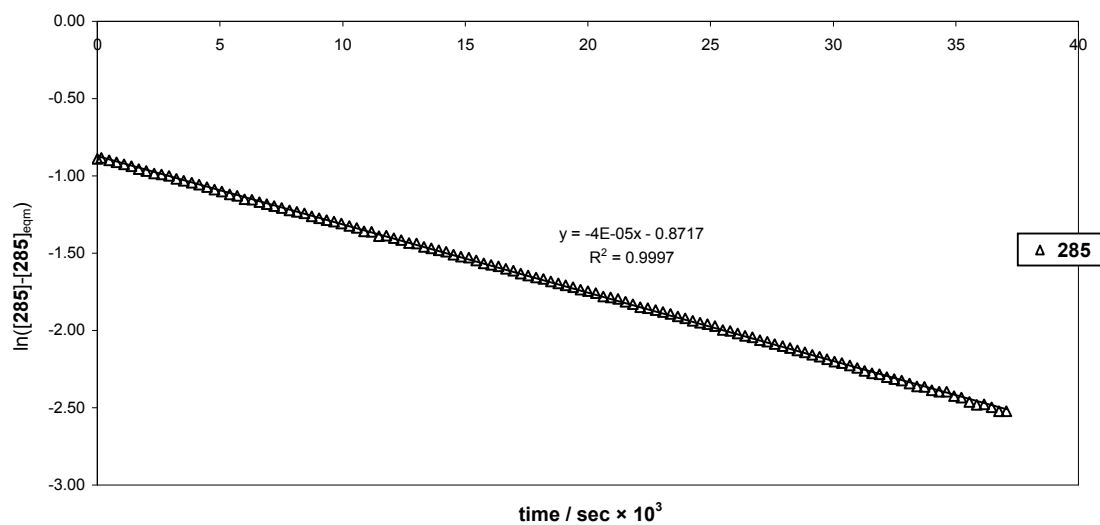
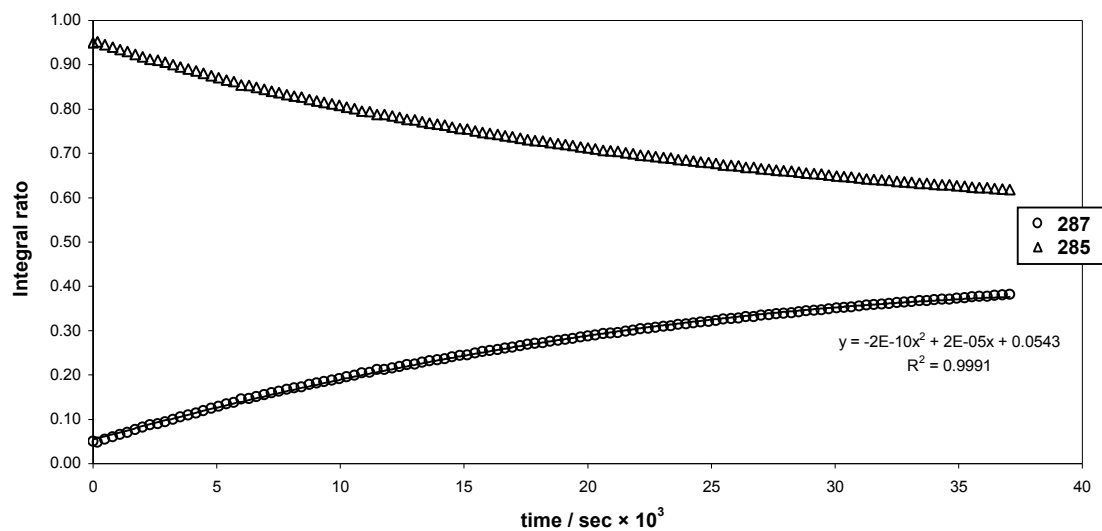
Experiment G2: Equilibration of 2-*exo*-hydroxy-3-*exo*-bornanyl acrylate **285** in purified DMSO-*d*₆ with *p*-TsoH under N₂ at **307 K**.

T/K	Mass/g	Conc./mol L ⁻¹	[287] _{eqm}	[285] _{eqm}	k_{-1}/k_{+1}	$k_{+1}+k_{-1}$	k_{-1}	k_{+1}
307	0.0135	0.120	0.471	0.529	0.89	9.22E-06	4.34E-06	4.88E-06



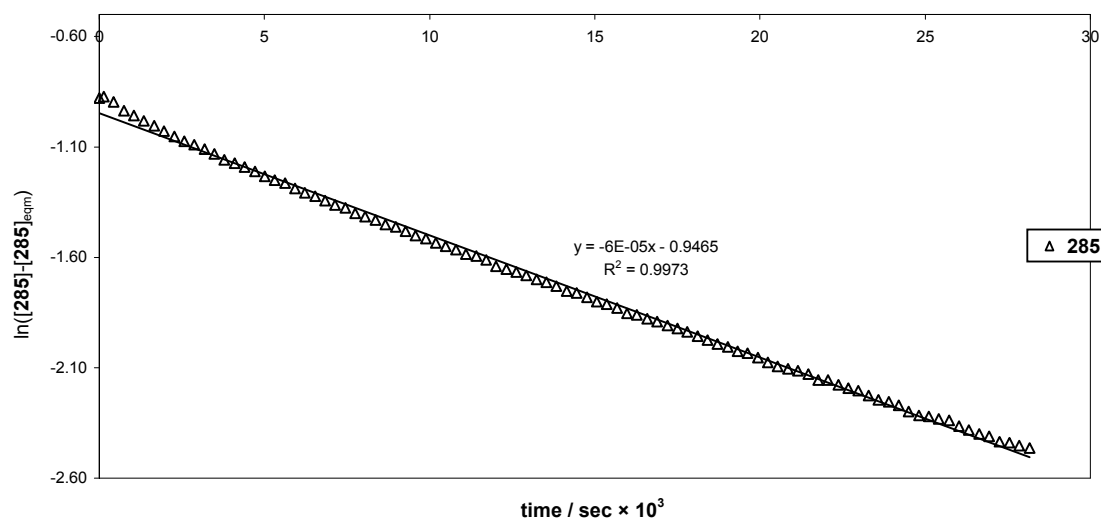
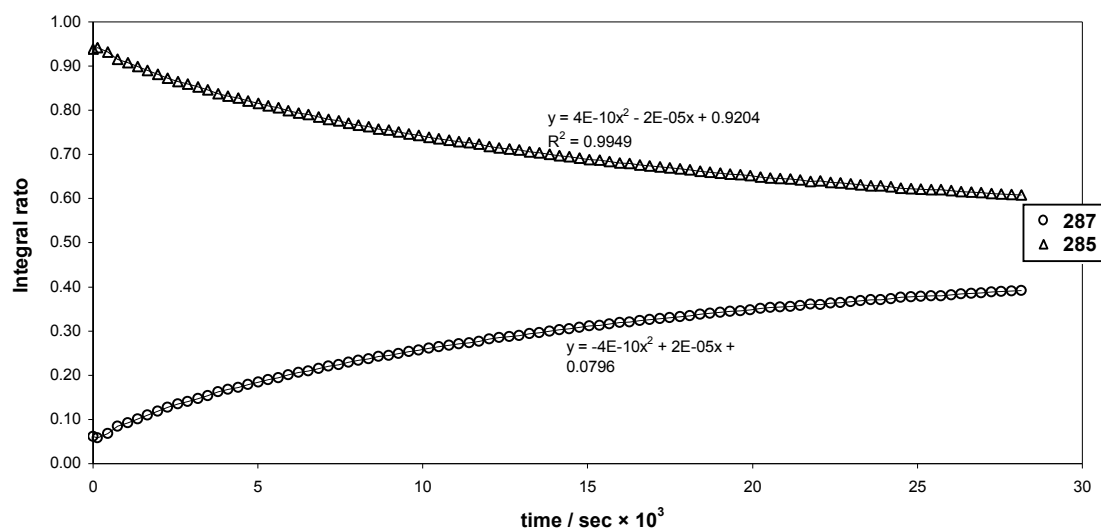
Experiment G3: Equilibration of 2-*exo*-hydroxy-3-*exo*-bornanyl acrylate **285** in purified DMSO-*d*₆ with *p*-TsOH under N₂ at **315 K**.

T/K	Mass/g	Conc./mol L ⁻¹	[287] _{eqm}	[285] _{eqm}	k_{-1}/k_{+1}	$k_{+1}+k_{-1}$	k_{-1}	k_{+1}
315	0.0135	0.120	0.462	0.538	0.86	4.42E-05	2.04E-05	2.38E-05



Experiment G4: Equilibration of 2-*exo*-hydroxy-3-*exo*-bornanyl acrylate **285** in purified DMSO-*d*₆ with *p*-TsOH under N₂ at **323 K**.

T/K	Mass/g	Conc./mol L ⁻¹	[287] _{eqm}	[285] _{eqm}	k_{-1}/k_{+1}	$k_{+1}+k_{-1}$	k_{-1}	k_{+1}
323	0.0096	0.086	0.476	0.524	0.91	5.53E-05	2.64E-05	2.90E-05



4. REFERENCES

1. T.D. Inch, *Synthesis*, 1970, 466-473.
2. J.M. Brown, S.G. Davies, G.W.J. Fleet and A.J. Pratt, *Chem. Br.*, 1989, 259.
3. J.D. Morrison, *Asymmetric Synthesis*, Academic Press, New York, 1984, **1**.
4. S.T. Handy, *Current Organic Chemistry*, 2000, **4**(4), 363.
5. J.W. Scott, *Asymmetric Synthesis*, ed J.D. Morrison and J.W. Scott, Academic Press, New York, 1984, **4**, 1.
6. G.R. Stephenson, *Advanced Asymmetric Synthesis*, Chapman-Hall, London, 1996, 4.
7. T. Katsuki and K.B. Sharpless, *J. Am. Chem. Soc.*, 1980, **102**, 5974.
8. J.D. Morrison and H.S. Mosher, *Asymmetric Organic Reactions*, Prentice-Hall Inc., Washington D.C., 1971, 165.
9. F. Maywald and P. Eilbracht, *Synlett.*, 1996, **4**, 380.
10. A.H. Hoveyda, D.A. Evans and G.C. Fu, *Chem. Rev.*, 1993, **93**, 1307.
11. G. Samuelsson, *Drugs of Natural Origin*, 1999, Swedish Pharmaceutical Press, Sweden, 259.
12. P.M. Dewick, *Medicinal Natural Products*, John Wiley and sons Ltd, England, 2002, 167.
13. T. Money, *Natural Product Reports*, 1985, 253.
14. H. Meerwein and K. van Emster, *Ber.* 1922, **55**, 2500.
15. J.H. Hutchinson, T. Money and S.E. Piper, *Can. J. Chem.*, 1986, **64**, 854.
16. V. Prelog, O. Ceder and M. Welhelm, *Helv. Chim. Acta*, 1955, **35**, 303.
17. I.V. Komarov, A. Monsees, R. Kadyrov, C. Fischer, U. Schmidt and A. Borner, *Tetrahedron Asymmetry*, 2002, **13**, 1615.
18. I.V. Komarov, M.V. Gorichko and M.Y. Kornilov, *Tetrahedron Asymmetry*, 1997, **8**(3), 435.
19. S-M. Hung, D-S. Lee and T-K. Yang, *Tetrahedron Asymmetry*, 1990, **1**, 873.
20. T-K. Yang, R-Y. Chen, D-S. Lee, W-S. Peng, Y-Z. Jiang, A-Q. Mi and T-T. Jong, *J. Org. Chem.*, 1994, **59**, 914.
21. W.C. Evans, J.M. Ridigion and J.L. Simonsen, *J. Chem. Soc.*, 1934, 137
22. W.C.M.C. Kokke, *J. Org. Chem.*, 1973, **38**, 2989.
23. E.P. Balskus, J. Menendez-Andino, R.M. Arbit and L.A. Paquette, *J. Org. Chem.*, 2001, **66**, 6695.

24. R.A. Chitenden and G.H. Cooper, *J. Chem. Soc.*, 1970, **149**, 49.
25. K. Tanaka, H. Osuga, and H. Suzuki, *Tetrahedron Asymmetry*, 1993, **4**, 1843.
26. P. Zhang and R.E. Gawley, *Tetrahedron Lett.* 1992, **33**, 2945.
27. E. Josephy and F. Radt, *Elsevier's Encyclopedia of Organic Chemistry*, Vol. 12A, Elsevier, Amsterdam, 1948.
28. J.L. Simonsen and L.N. Owen, *The Terpenes*, Vol II, 2nd ed., Cambridge University Press, 1948.
29. A. Pelter and S.H. Harper, *Rodd's Chemistry of Carbon Compounds*, Vol I, S. Coffey ed., Elsevier, Amsterdam, 1969, 136.
30. K. Maruoka, S. Hashimoto, Y. Kitagawa, H. Yamamoto and H. Nozaki, *J. Am. Chem. Soc.*, 1977, **99**, 7705.
31. J. Bredt, P. Engels, T. Lieser and H. Germer, *J. Prakt. Chem.*, 1923, **106**, 336.
32. M.S. Allen, N. Darby, P. Salisbury, E.R. Sigurdson and T. Money, *Can. J. Chem.*, 1979, 112.
33. C.R. Eck, R.W. Mills and T. Money, *J. Chem. Soc. Perkin Transactions 1*, 1975, 251.
34. F.S. Kipping and W.J. Pope, *J. Chem. Soc., Chem. Commun.*, 1993, **63**, 548.
35. W.L. Meyer, A.P. Lobo and R.N. McCarty, *J. Org. Chem.*, 1967, **32**, 1754.
36. E.J. Corey, S.W. Chow and R.A. Scherrer, *J. Am. Chem. Soc.*, 1957, **79**, 5773.
37. P.T. Kaye and W.E. Molema, *J. Chem. Soc., Chem. Commun.*, 1998, **22**, 2479.
38. Y-Y. Chu, C-S. Yu, C-J. Chen, K-S. Yang, J-C. Lain, C-H. Lin and K. Chen, *J. Org. Chem.*, 1999, **64**, 6993.
39. E.L. Eliel and W.J. Frazee, *J. Org. Chem.*, 1979, **44**, 3598.
40. O. De Lucci, C. Marchioro, G. Valle and G. Modena, *J. Chem. Soc., Chem. Commun.*, 1985, 878.
41. O. De Lucci, V. Lucchini, C. Marchioro, G. Valle and G. Modena, *J. Org. Chem.*, 1986, **51**, 1457.
42. P. Lipp and M. Holl, *Chem. Ber.*, 1938, **62**, 499.
43. Y. Asahina, T. Sano and T. Mayekawa, *ibid*, 1938, **71**, 312.
44. J. Wolinsky, D.R. Demmel and T. W. Gibson, *J. Org. Chem.*, 1967, **32**(7), 2087.
45. D.R. Drimmel and W.Y. Fu, *J. Org. Chem.*, 1973, **38**(21), 3778.
46. D. Solas and J. Wolinsky, *J. Org. Chem.*, 1983, **48**, 1988-1991.
47. J. Wolinsky and R.L. Marhenkel, *J. Org. Chem.*, 1975, **40**(12), 1766.
48. W. Oppolzer, C. Chapuis and M. Kelly, *Helv. Chim. Acta*, 1983, **66**, 2358.
49. W. Oppolzer, C. Chapuis and G. Berardinelli, *Helv. Chim. Acta*, 1984, **67**, 1397.

50. W. Oppolzer, *Helv. Chim. Acta*, 1984, **23**, 876.
51. W. Oppolzer, I. Rodriguez, J. Blagg and E. Walther, *J. Am. Chem. Soc.*, 1990, **112**, 2767.
52. W. Oppolzer, R. Moretti and S. Thomi, *Tetrahedron Lett.*, 1989, **30**, 6009.
53. W. Oppolzer, *Pure Appl. Chem.*, 1990, **62**, 1241.
54. W. Oppolzer, I. Rodriguez, J. Blagg and G. Berardinelli, *Helv. Chim. Acta*, 1989, **72**, 123.
55. W. Oppolzer, C. Starkemann, I. Rodriguez and G. Berardinelli, *Tetrahedron Lett.*, 1991, **32**, 61.
56. W. Oppolzer and P. Lienard, *Tetrahedron Lett.*, 1993, **34**, 4321
57. P.A. Smith, *Molecular Rearrangements*, Part I, ed. P de Mayo, Interscience, New York, 1963, 563 and 585.
58. K. Yamada, T. Kanekiyo, S. Tanaka, K. Naruchi and M. Yamamoto, *J. Am. Chem. Soc.*, 1981, **103**, 7003.
59. R.V. Stevens and F.C.A. Gaeta, *J. Am. Chem. Soc.*, 1977, **99**, 6105.
60. J. Hutchinson, S.E. Piper and T. Money, *J. Chem. Soc. Chem. Commun.*, 1984, 55.
61. W. Oppolzer, C. Robbiani and C. Battig, *Helv. Chim. Acta*, 1980, **63**, 2015.
62. B. Danieli and G. Palmisano, *Chem. Ind., London*, 1976, 565.
63. D.P.G. Hamon, G.F. Taylor and R.N. Young, *Synthesis*, 1975, 428.
64. D.H. Gustafson and W.F. Eрман, *J. Org. Chem.*, 1965, **30**, 1665.
65. R. Mahrwald, *Chem. Rev.*, 1999, **99**, 1095.
66. G.A. Olah, *Comprehensive Organic Chemistry*, Pergamon, NY, 1990, **3**, 293
67. W. Oppolzer, *Angew. Chem, Int. Ed. Engl.*, 1984, **23**, 876
68. N. Miyaura and A. Suzuki, *Chem. Rev.*, 1995, **95**, 2457
69. A.B. Baylis and M.E.D. Hillman, *German patent 2155113*, 1972; *Chem. Abstr.* 1972, **77**, 34174q., 1972.
70. K. Morita, Z. Sukuki and H. Hirose, *Bull. Chem. Soc. Jpn.*, 1968, **41**, 2815.
71. E. Ciganek, *Org. React.*, 1997, **51**, 201-350.
72. L.J. Brzezinski, S. Rafel and J.W. Leahy, *Tetrahedron*, 1997, **53**(48), 16423.
73. D. Basavaiah, A. Jaganmohan Rao and T. Satyanarayana, *Chem. Rev.*, 2003, **103**, 811.
74. D. Basavaiah, P.D. Rao and R.S. Hyma, *Tetrahedron*, 1996, **52**(24), 8001.
75. N.S. Isaacs, *Tetrahedron*, 1991, **47**, 8463.
76. M.K. Kundu, S.B. Mukherjee, N. Balu, R. Padmakumar and S.V. Bhat, *Synlett.*, 1994, 444.

77. S. Rafel and J.W. Leahy, *J. Org. Chem.*, 1997, **62**, 1521.
78. F. Ameer, S.E. Drewes, S. Freese and P.T. Kaye, *Synth. Commun.*, 1988, **18**, 495.
79. E.L.M. van Rosendaal, B.M.W. Voss and H.W. Schreen, *Tetrahedron*, 1993, **49**, 6931.
80. F. Roth, P. Gygax and G. Frater, *Tetrahedron Lett.*, 1992, **33**, 1045.
81. J.S. Hill and N.S. Isaacs, *J. Phys. Org. Chem.*, 1990, **3**, 285.
82. M.D. Evans and P.T. Kaye, *Synth. Commun.*, 1999, **29**, 2137.
83. M.L. Bode and P.T. Kaye, *Tetrahedron Lett.*, 1991, **32**, 5611.
84. L.V. Sabbagh, *PhD Thesis*, Rhodes University, 2000.
85. T.Cablewski, A.F. Faux and C.R. Strauss, *J. Org. Chem.*, 1994, **59**, 3408.
86. A.Gilbert, T.W. Heritage and N.S. Isaacs, *Tetrahedron Asymmetry*, 1991, **2**, 969.
87. G.P.H. Roos and P. Rampersadh, *Synth. Commun.*, 1993, **23**, 1261.
88. F. Ameer, S.E. Drewes, S. Freese and P.T. Kaye, *Synthetic Commun.*, 1988, **18**, 495.
89. T. Oishi, H. Oguri and M. Hirama, *Tetrahedron Asymmetry*, 1995, **6**(6), 1241.
90. I.E. Marco, P.R. Giles and N.J. Hindley, *Tetrahedron*, 1997, **53**(3), 1015.
91. B. Alcaide, P. Almendros and C. Aragoncillo, *Tetrahedron Lett.*, 1999, **40**, 7537.
92. P.R. Krishna, V. Kannan, G.V.M. Sharma and M.H.V. Ramana Raob, *Synlett.*, 2003, **6**, 888.
93. V.K. Aggarwal, A.M. Martin Castro, A. Mereu and H. Adams, *Tetrahedron Lett.*, 2002, **43**, 1577.
94. Y. Iwabuchi, M. Furukawa, T. Esumi and S. Hatakeyama, *J. Chem. Soc., Chem. Commun.*, 2001, 2030.
95. K-S Yang and K. Chen, *Org. Lett.*, 2000, **2**(6), 729.
96. S.E. Drewes S.D. Freese, N.D. Emslie and G.H.P. Roos, *Synth. Commun.*, 1988, **18**, 1565.
97. Y. Iwabuchi, T. Sugihara, T. Esumi and S. Hatakeyama, *Tetrahedron Lett.*, 2001, **42**, 7867.
98. Y. Iwabuchi, M. Nakatani, N. Yokoyama and S. Hatakeyama, *J. Am. Chem. Soc.*, , 1999, **121**, 10219.
99. M.D. Evans, *PhD Thesis*, Rhodes University, 1997.
100. J.M. Brown, I. Cutting, P.L. Evans and P.J. Maddox, *Tetrahedron Lett.*, 1986, **27**, 3307.
101. A.A. Khan, N.D. Emslie, S.E. Drewes, J.S. Field and N. Ramesar, *Chem. Ber.*, 1993, **126**, 1477.

102. L.J. Brzezinski, S. Rafel and J.W. Leahy, *J. Am. Chem. Soc.*, 1997, **119**, 4317.
103. S.E. Drewes, N.D. Emslie, J.S. Field, A.A. Khan and N. Ramesar, *Tetrahedron Lett.*, 1993, **34**, 1205.
104. S.E. Drewes, T. Manickum and G.H. P. Roos, *Synth. Commun.*, 1988, **18**, 1065.
105. T. Manickum and G.H. P. Roos, *S. Afr. J. Chem.*, 1994, **47**, 1.
106. E.P. Kundig, L-H Xu and B. Schnell, *Synlett.*, 1994, 413.
107. E.P. Kundig L-H Xu P. Romanens and G. Bernardinelli, *Tetrahedron Lett.*, 1993, **34**, 7049.
108. P.R. Krishna, V. Kannan, G.V.M. Sharma and A. Ilangovan, *Tetrahedron Asymmetry*, 2001, **12**, 829.
109. W.R. Roush, M. Adam, A.E. Walts and D.J. Harris, *J. Am. Chem. Soc.*, 1986, **108**, 3422.
110. D. Balan and H. Adofsson, *J. Org. Chem.*, 2001, **66**, 6498.
111. H. Richter and G. Jung, *Tetrahedron Lett.*, 1998, **39**, 2729.
112. J. Cai, Z. Zhou, G. Zhao and C. Tang, *Org. Lett.*, 2002, **4**(26), 4723.
113. H. Wynberg, *Recl. Trav. Chim. Pays-Bas*, 1981, **100**, 393.
114. K-S. Yang, W-D. Lee, J-F. Pan and K. Chen, *J. Org. Chem.*, 2003, **68**, 915.
115. R. Noyori, *Asymmetric Catalysis in Organic Synthesis*, Wiley, New York, 1994.
116. A.G.M. Barrett, A.S. Cook and A. Kamimura, *Chem. Commun.*, 1998, 2533.
117. V.K. Aggarwal, A. Mereu, G.J. Tarver and R.J. McCague, *J. Org. Chem.*, 1998, **63**, 7183.
118. T. Bauer and J. Gajewiak, *Tetrahedron*, 2003, 10009.
119. J.M. Brown and I. Cutting, *J. Chem. Soc, Chem. Commun.*, 1985, 578.
120. M. Kitamura, I. Kasahara, K. Manabe, R. Noyori and H. Takaya, *J. Org. Chem.*, 1988, **53**, 708.
121. B.M. Trost, H-C Tsui and F.D. Toste, *J. Am. Chem. Soc.*, 2000, **122**, 3534.
122. J.M. Matjila, *PhD Thesis*, Rhodes University, 1997, 15.
123. S.S. Ravindran, *PhD Thesis*, Rhodes University, 1994.
124. R. Klein, *MSc Thesis*, Rhodes University, 1999.
125. R.A. Learmonth, *PhD Thesis*, Rhodes University, 1990.
126. O. Mannasse, *Chem. Ber.*, 1902, **35**, 3811.
127. M.R. Banks, *Magn. Reson. Chem.*, 1992, **30**, 996.
128. V. Rautenstrauch, B. Willhalm, W. Thommen and U. Berger, *Helv. Chim. Acta*, 1981, **64**, 2109.

129. S.S. Pradhan, K.R. Thakker and A.T. McPhail, *Tetrahedron Lett.*, 1987, **28**, 1813.
130. M. Bonnat, J.O. Durand and M. Le Corre, *Tetrahedron: Asymmetry*, 1996, **7**(2), 559.
131. Y. Ito, T. Konoikie, T. Harada and J. Saegusa, *J. Am. Chem. Soc.*, 1977, **99**, 1487.
132. J. McNulty and M.J. Millar, *J. Org. Chem.*, 1999, **64**, 5312.
133. A. Krief and Hervesi, *Organoselenium Chem I*, Springer, NY, 1988, 76.
134. B.S. Furniss, A.J. Hammond, P.W.G Smith and A.R. Tratchell, *Vogel's Textbook of Practical Organic Chemistry*, 5th edn., 1989, 626.
135. E.J. Corey and Schaefer, *J. Am. Chem. Soc.*, , 1960, **82**, 918.
136. J. March, *Advanced Organic Chemistry*, 4th edn., John Wiley and Sons Ltd., 1992, 465.
137. E.C. Ashby, J.R. Boone, *J. Am. Chem. Soc.*, 1976, **98**, 5524.
138. L.Fieser and M.Fieser, Wiley Interscience, NY, 1967, **1**, 723.
139. P.N. Rylander, *Hydrogenation Methods*, Academic Press Limited, 1985, 72.
140. C.A.G. Haasnot, F.A.A.M. De Leeuw and C.Altona, *Tetrahedron*, 1980, **56**, 2783.
141. M.J. Karplus, *Chem. Phys.*, 1959, **30**, 11.
142. C.C Gomez and F.J.S. Lopez, Mestre-C, Beta: 3.9.9.0, 2004.
143. P.T. Kaye, A.R. Duggan, J.M. Matjila, W.E. Molema and S.S. Ravindran, *S. Afr. J. Chem.*, 2002, **55**, 111.
144. H.B. Kagan and J.C. Fiaud, *Top. Stereochem.*, 1978, **10**, 175.
145. W.S. Knowles, B.D. Vineyard, M.I. Sabacky and B.R. Stults, *Fundamental Research in Homogenous Catalysis*, ed. M.Tsutsui, vol. 3, Plenum, New York, 1979, 537.
146. T. Hayashi, A. Katsumara, M. Konishi and M. Kumada, *Tetrahedron Lett.*, 1979, 425.
147. P.T. Landsbury and A. Peterson, *J. Am. Chem. Soc.*, 1962, **84**, 1756.
148. D.C. Sarkar, A.R. Das and B.C. Ranu, *J. Org. Chem.*, 1990, **55**, 5799.
149. R. Noyori, *Science*, 1990, **248**, 1194.
150. R. Noyori and N. Takaya, *Acc. Chem. Res.*, 1990, **23**, 345.
151. K.Yamamoto, H. Fukushima and M. Nakazaki, *J. Chem. Soc., Chem. Commun.*, 1984, **14**, 1490.
152. R. Noyon, I. Tomino and Y. Tanimoto, *J. Am. Chem. Soc.*, 1979, **101**(11), 3129.
153. H.C. Brown. *et al.*, *J. Am. Chem. Soc.*, 1963, **85**, 2063, 2066 and 2072.
154. H.C. Brown, G. Zweifel and Ayyangar, *J. Am. Chem. Soc.*, 1964, **86**, 397.
155. K. Ding, A. Ishii and K. Mikami, *Angew. Chem, Int. Ed. Engl.*, 1999, **38**, 497
156. H. Budzikiewicz, C. Djerassi and D.H. Williams, Holden-Day Inc., San Francisco, 1967, 309 and 561.

157. J. Clayden, *Tetrahedron*, 2004, **60**, 4335.
158. W. Oppolzer, R. Moretti and C. Zhou, *Helv. Chim. Acta*, 1994, **77**, 2363.
159. Y. Elemen and U. Rognarsson, *J. Chem. Soc., Perkin Transactions 1*, 1995, **537**, 59.
160. G. Porzi and S. Sandri, *Tetrahedron Asymmetry*, 1996, **7**(1), 189.
161. V. Favero, G. Porzi and S. Sandri, *Tetrahedron Asymmetry*, 1997, **8**(4), 599.
162. G. Porzi, S. Sandri and P. Verrocchio, *Tetrahedron Asymmetry*, 1998, **9**, 119.
163. M. Bodansky and A. Bodansky, *Practice of Peptide Synthesis*, 1984.
164. J.M. Lacombe and A.A. Pavia, *J. Org. Chem.*, 1983, **48**, 2557.
165. Y.Ueda, C.E. Damas and B. Belleau, *Can. J. Chem.*, 1983, **61**, 6.
166. A. El-Achqar, M. Boumzebra, M-L. Roumestant and P. Viallefont, *Tetrahedron*, 1988, **44**(17), 5319.
167. R. Caputo, E. Corrado, C. Ferreri and G. Palumbo, *Synth. Commun.*, 1986, **16**, 1081.
168. P.N. Rylander, *Hydrogenation Methods*, Academic press Ltd., 1985, 160.
169. W. Carruthers, *Some Modern Methods of Organic Synthesis*, 1996, 3rd edn., Cambridge University Press, 1, 410, 457 and 484.
170. C. Catiwiela, M.D. Diaz-de-Villegas and J.A. Galvez, *Tetrahedron Asymmetry*, 1992, **3**(4), 567.
171. R.M. Silverstein and F.S. Webster, *Spectrometric Identification of Organic Compounds*, John Wiley and Sons Ltd, New York, 1998.
172. P-F. Xu Y-S. Chen, S-I. Lin and T-J. Lu, *J. Org. Chem.*, 2002, **67**, 2309.
173. P-F. Xu and T-J. Lu, *J. Org. Chem.*, 2003, **68**, 658.
174. W.E. Molema, *PhD Thesis*, Rhodes University, 1998, 67.
175. S.J. Angyal and R.J. Young, *Synthesis*, 1959, **81**, 5467.
176. I. Fleming in *Comprehensive Organic Synthesis*, ed., D.H.R. Barton and W.D. Ollis, Pergamon Press, Oxford, 1979, 309.
177. N. Greeves in *Comprehensive Organic Synthesis*, ed., B.M. Trost and I. Fleming, Pergamon Press, Oxford, 1991, **6**, 313, 632.
178. E.F.V. Scriven, *Chem. Soc. Rev.*, 1983, **12**, 129.
179. Y. Wu and W. Quintana, *Inorg. Chem.*, 1999, **38**, 2025.
180. A.R. Banks, R.F. Fibiger and T. Jones, *J. Org. Chem.*, 1977, **42**(24), 3965.
181. J.K. Kochi and G.S. Hammond, *J. Am. Chem. Soc.*, 1953, **75**, 3443.
182. W.S. Fones, *J. Org. Chem.*, 1949, **14**, 1099.
183. J. McMurry, *Organic Chemistry*, Brooks/Cole Publishing Co., 1992, 3rd edn., 1190.

184. J. Otera, *Esterification*; Wiley-VCH: Weinheim, 2003.
185. J. Otera, *Chem. Rev.*, 1993, **93**, 1449.
186. R.C. Larock, *Comprehensive Organic Transformations*, 2nd edn., VCH, New York, 1999, 269.
187. M.G. Stanton, *J. Org. Chem.*, 1997, **62**, 8240.
188. S. Bittner, *Tetrahedron Lett.*, 1975, 3871.
189. V. Tsikaris, V. Moussis, M. Sakarellos-Daitsiotis and C. Sakarellos, *Tetrahedron Lett.*, 2000, **41**, 8651.
190. T.M. Alam, M. Nyman, B.R. Cherry, J.M. Segall, and L.E. Lybarger, *J. Am. Chem. Soc.*, 2004, **126**, 5610.
191. S. Delbaere, J-C. Micheau and G. Vermeersch, *Org. Lett*, 2002, **4**(18), 3143.
192. C. Cossy, L. Helm, and A.E. Merbach, *Inorg. Chem.*, 1988, **27**, 1973.
193. W.H. Casey and B.L. Phillips, *Geochimica et Cosmochimica Acta*, 2001, **65**(5), 705.
194. B.L. Phillips, W.H. Casey and M. Karlsson, *Nature*, 2000, **404**, 379.
195. G. Furrer, M. Gfeller and B. Wehrli, *Geochimica et Cosmochimica Acta*, 1999, **63**(19/20), 3069.
196. A. Amirbahman, M. Gfeller and G. Furrer, *Geochimica et Cosmochimica Acta*, 2000, **64**(5), 911.
197. O. Mikko and L. Harri, *J. Org. Chem.*, 1997, **62**, 3246.
198. R.A. Marcus, *J. Phys. Chem.*, 1963, **67**, 853.
199. R.B. Jordan, *Reaction Mechanisms of Inorganic and Organometallic Systems*, 2nd edn., Oxford University Press, 1998.
200. C.H. Bamford, *Comprehensive Chemical Kinetics*, Vol. 2, Elsevier, 1969, 8-10, 343.
201. G.I. Brown, *Organic Chemistry*, Longman, London, 1988, 322.
202. K. Lobb, *unpublished work*, 2002.
203. R. Schmid and V.N. Sapunov, *Non-formal Kinetics, Monographs in Modern Chemistry*, Verlag Chemie, Weinheim, 1982, 20.
204. S. Glasstone, *Elements of Physical Chemistry*, McMillan and Co., London, 1961, 618-621.
205. J. Clayden, N. Greeves, S. Warren and P. Wothers, *Organic Chemistry*, Longman, London, 2001.
206. M. Polanyi and A.L. Szabo, *Trans. Faraday Soc.*, 1934, **30**, 508
207. J. B. Foresman and A. Frisch, *Exploring Chemistry with Electronic Structure Methods*, Gaussian inc., USA, 1996, 149 and 165.

- 208 M.L. Bender and R.J. Thomas, *J. Am. Chem. Soc.*, 1961, **83**, 4183.
- 209 F.M. Menger, *Tetrahedron*, 1983, **39**, 1013
- 210 C.K. Ingold, *Structure and Mechanism in Organic Chemistry*, 2nd edn., Cornell University Press: Ithaca, NY, 1969,
211. P. Bartlett, *Organic Synthesis*, 1965, **45**, 14.
212. W. Molema, *PhD Thesis*, Rhodes University, 1998, 166.
213. D.J. Procter, N.J. Archer, R.A. Needham, D. Bell, A.P. Marchington and C.M. Rayner, *Tetrahedron*, 1999, **55**(31), 9611.
214. H.C. Brown, *Tetrahedron*, 1957, **1**, 214.
215. J. Luche and A.L. Gemal, *J. Am. Chem. Soc.*, 1979, **101**, 5848.
216. L.G. Hamman and M. Koreeda, *Tetrahedron Lett.*, 1992, **33**, 6569.
217. K. Maruoka, Y. Araki and H. Yamanamoto, *J. Am. Chem. Soc.*, 1988, **110**, 2650.
218. H.C. Brown, E.J. Mead and B.C. Subba Rao, *Organic and Biological Chemistry*, 1955, 6209.
219. W. Oppolzer, M. Kelly and G. Bernardelli, *Tetrahedron Lett.*, 1984, **25**, 5889.
- 220, D.R. Drimmel and W.Y. Fu, *J. Org. Chem.*, 1973, **38**(21), 3782.
221. D. Solas and J. Wolinsky, *J. Org. Chem.*, 1983, **48**, 1988.
222. T.M.V.D. Pinho e Melo, A.L. Cardoso and A.M. d'A Rocha Gonsalves, *Tetrahedron*, 2003, **59**, 2345.
223. Gaussian 03, Revision B.05, M. J. Frisch, G.W. Trucks, H.B. Schlegel, G.E. Scuseria, M.A. Robb, J.R. Cheeseman, J.A. Montgomery, Jr., T. Vreven, K.N. Kudin, J.C. Burant, J.M. Millam, S.S. Iyengar, J. Tomasi, V. Barone, B. Mennucci, M. Cossi, G. Scalmani, N. Rega, G.A. Petersson, H. Nakatsuji, M. Hada, M. Ehara, K. Toyota, R. Fukuda, J. Hasegawa, M. Ishida, T. Nakajima, Y. Honda, O. Kitao, H. Nakai, M. Klene, X. Li, J.E. Knox, H.P. Hratchian, J.B. Cross, C. Adamo, J. Jaramillo, R. Gomperts, R.E. Stratmann, O. Yazyev, A.J. Austin, R. Cammi, C. Pomelli, J.W. Ochterski, P.Y. Ayala, K. Morokuma, G.A. Voth, P. Salvador, J.J. Dannenberg, V.G. Zakrzewski, S. Dapprich, A.D. Daniels, M.C. Strain, O. Farkas, D.K. Malick, A.D. Rabuck, K. Raghavachari, J.B. Foresman, J.V. Ortiz, Q. Cui, A. G. Baboul, S. Clifford, J. Cioslowski, B.B. Stefanov, G. Liu, A. Liashenko, P. Piskorz, I. Komaromi, R.L. Martin, D.J. Fox, T. Keith, M.A. Al-Laham, C.Y. Peng, A. Nanayakkara, M. Challacombe, P.M.W. Gill, B. Johnson, W. Chen, M.W. Wong, C. Gonzalez, and J.A. Pople, Gaussian, Inc., Pittsburgh PA, 2003.

224. J. Leonard, *Advanced Practical Organic Chemistry*, 1995, Blackie Academic, 162-163.
225. D.E. Ward, M. Sales and P.K. Sasmal, *J. Org. Chem.*, 2004, **69**, 4808.
226. L.A. Collett, M.T.Davies-Coleman and D.E.A. Rivett, *Phytochemistry*, 1998, **48**(4), 651.
227. K. Ishihara, M. Kubota, H. Kurihara and H. Yamamoto, *Tetrahedron*, 1996, **61**, 4560.
228. D. Bonafoux and I. Ojima, *Org. Lett.*, 2001, **3**(15), 2333.
229. M. Woltersdorf, R. Kranich and H. Schmalz, *Tetrahedron*, 1997, **53**(21), 7219.
230. Z. Cekovic and Z. Tokie, *Synthesis*, 1989, **8**, 610.
231. M. Schuman and V. Gouverneur, *Tetrahedron Lett.*, 2002, **43**, 3513.
232. K. Ishihara, M. Nakayama, S. Ohara and H. Yamamoto, *Tetrahedron*, 2002, **58**(41), 8179.
233. V.K Yadev and K.G. Babu, *J. Org. Chem.*, 2004, **69**, 577.
234. A. Filippi, N. A. Trout, P. Brunelle, W. Adcock, T.S. Sorensen and M. Speranza, *J. Am. Chem. Soc.*, 2001, **123**, 6396.
235. A Filippi, N.A. Trout, P.Brunelle, W. Adcock, T.S. Sorensen and M. Speranza, *J. Org. Chem.*, 2004, **69**(17), 5537.
236. B.W. Gung, *Chem. Rev.*, 1999, **99**, 1377.
237. N.G. Andersen, P.D. Ramsden, D. Che, M. Parvez and B.A. Keay, *Org. Lett.*, 1999, **1**(12), 2009.
238. N.G. Andersen, P.D. Ramsden, D. Che, M. Parvez, and B.A. Keay, *J. Org. Chem.*, 2001, **66**, 7478.
239. D.J. Ramon and M. Yus, *Tetrahedron Lett.*, 1998, **39**, 1239.
240. D.J. Ramon and M. Yus, *Tetrahedron*, 1998, **54**, 5651.
241. D.J. Ramon and M. Yus, *Tetrahedron Asymmetry*, 1997, **8**, 2479.
242. D.D. Perrin and W.L.F. Amarego, *Purification of Laboratory Chemicals*, Pergamon Press, Oxford, 3rd. edn., 1988.
243. Cerius², v. 4.0, BIOSYMM/Molecular Simulations Inc.
244. B. Pfrunder and C. Tamm, *Helv. Chim. Acta*, 1969, **52**, 1630.

5. APPENDIX I

5.1 CRYSTALLOGRAPHIC DATA FOR PHENYL 2-EXO-(3-CHLORO-PROPANOYLOXY)BORNANE-10-SULFONATE 308

Empirical Formula	$C_{19}H_{25}ClO_5S$	
Formula Weight	400.92	
Temperature (K)	113	
Wavelength	0.71073 Å	
Crystal System	Orthorhombic	
Space group	P2(1)2(1)2(1)	
Unit cell dimensions	a = 36.0852(7) Å	$\alpha = 90^\circ$
	b = 7.0606(2) Å	$\beta = 90^\circ$
	c = 7.5933(2) Å	$\gamma = 90^\circ$
Volume	1934.65(8) Å ³	
Z	4	
Density (calculated)	1.377 Mg/m ³	
F(000)	848	
Crystal Size	0.15 x 0.15 x 0.25 mm ³	
Theta range for data collection	2.3 - 27.9°	
Index ranges	-47<=h<=43, -9<=k<=9, -9<=l<=9	
Scan (Type & Range)	phi- and omega scans of 0.8-1.0°	
Reflections collected	10287	
Independent reflections	4103 [R(int) = 0.068]	
Absorption correction	Integration	
Min and Max transmission	0.0879 and 2.827	
Refinement method	Full-matrix, least squares on F ²	
Data / restraints / parameters	4103 / 0 / 237	
Goodness-of-fit on F ²	1.05	
Largest diff. peak and hole	-1.04 and 0.56 e.Å ⁻³	

6. APPENDIX II

6.1 KINETIC DATA FOR THE TRANSESTERIFICATION STUDIES

(See attached CD)